



*pathogens*

# Rotaviruses and Rotavirus Vaccines

---

Edited by

Celeste Donato and Julie Bines

Printed Edition of the Special Issue Published in *Pathogens*

# **Rotaviruses and Rotavirus Vaccines**



# Rotaviruses and Rotavirus Vaccines

Editors

**Celeste Donato**

**Julie Bines**

MDPI • Basel • Beijing • Wuhan • Barcelona • Belgrade • Manchester • Tokyo • Cluj • Tianjin



*Editors*

Celeste Donato	Julie Bines
Enteric Diseases	Enteric Diseases
Murdoch Children's Research	Murdoch Children's Research
Institute	Institute
Parkville	Parkville
Australia	Australia

*Editorial Office*

MDPI  
St. Alban-Anlage 66  
4052 Basel, Switzerland

This is a reprint of articles from the Special Issue published online in the open access journal *Pathogens* (ISSN 2076-0817) (available at: [www.mdpi.com/journal/pathogens/special\\_issues/rotaviruses\\_and\\_rotavirus\\_vaccines](http://www.mdpi.com/journal/pathogens/special_issues/rotaviruses_and_rotavirus_vaccines)).

For citation purposes, cite each article independently as indicated on the article page online and as indicated below:

LastName, A.A.; LastName, B.B.; LastName, C.C. Article Title. <i>Journal Name</i> <b>Year</b> , Volume Number, Page Range.
--

**ISBN 978-3-0365-2591-4 (Hbk)**

**ISBN 978-3-0365-2590-7 (PDF)**

© 2021 by the authors. Articles in this book are Open Access and distributed under the Creative Commons Attribution (CC BY) license, which allows users to download, copy and build upon published articles, as long as the author and publisher are properly credited, which ensures maximum dissemination and a wider impact of our publications.

The book as a whole is distributed by MDPI under the terms and conditions of the Creative Commons license CC BY-NC-ND.

# Contents

<b>About the Editors</b> . . . . .	vii
<b>Preface to "Rotaviruses and Rotavirus Vaccines"</b> . . . . .	ix
<b>Celeste M. Donato and Julie E. Bines</b> Rotaviruses and Rotavirus Vaccines Reprinted from: <i>Pathogens</i> <b>2021</b> , <i>10</i> , 959, doi:10.3390/pathogens10080959 . . . . .	1
<b>Bianca F. Middleton, Margie Danchin, Helen Quinn, Anna P. Ralph, Nevada Pingault, Mark Jones, Marie Estcourt and Tom Snelling</b> Retrospective Case-Control Study of 2017 G2P[4] Rotavirus Epidemic in Rural and Remote Australia Reprinted from: <i>Pathogens</i> <b>2020</b> , <i>9</i> , 790, doi:10.3390/pathogens9100790 . . . . .	7
<b>Celeste M. Donato, Nevada Pingault, Elena Demosthenous, Susie Roczo-Farkas and Julie E. Bines</b> Characterisation of a G2P[4] Rotavirus Outbreak in Western Australia, Predominantly Impacting Aboriginal Children Reprinted from: <i>Pathogens</i> <b>2021</b> , <i>10</i> , 350, doi:10.3390/pathogens10030350 . . . . .	19
<b>Jaime MacDonald, Michelle J. Groome, Janet Mans and Nicola Page</b> <i>FUT2</i> Secretor Status Influences Susceptibility to VP4 Strain-Specific Rotavirus Infections in South African Children Reprinted from: <i>Pathogens</i> <b>2020</b> , <i>9</i> , 795, doi:10.3390/pathogens9100795 . . . . .	39
<b>Peter N. Mwangi, Milton T. Mogotsi, Sebotsana P. Rasebotsa, Mapaseka L. Seheri, M. Jeffrey Mphahlele, Valantine N. Ndze, Francis E. Dennis, Khuzwayo C. Jere and Martin M. Nyaga</b> Uncovering the First Atypical DS-1-like G1P[8] Rotavirus Strains That Circulated during Pre-Rotavirus Vaccine Introduction Era in South Africa Reprinted from: <i>Pathogens</i> <b>2020</b> , <i>9</i> , 391, doi:10.3390/pathogens9050391 . . . . .	49
<b>Wairimu M. Maringa, Peter N. Mwangi, Julia Simwaka, Evans M. Mpabalwani, Jason M. Mwenda, Ina Peenze, Mathew D. Esona, M. Jeffrey Mphahlele, Mapaseka L. Seheri and Martin M. Nyaga</b> Molecular Characterisation of a Rare Reassortant Porcine-Like G5P[6] Rotavirus Strain Detected in an Unvaccinated Child in Kasama, Zambia Reprinted from: <i>Pathogens</i> <b>2020</b> , <i>9</i> , 663, doi:10.3390/pathogens9080663 . . . . .	67
<b>Matías Castells, Rubén Darío Caffarena, María Laura Casaux, Carlos Schild, Samuel Miño, Felipe Castells, Daniel Castells, Matías Victoria, Franklin Riet-Correa, Federico Giannitti, Viviana Parreño and Rodney Colina</b> Phylogenetic Analyses of Rotavirus A from Cattle in Uruguay Reveal the Circulation of Common and Uncommon Genotypes and Suggest Interspecies Transmission Reprinted from: <i>Pathogens</i> <b>2020</b> , <i>9</i> , 570, doi:10.3390/pathogens9070570 . . . . .	89
<b>Zoe Yandle, Suzie Coughlan, Jonathan Dean, Gráinne Tuite, Anne Conroy and Cillian F. De Gascun</b> Group A Rotavirus Detection and Genotype Distribution before and after Introduction of a National Immunisation Programme in Ireland: 2015–2019 Reprinted from: <i>Pathogens</i> <b>2020</b> , <i>9</i> , 449, doi:10.3390/pathogens9060449 . . . . .	107

<b>Meylin Bautista Gutierrez, Alexandre Madi Fialho, Adriana Gonçalves Maranhão, Fábio Correia Malta, Juliana da Silva Ribeiro de Andrade, Rosane Maria Santos de Assis, Sérgio da Silva e Mouta, Marize Pereira Miagostovich, José Paulo Gagliardi Leite and Tulio Machado Fumian</b> Rotavirus A in Brazil: Molecular Epidemiology and Surveillance during 2018–2019 Reprinted from: <i>Pathogens</i> 2020, 9, 515, doi:10.3390/pathogens9070515 . . . . .	123
<b>Mike J. Mwanga, Jennifer R. Verani, Richard Omoro, Jacqueline E. Tate, Umesh D. Parashar, Nickson Murunga, Elijah Gicheru, Robert F. Breiman, D. James Nokes and Charles N. Agoti</b> Multiple Introductions and Predominance of Rotavirus Group A Genotype G3P[8] in Kilifi, Coastal Kenya, 4 Years after Nationwide Vaccine Introduction Reprinted from: <i>Pathogens</i> 2020, 9, 981, doi:10.3390/pathogens9120981 . . . . .	139
<b>Arnold W. Lambisia, Sylvia Onchaga, Nickson Murunga, Clement S. Lewa, Steven Ger Nyanjom and Charles N. Agoti</b> Epidemiological Trends of Five Common Diarrhea-Associated Enteric Viruses Pre- and Post-Rotavirus Vaccine Introduction in Coastal Kenya Reprinted from: <i>Pathogens</i> 2020, 9, 660, doi:10.3390/pathogens9080660 . . . . .	155
<b>Sarah Thomas, Celeste M. Donato, Sokoveti Covea, Felisita T. Ratu, Adam W. J. Jenney, Rita Reyburn, Aalisha Sahu Khan, Eric Rafai, Varja Grabovac, Fatima Serhan, Julie E. Bines and Fiona M. Russell</b> Genotype Diversity before and after the Introduction of a Rotavirus Vaccine into the National Immunisation Program in Fiji Reprinted from: <i>Pathogens</i> 2021, 10, 358, doi:10.3390/pathogens10030358 . . . . .	169
<b>Tintu Varghese, Shainey Alokhit Khakha, Sidhartha Giri, Nayana P. Nair, Manohar Badur, Geeta Gathwala, Sanjeev Chaudhury, Shayam Kaushik, Mrutunjay Dash, Nirmal K. Mohakud, Rajib K. Ray, Prasantajyoti Mohanty, Chethrapilly Purushothaman Girish Kumar, Seshadri Venkatasubramanian, Rashmi Arora, Venkata Raghava Mohan, Jacqueline E. Tate, Umesh D. Parashar and Gagandeep Kang</b> Rotavirus Strain Distribution before and after Introducing Rotavirus Vaccine in India Reprinted from: <i>Pathogens</i> 2021, 10, 416, doi:10.3390/pathogens10040416 . . . . .	181
<b>Eva D. João, Benilde Munlela, Assucênio Chissaque, Jorfélia Chilaúle, Jerónimo Langa, Orvalho Augusto, Simone S. Boone, Elda Anapakala, Júlia Sambo, Esperança Guimarães, Diocreciano Bero, Marta Cassocera, Idalécia Cossa-Moiane, Jason M. Mwenda, Isabel Maurício, Hester G. O'Neill and Nilsa de Deus</b> Molecular Epidemiology of Rotavirus A Strains Pre- and Post-Vaccine (Rotarix®) Introduction in Mozambique, 2012–2019: Emergence of Genotypes G3P[4] and G3P[8] Reprinted from: <i>Pathogens</i> 2020, 9, 671, doi:10.3390/pathogens9090671 . . . . .	191
<b>Benilde Munlela, Eva D. João, Celeste M. Donato, Amy Strydom, Simone S. Boone, Assucênio Chissaque, Adilson F. L. Bauhofer, Jerónimo Langa, Marta Cassocera, Idalécia Cossa-Moiane, Jorfélia J. Chilaúle, Hester G. O'Neill and Nilsa de Deus</b> Whole Genome Characterization and Evolutionary Analysis of G1P[8] Rotavirus A Strains during the Pre- and Post-Vaccine Periods in Mozambique (2012–2017) Reprinted from: <i>Pathogens</i> 2020, 9, 1026, doi:10.3390/pathogens9121026 . . . . .	207

# About the Editors

## **Celeste Donato**

Dr Celeste Donato is a molecular virologist and senior research officer in the Enteric Diseases Group at the Murdoch Children's Research Institute in Melbourne, Australia. Dr Donato's research explores the epidemiology and evolution of viruses causing disease in humans and animal populations, including rotavirus, enterovirus, astrovirus, and influenza.

## **Julie Bines**

Professor Bines is the Victor and Loti Smorgon Professor of Paediatrics, Department of Paediatrics, The University of Melbourne, a paediatric gastroenterologist, and Head of Clinical Nutrition at the Royal Children's Hospital, Melbourne, Australia. Professor Bines also leads the Enteric Diseases research group at the Murdoch Children's Research Institute. Professor Bines has been involved across a breadth of activities related to rotavirus vaccines, including rotavirus vaccine development, vaccine clinical trials, pre- and post-licensure surveillance, and vaccine advocacy.



## Preface to “Rotaviruses and Rotavirus Vaccines”

The Rotavirus genus, within the *Reoviridae* virus family, encompasses a large and diverse population of viruses capable of causing disease in humans and a variety of animal species. Group A Rotavirus remains a leading cause of morbidity and mortality due to gastroenteritis in young children worldwide; it is estimated to have caused 128,500 deaths and 258,173,300 episodes of diarrhea among children under 5 years of age in 2016 alone. There has been a substantial decrease in the global burden of rotavirus disease over the last decade, which can be attributed to various public health measures such as improved sanitation, as well as the inclusion of rotavirus vaccines into the national immunisation programs of over 112 countries worldwide

Rotavirus is classified into G and P genotypes based on the two outer capsid proteins, VP7 and VP4, respectively. To date, 36 G types and 51 P types have been identified in humans and various animal species. The most common genotypes in humans are G1, G2, G3, G4, G9, and G12, in combination with P[4], P[6], and P[8]. The growing utilization of next-generation sequencing is expanding our knowledge of rotavirus genetic diversity through an increase in whole-genome sequencing. Rotavirus strains can evolve rapidly, employing numerous mechanisms including genetic drift and reassortment. Although rotavirus strains exhibit a degree of host species restriction, zoonotic transmission substantially increases the genetic diversity of strains causing human infection. Understanding changes to rotavirus epidemiology and genetic diversity in the vaccine era is critical to ensure the continued success of the global vaccination efforts.

The goal of this special edition of *Pathogens* was to bring together a breadth of information on rotavirus and rotavirus vaccines globally, highlighting rotavirus research from across the world which represents recent advances in our knowledge of vaccine effectiveness, rotavirus epidemiology, genotypic diversity, and genomic characterisation.

**Celeste Donato, Julie Bines**

*Editors*



Editorial

# Rotaviruses and Rotavirus Vaccines

Celeste M. Donato<sup>1,2,3,\*</sup>  and Julie E. Bines<sup>1,2,4</sup> 

<sup>1</sup> Enteric Diseases Group, Murdoch Children's Research Institute, Parkville, VIC 3052, Australia; jebines@unimelb.edu.au

<sup>2</sup> Department of Paediatrics, The University of Melbourne, Parkville, VIC 3052, Australia

<sup>3</sup> Department of Microbiology, Biomedicine Discovery Institute, Monash University, Clayton, VIC 3800, Australia

<sup>4</sup> Department of Gastroenterology and Clinical Nutrition, Royal Children's Hospital, Parkville, VIC 3052, Australia

\* Correspondence: celeste.donato@mcri.edu.au; Tel.: +61-(03)-99366715

**Keywords:** epidemiology; rotavirus vaccines; molecular phylogeny; virus evolution; zoonosis; vaccines; virology

Group A rotaviruses belong to the *Reoviridae* virus family and are classified into G and P genotypes based on the outer capsid proteins VP7 and VP4, respectively. To date, 36 G types and 51 P types have been characterised from humans and varied animal species [1]. The most prevalent genotypes in humans are G1, G2, G3, G4, G9, and G12, in combination with P[4], P[6], and P[8] [2,3]. A whole genome classification nomenclature has been developed to describe the genome constellation of strains; G<sub>x</sub>-P<sub>[x]</sub>-I<sub>x</sub>-R<sub>x</sub>-C<sub>x</sub>-M<sub>x</sub>-A<sub>x</sub>-N<sub>x</sub>-T<sub>x</sub>-E<sub>x</sub>-H<sub>x</sub>, denoting the VP7-VP4-VP6-VP1-VP2-VP3-NSP1-NSP2-NSP3-NSP4-NSP5/6 genes, with x referring to the various recognised genotypes for each gene. There are three major genotype constellations: Wa-like (G1-P[8]-I1-R1-C1-M1-A1-N1-T1-E1-H1), DS-1-like (G2-P[4]-I2-R2-C2-M2-A2-N2-T2-E2-H2), and AU-1-like (G3-P[9]-I3-R3-C3-M3-A3-N3-T3-E3-H3) [4].

Group A rotaviruses remain one of the principal aetiological agents of acute gastroenteritis in infants and young children worldwide. Rotavirus infection was estimated to have caused 128,500 deaths (95% uncertainty interval (UI), 104,500–155,600) and 258,173,300 episodes (95% UI, 193 million to 341 million) of diarrhea among children under 5 years of age in 2016 [5]. Rotavirus-associated mortality rates are highest in sub-Saharan Africa, Southeast Asia, and South Asia [5]. There has been a substantial decrease in the global burden of rotavirus disease over the last decade which can be attributed to varied public health measures such as improved sanitation, as well as the inclusion of rotavirus vaccines into the National Immunisation Programs of over 112 countries worldwide [6]. The implementation of rotavirus vaccines has been estimated to have averted more than 28,000 deaths (95% UI, 14,600–46,700) among children under 5 years of age in 2016 [5]. However, many low- and middle-income countries are yet to introduce rotavirus vaccines. The expanded use of the rotavirus vaccines, particularly in sub-Saharan Africa, could have prevented approximately 20% of all deaths attributable to diarrhea among children under 5 years of age in 2016 [5].

Four group A rotavirus vaccines; Rotarix<sup>®</sup> (GlaxoSmithKline, Rixenstart, Belgium), Rotasiil<sup>®</sup> (Serum Institute of India, Pune, India), RotaTeq<sup>®</sup> (Merck & Co, Pennsylvania, PA, USA) and Rotavac<sup>®</sup> (Bharat Biotech, Hyderabad, India) have been prequalified by the World Health Organization (WHO) for global use [7]. The most widely used vaccines are Rotarix, which is a monovalent vaccine comprised of a single human G1P[8] strain and RotaTeq, which is a pentavalent, human-bovine reassortant vaccine comprising G1P[5], G2P[5], G3P[5], G4P[5] and G6P[8] strains [8,9]. Rotasiil and Rotavac are primarily used in India. Rotasiil is a pentavalent, human-bovine reassortant vaccine comprised of G1P[5],



**Citation:** Donato, C.M.; Bines, J.E. Rotaviruses and Rotavirus Vaccines.

*Pathogens* **2021**, *10*, 959.

<https://doi.org/10.3390/pathogens10080959>

Received: 20 July 2021

Accepted: 28 July 2021

Published: 29 July 2021

**Publisher's Note:** MDPI stays neutral with regard to jurisdictional claims in published maps and institutional affiliations.



**Copyright:** © 2021 by the authors. Licensee MDPI, Basel, Switzerland. This article is an open access article distributed under the terms and conditions of the Creative Commons Attribution (CC BY) license (<https://creativecommons.org/licenses/by/4.0/>).

G2P[5], G3P[5], G4P[5], and G9[5] [10]. Rotavac is a monovalent vaccine comprised of a naturally occurring G9P[11] reassortant strain [11].

The goal of this special edition of *Pathogens* was to bring together a breadth of information on rotavirus and rotavirus vaccines globally to highlight rotavirus research from across the world that represent recent advances in our knowledge of vaccine effectiveness, rotavirus epidemiology, genotypic diversity, and genomic characterisation.

High rates of vaccine effectiveness have been reported in Europe, the USA and Australia [12,13]. However, suboptimal vaccine effectiveness, especially in the second year of life, has been noted in low- and middle-income countries in Africa and Latin America, as well as during outbreaks of rotavirus disease in the Australian Indigenous population [14,15]. The reasons why vaccine take and subsequent vaccine effectiveness are lower in some settings remains unclear. A range of factors have been implicated including higher rotavirus transmission rates, variations in gut microbiota, and host factors such as histo-blood group antigen (HBGA) and Lewis secretor antigens [15]. Middleton et al. conducted a retrospective case–control study to evaluate the performance of Rotarix and RotaTeq during a G2P[4] rotavirus epidemic in rural and remote Australia [16]. The majority of affected children were Aboriginal and/or Torres Strait Islander; populations that experience a disproportionately high burden of rotavirus disease. During this G2P[4] outbreak, there was some evidence of a protective effect among younger children under 12 months of age. However, the overall protective effect of either Rotarix or RotaTeq in this setting was weak. The study highlights that even within a high-income country, certain populations will experience differing vaccine effectiveness, which suggests that tailored vaccine strategies and public health measures may be required to better protect these populations until the reasons for suboptimal vaccine effectiveness can be elucidated and addressed [16]. The strain associated with this outbreak was characterised by Donato et al. and the demographics of the outbreak in Kimberley region of Western Australia was described [17]. Full genome sequencing revealed the outbreak variant exhibited the archetypal DS-1-like genome constellation: G2-P[4]-I2-R2-C2-M2-A2-N2-T2-E2-H2 and phylogenetic analysis revealed all genes were closely related to contemporary Japanese G2P[4] samples indicating a recent introduction into Australia rather than the outbreak variant having been derived from G2P[4] variants that had caused prior outbreaks in the region. The VP7 gene of the outbreak variant was compared to the G2 component of the RotaTeq vaccine, identifying mutations in known antigenic regions. However, these mutations are frequently observed in contemporary G2P[4] strains and are unlikely to be the sole reason that the outbreak occurred this population [17].

Host genetic factors such as HBGA status play a role in susceptibility to disease as well as response to vaccines. HBGA status varies across populations; with higher proportions of non-secretor phenotypes observed in African populations compared to other populations [18]. MacDonald et al. investigated FUT2-defined secretor status in children under 5 years-old hospitalised with rotavirus-related diarrhoea compared with rotavirus-negative controls [19]. The proportion of secretors in rotavirus-positive cases was significantly higher than in the rotavirus-negative controls. The rotavirus genotypes P[8] and P[4] were detected at significantly higher proportions in secretors compared to non-secretors. However, the P[6] genotype was observed at similar proportions amongst secretor and non-secretors [19]. Overall, this study suggests that HGBA status may partially influence rotavirus infection due to the VP4 protein, and may explain why rotavirus vaccines with P[8] strains exhibit suboptimal effectiveness in African populations [19].

Numerous mechanisms including genetic drift and reassortment contribute to rotavirus diversity. The segmented genome allows for reassortment both within and between human and animal strains, leading to the emergence of novel strains and unusual genotype combinations [20]. Reassortment is a key mechanism driving the evolution of rotavirus strains and reassortment between strains of different genotypes have been increasingly observed. The emergence of DS-1-like G1P[8] strains have been reported in several countries during the rotavirus vaccination era [21]. Mwangi et al. reported atypical DS-1-like G1P[8]

strains that circulated in 2008 during the pre-vaccine era in South Africa [22]. These strains emerged through reassortment events involving locally circulating South African strains and were not related to other atypical G1P[8] strains reported globally. This study highlighted the occurrence of independent, local reassortant events contributing to rotavirus diversity [22].

Zoonotic transmission also plays a critical role in the diversity of rotavirus strains detected in the human population. Maringa et al. described the full genome constellation of a human-porcine reassortant strain, RVA/Human-wt/ZMB/UFS-NGS-MRC-DPRU4723/2014/G5P[6], which was identified from an unvaccinated 12 month old male who had been hospitalised for gastroenteritis in Zambia [23]. The strain exhibited the genome constellation G5-P[6]-I1-R1-C1-M1-A8-N1-T1-E1-H1 and phylogenetic analysis revealed the genes were most closely related to porcine and porcine-like human strains [23]. Understanding the diversity of strains in various animal populations is important for animal health and farming practices, as well as being informative for the contextualisation of zoonotic transmission events. Castells et al. reported detection of rotavirus in calves reared for beef and dairy production in Uruguay [24]. Multiple genotypes associated with bovine disease were detected including G6P[11] (40.4%), G6P[5] (38.6%), G10P[11] (19.3%), as well as the uncommon genotype G24P[33] (1.8%) [24].

Long-term surveillance is critical in understanding the trends in rotavirus genotype diversity and distribution, as overinterpretation of short-term fluctuations in genotype prevalence can be misleading without a greater context of the natural, cyclic patterns in genotype replacement over time. This is especially critical when comparing trends in genotype distribution pre- and post-vaccine introduction. Genotype surveillance data in Australia and elsewhere has revealed changes in diversity, as well as temporal and geographic fluctuations over time following vaccine introduction [25,26]. Furthermore, differences in genotype diversity and dominance were observed when comparing vaccines by jurisdictions, suggesting that RotaTeq and Rotarix may exert different immunological pressures [25].

Yandle et al. described changes in the burden of rotavirus disease and genotype distribution in Ireland following vaccine introduction [27]. Rotavirus detection decreased by 91% in children aged 0–12 months between 2015/16 and 2018/19, and the once prominent seasonal peak in disease was reduced following Rotarix vaccine introduction in December 2016. The genotype distribution altered following vaccine introduction; the prevalence of G1P[8] which was dominant prior to vaccine introduction decreased while the prevalence of G2P[4] and G3P[8] increased. An increase in genotype diversity was also observed in the vaccine era, with the equine-like G3P[8] variant detected in Ireland [27]. The equine-like G3P[8] variant was also reported by Gutierrez et al., where it was the dominant genotype observed in Brazil in 2018 and 2019 [28]. This study also reported a significantly higher positivity rate among children aged >24–60 months compared to other age groups [28]. This shift in the age of rotavirus disease towards slightly older children has also been reported in other countries that have introduced rotavirus vaccines [26,29]. The equine-like G3P[8] variant was also reported by Mwangi et al., from the Kilifi region of Kenya in 2018; four years after Rotarix was introduced [30]. During this surveillance year, G3P[8] was the dominant genotype detected and the equine variant accounted for a small proportion of these G3P[8] cases, replacing G2P[4] and G1P[8] which had been predominant in the prior two years [30]. The epidemiological trends of enteric viruses pre- and post-rotavirus vaccine introduction were investigated in this region by Lambisia et al., describing rotavirus, norovirus (genogroup GII), adenovirus, astrovirus and sapovirus [31]. Following the introduction of Rotarix, the prevalence of rotavirus decreased whilst the prevalence of norovirus increased. The prevalence of adenovirus, astrovirus and sapovirus remained unchanged. This study also reported an increase in the median age of diarrhoea cases [31].

Rotarix was introduced into the Fiji National Immunisation Program in 2012 and has reduced the burden of rotavirus disease and hospitalisations in children under 5 years of

age. Ongoing rotavirus surveillance has been conducted in Fiji to investigate changes in genotype diversity, and Thomas et al. described patterns of rotavirus genotype diversity from 2005 to 2018 [32]. Prior to vaccine introduction, genotype dominance fluctuated annually and G1P[8] and G2P[4] were the dominant genotypes. In contrast to many countries that have reported an increase in rotavirus genotype diversity in the vaccine era, a decrease in diversity was observed in Fiji. G1P[8] and G2P[4] were not detected after 2015 and 2014, respectively. Similar to reports from Australia, G3P[8] and G12P[8] were frequently detected in the vaccine-era and the equine-like G3P[8] variants was transiently detected in between 2015–2016 [25,32].

Long-term surveillance pre- and post-vaccine introduction was also conducted at five sentinel sites in India between 2012 to 2020 by Varghese and colleagues [33]. The Rotavac vaccine was introduced in 2016 resulting in a decrease in rotavirus-associated hospitalisations. G1P[8] was the predominant genotyped reported in the pre-vaccination period, whereas G3P[8] became the dominant genotype in the post-vaccination period. Geographic variation in genotype distribution was noted between northern and southern sites [33].

João et al. also reported the prevalence of rotavirus genotypes, pre- (2012–2015) and post-vaccine (2016–2019) introduction in Mozambique [34]. In the three years prior to Rotarix vaccine introduction, G9P[8] was the predominant genotype with G1P[8], G2P[4] and G12P[4] also frequently detected. Following vaccine introduction G1P[8] remained a predominant genotype which is unusual as the prevalence of G1P[8] has been reported to dramatically decrease in most vaccine settings. The prevalence of G9P[8], G2P[4] and G12P[4] decreased while G9P[4] and G3P[4] emerged as prevalent genotypes [34]. A companion study from Munlela et al. described the whole genome characterisation and evolutionary analysis of Mozambican G1P[8] strains pre- and post-vaccine introduction [35]. The strains were collected between 2012 and 2017 and all exhibited a Wa-like genome constellation (G1-P[8]-I1-R1-C1-M1-A1-N1-T1-E1-H1). Phylogenetic analysis revealed the majority of strains clustered closely together in a conserved clade across the entire genome. No distinct clustering for pre- and post-vaccine strains were observed and strains appeared to have been derived from multiple introductions into Mozambique, potentially from India due to the high degree of genetic similarity across the genome. There was no discernible vaccine-induced selection pressure observed in this study [35].

The constant alternations in rotavirus genotype diversity and prevalence within countries and globally highlights the importance of on-going epidemiological and molecular surveillance programs. The increasing detection of unusual zoonotic and reassortant strains emphasises the necessity of whole genome sequencing and detailed phylogenetic analysis. Concerns remain that widespread vaccine use may shape the diversity of rotavirus strains and that vaccine-escape variants may emerge in some settings. Understanding the long-term patterns of rotavirus genotype distribution and evolution is critical in order to assess any changes observed following vaccine introduction given the tendency for natural temporal and geographic fluctuations in the absence of vaccines.

The continued surveillance and characterisation of rotavirus genotypes circulating in the vaccine era globally will provide important insights into epidemiology and strain diversity, ensuring the success of current and future vaccination programs. We express our sincere thanks to the authors and reviewers for their contribution to this very important topic. We also express our sincere gratitude to the Bill and Melinda Gates Foundation for providing funds to support the publication fees for the articles in this special edition.

**Funding:** This special edition was supported, in part, by the Bill & Melinda Gates Foundation [INV-017219]. Under the grant conditions of the Foundation, a Creative Commons Attribution 4.0 Generic License has already been assigned to the Author Accepted Manuscript version that might arise from the submissions to this special edition. The findings and conclusions contained within are those of the authors and do not necessarily reflect positions or policies of the Bill & Melinda Gates Foundation.

**Conflicts of Interest:** C.M.D. has served on advisory boards for GSK (2019, 2021), all payments were paid directly to an administrative fund held by Murdoch Children’s Research Institute. J.E.B. declares no competing interests.

## References

1. Rotavirus Classification Working Group. List of Accepted Genotypes. Available online: <https://rega.kuleuven.be/cev/viralmetagénomics/virus-classification/rcwg> (accessed on 10 June 2021).
2. Banyai, K.; Laszlo, B.; Duque, J.; Steele, A.D.; Nelson, E.A.; Gentsch, J.R.; Parashar, U.D. Systematic review of regional and temporal trends in global rotavirus strain diversity in the pre rotavirus vaccine era: Insights for understanding the impact of rotavirus vaccination programs. *Vaccine* **2012**, *30* (Suppl. 1), A122–A130. [CrossRef] [PubMed]
3. Doro, R.; Laszlo, B.; Martella, V.; Leshem, E.; Gentsch, J.; Parashar, U.; Banyai, K. Review of global rotavirus strain prevalence data from six years post vaccine licensure surveillance: Is there evidence of strain selection from vaccine pressure? *Infect. Genet. Evol.* **2014**, *28*, 446–461. [CrossRef] [PubMed]
4. Matthijnsens, J.; Ciarlet, M.; McDonald, S.M.; Attoui, H.; Banyai, K.; Brister, J.R.; Buesa, J.; Esona, M.D.; Estes, M.K.; Gentsch, J.R.; et al. Uniformity of rotavirus strain nomenclature proposed by the Rotavirus Classification Working Group (RCWG). *Arch. Virol.* **2011**, *156*, 1397–1413. [CrossRef] [PubMed]
5. Troeger, C.; Khalil, I.A.; Rao, P.C.; Cao, S.; Blacker, B.F.; Ahmed, T.; Armah, G.; Bines, J.E.; Brewer, T.G.; Colombara, D.V.; et al. Rotavirus Vaccination and the Global Burden of Rotavirus Diarrhea Among Children Younger Than 5 Years. *JAMA Pediatr.* **2018**, *172*, 958–965. [CrossRef]
6. World Health Organization. Vaccine in National Immunization Programme Update. Available online: [www.who.int/immunization/monitoring\\_surveillance/VaccineIntroStatus.pptx?ua=1](http://www.who.int/immunization/monitoring_surveillance/VaccineIntroStatus.pptx?ua=1) (accessed on 10 June 2021).
7. Burke, R.M.; Tate, J.E.; Kirkwood, C.D.; Steele, A.D.; Parashar, U.D. Current and new rotavirus vaccines. *Curr. Opin. Infect. Dis.* **2019**, *32*, 435–444. [CrossRef] [PubMed]
8. Vesikari, T.; Matson, D.O.; Dennehy, P.; Van Damme, P.; Santosham, M.; Rodriguez, Z.; Dallas, M.J.; Heyse, J.F.; Goveia, M.G.; Black, S.B.; et al. Safety and efficacy of a pentavalent human-bovine (WC3) reassortant rotavirus vaccine. *N. Engl. J. Med.* **2006**, *354*, 23–33. [CrossRef]
9. Vesikari, T.; Karvonen, A.; Puustinen, L.; Zeng, S.Q.; Szakal, E.D.; Delem, A.; De Vos, B. Efficacy of RIX4414 live attenuated human rotavirus vaccine in Finnish infants. *Pediatr. Infect. Dis. J.* **2004**, *23*, 937–943. [CrossRef]
10. Zade, J.K.; Kulkarni, P.S.; Desai, S.A.; Sabale, R.N.; Naik, S.P.; Dhare, R.M. Bovine rotavirus pentavalent vaccine development in India. *Vaccine* **2014**, *32* (Suppl. 1), A124–A128. [CrossRef]
11. Bhan, M.K.; Lew, J.F.; Sazawal, S.; Das, B.K.; Gentsch, J.R.; Glass, R.I. Protection conferred by neonatal rotavirus infection against subsequent rotavirus diarrhea. *J. Infect. Dis.* **1993**, *168*, 282–287. [CrossRef]
12. Kollaritsch, H.; Kundi, M.; Giaquinto, C.; Paulke-Korinek, M. Rotavirus vaccines: A story of success. *Clin. Microbiol. Infect.* **2015**, *21*, 735–743. [CrossRef]
13. Karafillakis, E.; Hassounah, S.; Atchison, C. Effectiveness and impact of rotavirus vaccines in Europe, 2006–2014. *Vaccine* **2015**, *33*, 2097–2107. [CrossRef] [PubMed]
14. Snelling, T.L.; Andrews, R.M.; Kirkwood, C.D.; Culvenor, S.; Carapetis, J.R. Case-control evaluation of the effectiveness of the G1P[8] human rotavirus vaccine during an outbreak of rotavirus G2P[4] infection in central Australia. *Clin. Infect. Dis.* **2011**, *52*, 191–199. [CrossRef] [PubMed]
15. Kirkwood, C.D.; Ma, L.F.; Carey, M.E.; Steele, A.D. The rotavirus vaccine development pipeline. *Vaccine* **2017**. [CrossRef]
16. Middleton, B.F.; Danchin, M.; Quinn, H.; Ralph, A.P.; Pingault, N.; Jones, M.; Estcourt, M.; Snelling, T. Retrospective Case-Control Study of 2017 G2P[4] Rotavirus Epidemic in Rural and Remote Australia. *Pathogens* **2020**, *9*, 790. [CrossRef] [PubMed]
17. Donato, C.M.; Pingault, N.; Demosthenous, E.; Roczo-Farkas, S.; Bines, J.E. Characterisation of a G2P[4] Rotavirus Outbreak in Western Australia, Predominantly Impacting Aboriginal Children. *Pathogens* **2021**, *10*, 350. [CrossRef] [PubMed]
18. Ferrer-Admetlla, A.; Sikora, M.; Laayouni, H.; Esteve, A.; Roubinet, F.; Blancher, A.; Calafell, F.; Bertranpetit, J.; Casals, F. A natural history of FUT2 polymorphism in humans. *Mol. Biol. Evol.* **2009**, *26*, 1993–2003. [CrossRef] [PubMed]
19. MacDonald, J.; Groome, M.J.; Mans, J.; Page, N. FUT2 Secretor Status Influences Susceptibility to VP4 Strain-Specific Rotavirus Infections in South African Children. *Pathogens* **2020**, *9*, 795. [CrossRef]
20. Taniguchi, K.; Urasawa, S. Diversity in rotavirus genomes. *Semin. Virol.* **1995**, *6*, 123–131. [CrossRef]
21. Jere, K.C.; Chaguzza, C.; Bar-Zeev, N.; Lowe, J.; Peno, C.; Kumwenda, B.; Nakagomi, O.; Tate, J.E.; Parashar, U.D.; Heyderman, R.S.; et al. Emergence of Double- and Triple-Gene Reassortant G1P[8] Rotaviruses Possessing a DS-1-Like Backbone after Rotavirus Vaccine Introduction in Malawi. *J. Virol.* **2018**, *92*. [CrossRef]
22. Mwangi, P.N.; Mogotsi, M.T.; Rasebotsa, S.P.; Seheri, M.L.; Mphahlele, M.J.; Ndze, V.N.; Dennis, F.E.; Jere, K.C.; Nyaga, M.M. Uncovering the First Atypical DS-1-like G1P[8] Rotavirus Strains That Circulated during Pre-Rotavirus Vaccine Introduction Era in South Africa. *Pathogens* **2020**, *9*, 391. [CrossRef]
23. Maringa, W.M.; Mwangi, P.N.; Simwaka, J.; Mpabalwani, E.M.; Mwenda, J.M.; Peenze, I.; Esona, M.D.; Mphahlele, M.J.; Seheri, M.L.; Nyaga, M.M. Molecular Characterisation of a Rare Reassortant Porcine-Like G5P[6] Rotavirus Strain Detected in an Unvaccinated Child in Kasama, Zambia. *Pathogens* **2020**, *9*, 663. [CrossRef] [PubMed]

24. Castells, M.; Caffarena, R.D.; Casaux, M.L.; Schild, C.; Miño, S.; Castells, F.; Castells, D.; Victoria, M.; Riet-Correa, F.; Giannitti, F.; et al. Phylogenetic Analyses of Rotavirus A from Cattle in Uruguay Reveal the Circulation of Common and Uncommon Genotypes and Suggest Interspecies Transmission. *Pathogens* **2020**, *9*, 570. [[CrossRef](#)] [[PubMed](#)]
25. Roczo-Farkas, S.; Kirkwood, C.D.; Cowley, D.; Barnes, G.L.; Bishop, R.F.; Bogdanovic-Sakran, N.; Boniface, K.; Donato, C.M.; Bines, J.E. The Impact of Rotavirus Vaccines on Genotype Diversity: A Comprehensive Analysis of 2 Decades of Australian Surveillance Data. *J. Infect. Dis.* **2018**, *218*, 546–554. [[CrossRef](#)] [[PubMed](#)]
26. Markkula, J.; Hemming-Harlow, M.; Salminen, M.T.; Savolainen-Kopra, C.; Pirhonen, J.; Al-Hello, H.; Vesikari, T. Rotavirus epidemiology 5–6 years after universal rotavirus vaccination: Persistent rotavirus activity in older children and elderly. *Infect. Dis.* **2017**, *49*, 388–395. [[CrossRef](#)]
27. Yandle, Z.; Coughlan, S.; Dean, J.; Tuite, G.; Conroy, A.; De Gascun, C.F. Group A Rotavirus Detection and Genotype Distribution before and after Introduction of a National Immunisation Programme in Ireland: 2015–2019. *Pathogens* **2020**, *9*, 449. [[CrossRef](#)] [[PubMed](#)]
28. Gutierrez, M.B.; Fialho, A.M.; Maranhão, A.G.; Malta, F.C.; Andrade, J.d.S.R.d.; Assis, R.M.S.d.; Mouta, S.d.S.e.; Miagostovich, M.P.; Leite, J.P.G.; Machado Fumian, T. Rotavirus A in Brazil: Molecular Epidemiology and Surveillance during 2018–2019. *Pathogens* **2020**, *9*, 515. [[CrossRef](#)]
29. Donato, C.M.; Roczo-Farkas, S.; Kirkwood, C.D.; Barnes, G.L.; Bines, J.E. Rotavirus disease and genotype diversity in older children and adults in Australia. *J. Infect. Dis.* **2020**. [[CrossRef](#)]
30. Mwanga, M.J.; Verani, J.R.; Omere, R.; Tate, J.E.; Parashar, U.D.; Murunga, N.; Gicheru, E.; Breiman, R.F.; Nokes, D.J.; Agoti, C.N. Multiple Introductions and Predominance of Rotavirus Group A Genotype G3P[8] in Kilifi, Coastal Kenya, 4 Years after Nationwide Vaccine Introduction. *Pathogens* **2020**, *9*, 981. [[CrossRef](#)]
31. Lambisia, A.W.; Onchaga, S.; Murunga, N.; Lewa, C.S.; Nyanjom, S.G.; Agoti, C.N. Epidemiological Trends of Five Common Diarrhea-Associated Enteric Viruses Pre- and Post-Rotavirus Vaccine Introduction in Coastal Kenya. *Pathogens* **2020**, *9*, 660. [[CrossRef](#)]
32. Thomas, S.; Donato, C.M.; Covea, S.; Ratu, F.T.; Jenney, A.W.J.; Reyburn, R.; Sahu Khan, A.; Rafai, E.; Grabovac, V.; Serhan, F.; et al. Genotype Diversity before and after the Introduction of a Rotavirus Vaccine into the National Immunisation Program in Fiji. *Pathogens* **2021**, *10*, 358. [[CrossRef](#)] [[PubMed](#)]
33. Varghese, T.; Alokith Khakha, S.; Giri, S.; Nair, N.P.; Badur, M.; Gathwala, G.; Chaudhury, S.; Kaushik, S.; Dash, M.; Mohakud, N.K.; et al. Rotavirus Strain Distribution before and after Introducing Rotavirus Vaccine in India. *Pathogens* **2021**, *10*, 416. [[CrossRef](#)] [[PubMed](#)]
34. João, E.D.; Munlela, B.; Chissaque, A.; Chilaúle, J.; Langa, J.; Augusto, O.; Boone, S.S.; Anapakala, E.; Sambo, J.; Guimarães, E.; et al. Molecular Epidemiology of Rotavirus A Strains Pre- and Post-Vaccine (Rotarix®) Introduction in Mozambique, 2012–2019: Emergence of Genotypes G3P[4] and G3P[8]. *Pathogens* **2020**, *9*, 671. [[CrossRef](#)] [[PubMed](#)]
35. Munlela, B.; João, E.D.; Donato, C.M.; Strydom, A.; Boone, S.S.; Chissaque, A.; Bauhofer, A.F.L.; Langa, J.; Cassocera, M.; Cossa-Moiane, I.; et al. Whole Genome Characterization and Evolutionary Analysis of G1P[8] Rotavirus A Strains during the Pre- and Post-Vaccine Periods in Mozambique (2012–2017). *Pathogens* **2020**, *9*, 1026. [[CrossRef](#)] [[PubMed](#)]

Article

# Retrospective Case-Control Study of 2017 G2P[4] Rotavirus Epidemic in Rural and Remote Australia

Bianca F. Middleton <sup>1,2,\*</sup> , Margie Danchin <sup>3,4,5</sup>, Helen Quinn <sup>6,7</sup>, Anna P. Ralph <sup>1,8</sup>, Nevada Pingault <sup>9</sup>, Mark Jones <sup>10</sup> , Marie Estcourt <sup>10</sup> and Tom Snelling <sup>1,11,12</sup>

- <sup>1</sup> Global and Tropical Health, Menzies School of Health Research, Charles Darwin University, Darwin 0810, Australia; Anna.Ralph@menzies.edu.au (A.P.R.); tom.snelling@sydney.edu.au (T.S.)
  - <sup>2</sup> Division of Women, Children and Youth, Royal Darwin Hospital, Darwin 0810, Australia
  - <sup>3</sup> Department of Paediatrics, University of Melbourne, Melbourne 3052, Australia; margie.danchin@rch.org.au
  - <sup>4</sup> Murdoch Children's Research Institute, Melbourne 3052, Australia
  - <sup>5</sup> Department of General Medicine, Royal Children's Hospital, Melbourne 3052, Australia
  - <sup>6</sup> The National Centre for Immunisation Research and Surveillance (NCIRS), The Children's Hospital at Westmead, Sydney 2145, Australia; helen.quinn@health.nsw.gov.au
  - <sup>7</sup> Faculty of Medicine and Health, Westmead Clinical School, The University of Sydney, Westmead 2145, Australia
  - <sup>8</sup> Division of Medicine, Royal Darwin Hospital, Darwin 0810, Australia
  - <sup>9</sup> Department of Health Western Australia, Communicable Disease Control Directorate, Perth 6004, Australia; nevada.pingault@health.wa.gov.au
  - <sup>10</sup> Health and Clinical Analytics, School of Public Health, The University of Sydney, Sydney 2006, Australia; mark.jones1@sydney.edu.au (M.J.); marie.estcourt@sydney.edu.au (M.E.)
  - <sup>11</sup> Wesfarmers Centre for Vaccine and Infectious Diseases, Telethon Kids Institute, Perth 6009, Australia
  - <sup>12</sup> School of Public Health, Curtin University, Perth 6102, Australia
- \* Correspondence: bianca.middleton@menzies.edu.au; Tel.: +61-4-0209-3321

Received: 24 August 2020; Accepted: 22 September 2020; Published: 26 September 2020



**Abstract:** Background: A widespread G2P[4] rotavirus epidemic in rural and remote Australia provided an opportunity to evaluate the performance of Rotarix and RotaTeq rotavirus vaccines, ten years after their incorporation into Australia's National Immunisation Program. Methods: We conducted a retrospective case-control analysis. Vaccine-eligible children with laboratory-confirmed rotavirus infection were identified from jurisdictional notifiable infectious disease databases and individually matched to controls from the national immunisation register, based on date of birth, Aboriginal status and location of residence. Results: 171 cases met the inclusion criteria; most were Aboriginal and/or Torres Strait Islander (80%) and the median age was 19 months. Of these cases, 65% and 25% were fully or partially vaccinated, compared to 71% and 21% of controls. Evidence that cases were less likely than controls to have received a rotavirus vaccine dose was weak, OR 0.79 (95% CI, 0.46–1.34). On pre-specified subgroup analysis, there was some evidence of protection among children <12 months (OR 0.48 [95% CI, 0.22–1.02]), and among fully vs. partially vaccinated children (OR 0.65 [95% CI, 0.42–1.01]). Conclusion: Despite the known effectiveness of rotavirus vaccination, a protective effect of either rotavirus vaccine during a G2P[4] outbreak in these settings among predominantly Aboriginal children was weak, highlighting the ongoing need for a more effective rotavirus vaccine and public health strategies to better protect Aboriginal children.

**Keywords:** rotavirus; rotavirus vaccines; vaccine effectiveness; case control

## 1. Introduction

Rotavirus is a leading cause of severe dehydrating diarrhoeal illness in children and continues to be responsible for the deaths of 118,000 to 183,000 children every year [1]. Many of these deaths occur in resource-poor settings [2].

In 2006, two oral rotavirus vaccines, Rotarix and RotaTeq, were licensed for use and in 2009 the World Health Organization endorsed their use globally [3]. Subsequent epidemiological studies have confirmed a strong protective effect of vaccination on rotavirus morbidity in high- and upper middle-income countries (vaccine efficacy [VE] >84%) [2]. However, in low-income countries, despite a large reduction in the absolute number of cases of gastroenteritis, measured vaccine efficacy has been lower (45–57%) and in some settings there is evidence of decreased protection in the second year of life [2,4–6].

The incorporation of rotavirus vaccines into the Northern Territory immunisation schedule in 2006 and then into the Australian National Immunisation Program (NIP) in 2007, resulted in a substantial and sustained decrease in rotavirus hospitalisations [7]. However, among Aboriginal and Torres Strait Islander children living in the hyperendemic settings of rural and remote Australia, the decrease in rotavirus hospitalisation was less dramatic and not sustained, with Aboriginal children living in the Northern Territory (NT) remaining more than 20 times more likely to be hospitalised with rotavirus than their non-Aboriginal counterparts [7]. An early vaccine effectiveness study in this setting also suggested reduced effectiveness against heterotypic strains and poor protection in the second year of life [8].

In 2017, an epidemic of G2P[4] rotavirus arose in the Northern Territory and subsequently spread to adjoining rural and remote regions of Western Australia (WA). These two jurisdictions cover a large geographic area which is sparsely populated; they have a higher proportion of resident Aboriginal and Torres Strait Islander people, many of whom live in rural and remote communities. The rotavirus epidemic occurred at a time when the Northern Territory exclusively administered Rotarix and Western Australia exclusively administered RotaTeq as part of the jurisdictional implementation of the NIP. We evaluated the protective effectiveness of both vaccines in these high-burden settings, ten years after the incorporation of rotavirus vaccines into the NIP.

## 2. Materials and Methods

### 2.1. Study Setting

The Alice Springs and Barkly regions of the Northern Territory, and the Kimberley, Pilbara and Goldfields regions of Western Australia are large but sparsely populated administrative health regions. Ranging from the semi-arid south, to the arid center and tropical north, these five regions encompass more than 2,500,000 km<sup>2</sup>, but are home to a combined total of just 174,000 people [9]. Children aged <5 years represent between 7–9% of the population, and between 5 and 41% of the population in each of these regions identify as being Aboriginal and/or Torres Strait Islander (hereafter respectfully referred to as 'Aboriginal') [9]. Many of these children live in towns or small remote communities. Rotarix and RotaTeq rotavirus vaccines have been licensed for use in Australia since June 2006. The Northern Territory immunisation program has funded the administration of Rotarix exclusively since October 2006. The Western Australian immunisation program funded the administration of Rotarix from July 2007 to June 2009, RotaTeq from July 2009 to June 2017, and Rotarix from July 2017.

### 2.2. Study Design

We conducted a retrospective, population-based, case control study of children age-eligible for at least 1 dose of rotavirus vaccine (those born after the introduction of Rotarix rotavirus vaccine to the NT schedule—after 1 July 2006 and aged  $\geq 6$  weeks, and those born after the introduction of RotaTeq rotavirus vaccine to the WA schedule—after 1 May 2009 and aged  $\geq 6$  weeks) who had laboratory positive and notified rotavirus infection during the 2017 G2P[4] rotavirus epidemic in the NT and WA.

Cases were individually matched to controls sampled from the national immunisation register. As a secondary analysis, we also compared cases who were age-eligible for full rotavirus vaccination (those born after 1 July 2006 and aged  $\geq 24$  weeks in the NT and those born after 1 May and aged  $\geq 32$  weeks in WA) with un-matched control children diagnosed with non-rotavirus gastrointestinal infections sampled from disease notification registers.

### *2.3. Data Sources*

Rotavirus is a notifiable disease in the NT and WA. Data regarding rotavirus cases and disease register controls were ascertained from the two jurisdictional-based notifiable infectious disease databases—The Northern Territory Notifiable Disease System (NTNDS) managed by the NT Centre for Disease Control, and the Western Australian Notifiable Infectious Disease Database (WANIDD) managed by the WA Department of Health.

To estimate baseline vaccine coverage in the case-referent population, matched population controls were sampled from the Australian Immunisation Register (AIR), a comprehensive population-based register which contains vaccination data for all children registered with Australia's universal health insurance scheme, Medicare (~99% of the population).

### *2.4. Participants*

#### *2.4.1. Population-Based Analysis*

Rotavirus cases were vaccine-eligible children aged  $\geq 6$  weeks with laboratory positive and notified rotavirus infection between 1 March and 30 June 2017. Cases were drawn from the Alice Springs and Barkly regions of the NT, and the Kimberley, Pilbara and Goldfields regions of WA. To be vaccine-eligible, children had to be born on or after 1 July 2006 in the NT (for Rotarix) and on or after 1 May 2009 in WA (for RotaTeq).

De-identified population controls were selected from the Australian Immunisation Register and matched to each case by date of birth ( $\pm 14$  days), Aboriginal status and location of residence (listed residential postcode within either the Alice Springs, Barkly, Pilbara, Goldfields or Kimberley regions). Up to 10 eligible controls were randomly selected for each case.

#### *2.4.2. Disease Register Analysis*

Rotavirus cases were selected as above, but because individual matching was not feasible, the analysis was restricted to children old enough to be fully vaccinated: age  $\geq 24$  weeks (for Rotarix) in the NT and  $\geq 32$  weeks (for RotaTeq) in WA.

Disease register controls were vaccine-eligible children (aged  $\geq 24$  weeks or  $\geq 32$  weeks in the NT and WA respectively), with microbiologically confirmed, non-rotavirus and non-vaccine preventable, notifiable gastrointestinal infections, notified between 1 January and 31 December 2017. Controls were selected from the Alice Springs and Barkly regions of the NT, and the Kimberley, Pilbara and Goldfields regions of WA. Non-rotavirus notifiable gastrointestinal infections included campylobacter, shigella, salmonella and cryptosporidium, and controls were excluded if they were also identified as a rotavirus case. Age, Aboriginal status, sex and location of residence were obtained from the disease register for inclusion in the regression analysis.

### *2.5. Immunisation Status*

The immunisation status of all rotavirus cases, population controls and disease register controls were determined from the Australian Immunisation Register (AIR). Full vaccination was defined as AIR-documented receipt of at least two doses of Rotarix for children living in the NT and at least three doses of RotaTeq for children living in WA. Partial vaccination was defined as AIR-documented receipt of one dose only of Rotarix for children living in the NT and either one or two doses only of RotaTeq for children living in WA. Unvaccinated children were defined as those registered on the

AIR, but without documented receipt of any rotavirus vaccines. In circumstances where a child had a vaccine dose recorded as dose two or dose three on the register, but where an earlier dose was not recorded, it was assumed the missing dose had been given [10]. A vaccine dose was considered administered on the date recorded as administered on the register (i.e., without any post-vaccination censoring). A vaccine dose was considered invalid if (1) administered too early (before six weeks of age or <28 days from prior vaccine dose), (2) it exceeded the recommended number of vaccine doses in the schedule (>2 doses of Rotarix or >3 doses of RotaTeq) or (3) the administered vaccine was different to the prior vaccine (mixed Rotarix/RotaTeq vaccination schedule). Children were excluded from selection as cases and controls if they had an invalid vaccine dose. Children were also excluded from the analysis if they were recorded as having received the non-programmatic vaccine for their resident jurisdiction (i.e., RotaTeq but living in the NT, or Rotarix but living in WA).

## *2.6. Statistical Analysis*

Conditional logistic regression was used to determine the odds ratio (OR) of vaccination for rotavirus cases compared with matched population controls from the immunisation register. Additional models were fit to compute the OR for any dose of vaccine (full and/or partial vaccination) vs none, full vaccination vs none, partial vaccination vs none, and full vs partial vaccination. Subgroup analyses were by jurisdiction (NT versus WA), and by age (<12 months versus  $\geq 12$  months).

For the disease register analysis, ordinary logistic regression was used to determine the odds ratio of vaccination for rotavirus cases compared with disease register controls. Age (months), sex, Aboriginal status (Aboriginal vs non-Aboriginal) and jurisdiction of residence (NT vs WA) were included in the model, together with an interaction term for Aboriginal status and jurisdiction of residence.

Assuming a baseline population vaccine coverage of 80%, we estimated that 80 matched sets of cases and population controls, with 10 controls for each case, would have at least 80% power to detect a significant real-world vaccine effectiveness of 45% (OR = 0.55).

All analysis was performed using Stata, version 15.1 (Stata).

## *2.7. Ethics Committee Approvals*

Approval was granted by the Central Australian Human Research Ethics Committee (CAHREC 18-3219), the Human Research Ethics Committee of the Northern Territory Department of Health and Menzies School of Health Research (HREC 18-3248), the Department of Health Western Australian Human Research Ethics Committee (DOH HREC 2018/30), the Western Australian Aboriginal Health Ethics Committee (HREC 891) and the Charles Darwin University Human Research Ethics Committee (H19040). Approval to access data held by the Australian Immunisation Register was granted by the Australian Government Department of Health.

## **3. Results**

The rotavirus epidemic occurred between 1 March and 30 June 2017. A total of 194 vaccine-eligible children aged  $\geq 6$  weeks were identified as rotavirus cases from which 171 were eligible for inclusion in the study (see Figure 1).

The median age of rotavirus infection was 19 months (range from 1 to 94 months). Most rotavirus cases were among children who identified as Aboriginal and/or Torres Strait Islander (NT 86%, WA 75%). Genotype results were available for only 60% of rotavirus cases, however, of those typed, all were G2P[4] strains. A total of 99 children were documented as having been hospitalised with rotavirus infection—78% of rotavirus cases in the NT and 39% of rotavirus cases in WA. Hospitalisation status was unknown for 15% of WA rotavirus cases (see Table 1).

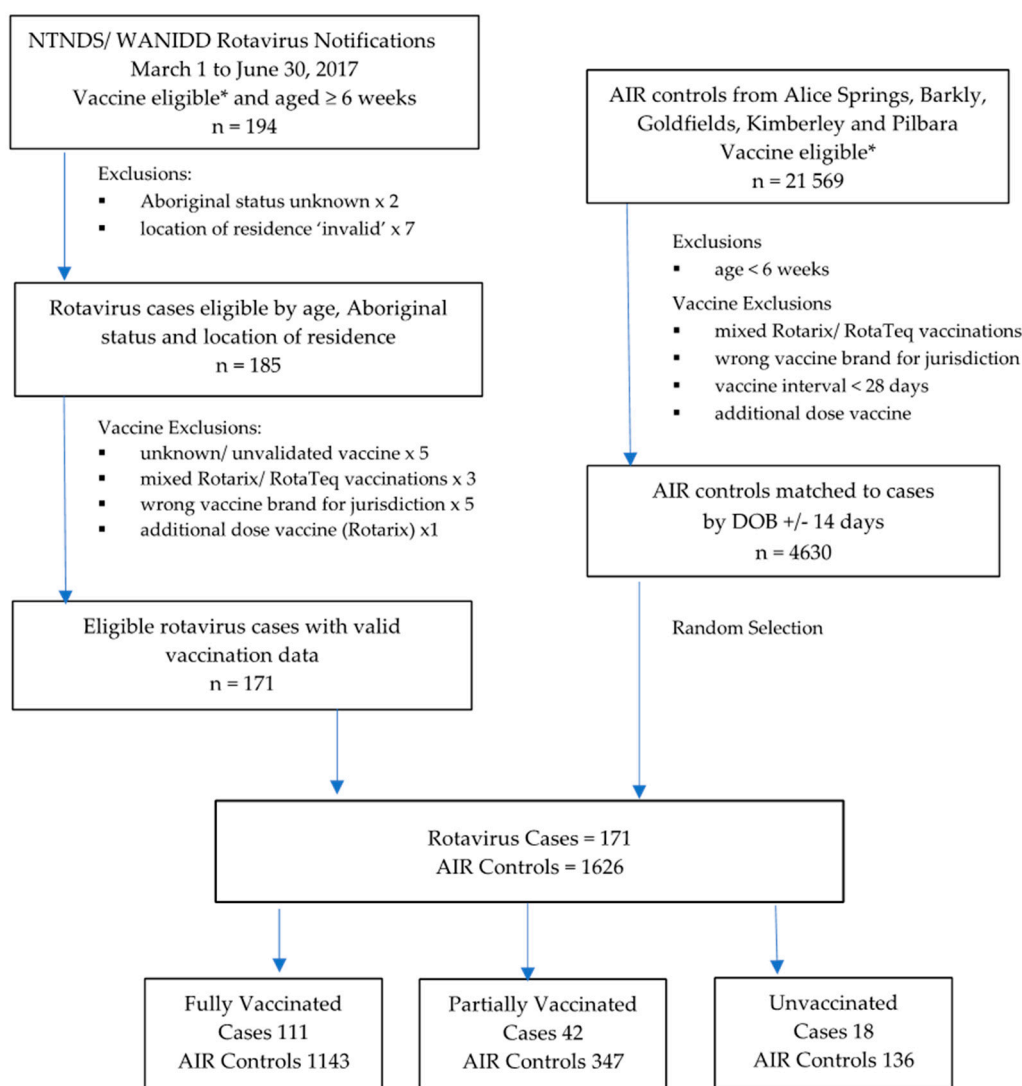


**Figure 1.** Selection of rotavirus cases and matched population controls from the Australian Immunisation Register. \* Vaccine-Eligible: children eligible by date of birth to have received at least one dose of Rotarix vaccine (those born after 1 July 2006 in the Northern Territory) or at least one dose of RotaTeq vaccine (those born after 1 May 2009 in Western Australia).

Among rotavirus cases, 65% were fully vaccinated, 25% partially vaccinated and 10% unvaccinated; among matched population controls from the immunisation register, 71% were fully vaccinated, 21% partially vaccinated and 8% unvaccinated. In the population-based analysis, the odds ratio of receipt of any doses of rotavirus vaccine versus none was 0.79 (95% CI, 0.46–1.34). For the NT and WA, the OR of any doses versus none was 1.10 (95% CI, 0.50–2.41) and 0.56 (95% CI, 0.27–1.16), respectively. For children aged <12 months and for children aged ≥12 months, the ORs were 0.48 (95% CI, 0.22–1.02) and 1.22 (95% CI, 0.55–2.73), respectively. The OR of full versus partial vaccination was 0.65 (95% CI, 0.42–1.01) (see Table 2 and Figure 2).

Of the 171 notified rotavirus cases above, 149 were age eligible for inclusion in the disease register analysis (aged ≥24 weeks or ≥32 weeks in the NT and WA, respectively). A total of 347 vaccine-eligible children were identified as having non-rotavirus gastrointestinal infections in the twelve-month period from 1 January and 31 December 2017. Of these children, 299 were eligible for inclusion (Supplementary Materials Figure S1). The median age of disease register controls was older than that of rotavirus cases, 29 months vs. 20 months (Supplementary Materials Table S1). Disease register controls were less

likely to be hospitalised than rotavirus cases (35% vs 58%) and, in WA, were less likely to identify as Aboriginal (41% vs 74%).

In the disease register analysis, 73%, 19% and 8% of cases were fully vaccinated, partially vaccinated and unvaccinated, respectively, compared with 83%, 12% and 5% of controls. The adjusted OR of any doses of rotavirus vaccine versus none was 0.58 (95% CI, 0.24–1.39); for WA and NT children, the adjusted ORs were 0.30 (95% CI, 0.09–0.98) and 1.40 (95% CI, 0.34–5.80), respectively, and for children aged <12 months and ≥12 months old, the adjusted ORs were 0.28 (95% CI, 0.03–2.83) and 0.81 (95% CI, 0.29–2.28), respectively. The adjusted OR of full vs. partial vaccination was 0.63 (95% CI, 0.35–1.13) (see Table 2 and Supplementary Materials Table S2).

**Table 1.** Baseline characteristics of rotavirus cases.

Characteristic	Rotavirus Cases	
	NT	WA
	n = 83	n = 88
<b>Age</b>		
Median age (months)	18	19
Age range (months)	1 to 72	1 to 94
6 weeks to <24 wks (NT only)	12 (14%)	
6 weeks to <32 wks (WA only)		10 (11%)
6 weeks to <1 year	25 (30%)	23 (26%)
1 year to <2 years	36 (44%)	34 (39%)
2 years to <3 years	11 (13%)	15 (17%)
3 years to <4 years	7 (8%)	5 (6%)
4 years to <5 years	3 (4%)	5 (6%)
≥5 years	1 (1%)	6 (6%)
<b>Sex</b>		
Female	42 (51%)	43 (49%)
Male	41 (49%)	45 (51%)
<b>Aboriginal Status</b>		
Aboriginal	71 (86%)	66 (75%)
Non-Aboriginal	12 (14%)	22 (25%)
<b>Location of Residence</b>		
Alice Springs	70 (84%)	
Barkly	13 (16%)	
Goldfields		17 (19%)
Kimberley		49 (56%)
Pilbara		22 (25%)
<b>Genotype</b>		
G2P[4]	44 (53%)	59 (67%)
Unknown	39 (47%)	29 (33%)
<b>Hospitalisation</b>		
Yes	65 (78%)	34 (39%)
No	18 (22%)	41 (46%)
Unknown		13 (15%)
<b>Vaccination</b>		
0 doses	8 (10%)	10 (11%)
1 doses	15 (18%)	8 (9%)
2 doses	60 (72%)	19 (22%)
3 doses		51 (58%)

**Table 2.** Odds ratio of vaccination in rotavirus cases versus controls in the population-based analysis and the disease register analysis.

Immunisation Status	Immunisation Register Analysis			Disease Register Analysis		
	Cases	Controls	Odds Ratio (95% CI)	Cases	Controls	Odds Ratio (95% CI)
<b>Any Dose vs. None</b>	n = 171	n = 1626	0.79 (0.46, 1.34)	n = 149	n = 299	0.58 (0.24, 1.39)
≥One Dose Vaccine	153	1490		137	283	
Unvaccinated	18	136		12	16	
<b>Any Dose vs. None NT (Rotarix)</b>	n = 83	n = 753	1.10 (0.50, 2.41)	n = 71	n = 123	1.40 (0.34, 5.80)
≥One Dose Vaccine	75	676		68	114	
Unvaccinated	8	77		3	9	
<b>Any Dose vs. None WA (RotaTeq)</b>	n = 88	n = 873	0.56 (0.27, 1.16)	n = 78	n = 176	0.30 (0.09, 0.98)
≥One Dose Vaccine	78	814		69	169	
Unvaccinated	10	59		9	7	
<b>Any Dose vs. None &lt; 12 mths</b>	n = 48	n = 449	0.48 (0.22, 1.02)	n = 26	n = 37	0.28 (0.03, 2.83)
≥One Dose Vaccine	37	392		21	36	
Unvaccinated	11	57		5	1	
<b>Any Dose vs. None ≥12mths</b>	n = 123	n = 1177	1.22 (0.55, 2.73)	n = 123	n = 262	0.81 (0.29, 2.28)
≥One Dose Vaccine	116	1098		116	247	
Unvaccinated	7	79		7	15	
<b>Full Dose vs. None</b>	n = 129	n = 1008	0.83 (0.43, 1.58)	n = 121	n = 264	0.55 (0.23, 1.32)
Fully Vaccinated	111	913		109	248	
Unvaccinated	18	95		12	16	
<b>Full Dose vs. None NT (Rotarix)</b>	n = 68	n = 529	2.06 (0.62, 6.83)	n = 61	n = 117	1.27 (0.31, 5.23)
Fully Vaccinated	60	469		58	108	
Unvaccinated	8	60		3	9	
<b>Full Dose vs. None WA (RotaTeq)</b>	n = 61	n = 479	0.40 (0.18, 0.93)	n = 60	n = 147	0.29 (0.09, 0.96)
Fully Vaccinated	51	444		51	140	
Unvaccinated	10	35		9	7	
<b>Full Dose vs. Partial Dose</b>	n = 153	n = 1350	0.65 (0.42, 1.01)	n = 137	n = 283	0.63 (0.35, 1.13)
Fully Vaccinated	111	1060		109	248	
Partially Vaccinated	42	290		28	35	

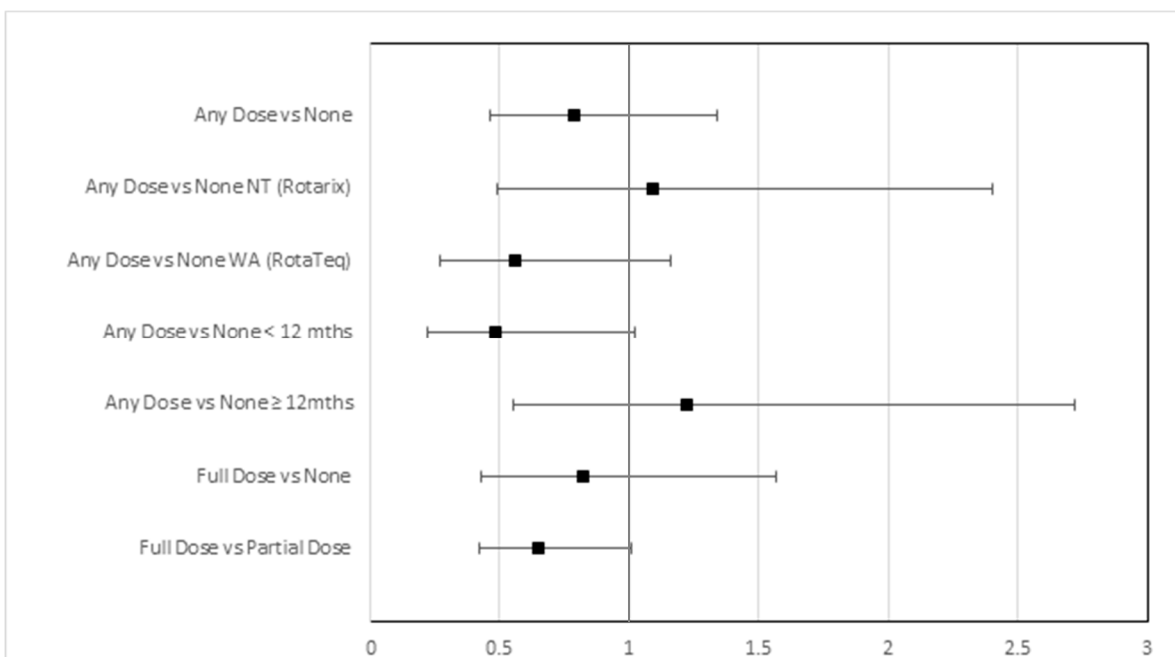


**Figure 2.** Odds ratio of vaccination in rotavirus cases versus controls in the population-based analysis.

Additional analyses were performed as requested after peer review—including restricting the population-based analysis to children age-eligible for full vaccination only (aged  $\geq 24$  weeks in the NT and  $\geq 32$  weeks in WA), restricting the population-based analysis to children aged  $< 5$  years and restricting the population-based analysis to Aboriginal children only. An additional analysis was also run without the ‘missing dose assumption’, i.e., in circumstances where a child had a vaccine dose recorded as dose two or three on the register but where an earlier dose was not recorded, the cases and controls were reclassified as ‘partially vaccinated’ (Supplementary Materials Table S3). This resulted in the reclassification of 26 population controls as partially vaccinated, but no change to the classification of rotavirus cases. The results of the additional analyses were broadly in keeping with the per-protocol analysis.

#### 4. Discussion

In the context of a G2P[4] rotavirus epidemic with 171 laboratory confirmed rotavirus notifications, we failed to find evidence that either rotavirus vaccine provided strong protection against rotavirus gastroenteritis. This contrasts with the large decrease in rotavirus morbidity and mortality observed globally in young children following the licensing of the oral two rotavirus vaccines, Rotarix and RotaTeq, in 2006 [2,7,11].

The 2017 G2P[4] rotavirus epidemic in the Northern Territory and adjoining regions of rural and remote Western Australia predominantly affected Aboriginal and Torres Strait Islander children (NT 86%, WA 75%). Two thirds of cases (65%) were fully vaccinated, and cases were only slightly less likely to have received a vaccine dose than matched population controls sampled from the immunisation register (OR of 0.79 is equivalent to a VE of 21% where  $VE = 1 - OR$ ). There was some evidence of protection among the subgroup of children  $< 12$  months old, although all 95% confidence intervals included one (no effect) and there was significant overlap in the confidence intervals across the subgroup analyses. We found little evidence of a protective effect for full vaccination overall (OR of full vs. no vaccination 0.83 (95% CI, 0.43, 1.58)), although there was some evidence that fully vaccinated children were better protected than unvaccinated children in Western Australia (OR of full vs no vaccination for WA 0.40 (95% CI, 0.18–0.93)). We also found some evidence that fully vaccinated children were moderately better protected than partially vaccinated children (OR of full vs. partial vaccination 0.65 (95% CI, 0.42–1.01)). These findings are consistent with recently published vaccine effectiveness studies evaluating the performance of Rotarix in New South Wales and both Rotarix/RotaTeq in Western Australia. In both studies, VE estimates were highest for fully vaccinated children aged  $< 12$  months, and there was evidence of increasing vaccine effectiveness with increasing doses of both Rotarix and RotaTeq vaccines [12,13].

Rotarix is a live, monovalent, attenuated oral rotavirus vaccine derived from the most common human rotavirus strain G1P[8], and RotaTeq is a pentavalent (G1, G2, G3, G4, P[8]) human–bovine reassortant vaccine [14]. While post-licensure studies have reported similar vaccine effectiveness levels for Rotarix and RotaTeq [2], very few studies have directly compared the effectiveness of each vaccine in the same setting or during the same outbreak [15–17]. While there is good evidence that RotaTeq is protective against G2P[4] strains [18], post-licensure studies have shown mixed results for the effectiveness of Rotarix against G2 strains [8,19] and in some jurisdictions using Rotarix, G2P[4] has emerged as the dominant circulating genotype [20–23]. An earlier study of a 2009 G2P[4] outbreak amongst NT Aboriginal infants failed to show that the rotavirus vaccine provided strong protection (OR 0.81 (95% CI, 0.32–2.05)) [8]. In our study, all rotavirus samples sent for genotypic analysis from the five administrative health regions between March and June 2017 were identified as G2P[4]. Given the epidemic was well-defined in time and geography, it is reasonable to assume that G2P[4] accounted for all epidemic cases; this study provides a unique opportunity to evaluate the performance of both Rotarix and RotaTeq during the same G2P[4] epidemic and in similar, albeit geographically distinct, populations. While the point estimate of the OR was consistently lower in the jurisdiction using Rotateq (consistent with better effectiveness), the confidence intervals were wide and overlapping.

Small rotavirus case numbers in both jurisdictions and programmatic differences in how cases are ascertained limit our ability to draw conclusions about the comparative effectiveness of the vaccines in this study.

While there was evidence of a protective effect among younger children, our estimates suggest that a strong protective effect of vaccination is unlikely among older children. The median age of rotavirus infection was 19 months with a substantial proportion of cases occurring among children aged 12–23 months (NT 44%, WA 39%). Decreased vaccine protection in the second year of life and persistent burden of rotavirus disease have been reported in other high-burden low-resource settings [2,5,24]. Possible determinants of poor vaccine response include high levels of maternally-derived, vaccine-neutralising anti-rotavirus antibodies, poor infant nutrition, intestinal microbiota imbalance, environmental enteropathy, comorbid infections such as HIV and a high diversity of circulating rotavirus strains [25]. In the population included in this study, children are very unlikely to have been HIV infected, but other infective comorbidities are common. Apart from reduced vaccine-induced protection, programmatic restrictions, including upper age-limits for rotavirus vaccine administration may also diminish the program. An early rotavirus vaccine, RRV-TV, caused intussusception in a small number of vaccinated older infants [26] and despite reassuring phase 3 clinical trial safety results, the manufacturers of Rotarix and RotaTeq have conservatively recommended upper age limits on the administration of their vaccines—24 weeks for Rotarix and 32 weeks for RotaTeq. In practice, this limits opportunity to complete the full vaccination schedule and eliminates the possibility of catch-up of missed vaccinations in later childhood [25]. Delayed and/or incomplete vaccination is more common among Australian Aboriginal children [27] and in one observational study, two-dose DTPa coverage increased by a further 16% after the upper age limit of rotavirus vaccine administration (from 75% to 91% in Aboriginal infants), whereas two-dose rotavirus vaccine coverage increased by only 3% (from 75% to 78% in Aboriginal infants) [28]. This suggests that relaxing the upper age restrictions for rotavirus vaccines, as recommended by WHO for countries with high rotavirus burden [3], could be considered as a strategy for improving vaccine uptake and schedule completion.

The validity of case-control methods is largely dependent on adequate control of confounders, that is, factors which are causally related to both vaccination and baseline risk of disease [29]. In our setting, vaccination coverage is influenced by age, Aboriginal status, geographical location and calendar time; age and Aboriginal status remain the two strongest baseline risk factors for rotavirus gastroenteritis requiring hospitalisation [7], and epidemics are clustered in geographic space and time. Our study therefore sought to control for these potential confounders by directly matching cases to population controls on age (date of birth), Aboriginal status and location of residence, and by confining the analysis to the defined outbreak period. In the disease register analysis, these factors were not matched but were captured and adjusted for in the regression analysis. This study could not directly measure socio-economic status for individual cases and controls, although Indigenous status and remoteness of residence may be considered surrogate measures, with the Alice Springs, Barkly, Kimberley and Goldfields regions encompassing some of the most socially disadvantaged regions in Australia, as measured by the Index of Relative Socioeconomic Advantage and Disadvantage.

While the jurisdiction-based notifiable infectious disease databases are believed to capture all laboratory-confirmed rotavirus cases during the epidemic, we acknowledge that not all children with rotavirus gastroenteritis present for medical care, are referred for testing, or complete testing when it is recommended. Rotavirus vaccines have been found to be more effective in preventing severe disease requiring hospitalisation than asymptomatic and other less severe forms of infection [2]. While we were not able to directly ascertain disease severity, most cases in this study are likely to have had either moderate or severe gastroenteritis because all sought medical care (in order to be hospitalised), and 78% and 39% were hospitalised in the NT and WA respectively.

It is also acknowledged that the propensity to seek medical care for rotavirus gastroenteritis symptoms may be associated with the propensity to access medical care for other reasons, including vaccination, and this is a potential source of bias in the population-based analysis which may have

caused us to underestimate vaccine protection. The disease register analysis is less likely to be affected by this bias because the vaccination status of rotavirus cases was compared to that of other children with (non-vaccine preventable), notifiable gastrointestinal clinical infections, i.e., children with clinical presentations which are likely to have been indistinguishable from rotavirus infection and who also underwent microbiological testing. The results of the disease register nested analysis were limited by small numbers, especially in the subgroup analyses, but were in broad agreement with the population-based analysis.

Rotavirus gastroenteritis cannot be reliably distinguished from other causes of non-bloody diarrhea on clinical grounds, and so only laboratory confirmed cases reported to the notifiable infectious disease databases were included. The sensitivity and specificity for detecting rotavirus in stool samples using commercially available EIA is high, although false positives and false negatives have been reported [30]. This is noted as a limitation of the nested disease register case-control study, where an assay error may result in misclassification of a case as a control, or vice versa, which would have caused us to underestimate vaccine protection.

While the Australian Immunisation Register provides credible individual and population-level data regarding vaccine coverage by vaccine type, date-of-birth, location of residence and Aboriginal status, controls were matched to cases based on their location of residence, as recorded on the register in October 2019, which may or may not accurately reflect their jurisdiction of residence between March and June 2017. It is unclear what, if any, bias this may have caused.

## 5. Conclusions

The incorporation of two rotavirus vaccines into the Australian NIP in 2007 has resulted in a substantial and sustained decrease in rotavirus morbidity across most of Australia, although Aboriginal and Torres Strait Islander children remain at increased risk of severe rotavirus disease requiring hospitalisation [7]. Our evaluation of the 2017 G2P[4] rotavirus epidemic in remote Australia suggests that rotavirus vaccination provided little protection against notifiable rotavirus disease for children living in rural and remote Australia, with the likely exception of children aged <12 months for whom moderate evidence of protection was found.

The admission of an additional 99 children with gastroenteritis to small regional and remote hospitals over fourteen weeks highlights the ongoing public health importance of rotavirus and the need for strategies to better protect Aboriginal children. Our data indicate a likely benefit from full rather than partial vaccination, underscoring the importance of completing the rotavirus schedule. Schedule completion could be enhanced by relaxing the upper age limit of rotavirus vaccination as has been recommended by the World Health Organisation for high-burden settings [3].

Our study also reports a high percentage of rotavirus cases in children aged 12–23 months and decreased vaccine protection among children older than 12 months. It is plausible that administering an additional or booster dose of rotavirus vaccine to slightly older children (beyond manufacturer upper age limit restrictions) may extend protection into the second year of life. Scheduling a third dose of Rotarix vaccine (at between 6 and 11 months old) is currently under investigation in the NT [31].

**Supplementary Materials:** The following are available online at <http://www.mdpi.com/2076-0817/9/10/790/s1>, Figure S1: Selection of rotavirus cases and un-matched disease register controls for disease register nested case-control study. Table S1. Baseline characteristics of rotavirus cases and disease register controls for the unmatched disease-register nested case-control study. Table S2. Odds Ratio of vaccination in rotavirus cases versus controls in the matched population-based analysis and the disease register nested analysis (full results). Table S3. Odds Ratio of vaccination in rotavirus cases versus controls in additional population-based analysis (i) children age-eligible for full vaccination only (aged  $\geq 24$  weeks in the NT and  $\geq 32$  weeks in WA), (ii) children aged <5 years only, (iii) Aboriginal children only, and (iv) 'missing dose assumption' removed.

**Author Contributions:** Conceptualization, T.S., M.D. and B.F.M.; methodology, T.S., M.D., H.Q., A.P.R. and M.E.; formal analysis, T.S. and B.F.M.; data curation, B.F.M. and H.Q.; writing—original draft preparation, B.F.M.; writing—review and editing, T.S., M.D., H.Q., A.P.R., M.E., N.P. and M.J.; supervision, T.S. and M.D.; project administration, B.F.M.; funding acquisition, B.F.M. All authors have read and agreed to the published version of the manuscript.

**Funding:** B.F.M. is supported by National Health and Medical Research Council (NHMRC) Post-Graduate Scholarship Grant (1134095), RACP Paediatrics and Child Health Division NHMRC Scholarship, Australian Academy of Science Douglas and Lola Douglas Scholarship. T.S. and A.P.R. are supported by a NHMRC Career Development Fellowship (1111657 and 1142011 respectively). M.D. is supported by a David Bickart Clinician Research Fellowship, University of Melbourne.

**Acknowledgments:** We acknowledge the support of the Menzies Child Health Indigenous Reference Group, the Kimberley Aboriginal Health Planning Forum and the Pilbara Aboriginal Health Planning Forum. We also acknowledge the support and assistance of Peter Markey and Heather Cook at the Northern Territory Centre for Disease Control, Paul Effler, Robyn Gibbs, Carolien Giele and Clare Huppertz from the Western Australian Communicable Disease Control Directorate, Rob Baird from Territory Pathology, and Julie Bines and Susie Roczo-Farkas from the Enteric Diseases Group, Murdoch Children's Research Institute.

**Conflicts of Interest:** The authors declare no conflict of interest.

## References

1. Troeger, C.; Khalil, I.A.; Rao, P.C.; Cao, S.; Blacker, B.F.; Ahmed, T.; Armah, G.; Bines, J.E.; Brewer, T.G.; Colombara, D.V.; et al. Rotavirus Vaccination and the Global Burden of Rotavirus Diarrhea among Children Younger Than 5 Years. *JAMA Pediatr.* **2018**, *172*, 958–965. [CrossRef] [PubMed]
2. Burnett, E.; Parashar, U.D.; Tate, J.E. Real-world effectiveness of rotavirus vaccines, 2006–2019: A literature review and meta-analysis. *Lancet Glob. Health* **2020**, *8*, e1195–e1202. [CrossRef]
3. WHO. Rotavirus vaccines WHO position paper: January 2013—Recommendations. *Vaccine* **2013**, *31*, 6170–6171. [CrossRef] [PubMed]
4. Armah, G.E.; Sow, S.O.; Breiman, R.F.; Dallas, M.J.; Tapia, M.D.; Feikin, D.R.; Binka, F.N.; Steele, A.D.; Laserson, K.F.; Ansah, N.A.; et al. Efficacy of pentavalent rotavirus vaccine against severe rotavirus gastroenteritis in infants in developing countries in sub-Saharan Africa: A randomised, double-blind, placebo-controlled trial. *Lancet* **2010**, *376*, 606–614. [CrossRef]
5. Madhi, S.A.; Cunliffe, N.A.; Steele, D.; Witte, D.; Kirsten, M.; Louw, C.; Ngwira, B.; Victor, J.C.; Gillard, P.H.; Chevart, B.B.; et al. Effect of human rotavirus vaccine on severe diarrhea in African infants. *N. Engl. J. Med.* **2010**, *362*, 289–298. [CrossRef]
6. Zaman, K.; Anh, D.D.; Victor, J.C.; Shin, S.; Yunus, M.; Dallas, M.J.; Podder, G.; Thiem, V.D.; Mai, L.T.P.; Luby, S.P.; et al. Efficacy of pentavalent rotavirus vaccine against severe rotavirus gastroenteritis in infants in developing countries in Asia: A randomised, double-blind, placebo-controlled trial. *Lancet* **2010**, *376*, 615–623. [CrossRef]
7. Dey, A.; Wang, H.; Menzies, R.; Macartney, K. Changes in hospitalisations for acute gastroenteritis in Australia after the national rotavirus vaccination program. *Med. J. Aust.* **2012**, *197*, 453–4547. [CrossRef]
8. Snelling, T.L.; Andrews, R.M.; Kirkwood, C.D.; Culvenor, S.; Carapetis, J.R. Case-control evaluation of the effectiveness of the G1P[8] human rotavirus vaccine during an outbreak of rotavirus G2P[4] infection in central Australia. *Clin. Infect. Dis.* **2011**, *52*, 191–199. [CrossRef]
9. ABS. 2016 Census QuickStats (SA3); Australian Bureau of Statistics: Canberra, Australia, 2017. Available online: <https://www.abs.gov.au/websitedbs/censushome.nsf/home/quickstats?opendocument&navpos=220> (accessed on 20 July 2020).
10. Hull, B.P.; Lawrence, G.; MacIntyre, C.R.; McIntyre, P.B. Estimating immunisation coverage: Is the 'third dose assumption' still valid? *Commun. Dis. Intell. Q. Rep.* **2003**, *27*, 357–361.
11. Field, E.J.; Vally, H.; Grimwood, K.; Lambert, S. Pentavalent rotavirus vaccine and prevention of gastroenteritis hospitalizations in Australia. *Pediatrics* **2010**, *126*, e506–e512. [CrossRef]
12. Fathima, P.; Snelling, T.L.; Gibbs, R.A. Effectiveness of rotavirus vaccines in an Australian population: A case-control study. *Vaccine* **2019**, *37*, 6048–6053. [CrossRef] [PubMed]
13. Maguire, J.E.; Glasgow, K.; Glass, K.; Roczo-Farkas, S.; Bines, J.E.; Sheppard, V.; Macartney, K.; Quinn, H.E. Rotavirus Epidemiology and Monovalent Rotavirus Vaccine Effectiveness in Australia: 2010–2017. *Pediatrics* **2019**, *144*, 1–10. [CrossRef] [PubMed]
14. Australian Technical Advisory Group on Immunisation (ATAGI). *Australian Immunisation Handbook*; Australian Government Department of Health: Canberra, Australia, 2018.
15. Payne, D.C.; Boom, J.A.; Staat, M.A.; Edwards, K.M.; Szilagyi, P.G.; Klein, E.J.; Selvarangan, R.; Azimi, P.H.; Harrison, C.; Moffatt, M.; et al. Effectiveness of pentavalent and monovalent rotavirus vaccines in concurrent use among US children <5 years of age, 2009–2011. *Clin. Infect. Dis.* **2013**, *57*, 13–20. [PubMed]

16. Castilla, J.; Beristain, X.; Martínez-Artola, V.; Ortega, A.N.; Cenoz, M.G.; Álvarez, N.; Polo, I.; Mazón, A.; Gil-Setas, A.; Barricarte, A. Effectiveness of rotavirus vaccines in preventing cases and hospitalizations due to rotavirus gastroenteritis in Navarre, Spain. *Vaccine* **2012**, *30*, 539–543. [CrossRef]
17. Muhsen, K.; Shulman, L.; Kasem, E.; Rubinstein, U.; Shachter, J.; Kremer, A.; Goren, S.; Zilberstein, I.; Chodick, G.; Ephros, M.; et al. Effectiveness of rotavirus vaccines for prevention of rotavirus gastroenteritis-associated hospitalizations in Israel: A case-control study. *Hum. Vaccines* **2010**, *6*, 450–454. [CrossRef]
18. Leshem, E.; Lopman, B.; Glass, R.; Gentsch, J.; Banyai, K.; Parashar, U.; Patel, M. Distribution of rotavirus strains and strain-specific effectiveness of the rotavirus vaccine after its introduction: A systematic review and meta-analysis. *Lancet Infect. Dis.* **2014**, *14*, 847–856. [CrossRef]
19. Correia, J.B.; Patel, M.M.; Nakagomi, O.; Montenegro, F.M.U.; Germano, E.M.; Correia, N.B.; Cuevas, L.E.; Parashar, U.D.; Cunliffe, N.A.; Nakagomi, T. Effectiveness of monovalent rotavirus vaccine (Rotarix) against severe diarrhea caused by serotypically unrelated G2P[4] strains in Brazil. *J. Infect. Dis.* **2010**, *201*, 363–369. [CrossRef]
20. Zeller, M.; Rahman, M.; Heylen, E.; De Coster, S.; De Vos, S.; Arijs, I.; Novo, L.; Verstappen, N.; Van Ranst, M.; Matthijssens, J. Rotavirus incidence and genotype distribution before and after national rotavirus vaccine introduction in Belgium. *Vaccine* **2010**, *28*, 7507–7513. [CrossRef]
21. Doro, R.; László, B.; Martella, V.; Leshem, E.; Gentsch, J.; Parashar, U.; Banyai, K. Review of global rotavirus strain prevalence data from six years post vaccine licensure surveillance: Is there evidence of strain selection from vaccine pressure? *Infect. Genet. Evol.* **2014**, *28*, 446–461. [CrossRef]
22. Roczo-Farkas, S.; Kirkwood, C.D.; Cowley, D.; Barnes, G.L.; Bishop, R.F.; Bogdanovic-Sakran, N.; Boniface, K.; Donato, C.M.; E Bines, J. The Impact of Rotavirus Vaccines on Genotype Diversity: A Comprehensive Analysis of 2 Decades of Australian Surveillance Data. *J. Infect. Dis.* **2018**, *218*, 546–554. [CrossRef]
23. Santos, V.S.; Nóbrega, F.A.; Soares, M.W.S.; Moreira, R.D.; Cuevas, L.E.; Gurgel, R.Q. Rotavirus Genotypes Circulating in Brazil Before and After the National Rotavirus Vaccine Program: A Review. *Pediatr. Infect. Dis. J.* **2018**, *37*, e63–e65. [CrossRef] [PubMed]
24. Patel, M.; Glass, R.I.; Jiang, B.; Santosham, M.; Lopman, B.; Parashar, U. A systematic review of anti-rotavirus serum IgA antibody titer as a potential correlate of rotavirus vaccine efficacy. *J. Infect. Dis.* **2013**, *208*, 284–294. [CrossRef] [PubMed]
25. Velasquez, D.E.; Parashar, U.; Jiang, B. Decreased performance of live attenuated, oral rotavirus vaccines in low-income settings: Causes and contributing factors. *Expert Rev. Vaccines* **2018**, *17*, 145–161. [CrossRef] [PubMed]
26. Peter, G.; Myers, M.G. Intussusception, rotavirus, and oral vaccines: Summary of a workshop. *Pediatrics* **2002**, *110*, e67. [CrossRef]
27. Moore, H.C.; Fathima, P.; Gidding, H.F.; De Klerk, N.; Liu, B.; Sheppard, V.; Effler, P.V.; Snelling, T.L.; McIntyre, P.; Blyth, C.C.; et al. Assessment of on-time vaccination coverage in population subgroups: A record linkage cohort study. *Vaccine* **2018**, *36*, 4062–4069. [CrossRef]
28. Fathima, P.; Gidding, H.F.; Snelling, T.L.; McIntyre, P.; Blyth, C.C.; Sheridan, S.; Liu, B.; De Klerk, N.; Moore, H.C. Timeliness and factors associated with rotavirus vaccine uptake among Australian Aboriginal and non-Aboriginal children: A record linkage cohort study. *Vaccine* **2019**, *37*, 5835–5843. [CrossRef]
29. Orenstein, W.A.; Bernier, R.H.; Hinman, A.R. Assessing vaccine efficacy in the field. Further observations. *Epidemiol. Rev.* **1988**, *10*, 212–241. [CrossRef]
30. Izzo, M.M.; Kirkland, P.D.; Gu, X.; Lele, Y.; Gunn, A.A.; House, J. Comparison of three diagnostic techniques for detection of rotavirus and coronavirus in calf faeces in Australia. *Aust. Vet. J.* **2012**, *90*, 122–129. [CrossRef] [PubMed]
31. Middleton, B.F.; Jones, M.A.; Waddington, C.S.; Danchin, M.; McCallum, C.; Gallagher, S.; Leach, A.J.; Andrews, R.; Kirkwood, C.; Cunliffe, N.; et al. The ORVAC trial protocol: A phase IV, double-blind, randomised, placebo-controlled clinical trial of a third scheduled dose of Rotarix rotavirus vaccine in Australian Indigenous infants to improve protection against gastroenteritis. *BMJ Open* **2019**, *9*, e032549. [CrossRef]



## Article

# Characterisation of a G2P[4] Rotavirus Outbreak in Western Australia, Predominantly Impacting Aboriginal Children

Celeste M. Donato<sup>1,2,3,\*</sup>, Nevada Pingault<sup>4</sup>, Elena Demosthenous<sup>1,3</sup>, Susie Roczo-Farkas<sup>1</sup>  
and Julie E. Bines<sup>1,2,5</sup>

- <sup>1</sup> Enteric Diseases Group, Murdoch Children's Research Institute, Parkville 3052, Australia; susie.roczofarkas@mcri.edu.au (S.R.-F.); jebines@unimelb.edu.au (J.E.B.)  
<sup>2</sup> Department of Paediatrics, The University of Melbourne, Parkville 3010, Australia  
<sup>3</sup> Department of Microbiology, Biomedicine Discovery Institute, Monash University, Clayton 3800, Australia  
<sup>4</sup> Department of Health Western Australia, Communicable Disease Control Directorate, Perth 6004, Australia; nevada.pingault@health.wa.gov.au  
<sup>5</sup> Department of Gastroenterology and Clinical Nutrition, Royal Children's Hospital, Parkville 3052, Australia  
\* Correspondence: celeste.donato@mcri.edu.au; Tel.: +61-03-9936-6715

**Abstract:** In May, 2017, an outbreak of rotavirus gastroenteritis was reported that predominantly impacted Aboriginal children  $\leq 4$  years of age in the Kimberley region of Western Australia. G2P[4] was identified as the dominant genotype circulating during this period and polyacrylamide gel electrophoresis revealed the majority of samples exhibited a conserved electropherotype. Full genome sequencing was performed on representative samples that exhibited the archetypal DS-1-like genome constellation: G2-P[4]-I2-R2-C2-M2-A2-N2-T2-E2-H2 and phylogenetic analysis revealed all genes of the outbreak samples were closely related to contemporary Japanese G2P[4] samples. The outbreak samples consistently fell within conserved sub-clades comprised of Hungarian and Australian G2P[4] samples from 2010. The 2017 outbreak variant was not closely related to G2P[4] variants associated with prior outbreaks in Aboriginal communities in the Northern Territory. When compared to the G2 component of the RotaTeq vaccine, the outbreak variant exhibited mutations in known antigenic regions; however, these mutations are frequently observed in contemporary G2P[4] strains. Despite the level of vaccine coverage achieved in Australia, outbreaks continue to occur in vaccinated populations, which pose challenges to regional areas and remote communities. Continued surveillance and characterisation of emerging variants are imperative to ensure the ongoing success of the rotavirus vaccination program in Australia.



**Citation:** Donato, C.M.; Pingault, N.; Demosthenous, E.; Roczo-Farkas, S.; Bines, J.E. Characterisation of a G2P[4] Rotavirus Outbreak in Western Australia, Predominantly Impacting Aboriginal Children. *Pathogens* **2021**, *10*, 350. <https://doi.org/10.3390/pathogens10030350>

Academic Editor: David Allen

Received: 9 February 2021

Accepted: 12 March 2021

Published: 16 March 2021

**Publisher's Note:** MDPI stays neutral with regard to jurisdictional claims in published maps and institutional affiliations.



**Copyright:** © 2021 by the authors. Licensee MDPI, Basel, Switzerland. This article is an open access article distributed under the terms and conditions of the Creative Commons Attribution (CC BY) license (<https://creativecommons.org/licenses/by/4.0/>).

**Keywords:** rotavirus; outbreak; Aboriginal; Indigenous; G2P[4]; gastroenteritis; Western Australia; whole genome sequencing; vaccine

## 1. Introduction

Group A rotaviruses, belonging to the Reoviridae virus family, remain one of the main aetiological agents of acute gastroenteritis in infants and young children worldwide, estimated to have caused 128,500 deaths and 258,173,300 episodes of diarrhea among children  $< 5$  years of age in 2016 [1]. The substantial decrease in the global burden of rotavirus disease over the last decade can be attributed to varied public health measures, such as improved sanitation, as well as the inclusion of rotavirus vaccines into the National Immunisation Programs (NIPs) of over 100 countries worldwide [2]. In Australia, the live-attenuated vaccines Rotarix<sup>®</sup> (monovalent, human G1P[8] strain) and RotaTeq<sup>®</sup> (pentavalent, human-bovine reassortant vaccine comprising G1P[5], G2P[5], G3P[5], G4P[5], and G6P[8] strains) were introduced into the NIP in mid-2007, with a state-based vaccine selection method in place up until mid-2017, after which a national tender process was initiated, with all states and territories now using Rotarix [3,4].

Group A rotavirus strains are classified into G and P genotypes based on the outer capsid proteins VP7 and VP4, respectively. To date, 36 G types and 51 P types have been characterised from humans and varied animal species [5]. The most prevalent genotypes in humans are G1, G2, G3, G4, G9, and G12, in combination with P[4], P[6], and P[8] [6,7]. A whole genome classification nomenclature has been developed to describe the genome constellation of strains; Gx-P[x]-Ix-Rx-Cx-Mx-Ax-Nx-Tx-Ex-Hx, denoting the VP7-VP4-VP6-VP1-VP2-VP3-NSP1-NSP2-NSP3-NSP4-NSP5/6 genes, with x referring to the various recognised genotypes for each gene. There are three major genotype constellations: Wa-like (G1-P[8]-I1-R1-C1-M1-A1-N1-T1-E1-H1), DS-1-like (G2-P[4]-I2-R2-C2-M2-A2-N2-T2-E2-H2), and AU-1-like (G3-P[9]-I3-R3-C3-M3-A3-N3-T3-E3-H3) [8].

Western Australia (WA) is the largest state in Australia and is sparsely populated, with 80% of the 2.5 million residents residing in the capital city of Perth. Approximately 4% of the WA population identify as Indigenous (hereafter respectfully referred to as Aboriginal to recognise that Aboriginal people are the original inhabitants of WA), the proportion is higher outside Perth [9]. The Kimberley (KIMB) is a remote region that encompasses an area of 421,451 square kilometres. In 2016, the population was 36,392, and 45% of the region's population identified as Aboriginal, living in towns and communities of varying sizes. The KIMB region has a younger population compared to other regions of WA, with a higher percentage of children aged 0–14 years (25%) [10]. For the period 2011–2015, the enteric disease notification rate (salmonellosis, cryptosporidiosis, rotavirus, campylobacteriosis, and shigellosis) for children in the KIMB region was 5.2 times higher than for all children in WA, with rotavirus accounting for 5% of notifications. For all enteric infection notifications, the rate for Aboriginal children was 2.4 times the non-Aboriginal rate [10].

Rotavirus became a notifiable disease in WA from July 2006 [11]. The Communicable Disease Control Directorate (CDCD) and Public Health Units (PHUs) in the Department of Health WA (WA Health) investigate clusters and outbreaks of rotavirus. Initially, Rotarix was used in WA, from July 2007 to February 2009, then vaccine selection was changed to RotaTeq. In July 2017, the rotavirus vaccine used in WA reverted back to Rotarix [12,13]. In 2017, the estimated vaccine coverage in eligible children <12 months of age was 83.5% in Aboriginal children nationally and 89.5% in non-Aboriginal children [14]. The vaccine coverage for WA was 81.5% in 2015, the most recent data available, compared to a national coverage of 85.4% [15].

Sporadic community-wide rotavirus outbreaks have occurred in different states and territories around Australia. Outbreaks due to G2P[4] strains occurred in Perth (1993), Melbourne (1994), and Sydney (2001) [16,17]. Widespread outbreaks impacting remote communities in the Northern Territory have occurred due to G2P[4] strains in 1993, 1999, 2004, and 2009 [18–22]. Outbreaks due to G2P[4] strains were reported in 2010 in South Australia and Western Australia [23]. An outbreak caused by G2P[4] occurred in New South Wales in 2012, predominantly impacting children aged 5–9 years [24]. In 2017, multiple G2P[4] outbreaks were reported in the Northern Territory, South Australia, and Western Australia [3].

The aim of this study was to describe the epidemiology and burden of disease during an outbreak of rotavirus in the metropolitan (METRO) region of Perth and the remote Kimberley (KIMB) region of WA in 2017. Whole genome sequencing was performed to characterise the rotavirus strain circulating during this outbreak and place it in the context of global strains.

## 2. Results

### 2.1. Descriptive Epidemiology

In 2017, there were 519 notified cases of rotavirus infection in WA (19.1 cases per 100,000 population), making rotavirus the third most commonly notified enteric infection in WA. A marked increase in rotavirus notifications was noted in the second quarter of

2017 (April/May/June, 2Q17), with 236 cases, compared to the five-year second quarter average (2012–2016) of 100.8 cases (Figure 1).

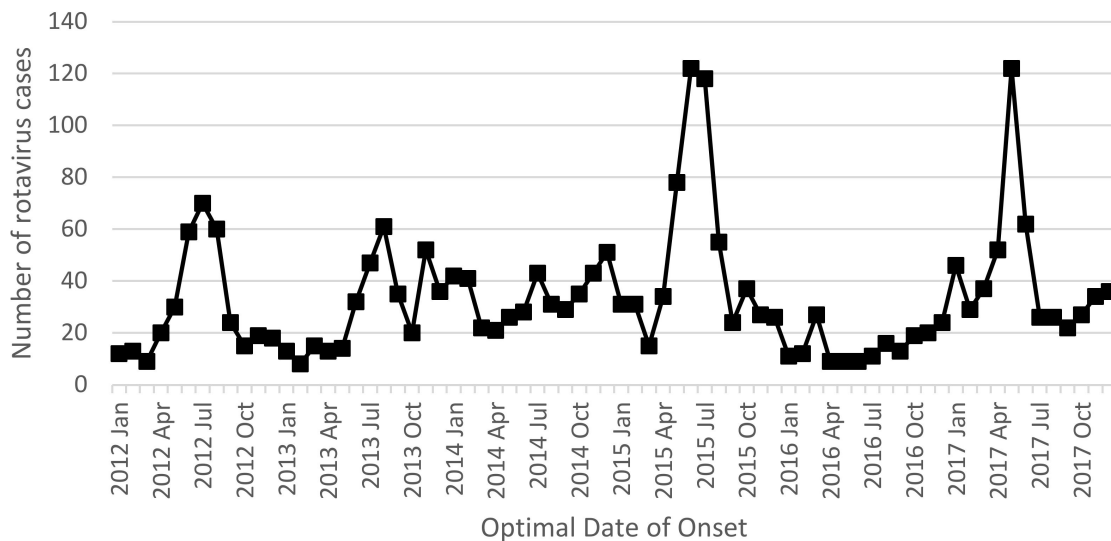


Figure 1. Monthly rotavirus notification rates between January 2012 and November 2017.

Within the 2Q17, the highest number of cases was seen in May ( $n = 122$ ), compared to 52 cases in April and 62 cases in June. Of the 122 cases in May, 80 were aged  $\leq 4$  years (Figure 2), with the majority of cases aged  $< 1$  year ( $n = 26$ ) and 1 year ( $n = 31$ ). While cases were seen in all PHUs, Aboriginal people from the KIMB ( $n = 46$ ) region and non-Aboriginal people from the metropolitan (METRO) region ( $n = 36$ ) were the two most affected groups (Figure 3). Examining children  $< 4$  years, Indigenous status, and PHU more closely, Aboriginal children from the KIMB region were disproportionately represented (40/80 cases) (Figure 4).

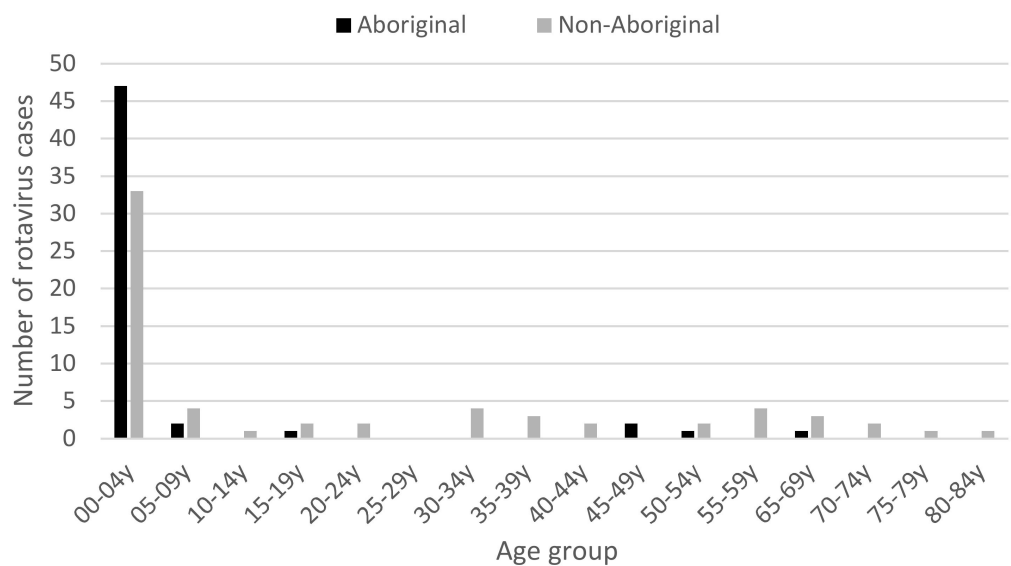
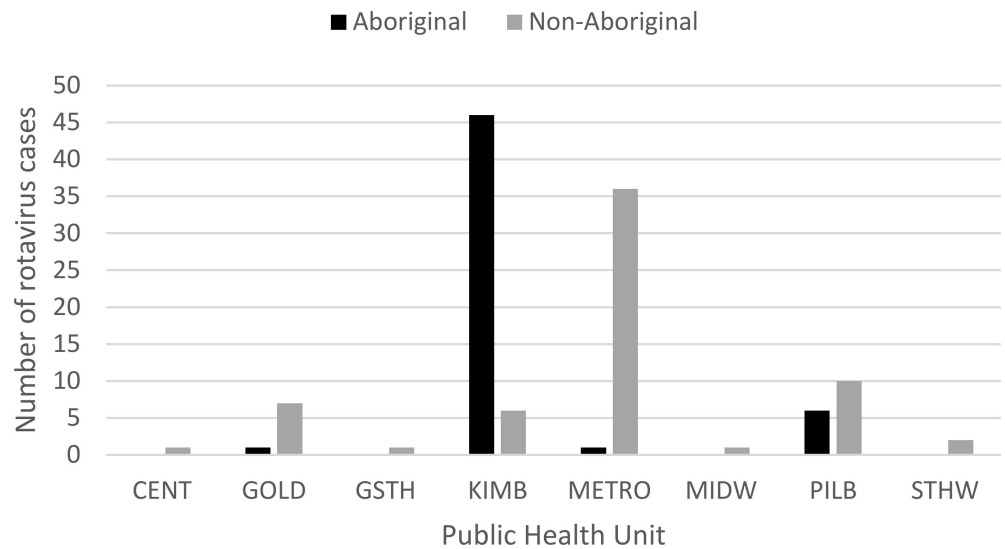
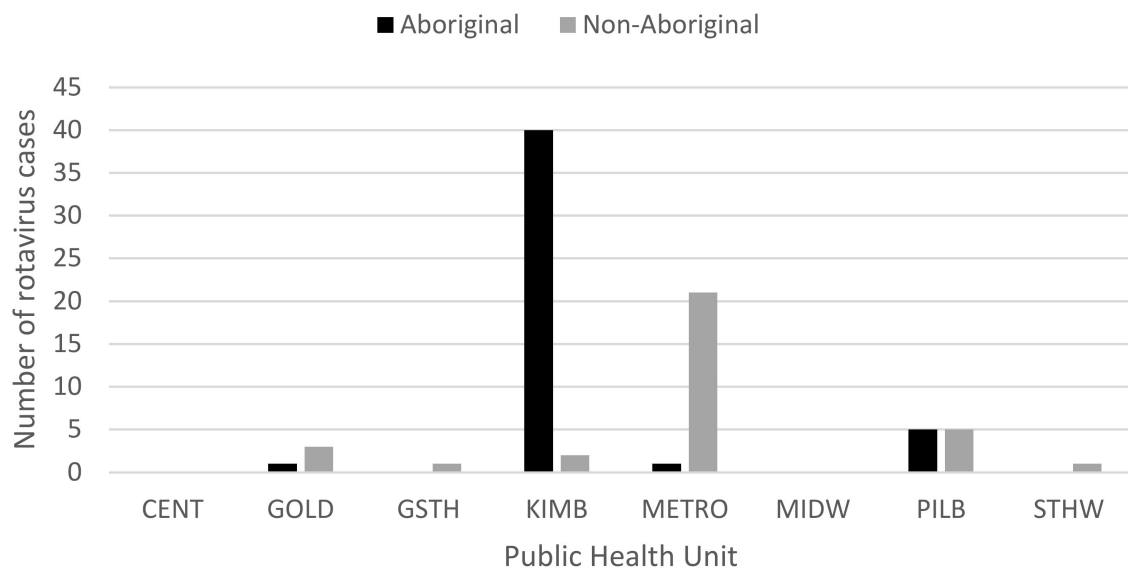


Figure 2. Distribution of the number of rotavirus cases in Western Australia in May, 2017 by age (years) and Indigenous status.



**Figure 3.** Distribution of the number of rotavirus cases from May, 2017, all ages, by Indigenous status and Public Health Unit (PHU) boundaries, reflecting WA Health administrative regions: Central/Wheatbelt (CENT), Goldfields (GOLD), Great Southern (GSTH), Kimberley (KIMB), Metropolitan Perth (METRO), Midwest (MIDW), Pilbara (PILB), and South West (STHW).



**Figure 4.** Distribution of rotavirus cases in May, 2017, aged  $\leq 4$  years, by Aboriginal status and Public Health Unit (PHU) boundaries, reflecting WA Health administrative regions: Central/Wheatbelt (CENT), Goldfields (GOLD), Great Southern (GSTH), Kimberley (KIMB), Metropolitan Perth (METRO), Midwest (MIDW), Pilbara (PILB), and South West (STHW).

Vaccination status was known for 97% of the total May cases (118/122). Of these, 41% were fully vaccinated (48/118), 24% were partially vaccinated (29/118), and 35% were not vaccinated (41/118) (Table 1). Only five of the unvaccinated cases were eligible to have been vaccinated, with the remaining 36 cases ineligible due to age.

Hospitalisation status was known for 78% of cases (95/122). For those with known hospitalisation status, 38% (36/95) were hospitalised as a result of their infection, of which 64% were Aboriginal people (23/36) and 36% were non-Aboriginal people (13/36). Children aged  $\leq 4$  years represented 86% of hospitalisations (31/36), of which Aboriginal children accounted for 71% (22/31). Of the hospitalised cases, 39% were fully vaccinated (14/36) and 36% were partially vaccinated (13/36). A further 22% were not vaccinated

(8/36), five of which were ineligible for vaccination due to age. Vaccination status was unknown for one case.

**Table 1.** Vaccination status of rotavirus cases from May 2017.

Genotype	Vaccination Status				Total
	Full	Partial	Eligible But Not Vaccinated	Ineligible Due to Age <sup>1</sup>	
G2P[4]	34	13	3	12	62
G3P[8]	1	0	0	2	3
G8P[8]	0	0	0	1	1
<b>Subtotal</b>	<b>35</b>	<b>13</b>	<b>3</b>	<b>15</b>	<b>66</b>
No data <sup>2</sup>	13	16	2	21	52
<b>Total May cases</b>	<b>48</b>	<b>29</b>	<b>5</b>	<b>36</b>	<b>118</b>

<sup>1</sup> Individuals  $\geq 11$  years of age were considered ineligible to have ever received a rotavirus vaccine dose based on age. <sup>2</sup> 52 samples were not sent to Murdoch Children's Research Institute for genotyping.

## 2.2. Genotyping

Cases were designated to the month of May based on the optimal date of onset (ODOO). Of the 122 cases from the month of May, a stool sample was available for 70 and were sent for genotype analysis at the National Rotavirus Reference Centre (NRRC), Murdoch Children's Research Institute in Melbourne, Australia. The predominant genotype identified was G2P[4] (94%, 66/70) (Table 2), with the majority of G2P[4] cases in the KIMB region (61%, 40/66). In the KIMB region, Aboriginal people were disproportionately represented, accounting for 90% of cases (36/40) (Table 2).

**Table 2.** Genotype results for 70 rotavirus positive samples (ODOO\* May, 2017).

Genotype	Region <sup>1</sup>	Aboriginal	Non- Aboriginal	Total
G2P[4]	GOLD	1	3	4
	KIMB	36	4	40
	METRO	1	8	9
	MIDW		1	1
	PILB	3	8	11
	STHW		1	1
<b>Total</b>		<b>41</b>	<b>25</b>	<b>66</b>
G3P[8]	METRO		3	3
G8P[8]	KIMB		1	1

<sup>1</sup> Public Health Unit (PHU) boundaries, reflecting WA Health administrative regions: Goldfields (GOLD), Kimberley (KIMB), Metropolitan Perth (METRO), Midwest (MIDW), Pilbara (PILB), and South West (STHW). \*ODOO: Optimal date of onset.

## 2.3. Vaccination and Hospitalisation Status of Genotyped Cases

Rotavirus vaccination information was available for 94% (66/70) of cases notified in May with genotyping results (Table 1). Of these, 53% (35/66) were fully vaccinated, 20% (13/66) were partially vaccinated, 4% (3/66) were not vaccinated but were eligible based on age, and 23% (15/66) were not vaccinated due to age (Table 1). Three quarters of G2P[4] cases were either fully or partially vaccinated (47/62). The majority of cases that were partially or fully vaccinated had received only the RotaTeq vaccine. Two fully vaccinated and one partially vaccinated case had received the Rotarix vaccine. Two fully vaccinated cases had received a combination of Rotarix and RotaTeq vaccines. Almost all Aboriginal cases had a known vaccination status (40/41); 60% (24/40) were fully vaccinated, 30% (12/40) were partially vaccinated, and 10% (4/20) were not vaccinated. Of the non-Aboriginal cases with known vaccination status (26/29), 42% (11/26) were fully vaccinated, 4% (1/26) were partially vaccinated, and 54% (14/26) were not vaccinated.

Hospitalisation status was known for 86% of the genotyped cases in May (60/70), with 19 cases hospitalised. Of these, 47% were fully vaccinated (9/19), 26% were partially vaccinated (5/19), 16% were not vaccinated (3/19), and vaccination status was unknown for two cases (10%).

#### 2.4. Sequence Analysis of G2P[4] Samples

A total of 38 G2P[4] samples were analysed using polyacrylamide gel electrophoresis to visualise the electropherotype pattern. The majority of samples had a highly similar electropherotype, indicating that a relatively conserved strain was circulating during the outbreak (data not shown).

Three samples were selected for whole genome sequencing, which were representative of the dominant electropherotype: RVA/Human-wt/AUS/WAPC2769/2017/G2P[4] (1-year-old, fully vaccinated, KIMB), RVA/Human-wt/AUS/WAPC2784/2017/G2P[4] (2-year-old, fully vaccinated child, METRO), and RVA/Human-wt/AUS/WAPC2824/2017/G2P[4] (3-year-old, fully vaccinated KIMB). The three samples exhibited the archetypal DS-1-like genome constellation: G2-P[4]-I2-R2-C2-M2-A2-N2-T2-E2-H2.

The 11 genes of each sample were successfully sequenced, with the exception of the VP2 gene of RVA/Human-wt/AUS/WAPC2769/2017/G2P[4] and RVA/Human-wt/AUS/WAPC2824/2017/G2P[4] for which only 69.7–70.3% of the open reading frame (ORF) could be determined. The sample volumes were exhausted, attempting to resolve the approximate 800-base pair (bp) region at the 3' prime end of the gene without success.

The coding regions of each gene of RVA/Human-wt/AUS/WAPC2784/2017/G2P[4] and RVA/Human-wt/AUS/WAPC2824/2017/G2P[4] were highly conserved, with RVA/Human-wt/AUS/WAPC2769/2017/G2P[4] displaying some minor variability: VP1 (99.81–99.94% nucleotide (nt) and 99.82–99.91% amino acid (aa) similarity), VP2 (99.84–100% nt and 99.84–100% aa similarity), VP3 (99.84–99.92% nt and 99.88–100% aa similarity), VP4 (99.79–99.91% nt and 99.61–99.87% aa similarity), VP6 (99.92–100% nt and 100% aa similarity), VP7 (99.89–100% nt and 99.69–100% aa similarity), NSP1 (99.86–99.93% nt and 100% aa similarity), NSP2 (99.90–100% nt and 100% aa similarity), NSP3 (99.47–99.79% nt and 99.39–99.68% aa similarity), NSP4 (99.62–99.81% nt and 99.43–100% aa similarity), and NSP5/6 (99.86–99.93% nt and 100% aa similarity).

#### 2.5. Phylogenetic Analysis

Phylogenetic analysis of the 11 genome segments was conducted to investigate the genetic relationships of the three outbreak samples RVA/Human-wt/AUS/WAPC2769/2017/G2P[4], RVA/Human-wt/AUS/WAPC2784/2017/G2P[4], and RVA/Human-wt/AUS/WAPC2824/2017/G2P[4] to previously characterised Australian samples and global strains (Figure 5a–k). In the VP7 tree, the outbreak samples clustered with contemporary G2P[4] samples from Japan and Taiwan detected in 2016 and 2017 shared 99.74–100% nt and 99.24–100% aa similarity (Figure 5a). The outbreak samples did not cluster closely to previously characterised Australian samples. The most closely related were two samples from Victoria detected in 2010, sharing 99.47–99.61% nt and 99.62–100% aa similarity (Figure 5a). In the VP4 tree, the outbreak samples clustered with the same contemporary G2P[4] samples from Japan as in the VP7 tree and shared 99.61–99.83% nt and 99.48–100% aa similarity (Figure 5b). Again, the outbreak samples did not cluster closely to previously characterised Australian samples; most closely related to the same two samples from Victoria (RVA/Human-wt/AUS/CK20040/2010/G2P[4] and RVA/Human-wt/AUS/CK20060/2010/G2P[4]) that shared 99.48–99.66% nt and 99.30–99.70% aa similarity (Figure 5b).



Figure 5. Cont.



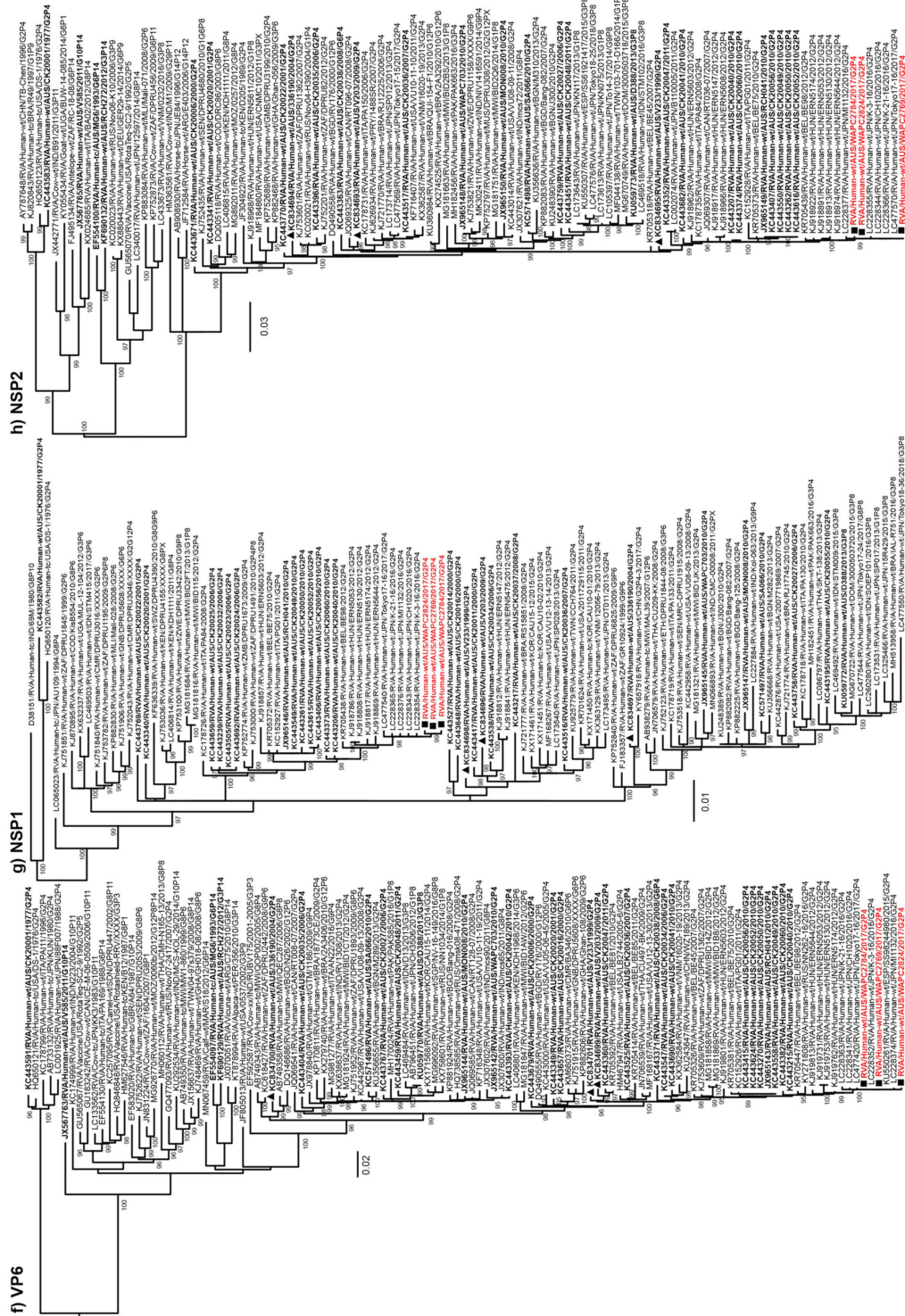
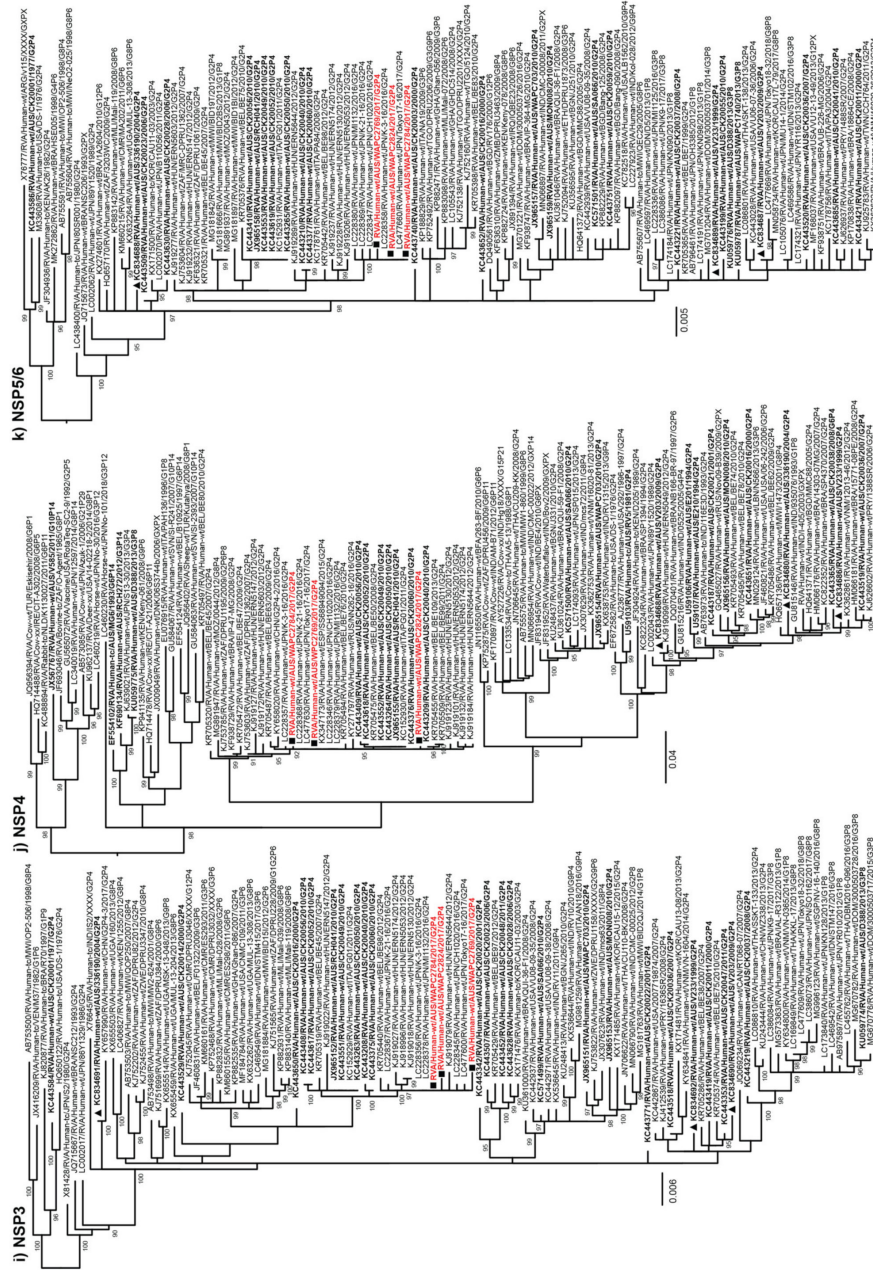


Figure 5. Cont.



**Figure 5.** Maximum likelihood phylogenetic trees of (a) VP7, (b) VP4, (c) VP1, (d) VP2, (e) VP3, (f) VP6, (g) NSP1, (h) NSP2, (i) NSP3, (j) NSP4, and (k) NSP5/6 2017 Western Australia outbreak G2P[4] samples. The position of strains sequenced in this study are highlighted in red and with square symbols, previously characterised G2P[4] outbreak samples from the Northern Territory detected in 1999, 2004, and 2010 are denoted with triangle symbols. All Australian samples are in bold. Ultrafast bootstrap values  $\geq 95\%$  are shown.

Across the VP1, VP2, VP3, and VP6 gene trees, the outbreak samples from this study continued to form conserved clusters with the contemporary Japanese samples RVA/Human-wt/JPN/MI1132/2016/G2P[4], RVA/Human-wt/JPN/K-21-16/2016/G2P[4], RVA/Human-wt/JPN/K-3-16/2016/G2P[4], RVA/Human-wt/JPN/Tokyo17-16/2017/G2P[4], and RVA/Human-wt/JPN/CH1020/2016/G2P[4] as observed in the VP7 and VP4 trees (Figure 5c–f). The samples RVA/Human-w/AUS/CK20040/2010/G2P[4] and RVA/Human-wt/AUS/CK20060/2010/G2P[4] were consistently the most closely related Australian samples to those from the 2017 outbreak. Across all trees, the 2017 outbreak samples fell within a clade that was comprised of a conserved group of G2P[4] strains from Belgium and Hungary that were detected in 2012, and the Australian samples RVA/Human-wt/AUS/CK20049/2010/G2P[4], RVA/Human-wt/AUS/CK20050/2010/G2P[4], RVA/Human-wt/AUS/CK20052/2010/G2P[4], RVA/Human-wt/AUS/CK20056/2010/G2P[4], and RVA/Human-wt/AUS/RCH041/2010/G2P[4].

Across the NSP1, NSP2, NSP3, NSP4, and NSP5 gene trees, the 2017 outbreak samples exhibited the same pattern across all trees: clustering with same group of contemporary Japanese samples, and falling within conserved clades comprised of G2P[4] strains from Belgium and Hungary that were detected in 2012, and Australian 2010 samples (Figure 5g–k).

The 2017 outbreak samples were not closely related to the samples RVA/Human-wt/AUS/V233/1999/G2P[4], RVA/Human-wt/AUS/336190/2004/G2P[4] and RVA/Human-wt/AUS/V203/2009/G2P[4], which were associated with prior outbreaks in the Northern Territory, often clustering in separate lineages or distinct clades. This suggests that the current outbreak variant was not derived from the prior G2P[4] outbreak variants that had undergone genetic drift or reassortment over the intervening years but were more closely related to a G2P[4] variant that has been detected in Japan, Hungary, and other regions of the world. It may be derived from the Australian 2010 G2P[4] variant that has undergone moderate genetic drift during global circulation.

#### 2.6. Comparison of the Outbreak Samples to the G2 VP7 Gene Component of the RotaTeq Vaccine

The VP7 gene of the 2017 outbreak samples possessed 93.37–99.48% nt and 94.79–95.01% aa similarity with the G2 VP7 gene of RotaTeq. The amino acid differences between the outbreak samples and RotaTeq were analysed and 16 residues differed between the G2 component of RotaTeq and the two outbreak samples RVA/Human-wt/AUS/WAPC2824/2017/G2P[4] and RVA/Human-wt/AUS/WAPC2769/2017/G2P[4]. RVA/Human-wt/AUS/WAPC2784/2017/G2P[4] had 17 residues that differed. The altered residues that fell between amino acid 78 and 312 were mapped to the surface of the VP7 monomer to highlight mutations in proximity to the VP7 antigenic epitopes 7-1a, 7-1b, and 7-2 [25] (Figure 6). Mutations were observed in all three samples in antigenic epitope regions: positions A87T and D96N in antigenic region 7-1a, and S213D in region 7-1b. Additionally, the mutation D145G in the antigenic epitope region 7-2 was observed in RVA/Human-wt/AUS/WAPC2784/2017/G2P[4]. The three outbreak samples exhibited the residues D96N and S213D, which are amino acid changes that have been shown to escape neutralisation with monoclonal antibodies [26].

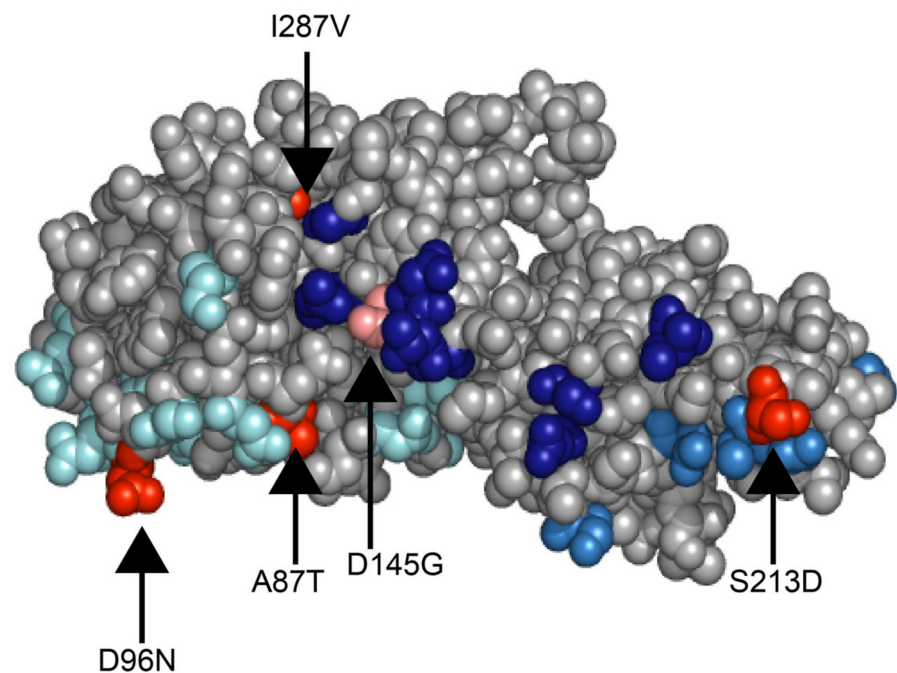


**Figure 6.** A surface representation of the VP7 monomer depicting the amino acid residues that differ between the 2017 G2P[4] WA outbreak samples and the G2 component of the RotaTeq vaccine strain (PDB ID: 3FMG). The antigenic epitopes are coloured as 7-1a in cyan, 7-1b in mid blue, and 7-2 in dark blue. The conserved residues that differ between the 2017 samples and the G2 component of the RotaTeq vaccine strain are shown in red and the residue that differed only in RVA/Human-wt/AUS/WAPC2784/2017/G2P[4] is shown in salmon.

### 3. Discussion

Rotavirus was gazetted as a notifiable disease in WA in 2006 in part to monitor the effectiveness of the rotavirus vaccine when it was added to the childhood immunisation schedule in Australia in mid-2007 [11]. The introduction of rotavirus vaccines has lessened the once prominent seasonality of rotavirus infection in Australia [27,28]. Following campylobacteriosis and salmonellosis, rotavirus was the third most commonly notified enteric infection in the population of WA in 2017 [29]. A large increase in rotavirus notifications was noted in the second quarter of 2017, with the highest number of cases noted in May, indicating an outbreak occurring prior to the onset of winter (Figure 1).

A total of 236 rotavirus notifications were recorded in the second quarter of 2017, compared to the five-year second quarter average of 100.8 notifications, highlighting the scale of the outbreak. The five-year second quarter average was somewhat skewed by an outbreak in the second quarter of 2015 (Figure 1) that affected all WA regions, and predominantly affected non-Aboriginal people. Multiple outbreaks related to child care and aged care facilities were noted during this time, with the predominant strain identified as G12P[8] [30].

In contrast to 2015, the increase in the second quarter of 2017 was noted to disproportionately affect young Aboriginal children in the KIMB region, which is in the north of the state. A number of towns and Aboriginal communities in the KIMB region were affected. The KIMB PHU investigated the increase in notifications, with assistance from local government environmental health officers. Several public health interventions were implemented as a result of their investigations, including the distribution of a public health alert to local hospitals and Aboriginal medical service providers, liaising with environmental health officers and community health staff to provide public health advice for affected communities, and an interview on local radio.

It is noteworthy that an increased burden of rotavirus disease was reported elsewhere in Australia for 2017. Multiple outbreaks were recorded across Australia, due to equine-like

G3P[8] in New South Wales and G8P[8] in New South Wales and Victoria [3]. In addition to the WA outbreak herein described, outbreaks due to G2P[4] were also reported in the Northern Territory (NT) and South Australia [3]. It is thought that the 2017 G2P[4] outbreak began in the NT and subsequently spread to rural and remote regions of WA adjacent to the border between these states [31]. A companion study described the weak protective effect of either Rotarix or RotaTeq vaccination in the setting of this outbreak [31]. Sub-optimal vaccine-effectiveness, particularly in the second year of life, has been reported in other high-burden, low-resource settings [32]. There are varied factors that could contribute to a reduced vaccine response, such as poor infant nutrition, the intestinal microbiota, co-morbid infections, as well as high levels of maternally derived anti-rotavirus antibodies [33].

The inclusion of rotavirus vaccines into the Australian NIP in 2007 has resulted in a considerable and sustained decrease in rotavirus morbidity across most of Australia, with a 71% decline in rotavirus-coded hospitalisations of children aged <5 years reported [34]. However, the observed decrease in hospitalisations has been less in Aboriginal and Torres Strait Islander children; they remain at greater risk of severe rotavirus disease requiring hospitalisation than their non-Indigenous counterparts [34]. Following rotavirus vaccine introduction in WA, significant declines in rotavirus-coded hospitalisation rates have been observed in all children aged <5 years, up to 79% among non-Aboriginal and up to 66% among Aboriginal children [35]. During the outbreak peak in May 2017 (122 cases), over a third of cases were hospitalised as a result of their infection, with Aboriginal people representing two thirds of these hospitalisations. As would be expected with rotavirus infection, the vast majority of cases hospitalised were  $\leq 4$  years of age, and Aboriginal children accounted for 71% of hospitalisations in this age group. Compared to their non-Indigenous counterparts, the paediatric Aboriginal population exhibit a greater burden of disease due to infections, and large, biannual rotavirus outbreaks have been reported in the Northern Territory [18–22]. Continued surveillance is critical to elucidate the complex factors that contribute to the occurrence of these outbreaks.

When the vaccination status of cases from the May peak was compared to hospitalisation status, vaccination did not appear to impact on whether a case was hospitalised. Fully or partially vaccinated children represented 75% of hospitalised cases (27/36) compared to unvaccinated eligible children accounting for 8% of hospitalised cases (3/36). Vaccination status was unknown for 3% of cases (1/36) and the remaining 14% of cases (5/36) were ineligible to have been vaccinated based on age. In May 2017, RotaTeq was the vaccine prescribed in the WA vaccination schedule and the vast majority of cases who were either fully or partially vaccinated were vaccinated with RotaTeq. Whilst a genotype-specific vaccine effectiveness has not been estimated for children in WA, the vaccine effectiveness of three doses of RotaTeq has been estimated at 82% (95% CI: 59–92) [36].

Full genome sequencing was performed on representative samples from the outbreak. These samples were found to be most closely related to Japanese G2P[4] strains detected in 2016 and 2017 across all genes in the genome. In one associated paper, these closely related samples were reported as minor G2P[4] variants circulating in the Mie prefecture in 2017 [37]. However, this variant was also detected in Tokyo in 2017, where G2P[4] was the dominant genotype, accounting for 40% of samples [38]. The outbreak samples also consistently clustered with Hungarian G2P[4] from 2012, where this genotype accounted for 13.5% of the samples genotyped in 2012 [39]. The WA outbreak samples clustered within a clade that also included G2P[4] strains from Australia that were circulating in 2010. These samples were collected during 2010–2011 when there was a substantial increase in G2P[4] strains in Australian states using the RotaTeq vaccine; G2P[4] strains replaced G1P[8] as the dominant genotype for the first time since vaccine introduction [23]. Overall, this suggests that the strain circulating during the 2017 WA outbreak is a global variant that was previously detected in Australia and has continued to be successfully transmitted in various regions around the world for over almost a decade. Based on the available sequencing, the majority of samples exhibit a relatively conserved genome that has not

undergone substantial reassortment, with the diversity observed indicative of genetic drift over the years. It is highly likely that this variant represents a re-introduction into Australia rather than reflecting genetic drift that has only occurred in the Australian population. The 2017 variant was not closely related to G2P[4] strains that had caused prior outbreaks in the Northern Territory in 1999, 2004, and 2009 [18].

The VP7 gene of the 2017 WA outbreak samples was compared to the G2 VP7 gene component of the RotaTeq vaccine. A total of 16 residues differed between the G2 component of RotaTeq and the two outbreak samples RVA/Human-wt/AUS/WAPC2824/2017/G2P[4] and RVA/Human-wt/AUS/WAPC2769/2017/G2P[4], and RVA/Human-wt/AUS/WAPC2784/2017/G2P[4] had 17 residues that differed. However, this is not unexpected as the RotaTeq G2 VP7 gene is derived from a strain that was circulating in 1992; global strains have undergone extensive genetic drift over the intervening years. Three of these altered residues in all three outbreak samples were observed in antigenic epitopes at positions A87T and D96N in antigenic region 7-1a, and S213D in region 7-1b [25]. Altered residue D145G in region 7-2 was only observed in RVA/Human-wt/AUS/WAPC2784/2017/G2P[4]. Residues D96N and S213D have been shown to escape neutralisation with monoclonal antibodies [26]. The observed altered residues A87T, D96N, and S213D have been observed in the majority of G2P[4] strains circulating globally over the last two decades [40]. In particular, mutations A87T, D96N, D145G, and S213D were observed in G2P[4] strains associated with outbreaks in children in Indonesia in 2018 and a nosocomial outbreak in adults within a German hospital [41,42]. Genetic drift in VP7 antigenic epitope regions could adversely impact the effectiveness of the RotaTeq vaccine against G2P[4] strains. However, large-scale studies combining genetic and antigenic characteristics of circulating variants are required to further elucidate this. It is possible that genetic drift between circulating variants and the vaccine strain, in combination with host-related facts that impact vaccine effectiveness in this population contribute to the occurrence of these outbreaks.

A limitation of this study was that a stool sample was available for 70/122 cases from the May peak. Not genotyping all samples could result in the proportion of the different genotypes being over- or underestimated. However, it does not alter the result that G2P[4] was the dominant genotype in the KIMB region as 41/53 samples were available and genotyped. The 70 samples available for genotyping were representative of the age distribution of rotavirus cases in WA during this period. However, more samples from Aboriginal cases were genotyped compared to non-Aboriginal cases (76% vs. 45%) and this could have overestimated the proportion of G2P[4] cases reported. Similarly, more samples were genotyped from the remote areas of the KIMB and PILB regions, which may also have overestimated the proportion of G2P[4] cases seen. Given this study largely focuses on the KIMB region, it is unlikely that this had any major impact on the overall results of the study.

## 4. Materials and Methods

### 4.1. Notification Data

Data on WA cases of rotavirus were obtained from the WA Notifiable Infectious Disease Database (WANIDD). The notifications contained in WANIDD are received from medical practitioners and pathology laboratories under the provisions of the Public Health Act 2016 and subsequent amendments, and are retained in WANIDD if national case definitions are met. Rotavirus was listed as a notifiable disease in WA in July 2006 [11]. Data was extracted from WANIDD by optimal date of onset (ODOO) for the time period 01/01/2012 to 31/12/2017 and exported to Microsoft<sup>®</sup> Excel 365 (Microsoft<sup>®</sup>, Version 1808, Redmond, WA, USA). The ODOO is a composite of the ‘true’ date of onset provided by the notifying doctor or obtained during case follow-up, the date of specimen collection for laboratory notified cases, and when neither of these dates is available, the date of notification by the doctor or laboratory, or the date of receipt of notification, whichever is earliest. Notification data are broken down by regions that are based on Public Health Unit (PHU) boundaries, reflecting WA Health administrative regions: Central/Wheatbelt

(CENT), Goldfields (GOLD), Great Southern (GSTH), Kimberley (KIMB), Metropolitan Perth (METRO), Midwest (MIDW), Pilbara (PILB), and South West (STHW).

#### 4.2. Vaccination Status

Records of vaccine administration were submitted to the Australian Immunisation Register (AIR) (curated by Services Australia, Australian Government). The AIR includes vaccines administered under the national immunisation program, school programs, and privately. CDCD staff accessed AIR to determine the rotavirus vaccine status of notified cases.

#### 4.3. Rotavirus Positive Faecal Samples

A total of 122 faecal samples collected from children and adults presenting to hospital or general practice clinics with severe gastroenteritis in Western Australia during May, 2017 were determined to be rotavirus positive by a local diagnostic laboratory. Seventy de-identified rotavirus positive specimens were sent to the National Rotavirus Reference Centre (NRRC) at the Murdoch Children's Research Institute. A further 27 samples did not have adequate remaining volume and were not sent for genotyping. There is no agreement with private pathology laboratories to forward samples for genotyping. As a result, 25/122 (20%) of samples were not genotyped. Where possible, metadata, including date of collection, date of birth, gender, and postcode, were collected. Samples were stored at  $-80\text{ }^{\circ}\text{C}$  until analysis, allocated a unique laboratory code, and entered into a REDCap database.

#### 4.4. Genotyping

Viral RNA was extracted from 10–20% (*w/v*) faecal extracts using the QIAamp Viral RNA mini extraction kit (QIAGEN, Hilden, Germany) according to the manufacturer's instructions. Rotavirus G- and P-genotyping was performed using a hemi-nested multiplex RT-PCR assay [43]. First-round RT-PCR reactions were performed using the One Step RT-PCR kit (QIAGEN, Germany), using the VP7 (VP7F/VP7R), or the VP4 primer pair (VP4F/VP4R) [44,45]. The second-round genotyping PCR reactions were performed using the AmpliTaq<sup>®</sup> DNA Polymerase with Buffer II (Applied Biosystems, Foster City, CA USA), together with specific oligonucleotide primers for G types (1, 2, 3, 4, 8, and 9) or P types ([4], [6], [8], [9], [10], and [11]) as previously described [4]. Gel electrophoresis of second-round PCR products was performed to determine the G- and P- genotype of each sample.

#### 4.5. Conformation of Vaccine-Line Strains

Sequencing of VP6 and VP7 genes was performed for suspect RotaTeq samples with mixed G types or were P non-typeable as previously described [18].

#### 4.6. Polyacrylamide Gel Electrophoresis

The 11 segments of rotavirus dsRNA were separated on 10% *w/v* polyacrylamide gel with 3% *w/v* polyacrylamide stacking gel at 25 mA for 16 h. The genome migration patterns (electropherotypes) were visualised by silver staining according to the established protocol [46].

#### 4.7. Whole Genome Sequencing

Each of the 11 genes were reverse transcribed and amplified by PCR using the OneStep RT-PCR Kit (QIAGEN, Hilden, Germany) using gene-specific sense and antisense primers (primer sequences available upon request). RNA was denatured and reverse transcribed for 30 min at  $45\text{ }^{\circ}\text{C}$ , followed by PCR activation for 15 min at  $95\text{ }^{\circ}\text{C}$ . Then, 40 cycles of amplification for 10 s at  $94\text{ }^{\circ}\text{C}$ , 1 min at  $55\text{ }^{\circ}\text{C}$ , and 3 min at  $68\text{ }^{\circ}\text{C}$ , followed by a final extension for 10 min at  $68\text{ }^{\circ}\text{C}$  were performed. The amplicons were gel purified using the Wizard<sup>®</sup> SV Gel and PCR Clean-Up System (Promega, Madison, WI, USA) according to the manufacturer's instructions.

The purified products were pooled in equimolar concentrations and subjected to standard library construction for Illumina sequencing using the Nextera XT DNA Library Preparation Kit following the manufacturer's recommendations for dual-indexed barcoding (Illumina Inc., San Diego, CA, USA). Normalised samples were pooled and sequenced using 500-cycle (2 × 250-bp paired-end) MiSeq reagent kits (v2; Illumina Inc., San Diego, CA, USA).

#### 4.8. Sequence Assembly

Raw reads were trimmed for quality and adapters using BBDuk Adapter/Quality Trimming Version 38.37, duplicate reads were removed using Dedupe Duplicate Read Remover version 38.37 and pair-end reads were merged using BBMerge Paired Read Merger version 38.37, all performed within Geneious Prime. Reads were mapped to reference rotavirus genomes using the Bowtie2 mapper within Geneious Prime [47].

#### 4.9. Assignment of Genotypes

The genotypes of each of the 11 genome segments were determined using the online RotaC v2.0 rotavirus genotyping tool (<http://rotac.regatools.be>, accessed on 18 January 2021) in accordance with the recommendations of the Rotavirus Classification Working Group (RCWG) [8].

#### 4.10. Phylogenetic Analysis

Nucleotide similarity searches were performed using the BLAST server on the GenBank database at the National Center for Biotechnology Information, USA ([www.ncbi.nlm.nih.gov](http://www.ncbi.nlm.nih.gov), accessed on 18 January 2021). The nucleotide and amino acid sequences of each gene were compared with sequences available in the GenBank database that possessed the entire open reading frame. Multiple nucleotide and amino acid alignments were constructed using the Multiple Sequence Comparison by Log Expectation (MUSCLE) algorithm in Geneious Prime [48].

The best-fit nucleotide substitution model for each gene tree were tested and selected in IQTREE v1.6 using the Bayesian Information Criteria [49]. The selected nucleotide substitution models were GTR+F+R3 (VP1, VP3), GTR+F+G4 (VP4), TIM+F+G4 (NSP1, NSP2, NSP3), TIM+F+I+G4 (VP2) TN+F+G4 (VP6, NSP4), and HKY+F+G4 (VP7, NSP5/6). The maximum likelihood trees were inferred using IQTREE v1.6 with the robustness of branches assessed by 1000 bootstrap replicates using the ultrafast bootstrap feature [50]. The resulting trees were visualised and edited in FigTree v1.4.4 (<http://tree.bio.ed.ac.uk/software/figtree/>, accessed on 18 January 2021). Nucleotide and amino acid distance matrixes were calculated using the p-distance algorithm in MEGAX [51]. Structural analysis of the VP7 protein (PDB ID: 3FMG) was performed using the PyMOL Molecular Graphics System, Version 1.2r3pre (Schrödinger, Inc, New York, NY, USA).

#### 4.11. Accession Numbers

The nucleotide sequences for genes described in this study have been deposited in GenBank under the accession numbers MW275246–MW275278.

## 5. Conclusions

This G2P[4] outbreak disproportionately impacted Aboriginal children ≤4 years of age in the remote Kimberley region of Western Australia. The G2P[4] variant circulating was closely related to contemporary Japanese G2P[4] samples, suggesting a global variant that exhibited the altered residues A87T, D96N, and S213D compared to the G2 component of the RotaTeq vaccine, residues that have been observed in the majority of G2P[4] strains circulating globally over the last two decades. Despite national vaccine coverage of 85.4%, outbreaks continue to occur in vaccinated populations in Australia, in particular impacting Aboriginal populations. These outbreaks pose particular challenges to regional areas and

remote communities. Continued surveillance and characterisation of emerging variants are imperative to ensure the ongoing success of the rotavirus vaccination program in Australia.

**Author Contributions:** Conceptualization, C.M.D., N.P. and S.R.-F.; Data curation, C.M.D., N.P. and S.R.-F.; Formal analysis, C.M.D., N.P. and S.R.-F.; Funding acquisition, C.M.D. and J.E.B.; Investigation, C.M.D., N.P. and S.R.-F.; Methodology, C.M.D., N.P., E.D. and S.R.-F.; Project administration, J.E.B.; Resources, C.M.D., N.P., S.R.-F. and J.E.B.; Software, C.M.D. and N.P.; Validation, C.M.D., N.P. and S.R.-F.; Visualization, C.M.D. and N.P.; Writing—original draft, C.M.D. and N.P.; Writing—review and editing, E.D., S.R.-F. and J.E.B. All authors have read and agreed to the published version of the manuscript.

**Funding:** This work was supported by the Australian National Health and Medical Research Council Project grant (1163346). The Australian Rotavirus Surveillance Program is supported by research grants from the vaccine companies Commonwealth Serum Laboratories (bioCSL)/Sequis (2010–2018) and the Australian Government Department of Health (2010–2018). Funding for this study was also provided by GlaxoSmithKline Biologicals SA (2010–2016, study ID116120 2017–2018). GlaxoSmithKline Biologicals SA was provided the opportunity to review a preliminary version of this manuscript for factual accuracy, but the authors are solely responsible for final content and interpretation. The authors received no financial support or other form of compensation related to the development of the manuscript. The Murdoch Children’s Research Institute is supported by the Victorian Government’s Operational Infrastructure Support program. CMD is supported through the Australian National Health and Medical Research Council with an Early Career Fellowship (1113269). The funders had no role in the design of the study; in the collection, analyses, or interpretation of data; in the writing of the manuscript, or in the decision to publish the results.

**Institutional Review Board Statement:** This activity has been reviewed by the Royal Children’s Hospital Human Research Ethics Office and assessed as a quality assurance and evaluation activity conducted on behalf of the Australian Government Department of Health and Western Australian Department of Health.

**Informed Consent Statement:** Patient consent was waived as data on WA cases of rotavirus were obtained from the WA Notifiable Infectious Disease Database (WANIDD). The notifications contained in WANIDD are received from medical practitioners and pathology laboratories under the provisions of the Public Health Act 2016 and subsequent amendments.

**Data Availability Statement:** The nucleotide sequences for genes described in this study have been deposited in GenBank under the accession numbers MW275246–MW275278.

**Acknowledgments:** The authors thank H. Tran for providing technical support, and S. Thomas for constructive feedback.

**Conflicts of Interest:** The Australian Rotavirus Surveillance Program is supported by research grants from the vaccine companies Commonwealth Serum Laboratories (bioCSL)/Sequis (2010–2018) and GlaxoSmithKline (2010–2016, study ID116120 2017–2018). C.M.D. has served on an advisory board for GSK (2019), all payments were paid directly to an administrative fund held by Murdoch Children’s Research Institute. All other authors declare no competing interests.

## References

1. Troeger, C.; Khalil, I.A.; Rao, P.C.; Cao, S.; Blacker, B.F.; Ahmed, T.; Armah, G.; Bines, J.E.; Brewer, T.G.; Colombara, D.V.; et al. Rotavirus Vaccination and the Global Burden of Rotavirus Diarrhea Among Children Younger Than 5 Years. *JAMA Pediatr.* **2018**, *172*, 958–965. [CrossRef]
2. World Health Organization. Vaccine in National Immunization Programme Update. Available online: [www.who.int/immunization/monitoring\\_surveillance/VaccineIntroStatus.pptx?ua=1](http://www.who.int/immunization/monitoring_surveillance/VaccineIntroStatus.pptx?ua=1) (accessed on 5 May 2020).
3. Roczo-Farkas, S.; Cowley, D.; Bines, J.E. Australian Rotavirus Surveillance Program: Annual Report, 2017. *Commun. Dis. Intell.* **2019**, *43*. [CrossRef] [PubMed]
4. Roczo-Farkas, S.; Kirkwood, C.D.; Cowley, D.; Barnes, G.L.; Bishop, R.F.; Bogdanovic-Sakran, N.; Boniface, K.; Donato, C.M.; Bines, J.E. The Impact of Rotavirus Vaccines on Genotype Diversity: A Comprehensive Analysis of 2 Decades of Australian Surveillance Data. *J. Infect. Dis.* **2018**, *218*, 546–554. [CrossRef] [PubMed]
5. Rotavirus Classification Working Group. List of Accepted Genotypes. Available online: <https://rega.kuleuven.be/cev/viralmetagenomics/virus-classification/rcwg> (accessed on 18 January 2021).

6. Bányai, K.; László, B.; Duque, J.; Steele, A.D.; Nelson, E.A.S.; Gentsch, J.R.; Parashar, U.D. Systematic review of regional and temporal trends in global rotavirus strain diversity in the pre rotavirus vaccine era: Insights for understanding the impact of rotavirus vaccination programs. *Vaccine* **2012**, *30*, A122–A130. [CrossRef]
7. Dóró, R.; László, B.; Martella, V.; Leshem, E.; Gentsch, J.; Parashar, U.; Bányai, K. Review of global rotavirus strain prevalence data from six years post vaccine licensure surveillance: Is there evidence of strain selection from vaccine pressure? *Infect. Genet. Evol.* **2014**, *28*, 446–461. [CrossRef]
8. Matthijnssens, J.; Ciarlet, M.; McDonald, S.M.; Attoui, H.; Banyai, K.; Brister, J.R.; Buesa, J.; Esona, M.D.; Estes, M.K.; Gentsch, J.R.; et al. Uniformity of rotavirus strain nomenclature proposed by the Rotavirus Classification Working Group (RCWG). *Arch. Virol.* **2011**, *156*, 1397–1413. [CrossRef] [PubMed]
9. Westphal, D.W.; Eastwood, A.; Levy, A.; Davies, J.; Huppatz, C.; Gilles, M.; Lyttle, H.; Williams, S.A.; Dowse, G.K. A protracted mumps outbreak in Western Australia despite high vaccine coverage: a population-based surveillance study. *Lancet Infect. Dis.* **2019**, *19*, 177–184. [CrossRef]
10. Anderson, C.; Bineham, N.; Lockwood, T.; Mukhtar, A.; Waenerberg, N. Kimberley Health Profile. 2018. Available online: [http://www.wacountry.health.wa.gov.au/fileadmin/sections/publications/Publications\\_by\\_topic\\_type/Reports\\_and\\_Profiles/Kimberley\\_Health\\_Profile\\_2018.pdf](http://www.wacountry.health.wa.gov.au/fileadmin/sections/publications/Publications_by_topic_type/Reports_and_Profiles/Kimberley_Health_Profile_2018.pdf) (accessed on 18 January 2021).
11. Government of Western Australia. Western Australia Government Gazette. Available online: [https://www.slp.wa.gov.au/gazette/gazette.nsf/searchgazette/E035CD6E603D90D4482571B80008A6AF/\\$file/gg130.pdf](https://www.slp.wa.gov.au/gazette/gazette.nsf/searchgazette/E035CD6E603D90D4482571B80008A6AF/$file/gg130.pdf) (accessed on 18 January 2021).
12. Australian Government Department of Health. Australian Technical Advisory Group on Immunisation. Available online: <https://www.health.gov.au/sites/default/files/atagi-rotateq-rotarix.pdf> (accessed on 18 January 2021).
13. Therapeutic Goods Administration. Rotavirus Vaccines Statement. Available online: <https://www.tga.gov.au/alert/rotavirus-vaccines-statement> (accessed on 22 January 2021).
14. Hull, B.; Hendry, A.; Dey, A.; Brotherton, J.; Macartney, K.; Beard, F. Annual Immunisation Coverage Report 2017. *Commun. Dis. Intell.* **2019**, *43*. [CrossRef] [PubMed]
15. Hull, B.; Hendry, A.; Dey, A.; Beard, F.; Brotherton, J.; McIntyre, P. Immunisation coverage annual report, 2015. *Commun. Dis. Intell.* **2019**, *43*. [CrossRef]
16. Bishop, R.F.; Masendycz, P.J.; Bugg, H.C.; Carlin, J.B.; Barnes, G.L. Epidemiological Patterns of Rotaviruses Causing Severe Gastroenteritis in Young Children throughout Australia from 1993 to 1996. *J. Clin. Microbiol.* **2001**, *39*, 1085–1091. [CrossRef]
17. Masendycz, P.; Bogdanovic-Sakran, N.; Palombo, E.; Bishop, R.; Barnes, G. Annual report of the Rotavirus Surveillance Programme, 1999/2000. *Commun. Dis. Intell.* **2000**, *24*, 195–198.
18. Donato, C.M.; Cowley, D.; Donker, N.C.; Bogdanovic-Sakran, N.; Snelling, T.L.; Kirkwood, C.D. Characterization of G2P[4] rotavirus strains causing outbreaks of gastroenteritis in the Northern Territory, Australia, in 1999, 2004 and 2009. *Infect. Genet. Evol.* **2014**, *28*, 434–445. [CrossRef]
19. Kirkwood, C.; Bogdanovic-Sakran, N.; Bishop, R.; Barnes, G.; Centre, N.R.R. Report of the Australian Rotavirus Surveillance Program 2003–2004. *Commun. Dis. Intell. Q. Rep.* **2004**, *28*, 481–485. [CrossRef]
20. Masendycz, P.; Bogdanovic-Sakran, N.; Kirkwood, C.; Bishop, R.; Barnes, G. Report of the Australian Rotavirus Surveillance Program, 2000/2001. *Commun. Dis. Intell. Q. Rep.* **2001**, *25*, 143–146.
21. Palombo, E.A.; Bugg, H.C.; Masendycz, P.J.; Coulson, B.S.; Barnes, G.L.; Bishop, R.F. Multiple-gene rotavirus reassortants responsible for an outbreak of gastroenteritis in central and northern Australia. *J. Gen. Virol.* **1996**, *77*, 1223–1227. [CrossRef] [PubMed]
22. Bishop, R.; Kirkwood, C. Rotavirus diarrhoea and Aboriginal Children. *Microbiol. Aust.* **2009**, *30*, 205–207. [CrossRef]
23. Donato, C.M.; Zhang, Z.A.; Donker, N.C.; Kirkwood, C.D. Characterization of G2P[4] rotavirus strains associated with increased detection in Australian states using the RotaTeq® vaccine during the 2010–2011 surveillance period. *Infect. Genet. Evol.* **2014**, *28*, 398–412. [CrossRef] [PubMed]
24. Kirkwood, C.D.; Roczo-Farkas, S.; Bishop, R.F.; Barnes, G.L.; Australian Rotavirus Surveillance, G. Australian Rotavirus Surveillance Program annual report, 2012. *Commun. Dis. Intell. Q. Rep.* **2014**, *38*, E29–E35.
25. Zeller, M.; Patton, J.T.; Heylen, E.; De Coster, S.; Ciarlet, M.; Van Ranst, M.; Matthijnssens, J. Genetic Analyses Reveal Differences in the VP7 and VP4 Antigenic Epitopes between Human Rotaviruses Circulating in Belgium and Rotaviruses in Rotarix and RotaTeq. *J. Clin. Microbiol.* **2012**, *50*, 966–976. [CrossRef]
26. Lazdins, I.; Coulson, B.S.; Kirkwood, C.; Dyal-Smith, M.; Masendycz, P.J.; Sonza, S.; Holmes, I.H. Rotavirus Antigenicity Is Affected by the Genetic Context and Glycosylation of VP7. *Virology* **1995**, *209*, 80–89. [CrossRef]
27. Newall, A.T.; MacIntyre, R.; Wang, H.; Hull, B.; Macartney, K. Burden of severe rotavirus disease in Australia. *J. Paediatr. Child Health* **2006**, *42*, 521–527. [CrossRef] [PubMed]
28. Clarke, M.F.; Davidson, G.P.; Gold, M.S.; Marshall, H.S. Direct and indirect impact on rotavirus positive and all-cause gastroenteritis hospitalisations in South Australian children following the introduction of rotavirus vaccination. *Vaccine* **2011**, *29*, 4663–4667. [CrossRef]
29. Combs, B.; Foster, N.; Pingault, N. Foodborne disease surveillance and outbreak investigations in Western Australia 2017 annual report. Department of Health: Perth, Western Australia, 2018. Available online: [https://ww2.health.wa.gov.au/Articles/F\\_I/Infectious-disease-data/Enteric-infection-reports-and-publications-OzFoodNet](https://ww2.health.wa.gov.au/Articles/F_I/Infectious-disease-data/Enteric-infection-reports-and-publications-OzFoodNet) (accessed on 22 January 2021).

30. Roczo-Farkas, S.; Kirkwood, C.D.; Bines, J.E.; Australian Rotavirus Surveillance, G. Australian Rotavirus Surveillance Program annual report, 2015. *Commun. Dis. Intell. Q. Rep.* **2016**, *40*, E527–E538. [[PubMed](#)]
31. Middleton, B.F.; Danchin, M.; Quinn, H.; Ralph, A.P.; Pingault, N.; Jones, M.; Estcourt, M.; Snelling, T. Retrospective Case-Control Study of 2017 G2P[4] Rotavirus Epidemic in Rural and Remote Australia. *Pathogens* **2020**, *9*, 790. [[CrossRef](#)] [[PubMed](#)]
32. Burnett, E.; Van Trang, N.; Rayamajhi, A.; Yousafzai, M.T.; Satter, S.M.; Anh, D.D.; Thapa, A.; Qazi, S.H.; Heffelfinger, J.D.; Hung, P.H.; et al. Preparing for safety monitoring after rotavirus vaccine introduction—Assessment of baseline epidemiology of intussusception among children <2 years of age in four Asian countries. *Vaccine* **2018**, *36*, 7593–7598. [[CrossRef](#)]
33. Velasquez, D.E.; Parashar, U.; Jiang, B. Decreased performance of live attenuated, oral rotavirus vaccines in low-income settings: Causes and contributing factors. *Expert Rev. Vaccines* **2018**, *17*, 145–161. [[CrossRef](#)]
34. Dey, A.; Wang, H.; Menzies, R.; Macartney, K. Changes in hospitalisations for acute gastroenteritis in Australia after the national rotavirus vaccination program. *Med. J. Aust.* **2012**, *197*, 453–457. [[CrossRef](#)] [[PubMed](#)]
35. Fathima, P.; Jones, M.A.; Moore, H.C.; Blyth, C.C.; Gibbs, R.A.; Snelling, T.L. Impact of Rotavirus Vaccines on Gastroenteritis Hospitalizations in Western Australia: A Time-series Analysis. *J. Epidemiol.* **2020**, JE20200066. [[CrossRef](#)]
36. Fathima, P.; Snelling, T.L.; Gibbs, R.A. Effectiveness of rotavirus vaccines in an Australian population: A case-control study. *Vaccine* **2019**, *37*, 6048–6053. [[CrossRef](#)]
37. Komoto, S.; Ide, T.; Negoro, M.; Tanaka, T.; Asada, K.; Umamoto, M.; Kuroki, H.; Ito, H.; Tanaka, S.; Ito, M.; et al. Characterization of unusual DS-1-like G3P[8] rotavirus strains in children with diarrhea in Japan. *J. Med. Virol.* **2018**, *90*, 890–898. [[CrossRef](#)] [[PubMed](#)]
38. Fujii, Y.; Oda, M.; Somura, Y.; Shinkai, T. Molecular Characteristics of Novel Mono-Reassortant G9P[8] Rotavirus A Strains Possessing the NSP4 Gene of the E2 Genotype Detected in Tokyo, Japan. *Jpn. J. Infect. Dis.* **2020**, *73*, 26–35. [[CrossRef](#)] [[PubMed](#)]
39. Dóró, R.; Mihalov-Kovács, E.; Marton, S.; László, B.; Deák, J.; Jakab, F.; Juhász, Á.; Kisfali, P.; Martella, V.; Melegh, B.; et al. Large-scale whole genome sequencing identifies country-wide spread of an emerging G9P[8] rotavirus strain in Hungary, 2012. *Infect. Genet. Evol.* **2014**, *28*, 495–512. [[CrossRef](#)] [[PubMed](#)]
40. Doan, Y.H.; Nakagomi, T.; Cunliffe, N.A.; Pandey, B.D.; Sherchand, J.B.; Nakagomi, O. The occurrence of amino acid substitutions D96N and S242N in VP7 of emergent G2P[4] rotaviruses in Nepal in 2004–2005: A global and evolutionary perspective. *Arch. Virol.* **2011**, *156*, 1969–1978. [[CrossRef](#)] [[PubMed](#)]
41. Utsumi, T.; Wahyuni, R.M.; Dinana, Z.; Gunawan, E.; Putra, A.S.D.; Mubawadi, T.; Soetjpto; Lusida, M.I.; Shoji, I. G2P[4] rotavirus outbreak in Belu, East Nusa Tenggara Province, Indonesia, 2018. *J. Infect. Public Health* **2020**, *13*, 1592–1594. [[CrossRef](#)]
42. Niendorf, S.; Ebner, W.; Marques, A.M.; Bierbaum, S.; Babikir, R.; Huzly, D.; Maaßen, S.; Grundmann, H.; Panning, M. Rotavirus outbreak among adults in a university hospital in Germany. *J. Clin. Virol.* **2020**, *129*, 104532. [[CrossRef](#)] [[PubMed](#)]
43. Gouvea, V.; Glass, R.I.; Woods, P.; Taniguchi, K.; Clark, H.F.; Forrester, B.; Fang, Z.Y. Polymerase chain reaction amplification and typing of rotavirus nucleic acid from stool specimens. *J. Clin. Microbiol.* **1990**, *28*, 276–282. [[CrossRef](#)]
44. Gómara, M.I.; Cubitt, D.; Desselberger, U.; Gray, J. Amino Acid Substitution within the VP7 Protein of G2 Rotavirus Strains Associated with Failure to Serotype. *J. Clin. Microbiol.* **2001**, *39*, 3796–3798. [[CrossRef](#)]
45. Simmonds, M.K.; Armah, G.; Asmah, R.; Banerjee, I.; Damanka, S.; Esona, M.; Gentsch, J.R.; Gray, J.J.; Kirkwood, C.; Page, N.; et al. New oligonucleotide primers for P-typing of rotavirus strains: Strategies for typing previously untypeable strains. *J. Clin. Virol.* **2008**, *42*, 368–373. [[CrossRef](#)]
46. Herring, A.J.; Inglis, N.F.; Ojeh, C.K.; Snodgrass, D.R.; Menzies, J.D. Rapid diagnosis of rotavirus infection by direct detection of viral nucleic acid in silver-stained polyacrylamide gels. *J. Clin. Microbiol.* **1982**, *16*, 473–477. [[CrossRef](#)]
47. Langmead, B.; Salzberg, S.L. Fast gapped-read alignment with Bowtie 2. *Nat. Methods* **2012**, *9*, 357–359. [[CrossRef](#)]
48. Edgar, R.C. MUSCLE: Multiple sequence alignment with high accuracy and high throughput. *Nucleic Acids Res.* **2004**, *32*, 1792–1797. [[CrossRef](#)] [[PubMed](#)]
49. Nguyen, L.-T.; Schmidt, H.A.; Von Haeseler, A.; Minh, B.Q. IQ-TREE: A Fast and Effective Stochastic Algorithm for Estimating Maximum-Likelihood Phylogenies. *Mol. Biol. Evol.* **2015**, *32*, 268–274. [[CrossRef](#)] [[PubMed](#)]
50. Minh, B.Q.; Nguyen, M.A.T.; Von Haeseler, A. Ultrafast Approximation for Phylogenetic Bootstrap. *Mol. Biol. Evol.* **2013**, *30*, 1188–1195. [[CrossRef](#)] [[PubMed](#)]
51. Kumar, S.; Stecher, G.; Li, M.; Nnyaz, C.; Tamura, K. MEGA X: Molecular evolutionary genetics analysis across computing platforms. *Mol. Biol. Evol.* **2018**, *35*, 1547–1549. [[CrossRef](#)]



Article

# FUT2 Secretor Status Influences Susceptibility to VP4 Strain-Specific Rotavirus Infections in South African Children

Jaime MacDonald <sup>1,2,\*</sup>, Michelle J. Groome <sup>3</sup>, Janet Mans <sup>2</sup> and Nicola Page <sup>1,2</sup> 

<sup>1</sup> National Institute for Communicable Diseases, Sandringham 2131, South Africa; nicolap@nicd.ac.za

<sup>2</sup> Department of Medical Virology, Faculty of Health Sciences, University of Pretoria, Pretoria 0001, South Africa; janet.mans@up.ac.za

<sup>3</sup> South African Medical Research Council, Vaccines and Infectious Diseases Analytics Research Unit, Faculty of Health Sciences, University of Witwatersrand, Johannesburg 2193, South Africa; groomem@rmpru.co.za

\* Correspondence: macdonaldjc@icloud.com; Tel.: +27-(0)-72-064-5721

Received: 31 July 2020; Accepted: 22 September 2020; Published: 27 September 2020



**Abstract:** Gastroenteritis is a preventable cause of morbidity and mortality worldwide. Rotavirus vaccination has significantly reduced the disease burden, but the sub-optimal vaccine efficacy observed in low-income regions needs improvement. Rotavirus VP4 ‘spike’ proteins interact with FUT2-defined, human histo-blood group antigens on mucosal surfaces, potentially influencing strain circulation and the efficacy of P[8]-based rotavirus vaccines. Secretor status was investigated in 500 children <5 years-old hospitalised with diarrhoea, including 250 previously genotyped rotavirus-positive cases (P[8] = 124, P[4] = 86, and P[6] = 40), and 250 rotavirus-negative controls. Secretor status genotyping detected the globally prevalent G428A single nucleotide polymorphism (SNP) and was confirmed by Sanger sequencing in 10% of participants. The proportions of secretors in rotavirus-positive cases (74%) were significantly higher than in the rotavirus-negative controls (58%;  $p < 0.001$ ). The rotavirus genotypes P[8] and P[4] were observed at significantly higher proportions in secretors (78%) than in non-secretors (22%), contrasting with P[6] genotypes with similar proportions amongst secretors (53%) and non-secretors (47%;  $p = 0.001$ ). This suggests that rotavirus interacts with secretors and non-secretors in a VP4 strain-specific manner; thus, secretor status may partially influence rotavirus VP4 wild-type circulation and P[8] rotavirus vaccine efficacy. The study detected a mutation (rs1800025) ~50 bp downstream of the G428A SNP that would overestimate non-secretors in African populations when using the TaqMan@SNP Genotyping Assay.

**Keywords:** rotavirus; secretor status; histo-blood group antigens; VP4 genotypes; *FUT2*; susceptibility; vaccines

## 1. Introduction

Gastroenteritis is a preventable cause of morbidity and mortality worldwide, and the burden predominantly exists in high-risk populations such as children under the age of five years in low-income regions [1]. Rotavirus is the most frequent aetiology of diarrhoeal illness and death in children <5 years-old, and it was responsible for 29% of global diarrhoeal deaths occurring in this age group in 2016 [2].

The introduction of oral rotavirus vaccines in >100 countries worldwide has significantly reduced the burden of rotavirus diarrhoea and resulted in a 38% overall reduction in childhood diarrhoeal hospitalisations globally [3,4]. However, rotavirus vaccine efficacy appears to vary significantly between high-income (85–98%) and low-income (50–64%) countries [5]. Eliciting an adequate immune response to oral vaccines is multifactorial but may be limited in low-income settings due to impoverished living conditions and increased exposure to pathogens [3]. In addition, the passive transfer of rotavirus maternal

antibodies during breastfeeding can influence the immune response elicited by oral rotavirus vaccines in young children [4]. Understanding the factors that have contributed to an observed lower rotavirus vaccine efficacy in these settings may alleviate the burden of rotavirus-associated mortality in children.

Host genetic factors have recently been proposed to influence susceptibility to enteric pathogens. The excretion of soluble human histo-blood group antigen (HBGA) structures in gut mucosal surfaces determines a host's 'secretor status,' controlled by the human *FUT2* gene. Non-secretor phenotypes with an inability to express soluble HBGAs due to mutations in the *FUT2* gene (such as the prevalent G428A SNP; rs601338) are present globally in varying proportions. Higher proportions of non-secretor phenotypes are observed in African populations (~30%) than in Asian populations (~5%) [6,7].

Antigenic HBGA structures present in the body can act as receptors for various pathogens to bind during infection [8,9]. *FUT2* secretor status can modulate infection because it defines the presence (secretor) or absence (non-secretor) of HBGA attachment factors excreted in the gut. Susceptibility to enteric norovirus infection has been associated with secretor status, where non-secretor phenotypes have been found to display a natural resistance to GII.4 norovirus strains [10–12]. It has been proposed that variations in secretor status phenotypes and subsequent differences in host-defined susceptibility may contribute to the circulation of rotavirus strains in a similar mechanism [13].

Interactions between rotavirus particles and HBGA receptors present in the gut can occur via the VP4 (VP8\* subunit) 'spike' protein on the surface of the virion [14]. Evidence of rotavirus VP4 strain-specific binding patterns between HBGAs and prevalent strains (P[8], P[4], and P[6]) has recently been noted [14]. Rotavirus P-types have distinct VP4 morphology that determines the presence or absence of HBGA-binding interfaces, allowing for different mechanisms of binding and entry of rotavirus particles to occur [13]. Studies have shown that rotavirus genotypes P[8]- and P[4]-bound complex and soluble HBGAs abundant in secretors, as well as an increased susceptibility to infection with these rotavirus strains in secretors. Non-secretors with an absence of HBGAs in the gut have been found to display a natural resistance to P[8] and P[4] strains with VP4 HBGA-binding interfaces [15–17]. Variations in host-defined secretor status can therefore influence susceptibility to infection with different rotavirus strains.

Rotavirus P[8] genotypes are responsible for more than 80% of human wild-type infections globally [15]. However, rotavirus circulation in Africa differs in strain diversity and prevalence, with more frequent cases of P[6] strains, which have reached 26% of all rotavirus strains circulating in African populations [18]. The proportions of naturally resistant non-secretors may alter the circulation of rotavirus P-types compared to that in global populations.

The Rotarix<sup>®</sup> and RotaTeq<sup>®</sup> rotavirus vaccines both contain P[8]-based strains or reassortants, and they provide protection through the replication of live-attenuated vaccine strains in the gut to induce a local immune response [4]. Associations between host-defined secretor status and susceptibility to infection with specific rotavirus strains pose interesting questions surrounding the lowered efficacy of P[8]-based rotavirus vaccines observed in some regions [19,20]. Emerging research has alluded to this idea [21–23], including the influence of the related *FUT3* Lewis host genetic factor [24–27], but further investigations are required. These data have contributed to the evidence that host genetic factors such as secretor status can influence infections by pathogens including rotavirus, as well as that strain-specific interaction mechanisms may occur [14,15,28].

The aim of this study was to investigate *FUT2*-defined secretor status in South African children <5 years-old hospitalised with diarrhoea and to examine the association between a host's genetic secretor status and rotavirus-associated hospitalisations. Understanding the relationship between pathogens such as rotavirus and the genetics of a population may identify avenues for improvements in vaccine efficacy to reduce the burden of rotavirus gastroenteritis.

## **2. Results**

Secretor genotypes were successfully determined for all 500 children selected for the study, and the total cohort comprised 65.8% (329) secretors with at least one functional *FUT2* allele and 34.2% (171) non-secretors with both *FUT2* alleles containing the G428A SNP.

Rotavirus-positive cases (RV+) comprised 74% (185/250) secretors (Se) and 26% (65/250) non-secretors, while rotavirus-negative controls (RV-) comprised 58% (144/250) secretors and 42% (106/250) non-secretors. The distributions of secretors versus non-secretors observed amongst cases and controls were significantly different ( $p < 0.001$ ).

Information on rotavirus genotyping from the Rotavirus Sentinel Surveillance Program (RSSP) database [29,30] showed that the rotavirus-positive cases ( $n = 250$ ) comprised 124 P[8] infections, 86 P[4] infections, and 40 P[6] infections (Supplementary Material). The proportions of secretors and non-secretors were compared amongst each VP4 strain within rotavirus-positive cases (Table 1). Rotavirus P[8] infections (79% secretors and 21% non-secretors) and P[4] infections (77% secretors and 23% non-secretors) had significantly different proportions of secretor phenotypes compared to P[6] infections (53% secretors and 47% non-secretors) ( $p = 0.001$  and  $p = 0.006$ , respectively). When considered together, rotavirus P[8] and P[4] infections (78% secretors and 22% non-secretors) had significantly different proportions of secretor phenotypes compared to P[6] infections (53% secretors and 47% non-secretors) ( $p = 0.001$ ).

**Table 1.** The distribution of secretors and non-secretors amongst VP4 genotypes P[8], P[4], and P[6] of rotavirus-positive cases (RV+;  $n = 250$ ).

Rotavirus Genotypes:	P[8] Infections ( $n = 124$ )	P[4] Infections ( $n = 86$ )	P[6] Infections ( $n = 40$ )
Secretors	79% (98/124)	77% (66/86)	52.5% (21/40)
Non-secretors	21% (26/124)	23% (20/86)	47.5% (19/40)
<i>p</i> -values for each comparison	P[8] vs. P[4]: $p = 0.693$		
	P[8] vs. P[6]: $p = 0.001$		
	P[4] vs. P[6]: $p = 0.006$		
	P[8] + P[4] vs. P[6]: $p = 0.001$		

The Sanger sequencing of the exon 2 region of the *FUT2* gene conducted for 10% of the cohort confirmed the presence of either functional *FUT2* alleles or G428A SNP alleles for 91% (48/53) of analysed specimens. Sequences of the *FUT2* exon 2 region from 12 homozygous secretors (SeSe), 24 heterozygous secretors (Sese), and 17 homozygous non-secretors (sese) were obtained and compared to RT-PCR G428A genotyping results. Five discrepant results were observed in which heterozygous secretor (Sese) individuals (one functional *FUT2* allele and one allele containing the non-functional G428A SNP) genotyped by Sanger sequencing were incorrectly genotyped by RT-PCR as non-secretors (both alleles containing the G428A SNP). A commonality between these discrepant specimens was an SNP mutation (rs1800025) ~50 bp downstream of the G428A SNP (Figure 1).

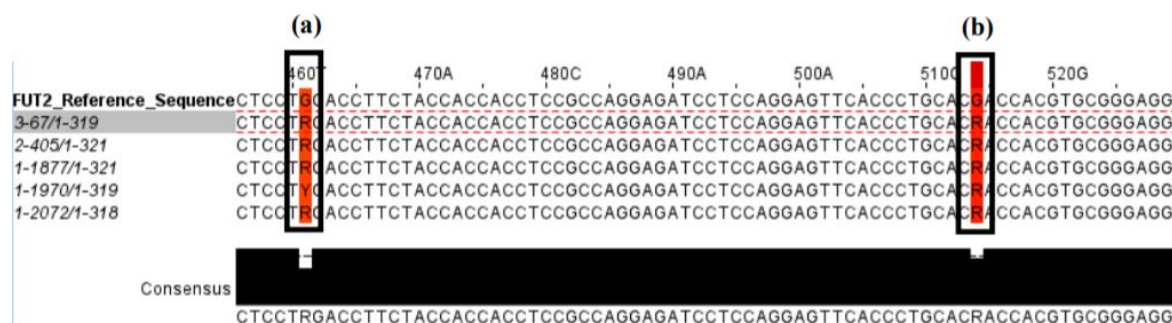


**Figure 1.** Sequence alignment of five participants where Sanger sequencing and RT-PCR genotyping results were discrepant. (a) The G428A SNP location displaying all discrepant sequences containing the two peaks ‘G’ and ‘A,’ as represented by an ‘R’ annotation. (b) The mutation site (rs1800025) located ~50 base pairs downstream of the G428A SNP, common in all discrepant results.

### 3. Discussion

The results from this study indicate that secretors were more susceptible to rotavirus infection, and non-secretors seemed to display a natural resistance. The absence of HBGAs in the gastric mucosa of non-secretors appeared to reduce susceptibility to rotavirus, possibly by limiting the attachment stage of binding and entry during rotavirus infection [31]. Despite this observation, non-secretors were present amongst rotavirus-positive cases, indicating that HBGA attachment may not be the only mechanism for rotavirus binding and subsequent entry. Early studies on rotavirus binding and entry described sialic acid as an attachment factor for some animal strains [32]. Alternative binding receptors such as sialic acid or yet unknown mechanisms could explain the presence of rotavirus infection in non-secretor individuals in our study.

Studies have shown that rotavirus VP4 (VP8\*) binds to HBGAs in a strain-specific manner [13]. Xu and colleagues showed that P[8] and P[4] rotavirus strains similarly bound to complex HBGAs via a  $\beta\beta$  binding domain, while more distantly related P[6] strains bound simple H-type 1 structures in a  $\beta\alpha$  binding domain [14]. In our study, a higher proportion of secretors was observed in P[8] (78%) and P[4] (76%) rotavirus infections compared to P[6] infections (53%). This suggested that secretors were significantly more susceptible to P[8] and P[4] strains than to P[6] strains ( $p < 0.01$ ), while non-secretors were more likely to be infected with P[6] strains. These strain-specific interactions may also influence the circulation of rotavirus strains within the South African population, as observed in other settings [15–17].

A correlation in the prevalence of rotavirus VP4 strains and HBGA genotypes suggested that the circulation of rotavirus may be partially modulated by their ability to bind to host-defined HBGA receptors. Globally, G1P[8] is the predominantly circulating rotavirus genotype, with ~74% of global strains containing the P[8] VP4 strain [18]. However, studies have shown that rotavirus strains in Africa are more diverse, with P[8] comprising 32% of rotavirus cases, P[4] comprising 13% of rotavirus cases, and P[6] comprising 26% of rotavirus cases [18]. In South Africa, P[6] strains were detected in 25% of rotavirus cases between 2003 and 2006, and they continue to circulate [30,33]. In this study, the higher proportion of non-secretors (34%), naturally resistant to P[8] and P[4] rotavirus infections, may explain the 16% detection of P[6] strains [17,34]. The *FUT2* genetics of a population may define the availability of host HBGA receptors for rotavirus infection, which could drive the epidemiology of rotavirus strain circulation in a region.

Discrepant results in Sanger sequencing revealed that five individuals were misclassified by RT-PCR as non-secretors (error rate 22.7%; 5/22), with sequencing identifying these five individuals as heterozygous secretors (Sese). The specimen sub-set comprised 58.5% secretors and 41.5% non-secretors based on RT-PCR genotyping, while the same specimens comprised 67.9% secretors and 32.1% non-secretors based on Sanger sequencing—an overall over-estimation of non-secretors of approximately 10%. This over-estimation of non-secretor genotypes is important to note for future studies, especially when using the TaqMan<sup>®</sup> SNP Genotyping Assay targeting the G428A SNP in an African population where non-secretors are frequent. The proportion of non-secretors (34%) observed in our cohort of 500 individuals correlated with other studies in African populations where higher frequencies of non-secretors were observed [35,36].

Misclassification by the commercial genotyping assay was hypothesised to be due to a mutation noted ~50 bp downstream of the G428A SNP position. The manufacturer confirmed that the mutation affected the primer binding of the reverse primer to the functional copy of the *FUT2* gene in the five heterozygous secretors, resulting in the absence of PCR product for the FAM-labelled probe (which detects the presence of the allele without the G428A SNP) to bind. Interestingly, the mutation was found in 9% of African populations compared to 2% in all populations in the 1000 genomes project [37]. Sanger sequencing remains an important tool to investigate host genetic factors such as secretor status, and further sequencing will be considered to examine the extent of the *FUT2* G514R mutation detected in this study.

Studies have indicated that secretor status can influence antibody titres to rotavirus [36], the incidence of gastrointestinal disease [38], and immune responses to rotavirus vaccines [28]. Rotarix<sup>®</sup> and RotaTeq<sup>®</sup> vaccines both contain P[8] vaccine constructs and require multiplication in intestinal cells to elicit local gut immunity [39,40]. The absence of HBGA attachment factors in non-secretors may reduce the replicative capacity of P[8] vaccine strains. The observation that non-secretors in Africa exhibit a natural resistance to wild-type P[8] strains may provide insights into the differences in vaccine efficacy across populations [5]. A study by Kazi and colleagues identified a link between the immune response to rotavirus P[8] vaccines and secretor status [28], and these associations have since been observed elsewhere [19,22,41]. Since patient sera were not collected as part of the RSSP, we could not investigate the direct effect of secretor status on rotavirus vaccine immune responses. Future studies investigating links between secretor status and variables such as vaccine immune responses, breastfeeding in young children, population genetics, and gut microbiome compositions, as well as alternative binding receptors for rotavirus entry, should be considered.

The limitations of this study include the small sample size of P[6] rotavirus cases available for further analysis (16%; 40/250). A larger sample size of rotavirus genotypes would be beneficial in confirming the relationship between specific rotavirus VP4 strains and secretor status. Another limitation of this study was the discordant results between RT-PCR genotyping and Sanger sequencing, resulting in the misclassification of heterozygous secretors by RT-PCR. Only 13% (22/171) of non-secretor genes were sequenced due to budget constraints, and additional funding will be sought to expand the sequencing of the *FUT2* gene of non-secretors in South Africa. A final limitation of this study was not including analysis of the related *FUT3* Lewis genes as it may also impact susceptibility to rotavirus infections. Future studies should consider the genetics of a cohort before utilising genotyping techniques, since alternative SNPs may be present which may skew results.

#### **4. Materials and Methods**

The South African RSSP enrolled children under the age of five years hospitalised for diarrhoea at various sites across South Africa (Protocol M091018, approved by the Human Research Ethics Committee (Medical) of the University of Witwatersrand). Diarrhoea was defined as three or more loose stools in past 24 h, with or without vomiting.

Informed consent was obtained from each child's parent or guardian prior to participation in the RSSP. Stool and dried blood spot (DBS) specimens were collected from enrolled participants, and each child's stool was screened as part of the RSSP for rotavirus group A (ProspecT<sup>™</sup> Rotavirus Microplate Assay, Oxoid, Basingstoke, UK). Rotavirus-positive cases were genotyped using conventional RT-PCR methods and primers for G-specific and P-specific genotypes to determine the GxP[x] rotavirus strain [42].

This sub-study was conducted in accordance with the Declaration of Helsinki, and the project entitled "Investigation of secretor status, rotavirus VP4 genotypes, and gastrointestinal microbiomes in cases of diarrhoea in South Africa" (Protocol number 222/2018) was approved by the Research Ethics Committee, Faculty of Health Sciences, University of Pretoria, in May 2018.

For this study, children enrolled in the RSSP between 2009 and 2017 with available DBS specimens were identified, and rotavirus-negative cases (n = 250) were randomly selected. Rotavirus GxP[x] genotypes were previously determined as part of the RSSP [30], and the rotavirus-positive subset (n = 250) was selected to represent the major rotavirus VP4 genotypes (P[8], P[4], and P[6]), with cases and controls selected randomly where possible.

Secretor status was investigated using DBS specimens. DNA from DBS specimens was extracted using a QIAamp DNA Mini kit (Qiagen Inc., Valencia, CA, USA) according to the manufacturer's instructions with one modification prior to extraction. The manufacturer's protocol was modified to improve lysis by incubating DBS cards (~1 cm diameter) in a 200 µL buffer ATL overnight at 37 °C, instead of at 85 °C for 10 min. Following extraction, DNA was stored at -40 °C at the Centre for Enteric Diseases (Virology), National Institute for Communicable Diseases.

Secretor status was determined by detecting the presence or absence of the *FUT2* G428A SNP using a Predesigned TaqMan<sup>®</sup> SNP Genotyping assay (Life Technologies Corporation, CA, USA, supplied by Thermo Fisher Scientific, Carlsbad, CA, USA) in a 10 µL reaction volume according to the manufacturer's instructions [27,43].

The Sanger sequencing of 10% of the cohort *FUT2* genes was performed to ensure that alternative non-secretor-causing SNPs, which may be undetected by this assay, were absent. The specimens were selected to include all secretor genotypes, with a slight selection bias towards heterozygous secretors (n = 19) and non-secretors (n = 22) compared to homozygous secretors (n = 12), as well as a range of cycle threshold values (Ct range of 10–39) obtained during RT-PCR. The coding exon 2 region of the *FUT2* gene was amplified using the FUT2Ex2F and FUT2Ex2R primers [7], cleaned using an ExoSAP-IT<sup>™</sup> PCR Product Cleanup protocol (Thermo Fisher), and sequenced using a BigDye<sup>™</sup> Terminator v3.1 Cycle Sequencing kit (Applied Biosystems, Life Technologies, Waltham, MA, USA) on an Applied Biosystems 3500xL Genetic Analyzer instrument (Applied Biosystems). Sequences were aligned to a *FUT2* protein-coding reference sequence (NG\_007511.1:11987-13018 *Homo sapiens* fucosyltransferase 2 (*FUT2*), RefSeqGene on chromosome 19) (NCBI) using Molecular Evolutionary Genetics Analysis software version 7.0.26 (MEGA7).

The sequences of the *FUT2* exon 2 region of 10% of the cohort were submitted to BankIt (National Center for Biotechnology Information, Bethesda, MD, USA), and the accession numbers are as follows: MW036696, MW036697, MW036698, MW036699, MW036700, MW036701, MW036702, MW036703, MW036704, MW036705, MW036706, MW036707, MW036708, MW036709, MW036710, MW036711, MW036712, MW036713, MW036714, MW036715, MW036716, MW036717, MW036718, MW036719, MW036720, MW036721, MW036722, MW036723, MW036724, MW036725, MW036726, MW036727, MW036728, MW036729, MW036730, MW036731, MW036732, MW036733, MW036734, MW036735, MW036736, MW036737, MW036738, MW036739, MW036740, MW036741, MW036742, MW036743, MW036744, MW036745, MW036746, MW036747, MW036748.

Statistical analyses using Chi-squared tests and univariate logistic regression models were performed using STATA version 14.0, where  $p < 0.05$  was considered significant (StataCorp College Station, TX, USA).

## 5. Conclusions

Rotavirus susceptibility appeared to be influenced by secretor status in this study of South African children hospitalised with acute diarrhoea. Secretors expressing HBGAs in gut mucosal surfaces were more likely to be infected with rotavirus, specifically the P[8] and P[4] strains, compared to non-secretors. Non-secretors, with an absence of HBGAs in the gut, appeared to be less susceptible to rotavirus P[8] and P[4] infections compared to secretors—thus, the P[6] genotype was more frequent in these individuals. Interactions between rotavirus and secretor status could provide insights into the circulation of rotavirus strains amongst genetically diverse populations. Insights into the potential causes of altered rotavirus susceptibility and subsequent vaccine efficacy will aid in minimising the burden of disease. Diarrhoeal deaths are preventable, and secretor status may be an important host genetic factor to help understand and improve rotavirus disease prevention. Finally, the choice of assay for detecting or classifying secretor status in different populations should be carefully considered because the tools currently available all have pros and cons associated with their use.

**Supplementary Materials:** The following are available online at <http://www.mdpi.com/2076-0817/9/10/795/s1>, File: Final DBS Cohort Results\_7.9.2020.

**Author Contributions:** Conceptualization, M.J.G., J.M. (Janet Mans) and N.P.; Data curation, J.M. (Jaime MacDonald); Formal analysis, M.J.G.; Funding acquisition, N.P.; Investigation, J.M. (Jaime MacDonald); Methodology, J.M. (Jaime MacDonald) and J.M. (Janet Mans); Project administration, N.P.; Resources, N.P.; Supervision, M.J.G., J.M. (Janet Mans) and N.P.; Validation, N.P.; Writing—original draft, J.M. (Jaime MacDonald); Writing—review & editing, M.J.G., J.M. (Janet Mans) and N.P. All authors have read and agreed to the published version of the manuscript.

**Funding:** This research was funded by the Rotavirus Surveillance grant (GSK E-Track 200238) and a bursary from the Poliomyelitis Research Foundation (Grant 19/48).

**Acknowledgments:** I would like to acknowledge the Centre for Enteric Diseases team at the National Institute for Communicable Diseases for facilitating and supporting this research.

**Conflicts of Interest:** The authors declare no conflict of interest. The funders had no role in the design of the study; in the collection, analyses, or interpretation of data; in the writing of the manuscript; or in the decision to publish the results.

## References

1. Troeger, C.; Forouzanfar, M.; Rao, P.C.; Khalil, I.; Brown, A.; Reiner, R.C.; Fullman, N.; Thompson, R.L.; Abajobir, A.; Ahmed, M.; et al. Estimates of global, regional, and national morbidity, mortality, and aetiologies of diarrhoeal diseases: A systematic analysis for the Global Burden of Disease Study 2015. *Lancet Infect. Dis.* **2017**, *17*, 909–948. [CrossRef]
2. Troeger, C.; Khalil, I.A.; Rao, P.C.; Cao, S.; Blacker, B.F.; Ahmed, T.; Armah, G.; Bines, J.E.; Brewer, T.G.; Colombara, D.V.; et al. Rotavirus vaccination and the global burden of rotavirus diarrhea among children younger than 5 years. *JAMA Pediatr.* **2018**, *172*, 958–965. [CrossRef] [PubMed]
3. Burnett, E.; Jonesteller, C.L.; Tate, J.E.; Yen, C.; Parashar, U.D. Global impact of rotavirus vaccination on childhood hospitalizations and mortality from diarrhea. *J. Infect. Dis.* **2017**, *215*, 1666–1672. [CrossRef] [PubMed]
4. Steele, A.D.; Victor, J.C.; Carey, M.E.; Tate, J.E.; Atherly, D.E.; Pecenka, C.; Diaz, Z.; Parashar, U.D.; Kirkwood, C.D. Experiences with rotavirus vaccines: Can we improve rotavirus vaccine impact in developing countries? *Hum. Vaccin. Immunother.* **2019**, *15*, 1215–1227. [CrossRef]
5. Velasquez, D.E.; Parashar, U.; Jiang, B. Decreased performance of live attenuated, oral rotavirus vaccines in low-income settings: Causes and contributing factors. *Expert Rev. Vaccines* **2018**, *17*, 145–161. [CrossRef]
6. Parker, E.P.K.; Ramani, S.; Lopman, B.A.; Church, J.A.; Iturriza-Gómara, M.; Prendergast, A.J.; Grassly, N.C. Causes of impaired oral vaccine efficacy in developing countries. *Future Microbiol.* **2018**, *13*, 97–118. [CrossRef]
7. Ferrer-Admetlla, A.; Sikora, M.; Laayouni, H.; Esteve, A.; Roubinet, F.; Blancher, A.; Calafell, F.; Bertranpetit, J.; Casals, F. A natural history of FUT2 polymorphism in humans. *Mol. Biol. Evol.* **2009**, *26*, 1993–2003. [CrossRef]
8. Ramani, S.; Hu, L.; Venkataram Prasad, B.V.; Estes, M.K. Diversity in rotavirus-host glycan interactions: A “sweet” spectrum. *Cell. Mol. Gastroenterol. Hepatol.* **2016**, *2*, 263–273. [CrossRef]
9. Monedero, V.; Buesa, J.; Rodríguez-Díaz, J. The interactions between host glycobiology, bacterial microbiota, and viruses in the gut. *Viruses* **2018**, *10*, 96. [CrossRef]
10. Van Trang, N.; Vu, H.T.; Le, N.T.; Huang, P.; Jiang, X.; Anh, D.D. Association between norovirus and rotavirus infection and histo-blood group antigen types in vietnamese children. *J. Clin. Microbiol.* **2014**, *52*, 1366–1374. [CrossRef]
11. Nordgren, J.; Sharma, S.; Kambhampati, A.; Lopman, B.; Svensson, L. Innate Resistance and Susceptibility to Norovirus Infection. *PLoS Pathog.* **2016**, *12*, 13–17. [CrossRef]
12. Nordgren, J.; Svensson, L. Genetic susceptibility to human norovirus infection: An update. *Viruses* **2019**, *11*, 226. [CrossRef] [PubMed]
13. Zhang, X.F.; Long, Y.; Tan, M.; Zhang, T.; Huang, Q.; Jiang, X.; Tan, W.F.; Li, J.D.; Hu, G.F.; Tang, S.; et al. P[8] and P[4] rotavirus infection associated with secretor phenotypes among children in south China. *Sci. Rep.* **2016**, *6*, 1–7. [CrossRef] [PubMed]
14. Xu, S.; Liu, Y.; Tan, M.; Zhong, W.; Zhao, D.; Jiang, X.; Michael, A. Molecular basis of P[6] and P[8] major human rotavirus VP8\* domain interactions with histo-blood group antigens. *BioRxiv* **2019**, 512301. [CrossRef]
15. Heylen, E.; Zeller, M.; Ciarlet, M.; Lawrence, J.; Steele, D.; Van Ranst, M.; Matthijssens, J. Human P[6] rotaviruses from sub-saharan Africa and southeast Asia are closely related to those of human P[4] and P[8] rotaviruses circulating worldwide. *J. Infect. Dis.* **2016**, *214*, 1039–1049. [CrossRef] [PubMed]
16. Gozalbo-Rovira, R.; Ciges-Tomas, J.R.; Vila-Vicent, S.; Buesa, J.; Santiso-Bellón, C.; Monedero, V.; Yebra, M.J.; Marina, A.; Rodríguez-Díaz, J. Unraveling the role of the secretor antigen in human rotavirus attachment to histo-blood group antigens. *PLOS Pathog.* **2019**, *15*, e1007865. [CrossRef] [PubMed]

17. Hu, L.; Sankaran, B.; Laucirica, D.R.; Patil, K.; Salmen, W.; Ferreon, A.C.M.; Tsoi, P.S.; Lasanajak, Y.; Smith, D.F.; Ramani, S.; et al. Glycan recognition in globally dominant human rotaviruses. *Nat. Commun.* **2018**, *9*, 1–12. [CrossRef]
18. Todd, S.; Page, N.A.; Duncan Steele, A.; Peenze, I.; Cunliffe, N.A. Rotavirus strain types circulating in Africa: Review of studies published during 1997–2006. *J. Infect. Dis.* **2010**, *202*, S34–S42. [CrossRef]
19. Armah, G.E.; Cortese, M.M.; Dennis, F.E.; Yu, Y.; Morrow, A.L.; McNeal, M.M.; Lewis, K.D.C.; Awuni, D.A.; Armachie, J.; Parashar, U.D. Rotavirus vaccine take in infants is associated with secretor status. *J. Infect. Dis.* **2019**, *219*, 746–749. [CrossRef]
20. Sharma, S.; Hagbom, M.; Svensson, L.; Nordgren, J. The Impact of Human Genetic Polymorphisms on Rotavirus Susceptibility, Epidemiology, and Vaccine Take. *Viruses* **2020**, *12*, 324. [CrossRef]
21. Bucardo, F.; Reyes, Y.; Rönnelid, Y.; González, F.; Sharma, S.; Svensson, L.; Nordgren, J. Histo-blood group antigens and rotavirus vaccine shedding in Nicaraguan infants. *Sci. Rep.* **2019**, *9*, 1–8. [CrossRef] [PubMed]
22. Pollock, L.E. Predictors of Vaccine Viral Replication, Immune Response and Clinical Protection Following Oral Rotavirus Vaccination in Malawian Children. Ph.D. Thesis, University of Liverpool, Liverpool, UK, 2018.
23. Clarke, E.; Desselberger, U. Correlates of protection against human rotavirus disease and the factors influencing protection in low-income settings. *Mucosal Immunol.* **2015**, *8*, 1–17. [CrossRef] [PubMed]
24. Wannhoff, A.; Folseraas, T.; Brune, M.; Rupp, C.; Friedrich, K.; Knierim, J.; Weiss, K.H.; Sauer, P.; Flechtenmacher, C.; Schirmacher, P.; et al. A common genetic variant of fucosyltransferase 2 correlates with serum carcinoembryonic antigen levels and affects cancer screening in patients with primary sclerosing cholangitis. *United Eur. Gastroenterol. J.* **2016**, *4*, 84–91. [CrossRef] [PubMed]
25. Colston, J.M.; Francois, R.; Pisanic, N.; Peñataro Yori, P.; McCormick, B.J.J.; Olortegui, M.P.; Gazi, M.A.; Svensen, E.; Ahmed, M.M.M.; Mduma, E.; et al. Effects of child and maternal histo-blood group antigen status on symptomatic and asymptomatic enteric infections in early childhood. *J. Infect. Dis.* **2019**, *220*, 151–162. [CrossRef] [PubMed]
26. Günaydin, G.; Nordgren, J.; Sharma, S.; Hammarstrom, L. Association of elevated rotavirus-specific antibody titers with HBGA secretor status in Swedish individuals: The FUT2 gene as a putative susceptibility determinant for infection. *Virus Res.* **2016**, *211*, 64–68. [CrossRef] [PubMed]
27. Bucardo, F.; Nordgren, J.; Reyes, Y.; Gonzalez, F.; Sharma, S.; Svensson, L. The Lewis A phenotype is a restriction factor for Rotateq and Rotarix vaccine-take in Nicaraguan children. *Sci. Rep.* **2018**, *8*, 1–8. [CrossRef]
28. Kazi, A.M.; Cortese, M.M.; Yu, Y.; Lopman, B.; Morrow, A.L.; Fleming, J.A.; McNeal, M.M.; Steele, A.D.; Parashar, U.D.; Zaidi, A.K.M.; et al. Secretor and salivary ABO blood group antigen status predict rotavirus vaccine take in infants. *J. Infect. Dis.* **2017**, *215*, 786–789. [CrossRef]
29. GERMS-SA. Annual Report 2017. Available online: <http://www.nicd.ac.za/index.php/publications/germs-annual-reports/> (accessed on 16 September 2020).
30. Page, N.A.; Seheri, L.M.; Groome, M.J.; Moyes, J.; Walaza, S.; Mphahlele, J.; Kahn, K.; Kapongo, C.N.; Zar, H.J.; Tempia, S.; et al. Temporal association of rotavirus vaccination and genotype circulation in South Africa: Observations from 2002 to 2014. *Vaccine* **2018**, *36*, 7231–7237. [CrossRef]
31. De Mattos, L.C. Structural diversity and biological importance of ABO, H, Lewis and secretor histo-blood group carbohydrates. *Brazilian J. Hematol. Hemotherapy* **2016**, *38*, 331–340. [CrossRef]
32. Isa, P.; Arias, C.F.; López, S. Role of sialic acids in rotavirus infection. *Glycoconj. J.* **2006**, *23*, 27–37. [CrossRef]
33. Seheri, L.M.; Page, N.; Dewar, J.B.; Geyer, A.; Nemarude, A.L.; Bos, P.; Esona, M.; Steele, A.D. Characterization and Molecular Epidemiology of Rotavirus Strains Recovered in Northern Pretoria, South Africa during 2003–2006. *J. Infect. Dis.* **2010**, *202*, S139–S147. [CrossRef] [PubMed]
34. Mwenda, J.M.; Ntoto, K.M.; Abebe, A.; Enweronu-laryea, C.; Amina, I.; Mchomvu, J.; Kisakye, A.; Mpabalwani, E.M.; Pazvakavambwa, I.; Armah, G.E.; et al. Burden and Epidemiology of Rotavirus Diarrhea in Selected African Countries: Preliminary Results from the African Rotavirus Surveillance Network. *J. Infect. Dis.* **2018**, *202*, 5–11. [CrossRef] [PubMed]
35. Thorne, L.; Nalwoga, A.; Mentzer, A.J.; De Rougemont, A.; Hosmillo, M.; Webb, E.; Nampijja, M.; Muhwezi, A.; Carstensen, T.; Gurdasani, D.; et al. The first norovirus longitudinal seroepidemiological study from sub-Saharan Africa reveals high seroprevalence of diverse genotypes associated with host susceptibility factors. *J. Infect. Dis.* **2018**, *218*, 716–725. [CrossRef] [PubMed]

36. Nordgren, J.; Sharma, S.; Bucardo, F.; Nasir, W.; Günaydin, G.; Ouermi, D.; Nitiema, L.W.; Becker-Dreps, S.; Simpon, J.; Hammarström, L.; et al. Both lewis and secretor status mediate susceptibility to rotavirus infections in a rotavirus genotype-dependent manner. *Clin. Infect. Dis.* **2014**, *59*, 1567–1573. [CrossRef] [PubMed]
37. Auton, A.; Abecasis, G.R.; Altshuler, D.M.; Durbin, R.M.; Abecasis, G.R.; Bentley, D.R.; Chakravarti, A.; Clark, A.G.; Donnelly, P.; Eichler, E.E.; et al. A global reference for human genetic variation. *Nature* **2015**, *526*, 68–74. [CrossRef]
38. Payne, D.C.; Currier, R.L.; Staat, M.A.; Sahni, L.C.; Selvarangan, R.; Halasa, N.B.; Englund, J.A.; Weinberg, G.A.; Boom, J.A.; Szilagyi, P.G.; et al. Epidemiologic association between FUT2 secretor status and severe rotavirus gastroenteritis in children in the United States. *JAMA Pediatr.* **2015**, *169*, 1040–1045. [CrossRef]
39. Yen, C.; Healy, K.; Tate, J.E.; Parashar, U.D.; Bines, J.; Neuzil, K.; Santosham, M.; Steele, A.D. Rotavirus vaccination and intussusception—Science, surveillance, and safety: A review of evidence and recommendations for future research priorities in low and middle income countries. *Hum. Vaccines Immunother.* **2016**, *12*, 2580–2589. [CrossRef]
40. Schellack, N.; Naested, C.; Schellack, G.; Meyer, H.; Motubatse, J.; Mamejja, K.; Makola, F. Schellack\_2017\_The management of rotavirus disease in children. *SA Pharm. J.* **2017**, *84*, 46–51.
41. Lee, B.; Dickson, D.M.; DeCamp, A.C.; Ross Colgate, E.; Diehl, S.A.; Uddin, M.I.; Sharmin, S.; Islam, S.; Bhuiyan, T.R.; Alam, M.; et al. Histo-blood group antigen phenotype determines susceptibility to genotype-specific rotavirus infections and impacts measures of rotavirus vaccine efficacy. *J. Infect. Dis.* **2018**, *217*, 1399–1407. [CrossRef]
42. World Health Organization (WHO). *Manual of Rotavirus Detection and Characterization Methods*; WHO: Geneva, Switzerland, 2009.
43. Thermo Fisher Scientific. *TaqMan® SNP Genotyping Assays: User Guide*; Thermo Fisher Scientific: Carlsbad, CA, USA, 2017.



© 2020 by the authors. Licensee MDPI, Basel, Switzerland. This article is an open access article distributed under the terms and conditions of the Creative Commons Attribution (CC BY) license (<http://creativecommons.org/licenses/by/4.0/>).



Article

# Uncovering the First Atypical DS-1-like G1P[8] Rotavirus Strains That Circulated during Pre-Rotavirus Vaccine Introduction Era in South Africa

Peter N. Mwangi <sup>1</sup>, Milton T. Mogotsi <sup>1</sup>, Sebotsana P. Rasebotsa <sup>1</sup>, Mapaseka L. Seheri <sup>2</sup>, M. Jeffrey Mphahlele <sup>3</sup>, Valantine N. Ndze <sup>4</sup> , Francis E. Dennis <sup>5</sup>, Khuzwayo C. Jere <sup>6,7</sup>  and Martin M. Nyaga <sup>1,\*</sup> 

<sup>1</sup> Next Generation Sequencing Unit, Division of Virology, Faculty of Health Sciences, University of the Free State, Bloemfontein 9300, South Africa; 2017219839@ufs4life.ac.za (P.N.M.); tmogotsi16@gmail.com (M.T.M.); RasebotsaS@ufs.ac.za (S.P.R.)

<sup>2</sup> Diarrhoeal Pathogens Research Unit, Sefako Makgatho Health Sciences University, Medunsa 0204, Pretoria, South Africa; mapaseka.seheri@smu.ac.za

<sup>3</sup> South African Medical Research Council, 1 Soutpansberg Road, Pretoria 0001, South Africa; Jeffrey.Mphahlele@mrc.ac.za

<sup>4</sup> Faculty of Health Sciences, University of Buea, P.O. Box 63, Buea, Cameroon; valentinengum@yahoo.com

<sup>5</sup> Noguchi Memorial Institute for Medical Research, University of Ghana, P.O. Box LG581, Legon, Ghana; FDennis@noguchi.ug.edu.gh

<sup>6</sup> Centre for Global Vaccine Research, Institute of Infection and Global Health, University of Liverpool, Ronald Ross Building, 8 West Derby Street, Liverpool L69 7BE, UK; Khuzwayo.Jere@liverpool.ac.uk

<sup>7</sup> Malawi-Liverpool-Wellcome Trust Clinical Research Programme, College of Medicine, University of Malawi, Blantyre 312225, Malawi

\* Correspondence: NyagaMM@ufs.ac.za; Tel.: +27-51-401-9158

Received: 13 April 2020; Accepted: 18 May 2020; Published: 20 May 2020



**Abstract:** Emergence of DS-1-like G1P[8] group A rotavirus (RVA) strains during post-rotavirus vaccination period has recently been reported in several countries. This study demonstrates, for the first time, rare atypical DS-1-like G1P[8] RVA strains that circulated in 2008 during pre-vaccine era in South Africa. Rotavirus positive samples were subjected to whole-genome sequencing. Two G1P[8] strains (RVA/Human-wt/ZAF/UFS-NGS-MRC-DPRU1971/2008/G1P[8] and RVA/Human-wt/ZAF/UFS-NGS-MRC-DPRU1973/2008/G1P[8]) possessed a DS-1-like genome constellation background (I2-R2-C2-M2-A2-N2-T2-E2-H2). The outer VP4 and VP7 capsid genes of the two South African G1P[8] strains had the highest nucleotide (amino acid) nt (aa) identities of 99.6–99.9% (99.1–100%) with the VP4 and the VP7 genes of a locally circulating South African strain, RVA/Human-wt/ZAF/MRC-DPRU1039/2008/G1P[8]. All the internal backbone genes (VP1–VP3, VP6, and NSP1–NSP5) had the highest nt (aa) identities with cognate internal genes of another locally circulating South African strain, RVA/Human-wt/ZAF/MRC-DPRU2344/2008/G2P[6]. The two study strains emerged through reassortment mechanism involving locally circulating South African strains, as they were distinctly unrelated to other reported atypical G1P[8] strains. The identification of these G1P[8] double-gene reassortants during the pre-vaccination period strongly supports natural RVA evolutionary mechanisms of the RVA genome. There is a need to maintain long-term whole-genome surveillance to monitor such atypical strains.

**Keywords:** atypical strains; genome constellation; reassortment; rotavirus; whole-genome characterization

## 1. Introduction

Diarrhea persists as a leading infectious mortality cause in children under the age of five worldwide [1]. Group A rotavirus (RVA) is the primary viral etiologic agent for acute gastroenteritis in children under five years of age [2], resulting in annual mortality cases ranging from 122,322 to 215,757 with an estimated 81% reported in sub-Saharan Africa and Southeast Asia [3,4]. To combat RVA diarrhea, especially in countries with high RVA disease burden, the World Health Organization (WHO) recommends incorporation of RVA vaccines into the national immunization programs alongside other childhood vaccines [5]. The WHO has prequalified four vaccines (Rotarix<sup>®</sup>, GlaxoSmithKline, Rixenstart, Belgium; RotaTeq<sup>®</sup>, Merck & Co, USA; ROTAVAC<sup>®</sup>, Bharat Biotech, Hyderabad, India and ROTASIL<sup>®</sup>, Serum Institute of India, Pune, India) for global use [6]. Two vaccines (Rotavin-M1<sup>®</sup>, POLYVAC, Hanoi, Vietnam and Lanzhou lamb rotavirus, Lanzhou Institute of Biological Products, Lanzhou, China) have been approved for national use in Vietnam and China, respectively [7,8]. Human neonatal RVA vaccine (RV3-BB) and bovine human reassortant RVA vaccine candidates as well as neonatal and non-replicating injectable vaccines are in the pipeline [9]. South Africa was the first African country to adopt the monovalent RVA vaccine (Rotarix<sup>®</sup>) in September 2009 into its Expanded Program on Immunization (EPI) (WHO, 2009), which culminated in a 77% reduction in RVA disease during the first year that the vaccine was introduced [10,11].

Rotaviruses belong to the *Reoviridae* family. The RV genome is composed of 11 segments of double-stranded RNA (dsRNA) encapsulated in a three-layered protein capsid. Six structural proteins (VP1–VP4, VP6, and VP7) and five or sometimes six non-structural proteins (NSP1–NSP5/NSP6) that encode the RV genome [2]. The outer capsid proteins, VP7 and VP4, which act as neutralizing agents, are universally applied in the binary classification of RV strains into G and P types, respectively [2]. The contemporary classification of RVA strains is based on whole-genome composition underpinned by the nucleotide homology cutoff values that have been determined for the open reading frame (ORF) of each gene segment [12,13]. The numbers of currently described genotypes are 36 G (VP7), 51 P (VP4), 26 I (VP6), 22 R (VP1), 20 C (VP2), 20 M (VP3), 31 A (NSP1), 22 N (NSP2), 22T (NSP3), 27 E (NSP4), and 22 H (NSP5) (<http://rega.kuleuven.be/cev/viralmetagénomics/virus-classification>).

The globally predominant RVA genotypes are G1P[8], G2P[4], G3P[8], G4P[8], G9P[8], and G12P[8] [14]. However, RVA strains variability by region is well documented [15]. In Africa, RVA genotypes such as G1P[6], G8P[4], G8P[6], G8P[8], and G9P[6] are substantially prevalent but uncommon elsewhere [14–17]. Additionally, G3P[8] and G4P[8] genotypes have been on the decline in Africa and have not been detected in many African countries for almost a decade aside from an impromptu emergence of equine-like G3P[6] and G3P[8] in Botswana and Eswatini [18]. RVAs are classified further into three genogroups: Wa-like, which bears a genotype 1 constellation (I1-R1-C1-M1-A1-N1-T1-E1-H1), DS-1-like, which bears genotype 2 constellation (I2-R2-C2-M2-A2-N2-T2-E2-H2), and a relatively minor AU-1-like characterized by genotype 3 constellation (I3-R3-C3-M3-A3-N3-T3-E3-H3) [19]. Typically, G1P[8], G3P[8], G4P[8], G9P[8], and G12P[8] RVA have a Wa-like genotype constellation, whereas G2P[4], G8P[4], and G8P[6] strains usually have a DS-1-like genotype constellation [19]. G1P[8] is the world's most prevalent genotype accountable for an estimated 50% of RVA infections [20]. The vast antigenic and genetic heterogeneity of G1P[8] strains contributes to the persistent recurrence of VP4 and VP7 protein variants, and the epidemiological fitness of some of these variants might be accountable for their global prevalence [21].

The segmented RNA genome of RVA facilitates reassortment and recombination events, and the error-prone RNA-dependent RNA polymerase promotes high mutation rates [2]. These evolutionary mechanisms lead to the emergence of novel strains and distinct lineages [22]. Intergenogroup reassortment of G1P[8] gene segments has been reported in Africa, Asia, and the Americas [23–27]. These atypical G1P[8] strains were first reported in Okayama Prefecture, Japan during 2012–2013 post-RVA vaccine surveillance of acute gastroenteritis and then in other prefectures, including Aichi, Akita, Kyoto, and Osaka [25–27]. Subsequent incidences were then reported during 2013 post-RVA vaccine surveillance in Phetchabun and Sukhothai provinces in Thailand [28,29] and in 2012–2013

during the pre-RVA vaccine period in Hanoi, Vietnam [30]. Although unpublished, sequence data of G1P[8] DS-1-like sequence strains isolated during pre-vaccine period between August–November 2012 in Palawan, Southwestern region of Philippines have been deposited in the GenBank database. Recently, for the first time in the Americas, G1P[8] DS-1-like strains were reported in 2013 during post-RVA vaccination period from the states of Sao Paulo and Goias in Brazil [23]. In Africa, Jere and colleagues reported the emergence of atypical G1P[8] strains during the post-RVA vaccination period in Blantyre, Malawi [24]. It is not definitively resolved whether these atypical G1P[8] strains are widespread. In addition, there is a paucity of information on whole-genome sequences of G1P[8] strains post-vaccine era with only a few countries performing full-genome characterization of the strain [15,21,31–35]. The African Enteric Viruses Genome Initiative (AEVGI) is conducting whole-genome characterization of country-specific pre- and post-vaccine RVA strains in Africa and has identified, for the first time in South Africa, atypical G1P[8] strains that were circulating before vaccine introduction. This study aimed to determine the genetic relationship and the evolutionary origin of these pre-vaccine atypical G1P[8] RVA strains.

## 2. Results

### 2.1. Nucleotide Sequencing

Illumina<sup>®</sup> MiSeq sequencing yielded  $14.7 \times 10^5$  reads (379 bp fragment size) and  $11.3 \times 10^5$  reads (364 bp fragment size) for strains RVA/Human-wt/ZAF/UFS-NGS-MRC-DPRU1971/2008/G1P[8] and RVA/Human-wt/ZAF/UFS-NGS-MRC-DPRU1973/G1P[8], respectively. All the sequences had a phred score of  $Q \geq 30$  (99.9% base calling accuracy).

### 2.2. Full-Genome Constellation Analysis

Whole-gene sequences of the 11 genes of strains, RVA/Human-wt/ZAF/UFS-NGS-MRC-DPRU1971/G1P[8] and RVA/Human-wt/ZAF/UFS-NGS-MRC-DPRU1973/G1P[8], were determined, and their genotype constellations were revealed as G1-P[8]-I2-R2-C2-M2-A2-N2-T2-E2-H2 (Table 1). The sizes of full-length segments 1 to 11 and their respective open reading frames (ORFs) for the two study strains were determined (Table 1). The ORF sequences for all the 11 genes of these two South African atypical G1P[8] strains were deposited in GenBank under accession numbers MT163245–MT163266.

**Table 1.** Whole genotype constellations of the South African DS-1-like G1P[8] rotavirus strains.

Gene Segment	VP7	VP4	VP6	VP1	VP2	VP3	NSP1	NSP2	NSP3	NSP4	NSP5
Base pair size for full length sequences	1062	2359	1355	3302	2684	2591	1566	1059	1066	751	810
Base pair size for the complete study strain ORF	978	2325	1191	3264	2637	2505	1458	951	939	525	600
RVA/Human-wt/ZAF/UFS-NGS-MRC-DPRU1971/2008/G1P[8]	G1	P[8]	I2	R2	C2	M2	A2	N2	T2	E2	H2
RVA/Human-wt/ZAF/UFS-NGS-MRC-DPRU1973/2008/G1P[8]	G1	P[8]	I2	R2	C2	M2	A2	N2	T2	E2	H2

Color codes indicate genogroup attribution. Green color represents the genotype associated with the Wa-like genogroup, while red color represents the genotype belonging to the DS-1-like genogroup. The nomenclature of the RV strains indicates RV group, species where the strain was isolated, name of the country where the strain was originally isolated, common name, year of isolation, and genotypes for genome segments four and nine as proposed by the Rotavirus Classification Working Group (RCWG) [12]. ORF = open reading frame.

### 2.3. Sequence and Phylogenetic Analysis

#### 2.3.1. Phylogenetic Analysis of VP7

Phylogenetically, the diversity of the VP7 G1 genes has been established through seven known lineages (I–VII) [36] (Figure 1). The VP7 genes of the atypical G1P[8] study strains, RVA/Human-wt/ZAF/UFS-NGS-MRC-DPRU1971/2008/G1P[8] and RVA/Human-wt/ZAF/UFS-NGS-MRC-DPRU1973/2008/G1P[8], clustered in genetic lineage I, which consisted of a global collection of G1

strains that circulated from 2002 to 2015 (Figure 1). In this lineage I, the two G1 study strains clustered closely together and shared almost absolute gene identities amongst themselves—nt (aa) 99.9% (100%) (Figure 1; Supplementary data 1 (S1)). Analysis of the G1 study strains with locally circulating South African strains retrieved from the GenBank identified the highest sequence identities of 99.8–99.9% (100%) with strain RVA/Human-wt/ZAF/MRC-DPRU1039/2008/G1P8 and clustered closely with this strain that was isolated the same year, 2008, as the two study strains (Figure 1). However, within the same lineage, the VP7 genes of the two G1 study strains from South Africa clustered distinctly away from the atypical G1P[8] strains reported in Brazil, Japan, Malawi, Philippines, Thailand, and Vietnam [22–26] and displayed overall nt (aa) similarities that ranged from 87.0–98.5% (87.1–98.8%) (Table S1 in Supplementary data 2 (S2)). Specifically, the nt (aa) similarities ranged from 96.9–97.0% (98.5%), 96.9–97.1% (98.5–98.8%), 87.0–98%5 (87.1–98.8), 96.5–96.8% (98.2–98.5%), 96.9–97.0% (98.8%), and 97.0–97.1% (96.9%) to the post-vaccination G1 atypical strains reported in Brazil, Japan, Philippines, Malawi, Thailand, and Vietnam, respectively (S1).

When the two South African G1 study strains were compared to the typical G1 strains selected globally, they displayed the highest nt (aa) similarities of 99.7–99.8% (100%) with a European strain, RVA/Human-wt/BEL/BEL00017/2006/G1P[8] (S1). The nt(aa) similarities comparison to representative strains from Africa (Eastern Africa, Southern Africa, and West Africa), America, Asia, Europe, and Oceania ranged from 93.9–97.6% (94.2–98.2%), 97.1–99.5% (98.2–100%), 97.1–97.9% (96.9–98.2%), 93.15–97.6% (94.8%–98.5%), 96.4–99.6% (97.8–99.7%), 99.7–99.8% (100%), and 93.7–98.4% (94.5–98.8%), respectively (Table S2 in S2). In addition, comparison of the VP7 genes of the two study strains to cognate gene sequence of the Rotarix<sup>®</sup> and RotaTeq<sup>®</sup> RV vaccine strains displayed nt (aa) identities that ranged from 94.2–94.3% (95.7%) and 91.0–91.1% (93.2%), respectively (S1).

#### Analysis of the VP7 Neutralization Epitopes

The VP7 genes contain three established neutralization epitopes: 7-1a, 7-1b, and 7-2. Twenty-nine amino acids (14 residues in 7-1a, 6 residues in 7-1b, and 9 residues in 7-2) define the three VP7 antigenic epitopes [37]. The VP7 neutralization epitope sites of the two South African study strains were aligned and mapped against cognate neutralization sites of the two RV vaccines, Rotarix<sup>®</sup>, and RotaTeq<sup>®</sup>. Four amino acid differences (N94S, S123N, K291R, and M217T) in the VP7 genes of the two South African study strains were identified relative to Rotarix<sup>®</sup> VP7 neutralization sites, while five amino acid differences (D97E, S123N, K291R, S147N, and M217T) were identified with comparison to RotaTeq<sup>®</sup> G1 antigenic sites (Figure 2). Antigenically, similar amino acid residues in the VP7 epitopes of the study strains were observed in the corresponding VP7 epitopes of the multiple atypical G1P[8] strains (Figure 2). The VP7 epitopes of the two South African G1 strains were contrasted with those of globally selected lineage I G1 strains. The analysis showed ten amino acid differences (T91N, S94N, D100N, D100E, N123S, R291K, T242A, N147D, L148F, and T217M) (Figure 2).

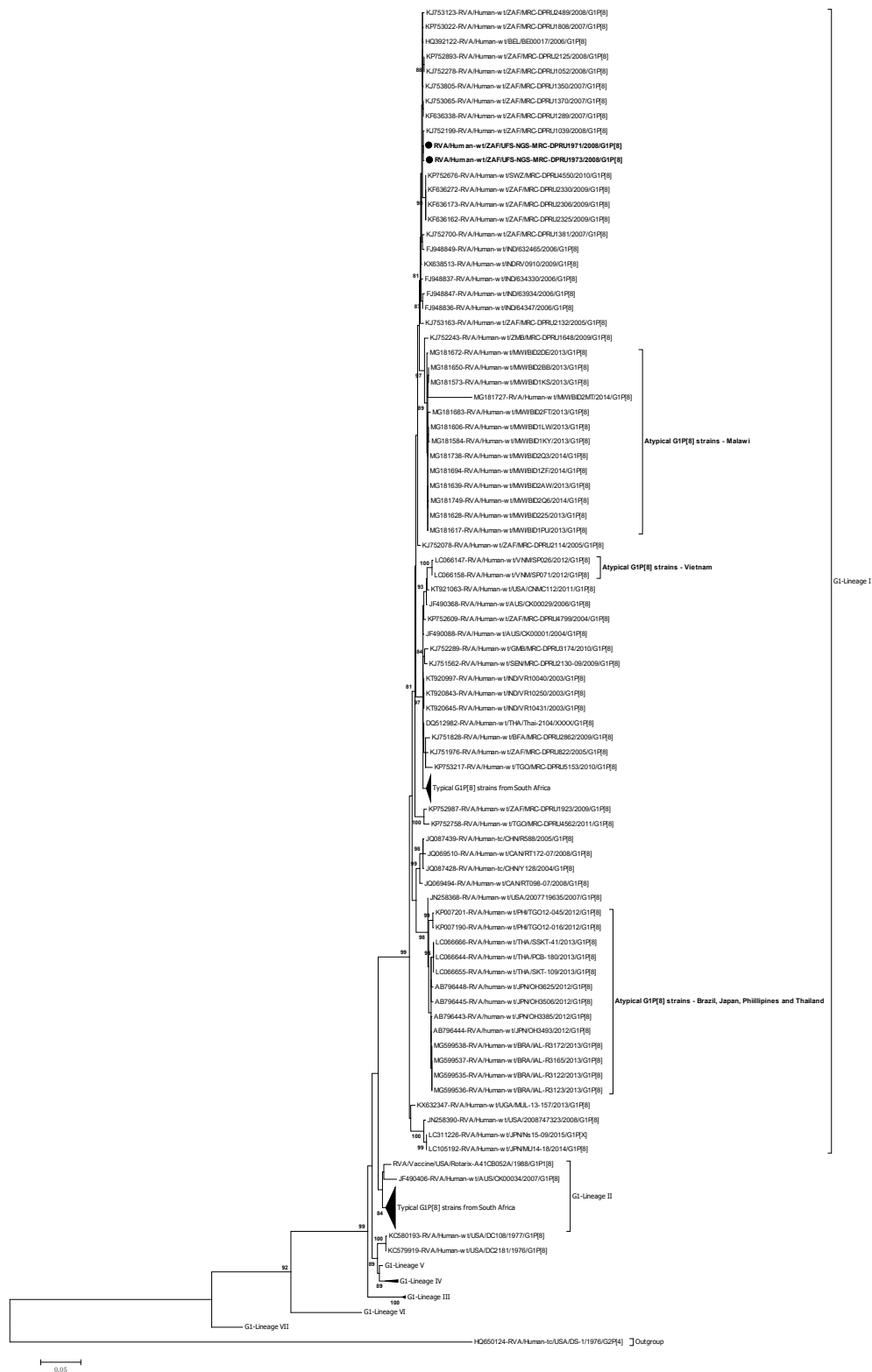


**Figure 1.** VP7 phylogenetic tree based on the full-length nucleotide sequences. Strains group A rotavirus (RVA)/Human-wt/ZAF/UFS-NGS-MRC-DPRU1971/2008/G1P[8] and RVA/Human-wt/ZAF/UFS-NGS-MRC-DPRU1973/2008/G1P[8] are identified by the black filled circular dots (●). Unusual G1P[8] strains from Malawi, Japan, Thailand, Vietnam, Brazil, and Philippine are indicated. Bootstrap values  $\geq 70\%$  are shown adjacent to each branch node. Each scale bar indicates the number of nucleotide substitutions per site.

	Strain	Lineage	Neutralization Epitopes																													
			7-1a												7-1b						7-2											
			87	91	94	96	97	98	99	100	104	123	125	129	130	291	201	211	212	213	238	242	143	145	146	147	148	190	217	221	222	264
Vaccine	RVA/Vaccine/USA/Rotarix-A41CB052A/1988/G1P1A[8]	II	T	T	N	G	E	W	K	D	Q	S	V	V	D	K	Q	N	V	D	N	T	K	D	Q	N	L	S	M	N	G	
strains	GU565057-RVA/Vaccine/USA/RotaTeq-WI79-9/1992/G1P7[5]	III	T	T	N	G	D	W	K	D	Q	S	V	V	D	K	Q	N	V	D	N	T	K	D	Q	S	L	S	M	N	G	
South Africa	RVA/Human-wt/ZAF/UFS-NGS-MRC-DPRU1971/2008/G1P[8]	I	T	T	S	G	E	W	K	D	Q	N	V	V	D	R	Q	N	V	D	N	T	K	D	Q	N	L	S	T	N	G	
	RVA/Human-wt/ZAF/UFS-NGS-MRC-DPRU1973/2008/G1P[8]	I	T	T	S	G	E	W	K	D	Q	N	V	V	D	R	Q	N	V	D	N	T	K	D	Q	N	L	S	T	N	G	
Vietnam	LC066147-RVA/Human-wt/VNM/SP026/2012/G1P[8]	I	T	T	N	G	E	W	K	D	Q	N	V	V	D	K	Q	N	V	D	N	T	K	D	Q	N	F	S	T	N	G	
	LC066158-RVA/Human-wt/VNM/SP071/2012/G1P[8]	I	T	T	N	G	E	W	K	D	Q	N	V	V	D	K	Q	N	V	D	N	T	K	D	Q	N	F	S	T	N	G	
	MG181738-RVA/Human-wt/MWI/BID2Q3/2014/G1P[8]	I	T	T	N	G	E	W	K	D	Q	N	V	V	D	R	Q	N	V	D	N	T	K	D	Q	N	L	S	T	S	G	
	MG181694-RVA/Human-wt/MWI/BID1Zf/2014/G1P[8]	I	T	T	N	G	E	W	K	D	Q	N	V	V	D	R	Q	N	V	D	N	T	K	D	Q	N	L	S	T	S	G	
	MG181617-RVA/Human-wt/MWI/BID1PU/2013/G1P[8]	I	T	T	N	G	E	W	K	D	Q	N	V	V	D	R	Q	N	V	D	N	T	K	D	Q	N	L	S	T	S	G	
	MG181639-RVA/Human-wt/MWI/BID2AW/2013/G1P[8]	I	T	T	N	G	E	W	K	D	Q	N	V	V	D	R	Q	N	V	D	N	T	K	D	Q	N	L	S	T	S	G	
	MG181628-RVA/Human-wt/MWI/BID225/2013/G1P[8]	I	T	T	N	G	E	W	K	D	Q	N	V	V	D	R	Q	N	V	D	N	T	K	D	Q	N	L	S	T	S	G	
	MG181749-RVA/Human-wt/MWI/BID2O6/2014/G1P[8]	I	T	T	N	G	E	W	K	D	Q	N	V	V	D	R	Q	N	V	D	N	T	K	D	Q	N	L	S	T	S	G	
	MG181650-RVA/Human-wt/MWI/BID2BB/2013/G1P[8]	I	T	T	N	G	E	W	K	D	Q	N	V	V	D	R	Q	N	V	D	N	T	K	D	Q	N	L	S	T	S	G	
	MG181573-RVA/Human-wt/MWI/BID1KS/2013/G1P[8]	I	T	T	N	G	E	W	K	D	Q	N	V	V	D	R	Q	N	V	D	N	T	K	D	Q	N	L	S	T	S	G	
	MG181606-RVA/Human-wt/MWI/BID1LW/2013/G1P[8]	I	T	T	N	G	E	W	K	D	Q	N	V	V	D	R	Q	N	V	D	N	T	K	D	Q	N	L	S	T	S	G	
	MG181594-RVA/Human-wt/MWI/BID1KY/2013/G1P[8]	I	T	T	N	G	E	W	K	D	Q	N	V	V	D	R	Q	N	V	D	N	T	K	D	Q	N	L	S	T	S	G	
	MG181672-RVA/Human-wt/MWI/BID2DE/2013/G1P[8]	I	T	T	N	G	E	W	K	D	Q	N	V	V	D	R	Q	N	V	D	N	T	K	D	Q	N	L	S	T	S	G	
	MG181683-RVA/Human-wt/MWI/BID2FT/2013/G1P[8]	I	T	T	N	G	E	W	K	D	Q	N	V	V	D	R	Q	N	V	D	N	T	K	D	Q	N	L	S	T	S	G	
	MG181727-RVA/Human-wt/MWI/BID2MT/2014/G1P[8]	I	T	T	S	N	E	W	E	N	Q	D	T	M	N	R	Q	N	V	D	N	T	K	D	Q	N	L	S	T	S	G	
	MG181661-RVA/Human-wt/MWI/BID2S/2013/G1P[8]	I	T	T	S	N	E	W	E	N	Q	D	T	M	N	R	Q	N	V	D	N	T	R	D	N	T	S	T	S	G		
	AB796443-RVA/human-wt/JPN/OH3385/2012/G1P[8]	I	T	T	S	G	E	W	K	D	Q	N	V	V	D	R	Q	N	V	D	N	T	K	D	Q	N	L	S	T	N	G	
	AB796444-RVA/human-wt/JPN/OH3493/2012/G1P[8]	I	T	T	S	G	E	W	K	D	Q	N	V	V	D	R	Q	N	V	D	N	T	K	D	Q	N	L	S	T	N	G	
	AB796445-RVA/human-wt/JPN/OH3506/2012/G1P[8]	I	T	T	S	G	E	W	K	D	Q	N	V	V	D	R	Q	N	V	D	N	T	K	D	Q	N	L	S	T	N	G	
	AB796448-RVA/human-wt/JPN/OH3625/2012/G1P[8]	I	T	T	S	G	E	W	K	D	Q	N	V	V	D	R	Q	N	V	D	N	T	K	D	Q	N	L	S	T	N	G	
Thailand	LC066655-RVA/Human-wt/THA/SKT-109/2013/G1P[8]	I	T	T	S	G	E	W	K	D	Q	N	V	V	D	R	Q	N	V	D	N	T	K	D	Q	N	L	S	T	N	G	
	LC066666-RVA/Human-wt/THA/SKT-41/2013/G1P[8]	I	T	T	S	G	E	W	K	D	Q	N	V	V	D	R	Q	N	V	D	N	T	K	D	Q	N	L	S	T	N	G	
	LC066644-RVA/Human-wt/THA/PCB-180/2013/G1P[8]	I	T	T	S	G	E	W	K	D	Q	N	V	V	D	R	Q	N	V	D	N	T	K	D	Q	N	L	S	T	N	G	
Philippines	KP007190-RVA/Human-wt/PHI/TGO12-016/2012/G1P[8]	I	T	T	S	G	E	W	K	D	Q	N	V	V	D	R	Q	N	V	D	N	T	K	D	Q	N	L	S	T	N	G	
	KP007201-RVA/Human-wt/PHI/TGO12-045/2012/G1P[8]	I	T	T	S	G	E	W	K	D	Q	N	V	V	D	R	Q	N	V	D	N	T	K	D	Q	N	L	S	T	N	G	
Brazil	MC599538-RVA/Human-wt/BRA/IAL-R3172/2013/G1P[8]	I	T	T	S	G	E	W	K	D	Q	N	V	V	D	R	Q	N	V	D	N	T	K	D	Q	N	L	S	T	N	G	
	MC599537-RVA/Human-wt/BRA/IAL-R3165/2013/G1P[8]	I	T	T	S	G	E	W	K	D	Q	N	V	V	D	R	Q	N	V	D	N	T	K	D	Q	N	L	S	T	N	G	
	MC599536-RVA/Human-wt/BRA/IAL-R3123/2013/G1P[8]	I	T	T	S	G	E	W	K	D	Q	N	V	V	D	R	Q	N	V	D	N	T	K	D	Q	N	L	S	T	N	G	
	MC599535-RVA/Human-wt/BRA/IAL-R3122/2013/G1P[8]	I	T	T	S	G	E	W	K	D	Q	N	V	V	D	R	Q	N	V	D	N	T	K	D	Q	N	L	S	T	N	G	
	KT921063-RVA/Human-wt/USA/CNMC112/2011/G1P[8]	I	T	T	N	G	E	W	K	D	Q	N	V	V	D	R	Q	N	V	D	N	T	K	D	Q	N	F	S	T	N	G	
	JF490368-RVA/Human-wt/Victoria/CK00029/2006/G1P[8]	I	T	T	N	G	E	W	K	D	Q	N	V	V	D	R	Q	N	V	D	N	T	K	D	Q	N	F	S	T	N	G	
	KT920997-RVA/Human-wt/IND/VR10040/2003/G1P[8]	I	T	T	S	G	E	W	K	D	Q	N	V	V	D	R	Q	N	V	D	N	T	K	D	Q	N	L	S	T	N	G	
	DO512982-RVA/Human-wt/THA/Thai-2104/XXXX/G1P[8]	I	T	T	S	G	E	W	K	D	Q	N	V	V	D	R	Q	N	V	D	N	T	K	D	Q	N	L	S	T	N	G	
	KJ752609-RVA/Human-wt/ZAF/MRC-DPRU4799/2004/G1P[8]	I	T	T	S	G	E	W	K	D	Q	N	V	V	D	R	Q	N	V	D	N	T	K	D	Q	N	F	S	T	N	G	
	KJ752288-RVA/Human-wt/SEN/MRC-DPRU2130-09/2009/G1P[8]	I	T	T	S	G	E	W	K	D	Q	N	V	V	D	R	Q	N	V	D	N	T	K	D	Q	N	D	L	S	T	N	G
	KF636217-RVA/Human-wt/ZAF/MRC-DPRU1544/2010/G1P[8]	I	T	T	S	G	E	W	K	D	Q	N	V	V	D	R	Q	N	V	D	N	T	A	K	D	Q	N	L	S	T	N	G
	KJ751828-RVA/Human-wt/BFA/MRC-DPRU2862/2009/G1P[8]	I	T	T	S	G	E	W	K	D	Q	N	V	V	D	K	Q	N	V	D	N	T	K	D	Q	N	L	S	T	N	G	
	KJ751976-RVA/Human-wt/ZAF/MRC-DPRU822/2005/G1P[8]	I	T	T	S	G	E	W	K	D	Q	N	V	V	D	K	Q	N	V	D	N	T	K	D	Q	N	L	S	T	N	G	
	KP752998-RVA/Human-wt/ZAF/MRC-DPRU832/2006/G1P[8]	I	T	T	S	G	E	W	K	D	Q	N	V	V	D	R	Q	N	V	D	N	T	K	D	Q	N	L	S	T	N	G	
	KJ751905-RVA/Human-wt/ZAF/MRC-DPRU1960/2008/G1P[8]	I	T	T	S	G	E	W	K	D	Q	N	V	V	D	R	Q	N	V	D	N	T	K	D	Q	N	L	S	T	N	G	
	KJ753220-RVA/Human-wt/ZAF/MRC-DPRU1327/2007/G1P[8]	I	T	T	S	G	E	W	K	D	Q	N	V	V	D	R	Q	N	V	D	N	T	K	D	Q	N	L	S	T	N	G	
	KJ752020-RVA/Human-wt/ZAF/MRC-DPRU6954/2011/G1P[8]	I	T	T	S	G	E	W	K	D	Q	N	V	V	D	R	Q	N	V	D	N	T	K	D	Q	N	L	S	T	N	G	
	KJ752333-RVA/Human-wt/ZAF/MRC-DPRU2198/2003/G1P[8]	I	T	T	N	G	E	W	K	D	Q	S	V	V	D	K	Q	N	V	D	N	T	K	D	Q	N	L	S	M	N	G	
	KJ753679-RVA/Human-wt/ZAF/MRC-DPRU1277/2004/G1P[8]	I	T	T	N	G	E	W	K	D	Q	S	V	V	D	K	Q	N	V	D	N	T	K	D	Q	N	L	S	M	N	G	
	KJ751795-RVA/Human-wt/ZAF/MRC-DPRU6113/2002/G1P[8]	I	T	T	N	G	E	W	K	D	Q	S	V	V	D	K	Q	N	V	D	N	T	K	D	Q	N	L	S	M	N	G	
	KP752676-RVA/Human-wt/SWZ/MRC-DPRU4550/2010/G1P[8]	I	T	T	S	G	E	W	K	D	Q	N	V	V	D	R	Q	N	V	D	N	T	K	D	Q	N	L	S	T	N	G	
	KJ752243-RVA/Human-wt/ZMB/MRC-DPRU1648/2009/G1P[8]	I	T	T	N	G	E	W	K	D	Q	N	V	V	D	R	Q	N	V	D	N	T	K	D	Q	N	L	S	T	N	G	
	KP753217-RVA/Human-wt/TGO/MRC-DPRU5153/2010/G1P[8]	I	T	T	S	G	E	W	K	D	Q	S	V	V	D	K	Q	N	V	D	N	T	K	D	Q	N	L	S	T	N	G	
	KX632347-RVA/Human-wt/UGA/MUL-13-157/2013/G1P[8]	I	T	T	S	G	E	W	K	D	Q	N	V	V	D	R	Q	N	V	D	N	T	K	D	Q	N	L	S	T	N	G	
	KJ752031-RVA/Human-wt/ETH/MRC-DPRU1843/2009/G1P[8]	I	T	T	N	G	E	W	K	D	N	Q	S	V	V	D	K	Q	N	V	D	N	T	K	D	Q	N	L	S	M	N	G
	JQ087439-RVA/Human-tc/CHN/R588/2005/G1P[8]	I	T	T	S	G	E	W	K	D	Q	N	V	V	D	R	Q	N	V	D	N	T	K	D	Q	N	L	S	T	N	G	
	JQ069494-RVA/Human-wt/CAN/RT098-07/2008/G1P[8]	I	T	T	S	G	E	W	K	D	Q	N	V	V	D	R	Q	N	V	D	N	T	K	D	Q	N	L	S	T	N	G	
	HQ392122-RVA/Human-wt/BEL/BE00017/2006/G1P[8]	I	T	T	S	G	E	W	K	D	Q	N	V	V	D	R	Q	N	V	D	N	T	K	D	Q	N	L	S	T	N	G	
	FJ498849-RVA/Human-wt/IND/632465/2006/G1P[8]	I	T	T	S	G	E	W	K	D	Q	N	V	V	D	R	Q	N	V	D	N	T	K	D	Q	N	L					

of the two South African strains with sequences of South African strains retrieved from the GenBank demonstrated the highest nt (aa) sequence identities of 99.6% (99.1–99.4%) with strain RVA/Human-wt/ZAF/MRC-DPRU1039/2008/G1P[8] (Figure 3). However, within the same lineage, the VP4 genes of the two atypical strains from South Africa segregated distinctly away from the atypical strains that have been detected in Brazil, Japan, Malawi, Philippines, Thailand, and Vietnam. They exhibited overall nt (aa) similarities that ranged from 95.2–98.0% (95.1–98.6%) (Table S1 in S2). Specifically, the nt (aa) similarities ranged from 97.6–97.8% (98.1–98.6), 98.2–98.5% (98.5%), 95.2–98.0% (95.1–98.2%), 97.7–97.8% (98.1–98.5%), 97.8–98.0% (97.7–98.2%), and 98.1–98.2% (97.9–98.3%) to the post-vaccination atypical strains reported in Brazil, Japan, Malawi, Philippines, Thailand, and Vietnam, respectively (S1). A comparison of the South African P[8] study strains characterized in this study with a global collection of P[8] strains showed their closeness, and the study strains shared the highest nt (aa) similarity of 99.5% (99.1–99.4%) to a Belgian strain, RVA/Human-wt/BEL/BEL00017/2006/G1P[8] (S1). Overall, the nt (aa) similarities in comparison to representative strains from Africa (Eastern Africa, Southern Africa, Western Africa), America, Asia, Europe, and Oceania ranged from 97.4–97.8% (97.8–98.2%), 86.7–99.1% (91.1–99.2%), 86.7–99.1% (91.1–99.2%), 86.6–99.4% (91.0–99.2%), 86.5–98.9% (91.1–98.7%), 86.8–99.5% (91.2–99.5%), and 86.5–98.5% (91.0%–98.6%), respectively. In addition, the comparison of the atypical VP4 genes to the P[8] genes of the Rotarix<sup>®</sup> and RotaTeq<sup>®</sup> vaccine strains displayed nt (aa) identities that ranged from 90.3–90.4% (93.9–94.2%) and 92.3% (95.2%), respectively (S1).

#### Analysis of the VP4 Neutralization Epitopes

The VP4 spike protein is cleaved by trypsin into two distinct structural proteins, VP8\* and VP5\* [2]. Analysis of the two South African study strains' VP4 sequences showed a conserved trypsin cleavage site (arginine) at positions 230, 240, and 581 [39]. Furthermore, the neutralization epitopes in the VP8\* and the VP5\* regions were analyzed. The VP8\* region has four (8-1 to 8-4) neutralization epitopes, while VP5\* has five (5-1 to 5-5) (Figure 4) [40]. Comparison of the two South African P[8] strains relative to the Rotarix<sup>®</sup> and the RotaTeq<sup>®</sup> P[8] sequences displayed 32 and 35 identical amino acid residues, respectively, spanning the VP4 antigenic epitopes (Figure 4). Amino acid differences between the two P[8] study strains and the P[8] component of vaccine strains were only identified in 8-1, 8-2, and 8-3 VP8\* epitopes. Five amino acid differences (E150D, N195G, S125N, S131R, and N135D) were identified in the study strains in relation to Rotarix<sup>®</sup> P[8] strain, while two amino acid differences (E150D and D195G) were identified relative to P[8] strain of RotaTeq<sup>®</sup> (Figure 4). Analysis with VP4 epitopes of other atypical G1P[8] strains identified similar amino acid residues with the exception of position 113 in the 8-3 epitope, whereby asparagine was observed in the study strains while other atypical strains had either an aspartate or serine at this position (Figure 4). Further analysis of the study strain's VP4 neutralization epitopes with corresponding VP4 neutralization epitopes of globally selected P[8]-lineage-III strains identified two amino acid differences (S146G and N113D) (Figure 4).

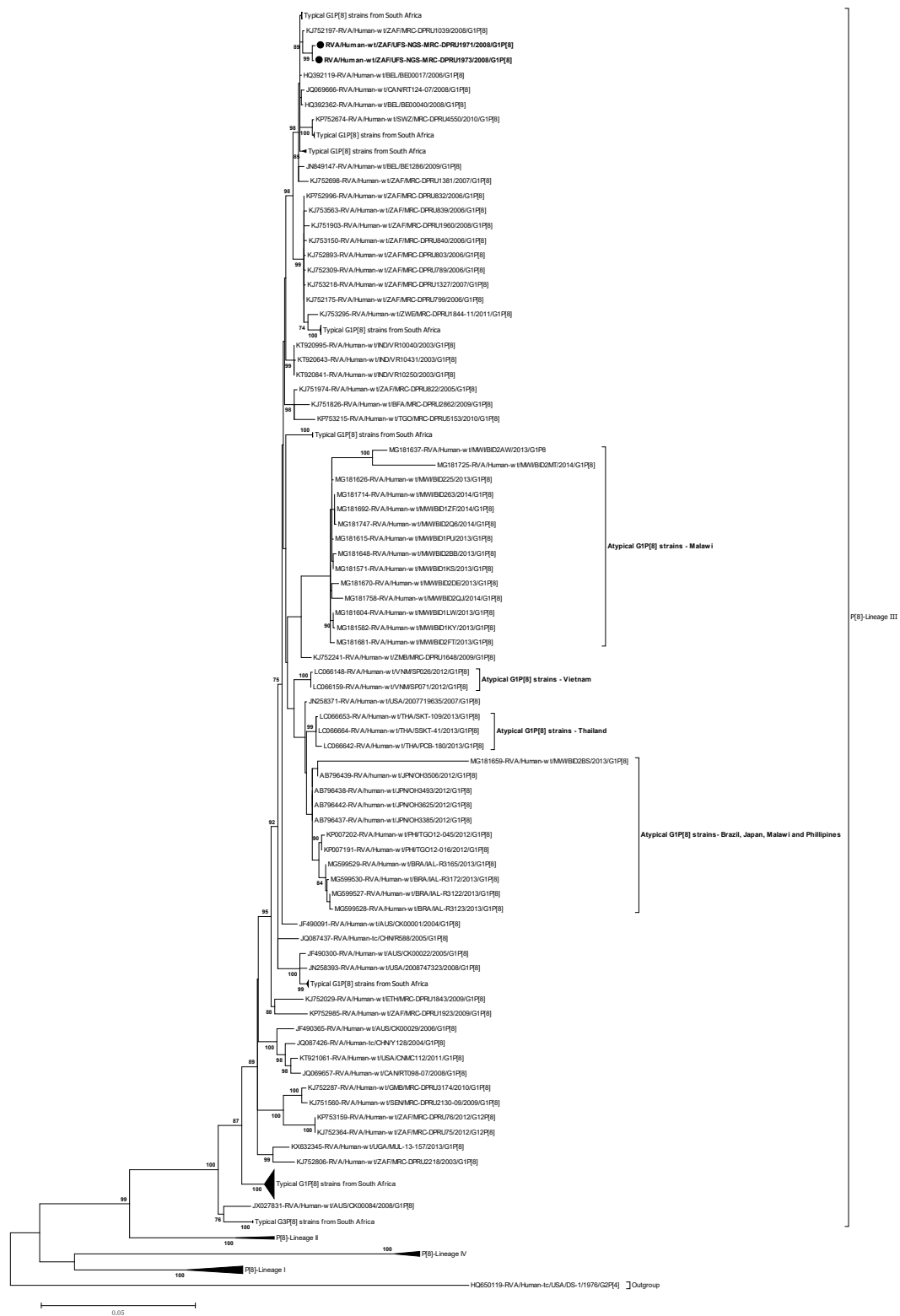


**Figure 3.** VP4 phylogenetic tree based on the full-length nucleotide sequences. Strains RVA/Human-wt/ZAF/UFS-NGS-MRC-DPRU1971/2008/G1P[8] and RVA/Human-wt/ZAF/UFS-NGS-MRC-DPRU1973/2008/G1P[8] are identified by the black filled circular dots (●). Unusual G1P[8] strains from Malawi, Japan, Thailand, Vietnam, Brazil, and Philippines are indicated. Bootstrap values  $\geq 70\%$  are shown adjacent to each branch node. Each scale bar indicates the number of nucleotide substitutions per site.

		Neutralization Epitopes																																							
		8-1							8-2							8-3							8-4							5-1				5-2		5-3		5-4		5-5	
		100	146	148	150	188	190	192	193	194	195	196	180	183	113	114	115	116	125	131	132	133	135	87	88	89	384	386	388	393	394	398	440	441	434	459	429	306			
Vaccine	RVA/Vaccine/USA/Rotarix/11/05/02/1980/G1P[8]	P[8]-H	D	S	Q	E	S	T	N	L	N	G	I	T	A	N	P	V	D	S	S	N	D	N	N	T	N	Y	F	I	W	P	G	R	T	P	E	L	R		
	GL/US65044-RVA/Vaccine/USA/RotaTeq/w/179-41/1992/G6P[8]	P[8]-H	D	S	Q	E	S	T	N	L	N	D	I	T	A	N	P	V	D	N	R	N	D	D	N	N	T	N	Y	F	L	W	P	G	R	T	P	E	L	R	
South Africa	RVA/Human-wt/ZAF/US-NGS-MRC-DPRU1971/2008/G1P[8]	P[8]-H	D	S	Q	D	S	T	N	L	N	G	I	T	A	N	P	V	D	N	R	N	D	D	N	N	T	N	Y	F	I	W	P	G	R	T	P	E	L	R	
	RVA/Human-wt/ZAF/US-NGS-MRC-DPRU1973/2008/G1P[8]	P[8]-H	D	S	Q	D	S	T	N	L	N	G	I	T	A	N	P	V	D	N	R	N	D	D	N	N	T	N	Y	F	I	W	P	G	R	T	P	E	L	R	
Vietnam	LC066148-RVA/Human-wt/VNM/SPO26/2012/G1P[8]	P[8]-H	D	S	Q	D	S	T	N	L	N	G	I	T	A	D	P	V	D	N	R	N	D	D	N	N	T	N	Y	F	I	W	P	G	R	T	P	E	L	R	
	LC066159-RVA/Human-wt/VNM/SPO71/2012/G1P[8]	P[8]-H	D	S	Q	D	S	T	N	L	N	G	I	T	A	D	P	V	D	N	R	N	D	D	N	N	T	N	Y	F	I	W	P	G	R	T	P	E	L	R	
	MG181948-RVA/Human-wt/MWI/BID258/2013/G1P[8]	P[8]-H	D	S	Q	D	S	T	N	L	N	S	I	T	A	D	P	V	D	N	R	N	D	D	N	N	T	N	Y	F	I	W	P	G	R	T	P	E	L	R	
	MG181815-RVA/Human-wt/MWI/BID1P/2013/G1P[8]	P[8]-H	D	S	Q	D	S	T	N	L	N	S	I	T	A	D	P	V	D	N	R	N	D	D	N	N	T	N	Y	F	I	W	P	G	R	T	P	E	L	R	
	MG181681-RVA/Human-wt/MWI/BID2F/2013/G1P[8]	P[8]-H	D	S	Q	D	S	T	N	L	N	S	I	T	A	D	P	V	D	N	R	N	D	D	N	N	T	N	Y	F	I	W	P	G	R	T	P	E	L	R	
	MG181626-RVA/Human-wt/MWI/BID225/2013/G1P[8]	P[8]-H	D	S	Q	D	S	T	N	L	N	S	I	T	A	D	P	V	D	N	R	N	D	D	N	N	T	N	Y	F	I	W	P	G	R	T	P	E	L	R	
	MG181714-RVA/Human-wt/MWI/BID263/2014/G1P[8]	P[8]-H	D	S	Q	D	S	T	N	L	N	S	I	T	A	D	P	V	D	N	R	N	D	D	N	N	T	N	Y	F	I	W	P	G	R	T	P	E	L	R	
	MG181692-RVA/Human-wt/MWI/BID12F/2014/G1P[8]	P[8]-H	D	S	Q	D	S	T	N	L	N	S	I	T	A	D	P	V	D	N	R	N	D	D	N	N	T	N	Y	F	I	W	P	G	R	T	P	E	L	R	
	MG181604-RVA/Human-wt/MWI/BID1LW/2013/G1P[8]	P[8]-H	D	S	Q	D	S	T	N	L	N	S	I	T	A	D	P	V	D	N	R	N	D	D	N	N	T	N	Y	F	I	W	P	G	R	T	P	E	L	R	
	MG181582-RVA/Human-wt/MWI/BID1K/2013/G1P[8]	P[8]-H	D	S	Q	D	S	T	N	L	N	S	I	T	A	D	P	V	D	N	R	N	D	D	N	N	T	N	Y	F	I	W	P	G	R	T	P	E	L	R	
Malawi	MG181571-RVA/Human-wt/MWI/BID1K5/2013/G1P[8]	P[8]-H	D	S	Q	D	S	T	N	L	N	S	I	T	A	D	P	V	D	N	R	N	D	D	N	N	T	N	Y	F	I	W	P	G	R	T	P	E	L	R	
	MG181747-RVA/Human-wt/MWI/BID2Q6/2014/G1P8	P[8]-H	D	S	Q	D	S	T	N	L	N	S	I	T	A	D	P	V	D	N	R	N	D	D	N	N	T	N	Y	F	I	W	P	G	R	T	P	E	L	R	
	MG181670-RVA/Human-wt/MWI/BID2D6/2013/G1P8	P[8]-H	D	S	Q	D	S	T	N	L	N	S	I	T	A	D	P	V	D	N	R	N	D	D	N	N	T	N	Y	F	I	W	P	G	R	T	P	E	L	R	
	MG181758-RVA/Human-wt/MWI/BID2Q/2014/G1P8	P[8]-H	D	S	Q	D	S	T	N	L	N	S	I	T	A	D	P	V	D	N	R	N	D	D	N	N	T	N	Y	F	I	W	P	G	R	T	P	E	L	R	
	MG181725-RVA/Human-wt/MWI/BID2M7/2014/G1P8	P[8]-H	D	S	Q	D	S	T	N	L	N	S	I	T	A	D	P	V	D	N	R	N	D	D	N	N	T	N	Y	F	I	W	P	G	R	T	P	E	L	R	
	MG181637-RVA/Human-wt/MWI/BID2AW/2013/G1P8	P[8]-H	D	S	Q	D	S	T	N	L	N	S	I	T	A	S	G	N	T	E	N	S																			
	MG181655-RVA/Human-wt/MWI/BID2S/2013/G1P8	P[8]-H	D	S	Q	D	S	T	N	L	N	S	I	T	A	D	P	V	D	N	R	N	D	D	N	N	T	N	Y	F	I	W	P	G	R	T	P	E	L	R	
	Atypical G1P[8]	AB796437-RVA/Human-wt/JPN/OH3385/2012/G1P[8]	P[8]-H	D	S	Q	D	S	T	N	L	N	G	I	T	A	D	P	V	D	N	R	N	D	D	N	N	T	N	-	-	-	-	-	-	-	-	-	-	-	
		AB796438-RVA/Human-wt/JPN/OH3493/2012/G1P[8]	P[8]-H	D	S	Q	D	S	T	N	L	N	G	I	T	A	D	P	V	D	N	R	N	D	D	N	N	T	N	-	-	-	-	-	-	-	-	-	-	-	
		AB796439-RVA/Human-wt/JPN/OH3506/2012/G1P[8]	P[8]-H	D	S	Q	D	S	T	N	L	N	G	I	T	A	D	P	V	D	N	R	N	D	D	N	N	T	N	-	-	-	-	-	-	-	-	-	-	-	
Japan	AB796442-RVA/Human-wt/JPN/OH3625/2012/G1P[8]	P[8]-H	D	S	Q	D	S	T	N	L	N	G	I	T	A	D	P	V	D	N	R	N	D	D	N	N	T	N	-	-	-	-	-	-	-	-	-	-	-		
	LC066653-RVA/Human-wt/THA/SKT-109/2013/G1P[8]	P[8]-H	D	S	Q	D	S	T	N	L	N	G	I	T	A	D	P	V	D	N	R	N	D	D	N	N	T	N	Y	F	I	W	P	G	R	T	P	E	L	R	
	LC066684-RVA/Human-wt/THA/SKT-41/2013/G1P[8]	P[8]-H	D	S	Q	D	S	T	N	L	N	D	I	T	A	D	P	V	D	N	R	N	D	D	N	N	T	N	Y	F	I	W	P	G	R	T	P	E	L	R	
Thailand	LC066642-RVA/Human-wt/THA/PCB-180/2013/G1P[8]	P[8]-H	D	S	Q	D	S	T	N	L	N	D	I	T	A	D	P	V	D	N	R	N	D	D	N	N	T	N	Y	F	I	W	P	G	R	T	P	E	L	R	
	KP007202-RVA/Human-wt/PHI/IG2-045/2012/G1P[8]	P[8]-H	D	S	Q	D	S	T	N	L	N	G	I	T	A	D	P	V	D	N	R	N	D	D	N	N	T	N	Y	F	I	W	P	G	R	T	P	E	L	R	
Philippines	KP007191-RVA/Human-wt/PHI/IG2-016/2012/G1P[8]	P[8]-H	D	S	Q	D	S	T	N	L	N	G	I	T	A	D	P	V	D	N	R	N	D	D	N	N	T	N	Y	F	I	W	P	G	R	T	P	E	L	R	
	MG59528-RVA/Human-wt/BRA/IAL-R3165/2013/G1P[8]	P[8]-H	D	S	Q	D	S	T	N	L	N	G	I	T	A	D	P	V	D	N	R	N	D	D	N	N	T	N	Y	F	I	W	P	G	R	T	P	E	L	R	
Brazil	MG59530-RVA/Human-wt/BRA/IAL-R3172/2013/G1P[8]	P[8]-H	D	S	Q	D	S	T	N	L	N	G	I	T	A	D	P	V	D	N	R	N	D	D	N	N	T	N	Y	F	I	W	P	G	R	T	P	E	L	R	
	MG59528-RVA/Human-wt/BRA/IAL-R3123/2013/G1P[8]	P[8]-H	D	S	Q	D	S	T	N	L	N	G	I	T	A	D	P	V	D	N	R	N	D	D	N	N	T	N	Y	F	I	W	P	G	R	T	P	E	L	R	
	MG59527-RVA/Human-wt/BRA/IAL-R3122/2013/G1P[8]	P[8]-H	D	S	Q	D	S	T	N	L	N	G	I	T	A	D	P	V	D	N	R	N	D	D	N	N	T	N	Y	F	I	W	P	G	R	T	P	E	L	R	
	KJ752276-RVA/Human-wt/ZAF/MRC-DPRU1052/2008/G1P[8]	P[8]-H	D	S	Q	D	S	T	N	L	N	G	I	T	A	N	P	V	D	N	R	N	D	D	N	N	T	N	Y	F	I	W	P	G	R	T	P	E	L	R	
	HO392119-RVA/Human-wt/BEL/BE000117/2006/G1P[8]	P[8]-H	D	S	Q	D	S	T	N	L	N	G	I	T	A	N	P	V	D	N	R	N	D	D	N	N	T	N	Y	F	I	W	P	G	R	T	P	E	L	R	
	JQ696966-RVA/Human-wt/CAN/R1124-07/2008/G1P[8]	P[8]-H	D	S	Q	D	S	T	N	L	N	G	I	T	A	N	P	V	D	N	R	N	D	D	N	N	T	N	Y	F	I	W	P	G	R	T	P	E	L	R	
	JN849147-RVA/Human-wt/BEL/BE1286/2009/G1P[8]	P[8]-H	D	S	Q	D	S	T	N	L	N	G	I	T	A	N	P	V	D	N	R	N	D	D	N	N	T	N	Y	F	I	W	P	G	R	T	P	E	L	R	
	KJ753121-RVA/Human-wt/ZAF/MRC-DPRU2489/2008/G1P[8]	P[8]-H	D	S	Q	D	S	T	N	L	N	G	I	T	A	N	P	V	D	N	R	N	D	D	N	N	T	N	Y	F	I	W	P	G	R	T	P	E	L	R	
	KJ752898-RVA/Human-wt/ZAF/MRC-DPRU1381/2007/G1P[8]	P[8]-H	D	S	Q	D	S	T	N	L	N	G	I	T	A	N	P	V	D	N	R	N	D	D	N	N	T	N	Y	F	I	W	P	G	R	T	P	E	L	R	
	KJ751974-RVA/Human-wt/ZAF/MRC-DPRU822/2005/G1P[8]	P[8]-H	D	S	Q	D	S	T	N	L	N	G	I	T	A	N	P	V	D	N	R	N	D	D	N	N	T	N	Y	F	I	W	P	G	R	T	P	E	L	R	
KP753215-RVA/Human-wt/GO/MRC-DPRU5153/2010/G1P[8]	P[8]-H	D	S	Q	D	S	T	N	L	N	G	I	T	A	N	P	V	D	N	R	N	D	D	N	N	T	N	Y	F	I	W	P	G	R	T	P	E	L	R		
KJ752241-RVA/Human-wt/ZMB/MRC-DPRU1949/2009/G1P[8]	P[8]-H	D	S	Q	D	S	T	N	L	N	S	I	T	A	D	P	V	D	N	R	N	D	D	N	N	T	N	Y	F	I	W	P	G	R	T	P	E	L	R		
KJ752598-RVA/Human-wt/ZAF/MRC-DPRU1211/2011/G1P[8]	P[8]-H	D	S	Q	D	S	T	N	L	N	G	I	T	A	D	P	V	D	N	R	N	D	D	N	N	T	N	Y	F	I	W	P	G	R	T	P	E	L	R		
JQ696957-RVA/Human-wt/CAN/R1098-07/2008/G1P[8]	P[8]-H	D	S	Q	D	S	T	N	L	N	G	I	T	A	D	P	V	D	N	R	N	D	D	N	N	T	N	Y	F	I	W	P	G	R	T	P	E	L	R		
JF490365-RVA/Human-wt/Victoria/CK0029/2006/G1P[8]	P[8]-H	D	S	Q	D	S	T	N	L	N	G	I	T	A	D	P	V	D	N	R	N	D	D	N	N	T	N	Y	F	I	W	P	G	R	T	P	E	L	R		
KP752985-RVA/Human-wt/ZAF/MRC-DPRU1923/2009/G1P[8]	P[8]-H	D	S	Q	D	S	T	N	L	N	G	I	T	A	D	P	V	D	N	R	N	D	D	N	N	T	N	Y	F	I	W	P	G	R	T	P	E	L	R		
KX632345-RVA/Human-wt/UGA/MUL-13-157/2013/G1P[8]	P[8]-H	D	S	Q	D	S	T	N	L	N	G																														

RVA/Human-wt/TGO/MRC-DPRU2206/2009/G3G9P[6], RVA/Human-wt/BEL/F01498/2009/G3P[6], and RVA/Human-wt/UGA/MUL-13-166/2013/G3P[6] for VP1–VP3 and VP6, respectively (S1).

#### 2.3.4. Phylogenetic Analysis of NSP1–NSP5

The NSP1–NSP5 genes of the two South African study strains were highly identical amongst each other with nt (aa) identity value of  $\geq 99.8\%$ , and clustered closely (Figures S5–S9). Close clustering with cognate genes of a locally circulating strain, RVA/Human-wt/ZAF/MRC-DPRU2344/2008/G2P[6], was observed for the all the NSP1–NSP5 genes, and they shared the highest nt (aa) similarities that ranged from  $\geq 99.5\text{--}100\%$  (99.4–100%) (S1). In contrast, the NSP1–NSP5 genes of the atypical study strains grouped distinctly away from cognate genes of atypical strains reported in Brazil, Japan, Philippines, Thailand, Vietnam, and Malawi and shared an overall nt (aa) similarities that ranged from  $\geq 89.0\text{--}99.8\%$  ( $\geq 94.3\text{--}100\%$ ) (Figures S5–S9 in S3; Table S1 in S2). Comparison of NSP1–NSP5 genes of the two South African study strains with corresponding selected reference strains collected globally demonstrated nt (aa) identities in the range of 98.6–100% (99.4–100%) with cognate A2, N2, T2, E2, and H2 genes of strains: RVA/Human-wt/BEL/F01498/2009/G3P[6], RVA/Human-wt/KEN/KDH1968/2014/G3P[6], RVA/Human-wt/GHA/GH018-08/2008/G8P[6], RVA/Human-wt/ZMB/MRC-DPRU1673/2009/G2P[4], and RVA/Human-wt/USA/2007769964/2007/G2P[4], respectively (S1).

#### 2.4. Reassortment Analysis

The concatenated genomes of strains RVA/Human-wt/ZAF/UFS-NGS-MRC-DPRU1971/2008/G1P[8] and RVA/Human-wt/ZAF/UFS-NGS-MRC-DPRU1973/2008/G1P[8] were compared with two South African strains RVA/Human-wt/ZAF/MRC-DPRU1039/2008/G1P[8] and RVA/Human-wt/ZAF/MRC-DPRU2344/G2P[6] (Figure 5). The two atypical South African study strains shared a highly conserved backbone with all genes exhibiting  $> 99.8\%$  nucleotide similarity. The VP7 and the VP4 genes of the two atypical strains shared the highest genetic similarities to RVA/Human-wt/ZAF/MRC-DPRU1039/2008/G1P[8]. However, the internal backbone genes were extremely diverse. The internal backbone genes of the atypical strains exhibited highest genetic similarity to RVA/Human-wt/ZAF/MRC-DPRU2344/G2P[6]. The results of this analysis suggest that the atypical G1P[8] strains were likely derived via reassortment events between contemporary, endemic South African strains.

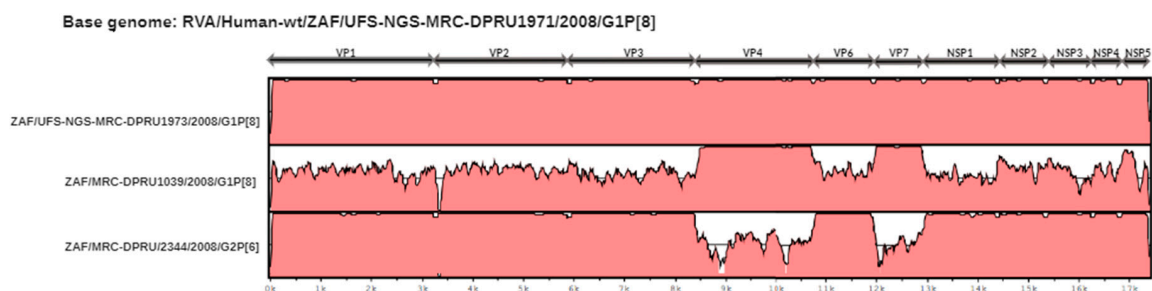


**Figure 5.** Nucleotide sequence similarities of the concatenated genome of RVA/Human-wt/ZAF/UFS-NGS-MRC-DPRU1971/2008/G1P[8] were compared with South African strains RVA/Human-wt/ZAF/UFS-NGS-MRC-DPRU1973/2008/G1P[8], RVA/Human-wt/ZAF/MRC-DPRU1039/2008/G1P[8], and RVA/Human-wt/ZAF/MRC-DPRU2344/G2P[6]. The left axis displays the strains, and rotavirus genome segment is included in the top scale. The bottom scale shows distance in kb.

### 3. Discussion

This study described the first pre-vaccine era atypical reassortant G1P[8] strains, whose outer gene segments (VP7 and VP4) expressed a Wa-like genotype, whereas the backbone genes expressed a DS-1-like genotype constellation. Analysis of the whole-genome constellation showed that genetic reassortment mechanism generated the DS-1-like G1P[8] strains. Rotavirus reassortment events are mainly facilitated by the segmentation inherent in the RV genome [2], which can generate rare

or novel RV strains and hence contribute to the vast RVA diversity [22]. Wa-like and DS-1-like intergenogroup reassortment events involving G1P[8] and DS-1-like genotype constellation have been described recently in six countries: Brazil, Japan, Philippines, Thailand, Vietnam, and Malawi [23–30]. According to literature, viable atypical reassortant strains can occur under natural conditions involving Wa-like G1P[8] or G3P[8] outer capsid genes expressing DS-1-like genetic background [41–44]. This study identified two DS-1-like G1P[8] strains in the course of the ongoing AEVGI whole-genome characterization of South African RVA strains. While reported in low frequencies and limited settings in Brazil (1.6% during 2013–2017 seasons) [22], Thailand (0.4% during 2012–2014 seasons) [27], and Vietnam (14% during 2012/2013 season) [28,29], 31–62% of these DS-1-like G1P[8] strains accounted for RVA positive strains circulating across selected regions in Japan [26], and 40% of randomly sampled post-vaccine samples were reported in Malawi [24]. Such atypical reassortant strains have the potential to predominate in circulation. G1P[4] strains suggested to have emerged from intergenogroup reassortment events accounted for 41% of RVA strains circulating in the peak months of the 2001 RVA season in Detroit, USA [45], whereas a surge in G3P[4] strains also presumed to have emerged from intergenogroup reassortment events were detected in Brazil at 36% [46] and in Ghana at 64% [47]. The two South African study strains were identified during the pre-RVA vaccination period in South Africa in contrast to the previously reported atypical strains found during the post-RVA vaccination period. This implies that the reassortment events that led to the emergence of the South African atypical G1P[8] strains may not necessarily be driven by vaccine-induced selective pressure but by natural evolutionary processes of RVA genome.

In order to identify the ancestral origin of these G1P[8] strains, assessment of whole-gene sequences and phylogenetic analysis showed that the outer capsid genes, VP7 and VP4, of strains RVA/Human-wt/ZAF/UFS-NGS-MRC-DPRU1971/2008/G1P[8] and RVA/Human-wt/ZAF/UFS-NGS-MRC-DPRU1973/2008/G1P[8] were 99.6–99.9% (99.1–100%) identical with South African strain RVA/Human-wt/ZAF/MRC-DPRU1039/2008/G1P[8] and clustered together in the same clade within the same. For the internal genes, the highest nucleotide identities were identified with cognate genes of another South African strain, RVA/Human-wt/ZAF/MRC-DPRU2344/2008/G2P[6], detected in the 2008 RVA season. Put together, it is probable that a locally circulating G2P[6] strain such as RVA/Human-wt/ZAF/MRC-DPRU2344/2008/G2P[6] with a DS-1-like backbone derived the VP7 and the VP4 genes from a locally co-circulating G1P[8] strain such as RVA/Human-wt/ZAF/MRC-DPRU1039/2008/G1P[8], generating the double-gene reassortants. Consequently, the results obtained in this study indicate that the two atypical South African G1P[8] strains were generated locally through genetic reassortment events. The generation of these reassortant double-gene strains tend to be independent of the events in which Brazilian, Japanese, Thai, Vietnamese, and Malawian DS-1-like G1P[8] strains were generated. The nine internal genes of the South African DS-1-like G1P[8] strains always clustered together with cognate genes of a locally circulating G2P[6] strain distinctly away from the cluster comprising Japanese, Thai, Philippines, and Malawi DS-1-like G1P[8] strains. Therefore, the South African DS-1-like G1P[8] strains emerged clonally from independent events, a phenomenon observed for the Malawian [24] and the Vietnamese [30] DS-1-like G1P[8] strains. In contrast, Brazilian, Japanese, and Thai G1P[8] DS-1-like strains were established to have been derived from a common ancestor [23,29].

Vaccine escape mutants can result due to mutations occurring in well-known VP7 neutralization epitope regions [48]. Host–antigen binding interactions involving human G1 strains are significantly impacted by mutations occurring at positions 94, 97, 147, and 291 [48]. The identified N94S substitution involving the substitution of asparagine (N) with a serine(S), which are both polar non-charged amino acid residues [49], may not significantly alter the overall morphology of the protein surface. However, since asparagine is usually N-glycosylated, there is a likely loss of glycosylation site, which could have a wide-ranging impact on the immunogenicity of the 7-1a epitope [50]. The D97E amino acid substitution involving polar negatively charged residues, aspartate (D) and glutamate (E), is likely to be a silent nucleotide change [49]. Similarly, a K291R substitution involving lysine (K), an amphipathic

polar amino acid, and arginine (R), a positively charged amino acid, is unlikely to have a far-reaching structural effect on the VP7 protein surfaces. However, M217T substitution was identified resulting in substitution of methionine, a non-polar residue to threonine, a polar amino acid residue, which could likely result in significant changes in biochemical properties of VP7 [49]. This M217T substitution was also present in earlier strains as well as some post-vaccine strains that were included for analysis, and the role it plays in driving epidemiological fitness of G1 strains is not fully resolved. In the host cell, trypsin-like proteases cleave the VP4 spike protein into two structural domains (VP8\* and VP5\*) [2]. Four surface-exposed antigenic epitopes (8-1 to 8-4) have been described in the VP8\* region, while five antigenic epitopes (5-1 to 5-5) in the VP5\* region have been documented [40]. The amino acid changes E150D, N195G, S125N, and N135D that were observed relative to the vaccine strains were conservative. However, a S131R substitution that resulted in a change in polarity might play a role in escape of host immunity [49]. Another amino acid substitution R131S resulting in a change in charge from positively charged amino acid to non-charged amino acid that was identified when comparison was made against globally selected lineage-III VP4 strains might impact vaccine escape effect [49].

#### **4. Materials and Methods**

##### *4.1. Ethics Approval*

The study was approved under ethics number UFS-HSD2018/0510/3107 by the Health Sciences Research Ethics Committee (HSREC) of the University of Free State, Bloemfontein, South Africa. The patient identities and demographics were de-linked from their unique laboratory identifiers to ensure confidentiality.

##### *4.2. Sample Collection*

Rotavirus positive stool samples from children under five years of age treated for gastroenteritis at Dr. George Mukhari Hospital, Pretoria North, South Africa and conventionally genotyped as G1P[8] were sourced from archival storage (2002 to 2017) of South Africa Medical Research Council—Diarrheal Pathogens Research Unit (MRC-DPRU), a WHO Rotavirus Regional Reference Laboratory (WHO-RRL) in Pretoria, South Africa. The two stool samples that were later genotyped as DS-1-like G1P[8] strains were collected from 6-month female and 12-month male children on 15 and 16 May 2008, respectively, from Soshanguve, Pretoria.

##### *4.3. Extraction and Purification of Double-Stranded RNA*

The extraction of RV ds-RNA was conducted by utilizing a previously described method [51], albeit with modifications (UFS-NGS unit extraction SOP). Briefly, a pea size (~100 mg) sample of stool was added to 200 µL of phosphate-buffered saline (PBS) solution, pH 7.2 (Sigma-Aldrich®, St Louis, MO, USA). The solution was mixed by pulse-vortexing for five seconds. A 1 mL volume of TRI-Reagent®-LS (Molecular Research Center, Inc, Cincinnati, OH, USA) was added and let to stand for five minutes. Phase separation was achieved by addition of 270 µL of chloroform (Sigma-Aldrich®, St Louis, MO, USA). Afterward, centrifugation for 13,000 revolutions per minute (RPM) was performed for 20 min at 4 °C in a temperature-controlled microcentrifuge (Eppendorf microcentrifuge 5427R, Hamburg, Germany). A volume of 1 mL isopropanol (Sigma-Aldrich®, St Louis, MO, USA) was added to the supernatant, and centrifugation was performed at 13,000 RPM for 30 min at room temperature. The supernatant was poured off, and the tubes were let to dry for 10 min, after which 95 µL of elution buffer (EB) from the MinElute Gel extraction kit (Qiagen, Hilden, Germany) was added. A 30 µL volume of 8M LiCl<sub>2</sub> (Sigma, St. Louis, MO, USA) was added, and the solution was precipitated for 16 h at 4 °C in a water bath in a Tupperware box. The MinElute gel extraction kit (Qiagen, Hilden, Germany) was used to purify the extracted RNA according to manufacturer's instructions, and 1% 0.5 X TBE agarose gel stained with Pronasafe (Condalab, UK) electrophoresis was used to verify the

integrity and the enrichment of dsRNA, which was visualized on a G:Box Syngene UV transilluminator (Syngene, Cambridge, UK).

#### *4.4. Synthesis and Purification of Complementary DNA (cDNA)*

The Maxima H Minus Double-Stranded cDNA Synthesis Kit (Thermo Fischer Scientific, Waltham, MA) was utilized to synthesize cDNA from the extracted viral RNA. Briefly, denaturation at 95 °C for 5 min of the extracted RNA was performed followed by addition of 1 µL of 100 µM Random Hexamer primer. Incubation was performed in a thermocycler at 65 °C for five minutes. The First-Strand Reaction mix (5 µL) and the First Strand Enzyme Mix (1 µL) were added, and the solution was incubated at 25 °C for 10 min followed by 2 h at 50 °C, and then the reaction was terminated by heating at 85 °C for 5 min. A volume of 55 µL of nuclease-free water, 20 µL of 5X Second Strand Reaction Mix, and 5 µL of Second Strand Reaction Mix was then added. The solution was then incubated at 16 °C for 60 min, after which the reaction was stopped by adding 6 µL 0.5M EDTA. A volume of 10 µL RNase I was then added, and the synthesized cDNA was incubated for five minutes at room temperature. Subsequently, the MSB® Spin PCRapace (Stratec) Purification Kit was used to purify the synthesized cDNA.

#### *4.5. DNA Library Preparation and Whole-Genome Sequencing*

The Nextera® XT DNA Library Preparation Kit (Illumina, San Diego, California, US) was utilized to prepare DNA libraries by following manufacturer's instructions. Briefly, the genomic DNA was tagmented by using the Nextera® transposome enzyme, and the tagmented DNA was subsequently amplified using a limited-cycle PCR program. The DNA libraries were cleaned-up using AMPure XP magnetic beads (Beckman Coulter, Pasadena, CA, USA) and 80% freshly prepared ethanol. The quantity of the DNA was determined using Qubit 2.0 fluorometer (Invitrogen, Carlsbad, CA, USA), and the quality of the libraries and the fragment sizes was assessed using Agilent 2100 BioAnalyzer® (Agilent Technologies, Waldbronn, Germany) by following the manufacturer's specified protocol. The Illumina MiSeq® sequencer (Illumina, San Diego, CA, USA) was utilized to perform paired-end nucleotide sequencing (301 × 2) for 600 cycles by using a MiSeq Reagent Kit v3 at the University of the Free State-Next Generation Sequencing (UFS-NGS) Unit, Bloemfontein, South Africa.

#### *4.6. Genome Assembly*

Geneious Prime® software, version 2019.1.1 (Biomatters, <https://www.geneious.com/>; [52]) was used for genome assembly. Briefly, for use with the reference mapping tools integrated in Geneious Prime version 2019.1.1, the default medium sensitivity parameter was selected to generate contigs from the FASTQ files data generated by the Illumina MiSeq® instrument. Complementary RV genome assembly was also performed using an in-house genome assembly pipeline and CLC Genomics Workbench 12 (<https://www.qiagenbioinformatics.com/>).

#### *4.7. Determination of Rotavirus Whole-Genotype Constellations*

The genotype of each gene segment was determined using Rota C, v 2.0 [13], an online server for genotyping RVA strains. This was used to generate the full genotype constellations for each RV strain.

#### *4.8. Phylogenetic Analyses*

Complete sequences for each gene segment were aligned and sequence comparisons performed as described previously [53–55]. Multiple sequence alignments were implemented utilizing the MUSCLE package in Molecular Evolutionary Genetics Analysis (MEGA) 6 software ([56]; <http://www.megasoftware.net/>). Upon alignment, the DNA Model Test program in MEGA 6 was used to determine the evolutionary model that best fits each gene sequence datasets. The models identified as best fitting with the sequence data for the indicated genes using the Corrected Akaike Information Criterion (AICc) were as follows: GTR+G+I (VP7, VP4, VP6, VP1, VP2, VP3, NSP1, NSP2, NSP3) and

HKY+G+I (NSP4 and NSP5). These models were utilized in maximum-likelihood trees' construction using MEGA 6 with 1000 bootstrap replicates to estimate branch support. Genetic distance matrices were prepared using the *p*-distance algorithm of MEGA 6 software [56]. In addition to the two whole-genome sequences of the strains in this study, other cognate sequences were acquired from GenBank ([57]; <http://www.ncbi.nlm.gov/genbank>). Further phylogenetic analysis by geographical regions Africa (Eastern Africa, Southern Africa, and West Africa), Asia, Americas, Europe, and Oceania was also performed. mVISTA software was used to visualize the comparative sequence similarities of concatenated whole-genome of genetically related strains [58].

## 5. Conclusions

Whole-gene analyses showed that the South African DS-1-like G1P[8] strains were generated involving locally circulating G2P[6] strains by acquiring the VP7 and the VP4 outer capsid proteins of locally co-circulating G1P[8] strains. Similar to their pre-vaccine era detection in Vietnam and Philippines, the identification of these atypical DS-1-like G1P[8] strains during the pre-vaccine period in South Africa, as opposed to their detection during post-vaccination era in selected settings in Brazil (Sao Paulo and Goias in 2013), Japan (Okayama, Aichi, Akita, Kyoto, and Osaka Prefectures in 2012), Thailand (Phetchabun and Sukhothai in 2013), and Malawi (Blantyre in 2013/2014), suggests that they originated from natural evolutionary processes of RVA genome. Whole-genome surveillance of RVA genotypes is imperative to understand the occurrence rate, the mechanisms that drive emergence of such atypical strains, and their epidemiological fitness as well as to assess the effect of vaccine selective pressure in shaping the antigenic landscape of RVA strains.

**Supplementary Materials:** The following are available online at <http://www.mdpi.com/2076-0817/9/5/391/s1>, Supplementary data 1 (S1): Identity matrices analysis for VP1, VP2, VP3, VP4, VP6, NSP1, NSP2, NSP3, NSP5 and NSP5 nucleotide and deduced amino acid identities among strains calculated by distance matrices using P-distance algorithm in MEGA 6. Supplementary data 2 (S2): Homology analysis summary containing Table S1 and Table S2. Supplementary data 3 (S3): Additional phylograms containing Figure S1:VP1, S2:VP2, S3:VP3, S4:VP6, S5:NSP1, S6:NSP2, S7:NSP3, S8:NSP4 and S9:NSP5.

**Author Contributions:** M.M.N., K.C.J., F.E.D. and V.N.N. conceptualized the main project. P.N.M., M.T.M., M.M.N. and S.P.R. performed the laboratory experiments. M.J.M. and M.L.S. facilitated the sample resources. Formal analysis was done by P.N.M. and M.M.N. Data curation was performed by P.N.M., M.T.M., M.M.N. and S.P.R. Writing of the original draft preparation was performed by P.N.M. Review of the drafts was performed by all co-authors. Supervision, funding acquisition and project administration was performed by M.M.N. All authors have read and agreed to the published version of the manuscript.

**Funding:** This research was principally funded by a grant awarded to M.M.N. by Bill and Melinda Gates Foundation (BMGF-OPP1180423\_2017). Other funding grants awarded to M.M.N. that funded this research include: South African Medical Research Council (SAMRC) through the Self-Initiated Research grant (SIR), Poliomyelitis Research Foundation (PRF-19/16) and National Research Foundation (NRF-120814).

**Acknowledgments:** Assistance in retrieval of the archived stool samples by Khutso Mothapo, Kebareng Rakau and Nonkululeko Magagula at the WHO-RRL in Pretoria, is hereby acknowledged. Assistance in laboratory work by Lesedi Mosime, Gilmore Pambuka and Teboho Mooko is duly acknowledged. Some aspects of data analysis guidance by Mathew Esona (CDC, Atlanta) and Felicity Burt is greatly acknowledged. Technical ICT support by Stephanus Riekert is also acknowledged.

**Conflicts of Interest:** The authors declare no conflict of interest.

## References

1. World Health Organization Causes of Mild Mortality. (WHO 2019). Available online: [https://www.who.int/gho/child\\_health/mortality/causes/en/](https://www.who.int/gho/child_health/mortality/causes/en/) (accessed on 20 August 2019).
2. Estes, M.K.; Greenberg, H.B. Rotaviruses. In *Fields Virology*; Knipe, D.M., Howley, P.M., Eds.; Wolters Kluwer Health/Lippincott, Williams and Wilkins: Philadelphia, PA, USA, 2013.
3. Troeger, C.; Khalil, I.A.; Rao, P.C.; Cao, S.; Blacker, B.F.; Ahmed, T.; Armah, G.; Bines, J.E.; Brewer, T.G.; Colombara, D.V.; et al. Rotavirus vaccination and the global burden of rotavirus diarrhea among children younger than 5 years. *JAMA Pediatr.* **2018**, *172*, 958–965. [CrossRef]

4. Tate, J.E.; Burton, A.H.; Boschi-Pinto, C.; Parashar, U.D.; World Health Organization–Coordinated Global Rotavirus Surveillance Network; Agocs, M.; Serhan, F.; de Oliveira, L.; Mwenda, J.M.; Mihigo, R.; et al. Global, regional, and national estimates of rotavirus mortality in children <5 years of age, 2000–2013. *Clin. Infect. Dis.* **2016**, *62* (Suppl. 2), S96–S105.
5. World Health Organization. Meeting of the immunization Strategic Advisory Group of Experts. *Wkly. Epidemiol. Rec.* **2009**, *84*, 220–236.
6. World Health Organization. WHO Prequalifies New Rotavirus Vaccine. Available online: [https://www.who.int/medicines/news/2018/prequalified\\_new-rotavirus\\_vaccine/en/](https://www.who.int/medicines/news/2018/prequalified_new-rotavirus_vaccine/en/) (accessed on 19 December 2019).
7. Anh, D.D.; Van Trang, N.; Thiem, V.D.; Anh, N.T.H.; Mao, N.D.; Wang, Y.; Jiang, B.; Hien, N.D.; Rotavin-M1 Vaccine Trial Group. A dose-escalation safety and immunogenicity study of a new live attenuated human rotavirus vaccine (Rotavin-M1) in Vietnamese children. *Vaccine* **2012**, *30*, A114–A121. [CrossRef]
8. Fu, C.; Wang, M.; Liang, J.; He, T.; Wang, D.; Xu, J. Effectiveness of Lanzhou lamb rotavirus vaccine against rotavirus gastroenteritis requiring hospitalization: A matched case-control study. *Vaccine* **2007**, *25*, 8756–8761. [CrossRef]
9. Kirkwood, C.D.; Steele, A.D. Rotavirus Vaccines in China. *Jama Netw. Open* **2018**, *1*, e181579. [CrossRef]
10. Madhi, S.A.; Cunliffe, N.A.; Steele, D.; Witte, D.; Kirsten, M.; Louw, C.; Ngwira, B.; Victor, J.C.; Gillard, P.H.; Chevart, B.B.; et al. Effect of human rotavirus vaccine on severe diarrhea in African infants. *N. Engl. J. Med.* **2010**, *362*, 289–298. [CrossRef]
11. Madhi, S.A.; Kirsten, M.; Louw, C.; Bos, P.; Aspinall, S.; Bouckenoghe, A.; Neuzil, K.M.; Steele, A.D. Efficacy and immunogenicity of two or three dose rotavirus-vaccine regimen in South African children over two consecutive rotavirus-seasons: A randomized, double-blind, placebo-controlled trial. *Vaccine* **2012**, *30*, A44–A51. [CrossRef]
12. Matthijssens, J.; Ciarlet, M.; McDonald, S.M.; Attoui, H.; Bányai, K.; Brister, J.R.; Buesa, J.; Esona, M.D.; Estes, M.K.; Gentsch, J.R.; et al. Uniformity of rotavirus strain nomenclature proposed by the Rotavirus Classification Working Group (RCWG). *Arch. Virol.* **2011**, *156*, 1397–1413. [CrossRef]
13. Maes, P.; Matthijssens, J.; Rahman, M.; Van Ranst, M. RotaC: A web-based tool for the complete genome classification of group A rotaviruses. *BMC Microbiol.* **2009**, *9*, 238. [CrossRef]
14. Dóro, R.; László, B.; Martella, V.; Leshem, E.; Gentsch, J.; Parashar, U.; Bányai, K. Review of global rotavirus strain prevalence data from six years post vaccine licensure surveillance: Is there evidence of strain selection from vaccine pressure? *Infect. Genet. Evol.* **2014**, *28*, 446–461. [CrossRef] [PubMed]
15. Banyai, K.; Mijatovic-Rustempasic, S.; Hull, J.J.; Esona, M.D.; Freeman, M.M.; Frace, A.M.; Bowen, M.D.; Gentsch, J.R. Sequencing and phylogenetic analysis of the coding region of six common rotavirus strains: Evidence for intragenogroup reassortment among co-circulating G1P[8] and G2P[4] strains from the United States. *J. Med. Virol.* **2011**, *83*, 532–539. [CrossRef] [PubMed]
16. Seheri, L.M.; Magagula, N.B.; Peenze, I.; Rakau, K.; Ndadza, A.; Mwenda, J.M.; Weldegebriel, G.; Steele, A.D.; Mphahlele, M.J. Rotavirus strain diversity in Eastern and Southern African countries before and after vaccine introduction. *Vaccine* **2018**, *36*, 7222–7230. [CrossRef]
17. Mwenda, J.M.; Ntoto, K.M.; Abebe, A.; Enweronu-Laryea, C.; Amina, I.; Mchomvu, J.; Kisakye, A.; Mpabalwani, E.M.; Pazvakavambwa, I.; Armah, G.E.; et al. Burden and epidemiology of rotavirus diarrhea in selected African countries: Preliminary results from the African Rotavirus Surveillance Network. *J. Infect. Dis.* **2010**, *202* (Suppl. 1), S5–S11. [CrossRef]
18. Seheri, L.M.; Ngomane, G.; Page, N.A.; Mokomane, M.; Maphalala, G.P.; Weldegebriel, G.; Peenze, I.; Magagula, N.B.; Nyaga, M.M.; Lisoga, J.; et al. Outbreak investigation of diarrheal disease in Botswana and Eswatini in 2018. In Proceedings of the 12th African Rotavirus Symposium, Johannesburg, South Africa, 30 July–1 August 2019.
19. Matthijssens, J.; Van Ranst, M. Genotype constellation and evolution of group A rotaviruses infecting humans. *Curr. Opin. Virol.* **2012**, *2*, 426–433. [CrossRef]
20. Do, L.P.; Nakagomi, T.; Otaki, H.; Agbemabiese, C.A.; Nakagomi, O.; Tsunemitsu, H. Phylogenetic inference of the porcine Rotavirus A origin of the human G1 VP7 gene. *Infect. Genet. Evol.* **2016**, *40*, 205–213. [CrossRef]
21. Santos, F.S.; Junior, E.S.; Guerra, S.F.S.; Lobo, P.S.; Junior, E.P.; Lima, A.B.F.; Vinente, C.B.G.; Chagas, E.H.N.; Justino, M.C.A.; Linhares, A.C.; et al. G1P[8] Rotavirus in children with severe diarrhea in the post-vaccine introduction era in Brazil: Evidence of reassortments and structural modifications of the antigenic VP7 and VP4 regions. *Infect. Genet. Evol.* **2019**, *69*, 255–266. [CrossRef]

22. Kirkwood, C.D. Genetic and antigenic diversity of human rotaviruses: Potential impact on vaccination programs. *J. Infect. Dis.* **2010**, *202* (Suppl. 1), S43–S48. [CrossRef]
23. Luchs, A.; da Costa, A.C.; Cilli, A.; Komninakis, S.C.V.; Carmona, R.D.C.C.; Morillo, S.G.; Sabino, E.C.; Timenetsky, M.D.C.S.T. First Detection of DS-1-like G1P[8] Double-gene Reassortant Rotavirus Strains on The American Continent, Brazil, 2013. *Sci. Rep.* **2019**, *9*, 2210. [CrossRef]
24. Jere, K.C.; Chaguza, C.; Bar-Zeev, N.; Lowe, J.; Peno, C.; Kumwenda, B.; Nakagomi, O.; Tate, J.E.; Parashar, U.D.; Heyderman, R.S.; et al. Emergence of double-and triple-gene reassortant G1P[8] rotaviruses possessing a DS-1-like backbone after rotavirus vaccine introduction in Malawi. *J. Virol.* **2018**, *92*, e01246-17. [CrossRef]
25. Fujii, Y.; Nakagomi, T.; Nishimura, N.; Noguchi, A.; Miura, S.; Ito, H.; Doan, Y.H.; Takahashi, T.; Ozaki, T.; Katayama, K.; et al. Spread and predominance in Japan of novel G1P[8] double-reassortant rotavirus strains possessing a DS-1-like genotype constellation typical of G2P[4] strains. *Infect. Genet. Evol.* **2014**, *28*, 426–433. [CrossRef]
26. Kuzuya, M.; Fujii, R.; Hamano, M.; Kida, K.; Mizoguchi, Y.; Kanadani, T.; Nishimura, K.; Kishimoto, T. Prevalence and molecular characterization of G1P[8] human rotaviruses possessing DS-1-like VP6, NSP4, and NSP5/6 in Japan. *J. Med. Virol.* **2014**, *86*, 1056–1064. [CrossRef] [PubMed]
27. Yamamoto, S.P.; Kaida, A.; Kubo, H.; Iritani, N. Gastroenteritis Outbreaks Caused by a DS-1-like G1P[8] Rotavirus Strain, Japan, 2012–2013. *Emerg. Infect. Dis.* **2014**, *20*, 1030. [CrossRef] [PubMed]
28. Komoto, S.; Tacharoenmuang, R.; Guntapong, R.; Ide, T.; Tsuji, T.; Yoshikawa, T.; Tharmaphornpilas, P.; Sangkitporn, S.; Taniguchi, K. Reassortment of human and animal rotavirus gene segments in emerging DS-1-like G1P[8] rotavirus strains. *PLoS ONE* **2016**, *11*, e0148416. [CrossRef] [PubMed]
29. Komoto, S.; Tacharoenmuang, R.; Guntapong, R.; Ide, T.; Haga, K.; Katayama, K.; Kato, T.; Ouchi, Y.; Kurahashi, H.; Tsuji, T.; et al. Emergence and characterization of unusual DS-1-like G1P[8] rotavirus strains in children with diarrhea in Thailand. *PLoS ONE* **2015**, *10*, e0141739. [CrossRef] [PubMed]
30. Nakagomi, T.; Nguyen, M.Q.; Gauchan, P.; Agbemabiese, C.A.; Kaneko, M.; Do, L.P.; Vu, T.D.; Nakagomi, O. Evolution of DS-1-like G1P[8] double-gene reassortant rotavirus A strains causing gastroenteritis in children in Vietnam in 2012/2013. *Arch. Virol.* **2017**, *162*, 739–748. [CrossRef] [PubMed]
31. Zeller, M.; Heylen, E.; Tamim, S.; McAllen, J.K.; Kirkness, E.F.; Akopov, A.; De Coster, S.; Van Ranst, M.; Matthijssens, J. Comparative analysis of the Rotarix™ vaccine strain and G1P[8] rotaviruses detected before and after vaccine introduction in Belgium. *PeerJ* **2017**, *5*, e2733. [CrossRef]
32. Magagula, N.B.; Esona, M.D.; Nyaga, M.M.; Stucker, K.M.; Halpin, R.A.; Stockwell, T.B.; Seheri, M.L.; Steele, A.D.; Wentworth, D.E.; Mphahlele, M.J. Whole genome analyses of G1P[8] rotavirus strains from vaccinated and non-vaccinated South African children presenting with diarrhea. *J. Med. Virol.* **2015**, *87*, 79–101. [CrossRef]
33. Shintani, T.; Ghosh, S.; Wang, Y.H.; Zhou, X.; Zhou, D.J.; Kobayashi, N. Whole genomic analysis of human G1P[8] rotavirus strains from different age groups in China. *Viruses* **2012**, *4*, 1289–1304. [CrossRef]
34. Arora, R.; Chitambar, S.D. Full genomic analysis of Indian G1P[8] rotavirus strains. *Infect. Genet. Evol.* **2011**, *11*, 504–511. [CrossRef]
35. Rahman, M.; Matthijssens, J.; Saiada, F.; Hassan, Z.; Heylen, E.; Azim, T.; Van Ranst, M. Complete genomic analysis of a Bangladeshi G1P[8] rotavirus strain detected in 2003 reveals a close evolutionary relationship with contemporary human Wa-like strains. *Infect. Genet. Evol.* **2010**, *10*, 746–754. [CrossRef] [PubMed]
36. Arista, S.; Giammanco, G.M.; De Grazia, S.; Ramirez, S.; Biundo, C.L.; Colomba, C.; Cascio, A.; Martella, V. Heterogeneity and temporal dynamics of evolution of G1 human rotaviruses in a settled population. *J. Virol.* **2006**, *80*, 10724–10733. [CrossRef] [PubMed]
37. Aoki, S.T.; Settembre, E.C.; Trask, S.D.; Greenberg, H.B.; Harrison, S.C.; Dormitzer, P.R. Structure of rotavirus outer-layer protein VP7 bound with a neutralizing Fab. *Science* **2009**, *324*, 1444–1447. [CrossRef] [PubMed]
38. Le, V.P.; Chung, Y.C.; Kim, K.; Chung, S.I.; Lim, I.; Kim, W. Genetic variation of prevalent G1P[8] human rotaviruses in South Korea. *J. Med. Virol.* **2010**, *82*, 886–896. [CrossRef] [PubMed]
39. Ciarlet, M.; Hyser, J.M.; Estes, M.K. Sequence Analysis of the VP4, VP6, VP7, and NSP4 Gene Products of the Bovine Rotavirus WC3. *Virus Genes* **2002**, *24*, 107–118. [CrossRef]
40. Zeller, M.; Patton, J.T.; Heylen, E.; De Coster, S.; Ciarlet, M.; Van Ranst, M.; Matthijssens, J. Genetic analyses reveal differences in the VP7 and VP4 antigenic epitopes between human rotaviruses circulating in Belgium and rotaviruses in Rotarix and RotaTeq. *J. Clin. Microbiol.* **2012**, *50*, 966–976. [CrossRef]

41. Guntapong, R.; Tacharoenmuang, R.; Singchai, P.; Upachai, S.; Sutthiwarakom, K.; Komoto, S.; Tsuji, T.; Tharmaphornpilas, P.; Yoshikawa, T.; Sangkitporn, S.; et al. Predominant prevalence of human rotaviruses with the G1P[8] and G8P[8] genotypes with a short RNA profile in 2013 and 2014 in Sukhothai and Phetchaboon provinces, Thailand. *J. Med. Virol.* **2017**, *89*, 615–620. [CrossRef]
42. Arana, A.; Montes, M.; Jere, K.C.; Alkorta, M.; Iturriza-Gómara, M.; Cilla, G. Emergence and spread of G3P[8] rotaviruses possessing an equine-like VP7 and a DS-1-like genetic backbone in the Basque Country (North of Spain), 2015. *Infect. Genet. Evol.* **2016**, *44*, 137–144. [CrossRef]
43. Cowley, D.; Donato, C.M.; Roczo-Farkas, S.; Kirkwood, C.D. Emergence of a novel equine-like G3P[8] inter-genogroup reassortant rotavirus strain associated with gastroenteritis in Australian children. *J. Gen. Virol.* **2016**, *97*, 403–410. [CrossRef]
44. Guerra, S.F.S.; Soares, L.S.; Lobo, P.S.; Júnior, E.T.P.; Júnior, E.C.S.; Bezerra, D.A.M.; Vaz, L.R.; Linhares, A.C.; Mascarenhas, J.D.A.P. Detection of a novel equine-like G3 rotavirus associated with acute gastroenteritis in Brazil. *J. Gen. Virol.* **2016**, *97*, 3131–3138. [CrossRef]
45. Abdel-Haq, N.M.; Thomas, R.A.; Asmar, B.I.; Zacharova, V.; Lyman, W.D. Increased prevalence of G1P[4] genotype among children with rotavirus-associated gastroenteritis in metropolitan Detroit. *J. Clin. Microbiol.* **2003**, *41*, 2680–2682. [CrossRef] [PubMed]
46. Rosa, M.E.S.; Pires, I.D.C.; Gouvea, V. 1998–1999 rotavirus seasons in Juiz de Fora, Minas Gerais, Brazil: Detection of an unusual G3P[4] epidemic strain. *J. Clin. Microbiol.* **2002**, *40*, 2837–2842. [CrossRef] [PubMed]
47. Asmah, R.H.; Green, J.; Armah, G.E.; Gallimore, C.I.; Gray, J.J.; Iturriza-Gómara, M.; Anto, F.; Oduro, A.; Binka, F.N.; Brown, D.W.; et al. Rotavirus G and P genotypes in rural Ghana. *J. Clin. Microbiol.* **2001**, *39*, 1981–1984. [CrossRef] [PubMed]
48. Coulson, B.S.; Kirkwood, C. Relation of VP7 amino acid sequence to monoclonal antibody neutralization of rotavirus and rotavirus monotype. *J. Virol.* **1991**, *65*, 5968–5974. [CrossRef]
49. Betts, M.J.; Russell, R.B. Amino acid properties and consequences of substitutions. *Bioinform. Genet.* **2003**, *317*, 289.
50. Caust, J.; Dyal-Smith, M.L.; Lazdins, I.; Holmes, I.H. Glycosylation, an important modifier of rotavirus antigenicity. *Arch. Virol.* **1987**, *96*, 123–134. [CrossRef]
51. Potgieter, A.C.; Page, N.A.; Liebenberg, J.; Wright, I.M.; Landt, O.; Van Dijk, A.A. Improved strategies for sequence-independent amplification and sequencing of viral double-stranded RNA genomes. *J. Gen. Virol.* **2009**, *90*, 1423–1432. [CrossRef]
52. Kearse, M.; Moir, R.; Wilson, A.; Stones-Havas, S.; Cheung, M.; Sturrock, S.; Buxton, S.; Cooper, A.; Markowitz, S.; Duran, C.; et al. Geneious Basic: An integrated and extendable desktop software platform for the organization and analysis of sequence data. *Bioinformatics* **2012**, *28*, 1647–1649. [CrossRef]
53. Esona, M.D.; Roy, S.; Rungsruriyachai, K.; Gautam, R.; Hermelijn, S.; Rey-Benito, G.; Bowen, M.D. Molecular characterization of a human G20P[28] rotavirus a strain with multiple genes related to bat rotaviruses. *Infect. Genet. Evol.* **2018**, *57*, 166–170. [CrossRef]
54. Esona, M.D.; Roy, S.; Rungsruriyachai, K.; Sanchez, J.; Vasquez, L.; Gomez, V.; Rios, L.A.; Bowen, M.D.; Vazquez, M. Characterization of a triple-recombinant, reassortant rotavirus strain from the Dominican Republic. *J. Gen. Virol.* **2017**, *98*, 134. [CrossRef]
55. Ward, M.L.; Mijatovic-Rustempasic, S.; Roy, S.; Rungsruriyachai, K.; Boom, J.A.; Sahni, L.C.; Baker, C.J.; Rench, M.A.; Wikswo, M.E.; Payne, D.C.; et al. Molecular characterization of the first G24P[14] rotavirus strain detected in humans. *Infect. Genet. Evol.* **2016**, *43*, 338–342. [CrossRef]
56. Tamura, K.; Stecher, G.; Peterson, D.; Filipski, A.; Kumar, S. MEGA6: Molecular evolutionary genetics analysis version 6.0. *Mol. Biol. Evol.* **2013**, *30*, 2725–2729. [CrossRef] [PubMed]
57. Benson, D.A.; Karsch-Mizrachi, I.; Lipman, D.J.; Ostell, J.; Rapp, B.A.; Wheeler, D.L. GenBank. *Nucleic Acids Res.* **2000**, *28*, 15–18. [CrossRef] [PubMed]
58. Mayor, C.; Brudno, M.; Schwartz, J.R.; Poliakov, A.; Rubin, E.M.; Frazer, K.A.; Pachter, L.S.; Dubchak, I. VISTA: Visualizing global DNA sequence alignments of arbitrary length. *Bioinformatics* **2000**, *16*, 1046–1047. [CrossRef] [PubMed]





Article

# Molecular Characterisation of a Rare Reassortant Porcine-Like G5P[6] Rotavirus Strain Detected in an Unvaccinated Child in Kasama, Zambia

Wairimu M. Maringa<sup>1</sup>, Peter N. Mwangi<sup>1</sup>, Julia Simwaka<sup>2</sup>, Evans M. Mpabalwani<sup>3</sup>, Jason M. Mwendu<sup>4</sup>, Ina Peenze<sup>5</sup>, Mathew D. Esona<sup>5</sup>, M. Jeffrey Mphahlele<sup>5,6</sup>, Mapaseka L. Seheri<sup>5</sup> and Martin M. Nyaga<sup>1,\*</sup> 

<sup>1</sup> Next Generation Sequencing Unit, Division of Virology, Faculty of Health Sciences, University of the Free State, Bloemfontein 9300, South Africa; makena96wairimu@gmail.com (W.M.M.); nthigapete@gmail.com (P.N.M.)

<sup>2</sup> Virology Laboratory, Department of Pathology & Microbiology, University Teaching Hospital, Adult and Emergency Hospital, Lusaka 10101, Zambia; juliachibumbya@gmail.com

<sup>3</sup> Department of Paediatrics & Child Health, School of Medicine, University of Zambia, Ridgeway, Lusaka RW50000, Zambia; evans.mpabalwani@unza.zm

<sup>4</sup> World Health Organization, Regional Office for Africa, Brazzaville P.O. Box 06, Congo; mwendaj@who.int

<sup>5</sup> Diarrhoeal Pathogens Research Unit, Faculty of Health Sciences, Sefako Makgatho Health Sciences University, Medunsa, Pretoria 0204, South Africa; ina.peenze@smu.ac.za (I.P.); mathew.esona@gmail.com (M.D.E.); Jeffrey.Mphahlele@mrc.ac.za (M.J.M.); mapaseka.seheri@smu.ac.za (M.L.S.)

<sup>6</sup> South African Medical Research Council, 1 Soutpansberg Road, Pretoria 0001, South Africa

\* Correspondence: NyagaMM@ufs.ac.za; Tel.: +27-51-401-9158

Received: 24 July 2020; Accepted: 14 August 2020; Published: 17 August 2020



**Abstract:** A human-porcine reassortant strain, RVA/Human-wt/ZMB/UFS-NGS-MRC-DPRU4723/2014/G5P[6], was identified in a sample collected in 2014 from an unvaccinated 12 month old male hospitalised for gastroenteritis in Zambia. We sequenced and characterised the complete genome of this strain which presented the constellation: G5-P[6]-I1-R1-C1-M1-A8-N1-T1-E1-H1. The genotype A8 is often observed in porcine strains. Phylogenetic analyses showed that VP6, VP7, NSP2, NSP4, and NSP5 genes were closely related to cognate gene sequences of porcine strains (e.g., RVA/Pig-wt/CHN/DZ-2/2013/G5P[X] for VP7) from the NCBI database, while VP1, VP3, VP4, and NSP3 were closely related to porcine-like human strains (e.g., RVA/Human-wt/CHN/E931/2008/G4P[6] for VP1, and VP3). On the other hand, the origin of the VP2 was not clear from our analyses, as it was not only close to both porcine (e.g., RVA/Pig-tc/CHN/SWU-1C/2018/G9P[13]) and porcine-like human strains (e.g., RVA/Human-wt/LKA/R1207/2009/G4P[6]) but also to three human strains (e.g., RVA/Human-wt/USA/1476/1974/G1P[8]). The VP7 gene was located in lineage II that comprised only porcine strains, which suggests the occurrence of independent porcine-to-human reassortment events. The study strain may have collectively been derived through interspecies transmission, or through reassortment event(s) involving strains of porcine and porcine-like human origin. The results of this study underline the importance of whole-genome characterisation of rotavirus strains and provide insights into interspecies transmissions from porcine to humans.

**Keywords:** whole-genome; genotype constellation; interspecies transmission; reassortment; porcine; porcine-like human

## 1. Introduction

Group A rotaviruses (RVA), of the family *Reoviridae*, are the number one viral pathogens causing severe diarrhoea in children below five years of age [1]. In 2016, an estimated 128,000 deaths in children below five years were due to RVA infections, 90% of which occurred in developing countries [2,3]. Similarly, RVA are the primary cause of acute gastroenteritis in new-born piglets [4].

Rotaviruses have a distinctive morphology which comprises a nonenveloped, three-layered icosahedral protein shell. The rotavirus genome within the protein shell comprises 11 segments of double-stranded (dsRNA) that encode six structural viral proteins (VP1 to VP4, VP6, and VP7) and five or six nonstructural proteins (NSP1 to NSP5/6) [1]. A binary classification system is used to distinguish RVA based on the antigenic properties of the outer shell proteins, VP7 and VP4, that determine the G-genotype and P-genotype, respectively [1]. Furthermore, RVA can be separated into two main genogroups and one minor genogroup according to a whole-genome classification system, whereby a specific genotype is assigned to the 11 gene segments. These genogroups represent the genotype constellations that are present in most human strains globally [5,6]. Genogroup 1 (Wa-like) bears the constellation I1-R1-C1-M1-A1-N1-T1-E1-H1 and is often associated with the G genotypes G1, G3, G4, G9, and G12 and P genotype P[8]. Genogroup 2 (DS-1-like) includes G2P[4] strains and bears the constellation I2-R2-C2-M2-A2-N2-T2-E2-H2. Lastly, the minor genogroup 3 (AU-1-like) bears the I3-R3-C3-M3-A3-N3-T3-E3-H3 constellation and includes G3P[9] strains [7]. As of 5th May 2020, the Rotavirus Classification Working Group had identified at least 36 G, 51 P, 26 I, 22 R, 20 C, 20 M, 31 A, 22 N, 22 T, 27 E, and 22 H genotypes [8]. The whole-genome classification system has made it possible to analyse and understand the origin of various strains, interspecies transmission, and animal–human reassortment events [9]. Human Wa-like strains and porcine rotavirus strains share a common origin, whereas DS-1-like and AU-1-like strains have a common origin with bovine and feline strains, respectively [5].

In humans, G1–G4, G9, and G12 along with P[4], P[6], and P[8] are the most frequently detected, globally [10–13]. On the contrary, in porcine, predominant genotypes are G3–G5, G9, and G11 along with P[6], P[7], and P[13] [4,14]. Porcine rotaviruses bear the constellation I5-R1-C1-M1-A8-N1-T1/T7-E1-H1 [5,15–20]. While human Wa-like RVA differ from porcine rotaviruses in some gene segments (VP4, VP6, VP7, and NSP1), they both appear to have genotype 1 in the VP1, VP2, VP3, NSP2, NSP3, NSP4, and NSP5 gene segments. Hence, the suggestion that human Wa-like and porcine RVAs have arisen from a common ancestor [5].

The findings that show animals can serve as potential reservoirs for genetically diverse rotavirus strains that can be passed on to humans have elicited a large amount of interest and topics for further research [21]. Several novel and rare animal-like or animal–human reassortant rotavirus strains have been identified globally [22–28]. The detection of animal strains in humans is presumed to be as a result of zoonotic transmission, along with reassortment, which contributes to the diversity of circulating RVA [4,29,30]. Inter- and intragenogroup reassortment may occur when multiple RVA simultaneously infect a host. This is attributed to the segmented nature of the rotavirus genome [1,31]. It is, therefore, necessary to continuously carry out the monitoring of animal RVA and the role they play in contributing to the diversity of circulating RVA in humans.

The G5, one of the most common porcine genotypes, has sporadically been identified in human populations in Brazil (G5P[X]), Cameroon (G5P[7] and G5P[8]), Argentina (G5P[8]), and the United Kingdom (G5P[X]) [32–36]. The P[6] is presumed to be of porcine origin. They have also been identified in human populations [37–40]. The first human G5P[6] strain, LL36755, was detected in a child who had acute gastroenteritis in China in 2007 [41]. Other G5P[6] strains were detected in Vietnam, Taiwan, Bulgaria, Japan, and Thailand [37,42–45]. To date, the whole-genome of only two human G5P[6] strains—Bulgarian BG620 (nt sequences unavailable in the DDBJ, EMBL, and GenBank data libraries as of 13 August 2020) and Japanese Ryukyu-1120 (full open reading frame, available in GenBank)—have been analysed [45,46].

Diarrhoea is a burden for the Zambian healthcare system, with about 33% of the extreme cases being attributable to RVA [47–49]. In an attempt to generate disease burden attributable to rotavirus diarrhoea in children, the Zambian Ministry of Health, with support from WHO, launched rotavirus surveillance at the University Teaching Hospital (UTH) in 2006 [50,51]. Surveillance data generated provided evidence of the burden of rotavirus diarrhoea that supported the introduction of the rotavirus vaccine, Rotarix<sup>®</sup>, as a pilot project in Lusaka, Zambia in 2012, and was later rolled out nationwide in November 2013 [50]. According to the estimates reported by the World Health Organization (WHO) and the United Nations International Children’s Emergency Fund (WHO/UNICEF), rotavirus vaccine coverage in Zambia has been consistently high for the last six years, increasing from 73% in 2014 to 90% in 2019 [52]. Over this period, a sustained and significant reduction in rotavirus-associated hospitalisations and mortality was observed in children under 5 years [51].

The African Rotavirus Surveillance Network, coordinated by the World Health Organization Regional Office for Africa (WHO/AFRO), is actively monitoring the diversity and distribution of RVA genotypes in children hospitalised with acute diarrhoea [53]. Initially, the network was established with four countries in 2006, and expanded to 29 countries by the end of 2016 [54,55]. The Diarrhoeal Pathogens Research Unit at Sefako Makgatho University in Pretoria (South Africa) and the Noguchi Memorial Institute for Medical Research in Accra (Ghana) are the two WHO Rotavirus Regional Reference Laboratories (RRLs) for the network that conducts monitoring of rotavirus epidemiology in Africa [55]. The WHO/AFRO is currently supporting the University of the Free State-Next Generation Sequencing (UFS-NGS) unit to undertake rotavirus surveillance of rotavirus strains that circulated in Zambia between 2013 and 2016 at the whole-genome level. A G5P[6] strain, UFS-NGS-MRC-DPRU4723, was identified among these strains and was analysed so as to elucidate its origin and evolution. The sample was collected in 2014 from an unvaccinated 12 month old male hospitalised for gastroenteritis at Arthur Davison Children’s Hospital in Ndola, Zambia.

## **2. Results**

### *2.1. Nucleotide Sequencing and Identity of the Strain*

Illumina<sup>®</sup> MiSeq sequencing exhibited a phred score of Q30 and collectively yielded 98.8 Mbs of data for this specific sample. The whole genome of RVA/Human-wt/ ZMB/UFS-NGS-MRC-DPRU4723/2014/G5P[6] was 18272 bps in size. The length and ORF of the 11 gene segments as determined by nucleotide sequencing are shown in Table 1. A BLASTn search was performed, and it appeared to exhibit maximum sequence identities of 95.7%–98.0% with porcine and human porcine-like strains (Table 1). Based on the whole genome classification system, RVA/Human-wt/ZMB/UFS-NGS-MRC-DPRU4723/2014/G5P[6] exhibited a G5-P[6]-I1-R1-C1-M1-A8-N1-T1-E1-H1 genotype constellation (Table 2). The genetic constellation of the study strain was compared to those of other G5 and non-G5 strains retrieved from the GenBank (Table 2).

**Table 1.** The segment and ORF lengths of strain UFS-NGS-MRC-DPRU4723 and the highest sequence identities obtained using the Basic Local Alignment Search Tool (BLAST).

GENOME SEGMENT Encoding	GenBank Accession no.	Segment Length	ORF Length	Results of Blast Search			
				Most Similar Strain	GenBank Accession no.	Similarity (%)	Reference
VP1	MT271025	3302	3267	GX54	KF041441	96.7	[56]
VP2	MT271026	2673	2673	R1207	LC389886	96.5	[57]
VP3	MT271027	2591	2508	R946	KF726060	95.7	[58]
VP4	MT271028	2359	2328	KisB332	KJ870903	98.0	[59]
NSP1	MT271029	1512	1482	NT0042	LC095894	98.1	[60]
VP6	MT271030	1356	1194	KYE-14-A048	KX988279	98.7	[29]
NSP3	MT271031	1076	942	12070-4	KX363287	97.1	[61]
NSP2	MT271032	954	954	YN	KJ466987	96.8	[https://www.ncbi.nlm.nih.gov/nucore/KJ466987]
VP7	MT271033	1054	981	JN-2	KT820777	98.0	[https://www.ncbi.nlm.nih.gov/nucore/KT820777]
NSP4	MT271034	751	528	14150-54	KX363354	97.7	[61]
NSP5	MT271035	644	594	R479	GU189559	97.6	[62]

## 2.2. Sequence and Phylogenetic Analysis

To investigate the potential origin of RVA/Human-wt/ZMB/UFS-NGS-MRC-DPRU4723/2014/G5P[6], phylogenetic trees were constructed for each of the 11 gene segments along with cognate gene sequences of RVA strains obtained from the GenBank.

### 2.2.1. Sequence and Phylogenetic Analysis of the VP7 Gene

Phylogenetically, there are three known VP7 G5 lineages (I-III) [63]. The VP7 genes of RVA/Human-wt/ZMB/UFS-NGS-MRC-DPRU4723/2014/G5P[6] clustered into lineage II, which consisted only of porcine G5 strains from mainly Asia and the Americas (Figure 1). The VP7 gene showed the highest nucleotide (nt) and amino acid (aa) identities with the Chinese porcine strains RVA/Pig-wt/CHN/DZ-2/2013/G5P[X] nt (aa), 98.6% (99.0%), and RVA/Pig-wt/CHN/JN-2/2014/G5P[X] 98.5% (99.0%) and was distantly related to the strains within lineage III with lower sequence identities (nt, 83.4%–86.5%; aa, 90.4%–94.5%) (Figure 1; Supplementary data 1). Overall, strains within lineage II exhibited sequence identities that were in the range nt, 89.6%–98.6%; aa, 92.4%–99.0% (Supplementary data 1).

The comparison of the amino acid sequence of RVA/Human-wt/ZMB/UFS-NGS-MRC-DPRU4723/2014/G5P[6] to reference G5 strains e.g., RVA/Pig-wt/THA/CMP-001-12/2012/G5P[13] (lineage I), RVA/Pig-wt/BRA/ROTA24/2013/G5P[6] (lineage II) and RVA/Human-wt/JPN/Ryukyu-1120/2011/G5P[6] (lineage III) within each of the three lineages revealed a high identity (range 90.0%–94.9% (Supplementary data 1; Supplementary data 2a). Numerous substitutions were identified in the nine VP7 variable regions, VR-1 to VR-9 [64]: VR-1 (I9V and I19V), VR-2 (V27T and V29T), VR-3 M/F39L, I40V, V41I, L/I43V, I/L/V47F, R49K, and A50T), VR-4 (K/A65T, V/M68A, M/A72T, and M/Q75T), VR-5/antigenic site A (N/S/D/T96A), VR-6 (I129V and D130E), VR-7/antigenic site B (N145D and A/V/E146G), VR-8/antigenic site C (L/S208T, A210T, T/V212I, S/A213I, I/M217T, V218I, and S220N), and VR-9/antigenic site F (A/M241T and S242N).

**Table 2.** Genotype natures of the 11 gene segments of Zambian strain UFS-NGS-MRC-DPRU4723 compared with those of selected human and porcine strains.

Strain	Genotype										
	VP7	VP4	VP6	VP1	VP2	VP3	NSP1	NSP2	NSP3	NSP4	NSP5
<b>RVA/Human-wt/ZMB/UFS-NGS-MRC-DPRU4723/2014/G5P[6]</b>	<b>G5</b>	<b>P[6]</b>	<b>I1</b>	<b>R1</b>	<b>C1</b>	<b>M1</b>	<b>A8</b>	<b>N1</b>	<b>T1</b>	<b>E1</b>	<b>H1</b>
RVA/Human-wt/BGR/BG260/2008/G5P[6] *	G5	P[6]	I1	R1	C1	M1	A8	N1	T1	E1	H1
RVA/Human-wt/JPN/Ryukyu-1120/2011/G5P[6]	G5	P[6]	I5	R1	C1	M1	A8	N1	T1	E1	H1
RVA/Human-wt/CHN/LL3354/2000/G5P[6]	G5	P[6]	I5	-	-	-	-	-	-	E1	-
RVA/Human-wt/CHN/LL4260/2001/G5P[6]	G5	P[6]	-	-	-	-	-	-	-	E1	-
RVA/Human-wt/CHN/LL36755/2003/G5P[6]	G5	P[6]	-	-	-	-	-	-	-	E1	-
RVA/Human-wt/VNM/KH210/2004/G5P[6]	G5	P[6]	-	-	-	-	-	-	-	E1	-
RVA/Human-wt/TWN/03-98P50/2009/G5P[6] *	G5	P[6]	I5	-	-	-	-	-	-	E1	-
RVA/Human-wt/CMR/6784/ARN/2000/G5P[7]	G5	P[7]	I5	R1	C1	M1	A1	N1	T1	E1	H1
RVA/Human-tc/BRA/IAL28/1992/G5P[8]	G5	P[8]	I5	R1	C1	M1	A1	N1	T1	E1	H1
RVA/Pig-tc/USA/OSU/1975/G5P[7]	G5	P[7]	I5	R1	C1	M1	A1	N1	T1	E1	H1
RVA/Pig-wt/BEL/12R002/2012/G5P[7]	G5	P[7]	I5	R1	C1	M1	A8	N1	T7	E1	H1
RVA/Pig-wt/JPN/BU2/2014/G5P[7]	G5	P[7]	I5	R1	C1	M1	A8	N1	T1	E1	H1
RVA/Human-tc/USA/Wa/1974/G1P[8]	G1	P[8]	I1	R1	C1	M1	A1	N1	T1	E1	H1
RVA/Human-tc/USA/DS-1/1976/G2P[4]	G2	P[4]	I2	R2	C2	M2	A2	N2	T2	E2	H2
RVA/Human-tc/JPN/AU-1/1982/G3P[9]	G3	P[9]	I3	R3	C3	M3	A3	N3	T3	E3	H3
RVA/Pig-wt/BEL/12R006/2012/G3P[6]	G3	P[6]	I5	R1	C1	M1	A8	N1	T1	E1	H1
RVA/Human-tc/GBR/ST3/1974/G4P[6]	G4	P[6]	I1	R1	C1	M1	A1	N1	T1	E1	H1
RVA/Pig-tc/USA/Gottfried/1975/G4P[6]	G4	P[6]	I1	R1	C1	M1	A8	N1	T1	E1	H1
RVA/Human-tc/CHN/R479/2004/G4P[6]	G4	P[6]	I5	R1	C1	M1	A1	N1	T7	E1	H1
RVA/Human-wt/CHN/E931/2008/G4P[6]	G4	P[6]	I1	R1	C1	M1	A8	N1	T1	E1	H1
RVA/Human-wt/COD/KisB332/2008/G4P[6]	G4	P[6]	I1	R1	C1	M1	A1	N1	T7	E1	H1
RVA/Human-wt/CHN/GX54/2010/G4P[6]	G4	P[6]	I1	R1	C1	M1	A8	N1	T1	E1	H1

Table 2. Cont.

Strain	Genotype										
	VP7	VP4	VP6	VP1	VP2	VP3	NSP1	NSP2	NSP3	NSP4	NSP5
RVA/Pig-wt/BEL/12R005/2012/G4P[7]	G4	P[7]	I5	R1	C1	M1	A8	N1	T7	E1	H1
RVA/Human-wt/BEL/BE2001/2009/G9P[6]	G9	P[6]	I5	R1	C1	M1	A8	N1	T7	E1	H1
RVA/Human-tc/USA/WI61/1983/G9P[8]	G9	P[8]	I1	R1	C1	M1	A1	N1	T1	E1	H1
RVA/Human-wt/BEL/B3458/2003/G9P[8]	G9	P[8]	I1	R1	C1	M1	A1	N1	T1	E1	H1
RVA/Human-tc/IND/mani-97/2006/G9P[19]	G9	P[19]	I5	R1	C1	M1	A8	N1	T1	E1	H1
RVA/Human-wt/BGD/Dhaka6/2001/G11P[25]	G11	P[25]	I1	R1	C1	M1	A1	N1	T1	E1	H1
RVA/Human-wt/VNM/30378/2009/G26P[19]	G26	P[19]	I5	R1	C1	M1	A8	N1	T1	E1	H1
RVA/Human-wt/BRA/rj24598/2015/G26P[19]	G26	P[19]	I5	R1	C1	M1	A8	N1	T1	E1	H1

Blue shading indicates the gene segments with genotypes identical to those of UFS-NGS-MRC-DPRU4723. Bold font indicates genotypes associated with porcine strains. “-” indicates that no sequence data were available in GenBank/EMBL/DDBJ data banks. \* Genotype assignment based on reports by [37] (strain 03-98sP50) and (strain BG260) [46]. To date, the nucleotide accession numbers for the 11 gene segments of strains 03-98sP50 and BG260 are not available in the GenBank, EMBL, or DDBJ data banks.

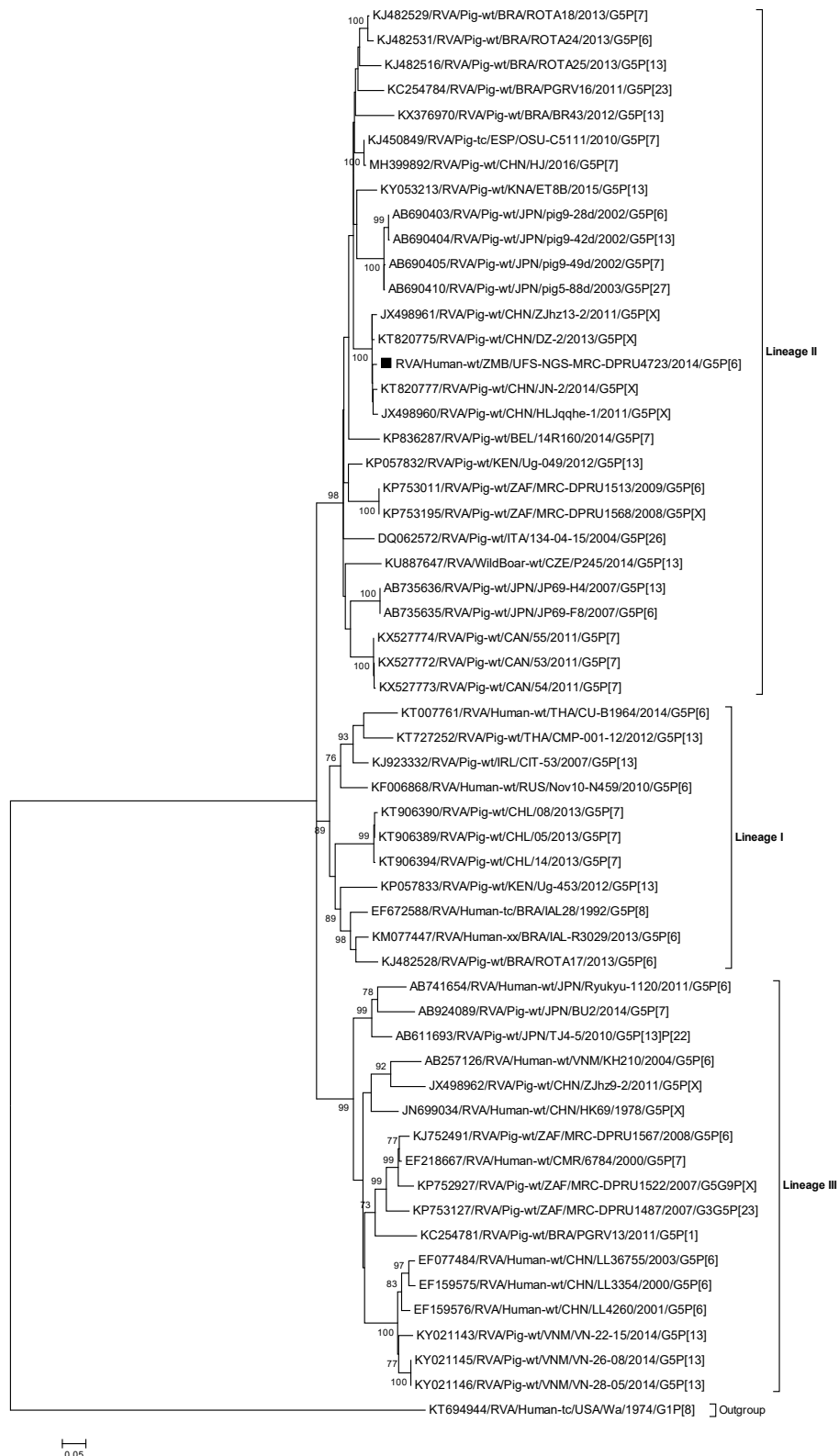


**Figure 1.** Phylogenetic tree constructed from the nucleotide sequences of the VP7 genes of strain RVA/Human-wt/ZMB/UFS-NGS-MRC-DPRU4723/2014/G5P[6] and representative strains. The position of strain RVA/Human-wt/ZMB/UFS-NGS-MRC-DPRU4723/2014/G5P[6] is shown by the black square (■). Reference strains obtained from GenBank are represented by accession number, strain name, country, and year of isolation. The three closest strains, as identified by BLASTn, are also included. Bootstrap values  $\geq 70\%$  are shown adjacent to each branch node. Scale bar: 0.05 substitutions per nucleotide.

### 2.2.2. Sequence and Phylogenetic Analysis of the VP4 Gene

The VP4 gene of RVA/Human-wt/ZMB/UFS-NGS-MRC-DPRU4723/2014/G5P[6] was phylogenetically compared to the already established five lineages (I-V) of genotype P[6] [65] (Figure 2). The P[6] gene of the study strain clustered into lineage V, which consisted of porcine and putative human porcine-like strains detected in parts of Europe and one African strain. A similarity analysis of the P[6] gene of the study strain with strains obtained from GenBank showed that the Zambian G5P[6] exhibited the highest sequence identity of 98.1% (98.3%) with a porcine-like human strain RVA/Human-wt/COD/KisB332/2008/G4P[6] from the Democratic Republic of Congo (Supplementary data 1). All the African strains clustered into a separate lineage, lineage I, with sequence identities of 85.7%–86.8% (92.5%–93.9%) (Supplementary data 1).

The deduced amino acid sequences of the VP4 gene of RVA/Human-wt/ZMB/UFS-NGS-MRC-DPRU4723/2014/G5P[6] along with the reference P[6] strain from each of the five lineages was compared (Supplementary data 2b). The reference strains shared high amino acid identities ranging from 91.0% to 98.3% (Supplementary data 1). Several amino acid changes were identified throughout the VP4 protein, and most of the substitutions were concentrated in the hypervariable region (amino acid 71–208) which houses the VR-3 (92–192) and includes a neutralization site at amino acid 135 [66,67]. Several amino acid substitutions were observed among the P[6] lineage I strains [65] at the VR-3 (L105I, V108I and T134S) and VR-8 (D602N) variable regions. Other amino acid substitutions were identified among the P[6] lineages at VR-1 (S30N), VR-2 (I61V), VR-3 (V112I, N114S, V130I, H182N and T189S), VR-4 (I280V), and VR-9 (E698K). The potential trypsin cleavage sites at residues 241 and 247 [68] were highly conserved in all the strains with three substitutions at positions 242 (I to V), 243 (A to T), and 244 (H to Y).

### 2.2.3. Phylogenetic Analysis of the VP6 Gene

The VP6 gene of RVA/Human-wt/ZMB/UFS-NGS-MRC-DPRU4723/2014/G5P[6] clustered closely with divergent African porcine strains from Uganda (RVA/Pig-wt/UGA/BUW-14-A003/2014/G3P[13], RVA/Pig-wt/UGA/KYE-14-A048/2014/G3P[13], and RVA/Pig-wt/UGA/KYE-14-A047/2014/G3P[13]) and a human porcine-like strain from the Democratic Republic of Congo (RVA/Human-wt/COD/KisB332/2008/G4P[6]) which displayed nt(aa) sequence identities ranging from 98.6% to 98.9% (98.9%–99.7%) (Figure 3, Supplementary data 1). Porcine-like Asian strains such as RVA/Human-wt/CHN/GX54/2010/G4P[6] and RVA/Human-wt/CHN/E931/2008/G4P[6] clustered separately, displaying identities of 88.7%–90.2% (97.5%–98.7%) (Supplementary data 1).

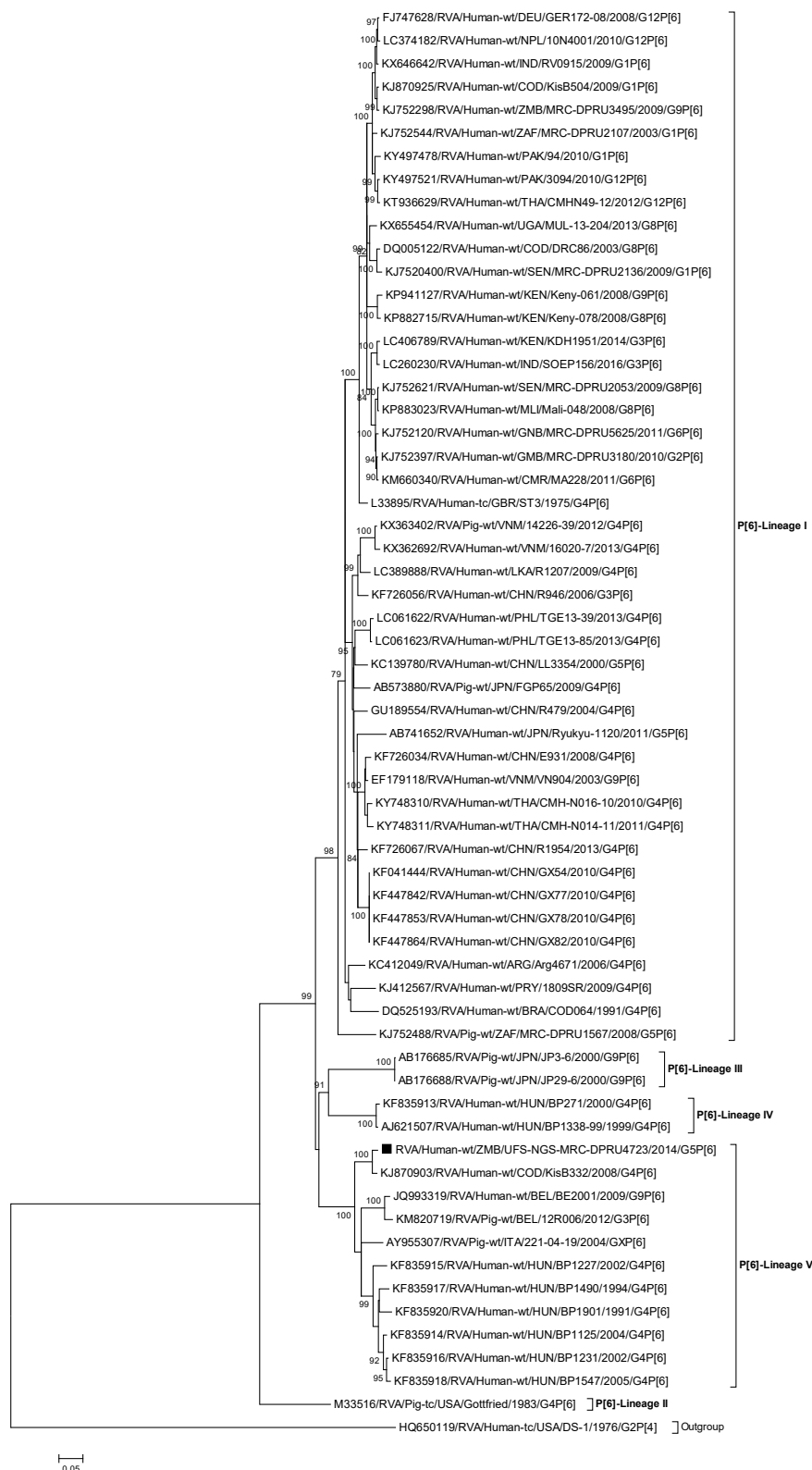


**Figure 2.** Phylogenetic tree constructed from the nucleotide sequences of the VP4 genes of strain RVA/Human-wt/ZMB/UFS-NGS-MRC-DPRU4723/2014/G5P[6] and representative strains. The position of strain RVA/Human-wt/ZMB/UFS-NGS-MRC-DPRU4723/2014/G5P[6] is shown by the black square (■). Reference strains obtained from GenBank are represented by accession number, strain name, country, and year of isolation. The three closest strains, as identified by BLASTn, are also included. Bootstrap values  $\geq 70\%$  are shown adjacent to each branch node. Scale bar: 0.05 substitutions per nucleotide.

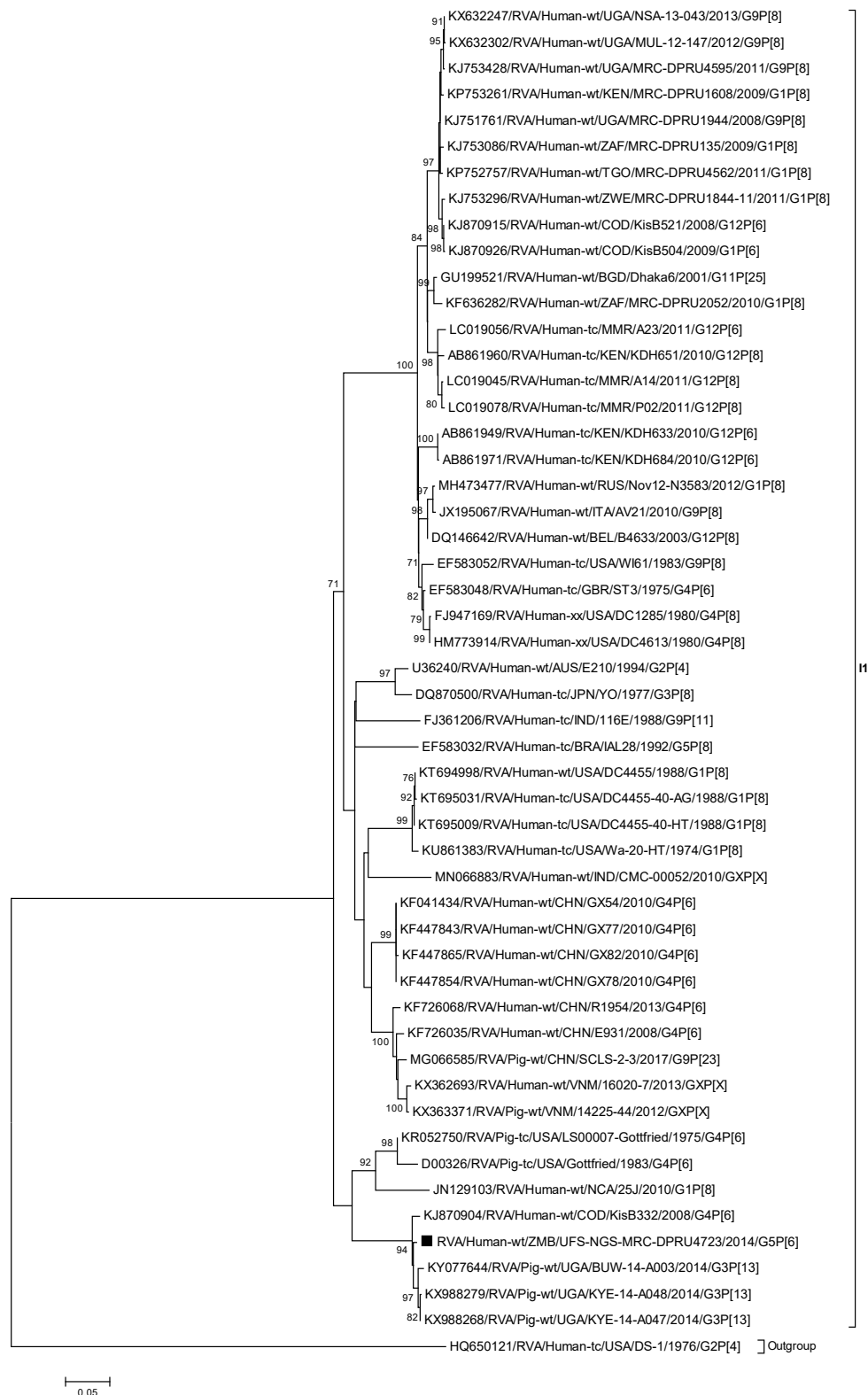


**Figure 3.** Phylogenetic tree constructed from the nucleotide sequences of the VP6 genes of strain RVA/Human-wt/ZMB/UFS-NGS-MRC-DPRU4723/2014/G5P[6] and representative strains. The position of strain RVA/Human-wt/ZMB/UFS-NGS-MRC-DPRU4723/2014/G5P[6] is shown by the black square (■). Reference strains obtained from GenBank are represented by accession number, strain name, country, and year of isolation. The three closest strains, as identified by BLASTn, are also included. Bootstrap values  $\geq 70\%$  are shown adjacent to each branch node. Scale bar: 0.05 substitutions per nucleotide.

#### 2.2.4. Phylogenetic Analysis of VP1 Gene

The VP1 gene of RVA/Human-wt/ZMB/UFS-NGS-MRC-DPRU4723/2014/G5P[6] clustered only with porcine and porcine-like human strains from Asia (China and Vietnam) (Supplementary data 3a). The VP1 gene exhibited a maximum nt (aa) sequence identity of 96.8% (98.9%) with the Chinese human porcine-like reassortant strains RVA/Human-wt/CHN/GX82/2010/G4P[6], RVA/Human-wt/CHN/GX78/2010/G4P[6], RVA/Human-wt/CHN/GX77/2010/G4P[6], and RVA/Human-wt/CHN/GX54/2010/G4P[6] (Supplementary data 1). Overall, the Asian strains within the cluster showed sequence identities of 94.1%–96.8% (97.9%–98.9%). Human non-porcine African strains clustered separately, with lower identities of 88.2%–88.8% (96.3%–97.3%) (Supplementary data 1).

#### 2.2.5. Phylogenetic Analysis of VP2 Gene

The VP2 gene of strain RVA/Human-wt/ZMB/UFS-NGS-MRC-DPRU4723/2014/G5P[6] fell into a distinct cluster predominantly composed of porcine and porcine-like human strains from Asia (China, India, Vietnam, South Korea, and Sri Lanka) (Supplementary data 3b). The VP2 gene of the study strain showed a maximum nt (aa) sequence identity of 96.6% (90.9%) with a Sri Lankan porcine-like human strain RVA/Human-wt/LKA/R1207/2009/G4P[6] (Supplementary data 1).

#### 2.2.6. Phylogenetic Analysis of VP3 Gene

The VP3 gene of strain RVA/Human-wt/ZMB/UFS-NGS-MRC-DPRU4723/2014/G5P[6] clustered in a lineage composed mainly of Asian (Asia and Thailand) porcine and porcine-like human strains (Supplementary data 3c), and exhibited the highest nt (aa) sequence identity with the Chinese porcine-like human strains—RVA/Human-wt/CHN/R946/2006/G3P[6], 95.8% (97.8%) and RVA/Human-wt/CHN/E931/2008/G4P[6], 95.7% (98.0%) (Supplementary data 1). The overall similarities of the Asian strains within the lineage ranged from 84.8% to 95.8% (92.7%–97.8%) (Supplementary data 1). Non-porcine African strains clustered separately and showed lower sequence identities of 84.1%–84.5% (92.1%–92.7%) (Supplementary data 1).

#### 2.2.7. Phylogenetic Analysis of NSP1 Gene

The NSP1 gene of strain RVA/Human-wt/ZMB/UFS-NSG-MRC-DPRU4723/2014/G5P[6] was assigned to a porcine genotype A8 and clustered among Asian (Vietnam, China, and Bangladesh) porcine and porcine-like human strains and an African (Ghana) porcine strain (Supplementary data 3d). The NSP1 gene of the study strain was closest to strain RVA/Human-tc/VNM/NT0042/2007/G4P[6] displaying a nt(aa) sequence identity of 98.2% (97.9%) (Supplementary data 1). The porcine and porcine-like human strains from Europe and the Americas clustered separately showing sequence identities of 84.2%–85.9% (85.4%–88.2%) and 84.1%–85.9% (83.7%–88.3%), respectively (Supplementary data 1).

#### 2.2.8. Phylogenetic Analysis of NSP2 Gene

The NSP2 gene of strain RVA/Human-wt/ZMB/UFS-NGS-MRC-DPRU4723/2014/G5P[6] clustered with Asian and European porcine and porcine-like human strains (Supplementary data 3e). The Nt(aa) similarity analysis showed that the NSP2 gene of the study strain was most similar to the Chinese porcine strains RVA/Pig-wt/CHN/YN/2012/GXP[X] and RVA/Pig-tc/CHN/SCMY-A3/2017/G9P[23]—96.8% (97.8%) (Supplementary data 1). Two African porcine strains, RVA/Pig-wt/ZAF/MRC-DPRU1487/2007/G3G5P[23] and RVA/Pig-wt/ZAF/MRC-DPRU1557/2008/G4G5P[23], were seen to cluster within the same lineage with sequence identities of 93.6%–93.7% (97.5%–97.8%) (Supplementary data 1).

#### 2.2.9. Phylogenetic Analysis of NSP3 Gene

The NSP3 gene of strain RVA/Human-wt/ZMB/UFS-NGS-MRC-DPRU4723/2014/G5P[6] clustered closely with porcine and porcine-like human strains mainly from Asia (Thailand and

Vietnam) and exhibited a maximum nt(aa) sequence identities of 96.5%–97.0% (98.4%–98.7%) with the strains RVA/Human-wt/VNM/30378/2009/G26P[19], RVA/Pig-wt/VNM/12070-4/2012/GXP[X], RVA/Human-wt/VNM/NT0205/2007/G4P[6], and RVA/Human-wt/VNM/NT0621/2008/G4P[6] (Supplementary data 1; Supplementary data 3f).

#### 2.2.10. Phylogenetic Analysis of NSP4 Gene

The NSP4 gene of strain RVA/Human-wt/ZMB/UFS-NGS-MRC-DPRU4723/2014/G5P[6] clustered with porcine and porcine-like human strains identified in Asia (China and Vietnam) and a porcine-like human strain from the Americas (Brazil) (Supplementary data 3g). In this cluster, the closest strains to UFS-NGS-MRC-DPRU4723 were the wild pig strains (RVA/WildBoar-wt/CZE/P828/2015/G9P[23] and RVA/WildBoar-wt/CZE/P830/2015/G9P[23]) from the Czech Republic, with nt(aa) sequence identities of 97.5% (98.3%) (Supplementary data 1). The Asian strains within the cluster showed nt(aa) similarities of 96.2%–97.3% (97.7%–98.9%). Porcine and porcine-like human strains from the Americas clustered separately and exhibited identities of 87.2%–96.4% (94.3%–98.9%) (Supplementary data 1).

#### 2.2.11. Phylogenetic Analysis of the NSP5 Gene

The NSP5 gene of strain RVA/Human-wt/ZMB/UFS-NGS-MRC-DPRU4723/2014/G5P[6] clustered with porcine strains from Asia and showed the highest nt(aa) sequence identity of 98.6% (100%) with the porcine strains RVA/Pig-wt/CHN/TM-a/2009/G3P[8] and RVA/Pig-tc/CHN/TM-a-P20/2018/G9P[23] identified in China (Supplementary data 1; Supplementary data 3h). Overall, the porcine and porcine-like human strains from Asia and the Americas displayed nt(aa) identities of in the range 94.8%–98.6% (98.0%–100%) and 93.9%–96.1% (95.9%–99.0%), respectively (Supplementary data 1).

### 2.3. Reassortment Analysis

The concatenated whole genome alignment of RVA/Human-wt/ZMB/UFS-NGS-MRC-DPRU4723/2014/G5P[6], together with the Japanese G5P[6] strain and selected Chinese porcine-like human P[6] strains, was visualised (Figure 4). The whole genome of the Zambian G5P[6] strain demonstrated a relatively high degree of conservation with the Japanese G5P[6] strain and the two Chinese G4P[6] strains. With the exception of VP7 and VP4, the genome of the Chinese strain E931 exhibited the overall highest genomic conservation to the study strain. With the exception of VP7, VP3, and NSP1 genes, the Chinese strain GX54 shared a highly conserved genome with the study strain. The Japanese strain Ryukyu-1120 demonstrated a highly similar genome to the study strain for seven of the 11 genes, the exceptions being VP1, VP3, VP6, and VP7. The results of this analysis confirmed the genetic similarity between RVA/Human-wt/ZMB/UFS-NGS-MRC-DPRU4723/2014/G5P[6] and Asian (Chinese) porcine-like human strains, hence suggesting that the Zambian G5P[6] strain may have been derived via reassortment events.

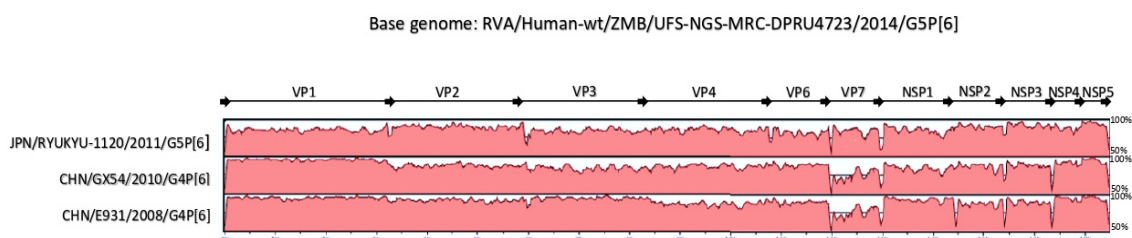


**Figure 4.** mVISTA whole genome nucleotide alignment comparing the Zambian G5P[6] strain (RVA/Human-wt/ZMB/UFS-NGS-MRC-DPRU4723/2014G5P[6]) with the G5P[6] strain from Japan (Ryukyu-1120), whose whole genome sequence had been determined, and with selected porcine-like human P[6] strains from China (GX54 and E931). Strain names are shown on the left, and the proteins VP1–VP4, VP6–VP7, and NSP1–NSP5 are indicated on the top. The bottom scale indicates distance in kb. Percentile values on the right indicate sequence-based similarity between the study strain and the respective reference strains. Shading indicates the level of conservation.

### 3. Discussion

The detection of genotype G5 in humans, which is typical for pigs, is possibly due to interspecies transmission [35,45]. In Zambia, as with many countries in Africa, humans and farm animals live in proximity. The interaction between humans and animals could be the primary cause for zoonotic transmission, which could result in genetic reassortments and perhaps other mechanisms of genetic diversity, ultimately leading to the introduction and spread of animal genotypes into human populations [69].

In this study, an analysis was conducted on a sample collected from a child admitted to a paediatric ward presenting with clinical symptoms (vomiting, diarrhoea, and fever) that are usually present during typical rotavirus infection. This raises the question whether such animal-derived strains are capable of mutating and effectively spreading within/across human populations as in the case of established typical Wa-like and DS-1-like genotype constellations, with the same magnitude of rotavirus disease severity. Furthermore, taking into consideration that the G5 and P[6] genotypes are not included in the currently available vaccines, the probability for such strains to have the potential to spread more swiftly from human to human may have implications for the effectiveness of current rotavirus vaccine candidates that are in use in African countries.

This study identified the complete genome of a reassortant porcine-like human strain, G5P[6], that showed the genotype constellation G5-P[6]-I1-R1-C1-M1-A8-N1-T1-E1-H1, which is commonly found in porcine and porcine-like human rotavirus strains [19]. RVA/Human-wt/ZMB/UFS-NGS-MRC-DPRU4723/2014/G5P[6] was found to share the same constellation (I1-R1-C1-M1-A8-N1-T1-E1-H1) with the archival porcine strain, Gottfried, and porcine-like human strains—BG260, E931, and GX54 [5,46,56,58]. In addition, porcine strains 12R002, 12R005, and 12R006, as well as porcine-like human strains Ryukyu-1120, mani-97, 30378, rj24598, and BE2001 shared the same constellation with strain RVA/Human-wt/ZMB/UFS-NGS-MRC-DPRU4723/2014/G5P[6] with the exception of VP6 (I5 instead of I1) and NSP3 (T7 instead of T1 gene segments) [20,25,26,45,70].

A phylogenetic analysis of RVA/Human-wt/ZMB/UFS-NGS-MRC-DPRU4723/2014/G5P[6] showed that this strain was a possible reassortant, as it was closely related to both porcine and porcine-like human strains, predominantly from Asia, than to typical human RVA strains. The VP6, VP7, NSP2, NSP4, and NSP5 segments of this strain showed a close similarity to porcine strains. Although the remaining gene segments (VP1, VP3, VP4, and NSP3) were closely related to human strains, all of these were porcine-like human strains [26,56,58–60,70]. With a genotype 1 (Wa-like) backbone, this finding is consistent with the hypothesis that human Wa-like strains and porcine strains have a common ancestor [5]. However, the origin of the VP2 gene of the study strain was not very definitive, as it was not only close to porcine and porcine-like human strains but also to three human strains (DC1476, DC582, and DC1127). Phylogenetically, the clusters of these three strains were shown to be distinctive from the genes of contemporary, wild-type human strains [71]. Notably, the VP7 gene of RVA/Human-wt/ZMB/UFS-NGS-MRC-DPRU4723/2014/G5P[6] was located in lineage II, which comprised only porcine strains, hence implying the possibility of porcine-to-human interspecies transmission [63]. Phylogenetic analysis of porcine and human P[6] strains indicated that both porcine and human P[6] strains were present in P[6] lineages I, III, and V, hence showing that human P[6] strains might have separately emerged from at least three porcine-to-human transmissions [65]. This finding supports the Zambian G5P[6] strain, as the VP4 gene clustered and shared high nucleotide and amino acid identities with lineage V of P[6] porcine and porcine-like human strains. The NSP1 gene was most similar to porcine-like human strains. However, it was revealed to have the porcine genotype A8. Taking this together, it is likely that RVA/Human-wt/ZMB/UFS-NGS-MRC-DPRU4723/2014/G5P[6] originated by zoonotic transmission, coupled with reassortment events.

Several amino acid changes were identified in the nine variable regions when the VP7 gene of the study strain was compared to other G5 strains within each of the three lineages [64]. Additionally, the previously described conserved N-glycosylation site at residues 69–71 within the variable region 4 (VR-4) was found to be conserved in all the G5 strains used in this analysis [64,72]. Four major

antigenic regions have been described for the VP7 protein in rotaviruses (A, B, C and F) [73,74]. Marked differences in the antigenic regions of RVA/Human-wt/ZMB/UFS-NGS-MRC-DPRU4723/2014/G5P[6] were seen when it was compared to other globally circulating G5 strains. Usually, antigenic regions A and C are said to be conserved within serotypes [75]. However, multiple substitutions were observed in these regions when comparing the Zambian G5 strain to other G5 strains globally.

The amino acid sequence for the VP4 gene was 775 amino acids long and displayed amino acid identity values ranging from 91.0% to 98.3% with the reference P[6] strains. Considering it has been established that strains with amino acid identities greater than 89% belong to the same P genotype [76], our findings show that RVA/Human-wt/ZMB/UFS-NGS-MRC-DPRU4723/2014/G5P[6] belongs to the genotype P[6]. The analysis of the amino acid sequences showed that the hypervariable region (amino acid 71-208) which houses the variable region 3 (VR-3) contained most of the substitutions. Furthermore, the potential trypsin cleavage sites [68] were conserved in all the P[6] strains. Several amino acid substitutions were observed among the lineage I P[6] strains. The presence of several amino acid changes in the VP4 gene of this strain compared to other circulating P[6] strains globally is in agreement with the hypothesis that the P[6] gene has been introduced to humans via independent reassortment events [40,65,77].

Rotaviruses are genetically diverse in nature and are host-species specific, suggesting that host species barriers and restrictions exist. However, rotaviruses of animal origin may cross the host species barrier and may acquire human rotavirus gene segments, which enables the viruses to efficiently spread across human populations [4]. In this regard, G5 rotavirus strains have sporadically been documented in Latin America, Asia, Europe, and Africa [33–37,41,45,46]. Porcine P[6] strains seem to pose a lesser species barrier to humans [20]. Even though the relationship between porcine and human rotaviruses has already been established [5], whole genome analysis in this study presented the possible occurrence of interspecies transmission and reassortment between human and porcine rotaviruses.

## **4. Materials and Methods**

### *4.1. Ethics Statement*

This is a subset of a major project which involved the whole genome characterisation of 133 specimens collected in Zambia from 2013 through 2016 as part of the surveillance supported by the WHO/AFRO (reference 2017/757922-0) in collaboration with the University of the Free State (UFS-NGS). Ethical clearance for the main project was obtained under ethics number HSREC130/2016(UFS-HSD2016/1082) from the Health Science Research Ethics Committee (HSREC), University of the Free State, Bloemfontein, South Africa. Furthermore, this specific study was approved by the HSREC under ethics number UFS-HSD2020/0277/2104.

### *4.2. Sample Collection*

The sample was collected in 2014 from an unvaccinated 12 month old male at Arthur Davidson Children's Hospital (ADCH) in Ndola, a rotavirus surveillance sentinel site. The child had travelled with parents from Kasama, a town in the Northern Province of Zambia which is approximately 760 km away from Ndola, Zambia. This child was admitted to a paediatric ward at ADCH, with gastroenteritis of four days duration and a history of fever. Frequency of vomiting and diarrhoea was three episodes and two episodes, respectively, in the previous 24 h. The level of dehydration was assessed as mild and the child received an oral rehydration solution and was discharged after a few days. The stool sample was screened using the enzyme immunoassay (EIA) technique for the presence of RVA antigen in the Virology laboratory in Lusaka. It was randomly picked and sent to the Diarrhoeal Pathogens Research Unit (DPRU), a World Health Organization Rotavirus Regional Reference Laboratory (WHO-RRL) in Pretoria, South Africa, as part of the WHO/AFRO annual rotavirus surveillance. Conventional genotyping was carried out at DPRU. Thereafter, the sample was shipped to the UFS-NGS unit for sequencing and whole-genome analysis.

#### 4.3. Viral dsRNA Extraction

The viral double-stranded RNA (dsRNA) was extracted from human stool suspensions using a previously described method with modifications [78]. Approximately 100 mg stool was suspended in 200  $\mu$ L phosphate-buffered saline (PBS) solution (Sigma-Aldrich<sup>®</sup>, St Louis, MO, United States). The faecal suspension was mixed with 900  $\mu$ L TRI Reagent<sup>®</sup> LS (Molecular Research Centre, Cincinnati, OH, United States) and homogenized for five minutes. A 300  $\mu$ L volume of chloroform (Sigma-Aldrich<sup>®</sup>, St Louis, MO, United States) was used to achieve phase separation, which was followed by centrifugation (Eppendorf microcentrifuge 5427 R, Germany) at 17,319 $\times$  *g* for 20 min at 4 °C. The supernatant was precipitated using 700  $\mu$ L ice-cold isopropanol (Sigma-Aldrich<sup>®</sup>, United States) and centrifuged (Eppendorf microcentrifuge 5427 R, Germany) at 17,319 $\times$  *g* for 30 min at 4 °C. The supernatant was discarded, and the tubes were air-dried for 5 min, followed by the precipitation of single-stranded RNA (ssRNA) using 30  $\mu$ L 8 M lithium chloride (Sigma, St Louis, MO, United States) at 4 °C for 16 h. The dsRNA was purified using the MinElute gel extraction kit (Qiagen, Hilden, Germany). RNA integrity was determined by electrophoresis on 1% TBE agarose gel stained with ethidium bromide (Sigma-Aldrich<sup>®</sup>, St Louis, MO, United States), which was visualised on a G: Box UV transilluminator (Syngene, Cambridge, United Kingdom).

#### 4.4. cDNA Synthesis and Purification

cDNA synthesis was carried out using the Maxima H Minus Double-stranded cDNA kit (Thermo Fisher Scientific, Waltham, MA, United States) according to the manufacturer's instructions with minor modifications captured at the UFS-NGS SOP, whereby the dsRNA was denatured at 95 °C for 5 min. First strand synthesis was carried out for two hours at 50 °C. Random hexamer primer was employed for cDNA synthesis. The cDNA was purified using the MSB<sup>®</sup> Spin PCRapace purification kit (Strattec, Invitex Molecular, Berlin, Germany).

#### 4.5. DNA Library Preparation and Illumina<sup>®</sup> MiSeq Sequencing

DNA libraries for Illumina<sup>®</sup> sequencing were prepared using the Nextera<sup>®</sup> XT DNA library preparation kit (Illumina, San Diego, CA, United States) according to the manufacturer's instructions. Briefly, DNA was tagged at 55 °C for five minutes followed by ligation to Illumina<sup>®</sup> sequencing index 1 and index 2 adapters by PCR amplification. Size selection and clean-up of the DNA libraries was performed using Agencourt AMPure XP beads (Beckman Coulter, South Kraemer Boulevard Brea, CA, United States). The quantity of DNA was determined on the Qubit 2.0 fluorimeter (Invitrogen, Carlsbad, CA, United States), and a quality check of the libraries was performed on a Bioanalyzer 2100 (Agilent Technologies, Santa Clara, CA, United States). After this, sequencing was performed on an Illumina<sup>®</sup> MiSeq sequencer (Illumina, San Diego, CA, United States) using a MiSeq reagent kit v3 for 600 cycles (2  $\times$  300 bp paired reads) with a 10% PhiX DNA control spike-in.

#### 4.6. Genome Assembly

The raw reads obtained in FASTQ format were assembled using Geneious Prime<sup>®</sup> 2019.2.1 (<https://www.geneious.com/>; [79]). Briefly, the paired-end reads were merged into single reads and trimmed to remove low quality and short reads. The reads were mapped to reference sequences obtained from GenBank. Consensus sequences covering the complete open reading frame (ORF) were submitted to the National Centre for Biotechnology Information (NCBI) GenBank and assigned accession numbers MT271025–MT271035. The ORF lengths were 3267 (VP1), 2673 (VP2), 2508 (VP3), 2328 (VP4), 1194 (VP6), 981 (VP7), 1482 (NSP1), 954 (NSP2), 942 (NSP3), 528 (NSP4), and 594 (NSP5).

#### 4.7. Assignment of Genotypes

The genotypes of each of the 11 rotavirus genome segments were determined using the online Virus Pathogen Resource (ViPR).

#### 4.8. Phylogenetic Analysis

Gene-specific multiple sequence alignments were made using the MAFFT plugin implemented in Geneious Prime<sup>®</sup> 2019.2.1 and the MUSCLE algorithm embedded in MEGA 6.06 (for the VP2 and NSP1 segments) [80,81]. Once aligned, the DNA Model Test program in MEGA 6.06 was used to identify the optimal evolutionary model for each genome segment [82]. Using an Akaike information criterion (corrected) (AICc), the following models were found to best fit the data: HKY+G+I (VP1), GTR+G+I (VP2, VP3, and VP4), T92+G (VP6, NSP1, NSP2, NSP3, NSP4, and NSP5), and T92+G+I (VP7). Maximum likelihood trees were constructed using the optimal models in MEGA version 6.06 [82,83] with 1000 bootstrap replicates to estimate branch support [84]. The shared nucleotide and amino acid sequence identities among strains were calculated for each gene using the *p*-distance algorithm in MEGA 6.06. Analysis and visualization of the aligned concatenated whole genomes was performed on the mVISTA online platform [85].

#### 5. Conclusions

In summary, RVA/Human-wt/ZMB/UFS-NGS-MRC-DPRU4723/2014/G5P[6] was a reassortant possessing gene segment of porcine and porcine-like human origin, and was closest to Asian strains. It is presumed that pigs play a crucial part as a source for new or newly-evolved emerging human rotaviruses. This highlights the need for continuous large-scale surveillance and whole genome analysis of circulating porcine and human rotaviruses. Furthermore, it was imperative to examine the prevalence of G5P[6] strains in Zambia. Eventually, this should result in a greater understanding of the genes that determine the transmission between hosts successfully as well as to gain insights on complex reassortment patterns between porcine and human rotaviruses.

**Supplementary Materials:** The following are available online at <http://www.mdpi.com/2076-0817/9/8/663/s1>. Supplementary data 1 (S1): Identity matrices for the VP1, VP2, VP3, VP4, VP6, VP7, NSP1, NSP2, NSP3, NSP4, and NSP5 nucleotide and deduced amino acid identities among strains calculated using the *p*-distance algorithm in MEGA 6.06. Supplementary data 2: Comparison of amino acid sequences. Supplementary data 3: Additional phylograms of the VP1, VP2, VP3, NSP1, NSP2, NSP3, NSP4 and NSP5.

**Author Contributions:** M.M.N., M.J.M., M.L.S., and J.M.M. conceptualised the main project. W.M.M., P.N.M., J.S., E.M.M., and M.M.N. performed the laboratory experiments. M.M.N., J.S., E.M.M., M.J.M., I.P., M.L.S., and J.M.M. facilitated the obtaining of the sample. Formal analysis was performed by W.M.M., M.D.E., and M.M.N. Data curation was performed by W.M.M., P.N.M., and M.M.N. Writing (original draft preparation) was performed by W.M.M. Review of the drafts was performed by all co-authors. Supervision, project administration, and funding acquisition was conducted by M.M.N. and J.M.M. All authors have read and agreed to the published version of the manuscript.

**Funding:** This research was principally funded by a grant awarded to M.M.N. by the World Health Organization (agreement number: UFS-AGR17-000378). Other sources of funding that supported the study were grants awarded to M.M.N.: the Bill and Melinda Gates Foundation (BMGF-OPP1180423\_2017), South African Medical Research Foundation through the Self-Initiated Research grant (SAMRC-SIR), National Research Foundation (NRF-120814), and a grant from the Poliomyelitis Research Foundation (PRF-19/95).

**Acknowledgments:** We greatly thank the Zambia team who assisted with sample collection and ELISA testing. We would like to thank Khutso Mothapo, Kebareng Rakau, and Nonkululeko Magagula at the WHO-RRL (Pretoria, South Africa) who assisted with the retrieval of samples. We would also like to thank Sebotsana Rasebotsa, Milton Mogotsi, Emmanuel Ayodeji, Teboho Mooko, and Gilmore Pambuka for their assistance with laboratory work. We are grateful to Stephanus Riekert for technical ICT support.

**Conflicts of Interest:** The authors declare no conflict of interest.

**Disclaimer:** The findings and conclusions in this report are those of the authors and do not necessarily represent the official position of the World Health Organization.

## References

1. Estes, M.K.; Greenberg, H.B. Rotaviruses. In *Fields Virology*, 6th ed.; Knipe, D.M., Howley, P.M., Eds.; Wolters Kluwer Health/Lippincott, Williams and Wilkins: Philadelphia, PA, USA, 2013; pp. 1347–1401.
2. Tate, J.E.; Burton, A.H.; Boschi-Pinto, C.; Parashar, U.D. World Health Organization—Coordinated Global Rotavirus Surveillance Network. Global, regional, and national estimates of rotavirus mortality in children <5 years of age, 2000–2013. *Clin. Infect. Dis.* **2016**, *62* (Suppl. 2), S96–S105. [CrossRef] [PubMed]
3. Troeger, C.; Khalil, I.A.; Rao, P.C.; Cao, S.; Blacker, B.F.; Ahmed, T.; Armah, G.; Bines, J.E.; Brewer, T.G.; Colombara, D.V.; et al. Rotavirus vaccination and the global burden of rotavirus diarrhoea among children younger than 5 years. *JAMA Pediatr.* **2018**, *172*, 958–965. [CrossRef] [PubMed]
4. Martella, V.; Bányai, K.; Matthijssens, J.; Buonavoglia, C.; Ciarlet, M. Zoonotic aspects of rotaviruses. *Vet. Microbiol.* **2010**, *140*, 246–255. [CrossRef] [PubMed]
5. Matthijssens, J.; Ciarlet, M.; Heiman, E.; Arijs, I.; Delbeke, T.; McDonald, S.M.; Palombo, E.A.; Iturriza-Gomara, M.; Maes, P.; Patton, J.T.; et al. Full genome-based classification of rotaviruses reveals a common origin between human Wa-like and porcine rotavirus strains and human DS-1-like and bovine rotavirus strains. *J. Virol.* **2008**, *82*, 3204–3219. [CrossRef]
6. Matthijssens, J.; Ciarlet, M.; McDonald, S.M.; Attoui, H.; Bányai, K.; Brister, J.R.; Buesa, J.; Esona, M.D.; Estes, M.K.; Gentsch, J.R.; et al. Uniformity of rotavirus strain nomenclature proposed by the Rotavirus Classification Working Group (RCWG). *Arch. Virol.* **2011**, *156*, 1397–1413. [CrossRef]
7. Matthijssens, J.; Van Ranst, M. Genotype constellation and evolution of group A rotaviruses infecting humans. *Curr. Opin. Virol.* **2012**, *2*, 426–433. [CrossRef]
8. RCWG. Rotavirus Classification Working Group—Laboratory of Viral Metagenomics. 2018. Available online: <https://rega.kuleuven.be/cev/viralmetagenomics/virus-classification/rcwg> (accessed on 5 May 2020).
9. Ghosh, S.; Kobayashi, N. Whole-genomic analysis of rotavirus strains: Current status and future prospects. *Future Microbiol.* **2011**, *6*, 1049–1065. [CrossRef]
10. Iturriza-Gómara, M.; Dallman, T.; Bányai, K.; Böttiger, B.; Buesa, J.; Diedrich, S.; Fiore, L.; Johansen, K.; Koopmans, M.; Korsun, N.; et al. Rotavirus genotypes co-circulating in Europe between 2006 and 2009 as determined by EuroRotaNet, a pan-European collaborative strain surveillance network. *Epidemiol. Infect.* **2011**, *139*, 895–909. [CrossRef]
11. Matthijssens, J.; Heylen, E.; Zeller, M.; Rahman, M.; Lemey, P.; Van Ranst, M. Phylodynamic analyses of rotavirus genotypes G9 and G12 underscore their potential for swift global spread. *Mol. Biol. Evol.* **2010**, *27*, 2431–2436. [CrossRef]
12. Patel, M.M.; Steele, D.; Gentsch, J.R.; Wecker, J.; Glass, R.I.; Parashar, U.D. Real-world impact of rotavirus vaccination. *Pediatr. Infect. Dis. J.* **2011**, *30*, 1–5. [CrossRef]
13. Rahman, M.; Matthijssens, J.; Yang, X.; Delbeke, T.; Arijs, I.; Taniguchi, K.; Iturriza-Gomara, M.; Iftekharuddin, N.; Azim, T.; Van Ranst, M. Evolutionary history and global spread of the emerging G12 human rotaviruses. *J. Virol.* **2007**, *81*, 2382–2390. [CrossRef] [PubMed]
14. Papp, H.; László, B.; Jakab, F.; Ganesh, B.; De Grazia, S.; Matthijssens, J.; Ciarlet, M.; Martella, V.; Bányai, K. Review of group A rotavirus strains reported in swine and cattle. *Vet. Microbiol.* **2013**, *165*, 190–199. [CrossRef] [PubMed]
15. Agbemabiese, C.A.; Nakagomi, T.; Gauchan, P.; Sherchand, J.B.; Pandey, B.D.; Cunliffe, N.A.; Nakagomi, O. Whole genome characterisation of a porcine-like human reassortant G26P[19] Rotavirus A strain detected in a child hospitalised for diarrhoea in Nepal, 2007. *Infect. Genet. Evol.* **2017**, *54*, 164–169. [CrossRef] [PubMed]
16. Kim, H.H.; Matthijssens, J.; Kim, H.J.; Kwon, H.J.; Park, J.G.; Son, K.Y.; Ryu, E.H.; Kim, D.S.; Lee, W.S.; Kang, M.I.; et al. Full-length genomic analysis of porcine G9P[23] and G9P[7] rotavirus strains isolated from pigs with diarrhoea in South Korea. *Infect. Genet. Evol.* **2012**, *12*, 1427–1435. [CrossRef] [PubMed]
17. Martel-Paradis, O.; Laurin, M.A.; Martella, V.; Sohal, J.S.; L’Homme, Y. Full-length genome analysis of G2, G9 and G11 porcine group A rotaviruses. *Vet. Microbiol.* **2013**, *162*, 94–102. [CrossRef]
18. Monini, M.; Zaccaria, G.; Ianiro, G.; Lavazza, A.; Vaccari, G.; Ruggeri, F.M. Full-length genomic analysis of porcine rotavirus strains isolated from pigs with diarrhoea in Northern Italy. *Infect. Genet. Evol.* **2014**, *25*, 4–13. [CrossRef]
19. Silva, F.D.; Gregori, F.; McDonald, S.M. Distinguishing the genotype 1 genes and proteins of human Wa-like rotaviruses vs. porcine rotaviruses. *Infect. Genet. Evol.* **2016**, *43*, 6–14. [CrossRef]

20. Theuns, S.; Heylen, E.; Zeller, M.; Roukaerts, I.D.; Desmarests, L.M.; Van Ranst, M.; Nauwynck, H.J.; Matthijssens, J. Complete genome characterisation of recent and ancient Belgian pig Group A rotaviruses and assessment of their evolutionary relationship with human rotaviruses. *J. Virol.* **2015**, *89*, 1043–1057. [CrossRef]
21. Doro, R.; Farkas, S.L.; Martella, V.; Banyai, K. Zoonotic transmission of rotavirus: Surveillance and control. *Expert Rev. Anti. Infect. Ther.* **2015**, *13*, 1337–1350. [CrossRef]
22. Cowley, D.; Donato, C.M.; Roczo-Farkas, S.; Kirkwood, C.D. Novel G10P[14] Rotavirus Strain, Northern Territory, Australia. *Emerg. Infect. Dis.* **2013**, *19*, 1324–1327. [CrossRef]
23. Komoto, S.; Tacharoenuang, R.; Guntapong, R.; Ide, T.; Sinchai, P.; Upachai, S.; Fukuda, S.; Yoshikawa, T.; Tharmaphornpilas, P.; Sangkitporn, S.; et al. Identification and characterisation of a human G9P[23] rotavirus strain from a child with diarrhoea in Thailand: Evidence for porcine-to-human interspecies transmission. *J. Gen. Virol.* **2017**, *98*, 532–538. [CrossRef] [PubMed]
24. Malasao, R.; Khamrin, P.; Kumthip, K.; Ushijima, H.; Maneekarn, N. Complete genome sequence analysis of rare G4P[6] rotavirus strains from human and pig reveals the evidence for interspecies transmission. *Infect. Genet. Evol.* **2018**, *65*, 357–368. [CrossRef] [PubMed]
25. Mukherjee, A.; Ghosh, S.; Bagchi, P.; Dutta, D.; Chattopadhyay, S.; Kobayashi, N.; Chawla-Sarkar, M. Full genomic analyses of human rotavirus G4P[4], G4P[6], G9P[19] and G10P[6] strains from north-eastern India: Evidence for interspecies transmission and complex reassortment events. *Clin. Microbiol. Infect.* **2011**, *17*, 1343–1346. [CrossRef] [PubMed]
26. My, P.V.; Rabaa, M.A.; Donato, C.; Cowley, D.; Phat, V.V.; Dung, T.T.; Anh, P.H.; Vinh, H.; Bryant, J.E.; Kellam, P.; et al. Novel porcine-like human G26P[19] rotavirus identified in hospitalised paediatric diarrhoea patients in Ho Chi Minh City, Vietnam. *J. Gen. Virol.* **2014**, *95*, 2727–2733. [CrossRef] [PubMed]
27. Quayle, O.; Roy, S.; Rungrsuriyachai, K.; Esona, M.D.; Xu, Z.; Tam, K.I.; Banegas, D.J.; Rey-Benito, G.; Bowen, M.D. Characterisation of a rare, reassortant human G10P[14] rotavirus strain detected in Honduras. *Mem. Inst. Oswaldo Cruz.* **2018**, *113*, 9–16. [CrossRef] [PubMed]
28. Tacharoenuang, R.; Komoto, S.; Guntapong, R.; Ide, T.; Singchai, P.; Upachai, S.; Fukuda, S.; Yoshida, Y.; Murata, T.; Yoshikawa, T.; et al. Characterisation of a G10P[14] rotavirus strain from a diarrhoeic child in Thailand: Evidence for bovine-to-human zoonotic transmission. *Infect. Genet. Evol.* **2018**, *63*, 43–57. [CrossRef]
29. Bwogi, J.; Jere, K.C.; Karamagi, C.; Byarugaba, D.K.; Namuwulya, P.; Baliraine, F.N.; Desselberger, U.; Iturriza-Gomara, M. Whole genome analysis of selected human and animal rotaviruses identified in Uganda from 2012 to 2014 reveals complex genome reassortment events between human, bovine, caprine and porcine strains. *PLoS ONE* **2017**, *12*, e0178855. [CrossRef]
30. Matthijssens, J.; Bilcke, J.; Ciarlet, M.; Martella, V.; Banyai, K.; Rahman, M.; Zeller, M.; Beutels, P.; Van Damme, P.; Van Ranst, M. Rotavirus disease and vaccination: Impact on genotype diversity. *Future Microbiol.* **2009**, *4*, 1303–1316. [CrossRef]
31. Nyaga, M.M.; Jere, K.C.; Esona, M.D.; Seheri, M.L.; Stucker, K.M.; Halpin, R.A.; Akopov, A.; Stockwell, T.B.; Peenze, I.; Diop, A.; et al. Whole genome detection of rotavirus mixed infections in human, porcine and bovine samples co-infected with various rotavirus strains collected from sub-Saharan Africa. *Infect. Genet. Evol.* **2015**, *31*, 321–334. [CrossRef]
32. Beards, G.; Graham, C. Temporal distribution of rotavirus G-serotypes in the West Midlands region of the United Kingdom, 1983–1994. *J. Diarrhoeal Dis. Res.* **1995**, *13*, 235–237.
33. Bok, K.; Castagnaro, N.; Borsa, A.; Nates, S.; Espul, C.; Fay, O.; Fabri, A.; Grinstein, S.; Miceli, I.; Matson, D.O.; et al. Surveillance for rotavirus in Argentina. *J. Med. Virol.* **2001**, *65*, 190–198. [CrossRef] [PubMed]
34. Esona, M.D.; Armah, G.E.; Geyer, A.; Steele, A.D. Detection of an unusual human rotavirus strain with G5P[8] specificity in a Cameroonian child with diarrhoea. *J. Clin. Microbiol.* **2004**, *42*, 441–444. [CrossRef] [PubMed]
35. Esona, M.D.; Geyer, A.; Banyai, K.; Page, N.; Aminu, M.; Armah, G.E.; Hull, J.; Steele, D.A.; Glass, R.I.; Gentsch, J.R. Novel human rotavirus genotype G5P[7] from child with diarrhoea, Cameroon. *Emerg. Infect. Dis.* **2009**, *15*, 83–86. [CrossRef] [PubMed]

36. Gouvea, V.; de Castro, L.; Timenetsky Mdo, C.; Greenberg, H.; Santos, N. Rotavirus serotype G5 associated with diarrhoea in Brazilian children. *J. Clin. Microbiol.* **1994**, *32*, 1408–1409. Erratum appears in *J. Clin. Microbiol.* **1994**, *32*, 1834. [CrossRef] [PubMed]
37. Hwang, K.P.; Wu, F.T.; Bányai, K.; Wu, H.S.; Yang, D.C.; Huang, Y.C.; Lin, J.S.; Hsiung, C.A.; Huang, J.C.; Jiang, B.; et al. Identification of porcine rotavirus-like genotype P[6] strains in Taiwanese children. *J. Med. Microbiol.* **2012**, *61*, 990–997. [CrossRef]
38. Lorenzetti, E.; Da Silva Medeiros, T.N.; Alfieri, A.F.; Alfieri, A.A. Genetic heterogeneity of wild-type G4P[6] porcine rotavirus strains detected in a diarrhoea outbreak in a regularly vaccinated pig herd. *Vet. Microbiol.* **2011**, *154*, 191–196. [CrossRef]
39. Martella, V.; Ciarlet, M.; Bányai, K.; Lorusso, E.; Cavalli, A.; Corrente, M.; Elia, G.; Arista, S.; Camero, M.; Desario, C.; et al. Identification of a novel VP4 genotype carried by a serotype G5 porcine rotavirus strain. *Virology* **2006**, *346*, 301–311. [CrossRef]
40. Nyaga, M.M.; Tan, Y.; Seheri, M.L.; Halpin, R.A.; Akopov, A.; Stucker, K.M.; Fedorova, N.B.; Shrivastava, S.; Duncan Steele, A.; Mwenda, J.M.; et al. Whole-genome sequencing and analyses identify high genetic heterogeneity, diversity and endemicity of rotavirus genotype P[6] strains circulating in Africa. *Infect. Genet. Evol.* **2018**, *63*, 79–88. [CrossRef]
41. Li, D.D.; Duan, Z.J.; Zhang, Q.; Liu, N.; Xie, Z.P.; Jiang, B.; Steele, D.; Jiang, X.; Wang, Z.S.; Fang, Z.Y. Molecular characterisation of unusual human G5P[6] rotaviruses identified in China. *J. Clin. Virol.* **2008**, *42*, 141–148. [CrossRef]
42. Ahmed, K.; Dang, D.A.; Nakagomi, O. Rotavirus G5P[6] in child with diarrhoea, Vietnam. *Emerg. Infect. Dis.* **2007**, *13*, 1232–1235. [CrossRef]
43. Chieochansin, T.; Vutithanachot, V.; Phumpholsup, T.; Posuwan, N.; Theamboonlers, A.; Poovorawan, Y. The prevalence and genotype diversity of Human Rotavirus A circulating in Thailand, 2011–2014. *Infect. Genet. Evol.* **2016**, *37*, 129–136. [CrossRef]
44. Duan, Z.J.; Li, D.D.; Zhang, Q.; Liu, N.; Huang, C.P.; Jiang, X.; Jiang, B.; Glass, R.; Steele, D.; Tang, J.Y.; et al. Novel human rotavirus of genotype G5P[6] identified in a stool specimen from a Chinese girl with diarrhoea. *J. Clin. Microbiol.* **2007**, *45*, 1614–1617. [CrossRef] [PubMed]
45. Komoto, S.; Maeno, Y.; Tomita, M.; Matsuoka, T.; Ohfu, M.; Yodoshi, T.; Akeda, H.; Taniguchi, K. Whole genomic analysis of a porcine-like human G5P[6] rotavirus strain isolated from a child with diarrhoea and encephalopathy in Japan. *J. Gen. Virol.* **2013**, *94*, 1568–1575. [CrossRef] [PubMed]
46. Mladenova, Z.; Papp, H.; Lengyel, G.; Kisfali, P.; Steyer, A.; Steyer, A.F.; Esona, M.D.; Iturriza-Gómara, M.; Bányai, K. Detection of rare reassortant G5P[6] rotavirus, Bulgaria. *Infect. Genet. Evol.* **2012**, *12*, 1676–1684. [CrossRef] [PubMed]
47. Chilengi, R.; Rudd, C.; Bolton, C.; Guffey, B.; Masumbu, P.K.; Stringer, J. Successes, challenges and lessons learned in accelerating introduction of rotavirus immunisation in Zambia. *World J. Vaccines* **2015**, *5*, 43–53. [CrossRef]
48. Zambia Ministry of Health. The 2012 Annual Health Statistical Bulletin. 2014. Available online: [https://www.moh.gov.zm/docs/reports/2012\\_Annual\\_Health\\_Statistical\\_Bulletin\\_Version\\_1.pdf](https://www.moh.gov.zm/docs/reports/2012_Annual_Health_Statistical_Bulletin_Version_1.pdf) (accessed on 18 March 2020).
49. Mpabalwani, M.; Oshitani, H.; Kasolo, F.; Mizuta, K.; Luo, N.; Matsubayashi, N.; Bhat, G.; Suzuki, H.; Numazaki, Y. Rotavirus gastro-enteritis in hospitalised children with acute diarrhoea in Zambia. *Ann. Trop. Paediatr.* **1995**, *15*, 39–43. [CrossRef]
50. Mpabalwani, E.M.; Simwaka, C.J.; Mwenda, J.M.; Mubanga, C.P.; Monze, M.; Matapo, B.; Parashar, U.D.; Tate, J.E. Impact of rotavirus vaccination on diarrhoeal Hospitalisations in children aged <5 Years in Lusaka, Zambia. *Clin. Infect. Dis.* **2016**, *62*, S183–S187. [CrossRef]
51. Mpabalwani, E.M.; Simwaka, J.C.; Mwenda, J.M.; Matapo, B.; Parashar, U.D.; Tate, J.E. Sustained impact of rotavirus vaccine on rotavirus hospitalisations in Lusaka, Zambia, 2009–2016. *Vaccine* **2018**, *36*, 7165–7169. [CrossRef]
52. WHO Vaccine-Preventable Diseases: Monitoring System. 2020 Global Summary. Available online: [https://apps.who.int/immunization\\_monitoring/globalsummary/countries?countrycriteria%5Bcountry%5D%5B%5D=ZMB](https://apps.who.int/immunization_monitoring/globalsummary/countries?countrycriteria%5Bcountry%5D%5B%5D=ZMB) (accessed on 7 August 2020).
53. Mwenda, J.M.; Tate, J.E.; Parashar, U.D.; Mihigo, R.; Agócs, M.; Serhan, F.; Nshimirimana, D. African Rotavirus Surveillance Network: A brief overview. *Pediatr. Infect. Dis. J.* **2014**, *33*, S6–S8. [CrossRef]

54. Mwenda, J.M.; Burke, R.M.; Shaba, K.; Mihigo, R.; Tevi-Benissan, M.C.; Mumba, M.; Biey, J.N.; Cheikh, D.; Poy, A.; Zawaira, F.R.; et al. Implementation of rotavirus surveillance and vaccine introduction—World Health Organization African region, 2007–2016. *Morb. Mortal. Wkly. Rep.* **2017**, *66*, 1192–1196. [CrossRef]
55. Mwenda, J.M.; Ntoto, K.M.; Abebe, A.; Enweronu-Laryea, C.; Amina, I.; Mchomvu, J.; Kisakye, A.; Mpabalwani, E.M.; Pazvakavambwa, I.; Armah, G.E.; et al. Burden and epidemiology of rotavirus diarrhoea in selected African countries: Preliminary results from the African Rotavirus Surveillance Network. *J. Infect. Dis.* **2010**, *202*, S5–S11. [CrossRef] [PubMed]
56. Dong, H.J.; Qian, Y.; Huang, T.; Zhu, R.N.; Zhao, L.Q.; Zhang, Y.; Li, R.C.; Li, Y.P. Identification of circulating porcine-human reassortant G4P[6] rotavirus from children with acute diarrhoea in China by whole genome analyses. *Infect. Genet. Evol.* **2013**, *20*, 155–162. [CrossRef] [PubMed]
57. Yahiro, T.; Takaki, M.; Chandrasena, T.G.A.; Rajindrajith, S.; Iha, H.; Ahmed, K. Human-porcine reassortant rotavirus generated by multiple reassortment events in a Sri Lankan child with diarrhoea. *Infect. Genet. Evol.* **2018**, *65*, 170–186. [CrossRef] [PubMed]
58. Zhou, X.; Wang, Y.H.; Ghosh, S.; Tang, W.F.; Pang, B.B.; Liu, M.Q.; Peng, J.S.; Zhou, D.J.; Kobayashi, N. Genomic characterisation of G3P[6], G4P[6] and G4P[8] human rotaviruses from Wuhan, China: Evidence for interspecies transmission and reassortment events. *Infect. Genet. Evol.* **2015**, *33*, 55–71. [CrossRef] [PubMed]
59. Heylen, E.; Likelele, B.B.; Zeller, M.; Stevens, S.; De Coster, S.; Conceição-Neto, N.; Van Geet, C.; Jacobs, J.; Ngbondanda, D.; Van Ranst, M.; et al. Rotavirus surveillance in Kisangani, the Democratic Republic of the Congo, reveals a high number of unusual genotypes and gene segments of animal origin in non-vaccinated symptomatic children. *PLoS ONE* **2014**, *9*, e100953. [CrossRef] [PubMed]
60. Kaneko, M.; Do, L.P.; Doan, Y.H.; Nakagomi, T.; Gauchan, P.; Agbemabiese, C.A.; Dang, A.D.; Nakagomi, O. Porcine-like G3P[6] and G4P[6] rotavirus A strains detected from children with diarrhoea in Vietnam. *Arch. Virol.* **2018**, *163*, 2261–2263. [CrossRef] [PubMed]
61. Phan, M.V.; Anh, P.H.; Cuong, N.V.; Munnink, B.B.; Hoek, L.; My, P.T.; Tri, T.N.; Bryant, J.E.; Baker, S.; Thwaites, G.; et al. Unbiased whole-genome deep sequencing of human and porcine stool samples reveals circulation of multiple groups of rotaviruses and a putative zoonotic infection. *Virus Evol.* **2016**, *2*, 1–15. [CrossRef]
62. Wang, Y.H.; Kobayashi, N.; Zhou, D.J.; Yang, Z.Q.; Zhou, X.; Peng, J.S.; Zhu, Z.R.; Zhao, D.F.; Liu, M.Q.; Gong, J. Molecular epidemiologic analysis of group A rotaviruses in adults and children with diarrhoea in Wuhan city, China, 2000–2006. *Arch. Virol.* **2007**, *152*, 669–685. [CrossRef]
63. da Silva, M.F.; Tort, L.F.; Gómez, M.M.; Assis, R.M.; Volotão, E.d.M.; de Mendonça, M.C.; Bello, G.; Leite, J.P. VP7 Gene of human rotavirus A genotype G5: Phylogenetic analysis reveals the existence of three different lineages worldwide. *J. Med. Virol.* **2011**, *83*, 357–366. [CrossRef]
64. Green, K.Y.; Hoshino, Y.; Ikegami, N. Sequence analysis of the gene encoding the serotype-specific glycoprotein (VP7) of two new human rotavirus serotypes. *Virology* **1989**, *168*, 429–433. [CrossRef]
65. Martella, V.; Bányai, K.; Ciarlet, M.; Iturriza-Gómara, M.; Lorusso, E.; De Grazia, S.; Arista, S.; Decaro, N.; Elia, G.; Cavalli, A.; et al. Relationships among porcine and human P[6] rotaviruses: Evidence that the different human P[6] lineages have originated from multiple interspecies transmission events. *Virology* **2006**, *344*, 509–519. [CrossRef] [PubMed]
66. Burke, B.; Bridger, J.C.; Desselberger, U. Temporal correlation between a single amino acid change in the VP4 of a porcine rotavirus and a marked change in pathogenicity. *Virology* **1994**, *202*, 754–759. [CrossRef] [PubMed]
67. Mackow, E.R.; Shaw, R.D.; Matsui, S.M.; Vo, P.T.; Dang, M.N.; Greenberg, H.B. The rhesus rotavirus gene encoding protein VP3: Location of amino acids involved in homologous and heterologous rotavirus neutralization and identification of a putative fusion region. *Proc. Natl. Acad. Sci. USA* **1988**, *85*, 645–649. [CrossRef] [PubMed]
68. Arias, C.F.; Romero, P.; Alvarez, V.; López, S. Trypsin activation pathway of rotavirus infectivity. *J. Virol.* **1996**, *70*, 5832–5839. [CrossRef] [PubMed]
69. Steyer, A.; Poljšak-Prijatelj, M.; Barlič-Maganja, D.; Marin, J. Human, porcine and bovine rotaviruses in Slovenia: Evidence of interspecies transmission and genome reassortment. *J. Gen. Virol.* **2008**, *89*, 1690–1698. [CrossRef]

70. Zeller, M.; Heylen, E.; De Coster, S.; Van Ranst, M.; Matthijssens, J. Full genome characterisation of a porcine-like human G9P[6] rotavirus strain isolated from an infant in Belgium. *Infect. Genet. Evol.* **2012**, *12*, 1492–1500. [CrossRef]
71. Zhang, S.; McDonald, P.W.; Thompson, T.A.; Dennis, A.F.; Akopov, A.; Kirkness, E.F.; Patton, J.T.; McDonald, S.M. Analysis of human rotaviruses from a single location over an 18-Year time span suggests that protein co-adaptation influences gene constellations. *J. Virol.* **2014**, *88*, 9842–9863. [CrossRef]
72. Ciarlet, M.; Ludert, J.E.; Liprandi, F. Comparative amino acid sequence analysis of the major outer capsid protein (VP7) of porcine rotaviruses with G3 and G5 serotype specificities isolated in Venezuela and Argentina. *Arch. Virol.* **1995**, *140*, 437–451. [CrossRef]
73. Dyal-Smith, M.L.; Lazdins, I.; Tregear, G.W.; Holmes, I.H. Location of the major antigenic sites involved in rotavirus serotype-specific neutralisation. *Proc. Natl. Acad. Sci. USA* **1986**, *83*, 3465–3468. [CrossRef]
74. Kobayashi, N.; Taniguchi, K.; Urasawa, S. Analysis of the newly identified neutralisation epitopes on VP7 of human rotavirus serotype 1. *J. Gen. Virol.* **1991**, *72*, 117–124. [CrossRef]
75. Green, K.Y.; Sears, J.F.; Taniguchi, K.; Midthun, K.; Hoshino, Y.; Gorziglia, M.; Nishikawa, K.; Urasawa, S.; Kapikian, A.Z.; Chanock, R.M. Prediction of human rotavirus serotype by nucleotide sequence analysis of the VP7 protein gene. *J. Virol.* **1988**, *62*, 1819–1823. [CrossRef] [PubMed]
76. Gorziglia, M.; Larralde, G.; Kapikian, A.Z.; Chanock, R.M. Antigenic relationships among human rotaviruses as determined by outer capsid protein VP4. *Proc. Natl. Acad. Sci. USA* **1990**, *87*, 7155–7159. [CrossRef] [PubMed]
77. Bányai, K.; Martella, V.; Jakab, F.; Meleg, B.; Szűcs, G. Sequencing and phylogenetic analysis of human genotype P[6] rotavirus strains detected in Hungary provides evidence for genetic heterogeneity within the P[6] VP4 gene. *J. Clin. Microbiol.* **2004**, *42*, 4338–4343. [CrossRef]
78. Potgieter, A.C.; Page, N.A.; Liebenberg, J.; Wright, I.M.; Landt, O.; van Dijk, A.A. Improved strategies for sequence-independent amplification and sequencing of viral double-stranded RNA genomes. *J. Gen. Virol.* **2009**, *90*, 1423–1432. [CrossRef]
79. Kearse, M.; Moir, R.; Wilson, A.; Stones-Havas, S.; Cheung, M.; Sturrock, S.; Buxton, S.; Cooper, A.; Markowitz, S.; Duran, C.; et al. Geneious Basic: An integrated and extendable desktop software platform for the organization and analysis of sequence data. *Bioinformatics* **2012**, *28*, 1647–1649. [CrossRef] [PubMed]
80. Edgar, R.C. MUSCLE: A multiple sequence alignment method with reduced time and space complexity. *BMC Bioinform.* **2004**, *5*, 1–19. [CrossRef]
81. Katoh, K.; Standley, D.M. MAFFT multiple sequence alignment software version 7: Improvements in performance and usability. *Mol. Biol. Evol.* **2013**, *30*, 772–780. [CrossRef]
82. Tamura, K.; Stecher, G.; Peterson, D.; Filipiński, A.; Kumar, S. MEGA 6: Molecular evolutionary genetics analysis version 6.0. *Mol. Biol. Evol.* **2013**, *30*, 2725–2729. [CrossRef]
83. Guindon, S.; Gascuel, O. A simple, fast, and accurate algorithm to estimate large phylogenies by maximum likelihood. *Syst. Biol.* **2003**, *52*, 696–704. [CrossRef]
84. Felsenstein, J. Confidence Limits on Phylogenies: An approach using the bootstrap. *Evolution* **1985**, *39*, 783–791. [CrossRef]
85. Frazer, K.A.; Pachter, L.; Poliakov, A.; Rubin, E.M.; Dubchak, I. VISTA: Computational tools for comparative genomics. *Nucleic Acids Res.* **2004**, *32*, 273–279. [CrossRef] [PubMed]



© 2020 by the authors. Licensee MDPI, Basel, Switzerland. This article is an open access article distributed under the terms and conditions of the Creative Commons Attribution (CC BY) license (<http://creativecommons.org/licenses/by/4.0/>).



Article

# Phylogenetic Analyses of Rotavirus A from Cattle in Uruguay Reveal the Circulation of Common and Uncommon Genotypes and Suggest Interspecies Transmission

Matías Castells <sup>1,2,\*</sup> , Rubén Darío Caffarena <sup>2,3</sup> , María Laura Casaux <sup>2</sup>, Carlos Schild <sup>2</sup>, Samuel Miño <sup>4</sup> , Felipe Castells <sup>5</sup>, Daniel Castells <sup>6</sup>, Matías Victoria <sup>1</sup>, Franklin Riet-Correa <sup>2</sup>, Federico Giannitti <sup>2</sup>, Viviana Parreño <sup>4</sup> and Rodney Colina <sup>1,\*</sup>

<sup>1</sup> Laboratorio de Virología Molecular, CENUR Litoral Norte, Centro Universitario de Salto, Universidad de la República, Rivera 1350, Salto 50000, Uruguay; matvicmon@yahoo.com

<sup>2</sup> Instituto Nacional de Investigación Agropecuaria (INIA), Plataforma de Investigación en Salud Animal, Estación Experimental la Estanzuela, Ruta 50 km 11, Colonia 70000, Uruguay; rdcaffarena@gmail.com (R.D.C.); mlcasaux@gmail.com (M.L.C.); schild.co@gmail.com (C.S.); frcorrea@inia.org.uy (F.R.-C.); fgiannitti@inia.org.uy (F.G.)

<sup>3</sup> Facultad de Veterinaria, Universidad de la República, Alberto Lasplaces 1620, Montevideo 11600, Uruguay

<sup>4</sup> Sección de Virus Gastroentéricos, Instituto de Virología, CICVyA, INTA Castelar, Buenos Aires 1686, Argentina; mino.samuel@inta.gob.ar (S.M.); vivipar3015@gmail.com (V.P.)

<sup>5</sup> Doctor en Veterinaria en Ejercicio Libre, Asociado al Laboratorio de Virología Molecular, CENUR Litoral Norte, Centro Universitario de Salto, Universidad de la República, Rivera 1350, Salto 50000, Uruguay; felicastells@gmail.com

<sup>6</sup> Centro de Investigación y Experimentación Dr. Alejandro Gallinal, Secretariado Uruguayo de la Lana, Ruta 7 km 140, Cerro Colorado, Florida 94000, Uruguay; castells@adinet.com.uy

\* Correspondence: matiascastellsbauer@gmail.com (M.C.); rodneycolina1@gmail.com (R.C.); Tel.: +598-4734-2924 (M.C. & R.C.)

Received: 7 April 2020; Accepted: 30 June 2020; Published: 14 July 2020



**Abstract:** Uruguay is one of the main exporters of beef and dairy products, and cattle production is one of the main economic sectors in this country. Rotavirus A (RVA) is the main pathogen associated with neonatal calf diarrhea (NCD), a syndrome that leads to significant economic losses to the livestock industry. The aims of this study are to determine the frequency of RVA infections, and to analyze the genetic diversity of RVA strains in calves in Uruguay. A total of 833 samples from dairy and beef calves were analyzed through RT-qPCR and sequencing. RVA was detected in 57.0% of the samples. The frequency of detection was significantly higher in dairy (59.5%) than beef (28.4%) calves ( $p < 0.001$ ), while it did not differ significantly among calves born in herds that were vaccinated (64.0%) or not vaccinated (66.7%) against NCD. The frequency of RVA detection and the viral load were significantly higher in samples from diarrheic (72.1%, 7.99 log<sub>10</sub> genome copies/mL of feces) than non-diarrheic (59.9%, 7.35 log<sub>10</sub> genome copies/mL of feces) calves ( $p < 0.005$  and  $p = 0.007$ , respectively). The observed G-types (VP7) were G6 (77.6%), G10 (20.7%), and G24 (1.7%), while the P-types were P[5] (28.4%), P[11] (70.7%), and P[33] (0.9%). The G-type and P-type combinations were G6P[11] (40.4%), G6P[5] (38.6%), G10P[11] (19.3%), and the uncommon genotype G24P[33] (1.8%). VP6 and NSP1-5 genotyping were performed to better characterize some strains. The phylogenetic analyses suggested interspecies transmission, including transmission between animals and humans.

**Keywords:** rotavirus; bovine; genotypes; interspecies transmission; diarrhea

## 1. Introduction

Neonatal calf diarrhea (NCD) is a syndrome of worldwide distribution and the major cause of mortality of dairy calves before weaning [1]. NCD has a negative impact on animal welfare and leads to significant economic losses to the livestock industry [2–5].

Rotavirus A (RVA) is the main pathogen associated with NCD [6,7]. RVA (species *Rotavirus A*; genus *Rotavirus*; subfamily *Sedoreovirinae*; family *Reoviridae*) is a nonenveloped virus with a triple-layered capsid and a genome composed of 11 segments of double-stranded RNA [8]. RVA is widespread in dairy farms in Uruguay, and viable viral particles have been detected in sources of drinking water used for calves [9], suggesting water contamination and waterborne transmission.

Rotaviruses are classified by a binary system of G and P types for VP7 and VP4, respectively, determined by sequence analyses. In 2008, a complete genome classification system, named genotype constellation, assigning a specific genotype to each of the 11 genome segments was developed [10]. The VP7-VP4-VP6-VP1-VP2-VP3-NSP1-NSP2-NSP3-NSP4-NSP5/6 genes of rotavirus strains are classified using the abbreviations Gx-P[x]-Ix-Rx-Cx-Mx-Ax-Nx-Tx-Ex-Hx (where x is the genotype number), respectively.

Recently, since the inclusion of gene segments other than VP7 and VP4 in molecular analyses, gene reassortment has been described as a common event in RVA, sometimes between virus strains originated from different hosts, suggesting interspecies transmission [10–13].

Surveys describing the epidemiology of RVA in cattle in South America are mainly restricted to Brazil and Argentina; no published data about RVA epidemiology in Uruguayan calves are available. However, other viruses such as bovine coronavirus and bovine astrovirus have been detected in Uruguay [14,15].

Uruguay is one of the main exporters of beef [16] and dairy products [17]. Furthermore, cattle production is one of the main economic sectors in this country, with almost 12 million head of cattle accounting for 33% of the total exports [18]. The aims of this study are to determine the frequency of RVA infections and to analyze the genetic diversity of the RVA strains detected in Uruguayan calves.

## 2. Results

### 2.1. Detection Frequency of RVA in Uruguayan Calves

Rotavirus A was detected in 57.0% (475/833) of the analyzed samples. The frequency of detection was significantly higher in dairy (59.5%, 456/766) than beef (28.4%, 19/67) calves (OR: 3.72, 95% CI: 2.14–6.44;  $p < 0.000001$ ; Figure 1a). The frequency of RVA detection in live calves was higher (58.0%, 444/766) than in deceased calves (46.3%, 31/67), although this difference was not statistically significant ( $p = 0.06$ ; Figure 1b). The frequency of detection in dairy calves born in herds that vaccinated (64.0%, 144/225) or did not vaccinate dams (66.7%, 164/246) against NCD did not differ significantly ( $p = 0.5$ ; Figure 1c). The frequency of RVA detection was significantly higher in samples from diarrheic (72.1%, 173/240) than non-diarrheic (59.9%, 163/272) dairy calves (OR: 1.73, 95% CI: 1.19–2.50;  $p < 0.005$ ; Figure 1d). No seasonal distribution was observed in RVA detection (data not shown).

Rotavirus A was detected in 58.8% (87/148), 70.6% (142/201), 68.2% (75/110), and 52.9% (18/34) of dairy calves in the first, second, third, and fourth weeks of life, respectively (Table 1). Statistically significant differences were observed between the second and the first weeks of age (OR: 1.69, 95% CI: 1.08–2.64;  $p = 0.02$ ), and between the second and the fourth weeks of age (OR: 2.14, 95% CI: 1.02–4.48;  $p = 0.04$ ). The mean age in days of RVA-positive dairy calves was significantly lower in diarrheic than nondiarrheic calves ( $p = 0.02$ ; Table 1).

The RVA viral load was significantly higher in diarrheic than nondiarrheic dairy calves ( $p = 0.007$ ; Table 1), ranging between  $1.14 \times 10^4$  and  $7.36 \times 10^{12}$  genome copies/milliliter (gc/mL) of feces. In all four age groups, the frequency of RVA detection was higher in diarrheic than nondiarrheic dairy calves: 69.0% (40/58) vs. 52.2% (47/90) in the first week, 72.1% (98/136) vs. 67.7% (44/65) in the second week, 68.8% (22/32) vs. 67.9% (53/78) in the third week, and 85.7% (6/7) vs. 44.4% (12/27) in the fourth week

of age. A statistically significant difference was observed only within the first week (OR: 2.03, 95% CI: 1.01–4.07;  $p = 0.04$ ).

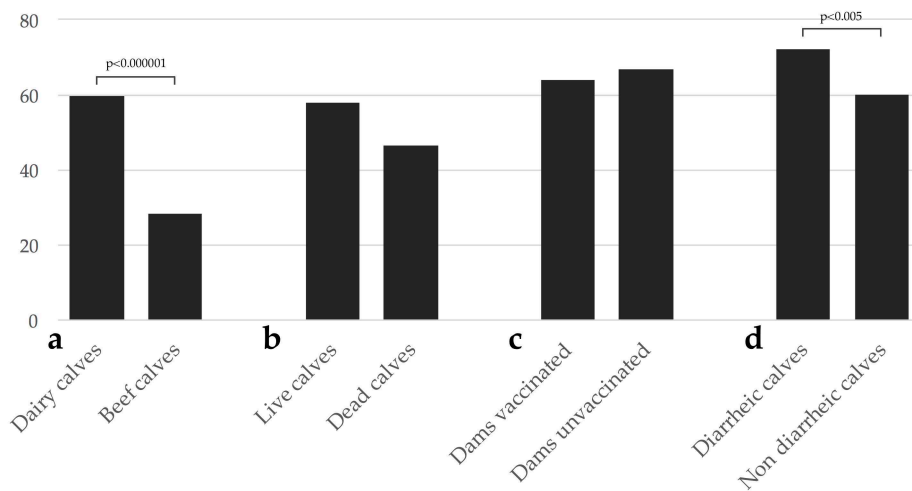


**Figure 1.** Frequency of Rotavirus A (RVA) detection in calves. (a) Frequency of RVA detection in dairy vs. beef calves; (b) frequency of RVA detection in live vs. deceased calves; (c) frequency of RVA detection in calves from vaccinated <sup>a</sup> vs. unvaccinated dairy herds; (d) frequency of RVA detection in diarrheic vs. non diarrheic dairy calves. Comparisons with statistically significant differences are indicated. <sup>a</sup> Most of the vaccines against neonatal calf diarrhea available in Uruguay include two RVA strains.

**Table 1.** Frequency of RVA detection and viral load in feces of diarrheic and nondiarrheic calves.

	Calves Age					
	Mean Age <sup>a</sup>	Viral Load <sup>b</sup>	First Week	Second Week	Third Week	Fourth Week
Diarrheic	11.9 <sup>1</sup>	7.99 <sup>2</sup>	69.0 <sup>3</sup>	72.1	68.8	85.7
Non-diarrheic	13.5 <sup>1</sup>	7.35 <sup>2</sup>	52.2 <sup>3</sup>	67.7	67.9	44.4
Total	12.7	7.67	58.8 <sup>4</sup>	70.6 <sup>4,5</sup>	68.2	52.9 <sup>5</sup>

<sup>a</sup> Mean age in days of RVA-positive calves. <sup>b</sup> Mean RVA viral load expressed as log<sub>10</sub> of RVA genome copies per milliliter of feces. Equal numbers in superscript refer to values with statistically significant differences ( $p < 0.05$ ).

### 2.2. VP7 and VP4 Genotyping

We obtained 58 and 116 sequences for VP7 and VP4, respectively. The detected G-types (VP7) were G6 (77.6%, 45/58), G10 (20.7%, 12/58), and G24 (1.7%, 1/58), while the P-types (VP4) were P[5] (28.4%, 33/116), P[11] (70.7%, 82/116), and P[33] (0.9%, 1/116). The following G- and P-type combinations were obtained for 57 strains: G6P[11] (40.4%, 23/57), G6P[5] (38.6%, 22/57), G10P[11] (19.3%, 11/57), and G24P[33] (1.8%, 1/57). Furthermore, 60 strains had undetermined G- or P-type: GXP[11] (80.0%, 48/60), GXP[5] (18.3%, 11/60), and G10P[X] (1.7%, 1/60).

### 2.3. VP6 and NSP1-5 Genotyping

Ten samples, including representative VP7 and VP4 genotype combinations observed, were selected for VP6 and NSP1-5 gene characterization: 2 G6P[5], 2 G6P[11], 2 G10P[11], 2 GXP[11], 1 G10P[X], and 1 G24P[33] (Table 2). All the strains were I2 (VP6), N2 (NSP2), and E12 (NSP4). Nine were H3 and one could not be determined HX (NSP5). Five strains were A3, four were A13, and one could not be determined AX (NSP1). Eight strains were T6, one was T9, and one could not be determined TX (NSP3).

**Table 2.** Genotype constellation of 10 RVA strains from Uruguayan calves.

Strain	VP7	VP4	VP6	NSP1	NSP2	NSP3	NSP4	NSP5
RVA/Cow-wt/URY/LVMS781/2015/G6P[5]	G6	P[5]	I2	AX	N2	T6	E12	H3
RVA/Cow-wt/URY/LVMS1788/2016/GxP[11]	GX	P[11]	I2	A3	N2	T6	E12	H3
RVA/Cow-wt/URY/LVMS1812/2016/G6P[5]	G6	P[5]	I2	A3	N2	T6	E12	H3
RVA/Cow-wt/URY/LVMS1837/2016/G10P[11]	G10	P[11]	I2	A13	N2	TX	E12	H3
RVA/Cow-wt/URY/LVMS2625/2016/G10P[11]	G10	P[11]	I2	A13	N2	T6	E12	H3
RVA/Cow-wt/URY/LVMS3024/2016/G24P[33]	G24	P[33]	I2	A13	N2	T9	E12	H3
RVA/Cow-wt/URY/LVMS3027/2016/G6P[11]	G6	P[11]	I2	A3	N2	T6	E12	H3
RVA/Cow-wt/URY/LVMS3031/2016/G6P[11]	G6	P[11]	I2	A3	N2	T6	E12	H3
RVA/Cow-wt/URY/LVMS3053/2016/G10P[x]	G10	P[X]	I2	A13	N2	T6	E12	HX
RVA/Cow-wt/URY/LVMS3206/2016/GxP[11]	GX	P[11]	I2	A3	N2	T6	E12	H3

Uncommon genotypes are shadowed in grey.

#### 2.4. Phylogenetic Analyses

The phylogenetic analyses showed an intricate genetic scenario. The analyses of the VP7 gene showed that G6 and G10 Uruguayan strains clustered in two and one different lineages, respectively, with sequences obtained from cattle. Specifically, the G6P[5] Uruguayan strains clustered in one lineage (split into two sublineages) with Argentinian strains, and the G6P[11] Uruguayan strains clustered separately in a lineage with Slovenian strains (Figure 2). The G10 Uruguayan strains clustered in a lineage (split into two sublineages) with Argentinian strains (Figure 3). Brazilian G6 and G10 strains clustered separately with Uruguayan and Argentinian G6 and G10 strains.

The phylogenetic analyses of the VP4 gene showed that P[5] Uruguayan strains clustered in a lineage with Argentinian G6P[5] strains obtained from cattle, and Brazilian P[5] strains clustered separate (Figure 4). The P[11] Uruguayan strains clustered in three lineages with sequences obtained from cattle, two of the lineages were comprised of G6 and G10 Argentinian strains (and one of these lineages is split into two sublineages), and the other lineage comprised of G6P[11] Brazilian strains, although P[11] Uruguayan strains were distinct to the majority of the Brazilian P[11] strains (Figure 5).

In the phylogenetic tree of the NSP1 gene, we observed that Uruguayan strains clustered in three different genetic lineages of the genotype A3: one jointly with human strains from Paraguay and Brazil, another with Italian and Belgian human strains, and another with a goat strain from Argentina and, in one genetic lineage of the genotype A13, with an Argentinian strain from a cow (Figure S1).

The phylogenetic analysis of the NSP2 gene showed that the Uruguayan strains were clustered in two separate lineages: one with Argentinian strains from cow and goat, and the other with strains from guanaco and vicuña from Argentina and strains from humans from Australia (Figure S2).

On the other hand, the phylogenetic analysis of the NSP3 gene showed that the T6 Uruguayan strains were clustered in three sublineages within one lineage: one together with strains distributed worldwide (including vaccine strains), one with Argentinian (vicuña and guanaco), Japanese (cow), Slovenian (human), and Paraguayan (human) strains, and the third with a goat strain from Argentina and a human strain from Belgium. The T9 strain clustered with the other four T9 strains detected so far (from Japan and the USA; Figure S3).

For the NSP4 gene, we observed that besides the Uruguayan strains obtained in our study, only sequences from South America were available. The phylogenetic analysis showed that Uruguayan strains clustered in four different lineages together with strains from several host species (cows, guanacos, horses, goats, and humans), all from this subcontinent (Figure S4).

The phylogenetic analysis of the NSP5 gene showed that the Uruguayan strains were clustered in three sublineages within one lineage: one together with strains distributed worldwide in several host species), other with an Argentinian strain from a cow and a Paraguayan strain obtained from a human, and another with a strain from a guanaco from Argentina, a strain from a yak from China, and a strain from a human from Hungary (Figure S5).

Lastly, the phylogenetic analysis of the VP6 gene showed that the Uruguayan strains were clustered in three lineages: one conformed only with Uruguayan strains, another lineage with an Argentinian strain from a cow, and another lineage with South American strains from various hosts

(human, llama, sheep, and goat), Japanese strains from human and cow, and a roe deer Slovenian strain (Figure S6).

VP7



**Figure 2.** Maximum likelihood tree of the G6 genotype of the VP7 gene. The best nucleotide substitution model (TIM2 + I + G) and the maximum likelihood tree were obtained with W-IQ-TREE. Uruguayan strains are shown in red. Shimodaira–Hasegawa approximate likelihood-ratio test (SH-aLRT) values  $\geq 80$  are shown.

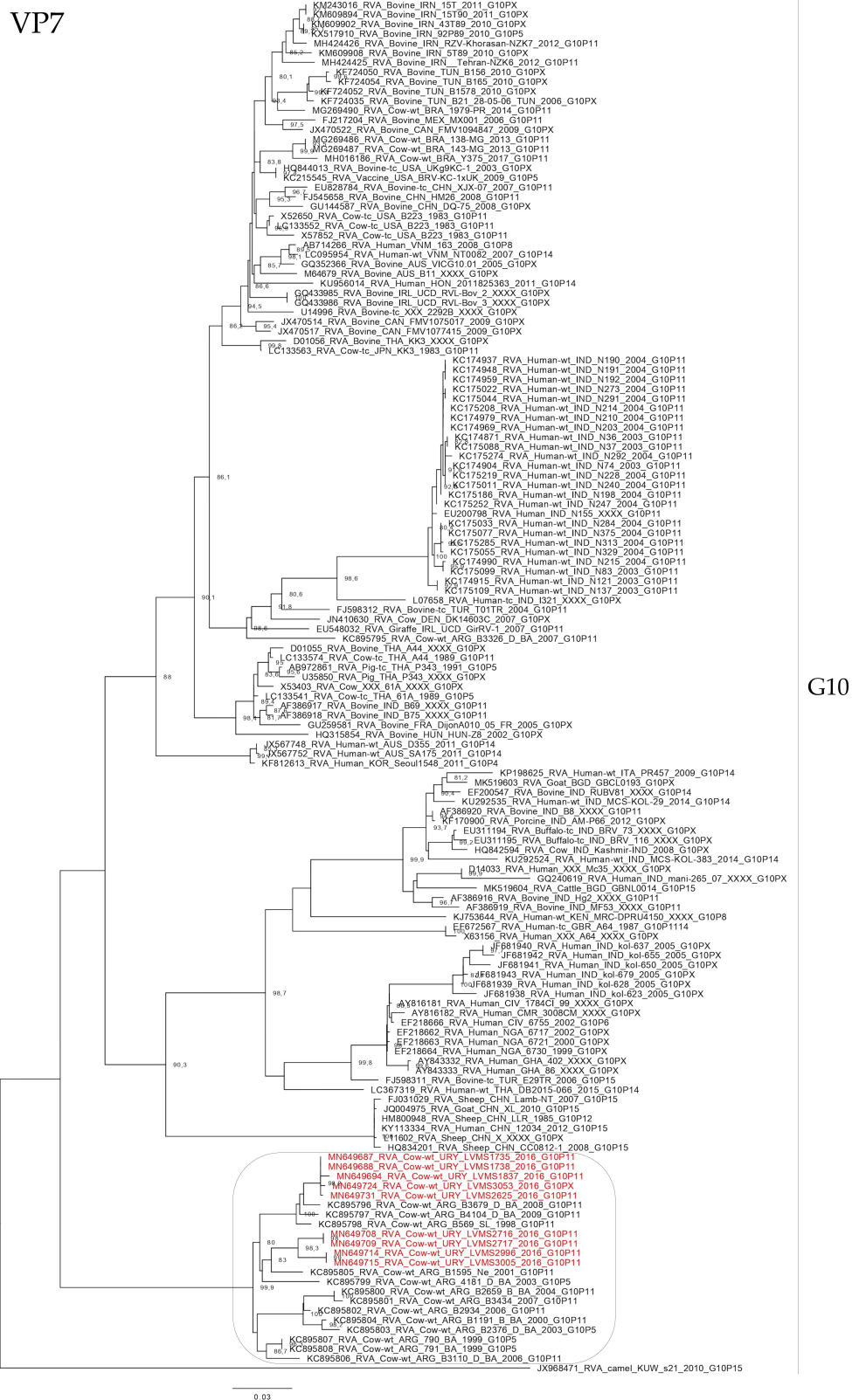


**Figure 3.** Maximum likelihood tree of the G10 genotype of the VP7 gene. The best nucleotide substitution model (TPM3 + G) and the maximum likelihood tree were obtained with W-IQ-TREE. Uruguayan strains are shown in red. SH-aLRT values  $\geq 80$  are shown.

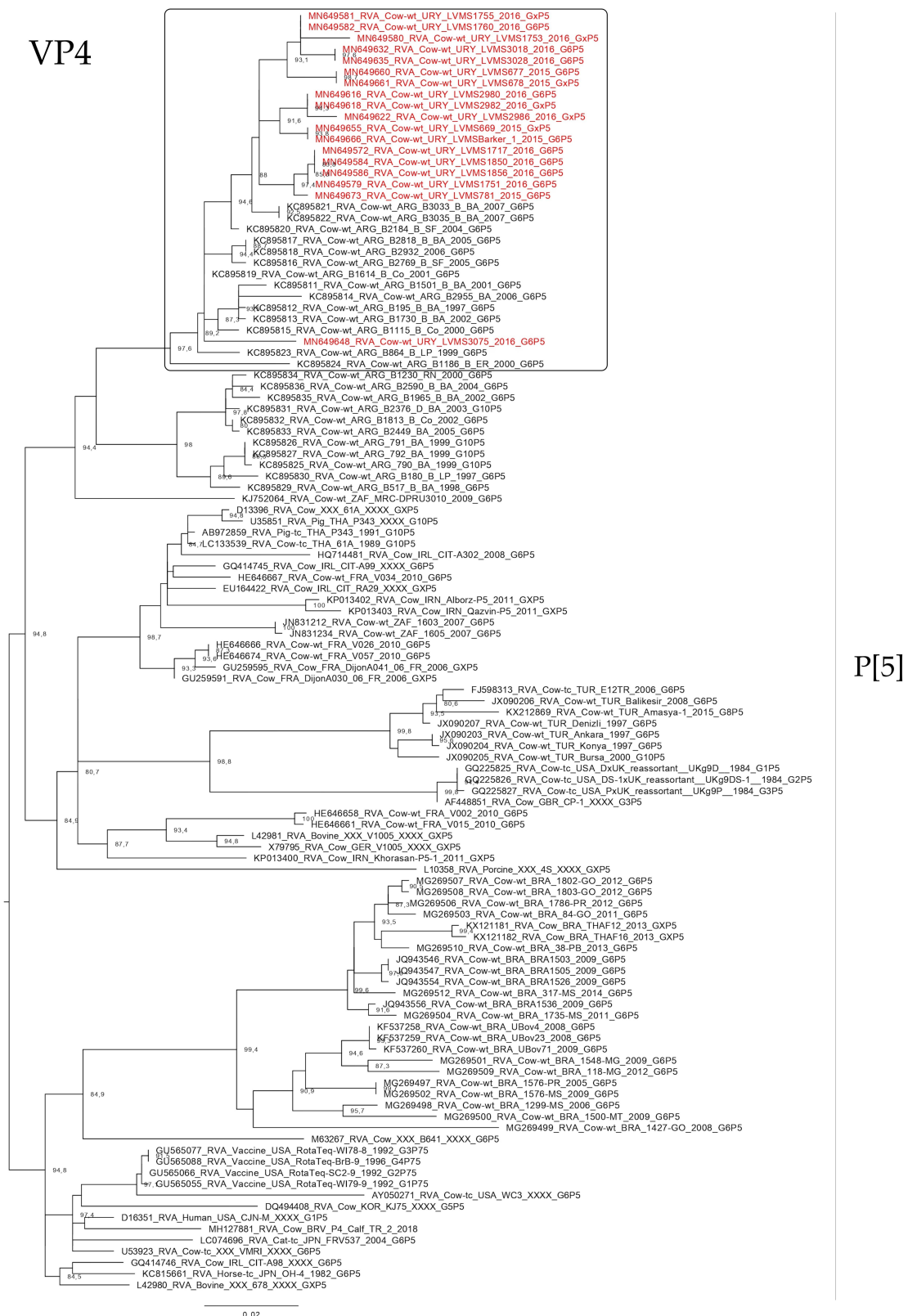
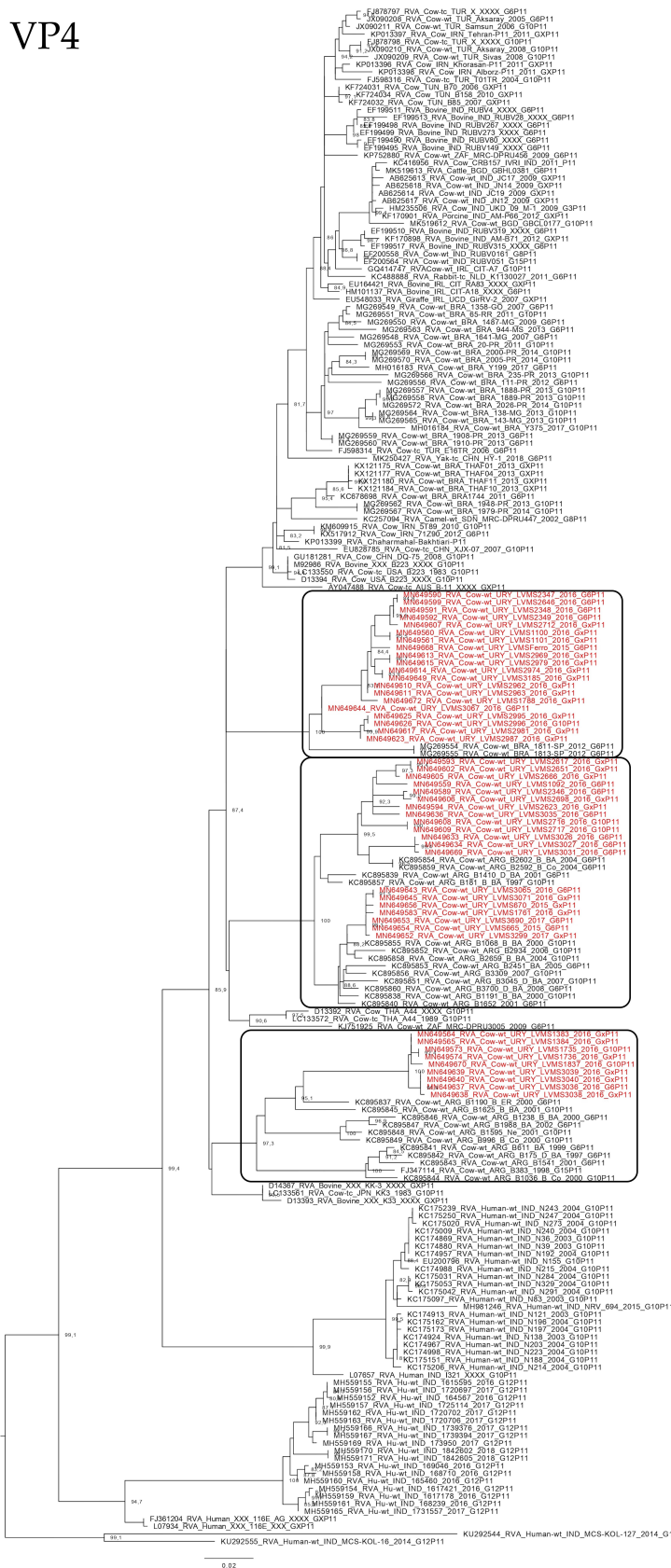


**Figure 4.** Maximum likelihood tree of the P[5] genotype of the VP4 gene. The best nucleotide substitution model (TIM + G) and the maximum likelihood tree were obtained with W-IQ-TREE. Uruguayan strains are shown in red. SH-aLRT values  $\geq 80$  are shown.

VP4



P[11]

**Figure 5.** Maximum likelihood tree of the P[11] genotype of the VP4 gene. The best nucleotide substitution model (TPM3u + G) and the maximum likelihood tree were obtained with W-IQ-TREE. Uruguayan strains are shown in red. SH-aLRT values  $\geq 80$  are shown.

### 3. Discussion

Rotavirus A was detected in feces and intestinal contents collected from dairy and beef calves with a frequency of 57%, which was higher than reports from Argentina and Brazil (17–42%) [19–22], and other geographic regions (20–49%) [7,23–25]. On the other hand, in Australia, the frequency of RVA detection was 80%, which is higher than the detected in our study [6]. Interestingly, most of the mentioned studies were conducted by assays different than RT-qPCR, except the one conducted in Australia. It is well documented that the RT-qPCR for RVA detection has a higher sensitivity than other assays, reducing the risk of false-negatives (i.e., ELISA, electron microscopy, PAGE, immunochromatography, and conventional PCR) [6,26–28], which could explain the higher frequency observed in Uruguay when compared with neighboring countries while reducing the risk of false-positive results, also given its higher specificity. Furthermore, the use of RT-qPCR, which is known to detect very few genomic copies, allows pathogen detection in clinical and subclinical calves. In addition, in many field situations, the time of onset of diarrhea is not known, so the peak of pathogen shedding may have already passed, or the infection could be just settling down by the time of sampling [29]. The limit of detection in our study ( $10^4$  gc/mL of feces) and the higher RVA viral load in diarrheic than nondiarrheic calves are in agreement with the stated by Torres-Medina et al. [29]. On the other hand, we also observed high viral loads in some nondiarrheic calves.

Infection with RVA has long been associated with diarrhea [29–31], as observed in our study, where RVA detection was more frequent in diarrheic than in nondiarrheic calves, independently of their age (up to 4 weeks). Concerning the calves' age, we observed that the proportion of calves shedding RVA was higher in the second and third weeks of age, as observed in Brazil [19,32] and elsewhere [33]. In addition, the mean age of RVA-positive calves in our study is similar to the age reported previously [31], and we observed that diarrheic calves positive for RVA were younger than nondiarrheic calves, indicating that calves are exposed to this pathogen early after birth.

Although the sampling between beef and dairy farms was unequal, our results indicate that the circulation of RVA was higher in dairy than beef calves. This contrasts with the reported results in neighboring countries, where RVA was more frequently detected in beef than dairy calves [19,20] or in a similar frequency [21]. Our results also contrast with those observed in a study conducted in Australia [6].

A common practice used to prevent NCD is the vaccination of pregnant cows/heifers during the last stage of pregnancy to protect the calves by the transference of passive maternal antibodies through colostrum intake. Most available vaccines in the Uruguayan market include bovine rotavirus A strains (most of them include two strains, G6 and G10, as detailed by the manufacturers). In this study, we observed a similar frequency of RVA detection in calves from vaccinated and unvaccinated herds. Failure in the protection against RVA infection by the vaccine was reported in studies conducted in Argentina and Brazil [34–37]; although vaccines are not effective in preventing RVA infection, they significantly reduce morbidity, the severity of diarrhea, and mortality related to RVA [38].

In this study, we determined the RVA genotypes circulating in calves in Uruguay. Overall, the VP7 and VP4 genotypes observed in this country are the most prevalent in cattle worldwide [39], although, unexpectedly, we detected a G24P[33] strain, which thus far had only been reported from an asymptomatic cow and her calf in Japan [11]. The G24P[33] strain detected in Uruguay was obtained from a 10-day-old asymptomatic dairy calf sampled in August 2016.

Regarding the VP6 and NSP1-5 genotyping, the Uruguayan strains, including the G24P[33], showed a relatively conserved genotype constellation I2-A3/A13-N2-T6/T9-E12-H3, corresponding to VP6 and NSP1-5 genotypes, respectively. These genotypes are commonly found in cattle, with the exception of T9 [40]. The T9 genotype has been sporadically detected in two cows from Japan [11], in a child from Japan [41], and in a child from the USA [42]. This genotype has been associated with atypical VP7 and VP4 genotypes (G21P[29], G24P[33], G8P[14], and G24P[14]). In this study, we observed the T9 genotype associated with G24P[33]. In-depth analysis of the RVA/Cow-wt/URY/LVMS3024/2016/G24P[33] strain revealed almost the same genotype constellation as the RVA/Cow-wt/JPN/Dai-10/2007/G24P[33] strain

from Japan, with the unusual G24, P[33], and T9 genotypes. The only difference was observed in the NSP4 gene that was E12 in the Uruguayan strain and E2 in the Japanese. It is interesting to note that all the Uruguayan strains were E12, a genotype widely detected in cattle [12], guanacos [12], horses [43,44], goats [45], and children [46,47] in South America. This reinforces the notion that the E12 genotype may be restricted to South America, as previously postulated [44].

The rare G24P[33] strain detected in our study represented a challenge. The G24, P[33], and T9 genotypes observed in this strain provides information for a possible introduction of the virus from Japan to Uruguay, or vice versa. The expansion of the Wagyu beef industry beyond Japan [48] could have influenced the dispersion of some RVA strains through live cattle exports. On the other hand, the E12 genotype in the Uruguayan G24P[33] strain and E2 genotype in the Japanese G24P[33] strain represented a probable gene reassortment, which is a more plausible scenario than the emergence of two independent strains with the same rare genotype constellation except for NSP4. Further studies should be conducted to determine the evolution and possible emergence of these rare genotypes.

In the phylogenetic analyses of all the genes, it can be observed that Uruguayan strains clustered mainly with South American strains. The only gene that did not show any South American-specific lineage was NSP3, in which the Uruguayan strains clustered mainly with Argentinian strains, but also with strains from other continents. These data, together with the identification of the E12 genotype in all the Uruguayan sequences, suggest a South American origin of RVA lineages [44]. Furthermore, the phylogenetic analyses showed an intricate pattern of diversity, with evidence of gene reassortments, interspecies transmission, local dispersion of some strains, and circulation of strains that are most prevalent in cattle worldwide.

The analyses of VP7 and VP4 showed a conserved pattern with all the Uruguayan strains clustering, with strains detected only in cattle and mainly from Argentina, indicating a probable host species and geographic linkage. Due to the shortage of G24 and P[33] sequences in the database (2 and 1, respectively), no phylogenetic analyses were performed for these genotypes. In the VP7 and VP4 phylogenetic analysis, the majority of strains characterized in this study clustered closely with strains detected in Argentinian cattle. The exceptions were one G6 lineage that clustered with European strains isolated from cattle, and one in P[11] sublineage that clustered with Brazilian strains isolated from cattle. There is a clear phylogenetic relationship between the strains detected in the cattle in Uruguay and Argentina, whereas Brazilian strains were, in general, phylogenetically distant from the Uruguayan strains. In addition, Uruguayan strains clustered together among themselves, suggesting that limited introductions of RVA into the country have occurred, but the strains were widely dispersed in the cattle. A possible explanation for the genetic similarity between the Uruguayan and Argentinian strains and their divergence to the Brazilian strains could be explained, in part, by the breed of cattle. In Uruguay and Argentina, most of the cattle breeds are *Bos taurus*, while in Brazil, there are mostly *Bos indicus* or *Bos indicus* x *Bos taurus* crosses. Although it has not been studied in cattle, different human subpopulations appeared to have different susceptibility infection and clinical disease, and this susceptibility is dependent on the rotavirus genotype, and in some cases, it also depends on different rotavirus strains of the same genotype [49].

Based on the phylogenetic analyses, we observed evidence of gene reassortment and interspecies transmission events. Regarding the former event, in addition to the previously mentioned gene reassortment of the G24P[33] strain, strong evidence was observed in the strains RVA/Cow-wt/URY/LVMS1812/2016/G6P[5] and RVA/Cow-wt/URY/LVMS3206/2016/GxP[11] because both strains clustered together in all the genes, except in VP4 (which showed different genotypes, (P[5] and P[11], respectively), indicating that a possible gene reassortment event may have occurred. Another piece of evidence was observed in the RVA/Cow-wt/URY/LVMS1788/2016/GxP[11] strain because it clustered together with other Uruguayan strains in most of the genes, except in NSP1 and NSP3 genes, which clustered alone in different genetic lineages, also suggesting a gene reassortment event. Furthermore, the strain RVA/Cow-wt/URY/LVMS1837/2016/G10P[11] clustered together with RVA/Cow-wt/URY/LVMS2625/2016/G10P[11] and RVA/Cow-wt/URY/LVMS3053/2016/G10P[x] in most of the genes, but clustered

separately in distant genetic lineages in NSP2 and NSP5; this was probably due to gene reassortment. On the other hand, an interesting observation was that, in general, G6 strains tended to cluster together in most of the genes, and the same was observed for the G10 strains, with the exceptions aforementioned.

Regarding interspecies transmission, we observed that in the analyses of VP7 and VP4, all the Uruguayan strains clustered with other bovine strains, so these gene segments seem to be more host-specific than the other genes. On the other hand, and based on the phylogenetic analyses, we observed evidence suggesting interspecies transmission because the bovine strains detected in Uruguay closely clustered with strains detected in other host species. We observed that bovine Uruguayan strains A13 (NSP1 gene) clustered together with strains isolated from humans and a goat, possibly indicating events of interspecies transmission. Two lineages showed a close relationship between Uruguayan bovine strains and human strains (from South America and Europe); these human strains were reported to be Artiodactyl-like and a product of interspecies transmission [10,47,50], as well as the goat strain of a third lineage [45], which is in accordance with our results. In the NSP2-5 and VP6 genes, we observed that the Uruguayan bovine strains clustered in some lineages with strains isolated from other host species (human, goat, guanaco, vicuna, roe deer, llama, and sheep), mainly from South America, that were proposed to be originated by interspecies transmission [12,45,47,51], again in accordance with our results. Another piece of evidence supporting this event was observed in the NSP4; all the RVA strains detected in South America were E12, independent of the host species where they were isolated (horse, cow, guanaco, human, goat), suggesting interspecies transmission and fixation of this genotype in South America [44]. The interspecies transmission of RVA is widely documented [10–13], and our results support this event. In South America, it is common to raise different livestock species on the same farm in close contact with humans [45], which increases the possibility of interspecies transmission. Our results support that interspecies transmission is a common event in South America, including the possibility of zoonotic transmission [45,51,52].

Lastly, our study had some limitations. In Uruguay, dairy farming is concentrated in the southwest region and calves are raised under intensive production systems that facilitated the collection of the samples, while beef calves are mostly bred in extensive production systems and dispersed throughout the country, which hindered the access to samples. This resulted in an overrepresentation of dairy (92%) versus beef (8%) samples in our study. Another limitation was that we had no spiked control to determine if there was inhibition of the qPCR, which may lead to false-negatives. Regarding coinfections, the methodology used has the limitation that sequences obtained from a single animal would have only represented the predominant strain and/or sequences with multiple traces that were not included in the study. It is important to mention that, from our analyses, we could not determine the route nor the time in which the gene reassortment and the interspecies transmission events took place.

## **4. Materials and Methods**

### *4.1. Samples*

Fecal samples of 766 live calves and intestinal contents from 67 naturally-deceased calves were collected from 833 different calves from dairy and beef herds in Uruguay between 2015 and 2018. Sampled herds were distributed in 10 of the 19 regions of the country (Figure 6), and throughout the year, including samples collected in the four climate seasons. In addition, 766 samples were from dairy calves, and 67 from beef calves. We compared the frequency of the RVA infection between groups only for dairy calves. A total of 240 dairy calves had diarrhea at the time of sampling, while 272 were nondiarrheic dairy calves (this information was unavailable for 321 calves). The distribution by age in the first, second, third, and fourth weeks of life was 148, 201, 110, and 34 dairy calves, respectively (the age was unavailable for 340 calves). A total of 225 calves were from dairy herds vaccinated against NCD and 246 calves were from nonvaccinated dairy herds (herd vaccination history was unavailable for 362 calves).



**Figure 6.** Map of Uruguay, the regions from which samples were collected shown in grey.

#### 4.2. Sample Suspension, RNA Extraction, Reverse Transcription, Detection and Quantification of RVA

Samples were diluted 1:10 (*v:v*) in phosphate-buffered saline solution, centrifuged at 3000× *g* for 20 min at 4 °C, and supernatants were collected and stored at −80 °C. Viral RNA was extracted using a QIAamp® cadof® Pathogen Mini Kit (Qiagen®, Hilden, Germany), following the manufacturer’s instructions. Reverse transcription (RT) was carried out with RevertAid® Reverse Transcriptase (Thermo Fisher Scientific®, Waltham, MA, USA) and random hexamers primers (Qiagen®), following the manufacturer’s instructions. All RNAs and cDNAs were stored at −80 °C until further viral analyses. Screening and quantification of the samples for RVA identification were carried out through a quantitative polymerase chain reaction (qPCR) targeted to the NSP3 gene, as described elsewhere [9]. Briefly, 12.5 µL of SensiFAST™ Probe No-ROX Kit (Bioline®, London, UK), 5.0 µL of nuclease-free water, 1.0 µL of 10 µM forward primer, 1.0 µL of 10 µM reverse primer, 0.5 µL of 10 µM probe, and 5 µL of cDNA were mixed in 0.2-mL PCR tubes. All samples were analyzed in duplicate. In order to validate the complete process, an RVA-positive (G6P[5] strain) and an RVA-negative fecal sample were used as positive and negative controls, respectively.

#### 4.3. Rotavirus A Genotyping

Quantitative-PCR positive samples were subsequently subjected to amplification of VP7 and VP4 (VP8\*). Briefly, 12.5 µL of MangoMix™ (Bioline®), 5 µL of cDNA, 5.5 µL of nuclease-free water, 1 µL of dimethyl sulfoxide, 0.5 µL of 20 µM forward primer and 0.5 µL of 20 µM reverse primer were mixed in 0.2-mL PCR tubes. Forward and reverse primers for VP7 and VP4 (VP8\*) amplification are described elsewhere [20,53]. In addition, 10 samples, including representative VP7 and VP4 genotype combinations observed in this study, were selected for VP6 and NSP1-5 gene characterization. Primers and cycling conditions were used, as described elsewhere [10], and PCR reagents were used, as described above. Genotyping was performed using the web-based genotyping tool RotaC v2.0 [54].

#### 4.4. PCR Product Purification, Sequencing, and GenBank Accession Numbers

PCR products were visualized in 1–2% agarose gels and positive samples were purified using PureLink™ Quick Gel Extraction and PCR Purification Combo Kit (Invitrogen®, Carlsbad, CA, USA),

according to the manufacturer's instructions. Both cDNA strands were sequenced by Macrogen Inc. (Seoul, Korea). Sequences were deposited in GenBank with accession numbers: MN649559—MN649674 (VP4), MN649675—MN649732 (VP7), MN649733—MN649742 (VP6), MN649743—MN649751 (NSP1), MN649752—MN649761 (NSP2), MN649762—MN649770 (NSP3), MN649771—MN649780 (NSP4), and MN649781—MN649789 (NSP5).

#### 4.5. Phylogenetic Analysis

All the available sequences corresponding to the genotypes observed in the RVA strains detected in this study, previously determined with RotaC, were downloaded from the Virus Variation Resource (<http://www.ncbi.nlm.nih.gov/genome/viruses/variation/>) [55]. A dataset was created for each genotype, and multiple sequence alignments were obtained using Clustal W implemented in MEGA 7 software [56]. The final alignment of each gene comprised all the worldwide sequences that covered the length of the sequences obtained in this study. The length of the sequences and the nucleotide position, involved in the phylogenetic analysis of each gene, are detailed in Table 3. The nucleotide substitution models that best fit each dataset (Table 3) and the maximum likelihood trees were obtained using W-IQ-TREE (available at <http://iqtree.cibiv.univie.ac.at>) [57]. The branches support was estimated with the Shimodaira–Hasegawa-approximate likelihood-ratio test (SH-aLRT) [58]. Trees were visualized in FigTree (<http://tree.bio.ed.ac.uk/software/figtree/>).

**Table 3.** Information about the final alignments obtained for the phylogenetic analyses.

	NSP1	NSP2	NSP3	NSP4	NSP5	VP4 (P[5])	VP4 (P[11])	VP6	VP7 (G6)	VP7 (G10)
Sequences length *	1005	954	917	528	597	645	654	1143	852	837
Genomic position *	165–1169	Complete ORF	47–963	Complete ORF	Complete ORF	130–774	124–795	Complete ORF	121–972	73–909
Best nucleotide substitution model	TIM + I + G	TIM + G	TIM3 + G	HKY + G	TN + I + G	TIM + G	TPM3u + G	TIM + I + G	TIM2 + I + G	TPM3 + G

\* Reference strain: WC3.

#### 4.6. Statistical Analyses

Data were organized and graphics were generated using Microsoft® Office Excel. Categorical data were evaluated with RStudio v1.0.136 software through Pearson's chi-squared tests. Odds ratios (OR) and 95% confidence intervals (CI) were calculated with jamovi software (available at <https://www.jamovi.org/>). Viral load values (genome copies/milliliter of feces) were log10 transformed. For the viral load and mean age analyses, the Shapiro–Wilk test was performed, rejecting the normality of the data, so the Mann–Whitney U test was performed with the same software. For all tests, differences were considered statistically significant if the obtained *p*-value was < 0.05.

## 5. Conclusions

Rotavirus A is widespread in cattle in Uruguay and is associated with diarrhea in calves, with a peak of viral shedding at 2–3 weeks of age, and higher viral shedding in diarrheic versus non-diarrheic calves. Even though the main genotypes observed in this country are the most prevalent worldwide, a rare strain was detected with a G24-P[33]-I2-A13-N2-T9-E12-H3 genotype constellation. The E12 genotype detected in all strains, regardless of the VP7 and VP4 genotypes, appears to be a South American geographic marker. An intricate genetic scenario was evidenced, with gene reassortment and interspecies transmission events, including transmission between animals and humans.

**Supplementary Materials:** The following are available online at <http://www.mdpi.com/2076-0817/9/7/570/s1>, Figure S1: Maximum likelihood tree of the NSP1 gene. The best nucleotide substitution model (TIM + I + G) and the maximum likelihood tree were obtained with W-IQ-TREE. Uruguayan strains are shown in different colors. SH-aLRT values  $\geq 80$  are shown. Figure S2: Maximum likelihood tree of the NSP2 gene. The best nucleotide substitution model (TIM + G) and the maximum likelihood tree were obtained with W-IQ-TREE. Uruguayan strains are shown in different colors. SH-aLRT values  $\geq 80$  are shown. Figure S3: Maximum likelihood tree of the NSP3 gene. The best nucleotide substitution model (TIM3 + G) and the maximum likelihood tree were obtained with W-IQ-TREE. Uruguayan strains are shown in different colors. SH-aLRT values  $\geq 80$  are shown.

Figure S4: Maximum likelihood tree of the NSP4 gene. The best nucleotide substitution model (HKY + G) and the maximum likelihood tree were obtained with W-IQ-TREE. Uruguayan strains are shown in different colors. SH-aLRT values  $\geq 80$  are shown. Figure S5: Maximum likelihood tree of the NSP5 gene. The best nucleotide substitution model (TN + I + G) and the maximum likelihood tree were obtained with W-IQ-TREE. Uruguayan strains are shown in different colors. SH-aLRT values  $\geq 80$  are shown. Figure S6: Maximum likelihood tree of the VP6 gene. The best nucleotide substitution model (TIM + I + G) and the maximum likelihood tree were obtained with W-IQ-TREE. Uruguayan strains are shown in different colors. SH-aLRT values  $\geq 80$  are shown.

**Author Contributions:** Conceptualization, M.C. and R.C.; methodology, M.C., R.D.C., M.L.C., C.S., S.M., F.C. and D.C.; resources, M.C., F.R.-C., F.G., V.P. and R.C.; writing—original draft preparation, M.C.; writing—review and editing, M.C., R.D.C., M.L.C., S.M., F.C., D.C., M.V., F.R.-C., F.G., V.P. and R.C.; funding acquisition, M.C., F.R.-C. and R.C. All authors have read and agreed to the published version of the manuscript.

**Funding:** This research was funded by “Instituto Nacional de Investigación Agropecuaria” (INIA), grant number PL\_015 N-15156 and N-23398, and by the “Universidad de la República” program “Polo de Desarrollo Universitario”. The APC was funded by “Universidad de la República”.

**Acknowledgments:** M.C. acknowledges support from the “Agencia Nacional de Investigación e Innovación” (ANII) through a PhD scholarship, and “Comisión Sectorial de Investigación Científica” (CSIC) and ANII for mobility fellowships.

**Conflicts of Interest:** The authors declare no conflict of interest. The funders had no role in the design of the study; in the collection, analyses, or interpretation of data; in the writing of the manuscript, or in the decision to publish the results.

## References

1. Urie, N.J.; Lombard, J.E.; Shivley, C.B.; Koprak, C.A.; Adams, A.E.; Earleywine, T.J.; Olson, J.D.; Garry, F.B. Preweaned heifer management on US dairy operations: Part V. Factors associated with morbidity and mortality in preweaned dairy heifer calves. *J. Dairy Sci.* **2018**, *101*, 9229–9244. [CrossRef]
2. Waltner-Toews, D.; Martin, S.W.; Meek, A.H. The effect of early calthood health status on survivorship and age at first calving. *Can. J. Vet. Res.* **1986**, *50*, 314–317. [PubMed]
3. Donovan, G.A.; Dohoo, I.R.; Montgomery, D.M.; Bennett, F.L. Calf and disease factors affecting growth in female Holstein calves in Florida, USA. *Prev. Vet. Med.* **1998**, *33*, 1–10. [CrossRef]
4. Østerås, O.; Solbu, H.; Refsdal, A.O.; Roalkvam, T.; Filseth, O.; Minsaas, A. Results and evaluation of thirty years of health recordings in the Norwegian dairy cattle population. *J. Dairy Sci.* **2007**, *90*, 4483–4497. [CrossRef]
5. Windeyer, M.C.; Leslie, K.E.; Godden, S.M.; Hodgins, D.C.; Lissemore, K.D.; LeBlanc, S.J. Factors associated with morbidity, mortality, and growth of dairy heifer calves up to 3 months of age. *Prev. Vet. Med.* **2014**, *113*, 231–240. [CrossRef] [PubMed]
6. Izzo, M.M.; Kirkland, P.D.; Mohler, V.L.; Perkins, N.R.; Gunn, A.A.; House, J.K. Prevalence of major enteric pathogens in Australian dairy calves with diarrhoea. *Aust. Vet. J.* **2011**, *89*, 167–173. [CrossRef]
7. Al Mawly, J.; Grinberg, A.; Prattley, D.; Moffat, J.; French, N. Prevalence of endemic enteropathogens of calves in New Zealand dairy farms. *N. Z. Vet. J.* **2015**, *63*, 147–152. [CrossRef]
8. Estes, M.; Greenberg, H. Rotaviruses. In *Fields Virology*, 6th ed.; Knipe, D.M., Howley, P.M., Cohen, J.I., Griffin, D.E., Lamb, R.A., Martin, M.A., Racaniello, V.R., Roizman, B., Eds.; Wolters Kluwer Business/Lippincott Williams and Wilkins: Philadelphia, PA, USA, 2013.
9. Castells, M.; Schild, C.; Caffarena, D.; Bok, M.; Giannitti, F.; Armendano, J.; Riet-Correa, F.; Victoria, M.; Parreño, V.; Colina, R. Prevalence and viability of group A rotavirus in dairy farm water sources. *J. Appl. Microbiol.* **2018**, *124*, 922–929. [CrossRef]
10. Matthijnssens, J.; Ciarlet, M.; Heiman, E.; Arijs, I.; Delbeke, T.; McDonald, S.M.; Palombo, E.A.; Iturriza-Gómara, M.; Maes, P.; Patton, J.T.; et al. Full genome-based classification of rotaviruses reveals a common origin between human Wa-Like and porcine rotavirus strains and human DS-1-like and bovine rotavirus strains. *J. Virol.* **2008**, *82*, 3204–3219. [CrossRef]
11. Abe, M.; Ito, N.; Masatani, T.; Nakagawa, K.; Yamaoka, S.; Kanamaru, Y.; Suzuki, H.; Shibano, K.; Arashi, Y.; Sugiyama, M. Whole genome characterization of new bovine rotavirus G21P[29] and G24P[33] strains provides evidence for interspecies transmission. *J. Gen. Virol.* **2011**, *92*, 952–960. [CrossRef]

12. Matthijnssens, J.; Potgieter, C.A.; Ciarlet, M.; Parreño, V.; Martella, V.; Bányai, K.; Garaicoechea, L.; Palombo, E.A.; Novo, L.; Zeller, M.; et al. Are human P[14] rotavirus strains the result of interspecies transmissions from sheep or other ungulates that belong to the mammalian order Artiodactyla? *J. Virol.* **2009**, *83*, 2917–2929. [CrossRef] [PubMed]
13. Matthijnssens, J.; Rahman, M.; Martella, V.; Xuelei, Y.; De Vos, S.; De Leener, K.; Ciarlet, M.; Buonavoglia, C.; Van Ranst, M. Full genomic analysis of human rotavirus strain B4106 and lapine rotavirus strain 30/96 provides evidence for interspecies transmission. *J. Virol.* **2006**, *80*, 3801–3810. [CrossRef]
14. Castells, M.; Giannitti, F.; Caffarena, R.D.; Casaux, M.L.; Schild, C.; Castells, D.; Riet-Correa, F.; Victoria, M.; Parreño, V.; Colina, R. Bovine coronavirus in Uruguay: Genetic diversity, risk factors and transboundary introductions from neighboring countries. *Arch. Virol.* **2019**, *164*, 2715–2724. [CrossRef] [PubMed]
15. Castells, M.; Bertoni, E.; Caffarena, R.D.; Casaux, M.L.; Schild, C.; Victoria, M.; Riet-Correa, F.; Giannitti, F.; Parreño, V.; Colina, R. Bovine astrovirus surveillance in Uruguay reveals high detection rate of a novel *Mamastrovirus* species. *Viruses* **2019**, *12*, 32. [CrossRef] [PubMed]
16. Food and Agriculture Organization of the United Nations. *Meat Market Review*; FAO: Rome, Italy, 2018.
17. International Dairy Federation. The World Dairy Situation 2013. In *Bulletin of the International Dairy Federation 470/2013*; International Dairy Federation: Schaerbeek, Belgium, 2013.
18. DIEA. Anuario Estadístico Agropecuario. 2018. Available online: [https://descargas.mgap.gub.uy/DIEA/Anuarios/Anuario2018/Anuario\\_2018.pdf](https://descargas.mgap.gub.uy/DIEA/Anuarios/Anuario2018/Anuario_2018.pdf) (accessed on 19 March 2020).
19. Alfieri, A.A.; Parazzi, M.E.; Takiuchi, E.; Médici, K.C.; Alfieri, A.F. Frequency of group A rotavirus in diarrhoeic calves in Brazilian cattle herds, 1998–2002. *Trop. Anim. Health Prod.* **2006**, *38*, 521–526. [CrossRef] [PubMed]
20. Garaicoechea, L.; Bok, K.; Jones, L.R.; Combessies, G.; Odeón, A.; Fernandez, F.; Parreño, V. Molecular characterization of bovine rotavirus circulating in beef and dairy herds in Argentina during a 10-year period (1994–2003). *Vet. Microbiol.* **2006**, *118*, 1–11. [CrossRef] [PubMed]
21. Badaracco, A.; Garaicoechea, L.; Rodríguez, D.; Uriarte, E.L.; Odeón, A.; Bilbao, G.; Galarza, R.; Abdala, A.; Fernandez, F.; Parreño, V. Bovine rotavirus strains circulating in beef and dairy herds in Argentina from 2004 to 2010. *Vet. Microbiol.* **2012**, *158*, 394–399. [CrossRef]
22. Da Silva Medeiros, T.N.; Lorenzetti, E.; Alfieri, A.F.; Alfieri, A.A. G and P genotype profiles of rotavirus A field strains circulating in beef and dairy cattle herds in Brazil, 2006–2015. *Comp. Immunol. Microbiol. Infect. Dis.* **2019**, *64*, 90–98. [CrossRef]
23. Madadgar, O.; Nazaktabar, A.; Keivanfar, H.; Zahraei Salehi, T.; Lotfollah Zadeh, S. Genotyping and determining the distribution of prevalent G and P types of group A bovine rotaviruses between 2010 and 2012 in Iran. *Vet. Microbiol.* **2015**, *179*, 190–196. [CrossRef]
24. Pourasgari, F.; Kaplon, J.; Karimi-Naghlani, S.; Fremy, C.; Otarod, V.; Ambert-Balay, K.; Mirjalili, A.; Pothier, P. The molecular epidemiology of bovine rotaviruses circulating in Iran: A two-year study. *Arch. Virol.* **2016**, *161*, 3483–3494. [CrossRef] [PubMed]
25. Mohamed, F.F.; Mansour, S.M.G.; El-Araby, I.E.; Mor, S.K.; Goyal, S.M. Molecular detection of enteric viruses from diarrheic calves in Egypt. *Arch. Virol.* **2017**, *162*, 129–137. [CrossRef] [PubMed]
26. Pang, X.L.; Lee, B.; Boroumand, N.; Leblanc, B.; Preiksaitis, J.K.; Yu Ip, C.C. Increased detection of rotavirus using a real time reverse transcription-polymerase chain reaction (RT-PCR) assay in stool specimens from children with diarrhea. *J. Med. Virol.* **2004**, *72*, 496–501. [CrossRef] [PubMed]
27. Gutiérrez-Aguirre, I.; Steyer, A.; Boben, J.; Gruden, K.; Poljsak-Prijatelj, M.; Ravnikar, M. Sensitive detection of multiple rotavirus genotypes with a single reverse transcription-real-time quantitative PCR assay. *J. Clin. Microbiol.* **2008**, *46*, 2547–2554. [CrossRef] [PubMed]
28. De La Cruz Hernández, S.I.; Anaya Molina, Y.; Gómez Santiago, F.; Terán Vega, H.L.; Monroy Leyva, E.; Méndez Pérez, H.; García Lozano, H. Real-time RT-PCR, a necessary tool to support the diagnosis and surveillance of rotavirus in Mexico. *Diagn. Microbiol. Infect. Dis.* **2018**, *90*, 272–276. [CrossRef]
29. Torres-Medina, A.; Schlafer, D.H.; Mebus, C.A. Rotaviral and coronaviral diarrhea. *Vet. Clin. N. Am. Food Anim. Pract.* **1985**, *1*, 471–493. [CrossRef]
30. Foster, D.M.; Smith, G.W. Pathophysiology of diarrhea in calves. *Vet. Clin. N. Am. Food Anim. Pract.* **2009**, *25*, 13–36. [CrossRef] [PubMed]
31. Blanchard, P.C. Diagnostics of dairy and beef cattle diarrhea. *Vet. Clin. N. Am. Food Anim. Pract.* **2012**, *28*, 443–464. [CrossRef]

32. Coura, F.M.; Freitas, M.D.; Ribeiro, J.; de Leme, R.A.; de Souza, C.; Alfieri, A.A.; Facury Filho, E.J.; de Carvalho, A.Ú.; Silva, M.X.; Lage, A.P.; et al. Longitudinal study of *Salmonella* spp., diarrheagenic *Escherichia coli*, Rotavirus, and Coronavirus isolated from healthy and diarrheic calves in a Brazilian dairy herd. *Trop. Anim. Health Prod.* **2015**, *47*, 3–11. [CrossRef]
33. Saif, L.J.; Smith, K.L. Enteric viral infections of calves and passive immunity. *J. Dairy Sci.* **1985**, *68*, 206–228. [CrossRef]
34. Badaracco, A.; Garaicoechea, L.; Matthijssens, J.; Louge Uriarte, E.; Odeón, A.; Bilbao, G.; Fernandez, F.; Parra, G.I.; Parreño, V. Phylogenetic analyses of typical bovine rotavirus genotypes G6, G10, P[5] and P[11] circulating in Argentinean beef and dairy herds. *Infect. Genet. Evol.* **2013**, *18*, 18–30. [CrossRef] [PubMed]
35. Barreiros, M.A.; Alfieri, A.F.; Médiçi, K.C.; Leite, J.P.; Alfieri, A.A. G and P genotypes of group A rotavirus from diarrhoeic calves born to cows vaccinated against the NCDV (P[1], G6) rotavirus strain. *J. Vet. Med. B Infect. Dis. Vet. Public Health* **2004**, *51*, 104–109. [CrossRef]
36. Da Silva Medeiros, T.N.; Lorenzetti, E.; Alfieri, A.F.; Alfieri, A.A. Phylogenetic analysis of a G6P[5] bovine rotavirus strain isolated in a neonatal diarrhea outbreak in a beef cattle herd vaccinated with G6P[1] and G10P[11] genotypes. *Arch. Virol.* **2015**, *160*, 447–451. [CrossRef] [PubMed]
37. Rocha, T.G.; Silva, F.D.; Gregori, F.; Alfieri, A.A.; Buzinaro, M.D.; Fagliari, J.J. Longitudinal study of bovine rotavirus group A in newborn calves from vaccinated and unvaccinated dairy herds. *Trop. Anim. Health Prod.* **2017**, *49*, 783–790. [CrossRef] [PubMed]
38. Parreño, V.; Béjar, C.; Vagnozzi, A.; Barrandeguy, M.; Costantini, V.; Craig, M.I.; Yuan, L.; Hodgins, D.; Saif, L.; Fernández, F. Modulation by colostrum-acquired maternal antibodies of systemic and mucosal antibody responses to rotavirus in calves experimentally challenged with bovine rotavirus. *Vet. Immunol. Immunopathol.* **2004**, *100*, 7–24. [CrossRef]
39. Papp, H.; László, B.; Jakab, F.; Ganesh, B.; De Grazia, S.; Matthijssens, J.; Ciarlet, M.; Martella, V.; Bányai, K. Review of group A rotavirus strains reported in swine and cattle. *Vet. Microbiol.* **2013**, *165*, 190–199. [CrossRef] [PubMed]
40. Komoto, S.; Pongsuwanna, Y.; Tacharoenmuang, R.; Guntapong, R.; Ide, T.; Higo-Moriguchi, K.; Tsuji, T.; Yoshikawa, T.; Taniguchi, K. Whole genomic analysis of bovine group A rotavirus strains A5-10 and A5-13 provides evidence for close evolutionary relationship with human rotaviruses. *Vet. Microbiol.* **2016**, *195*, 37–57. [CrossRef] [PubMed]
41. Okitsu, S.; Hikita, T.; Thongprachum, A.; Khamrin, P.; Takanashi, S.; Hayakawa, S.; Maneekarn, N.; Ushijima, H. Detection and molecular characterization of two rare G8P[14] and G3P[3] rotavirus strains collected from children with acute gastroenteritis in Japan. *Infect. Genet. Evol.* **2018**, *62*, 95–108. [CrossRef]
42. Ward, M.L.; Mijatovic-Rustempasic, S.; Roy, S.; Rungsriruriyachai, K.; Boom, J.A.; Sahni, L.C.; Baker, C.J.; Rench, M.A.; Wikswo, M.E.; Payne, D.C.; et al. Molecular characterization of the first G24P[14] rotavirus strain detected in humans. *Infect. Genet. Evol.* **2016**, *43*, 338–342. [CrossRef]
43. Garaicoechea, L.; Miño, S.; Ciarlet, M.; Fernández, F.; Barrandeguy, M.; Parreño, V. Molecular characterization of equine rotaviruses circulating in Argentinean foals during a 17-year surveillance period (1992–2008). *Vet. Microbiol.* **2011**, *148*, 150–160. [CrossRef]
44. Matthijssens, J.; Miño, S.; Papp, H.; Potgieter, C.; Novo, L.; Heylen, E.; Zeller, M.; Garaicoechea, L.; Badaracco, A.; Lengyel, G.; et al. Complete molecular genome analyses of equine rotavirus A strains from different continents reveal several novel genotypes and a largely conserved genotype constellation. *J. Gen. Virol.* **2012**, *93 Pt 4*, 866–875. [CrossRef]
45. Louge Uriarte, E.L.; Badaracco, A.; Matthijssens, J.; Zeller, M.; Heylen, E.; Manazza, J.; Miño, S.; Van Ranst, M.; Odeón, A.; Parreño, V. The first caprine rotavirus detected in Argentina displays genomic features resembling virus strains infecting members of the Bovidae and Camelidae. *Vet. Microbiol.* **2014**, *171*, 189–197. [CrossRef] [PubMed]
46. Volotão, E.M.; Soares, C.C.; Maranhão, A.G.; Rocha, L.N.; Hoshino, Y.; Santos, N. Rotavirus surveillance in the city of Rio de Janeiro-Brazil during 2000–2004: Detection of unusual strains with G8P[4] or G10P[9] specificities. *J. Med. Virol.* **2006**, *78*, 263–272. [CrossRef] [PubMed]
47. Martinez, M.; Phan, T.G.; Galeano, M.E.; Russomando, G.; Parreno, V.; Delwart, E.; Parra, G.I. Genomic characterization of a rotavirus G8P[1] detected in a child with diarrhea reveal direct animal-to-human transmission. *Infect. Genet. Evol.* **2014**, *27*, 402–407. [CrossRef]

48. Gotoh, T.; Nishimura, T.; Kuchida, K.; Mannen, H. The Japanese Wagyu beef industry: Current situation and future prospects—A review. *Asian Australas. J. Anim. Sci.* **2018**, *31*, 933–950. [CrossRef] [PubMed]
49. Sharma, S.; Hagbom, M.; Svensson, L.; Nordgren, J. The Impact of Human Genetic Polymorphisms on Rotavirus Susceptibility, Epidemiology, and Vaccine Take. *Viruses* **2020**, *12*, 324. [CrossRef] [PubMed]
50. Gómez, M.M.; Resque, H.R.; de Mello Volotao, E.; Rose, T.L.; da Silva, M.F.; Heylen, E.; Zeller, M.; Matthijnsens, J.; Leite, J.P. Distinct evolutionary origins of G12P[8] and G12P[9] group A rotavirus strains circulating in Brazil. *Infect. Genet. Evol.* **2014**, *28*, 385–388. [CrossRef]
51. Rojas, M.; Dias, H.G.; Gonçalves, J.L.S.; Manchego, A.; Rosadio, R.; Pezo, D.; Santos, N. Genetic diversity and zoonotic potential of rotavirus A strains in the southern Andean highlands, Peru. *Transbound. Emerg. Dis.* **2019**, *66*, 1718–1726. [CrossRef]
52. Matthijnsens, J.; Rahman, M.; Van Ranst, M. Two out of the 11 genes of an unusual human G6P[6] rotavirus isolate are of bovine origin. *J. Gen. Virol.* **2008**, *89*, 2630–2635. [CrossRef]
53. Gouvea, V.; Santos, N.; Timenetsky Mdo, C. VP4 typing of bovine and porcine group A rotaviruses by PCR. *J. Clin. Microbiol.* **1994**, *32*, 1333–1337. [CrossRef]
54. Maes, P.; Matthijnsens, J.; Rahman, M.; Van Ranst, M. RotaC: A web-based tool for the complete genome classification of group A rotaviruses. *BMC Microbiol.* **2009**, *9*, 238. [CrossRef]
55. Hatcher, E.L.; Zhdanov, S.A.; Bao, Y.; Blinkova, O.; Nawrocki, E.P.; Ostapchuck, Y.; Schäffer, A.A.; Brister, J.R. Virus Variation Resource—Improved response to emergent viral outbreaks. *Nucleic Acids Res.* **2017**, *45*, D482–D490. [CrossRef] [PubMed]
56. Kumar, S.; Stecher, G.; Tamura, K. MEGA7: Molecular Evolutionary Genetics Analysis Version 7.0 for Bigger Datasets. *Mol. Biol. Evol.* **2016**, *33*, 1870–1874. [CrossRef] [PubMed]
57. Trifinopoulos, J.; Nguyen, L.T.; von Haeseler, A.; Minh, B.Q. W-IQ-TREE: A fast online phylogenetic tool for maximum likelihood analysis. *Nucleic Acids Res.* **2016**, *44*, W232–W235. [CrossRef]
58. Guindon, S.; Dufayard, J.F.; Lefort, V.; Anisimova, M.; Hordijk, W.; Gascuel, O. New algorithms and methods to estimate maximum-likelihood phylogenies: Assessing the performance of PhyML 3.0. *Syst. Biol.* **2010**, *59*, 307–321. [CrossRef] [PubMed]



© 2020 by the authors. Licensee MDPI, Basel, Switzerland. This article is an open access article distributed under the terms and conditions of the Creative Commons Attribution (CC BY) license (<http://creativecommons.org/licenses/by/4.0/>).



Article

# Group A Rotavirus Detection and Genotype Distribution before and after Introduction of a National Immunisation Programme in Ireland: 2015–2019

Zoe Yandle \* , Suzie Coughlan, Jonathan Dean, Gráinne Tuite, Anne Conroy and Cillian F. De Gascun

UCD National Virus Reference Laboratory, University College Dublin, Dublin 4, Ireland; suzie.coughlan@ucd.ie (S.C.); jonathan.dean@ucd.ie (J.D.); grainne.tuite@ucd.ie (G.T.); anne.conroy@ucd.ie (A.C.); cillian.degascun@ucd.ie (C.F.D.G.)

\* Correspondence: zyandle@ucd.ie; Tel.: +353-1-716-4401

Received: 19 May 2020; Accepted: 5 June 2020; Published: 7 June 2020



**Abstract:** Immunisation against rotavirus infection was introduced into Ireland in December 2016. We report on the viruses causing gastroenteritis before (2015–2016) and after (2017–2019) implementation of the Rotarix vaccine, as well as changes in the diversity of circulating rotavirus genotypes. Samples from patients aged  $\leq 5$  years ( $n = 11,800$ ) were received at the National Virus Reference Laboratory, Dublin, and tested by real-time RT-PCR for rotavirus, Rotarix, norovirus, sapovirus, astrovirus, and enteric adenovirus. Rotavirus genotyping was performed either by multiplex or hemi-nested RT-PCR, and a subset was characterised by sequence analysis. Rotavirus detection decreased by 91% in children aged 0–12 months between 2015/16 and 2018/19. Rotarix was detected in 10% of those eligible for the vaccine and was not found in those aged  $>7$  months. Rotavirus typically peaks in March–May, but following vaccination, the seasonality became less defined. In 2015–16, G1P[8] was the most common genotype circulating; however, in 2019 G2P[4] was detected more often. Following the introduction of Rotarix, a reduction in numbers of rotavirus infections occurred, coinciding with an increase in genotype diversity, along with the first recorded detection of an equine-like G3 strain in Ireland.

**Keywords:** gastroenteritis; rotavirus; Rotarix; pediatric; diagnostics; molecular epidemiology; G3P[8]; equine-like

## 1. Introduction

Rotavirus is a leading cause of pediatric acute gastroenteritis, causing fever, vomiting, and diarrhoea. Mortality rates are highest in low income developing countries, where it causes approximately 128,000 fatal cases per year in those under five years old [1,2]. With the availability of rotavirus vaccines, the rate of global hospitalisations due to rotavirus or acute gastroenteritis, as well as deaths due to acute gastroenteritis, has decreased [3]. In Europe, pediatric rotavirus infection results in approximately 75,000–150,000 hospitalisations annually, with 2–4 times more children seeking out-patient medical care [4]. In Ireland, average crude incidence rates were 55 per 100,000 population in the 2007–2015 period [5], with hospitalisation rates of approximately 1190 per 100,000 [6], compared to the majority of EU member states, which report rates of 300–600 per 100,000 [4].

In 2009, the World Health Organisation (WHO) recommended global rotavirus vaccination [7] and, in Europe, 13 countries include it in their universal immunisation programmes, with a further five offering the vaccine for certain risk groups, specific regions, or requiring partial payment [8].

Two licensed live-attenuated vaccines are available in Europe; the pentavalent bovine-human reassortment rotavirus vaccine, RotaTeq (Merck & Co., West Point, PA, USA), and the human monovalent vaccine, Rotarix (GlaxoSmithKline, Rixensart, Belgium). In December 2016, Rotarix was introduced into the Irish national immunisation programme, with the vaccine administered in two doses at 2 and 4 months of age. Most recent figures (Q3, 2019) show the national uptake of the vaccine is 89% [9]. Rotavirus is a notifiable disease in Ireland, and laboratory confirmed cases are reported to the Health Protection Surveillance Centre. Effectiveness of both RotaTeq and Rotarix has been well documented, with the UK, Germany, and Belgium reporting an approximate 85% reduction in the presentation of severe rotavirus disease following vaccination [10–12].

Rotaviruses are double stranded RNA viruses containing 11 genome segments. There are 10 groups, A–J, defined by the middle VP6 capsid antigen, [13] two of which (I and J) were recently discovered in dogs and bats, respectively [14,15]. However, in humans, the majority of infections are caused by Group A rotavirus. Classification is a binary system depending on the expression of two outer proteins; the G and P-type, encoded by VP7 and VP4, respectively. Full genome analysis (where the VP7-VP4-VP6-VP1-VP2-VP3-NSP1-NSP2-NSP3-NSP4-NSP5/6 genes of rotavirus (RV) strains are described using the abbreviations Gx-P[x]-Ix-Rx-Cx-Mx-Ax-Nx-Tx-Ex-Hx), is required to monitor the evolution of the virus and detect reassortment [16].

Despite the theoretical possibility for numerous rotavirus G/P constellations, six account for 80–90% of circulating genotypes, namely G1P[8], G2P[4], G3P[8], G4P[8], G9P[8] and G12P[8]. Distribution of these commonly detected genotypes can vary by year, country, and age [17]. Despite the natural fluctuation of genotype diversity, increasing data suggest that the changes may be due to the impact of strain-specific vaccines [18]. Both in Belgium and the UK, before immunisation, G1P[8] was the most common circulating genotype; however, following vaccination, G2P[4] has been more frequently detected [19,20]. In Finland, following the introduction of RotaTeq, G9P[8] and G12P[8] have now become the main genotypes, where, previously, G1P[8] dominated [21]. However, changes in genotype distribution also occurs in countries with no immunisation [22,23], so whether the vaccine directly leads to a change in genotype diversity remains unclear [24,25].

Surveillance of rotavirus genotypes has been recommended by the WHO in countries with immunisation programmes to detect and monitor strain variation and ensure vaccine effectiveness is maintained [26]. The surveillance network, EuroRotaNet, has been monitoring rotavirus diversity in 12 European countries and has reported an increase in diversity since vaccination [17,27]. As Ireland is not currently part of any European or global surveillance network, we aim to fill that current gap of knowledge.

The purpose of this study is two-fold; firstly, to report on the viruses causing gastroenteritis, including rotavirus, 2 years prior and 3 years post implementation of the Rotarix immunisation programme, and, secondly, to describe the diversity of rotavirus genotypes in Ireland.

## **2. Results**

### *2.1. Sample Demographics*

Ireland has a population of 4.8 million with 36% of people living in the eastern health region, which includes Dublin, the surrounding areas, and the country's largest children's hospitals [28]. The National Virus Reference Laboratory (NVRL), Dublin, provides a diagnostic and reference service for all health care regions, though testing is also provided in regional hospitals.

This study analyzed the results from pediatric ( $\leq 5$  years) patient samples received at the NVRL between 1 January 2015 and 31 December 2019 for the investigation of viral gastroenteritis. In total, 11,800 faecal samples were included in the analysis, 5267 (45%) from females, 6511 (55%) from males, and 22 (0.2%) for which details were not provided. Samples tested were predominantly from the eastern health region 10,644/11,800 (90%), and of these 10,180/10,644 (96%) were from a children's hospital. Other samples were from the northern 672/11,800 (6%), western 204/11,800 (2%), midlands 139/11,800

(1%), and southern health regions 141/11,800 (1%). As vaccine history was not available for each patient, cohorts are described as vaccine-eligible, using age as a proxy for vaccination status.

During 2015 to 2019, there were 312,013 births recorded in Ireland; 159,821 males (51.2%) and 152,192 females (48.8%). To establish how representative the samples tested were, the percentage of the annual birth cohort investigated for the detection of viruses causing gastroenteritis was calculated for those aged 0–12 months in each year. In 2015, 2280/65,536 (3.5%) were tested, in 2016 2065/63,841 (3.3%) were tested, in 2017 760/61,824 (1.2%) were tested, in 2018 587/61,016 (1%) were tested, and in 2019 608/59,796 (1%) were tested.

## 2.2. Detection of Viral Pathogens

The most frequently detected viral pathogen in 2015 and 2016 was rotavirus, followed by norovirus. Norovirus has been detected in approximately 12% of samples each year, whereas enteric adenovirus (adenovirus subgenus F), sapovirus, and astrovirus were detected in 2.8–6.3% of samples from 2015–2019 (Table 1). The number of samples with no virus detected ranged from 51.4% to 65.0%, depending on the year.

**Table 1.** Laboratory results for the investigation of viral gastroenteritis in 11,800 samples tested at the National Virus Reference Laboratory (NVRL), aged 0–5 years in 2015–2019.

Virus Detected	Results (%) by Year					Total
	2015	2016	2017	2018	2019	
Rotavirus-wild-type	662 (15.03)	519 (13.09)	250 (15.49)	53 (4.42)	70 (5.93)	1554
Rotavirus-Rotarix	0 (0.00)	1 (0.03)	61 (3.78)	49 (4.08)	69 (5.84)	180
Norovirus	482 (10.94)	492 (12.41)	210 (13.01)	158 (13.17)	141 (11.94)	1483
Adenovirus F	156 (3.54)	155 (3.91)	101 (6.26)	64 (5.33)	47 (3.98)	523
Sapovirus	202 (4.59)	167 (4.21)	85 (5.27)	72 (6.00)	33 (2.79)	559
Astrovirus	197 (4.47)	121 (3.05)	77 (4.77)	68 (5.67)	53 (4.49)	516
No virus detected	2705 (61.42)	2511 (63.31)	830 (51.43)	736 (61.33)	768 (65.03)	7550
Total samples tested	4199	3787	1499	1159	1156	
Total results	4404 <sup>a</sup>	3966 <sup>b</sup>	1614 <sup>c</sup>	1200 <sup>d</sup>	1181 <sup>e</sup>	

<sup>a</sup> 185 dual infections, 10 triple infections <sup>b</sup> 154 dual infections, 11 triple infections, 1 quadruple infection, <sup>c</sup> 93 dual infections, 8 triple infections, 2 quadruple infections <sup>d</sup> 41 dual infections <sup>e</sup> 25 dual infections. Additional viruses detected in Rotarix samples, 2017: norovirus n = 3, adenovirus F n = 1, astrovirus n = 2; 2018: norovirus n = 8, adenovirus F n = 1; 2019: norovirus n = 3, sapovirus n = 1, astrovirus n = 1.

There were 1753 samples tested from vaccine-eligible children in 2017–2019, and of these 43 (2.5%) had wild-type rotavirus, 179 (10.2%) had Rotarix, 257 (14.7%) had norovirus, 113 (6.4%) had adenovirus F, 97 (5.5%) had sapovirus, and 95 (5.4%) had astrovirus detected. In this group, there were 70 dual infections and 1039 (59.3%) samples had no detectable virus.

## 2.3. Detection of Wild-Type Rotavirus

The median age of those testing positive for rotavirus in the pre-vaccine era, 2015–2016 (n = 1181), was significantly lower at 1.19 years (interquartile range (IQR) 0.64–1.85), compared to the median in the entire 3 years post-vaccine, 2017–2019 (n = 373) at 1.85 years (IQR 1.12–2.84)  $p < 0.0001$  (Table 2).

In the 2015/16 pre-vaccine era, a total of 485/4345 (11.2%) children aged 0–1 year had detectable wild-type rotavirus. This compares with 12/1195 (1.0%) in the post-vaccine 2018 and 2019 era, representing a 91.1% relative decrease in the number of wild-type rotavirus detected in this age range. The 1–2-year age group showed a relative reduction of 79.1% when 2015/16 was compared with 2018/19; 444/1691 (26.3%) compared to 28/505 (5.5%), respectively. This contrasts with the 5–6-year age group, which showed an increase in the detection of rotavirus from 20/324 (6.2%) to 12/96 (12.5%).

**Table 2.** Number of wild-type rotavirus positive cases by age group in the pre-vaccine years (2015–2016) compared to the post-vaccine years (2017–2019).

Year	Number of Wild-Type Rotavirus Positive Samples/Total Number of Samples Tested (%)							Median Age (IQR)	
	0–1 Year	1–2 Years	2–3 Years	3–4 Years	4–5 Years	5–6 Years	Total		
Pre-vaccine	2015	285/2280 (12.5)	227/899 (25.3)	90/413 (21.8)	35/213 (16.4)	17/213 (8.0)	8/181 (4.4)	662/4199 (15.8)	1.17 (0.5–1.9)
	2016	200/2065 (9.7)	217/792 (27.4)	55/427 (12.9)	24/224 (10.7)	11/136 (8.1)	12/143 (8.4)	519/3787 (13.7)	1.22 (0.8–1.8)
Post-vaccine	2017	57/760 (7.5)	110/374 (29.4)	49/144 (34.0)	19/105 (18.1)	6/55 (10.9)	9/61 (14.8)	250/1499 (16.7)	1.59 (1.0–2.4)
	2018	8/587 (1.4)	12/272 (4.4)	23/125 (18.4)	2/62 (3.2)	3/59 (5.1)	5/54 (9.2)	53/1159 (4.6)	2.24 (1.6–2.9)
	2019	4/608 (0.7)	16/233 (6.9)	16/129 (12.4)	21/86 (24.4)	6/58 (10.3)	7/42 (16.7)	70/1156 (6.1)	2.90 (1.9–3.5)

Interquartile range (IQR).

### 2.4. Seasonal Variation of Wild-Type Rotavirus

Prior to vaccination, rotavirus was a seasonal infection. In 2015, the season ran from weeks 1–29, peaking in week 11; in 2016 from weeks 11–27, peaking in week 19; and in 2017 from weeks 2–30, peaking in week 11. However, in 2018 and 2019, there was no clear seasonal onset and end, and rotavirus was most frequently detected in weeks 14 and 22, respectively (Figure 1).

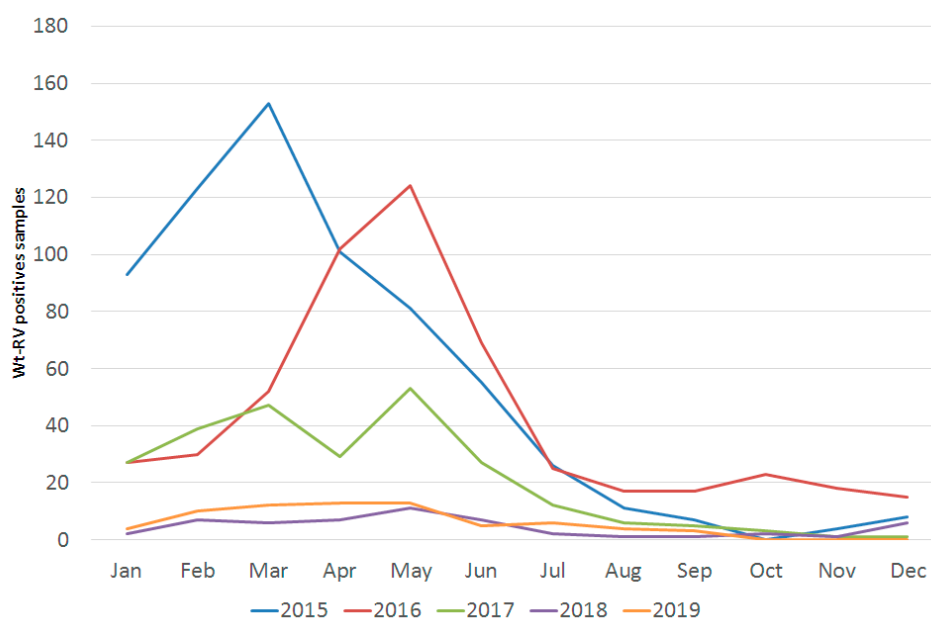


**Figure 1.** Number of wild-type rotavirus (Wt-RV) cases detected by month, 2015–2019.

### 2.5. Detection of Vaccine-Derived Rotavirus (Rotarix)

Of all 3814 samples tested in 2017–2019, 1753 (46.0%) were eligible for the vaccine, and Rotarix was detected in 179/1753 (10.2%) of these (Table 1). In addition, one sample from a vaccine eligible patient was received and tested in December 2016 and found to be positive for Rotarix. In 20/180 (11.1%) of Rotarix-positive samples, another virus was detected, most commonly norovirus.

The age at which Rotarix was most frequently detected was 2 months (Table 3). Rotarix was not detected in any samples from patients older than 7 months of age.

**Table 3.** Detection of Rotarix by age.

	Age					
	2 mts	3 mts	4 mts	5 mts	6 mts	7 mts
Rotarix detected/total number Rotarix detected (%)	99/180 (55.0)	41/180 (22.8)	26/180 (14.4)	11/180 (6.1)	2/180 (1.1)	1/180 (0.6)

### 2.6. Distribution of Genotypes in Ireland

In total, 786/1554 (51%) samples with detectable wild-type rotavirus were genotyped. Of these, 728 (93%) were from the eastern health board, 33 (4%) northern, 14 (2%) western, 8 (1%) southern, and 3 (0.4%) from the midlands. No significant correlation was observed between genotype and region or age (data not shown).

As the total numbers of rotavirus cases decreased following the introduction of immunization in December 2016, the proportion of samples genotyped was increased to reliably detect significant changes. In 2015, 293/662 (44%), and in 2016, 242/519 (47%) positive samples were genotyped, while in 2017, 135/250 (54%), in 2018, 48/53 (91%), and in 2019, 68/70 (97%) were genotyped.

### 2.7. Comparison of the Genotype Diversity Pre- and Post-Vaccine

G1P[8] was the most common genotype detected in 2015, 2016, and 2017 (Table 4). Conversely, G2P[4] was the most frequently detected genotype in 2019 (Figure 2). G3P[4], G8P[8], G9P[4], G12P[6], and G2P[8] remain uncommon genotypes in Ireland, detected in five, two, four, two, and one samples, respectively, over the 5-year period.

**Table 4.** Comparison of genotype diversity between the pre-vaccine (2015–2016) and post-vaccine (2017–2019) eras. Confidence interval (CI) significance 0.95. Comparison of the genotype proportion between pre- and post-vaccine year groups by Chi-square  $p < 0.05$ .

Genotype	Pre-Vaccinen (%)		Post-Vaccinen (%)			Pre-Vaccine Data Combined		Post-Vaccine Data Combined		Pre vs. Post $p =$
	2015	2016	2017	2018	2019	n (%)	CI 95%	n (%)	CI 95%	
G1P[8]	125 (42.7)	172 (71.1)	70 (51.9)	7 (14.6)	3 (4.4)	297 (55.5)	51.3–59.7	80 (31.9)	26.4–37.9	<0.0001
G2P[4]	6 (2.0)	16 (6.6)	15 (11.1)	7 (14.6)	27 (39.7)	22 (4.1)	2.7–6.2	49 (19.5)	15.1–24.9	<0.0001
G3P[8]	10 (3.4)	9 (3.7)	17 (12.6)	7 (14.6)	16 (23.5)	19 (3.6)	2.3–5.5	40 (15.9)	11.9–21.0	<0.0001
G4P[8]	64 (21.8)	0 (0.0)	6 (4.4)	11 (23.0)	0 (0.0)	64 (12.0)	9.5–15.0	17 (6.8)	4.3–10.6	0.0257
G9P[8]	69 (23.5)	34 (14.1)	20 (14.8)	10 (20.9)	4 (5.9)	103 (19.3)	16.1–22.8	34 (13.6)	9.9–18.3	0.0493
G12P[8]	3 (1.0)	4 (1.7)	0 (0.0)	1 (2.1)	5 (7.4)	7 (1.3)	0.1–2.7	6 (2.4)	1.1–5.1	0.2675
Mixed	7 (2.4)	3 (1.2)	1 (0.7)	1 (2.1)	4 (5.9)	10 (1.9)	1–3.4	6 (2.4)	1.1–5.1	0.0014
Uncommon	2 (0.7)	2 (0.8)	1 (0.7)	1 (2.1)	8 (11.8)	4 (0.8)	0.03–1.9	10 (4.0)	2.2–7.2	0.6295
Untypable	7 (2.4)	2 (0.8)	5 (3.7)	3 (6.3)	1 (1.5)	9 (1.7)	0.9–3.2	9 (3.6)	1.9–6.7	n/a
Total	293 (100)	242 (100)	135 (100)	48 (100)	68 (100)	535 (100)	n/a	251 (100)	n/a	n/a

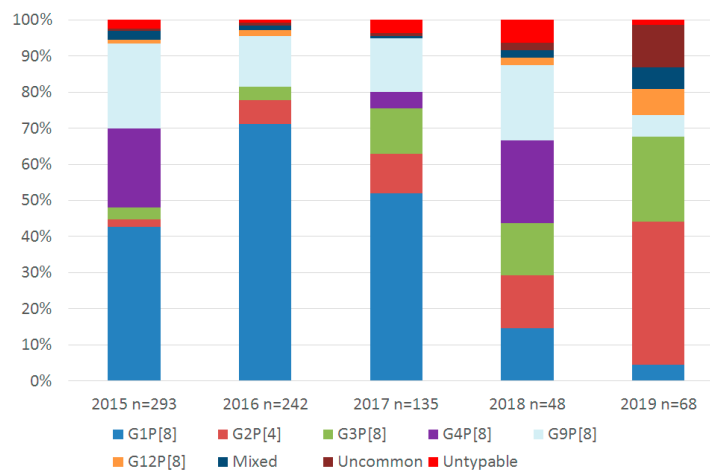


**Figure 2.** Genotype diversity in Ireland 2015–2019. Data are presented as the proportion (%) of a specific genotype compared to the total genotype results. Uncommon genotypes: <1% of total results, 2015: G9P[4] n = 2; 2016: G12P[6] n = 2; 2017: G8P[8] n = 1. 2018: G3P[4] n = 1; 2019: G2P[8] n = 1, G3P[4] n = 4, G8P[8] n = 1, G9P[4] n = 2. Mixed genotypes: those with >1 G or P-type, 2015: G1/4P[8] n = 7; 2016: G8/12P[8] n = 1, G2/3P[8] n = 1, G2/9 P[4/8] n = 1; 2017: G1/3P[8] n = 1; 2018: G1/3P[8] n = 1; 2019: G8/12P[8] n = 2, G3/12P[8] n = 1, G8P[8] n = 1, G9/12P[8] n = 1. Untypable results are those where either the G or P type was untypable.

## 2.8. Detection of Human and Equine-Like Rotavirus G3

G3P[8] was detected in 19/535 (4%) of genotyped samples in 2015–2016, compared to 40/251 (16%) in 2017–2019, a significant increase ( $p < 0.0001$ ), whilst the uncommon G3P[4] was only detected in the post-vaccine era. Four G3 strains were detected as a mixed infection. Of the 68 G3 types (63 P[8] and 5 P[4]), 17 were selected for sequencing of the VP7 gene, which identified two G3P[8] samples from 2018, containing viruses that clustered within the equine-like G3 lineage and the remaining 15 G3 samples clustered within the human lineage (Figure 3).

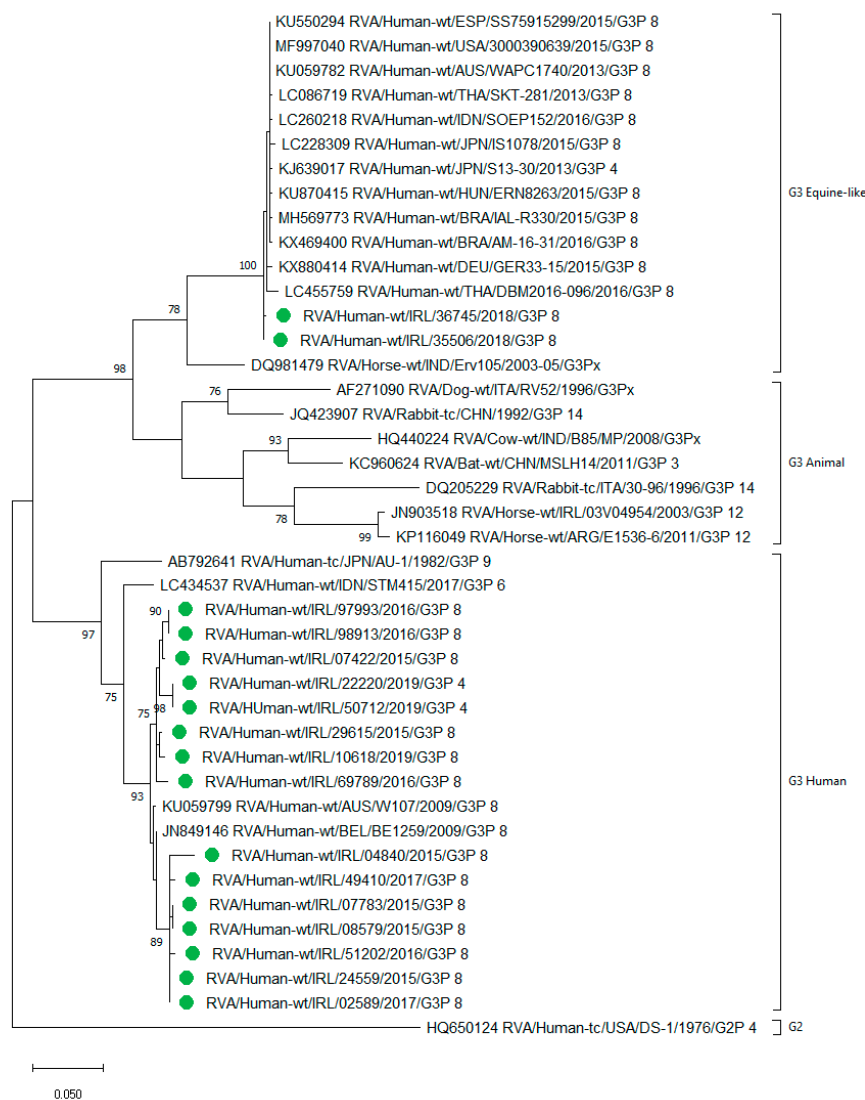


**Figure 3.** Phylogenetic tree of VP7 G3 rotavirus gene sequences. The tree was constructed by using the maximum likelihood method and the Tamura-Nei model [29]. Bootstrap values (1000 replicates) above 75% are shown. The tree is drawn to scale, with branch lengths measured in the number of substitutions per site. This analysis shows 46 nucleotide sequences; 17 from Irish strains identified in this study (colour coded with green circle) and 29 from reference strains in GenBank. Phylogenetic analyses were conducted in MEGA X [30].

## 2.9. Genotypes Detected in Rotavirus Positive Samples from Those of Vaccine-Eligible Age

There are six common genotypes circulating in Europe, namely, G1P[8], G2P[4], G3P[8], G4P[8], G9P[8], and G12P[8] [17], and all other genotypes are considered uncommon. Of the 43 samples with detectable wild-type rotavirus and of vaccine-eligible age, 37 were genotyped by RT-PCR (Table 5).

Of these, 30/37 (81.1%) had a common genotype, 4/37 (10.8%) had an uncommon genotype, 2/37 (5.4%) had a mixed infection, and one sample (2.7%) could not be fully genotyped. Ten of the 37 samples (27.0%) had G3 genotype detected (seven P[8] and three P[4]).

**Table 5.** Wild-type rotavirus genotypes detected in the age group eligible for the vaccine. Six additional samples had detectable wild-type rotavirus but were unavailable for genotyping.

Genotype	Classification of Genotype	Number of Samples (%)
G1P[8]	Common	5 (13.5)
G2P[4]	Common	11 (29.7)
G3P[8]	Common	6 (16.2)
G4P[8]	Common	1 (2.7)
G9P[8]	Common	4 (10.8)
G12P[8]	Common	3 (8.1)
G3P[4]	Uncommon	3 (8.1)
G9P[4]	Uncommon	1 (2.7)
G1/3 P[8]	Mixed	1 (2.7)
G9/12 P[8]	Mixed	1 (2.7)
G9 P untypable	Untypable	1 (2.7)
Total		37 (100)

### 3. Discussion

This study describes the reduction in rotavirus detection following implementation of a national immunization program for all children in Ireland, as well as previously unknown data regarding the extent of genotype diversity during 2015–2019. Our study shows that the largest reduction in the detection of rotavirus occurred in those aged 0–12 months, where a relative decrease of 91% was achieved between 2015/16 and 2018/19. Although the vaccine status was unknown in detail, the effectiveness of the vaccination program has been clearly shown. Our results support the national data collated by the Health Protection Surveillance Centre (HPSC), where a crude incidence rate (CIR) of rotavirus for all age groups was 13.3 per 100,000 population in 2018, representing a decrease of 76%, compared to the mean CIR during 2008–2017 of 55.5 per 100,000 [5]. In addition, since the introduction of the vaccine, there was a reduction in visits to three large pediatric emergency departments with acute gastroenteritis, where median weekly presentations in 2017–2018 (126; interquartile range (IQR), 103–165) were lower than in 2012–2016 (160; IQR 128–214) ( $p < 0.001$ ) [31]. Furthermore, an 86% (95% CI 79.3–90.2%) decrease in hospitalizations due to rotavirus has been reported nationally in those aged <1 year [32]. In our study, we found that the median age of wild-type rotavirus infection significantly increased in the years following vaccination, from 1.2 years in 2015 to 2.9 years in 2019 ( $p < 0.0001$ ). This is consistent with the findings of other researchers, who also noted the later age of infection in the post-vaccine era [11,33]. In Ireland, vaccination uptake is recorded by individual General Practitioners and health care professionals which are submitted to the HPSC on a quarterly basis. Vaccine uptake data from Q1 2017 to Q3 2017 was unavailable, but the evidence suggests that this must have been suboptimal as there was little change in rotavirus detection in those aged 0–1 year in 2016 compared to 2017 (9.7% versus 7.5%, respectively). The substantial increase in rotavirus infection in the post-vaccine years in the 5–6-year age group who would not be eligible for the vaccine was also somewhat surprising. Although the number of children tested in this age group were lower in the post-vaccine compared to pre-vaccine years, the proportion of positives was almost double (6.2% versus 12.5%). The short timeframe is a limitation of this study; however, collection of data is ongoing, and it will be of interest to follow up on the impact of vaccination on rotavirus detection in all age groups in the post-vaccine era. A further finding in our data is a diminution of the characteristic rotavirus seasonal pattern, a phenomenon that has been noted by others following introduction of the rotavirus vaccine [17,34].

The live-attenuated vaccine Rotarix replicates in the gut of the recipient and is excreted, albeit at lower amounts compared to a wild-type infection [35]. We detected Rotarix in 10% of patients who

were of vaccine-eligible age and, as rotavirus is notifiable in Ireland, this highlights the importance of differentiating between wild-type and vaccine-derived viruses, particularly when screening with a sensitive method, such as RT-PCR. By not excluding vaccine-derived rotavirus from diagnostic tests, there may be an over-estimation of rotavirus disease burden and unnecessary clinical intervention [36–38]. We identified 180 samples with detectable Rotarix, 20 (11%) of which had another virus detected, the most common being norovirus. We found norovirus to be the second most common pathogen detected after rotavirus in 2015/16, which then became the most common cause of viral gastroenteritis in our study group in the post-vaccine era. Our results are consistent with that observed in earlier studies, where norovirus is now the leading cause of viral gastroenteritis in those vaccinated for rotavirus [39–41]. Of note, sapovirus, astrovirus, and enteric adenovirus were detected in similar proportions over the 5-year time period and demonstrated no increase or decrease in detection rates following Rotarix introduction. Depending on the year, we report that 51–65% had no detectable viral pathogen. This apparent diagnostic gap highlights a further limitation of this study, in that it is quite possible that parallel samples were sent for the investigation of bacterial or parasitic pathogens, which are common causes of gastroenteritis [42,43]. Unfortunately, we did not have access to these results. In addition, other viruses, such as bocavirus, enterovirus, and parechoviruses, which may cause gastroenteritis, would not have been detected by our routine screening test.

Prior to the introduction of Rotarix, we found the circulating genotypes in Ireland were comparable to other European countries, with G1P[8] being the most commonly detected. The findings of the current study are consistent with those observed in several earlier reports from samples tested in Ireland from 1995 to 2009, where it was reported that the most commonly detected genotype was G1P[8], with fluctuating levels of G2P[4], G3P[8], G4P[8], and G9P[8] [44–49]. The current study matches those findings. However, we can report that the diversity of genotypes increased in the years following the introduction of a vaccine and that, in 2018/19, G1P[8] was no longer the most common genotype. Furthermore, genotypes detected in children eligible for the vaccine was more varied than those detected in the vaccine-ineligible cohort. With regards to wild-type and vaccine rotavirus strains, they can be described in terms of being homotypic, partly heterotypic, and fully heterotypic based on the G and P proteins. For instance, the monovalent G1P[8] Rotarix vaccine is homotypic to other circulating G1P[8] strains (both proteins are the same), G12P[8] is partly heterotypic (one protein different), and G2P[4] is fully heterotypic (both G and P proteins are different) [50]. Rotarix provides exposure to G1P[8] rotavirus among infants, with protection that is likely to be higher against homotypic strains than heterotypic strains, such as G2P[4]. This suggests that natural infection leading to disease is more likely to be caused by such heterotypic strains [19,51] and that a vaccinated population could possibly drive selective pressure, increasing the likelihood of these genotypes to circulate in the community [52,53]. That being said, the monovalent vaccine Rotarix provides significant protection from G1, G2, G3, G4, and G9, and efficacy against severe G2 rotavirus gastroenteritis was as high as for other rotavirus types [54]. Clearly, the immune response to rotavirus infection is a complex issue, with a previous report suggesting that type-specific neutralizing antibodies induced by the vaccine against VP7/VP4 epitopes are not solely responsible for a protective effect [55]. The report proposes that, as there are a limited number of diverse circulating strains worldwide, these antibodies are not driving long-term selective pressure, which itself would favor antigenic drift or the emergence of novel genotypes.

Interestingly, the genotype G12P[8] was not circulating widely at the time of Rotarix and RotaTeq vaccine development; however, it has now become established as an increasingly common genotype [17]. A large study in the USA found G12P[8] more frequently than any other rotavirus genotype in fully vaccinated children [56]. Another example of an uncommon genotype becoming more prevalent is the recently emerged equine-like G3 strain, first identified in Japan in 2013 [57] but now detected world-wide [58–60]. We identified, for the first time in Ireland, two samples from 2018 that clustered within the equine-like G3 lineage. A further 15 G3 samples were sequenced and all clustered in the human lineage, suggesting that the equine-like lineage has not yet become established in Ireland compared to other countries [59,61]. Of note, five of the uncommon human G3P[4] strains were

also identified in our study in 2018–2019, and this strain has been detected before in Ireland in 2006/07 [48]. The detection of uncommon genotypes, along with the additional potential for zoonotic reassortment [62,63], reinforces the WHO recommendation for surveillance, emphasising the need for continued monitoring of rotavirus vaccine efficacy against emerging rotavirus.

Several important limitations need to be considered for our study group. Firstly, the results are somewhat biased due to the observational nature of the study and samples tested would have been from those with moderate to severe gastroenteritis that warranted clinical investigation. In addition, there was no denominator for the population not suffering from symptoms of viral gastroenteritis, so we are unable to calculate incidence and prevalence of rotavirus infection. Furthermore, with no access to vaccination data, it was not possible to determine vaccine effectiveness rates or describe definitive vaccine failures. However, due to the large data set ( $n = 11,800$ ), we can show relative reductions in the detection of rotavirus and the changes in the diversity of circulating genotypes. The geographical distribution of samples is nationwide, although the data are skewed to some extent due to the density of the population in Dublin and the location of the main children's hospitals, and therefore samples were predominantly from the eastern health region. It should also be noted that the number of samples tested has decreased year on year. The reason for this may be the decrease in symptomatic children or the increase in localized testing and possible availability of point of care assays. Finally, it was not possible to categorize samples as the community or hospital acquired and we could not identify samples belonging to outbreaks.

We have shown that rotavirus continues to circulate in the pediatric population, albeit in low numbers, and this is expected to decrease further with the increasing cohort of vaccinated children. Binary genotypic classification is useful to establish circulating genotypes and can be used for reassortment studies of the VP7 and VP4 encoding genes; however, whole genome genotyping is required for a more detailed analysis of the virus. Indeed, a future aim from this ongoing study is to perform whole genome sequencing from samples in this dataset to allow identification of possible reassortment of non VP7/VP4 genes or mutation events. In addition, all samples identified as G3 will be categorized as either equine-like or of human lineage. By collaborating with clinicians at the children's hospitals, it is hoped that any sample from a child with rotavirus with a full or partial vaccine history will be referred to the NVRL for whole genome sequencing to establish definitive strains circulating in this group of children.

In conclusion, we describe the detection and characterization of rotavirus in pediatric samples circulating in Ireland over a 5-year time period. We show that, following the introduction of Rotarix, there is a relative reduction in the number of rotavirus infections diagnosed, coinciding with an increase in genotype diversity, along with the first recorded detection of an equine-like G3 strain in Ireland.

## **4. Materials and Methods**

### *4.1. Study Design*

This opportunistic study presents the results of faecal samples from pediatric samples ( $\leq 5$  years) investigated for viral gastroenteritis at the National Virus Reference Laboratory (NVRL), Dublin, Ireland. Test results for wild-type rotavirus, vaccine-derived rotavirus (Rotarix), norovirus, sapovirus, astrovirus, and enteric adenovirus subgenus F were obtained with genotype and sequence results, if available. Samples dated 1 January 2015 to 31 December 2019 were included in the study. Samples dated 1 January 2015 to 31 December 2016 were designated as "pre-vaccine". The first doses of Rotarix were given for those aged 2 months from the 1 December 2016. Only one sample was received from a 2-month old in December 2016, and this patient had detectable Rotarix. Samples dated 1 January 2017 to 31 December 2019 were designated as "post-vaccine". Routine testing for Rotarix was introduced into the NVRL from 11 December 2017. Rotavirus-positive samples received from 1 December 2016 to 10 December 2017 were tested for Rotarix, retrospectively.

#### *4.2. Annual Birth Cohort in Ireland*

The Central Office of Statistics provides the annual number of births in Ireland [64]. The number of annual births by year are: 2015: 65,536 (33,480 males, 32,056 females); 2016: 63,841 (32,709 males, 31,132 females); 2017: 61,824 (31,779 males, 30,045 females); 2018: 61,016 (31,298 males, 29,718 females); 2019: 59,796 (30,555 males, 29,241 females,). Data for 2018 and 2019 are provisional. The overall male: female ratio for 2015–2019 was 1.1: 1 (51.2% versus 48.8%).

#### *4.3. Data Analysis*

Data were extracted from the NVRL Laboratory Information Management System and analyzed in Excel. All samples were assumed to be from symptomatic patients. Samples with no date of birth recorded or duplicate samples were excluded from the study. Patients were de-identified, and the variables recorded in the database were patients' age at sample collection, sex, sample date, geographical region, and test result(s). Geographical regions were categorized as eastern (which includes Dublin), western, southern (south and south-east), northern (north-west and north-east), and midlands (midlands and mid-west), as defined by the Health Service Executive areas used by the Health Protection Surveillance Centre [5].

#### *4.4. Sampling Strategy for Genotyping and Sequencing of Samples*

To determine the sample size required to reliably detect a change in genotype frequency, a sample size calculator was used (CL95%, [www.openepi.com](http://www.openepi.com)), and then a random selection of wild-type rotavirus samples was selected for genotyping. In addition, all uncommon genotypes and a random subset of genotyped samples was selected for sequencing of VP7 and VP4 genes. A subset of those identified as G3 and were sequenced and analyzed to determine a human or equine-like lineage.

#### *4.5. Seasonality*

Seasonal onset, peak, and end were calculated: Onset: First of 2 consecutive weeks, where the median percentage of positive results was >10%. Peak: Week with the highest proportion of positive samples. End: Last of two consecutive weeks, where the median percentage was <10%. Denominator: total samples tested; numerator: the number of positive samples.

#### *4.6. Vaccine Eligibility*

The vaccine status was unknown, and patients were categorised by vaccine eligibility. Vaccine-eligible samples were those born after 1 October 2016 and were  $\geq 2$  months of age. Vaccine-ineligible samples were those born after 1 October 2016 and were <2 months of age or were born prior to 1 October 2016 and were aged 0–5 years of age.

#### *4.7. Laboratory Methods*

Upon receipt into the laboratory, approximately 20% *w/v* suspension of the fecal sample was prepared in 400  $\mu$ L Stool Transport and Recovery Buffer (Roche) and 400  $\mu$ L external lysis buffer (Roche). A total of 450  $\mu$ L of the suspension was extracted by Roche MagNAPure 96 and eluted into 100  $\mu$ L. During extraction, Brome Mosaic Virus RNA (University of Indiana) was added as an internal control (IC) at 1 pg/ $\mu$ L to the sample prior to extraction. The eluates were tested in five one-step RT-PCR assays, as previously described [65–70]. Briefly, eluates were tested in a 25  $\mu$ L or 10  $\mu$ L reaction mixture (depending on the 96- or 384-well format, respectively), containing 2 $\times$  Superscript<sup>TM</sup> III Platinum One-Step qRT-PCR mix (Invitrogen), as per product insert. Final concentrations of primers and probes ranged from 80 nM to 400 nM, depending on the target. Each sample eluate was tested by five (RT-)PCR reactions, namely: (i) norovirus G1/G2/IC; (ii) adenovirus F/pan-rotavirus/IC; (iii) Rotarix; iv) astrovirus/IC; v) sapovirus/IC. Amplification was performed on the ABI 7500 Fast (96-well format) or the ABI Vii7 (384-well format) instrument under the following conditions: 15 mins 50 °C, 2 mins 95 °C,

38 cycles of 15 secs 95 and 30 secs 60 °C (56 °C for norovirus). Amplification data was collected and analyzed with Sequence Detection Software version 2.3 or the ViiA7 software version 1.2.1 (both from Applied Biosystems).

Genotyping was either by a multiplex RT-PCR [71,72] or by hemi-nested RT-PCR, as described previously [73], with fragment visualization and size determination performed on the TapeStation (Agilent software, version 2200). Samples with an indeterminate G or P type were tested by both methods before being categorized as untypable. A selection of genotypes were confirmed by Sanger sequencing of the VP7 and VP4 genes, using previously described methods [73] on the ABI 3500Dx genetic analyzer (Applied Biosystems) and typed using the RotaC typing tool [74] or by the Basic Local Alignment and Search Tool, BLAST (<http://www.ncbi.nlm.nih.gov/blast/Blast.cgi>). G3 VP7 sequences (450 nucleotides) were aligned with appropriate reference sequences using ClustalW. Phylogenetic analyses were conducted in MEGA X [30] using the maximum likelihood method, with 1000 bootstrap replicates, based on the Tamura-Nei model [29]. This model was selected as it generated the lowest Bayesian information criterion (BIC) score in MEGA X.

#### 4.8. GenBank Accession Numbers

Partial VP7 fragments of the equine-like G3 strains identified in this study were deposited in GenBank under the following accession numbers: strains; MT475885 and MT475886, whereas the human-lineage G3 VP7 fragments were MT537569-537583.

#### 4.9. Statistical Analysis

The study was observational and therefore most data presented was descriptive. The median age of rotavirus infection in the pre- and post-vaccination groups was compared using Mann–Whitney *U* test. The Chi-square test for proportions was used to compare genotypes in the pre- and post-vaccination groups. *P* values for both tests of  $\leq 0.05$  were considered statistically significant. Confidence intervals (95%) were calculated using the Wilson method for a proportion of the genotypes detected. Statistical analysis was performed using SPSS 26 (IBM Corp; Armonk, NY, USA) software or [www.openepi.com](http://www.openepi.com).

#### 4.10. Ethical Statement

All procedures performed in studies involving human participants were in accordance with the ethical standards of the institutional and/or research committee and with the 1964 Helsinki declaration and its later amendments or comparable standards. This study was approved for ethical exemption by University College, Dublin LS-E-17-09.

**Author Contributions:** Conceptualization, Z.Y., S.C., and C.F.D.G.; data curation, S.C.; formal analysis, Z.Y.; investigation, Z.Y. and S.C.; methodology, Z.Y., S.C., and C.F.D.G.; project administration, Z.Y. and S.C.; resources, Z.Y., G.T., A.C., and C.F.D.G.; supervision, S.C. and C.F.D.G.; validation, Z.Y., S.C., and C.F.D.G.; visualization, Z.Y., S.C., and C.F.D.G.; writing—original draft, Z.Y.; Writing—review and editing, Z.Y., S.C., J.D., G.T., and C.F.D.G. All authors have read and agreed to the published version of the manuscript.

**Funding:** This research received no external funding

**Acknowledgments:** The authors would like to thank all clinicians and general practitioners for referring samples to the National Virus Reference Laboratory, Dublin, and to acknowledge the hard work of all the laboratory staff for processing and testing samples for the gastroenteritis screen.

**Conflicts of Interest:** The authors declare no conflict of interest.

## References

1. Hungerford, D.; Smith, K.; Tucker, A.; Iturriza-Gomara, M.; Vivancos, R.; McLeonard, C.; N, A.C.; French, N. Population effectiveness of the pentavalent and monovalent rotavirus vaccines: A systematic review and meta-analysis of observational studies. *BMC Infect. Dis.* **2017**, *17*, 569. [CrossRef] [PubMed]

2. Troeger, C.; Blacker, B.; Khalil, I. Estimates of the global, regional, and national morbidity, mortality, and aetiologies of diarrhoea in 195 countries: A systematic analysis for the Global Burden of Disease Study 2016. *Lancet. Infect. Dis.* **2018**, *18*, 1211–1228. [CrossRef]
3. Burnett, E.; Parashar, U.D.; Tate, J.E. Global impact of rotavirus vaccination on diarrhea hospitalizations and deaths among children < 5 years old: 2006–2019. *J. Infect. Dis.* **2020**. [CrossRef] [PubMed]
4. European Centre for Disease Prevention and Control. *ECDC Report: Expert Opinion on Rotavirus Vaccination in Infancy*; ECDC: Stockholm, Sweden, 2017.
5. HSE Health Protection Surveillance Centre. *Rotavirus 2018 Annual Epidemiological Report*; HSE HPSC: Dublin, Ireland, 2019.
6. Lynch, M.; O'Halloran, F.; Whyte, D.; Fanning, S.; Cryan, B.; Glass, R.I. Rotavirus in Ireland: National estimates of disease burden, 1997 to 1998. *Pediatric Infect. Dis. J.* **2001**, *20*, 693–698. [CrossRef]
7. World Health Organization. Global Advisory Committee on Vaccine Safety, report of meeting held 17–18 June 2009. *Wkly. Epidemiol. Rec.* **2009**, *84*, 213–236.
8. Poelaert, D.; Pereira, P.; Gardner, R.; Standaert, B.; Benninghoff, B. A review of recommendations for rotavirus vaccination in Europe: Arguments for change. *Vaccine* **2018**, *36*, 2243–2253. [CrossRef]
9. Health Protection Surveillance Centre. Available online: <https://www.hpsc.ie/az/vaccinepreventable/vaccination/immunisationuptakestatistics/immunisationuptakestatisticsat12and24monthsofage/> (accessed on 10 March 2020).
10. Walker, J.L.; Andrews, N.J.; Atchison, C.J.; Collins, S.; Allen, D.J.; Ramsay, M.E.; Ladhani, S.N.; Thomas, S.L. Effectiveness of oral rotavirus vaccination in England against rotavirus-confirmed and all-cause acute gastroenteritis. *Vaccine: X* **2019**, *1*, 100005. [CrossRef]
11. Pietsch, C.; Liebert, U.G. Rotavirus vaccine effectiveness in preventing hospitalizations due to gastroenteritis: A descriptive epidemiological study from Germany. *Clin. Microbiol. Infect.* **2019**, *25*, 102–106. [CrossRef]
12. Braeckman, T.; Van Herck, K.; Meyer, N.; Pircon, J.Y.; Soriano-Gabarro, M.; Heylen, E.; Zeller, M.; Azou, M.; Capiiau, H.; De Koster, J.; et al. Effectiveness of rotavirus vaccination in prevention of hospital admissions for rotavirus gastroenteritis among young children in Belgium: Case-control study. *BMJ* **2012**, *345*, e4752. [CrossRef]
13. Matthijnssens, J.; Otto, P.H.; Ciarlet, M.; Desselberger, U.; Van Ranst, M.; Johne, R. VP6-sequence-based cutoff values as a criterion for rotavirus species demarcation. *Arch. Virol.* **2012**, *157*, 1177–1182. [CrossRef]
14. Mihalov-Kovács, E.; Gellért, Á.; Marton, S.; Farkas, S.L.; Fehér, E.; Oldal, M.; Jakab, F.; Martella, V.; Bányai, K. Candidate new rotavirus species in sheltered dogs, Hungary. *Emerg. Infect. Dis.* **2015**, *21*, 660–663. [CrossRef] [PubMed]
15. Bányai, K.; Kemenesi, G.; Budinski, I.; Földes, F.; Zana, B.; Marton, S.; Varga-Kugler, R.; Oldal, M.; Kurucz, K.; Jakab, F. Candidate new rotavirus species in Schreiber's bats, Serbia. *Infect. Genet. Evol.* **2017**, *48*, 19–26. [CrossRef] [PubMed]
16. Matthijnssens, J.; Ciarlet, M.; Heiman, E.; Arijs, I.; Delbeke, T.; McDonald, S.M. Full genome-based classification of rotaviruses reveals a common origin between human Wa-Like and porcine rotavirus strains and human DS-1-like and bovine rotavirus strains. *J. Virol.* **2008**, *82*. [CrossRef] [PubMed]
17. Hungerford, D.; Vivancos, R.; EuroRotaNet Network Members. In-season and out-of-season variation of rotavirus genotype distribution and age of infection across 12 European countries before the introduction of routine vaccination, 2007/08 to 2012/13. *Eurosurveillance* **2016**, *21*. [CrossRef] [PubMed]
18. Roczo-Farkas, S.; Kirkwood, C.D.; Cowley, D.; Barnes, G.L.; Bishop, R.F.; Bogdanovic-Sakran, N.; Boniface, K.; Donato, C.M.; Bines, J.E. The Impact of Rotavirus Vaccines on Genotype Diversity: A Comprehensive Analysis of 2 Decades of Australian Surveillance Data. *J. Infect. Dis.* **2018**, *218*, 546–554. [CrossRef] [PubMed]
19. Hungerford, D.; Allen, D.J.; Nawaz, S.; Collins, S.; Ladhani, S.; Vivancos, R.; Iturriza-Gomara, M. Impact of rotavirus vaccination on rotavirus genotype distribution and diversity in England, September 2006 to August 2016. *Eurosurveillance* **2019**, *24*, 1700774. [CrossRef]
20. Zeller, M.; Rahman, M.; Heylen, E.; De Coster, S.; De Vos, S.; Arijs, I.; Novo, L.; Verstappen, N.; Van Ranst, M.; Matthijnssens, J. Rotavirus incidence and genotype distribution before and after national rotavirus vaccine introduction in Belgium. *Vaccine* **2010**, *28*, 7507–7513. [CrossRef]
21. Markkula, J.; Hemming-Harlow, M.; Salminen, M.T.; Savolainen-Kopra, C.; Pirhonen, J.; Al-Hello, H.; Vesikari, T. Rotavirus epidemiology 5–6 years after universal rotavirus vaccination: Persistent rotavirus activity in older children and elderly. *Infect. Dis.* **2017**, *49*, 388–395. [CrossRef]

22. Kaplon, J.; Grangier, N.; Pillet, S.; Minoui-Tran, A.; Vabret, A.; Wilhelm, N.; Prieur, N.; Lazrek, M.; Alain, S.; Mekki, Y.; et al. Predominance of G9P[8] rotavirus strains throughout France, 2014–2017. *Clin. Microbiol. Infect.* **2018**, *24*, 660.e661–660.e664. [CrossRef]
23. Verberk, J.D.M.; Bruijning-Verhagen, P.; Melker, H.E. Rotavirus in the Netherlands: Background information for the Health Council. *RIVM* 2017. [CrossRef]
24. Matthijssens, J.; Nakagomi, O.; Kirkwood, C.D.; Ciarlet, M.; Desselberger, U.; Ranst, M.V. Group A rotavirus universal mass vaccination: How and to what extent will selective pressure influence prevalence of rotavirus genotypes? *Expert Rev. Vaccines* **2012**, *11*, 1347–1354. [CrossRef] [PubMed]
25. Matthijssens, J.; Bilcke, J.; Ciarlet, M.; Martella, V.; Bányai, K.; Rahman, M.; Zeller, M.; Beutels, P.; Van Damme, P.; Van Ranst, M. Rotavirus disease and vaccination: Impact on genotype diversity. *Future Microbiol.* **2009**, *4*, 1303–1316. [CrossRef] [PubMed]
26. World Health Organization. Available online: [https://www.who.int/immunization/monitoring\\_surveillance/burden/estimates/rotavirus/Rota\\_virus\\_Q5\\_mortality\\_estimates\\_external\\_review\\_report\\_2006\\_may.pdf?ua=1](https://www.who.int/immunization/monitoring_surveillance/burden/estimates/rotavirus/Rota_virus_Q5_mortality_estimates_external_review_report_2006_may.pdf?ua=1) (accessed on 20 January 2020).
27. Iturriza-Gomara, M.; Dallman, T.; Banyai, K.; Bottiger, B.; Buesa, J.; Diedrich, S.; Fiore, L.; Johansen, K.; Koopmans, M.; Korsun, N.; et al. Rotavirus genotypes co-circulating in Europe between 2006 and 2009 as determined by EuroRotaNet, a pan-European collaborative strain surveillance network. *Epidemiol. Infect.* **2011**, *139*, 895–909. [CrossRef] [PubMed]
28. Central Statistics Office. Available online: <https://www.cso.ie/en/statistics/population> (accessed on 8 May 2020).
29. Tamura, K.; Nei, M. Estimation of the number of nucleotide substitutions in the control region of mitochondrial DNA in humans and chimpanzees. *Mol. Biol. Evol.* **1993**, *10*, 512–526. [CrossRef]
30. Kumar, S.; Stecher, G.; Li, M.; Nnyaz, C.; Tamura, K. MEGA X: Molecular Evolutionary Genetics Analysis across Computing Platforms. *Mol. Biol. Evol.* **2018**, *35*, 1547–1549. [CrossRef]
31. Coveney, J.; Barrett, M.; Fitzpatrick, P.; Kandamany, N.; McNamara, R.; Koe, S.; Okafor, I. National rotavirus vaccination programme implementation and gastroenteritis presentations: The paediatric emergency medicine perspective. *Ir. J. Med. Sci.* **2019**, *189*, 327–332. [CrossRef]
32. Burns, H.E.; Collins, A.M.; Fallon, U.B.; Marsden, P.V.; Ni Shuilleabhain, C.M. Rotavirus vaccination impact, Ireland, implications for vaccine confidence and screening. *Eur. J. Public Health* **2020**, 281–285. [CrossRef]
33. Shim, J.O.; Chang, J.Y.; Shin, S.; Moon, J.S.; Ko, J.S. Changing distribution of age, clinical severity, and genotypes of rotavirus gastroenteritis in hospitalized children after the introduction of vaccination: A single center study in Seoul between 2011 and 2014. *BMC Infect. Dis.* **2016**, *16*, 287. [CrossRef]
34. Tate, J.E.; Panozzo, C.A.; Payne, D.C.; Patel, M.M.; Cortese, M.M.; Fowlkes, A.L.; Parashar, U.D. Decline and change in seasonality of US rotavirus activity after the introduction of rotavirus vaccine. *Pediatrics* **2009**, *124*, 465–471. [CrossRef]
35. Yandle, Z.; Coughlan, S.; Drew, R.J.; Cleary, J.; De Gascun, C. Diagnosis of rotavirus infection in a vaccinated population: Is a less sensitive immunochromatographic method more suitable for detecting wild-type rotavirus than real-time RT-PCR? *J. Clin. Virol.* **2018**, *109*, 19–21. [CrossRef]
36. Gower, C.M.; Dunning, J.; Nawaz, S.; Allen, D.; Ramsay, M.E.; Ladhani, S. Vaccine-derived rotavirus strains in infants in England. *Arch. Dis. Child.* **2019**, *105*, 1–5. [CrossRef] [PubMed]
37. Whiley, D.M.; Ye, S.; Tozer, S.; Clark, J.E.; Bletchly, C.; Lambert, S.B.; Grimwood, K.; Nimmo, G.R. Over-diagnosis of rotavirus infection in infants due to detection of vaccine virus. *Clin. Infect. Dis.* **2019**, ciz1196. [CrossRef] [PubMed]
38. McAuliffe, G.N.; Taylor, S.L.; Moore, S.; Hewitt, J.; Upton, A.; Howe, A.S.; Best, E.J. Suboptimal performance of rotavirus testing in a vaccinated community population should prompt laboratories to review their rotavirus testing algorithms in response to changes in disease prevalence. *Diagn. Microbiol. Infect. Dis.* **2019**, *93*, 203–207. [CrossRef] [PubMed]
39. Hemming, M.; Räsänen, S.; Huhti, L.; Paloniemi, M.; Salminen, M.; Vesikari, T. Major reduction of rotavirus, but not norovirus, gastroenteritis in children seen in hospital after the introduction of RotaTeq vaccine into the National Immunization Programme in Finland. *Eur. J. Pediatr.* **2013**, *172*, 739–746. [CrossRef]
40. Bucardo, F.; Reyes, Y.; Svensson, L.; Nordgren, J. Predominance of norovirus and sapovirus in Nicaragua after implementation of universal rotavirus vaccination. *PLoS ONE* **2014**, *9*, e98201. [CrossRef]

41. Koo, H.L.; Neill, F.H.; Estes, M.K.; Munoz, F.M.; Cameron, A.; DuPont, H.L.; Atmar, R.L. Noroviruses: The Most Common Pediatric Viral Enteric Pathogen at a Large University Hospital After Introduction of Rotavirus Vaccination. *J. Pediatric Infect. Dis. Soc.* **2013**, *2*, 57–60. [CrossRef]
42. Steyer, A.; Jevšnik, M.; Petrovec, M.; Pokorn, M.; Grosek, Š.; Fratnik Steyer, A.; Šoba, B.; Uršič, T.; Cerar Kišek, T.; Kolenc, M.; et al. Narrowing of the Diagnostic Gap of Acute Gastroenteritis in Children 0–6 Years of Age Using a Combination of Classical and Molecular Techniques, Delivers Challenges in Syndromic Approach Diagnostics. *Pediatric Infect. Dis. J.* **2016**, *35*, e262–e270. [CrossRef]
43. Donaldson, A.L.; Clough, H.E.; O’Brien, S.J.; Harris, J.P. Symptom profiling for infectious intestinal disease (IID): A secondary data analysis of the IID2 study. *Epidemiol. Infect.* **2019**, *147*, e229. [CrossRef]
44. O’Mahony, J.; Foley, B.; Morgan, S.; Morgan, J.G.; Hill, C. VP4 and VP7 genotyping of rotavirus samples recovered from infected children in Ireland over a 3-year period. *J. Clin. Microbiol.* **1999**, *37*, 1699–1703. [CrossRef]
45. O’Halloran, F.; Lynch, M.; Cryan, B.; O’Shea, H.; Fanning, S. Molecular characterization of rotavirus in Ireland: Detection of novel strains circulating in the population. *J. Clin. Microbiol.* **2000**, *38*, 3370–3374. [CrossRef]
46. Reidy, N.; O’Halloran, F.; Fanning, S.; Cryan, B.; O’Shea, H. Emergence of G3 and G9 rotavirus and increased incidence of mixed infections in the southern region of Ireland 2001–2004. *J. Med Virol.* **2005**, *77*, 571–578. [CrossRef] [PubMed]
47. Lennon, G.; Reidy, N.; Cryan, B.; Fanning, S.; O’Shea, H. Changing profile of rotavirus in Ireland: Predominance of P[8] and emergence of P[6] and P[9] in mixed infections. *J. Med Virol.* **2008**, *80*, 524–530. [CrossRef] [PubMed]
48. Collins, P.J.; Mulherin, E.; O’Shea, H.; Cashman, O.; Lennon, G.; Pidgeon, E.; Coughlan, S.; Hall, W.; Fanning, S. Changing patterns of rotavirus strains circulating in Ireland: Re-emergence of G2P[4] and identification of novel genotypes in Ireland. *J. Med Virol.* **2015**, *87*, 764–773. [CrossRef] [PubMed]
49. Cashman, O.; Collins, P.J.; Lennon, G.; Cryan, B.; Martella, V.; Fanning, S.; Staines, A.; O’Shea, H. Molecular characterization of group A rotaviruses detected in children with gastroenteritis in Ireland in 2006–2009. *Epidemiol. Infect.* **2012**, *140*, 247–259. [CrossRef]
50. Bernstein, D.I. Rotavirus Vaccines: Mind Your Ps and Gs. *J. Infect. Dis.* **2018**, *218*, 519–521. [CrossRef]
51. Matthijnssens, J.; Zeller, M.; Heylen, E.; De Coster, S.; Vercauteren, J.; Braeckman, T.; Van Herck, K.; Meyer, N.; Pirçon, J.Y.; Soriano-Gabarro, M.; et al. Higher proportion of G2P[4] rotaviruses in vaccinated hospitalized cases compared with unvaccinated hospitalized cases, despite high vaccine effectiveness against heterotypic G2P[4] rotaviruses. *Clin. Microbiol. Infect.* **2014**, *20*, O702–O710. [CrossRef]
52. Pitzer, V.E.; Bilcke, J.; Heylen, E.; Crawford, F.W.; Callens, M.; De Smet, F.; Van Ranst, M.; Zeller, M.; Matthijnssens, J. Did Large-Scale Vaccination Drive Changes in the Circulating Rotavirus Population in Belgium? *Sci. Rep.* **2015**, *5*, 18585. [CrossRef]
53. Zeller, M.; Donato, C.; Trovão, N.S.; Cowley, D.; Heylen, E.; Donker, N.C.; McAllen, J.K.; Akopov, A.; Kirkness, E.F.; Lemey, P.; et al. Genome-Wide Evolutionary Analyses of G1P[8] Strains Isolated Before and After Rotavirus Vaccine Introduction. *Genome Biol. Evol.* **2015**, *7*, 2473–2483. [CrossRef]
54. Vesikari, T.; Karvonen, A.; Prymula, R.; Schuster, V.; Tejedor, J.C.; Cohen, R.; Meurice, F.; Han, H.H.; Damaso, S.; Bouckenoghe, A. Efficacy of human rotavirus vaccine against rotavirus gastroenteritis during the first 2 years of life in European infants: Randomised, double-blind controlled study. *Lancet* **2007**, *370*, 1757–1763. [CrossRef]
55. Clarke, E.; Desselberger, U. Correlates of protection against human rotavirus disease and the factors influencing protection in low-income settings. *Mucosal Immunol.* **2015**, *8*, 1–17. [CrossRef]
56. Ogden, K.M.; Tan, Y.; Akopov, A.; Stewart, L.S.; McHenry, R.; Fonnesbeck, C.J.; Piya, B.; Carter, M.H.; Fedorova, N.B.; Halpin, R.A.; et al. Multiple introductions and antigenic mismatch with vaccines may contribute to increased predominance of G12P[8] rotaviruses in the United States. *J. Virol.* **2018**. [CrossRef] [PubMed]
57. Malasao, R.; Saito, M.; Suzuki, A.; Imagawa, T.; Nukiwa-Soma, N.; Tohma, K.; Liu, X.; Okamoto, M.; Chaimongkol, N.; Dapat, C.; et al. Human G3P[4] rotavirus obtained in Japan, 2013, possibly emerged through a human–equine rotavirus reassortment event. *Virus Genes* **2015**, *50*, 129–133. [CrossRef] [PubMed]
58. Esposito, S.; Camilloni, B.; Bianchini, S.; Ianiro, G.; Polinori, I.; Farinelli, E.; Monini, M.; Principi, N. First detection of a reassortant G3P[8] rotavirus A strain in Italy: A case report in an 8-year-old child. *Virol. J.* **2019**, *16*, 64. [CrossRef] [PubMed]

59. Tacharoenmuang, R.; Komoto, S.; Guntapong, R.; Upachai, S.; Singchai, P.; Ide, T.; Fukuda, S.; Ruchusatsawast, K.; Sriwantana, B.; Tatsumi, M.; et al. High prevalence of equine-like G3P[8] rotavirus in children and adults with acute gastroenteritis in Thailand. *J. Med Virol.* **2020**, *92*, 174–186. [CrossRef]
60. Pietsch, C.; Liebert, U.G. Molecular characterization of different equine-like G3 rotavirus strains from Germany. *Infect. Genet. Evol.* **2018**, *57*, 46–50. [CrossRef]
61. Cowley, D.; Donato, C.M.; Roczo-Farkas, S.; Kirkwood, C.D. Emergence of a novel equine-like G3P[8] inter-genogroup reassortant rotavirus strain associated with gastroenteritis in Australian children. *J. Gen. Virol.* **2016**, *97*, 403–410. [CrossRef]
62. Kumar, N.; Malik, Y.S.; Sharma, K.; Dhama, K.; Ghosh, S.; Banyai, K.; Kobayashi, N.; Singh, R.K. Molecular characterization of unusual bovine rotavirus A strains having high genetic relatedness with human rotavirus: Evidence for zoonanthroponotic transmission. *Zoonoses Public Health* **2018**, *65*, 431–442. [CrossRef]
63. Tamim, S.; Matthijssens, J.; Heylen, E.; Zeller, M.; Van Ranst, M.; Salman, M.; Hasan, F. Evidence of zoonotic transmission of VP6 and NSP4 genes into human species A rotaviruses isolated in Pakistan in 2010. *Arch. Virol.* **2019**, *164*, 1781–1791. [CrossRef]
64. Central Statistics Office. Available online: <https://www.cso.ie/en/statistics/birthsdeathsandmarriages> (accessed on 30 May 2020).
65. Gautam, R.; Esona, M.D.; Mijatovic-Rustempasic, S.; Ian Tam, K.; Gentsch, J.R.; Bowen, M.D. Real-time RT-PCR assays to differentiate wild-type group A rotavirus strains from Rotarix(®) and RotaTeq(®) vaccine strains in stool samples. *Hum. Vaccines Immunother.* **2014**, *10*, 767–777. [CrossRef]
66. Kageyama, T.; Kojima, S.; Shinohara, M.; Uchida, K.; Fukushi, S.; Hoshino, F.B.; Takeda, N.; Katayama, K. Broadly reactive and highly sensitive assay for Norwalk-like viruses based on real-time quantitative reverse transcription-PCR. *J. Clin. Microbiol.* **2003**, *41*, 1548–1557. [CrossRef]
67. Tiemessen, C.T.; Nel, M.J. Detection and typing of subgroup F adenoviruses using the polymerase chain reaction. *J. Virol. Methods* **1996**, *59*, 73–82. [CrossRef]
68. Oka, T.; Katayama, K.; Hansman, G.S.; Kageyama, T.; Ogawa, S.; Wu, F.T.; White, P.A.; Takeda, N. Detection of human sapovirus by real-time reverse transcription-polymerase chain reaction. *J. Med. Virol.* **2006**, *78*, 1347–1353. [CrossRef] [PubMed]
69. Logan, C.; O’Leary, J.J.; O’Sullivan, N. Real-time reverse transcription PCR detection of norovirus, sapovirus and astrovirus as causative agents of acute viral gastroenteritis. *J. Virol. Methods* **2007**, *146*, 36–44. [CrossRef] [PubMed]
70. Freeman, M.M.; Kerin, T.; Hull, J.; McCaustland, K.; Gentsch, J. Enhancement of detection and quantification of rotavirus in stool using a modified real-time RT-PCR assay. *J. Med Virol.* **2008**, *80*, 1489–1496. [CrossRef] [PubMed]
71. Gautam, R.; Mijatovic-Rustempasic, S.; Esona, M.D.; Tam, K.I.; Quaye, O.; Bowen, M.D. One-step multiplex real-time RT-PCR assay for detecting and genotyping wild-type group A rotavirus strains and vaccine strains (Rotarix(R) and RotaTeq(R)) in stool samples. *PeerJ* **2016**, *4*, e1560. [CrossRef] [PubMed]
72. Andersson, M.; Lindh, M. Rotavirus genotype shifts among Swedish children and adults—Application of a real-time PCR genotyping. *J. Clin. Virol.* **2017**, *96*, 1–6. [CrossRef]
73. World Health Organization. Method 16: G and P genotyping. In *Manual of Rotavirus Detection and Characterization Methods*; WHO/IVB/08.17; WHO: Geneva, Switzerland, 2009; pp. 91–98.
74. Maes, P.; Matthijssens, J.; Rahman, M.; Van Ranst, M. RotaC: A web-based tool for the complete genome classification of group A rotaviruses. *BMC Microbiol.* **2009**, *9*, 238. [CrossRef]



© 2020 by the authors. Licensee MDPI, Basel, Switzerland. This article is an open access article distributed under the terms and conditions of the Creative Commons Attribution (CC BY) license (<http://creativecommons.org/licenses/by/4.0/>).



Article

# Rotavirus A in Brazil: Molecular Epidemiology and Surveillance during 2018–2019

Meylin Bautista Gutierrez, Alexandre Madi Fialho, Adriana Gonçalves Maranhão, Fábio Correia Malta, Juliana da Silva Ribeiro de Andrade, Rosane Maria Santos de Assis, Sérgio da Silva e Mouta, Marize Pereira Miagostovich, José Paulo Gagliardi Leite and Tulio Machado Fumian \* 

Laboratory of Comparative and Environmental Virology, Oswaldo Cruz Institute, Oswaldo Cruz Foundation, Avenida Brasil 4365, Rio de Janeiro 21040-900, Brazil; meylin.gutierrez@ioc.fiocruz.br (M.B.G.); amfialho@ioc.fiocruz.br (A.M.F.); adriana.maranhao@ioc.fiocruz.br (A.G.M.); fabio.malta@ioc.fiocruz.br (F.C.M.); juliana@ioc.fiocruz.br (J.d.S.R.d.A.); rmsassis@ioc.fiocruz.br (R.M.S.d.A.); mouta@ioc.fiocruz.br (S.d.S.e.M.); marizepm@ioc.fiocruz.br (M.P.M.); jpgleite@ioc.fiocruz.br (J.P.G.L.)

\* Correspondence: tuliomf@ioc.fiocruz.br or fumiantm@gmail.com; Tel.: +55-(21)-25621817

Received: 12 May 2020; Accepted: 7 June 2020; Published: 27 June 2020



**Abstract:** Rotavirus A (RVA) vaccines succeeded in lowering the burden of acute gastroenteritis (AGE) worldwide, especially preventing severe disease and mortality. In 2019, Brazil completed 13 years of RVA vaccine implementation (Rotarix™) within the National Immunization Program (NIP), and as reported elsewhere, the use of Rotarix™ in the country has reduced childhood mortality and morbidity due to AGE. Even though both marketed vaccines are widely distributed, the surveillance of RVA causing AGE and the monitoring of circulating genotypes are important tools to keep tracking the epidemiological scenario and vaccines impact. Thus, our study investigated RVA epidemiological features, viral load and G and P genotypes circulation in children and adults presenting AGE symptoms in eleven states from three out of five regions in Brazil. By using TaqMan®-based one-step RT-qPCR, we investigated a total of 1536 stool samples collected from symptomatic inpatients, emergency department visits and outpatients from January 2018 to December 2019. G and P genotypes of RVA-positive samples were genetically characterized by multiplex RT-PCR or by nearly complete fragment sequencing. We detected RVA in 12% of samples, 10.5% in 2018 and 13.7% in 2019. A marked winter/spring seasonality was observed, especially in Southern Brazil. The most affected age group was children aged >24–60 months, with a positivity rate of 18.8% ( $p < 0.05$ ). Evaluating shedding, we found a statistically lower RVA viral load in stool samples collected from children aged up to six months compared to the other age groups ( $p < 0.05$ ). The genotype G3P[8] was the most prevalent during the two years (83.7% in 2018 and 65.5% in 2019), and nucleotide sequencing of some strains demonstrated that they belonged to the emergent equine-like G3P[8] genotype. The dominance of an emergent genotype causing AGE reinforces the need for continuous epidemiological surveillance to assess the impact of mass RVA immunization as well as to monitor the emergence of novel genotypes.

**Keywords:** acute gastroenteritis; rotavirus A; incidence; genotyping; Brazil

## 1. Introduction

Acute gastroenteritis (AGE) remains as a major cause of mortality in children under five years old worldwide [1,2]. Among the AGE-causing pathogens, rotavirus A (RVA) is one of the leading agents, responsible for approximately 200,000 deaths per year among children <5 years old in developing countries [3–5]. Regarding severe disease, RVA accounts for around 20% and 40% of all AGE-hospitalization in countries with and without RVA vaccines implemented, respectively [6,7].

Currently, four World Health Organization (WHO)-prequalified live-attenuated oral RVA vaccines are available internationally—Rotarix™, RotaTeq™, Rotavac™, and RotaSiil™—and over 100 countries have introduced one of these vaccines into their national immunization program [8] (<https://www.who.int/immunization/diseases/rotavirus/en/>).

Rotaviruses belong to the *Reoviridae* family, genus *Rotavirus*. While nine rotaviruses species have been described (A–I), RVA is by far the most important species infecting humans worldwide [9,10]. The non-enveloped triple-layered viral particle has 70–75 nm in diameter with 11 segmented double-stranded RNA (dsRNA) genes, encoding for six structural (VP1–VP4, VP6, VP7) and depending on the strain, five or six non-structural proteins (NSP1–NSP5 or NSP6) [11]. Genetically, RVA is classified into G- and P-types, based on nucleotide sequence of genomic segments coding VP7 and VP4 proteins (binary classification), and currently there have been described 36 G- and 51 P-types [12]. Although many G and P combination would be possible to emerge, a few genotypes (G1P[8], G2P[4], G3P[8], G4P[8], G9P[8], and G12P[8]) have prevailed worldwide causing the majority of RVA infections in children [13–15].

Brazil has implemented the Rotarix™ vaccine in the National Immunization Program (NIP) in March 2006, which led to a significant reduction of diarrhea-associated mortality and hospitalization [16–18]. Linhares et al. [19] demonstrated the higher effectiveness of Rotarix™ among Brazilian infants aged up to 12 months and decreasing in older children. Concerning the genotype distribution in Brazil after the introduction of Rotarix™, G2P[4] was by far the most prevalent genotype detected until 2010. From 2011 onwards, a gradual decrease in the prevalence of G2P[4] was observed, being replaced by G3, G9, and G12 harboring a P[8]-type [20–23]. Nevertheless, unusual RVA genotypes have been frequently detected, such as: G3[P6], G12[P6], G8P[4], and G8P[6] and more recently the equine-like G3P[8] [17,23,24]. Similarly, recent studies from other countries have reported the detection of rare RVA genotype combination [25–28].

It has been demonstrated that the distribution of RVA genotypes over the years is characterized by natural and cyclical genotype fluctuations [20,29,30]. However, the selective pressure due to mass RVA vaccination could favor specific G and P combinations [9,31]. Therefore, the new and dynamic epidemiological scenario reinforces the need to continuously document RVA prevalence in AGE cases, molecular epidemiology and the potential emergence of unusual genotypes.

Our study investigated RVA prevalence, features and the molecular characterization of G and P genotypes among patients with AGE from three regions (Southern, Southeastern and Northeastern) in Brazil, 2018–2019. RVA was detected and quantified by quantitative RT-PCR (RT-qPCR) from diarrheic stool samples received from eleven Brazilian states, and G and P genotypes were determined by multiplex one-step RT-PCR or sequencing.

## **2. Materials and Methods**

### *2.1. Stool Collection and Ethics Statements*

This study included stool samples that were collected between January 2018 and December 2019 from children and adults with symptoms of AGE, characterized as  $\geq$ three liquid/semi liquid evacuations in a 24 h period. Inpatients and outpatients diarrheic stool samples were collected from eleven states from three regions of Brazil: Southern, Southeastern, and Northeastern. Samples were systematically sent together with clinical-epidemiological records to the Regional Rotavirus Reference Laboratory—Laboratory of Comparative and Environmental Virology (RRRL–LVCA). The laboratory is part of the ongoing national network for AGE surveillance and coordinated by General Coordination of Public Health Laboratories, Brazilian Ministry of Health.

This study is approved by the Ethics Committee of the Oswaldo Cruz Foundation (FIOCRUZ), number CAAE: 94144918.3.0000.5248. The surveillance is performed through a hierarchical network in which samples are provided by medical request in hospitals and health centers, monitored by the Brazilian Unified Health System (SUS). Patients' data were maintained anonymously and securely.

## 2.2. Viral RNA Extraction

Viral RNA was purified from 140 µL of clarified stool suspension (10% *w/v*) prepared with Tris-calcium buffer (pH = 7.2). Samples were subjected to an automatic nucleic acid extraction procedure using a QIAamp® Viral RNA Mini kit (QIAGEN, CA, USA) and a QIAcube® automated system (QIAGEN), according to the manufacturer's instructions. RVA RNA was eluted in 60 µL of the elution buffer AVE. The isolated RNA was immediately stored at −80 °C until the molecular analysis. In each extraction procedure, RNase/DNase-free water was used as negative control.

## 2.3. RVA Detection and Quantification

RVA was detected and quantified by using a TaqMan®-based quantitative one step PCR (RT-qPCR) with primers and probe targeting the conserved NSP3 segment, according to Zeng et al. (2008). Briefly, RT-qPCR reactions were performed with 5 µL of the extracted RNA in a final volume of 25 µL using the SuperScript™ III Platinum™ One-Step qRT-PCR Kit (ThermoFisher Scientific, Invitrogen Division, Carlsbad, CA, USA) in the Applied Biosystems® 7500 Real-Time PCR System (Applied Biosystems, Foster City, CA, USA). NSP3 primers and probe final concentrations used were 0.8 and 0.5 µM, respectively. The thermal cycling conditions were carried out as follows: RT step at 55 °C for 30 min, an initial denaturation step at 95 °C for 10 min and 40 cycles of PCR amplification at 95 °C for 15 s and 60 °C for 1 min. Samples that crossed the threshold line showing a characteristic sigmoid curve were regarded as positive. All runs included negative and non-template controls, and a standard curve with serial dilutions ( $10^6$ – $10^1$ ) of double-stranded DNA fragments (gBlock® Gene Fragment, Integrated DNA Technologies, Iowa, USA) containing the RVA NSP3 target region to ensure the correct interpretation of the results throughout the study. RVA viral loads were expressed as genome copies per gram (GC/g) of stool.

## 2.4. Genotyping and Sequencing

RVA-positive samples obtained by RT-qPCR were G- and P-genotyped using a one-step multiplex RT-PCR. The reactions were performed using the Qiagen One Step RT-PCR kit (Qiagen), using forward conserved primers VP7uF or VP4uF and specific reverse primers for G types G1, G2, G3, G4, G9, and G12, or P types P[4], P[6], P[8], P[9], and P[10] as recommended by the Centers for Disease Control and Prevention, USA. The G- and P-genotypes were assigned based on different amplicon sizes [base pairs (bp)] using agarose gel analysis. Sanger sequencing was also used to characterize the nucleotide (nt) sequence of specific strains, such as non-typeable samples or the equine-like G3, using consensus primers directed to the conserved regions within the VP4 and VP7 genes. The amplicons fragments of 876 bp and 881 bp for VP4 and VP7, respectively, were purified using the ExoSAP clean-up kit (ThermoFisher Scientific) and sent to the FIOCRUZ Institutional Platform for DNA sequencing (PDTIS). All primers used for RVA genotyping were based on previously studies [32–34].

## 2.5. Phylogenetic Analysis

Chromatogram analysis and consensus sequences were obtained using Geneious Prime (Biomatters Ltd., Auckland, New Zealand). RVA genotypes were confirmed in terms of closest homology sequence using Basic Local Alignment Search Tool (BLAST). Phylogenetic trees were constructed using the maximum likelihood method and the Kimura two-parameter model (2000 bootstrap replications for branch support) in MEGA X v. 10.1.7 [35], with RVA reference sequences obtained from the National Center for Biotechnology Information (NCBI) database. Nucleotide sequences obtained from clinical samples were submitted to NCBI GenBank (accession numbers: MT386419 to MT386453).

## 2.6. Statistical Analysis

Statistical analyses were performed using GraphPad Prism software v. 8.4.1 (GraphPad Software, San Diego, CA, USA). As appropriate, Mann–Whitney U test, Chi-squared or Fisher test was used to

assess significant difference between RVA detection rates, years of collecting samples and age groups, as well as to compare RVA viral load according to different age groups. A  $p$  value  $< 0.05$  was considered to be statistically significant.

### 3. Results

#### 3.1. Rotavirus A Epidemiology

During the two-year period of this study (2018–2019), a total of 1536 stool samples were collected from symptomatic inpatients with AGE (1161 and 375 from children and adults, respectively). Overall, we detected RVA in 12% of samples ( $n = 185$ ), 10.5% in 2018 and 13.7% in 2019. We observed a slight increase in RVA incidence in 2019, but without statistical significance ( $p = 0.053$ ). Except for three months in 2018 (April, June, and December), RVA circulated year-round, with monthly detection rates varying from 1.6% to 36.7% in May 2018 and September 2019, respectively (Figure 1A). In relation to seasonal patterns, we observed higher RVA circulation during winter/spring months, especially marked in Southern region states (Figure 1B,C), whilst RVA detections were lowest in autumn months.

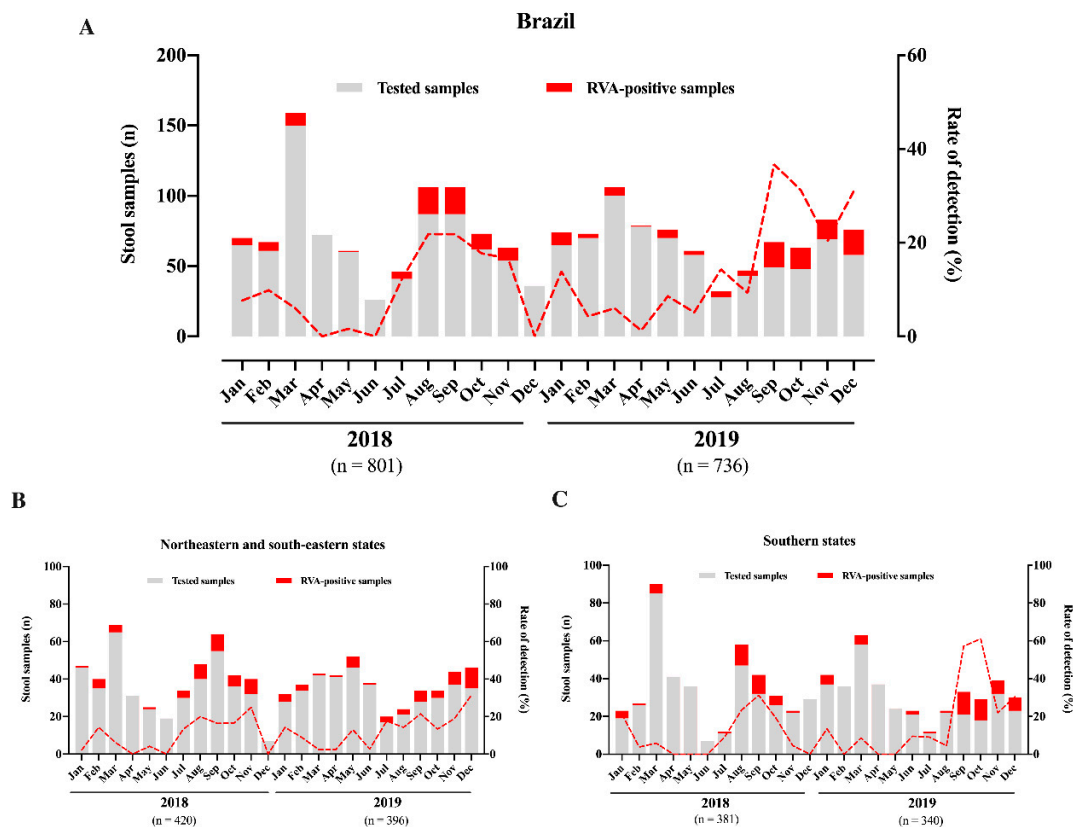


**Figure 1.** Monthly distribution of tested acute gastroenteritis samples, rotavirus A (RVA)-positive samples and RVA detection rates in Brazil (A), Northeastern and South-eastern states (B), and Southern states (C), during 2018–2019.

In regard to regional analysis, higher RVA prevalence was observed in the Northeast region (18.7%) compared to Southeastern and Southern regions (3.4% and 12.5%, respectively). Comparing the two year of the study, RVA detection rates were higher in 2019 for the three regions, but only with statistical significance in Southeastern region ( $p = 0.022$ ). Table 1 shows detailed analysis by regions and states. It is interesting to note that the two states of Southern region (Santa Catarina and Rio Grande do Sul) accounted for almost half of the AGE cases and RVA-positive samples (Figure 2).

**Table 1.** Number of tested and rotavirus-positive fecal samples through laboratory-based surveillance by region and state in Brazil during 2018 and 2019.

Region/State	No. of Fecal Samples: Positive/Tested (%)			p-Value (Chi-Square Test)
	Total	2018	2019	
<b>Southeast</b>	14/381 (3.7)	2/168 (1.2)	12/213 (5.6)	0.022
Espírito Santo		1/56	2/101	
Minas Gerais		1/75	-	
Rio de Janeiro		-	10/79	
<b>Northeast</b>	81/434 (18.7)	44/252 (17.5)	37/182 (20.3)	0.452
Bahia		1/98	2/95	
Maranhão		1/8	1/1	
Paraíba		20/37	-	
Pernambuco		19/68	30/61	
Rio Grande do Norte		-	1/5	
Sergipe		3/41	3/20	
<b>South</b>	90/720 (12.5)	39/381 (10.2)	51/340 (15)	0.053
Rio Grande do Sul		16/168	38/181	
Santa Catarina		23/213	13/159	

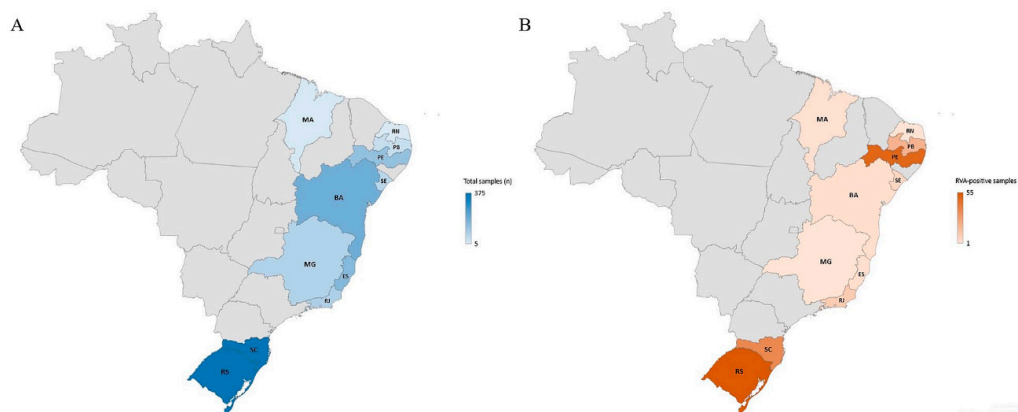


**Figure 2.** Map of Brazil highlighting the eleven states with sentinel surveillance service attended by the Rotavirus Regional Reference Laboratory, IOC, FIOCRUZ. Number of tested samples (A) and number of RVA-positive samples (B).

Most of stool samples received were from children less than five years old, representing 72.1% (1108/1536) of the AGE cases. RVA detection rate was significantly higher among children aged between 24 and 60 months (18.8%) compared to the other age groups, where detection rates varied from 9.3% to 12.1% (Table 2). We also analyzed RVA viral load (GC/g of stool) among different age groups. The median values of RVA viral loads varied from 4.2 to 6.8 log<sub>10</sub> GC/g among the different age groups. RVA-positive samples showed viral load values statistically lower in AGE cases among children ≤6 months compared to older patients (*p* < 0.05) (Figure 3).

**Table 2.** Number of tested and rotavirus-positive fecal samples through laboratory-based surveillance by age group in Brazil during 2018–2019.

Age Group (Months)	No. of Fecal Samples: Positive/Tested (%)			p-Value * (Chi-Square Test)
	2018	2019	Total	
0–6	16/122 (13.1)	9/101 (8.9)	25/223 (11.2)	0.0153
>6–12	10/133 (7.5)	14/116 (12)	24/249 (9.6)	0.0021
>12–24	17/203 (8.3)	18/173 (10.4)	35/376 (9.3)	0.0003
>24–60	26/141 (18.4)	23/119 (19.3)	49/260 (18.8)	-
>60	16/202 (7.9)	36/227 (15.8)	52/428 (12.1)	0.0109

\* *p*-values were calculated between the age group of >24–60 and each other. All other combinations were not statistically different.

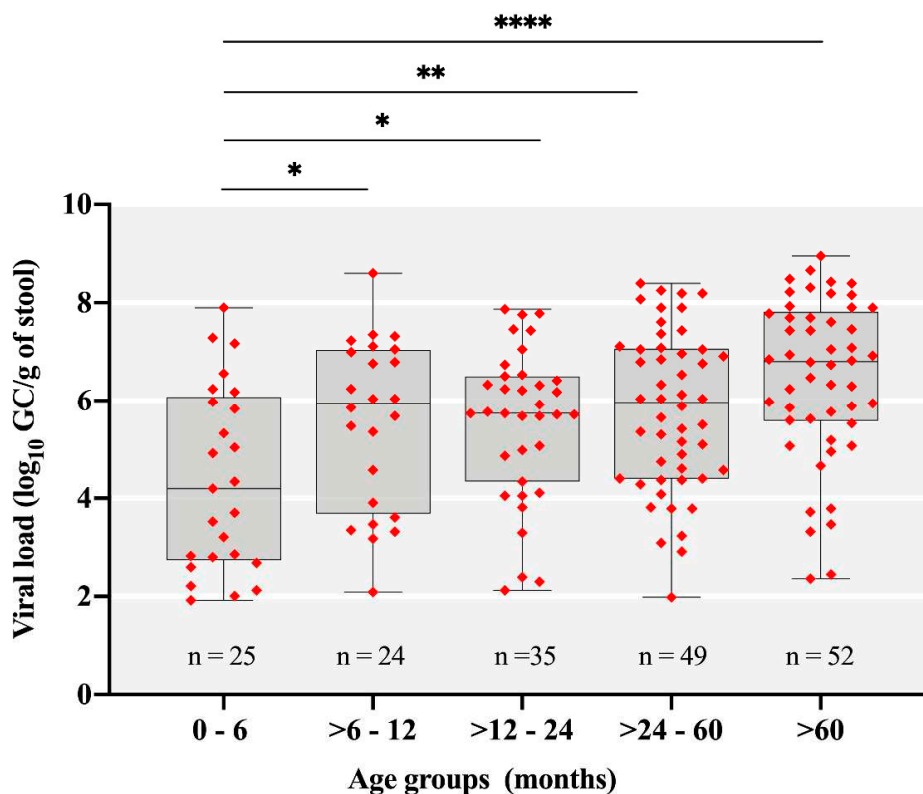


**Figure 3.** Rotavirus A (RVA) viral load expressed as  $\log_{10}$  genome copies per gram of stool ( $\log_{10}$  GC/g) among different age groups in Brazil, 2018–2019. Box-and-whisker plots show the first and third quartiles (equivalent to the 5th and 95th percentiles), the median (the horizontal line in the box), and range of  $\log_{10}$  GC/g values. \*  $p \leq 0.05$ ; \*\*  $p \leq 0.01$ ; \*\*\*\*  $p \leq 0.0001$ .

### 3.2. RVA Genotyping

A total of 186 RVA-positive samples were subjected to G and P genotyping by one-step multiplex RT-PCR. From these, 167 samples (89%) were successfully genotyped; 80 from 2018 and 87 from 2019. We characterized seven different RVA genotypes circulating during this study: G3P[8], G3P[6], G9P[8], G1P[8], G2P[6], G12P[6], and G6P[8]. G3P[8] was detected year-round and was by far, the most prevalent genotype, accounting for 83.8% ( $n = 67$ ) of genotyped samples in 2018 and 65.5% ( $n = 57$ ) in 2019 (Figure 4). Two other usual RVA genotypes were detected, but in lower prevalence—G1P[8] detected in one sample in 2018 and 2019, and G9P[8] detected in two and eight samples from 2018 and 2019, respectively. We also detected unusual G/P combinations, especially in 2019, as follows: G3P[6] in 6.3% of samples from 2018; G6P[8], G12P[6], and G2P[6] in 13.8%, 4.6% and 1.2% of samples from 2019 (Figure 4). G or P non-typed (NT) samples (GNTP8, GNTP6, and G3P[NT]) accounted for 5.4% of samples, and were represented mostly by samples with low RVA viral load (high Ct values).

In addition to RT-PCR genotyping, we sequenced some of the RVA-positive samples in order to get detailed information of the circulating strains and their respective lineages. We successfully obtained 22 and 21 consensus sequences of VP7 and VP4 genes, respectively. Phylogenetic analysis of the VP7 gene confirmed the characterization of Brazilian strains belonging to G3 and G6. Eighteen G3 strains from both years and from the three Brazilian regions were sequenced. From these, 94.4% ( $n = 17$ ) of sequences clustered within the lineage 1, represented by equine-like G3P[8] strains. Our sequences were genetically related to previously detected equine-like G3P[8] strains from Brazil (KX469400) and other countries, such as Germany (KY000546), Slovakia (MN203563), Dominican Republic (MG652313), and Japan (LC47366). One G3 sequence clustered within lineage 3 that comprises the Wa-like G3P[8] group. The Brazilian Wa-like G3 sequence was closely related to strains from Brazil (KJ454454), Argentina (KJ583190 and KJ583201) and Hungary (JQ693568), with nt similarity varying from 98.4

to 99.8% (Figure 5A). The four G6 strains sequenced in our study, harboring a P[8]-type, clustered within lineage 1 showing moderate nt identity (97.8–98.1%) with G6P[8] strains detected in Bulgaria (KM590371 and KM590373) and with G6P[9] strains from Germany (KX880436) and Italy (KC152917). None of our G6 sequences clustered within the G6 lineage 3, that comprises human-bovine reassortant strains (Figure 5A).

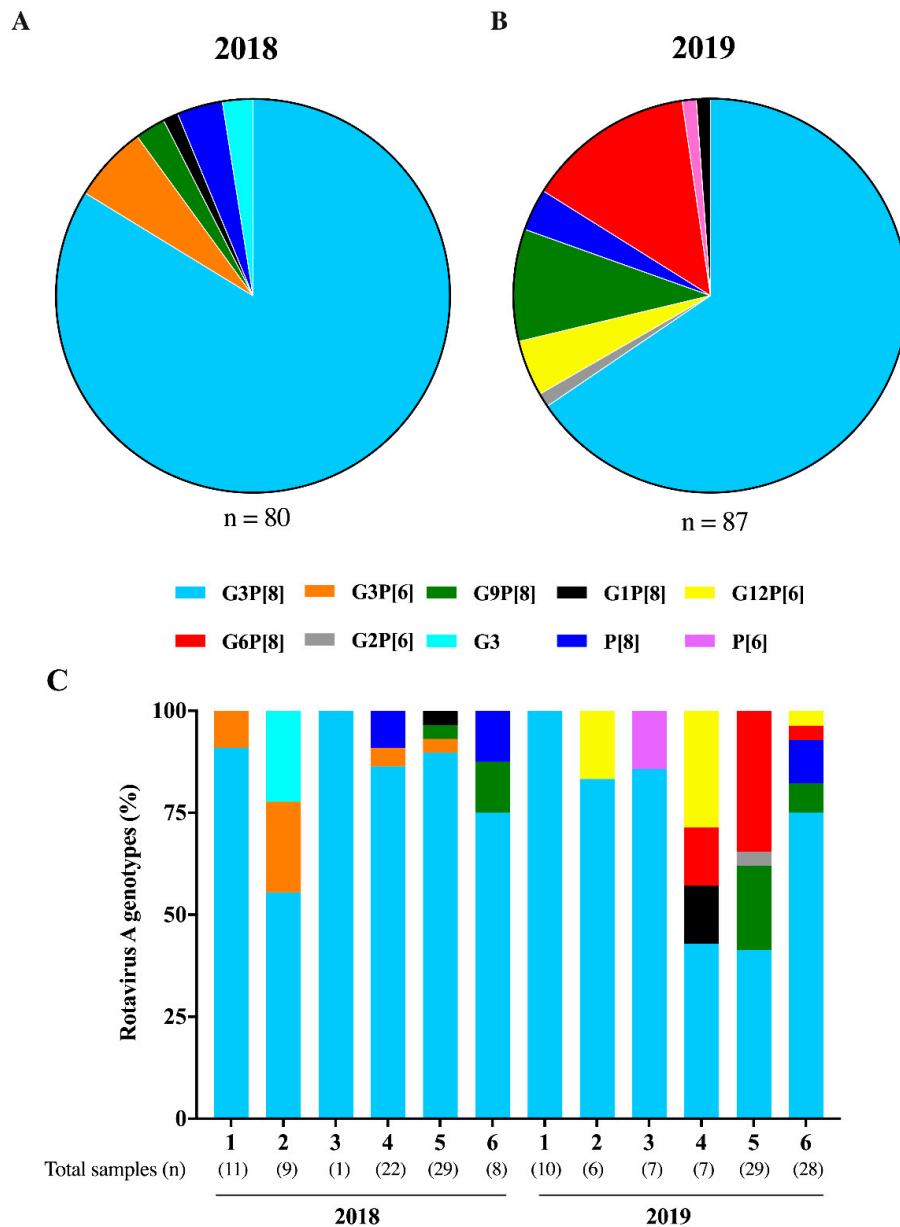


**Figure 4.** Rotavirus A (RVA) genotypes distribution in Brazil, 2018 (A) and 2019 (B). Bi-monthly genotypes circulation during the two-year of study (C).

Phylogenetic analysis of 21 sequences of VP4 gene, demonstrated that, except for one, all P[8] Brazilian strains harboring two different G-types (G3 and G6) grouped into lineage 3. The 20 strains were closely related (99.2–99.6% of nt similarity) to P[8]-3 Brazilian strains isolated in 2016 (KX469415 and MH569765) and strains from other countries, such as USA (MF997038), Japan (LC477395), Spain (KU550282), Australia (KU059769), and Italy (MK158257). One strain was characterized into P[6] lineage 1, and was closely related (99.5–99.7% of nt similarity) to strains detected in Argentina (KJ583199), Iraq (JX891397), and China (MG78835) (Figure 5B).



#### 4. Discussion

In this study, we provide laboratory-based RVA national surveillance in eleven states from three regions in Brazil, during 2018–2019. We tested 1536 AGE stool samples and found an overall RVA-positivity of 12%. RVA detection rates were higher during winter/spring months and among children aged 24–60 months. By far, G3P[8] was the most frequently detected genotype, and showed a year-round circulation.

Despite the development of vaccines, RVA are still a major cause of severe AGE in infants worldwide [5]. Here, we detected RVA in 10.5% and 13.7% of samples from 2018 and 2019, respectively. In Brazil, after Rotarix™ implementation, different studies have investigated RVA circulation among AGE cases. A study from the Enteric Diseases Laboratory at Adolfo Lutz Institute, one of the three Brazilian Reference Laboratory for RVA surveillance, reported annual RVA prevalence varying from 9.9% to 25.3% during 2013–2017, with AGE samples from five states in the Midwestern and part of the Southeastern and Southern regions [24]. A previous study from our group demonstrated an overall RVA positivity of 20.8% among children up to 12 years old between 2006 and 2017, with annual detection rates varying between 5% to 35% [20]. Studies conducted at Evandro Chagas Institute, the national and regional reference center for RVA surveillance in Northern Brazil, demonstrated RVA positivity rates of 33% in samples from six states from North Brazil, 2011–2012 [23], and 24.2% in samples collected between June 2012 and June 2015 [36]. However, it is worth mentioning that both studies involved children hospitalized for severe AGE. In Argentina, RVA positivity decreased from 26.8% to 13.6% comparing the pre- and post-vaccination periods [37]. Other studies performed elsewhere have described RVA detection rates varying from 8.4% to 23.2% [38–42].

RVA seasonality has been well defined, especially for temperate climate countries, where RVA peaks during dry and cold months. In tropical areas, RVA circulates year-round without marked peaks of infections [43,44]. In Brazil, we observed a year-round RVA circulation without marked seasonality, but high detection rates of RVA was observed during winter/spring months, in agreement with other studies [42,45]. RVA highest detection rate was observed in September 2019 (36.7%) in line with findings observed over a 21-year period in Brazil [20], and also with Luchs et al. [46] that demonstrated the peak of RV incidence in September during a five-year RVA surveillance study (2007–2012) in Brazil. As a continental-size country, we analyzed separately, RVA circulation in Southern states in comparison with Southeastern and Northeastern states (Figure 1B,C). We observed more clear peaks of RVA infections in winter/spring months (June 21st to December 20th) in Southern states (Rio Grande do Sul—RS, and Santa Catarina—SC) compared to Southeastern and Northeastern Brazil. This could be explained as both RS and SC states are in a subtropical area, characterized by different climate pattern compared to the other states. A three-year study conducted in Vietnam to assess RVA epidemiology in AGE cases also demonstrated varied seasonally positivity, with different RVA-detection peaks among the three regions analyzed—North, Central, and South [47]. The fact that RVA usually peaks in September in Brazil, observed here and by others [20,46], is an important information to authorities to prepare strategies to reduce AGE impacts in the health system.

Regarding RVA infections among different age groups, we observed a significantly high positivity rate among children aged >24 and 60 months compared to other age groups. This shifting in the age of children more affected by RVA illness (older children) has been observed, especially in countries that have introduced RVA mass vaccination. Our data are consistent with previous findings reported from Brazil [20] and the USA [48,49]. In contrast, countries where RVA vaccines are yet to be introduced into national immunization programs, have reported the majority of RVA positive children (~90%) within the first 2 years of life [44,47]. By analyzing RVA shedding among the age groups, we found a statistically lower viral load among children less than six months (Figure 3). We believe that this lower viral load could be mostly explained by the passive protection mediated by breast milk maternal antibodies [50], but also by the higher effectiveness and prompt immune response generated by Rotarix™ after the oral doses administered at the age of 2 and 4 months [17]. However, this second hypothesis alone could not explain the high viral load among children aged >6 and 12 months. In addition, high Ct

values could indicate less severe disease [51]. In that study, authors demonstrated that the severity of diarrhea, determined by the Vesikari score, was significantly and negatively associated with Ct values of children stool samples.

Regarding RVA genotype characterization, we successfully identified G- and P-types in 89% of positive samples, by one-step multiplex RT-PCR and sequencing. By far, G3P[8] was the most prevalent genotype in both years. The phylogenetic analysis of the VP7 gene revealed that the majority of the Brazilian strains sequenced (94%) belong to the equine-like G3 genotype (G3-1). Moreover, all the P[8] strains sequenced clustered within the P[8]-3 lineage. This P[8]-3, harboring a G12-type, was the dominant strain in Brazil in 2014, detected in 75% of genotyped samples [52].

Emergent equine-like DS-1-like G3P[8] RVA strains were firstly identified in children with AGE in Australia in 2013 [53]. From 2013 onwards, the equine-like G3P[8] DS-1-like genotype has spread and become endemic worldwide [54–60]. In Brazil, the first evidence of the circulation of equine-like G3P[8] date from 2015, when Luchs et al. [24] detected the reassortant RVA strain in a touristic city of Southern Brazil, Foz do Iguaçu, that borders Argentina and Paraguay. Subsequently, these novel viruses quickly spread to other states in Brazil, being the most prevalent genotype in 2017 (66.2%). The occurrence of DS-1-like G3P[8] RVA strains was also reported in Amazon region, Northern Brazil in 2016 [60]. In the previous study from our group, we demonstrated the increase of G3P[8] from 2015, peaking in the last year of the study—2017. However, it was not investigated whether they belonged to the DS-1-like RVA group [20]. More recently, countries such as Australia, Italy and Pakistan, have demonstrated the high prevalence of the emergent equine-like G3P[8] genotype [42,45,61].

Atypical genotypes G3P[6], G6P[8], G2P[6], and G12P[6] were also detected as minor genotypes in our study. The phylogenetic analysis of the VP7 gene demonstrated that Brazilian G6-1 strains were closely related to strains circulating in Bulgaria and Italy [62,63]. The genotype G12P[6] characterized in our study has been frequently detected in Nepal, with detection rates of 46.4% in 2013 and 36% in 2014, among AGE cases in children less than five years of age [64,65]. Unexpectedly, we did not detect the former dominant G2P[4] genotype. In Brazil, after Rotarix™ implementation in March 2006, this genotype has been the most frequently detected until 2015 [66], however, the recently low prevalence of G2P[4] viruses could be explained a cyclical pattern of circulation along with the herd induced homotypic immunity and depletion of the susceptible population [20].

A major strength of our study is that we included data from eleven states, representing around 100 million inhabitants (almost half of Brazilian population). Albeit, this could be considered as a major limitation as well, since the variability in reporting and collecting AGE cases by states generates surveillance biases. Another limitation is that important RVA genes, such as VP6 and NSP4, were not characterized. Nevertheless, future studies approaching a more complete genetic characterization of G3P[8] strains, as well as unusual genotypes detected here (G3P[6] and G12P[6]) will be performed, in order to monitor RVA genotypes spread and evolution over time.

In conclusion, we found a 12% of RVA-positivity in AGE cases from Brazil, and according to global trends, the equine-like G3P[8] was the dominant genotype in 2018 and 2019. The constant shifting of RVA genotypes circulation and the potential emergence of unusual/reassortant strains reinforces the importance and the need for continuous country-based epidemiological and molecular surveillance programs.

**Author Contributions:** Conceptualization, M.B.G., M.P.M., J.P.G.L., and T.M.F.; methodology, M.B.G., A.M.F., A.G.M., F.C.M., J.d.S.R.d.A., R.M.S.d.A., and S.d.S.e.M.; formal analysis, M.B.G. and T.M.F.; investigation, M.B.G., F.C.M., J.d.S.R.d.A., R.M.S.d.A., and T.M.F.; writing—original draft preparation, M.B.G. and T.M.F.; writing—review and editing, T.M.F., M.P.M., J.P.G.L., A.M.F., A.G.M., F.C.M., J.d.S.R.d.A., R.M.S.d.A., and S.d.S.e.M.; supervision, T.M.F.; project administration, T.M.F.; M.P.M., and J.P.G.L.; funding acquisition, T.M.F. and J.P.G.L. All authors have read and agreed to the published version of the manuscript.

**Funding:** This work was supported by The Brazilian National Council for Scientific and Technological Development (CNPq) (Programa Universal grant no. 424376/2016-4) and (Programa Estratégico de Apoio à Pesquisa em Saúde—PAPES VII grant no. 401795/2015-2—FIOCRUZ/CNPq), Carlos Chagas Filho Foundation for Research Support of the State of Rio de Janeiro (FAPERJ) (grant no. 202.796/2019—Jovem Cientista do Nosso Estado, TMF; grant no. 202.779/2018—Cientista do Nosso Estado, JPGL) and PAEF-2—Oswaldo Cruz Institute. Further support was given by CGLab. We are grateful for support from the Coordination for the Improvement of Higher Education Personnel (CAPES—PrInt-Fiocruz-CAPES program).

**Acknowledgments:** We would like to thank the Rotavirus Surveillance System, coordinated by the Coordenação Geral de Laboratórios de Saúde Pública (CGLab), Brazilian Ministry of Health, and the State Central Laboratories involved in the study.

**Conflicts of Interest:** The authors declare no conflict of interest.

## References

1. WHO | Levels and Trends in Child Mortality Report 2019. Available online: [https://www.who.int/maternal\\_child\\_adolescent/documents/levels\\_trends\\_child\\_mortality\\_2019/en/](https://www.who.int/maternal_child_adolescent/documents/levels_trends_child_mortality_2019/en/) (accessed on 2 May 2020).
2. Liu, L.; Qian, Y.; Zhang, Y.; Zhao, L.; Jia, L.; Dong, H. Epidemiological aspects of rotavirus and adenovirus in hospitalized children with diarrhea: A 5-year survey in Beijing. *BMC Infect. Dis.* **2016**, *16*, 508. [CrossRef] [PubMed]
3. Bányai, K.; Estes, M.K.; Martella, V.; Parashar, U.D. Viral gastroenteritis. *Lancet* **2018**, *392*, 175–186. [CrossRef]
4. Troeger, C.; Khalil, I.A.; Rao, P.C.; Cao, S.; Blacker, B.F.; Ahmed, T.; Armah, G.; Bines, J.E.; Brewer, T.G.; Colombara, D.V.; et al. Rotavirus Vaccination and the Global Burden of Rotavirus Diarrhea Among Children Younger Than 5 Years. *JAMA Pediatr.* **2018**, *172*, 958–965. [CrossRef]
5. Tate, J.E.; Burton, A.H.; Boschi-Pinto, C.; Parashar, U.D.; World Health Organization—Coordinated Global Rotavirus Surveillance Network. Global, Regional, and National Estimates of Rotavirus Mortality in Children <5 Years of Age, 2000–2013. *Clin. Infect. Dis.* **2016**, *62*, S96–S105. [CrossRef]
6. Burnett, E.; Parashar, U.D.; Tate, J.E. Global impact of rotavirus vaccination on diarrhea hospitalizations and deaths among children <5 years old: 2006–2019. *J. Infect. Dis.* **2020**. [CrossRef]
7. Aliabadi, N.; Antoni, S.; Mwenda, J.M.; Weldegebriel, G.; Biey, J.N.M.; Cheikh, D.; Fahmy, K.; Tebeb, N.; Ashmony, H.A.; Ahmed, H.; et al. Global impact of rotavirus vaccine introduction on rotavirus hospitalisations among children under 5 years of age, 2008–2016: Findings from the Global Rotavirus Surveillance Network. *Lancet Glob. Health* **2019**, *7*, e893–e903. [CrossRef]
8. Burke, R.M.; Tate, J.E.; Kirkwood, C.D.; Steele, A.D.; Parashar, U.D. Current and new rotavirus vaccines. *Curr. Opin. Infect. Dis.* **2019**, *32*, 435–444. [CrossRef] [PubMed]
9. Matthijnssens, J.; Van Ranst, M. Genotype constellation and evolution of group A rotaviruses infecting humans. *Curr. Opin. Virol.* **2012**, *2*, 426–433. [CrossRef]
10. Dóro, R.; Farkas, S.L.; Martella, V.; Bányai, K. Zoonotic transmission of rotavirus: Surveillance and control. *Expert Rev. Anti. Infect. Ther.* **2015**, *13*, 1337–1350. [CrossRef] [PubMed]
11. Matthijnssens, J.; Ciarlet, M.; Heiman, E.; Arijs, I.; Delbeke, T.; McDonald, S.M.; Palombo, E.A.; Iturriza-Gómara, M.; Maes, P.; Patton, J.T.; et al. Full genome-based classification of rotaviruses reveals a common origin between human Wa-Like and porcine rotavirus strains and human DS-1-like and bovine rotavirus strains. *J. Virol.* **2008**, *82*, 3204–3219. [CrossRef]
12. Rotavirus Classification Working Group: RCWG. Available online: <https://rega.kuleuven.be/cev/viralmetagénomics/virus-classification/rcwg> (accessed on 10 May 2020).
13. Dóro, R.; László, B.; Martella, V.; Leshem, E.; Gentsch, J.; Parashar, U.; Bányai, K. Review of global rotavirus strain prevalence data from six years post vaccine licensure surveillance: Is there evidence of strain selection from vaccine pressure? *Infect. Genet. Evol.* **2014**, *28*, 446–461. [CrossRef]
14. Bányai, K.; László, B.; Duque, J.; Steele, A.D.; Nelson, E.A.S.; Gentsch, J.R.; Parashar, U.D. Systematic review of regional and temporal trends in global rotavirus strain diversity in the pre rotavirus vaccine era: Insights for understanding the impact of rotavirus vaccination programs. *Vaccine* **2012**, *30*, A122–A130. [CrossRef] [PubMed]

15. Iturriza-Gómara, M.; Dallman, T.; Bányai, K.; Böttiger, B.; Buesa, J.; Diedrich, S.; Fiore, L.; Johansen, K.; Koopmans, M.; Korsun, N.; et al. Rotavirus genotypes co-circulating in Europe between 2006 and 2009 as determined by EuroRotaNet, a pan-European collaborative strain surveillance network. *Epidemiol. Infect.* **2011**, *139*, 895–909. [CrossRef] [PubMed]
16. de A. Mendes, P.S.; da C. Ribeiro, H.; Mendes, C.M.C. Temporal trends of overall mortality and hospital morbidity due to diarrheal disease in Brazilian children younger than 5 years from 2000 to 2010. *J. Pediatr. (Rio J.)* **2013**, *89*, 315–325. [CrossRef] [PubMed]
17. Gurgel, R.Q.; Alvarez, A.D.J.; Rodrigues, A.; Ribeiro, R.R.; Dolabella, S.S.; Da Mota, N.L.; Santos, V.S.; Iturriza-Gómara, M.; Cunliffe, N.A.; Cuevas, L.E. Incidence of Rotavirus and Circulating Genotypes in Northeast Brazil during 7 Years of National Rotavirus Vaccination. *PLoS ONE* **2014**, *9*. [CrossRef]
18. Gurgel, R.G.; Bohland, A.K.; Vieira, S.C.F.; Oliveira, D.M.P.; Fontes, P.B.; Barros, V.F.; Ramos, M.F.; Dove, W.; Nakagomi, T.; Nakagomi, O.; et al. Incidence of rotavirus and all-cause diarrhea in northeast Brazil following the introduction of a national vaccination program. *Gastroenterology* **2009**, *137*, 1970–1975. [CrossRef] [PubMed]
19. Linhares, A.C.; Velázquez, F.R.; Pérez-Schael, I.; Sáez-Llorens, X.; Abate, H.; Espinoza, F.; López, P.; Macías-Parra, M.; Ortega-Barría, E.; Rivera-Medina, D.M.; et al. Efficacy and safety of an oral live attenuated human rotavirus vaccine against rotavirus gastroenteritis during the first 2 years of life in Latin American infants: A randomised, double-blind, placebo-controlled phase III study. *Lancet* **2008**, *371*, 1181–1189. [CrossRef]
20. Carvalho-Costa, F.A.; de Assis, R.M.S.; Fialho, A.M.; Araújo, I.T.; Silva, M.F.; Gómez, M.M.; Andrade, J.S.; Rose, T.L.; Fumian, T.M.; Volotão, E.M.; et al. The evolving epidemiology of rotavirus A infection in Brazil a decade after the introduction of universal vaccination with Rotarix®. *BMC Pediatr.* **2019**, *19*, 42. [CrossRef]
21. Carvalho-Costa, F.A.; de M. Volotão, E.; de Assis, R.M.S.; Fialho, A.M.; da S.R. de Andrade, J.; Rocha, L.N.; Tort, L.F.L.; da Silva, M.F.M.; Gómez, M.M.; de Souza, P.M.; et al. Laboratory-based rotavirus surveillance during the introduction of a vaccination program, Brazil, 2005–2009. *Pediatr. Infect. Dis. J.* **2011**, *30*, S35–S41. [CrossRef]
22. Luchs, A.; do C.S.T. Timenetsky, M. Group A rotavirus gastroenteritis: Post-vaccine era, genotypes and zoonotic transmission. *Einstein (Sao Paulo)* **2016**, *14*, 278–287. [CrossRef] [PubMed]
23. da Silva Soares, L.; de Fátima Dos Santos Guerra, S.; do Socorro Lima de Oliveira, A.; da Silva Dos Santos, F.; de Fátima Costa de Menezes, E.M.; Mascarenhas, J.; d’Arc, P.; Linhares, A.C. Diversity of rotavirus strains circulating in Northern Brazil after introduction of a rotavirus vaccine: High prevalence of G3P[6] genotype. *J. Med. Virol.* **2014**, *86*, 1065–1072. [CrossRef]
24. Luchs, A.; da Costa, A.C.; Cilli, A.; Komninakis, S.C.V.; de C.C. Carmona, R.; Boen, L.; Morillo, S.G.; Sabino, E.C.; do C.S.T. Timenetsky, M. Spread of the emerging equine-like G3P[8] DS-1-like genetic backbone rotavirus strain in Brazil and identification of potential genetic variants. *J. Gen. Virol.* **2019**, *100*, 7–25. [CrossRef] [PubMed]
25. Jing, Z.; Zhang, X.; Shi, H.; Chen, J.; Shi, D.; Dong, H.; Feng, L. A G3P[13] porcine group A rotavirus emerging in China is a reassortant and a natural recombinant in the VP4 gene. *Transbound. Emerg. Dis.* **2018**, *65*, e317–e328. [CrossRef] [PubMed]
26. Komoto, S.; Tacharoenmuang, R.; Guntapong, R.; Ide, T.; Sinchai, P.; Upachai, S.; Fukuda, S.; Yoshikawa, T.; Tharmaphornpilas, P.; Sangkitporn, S.; et al. Identification and characterization of a human G9P[23] rotavirus strain from a child with diarrhoea in Thailand: Evidence for porcine-to-human interspecies transmission. *J. Gen. Virol.* **2017**, *98*, 532–538. [CrossRef] [PubMed]
27. Quayé, O.; Roy, S.; Rungsririyachai, K.; Esona, M.D.; Xu, Z.; Tam, K.I.; Banegas, D.J.C.; Rey-Benito, G.; Bowen, M.D. Characterisation of a rare, reassortant human G10P[14] rotavirus strain detected in Honduras. *Mem. Inst. Oswaldo Cruz* **2018**, *113*, 9–16. [CrossRef]
28. Tacharoenmuang, R.; Komoto, S.; Guntapong, R.; Ide, T.; Singchai, P.; Upachai, S.; Fukuda, S.; Yoshida, Y.; Murata, T.; Yoshikawa, T.; et al. Characterization of a G10P[14] rotavirus strain from a diarrheic child in Thailand: Evidence for bovine-to-human zoonotic transmission. *Infect. Genet. Evol.* **2018**, *63*, 43–57. [CrossRef]
29. Gentsch, J.R.; Parashar, U.D.; Glass, R.I. Impact of rotavirus vaccination: The importance of monitoring strains. *Future Microbiol.* **2009**, *4*, 1231–1234. [CrossRef]

30. Matthijnssens, J.; Bilcke, J.; Ciarlet, M.; Martella, V.; Bányai, K.; Rahman, M.; Zeller, M.; Beutels, P.; Van Damme, P.; Van Ranst, M. Rotavirus disease and vaccination: Impact on genotype diversity. *Future Microbiol.* **2009**, *4*, 1303–1316. [CrossRef]
31. Roczo-Farkas, S.; Kirkwood, C.D.; Cowley, D.; Barnes, G.L.; Bishop, R.F.; Bogdanovic-Sakran, N.; Boniface, K.; Donato, C.M.; Bines, J.E. The Impact of Rotavirus Vaccines on Genotype Diversity: A Comprehensive Analysis of 2 Decades of Australian Surveillance Data. *J. Infect. Dis.* **2018**, *218*, 546–554. [CrossRef]
32. Esona, M.D.; Gautam, R.; Tam, K.I.; Williams, A.; Mijatovic-Rustempasic, S.; Bowen, M.D. Multiplexed one-step RT-PCR VP7 and VP4 genotyping assays for rotaviruses using updated primers. *J. Virol. Methods* **2015**, *223*, 96–104. [CrossRef]
33. Gómara, M.I.; Cubitt, D.; Desselberger, U.; Gray, J. Amino acid substitution within the VP7 protein of G2 rotavirus strains associated with failure to serotype. *J. Clin. Microbiol.* **2001**, *39*, 3796–3798. [CrossRef] [PubMed]
34. Gentsch, J.R.; Glass, R.I.; Woods, P.; Gouvea, V.; Gorziglia, M.; Flores, J.; Das, B.K.; Bhan, M.K. Identification of group A rotavirus gene 4 types by polymerase chain reaction. *J. Clin. Microbiol.* **1992**, *30*, 1365–1373. [CrossRef] [PubMed]
35. Kumar, S.; Stecher, G.; Li, M.; Nnyaz, C.; Tamura, K. MEGA X: Molecular Evolutionary Genetics Analysis across Computing Platforms. *Mol. Biol. Evol.* **2018**, *35*, 1547–1549. [CrossRef] [PubMed]
36. Justino, M.C.A.; Campos, E.A.; Mascarenhas, J.D.P.; Soares, L.S.; de F.S. Guerra, S.; Furlaneto, I.P.; Pavão, M.J.C.; Maciel, T.S.; Farias, F.P.; Bezerra, O.M.; et al. Rotavirus antigenemia as a common event among children hospitalised for severe, acute gastroenteritis in Belém, northern Brazil. *BMC Pediatr.* **2019**, *19*, 193. [CrossRef] [PubMed]
37. Degiuseppe, J.I.; Stupka, J.A. First assessment of all-cause acute diarrhoea and rotavirus-confirmed cases following massive vaccination in Argentina. *Epidemiol. Infect.* **2018**, *146*, 1948–1954. [CrossRef]
38. Junaid, S.A.; Umeh, C.; Olabode, A.O.; Banda, J.M. Incidence of rotavirus infection in children with gastroenteritis attending Jos university teaching hospital, Nigeria. *Virol. J.* **2011**, *8*, 233. [CrossRef]
39. Nordgren, J.; Bonkougou, I.J.O.; Nitiema, L.W.; Sharma, S.; Ouermi, D.; Simpore, J.; Barro, N.; Svensson, L. Rotavirus in diarrheal children in rural Burkina Faso: High prevalence of genotype G6P[6]. *Infect. Genet. Evol.* **2012**, *12*, 1892–1898. [CrossRef]
40. Umair, M.; Abbasi, B.H.; Sharif, S.; Alam, M.M.; Rana, M.S.; Mujtaba, G.; Arshad, Y.; Fatmi, M.Q.; Zaidi, S.Z. High prevalence of G3 rotavirus in hospitalized children in Rawalpindi, Pakistan during 2014. *PLoS ONE* **2018**, *13*, e0195947. [CrossRef]
41. Halasa, N.; Piya, B.; Stewart, L.S.; Rahman, H.; Payne, D.C.; Woron, A.; Thomas, L.; Constantine-Renna, L.; Garman, K.; McHenry, R.; et al. The Changing Landscape of Pediatric Viral Enteropathogens in the Post-Rotavirus Vaccine Era. *Clin. Infect. Dis.* **2020**. [CrossRef]
42. Rovida, F.; Nepita, E.V.; Giardina, F.; Piralla, A.; Campanini, G.; Baldanti, F. Rotavirus molecular epidemiology in hospitalized patients, Northern Italy, 2015–2018. *New Microbiol.* **2020**, *43*, 1–5.
43. Levy, K.; Hubbard, A.E.; Eisenberg, J.N.S. Seasonality of rotavirus disease in the tropics: A systematic review and meta-analysis. *Int. J. Epidemiol.* **2009**, *38*, 1487–1496. [CrossRef] [PubMed]
44. Samdan, A.; Ganbold, S.; Gunteev, O.; Orosoo, S.; Javzandorj, N.; Gongor, A.; Enkhtuvshin, A.; Demberelsuren, S.; Abdul, W.; Jee, Y.; et al. Hospital-based surveillance for rotavirus diarrhea in Ulaanbaatar, Mongolia, April 2009 through March 2016. *Vaccine* **2018**, *36*, 7883–7887. [CrossRef] [PubMed]
45. Sadiq, A.; Bostan, N.; Bokhari, H.; Matthijnssens, J.; Yinda, K.C.; Raza, S.; Nawaz, T. Molecular characterization of human group A rotavirus genotypes circulating in Rawalpindi, Islamabad, Pakistan during 2015–2016. *PLoS ONE* **2019**, *14*. [CrossRef]
46. Luchs, A.; Cilli, A.; Morillo, S.G.; de C.C. Carmona, R.; do C.S.T. Timenetsky, M. ROTAVIRUS GENOTYPES CIRCULATING IN BRAZIL, 2007–2012: IMPLICATIONS FOR THE VACCINE PROGRAM. *Rev. Inst. Med. Trop. Sao Paulo* **2015**, *57*, 305–313. [CrossRef]
47. Huyen, D.T.T.; Hong, D.T.; Trung, N.T.; Hoa, T.T.N.; Oanh, N.K.; Thang, H.V.; Thao, N.T.T.; Hung, D.M.; Iijima, M.; Fox, K.; et al. Epidemiology of acute diarrhea caused by rotavirus in sentinel surveillance sites of Vietnam, 2012–2015. *Vaccine* **2018**, *36*, 7894–7900. [CrossRef]

48. Hull, J.J.; Teel, E.N.; Kerin, T.K.; Freeman, M.M.; Esona, M.D.; Gentsch, J.R.; Cortese, M.M.; Parashar, U.D.; Glass, R.I.; Bowen, M.D.; et al. United States rotavirus strain surveillance from 2005 to 2008: Genotype prevalence before and after vaccine introduction. *Pediatr. Infect. Dis. J.* **2011**, *30*, S42–S47. [CrossRef]
49. Desai, R.; Parashar, U.D.; Lopman, B.; de Oliveira, L.H.; Clark, A.D.; Sanderson, C.F.B.; Tate, J.E.; Matus, C.R.; Andrus, J.K.; Patel, M.M. Potential intussusception risk versus health benefits from rotavirus vaccination in Latin America. *Clin. Infect. Dis.* **2012**, *54*, 1397–1405. [CrossRef]
50. Clarke, E.; Desselberger, U. Correlates of protection against human rotavirus disease and the factors influencing protection in low-income settings. *Mucosal. Immunol.* **2015**, *8*, 1–17. [CrossRef]
51. Kang, G.; Iturriza-Gomara, M.; Wheeler, J.G.; Crystal, P.; Monica, B.; Ramani, S.; Primrose, B.; Moses, P.D.; Gallimore, C.I.; Brown, D.W.; et al. Quantitation of Group A Rotavirus by Real-Time Reverse-Transcription-Polymerase Chain Reaction. *J. Med. Virol.* **2004**, *73*, 118–122. [CrossRef]
52. da Silva, M.F.M.; Fumian, T.M.; de Assis, R.M.S.; Fialho, A.M.; Carvalho-Costa, F.A.; da Silva Ribeiro de Andrade, J.; Leite, J.P.G. VP7 and VP8\* genetic characterization of group A rotavirus genotype G12P[8]: Emergence and spreading in the Eastern Brazilian coast in 2014. *J. Med. Virol.* **2017**, *89*, 64–70. [CrossRef]
53. Kirkwood, C.D.; Roczo-Farkas, S.; Australian Rotavirus Surveillance Group. Australian Rotavirus Surveillance Program annual report, 2013. *Commun. Dis. Intell. Q Rep.* **2014**, *38*, E334–E342.
54. Arana, A.; Montes, M.; Jere, K.C.; Alkorta, M.; Iturriza-Gómara, M.; Cilla, G. Emergence and spread of G3P[8] rotaviruses possessing an equine-like VP7 and a DS-1-like genetic backbone in the Basque Country (North of Spain), 2015. *Infect. Genet. Evol.* **2016**, *44*, 137–144. [CrossRef] [PubMed]
55. Dóro, R.; Marton, S.; Bartókné, A.H.; Lengyel, G.; Agócs, Z.; Jakab, F.; Bányai, K. Equine-like G3 rotavirus in Hungary, 2015—Is it a novel intergenogroup reassortant pandemic strain? *Acta. Microbiol. Immunol. Hung.* **2016**, *63*, 243–255. [CrossRef]
56. Perkins, C.; Mijatovic-Rustempasic, S.; Ward, M.L.; Cortese, M.M.; Bowen, M.D. Genomic Characterization of the First Equine-Like G3P[8] Rotavirus Strain Detected in the United States. *Genome. Announc.* **2017**, *5*. [CrossRef]
57. Kikuchi, W.; Nakagomi, T.; Gauchan, P.; Agbemabiese, C.A.; Noguchi, A.; Nakagomi, O.; Takahashi, T. Detection in Japan of an equine-like G3P[8] reassortant rotavirus A strain that is highly homologous to European strains across all genome segments. *Arch. Virol.* **2018**, *163*, 791–794. [CrossRef]
58. Komoto, S.; Ide, T.; Negoro, M.; Tanaka, T.; Asada, K.; Umamoto, M.; Kuroki, H.; Ito, H.; Tanaka, S.; Ito, M.; et al. Characterization of unusual DS-1-like G3P[8] rotavirus strains in children with diarrhea in Japan. *J. Med. Virol.* **2018**, *90*, 890–898. [CrossRef]
59. Pietsch, C.; Liebert, U.G. Molecular characterization of different equine-like G3 rotavirus strains from Germany. *Infect. Genet. Evol.* **2018**, *57*, 46–50. [CrossRef] [PubMed]
60. Guerra, S.F.S.; Soares, L.S.; Lobo, P.S.; Penha Júnior, E.T.; Sousa Júnior, E.C.; Bezerra, D.A.M.; Vaz, L.R.; Linhares, A.C.; Mascarenhas, J.D.P. Detection of a novel equine-like G3 rotavirus associated with acute gastroenteritis in Brazil. *J. Gen. Virol.* **2016**, *97*, 3131–3138. [CrossRef]
61. Maguire, J.E.; Glasgow, K.; Glass, K.; Roczo-Farkas, S.; Bines, J.E.; Sheppeard, V.; Macartney, K.; Quinn, H.E. Rotavirus Epidemiology and Monovalent Rotavirus Vaccine Effectiveness in Australia: 2010–2017. *Pediatrics* **2019**, *144*. [CrossRef]
62. Ianiro, G.; Delogu, R.; Camilloni, B.; Lorini, C.; Ruggeri, F.M.; Fiore, L. Detection of unusual G6 rotavirus strains in Italian children with diarrhoea during the 2011 surveillance season. *J. Med. Virol.* **2013**, *85*, 1860–1869. [CrossRef]
63. Mladenova, Z.; Nawaz, S.; Ganesh, B.; Iturriza-Gomara, M. Increased detection of G3P[9] and G6P[9] rotavirus strains in hospitalized children with acute diarrhea in Bulgaria. *Infect. Genet. Evol.* **2015**, *29*, 118–126. [CrossRef]
64. Ansari, S.; Sherchand, J.B.; Rijal, B.P.; Parajuli, K.; Mishra, S.K.; Dahal, R.K.; Shrestha, S.; Tandukar, S.; Chaudhary, R.; Kattel, H.P.; et al. Characterization of rotavirus causing acute diarrhoea in children in Kathmandu, Nepal, showing the dominance of serotype G12. *J. Med. Microbiol.* **2013**, *62*, 114–120. [CrossRef] [PubMed]

65. Dhital, S.; Sherchand, J.B.; Pokhrel, B.M.; Parajuli, K.; Shah, N.; Mishra, S.K.; Sharma, S.; Kattel, H.P.; Khadka, S.; Khatiwada, S.; et al. Molecular epidemiology of Rotavirus causing diarrhea among children less than five years of age visiting national level children hospitals, Nepal. *BMC Pediatr.* **2017**, *17*, 101. [CrossRef] [PubMed]
66. Santos, V.S.; Gurgel, R.Q.; Cavalcante, S.M.M.; Kirby, A.; Café, L.P.; Souto, M.J.; Dolabella, S.S.; de Assis, M.R.; Fumian, T.M.; Miagostovich, M.P.; et al. Acute norovirus gastroenteritis in children in a highly rotavirus-vaccinated population in Northeast Brazil. *J. Clin. Virol.* **2017**, *88*, 33–38. [CrossRef]



© 2020 by the authors. Licensee MDPI, Basel, Switzerland. This article is an open access article distributed under the terms and conditions of the Creative Commons Attribution (CC BY) license (<http://creativecommons.org/licenses/by/4.0/>).



Article

# Multiple Introductions and Predominance of Rotavirus Group A Genotype G3P[8] in Kilifi, Coastal Kenya, 4 Years after Nationwide Vaccine Introduction

Mike J. Mwangi <sup>1</sup>, Jennifer R. Verani <sup>2,3</sup>, Richard Omoro <sup>4</sup>, Jacqueline E. Tate <sup>3</sup>, Umesh D. Parashar <sup>3</sup>, Nickson Murunga <sup>1</sup>, Elijah Gicheru <sup>1</sup>, Robert F. Breiman <sup>5</sup>, D. James Nokes <sup>1,6</sup> and Charles N. Agoti <sup>1,7,\*</sup>

<sup>1</sup> Kenya Medical Research Institute (KEMRI)-Wellcome Trust Research Programme, off Hospital Road, Kilifi 80108, Kenya; mikemwanga6@gmail.com (M.J.M.); nmurunga@kemri-wellcome.org (N.M.); egicheru@kemri-wellcome.org (E.G.); jnokes@kemri-wellcome.org (D.J.N.)

<sup>2</sup> Centers for Disease Control and Prevention (CDC), KEMRI Complex, off Mbagathi Way, Village Market, Nairobi 00621, Kenya; qzr7@cdc.gov

<sup>3</sup> Centers for Disease Control and Prevention (CDC), Atlanta, GA 30333, USA; jqt8@cdc.gov (J.E.T.); uap2@cdc.gov (U.D.P.)

<sup>4</sup> KEMRI, Center for Global Health Research (KEMRI-CGHR), Kisumu 00202, Kenya; omorerichard@gmail.com

<sup>5</sup> Hubert Department of Global Health, Rollins School of Public Health, Emory University, Atlanta, GA 30322, USA; rfbreiman@emory.edu

<sup>6</sup> School of Life Sciences and Zeeman Institute (SBIDER), The University of Warwick, Coventry CV4 7AL, UK

<sup>7</sup> School of Health and Human Sciences, Pwani University, Kilifi 80108, Kenya

\* Correspondence: cnyaigoti@kemri-wellcome.org

Received: 20 October 2020; Accepted: 20 November 2020; Published: 24 November 2020



**Abstract:** Globally, rotavirus group A (RVA) remains a major cause of severe childhood diarrhea, despite the use of vaccines in more than 100 countries. RVA sequencing for local outbreaks facilitates investigation into strain composition, origins, spread, and vaccine failure. In 2018, we collected 248 stool samples from children aged less than 13 years admitted with diarrheal illness to Kilifi County Hospital, coastal Kenya. Antigen screening detected RVA in 55 samples (22.2%). Of these, VP7 (G) and VP4 (P) segments were successfully sequenced in 48 (87.3%) and phylogenetic analysis based on the VP7 sequences identified seven genetic clusters with six different GP combinations: G3P[8], G1P[8], G2P[4], G2P[8], G9P[8] and G12P[8]. The G3P[8] strains predominated the season ( $n = 37$ , 67.2%) and comprised three distinct G3 genetic clusters that fell within Lineage I and IX (the latter also known as equine-like G3 Lineage). Both the two G3 lineages have been recently detected in several countries. Our study is the first to document African children infected with G3 Lineage IX. These data highlight the global nature of RVA transmission and the importance of increasing global rotavirus vaccine coverage.

**Keywords:** gastroenteritis; rotavirus; G3[P8]; phylogenetics; equine-like

## 1. Introduction

Following progressive introduction of rotavirus vaccines into national immunization programs (NIP) of more than 100 countries since 2006, a significant decline of rotavirus group A (RVA) disease burden has occurred [1,2]. However, despite these successes, RVA remains a leading cause of diarrhea morbidity and mortality [3,4], resulting in an estimated 128,500 deaths annually among under-5-year-olds, a majority occurring in low-income settings [5]. Consistently, licensed oral RVA

vaccines have underperformed in low-income settings compared with high-income settings [6,7]. After monovalent Rotarix<sup>®</sup> vaccine was introduced into Kenya's NIP in July 2014, with doses given at 6 and 10 weeks of life, a multi-site case-control study found an overall 2-dose vaccine effectiveness of only 64% (95% confidence interval (CI): 35–80%) in under-5-year-olds [8]. In England, the same vaccine showed effectiveness of 77% (95% CI: 66–85%) [9].

In humans, RVA immunity is partly conferred by neutralizing antibodies directed against the VP4 (protease-sensitive) and VP7 (glycoprotein) viral capsid surface proteins that define P and G types, respectively [10]. These two viral proteins are highly diverse, with up to 36 different G and 51 different P types recorded to-date [11], some of which predominantly infect non-human animal species [12]. Among other factors, the higher number of co-circulating GP genotypes in low-income settings has been proposed to be a potential contributor to rotavirus vaccine underperformance [6].

Currently, there are four licensed and WHO pre-qualified RVA vaccines; all live attenuated and administered orally, but with different strain compositions. These are monovalent Rotarix<sup>®</sup> (G1P[8]), pentavalent RotaTeq<sup>®</sup> (5 reassortant viruses; G1, G2, G3, G4 and G6 genotypes in combination with P[8]), monovalent ROTAVAC<sup>®</sup> (G9P[11]) and pentavalent ROTASIIL<sup>®</sup> (5 reassortant viruses; G1, G2, G3, G4 and G9). All four vaccines were shown to be largely cross-protective against heterotypic strains in both clinical trials and following vaccine implementation in several settings [6,13]. Paradoxically, post-vaccine rollout, outbreaks caused by strains heterotypic to the vaccine in use have been sometimes reported in countries, occurring in patterns seeming to be influenced by the vaccine regimen in use [14–16].

Recent genotyping studies of RVA have found increased proportions of G2P[4], G3P[8] and G12P[8] genotypes in rotavirus vaccinating countries [14,16–18]. These genotypes appeared to play only a minor role in the pre-vaccine era; thus, their increasing prevalence is consistent with increased capacity in escaping vaccine immunity [12,19]. Furthermore, there have been several reports of human infection with equine-like G3 viruses suggestive of greater human vulnerability to antigenically novel RVA strains [20–29]. At the Kenya Medical Research Institute (KEMRI)—Wellcome Trust Research Programme (KWTRP), we have maintained a RVA surveillance at Kilifi County Hospital (KCH), located in rural coastal Kenya since 2009 [30]. The aim of the current analysis was to determine the genetic relatedness of the strains that were in circulation in the 2018 RVA season in Kilifi, their origins, global phylogenetic context, and role in the local sub-optimal vaccine performance.

## **2. Results**

### *2.1. Study Population Characteristics*

Between January and December 2018, 384 children aged less than 13 years were admitted to KCH with diarrhea as one of their illness symptoms. Of these, 208 (54.2%) were Kilifi Health and Demographic surveillance system (KHDSS) area residents (Figure S1). A stool sample was obtained from 248 (64.6%). The main reasons for non-sampling were death ( $n = 13$ ), discharge or transfer before sample collection ( $n = 22$ ), consent refusal ( $n = 52$ ), or other ( $n = 16$ ). Among study eligible children ( $n = 384$ ), the distribution of the sampled and not sampled children differed significantly across age strata ( $p = 0.002$ ) and discharge outcome ( $p < 0.001$ ), Table 1. The distribution of the sampled and not sampled children were similar across sexes and by rotavirus vaccine eligibility status. The majority of the eligible participants were aged less than 2 years (68.2%) and were age eligible to have received one or two doses of rotavirus vaccine (83.6%). By EIA testing, RVA was detected in 55 children (22.2%), Figure 1a, 32 (58.1%) of which were KHDSS area residents. Fifty-one (92.7%) of the RVA positive children were age eligible to have received two doses of the RVA vaccine. Of these, the vaccination status was known for 36 (70.6%), of which 29 (80.6%) were confirmed to have received two doses of Rotarix<sup>®</sup> vaccine while the remainder (19.4%) received one dose, Table 1.

**Table 1.** A comparison of demographic characteristics of children with diarrhea admitted to Kilifi County Hospital (KCH) that were sampled versus those who were not sampled in 2018 and those that were RVA positive versus those that were RVA negative.

Characteristic	All (%)	Sampled (%)	Unsampled (%)	<i>p</i> Value <sup>§</sup>	RVA + ve (%)	RVA - ve (%)	<i>p</i> Value *
Number of patients	384	248 (64.6)	136 (35.4)		55 (22.2)	193 (77.8)	
Sex				0.728			0.008
Male	210 (54.7)	134 (54.0)	76 (55.9)		21 (9.8)	113 (58.6)	
Female	174 (45.3)	114 (46.0)	60 (44.1)		34 (61.8)	80 (41.5)	
Age							
Mean (SD) <sup>¶</sup>	27.4 (29.9)	26.4 (31.8)	29.3 (26.1)	0.352	19.6 (15.0)	28.3 (35.0)	0.073
Median (IQR) <sup>§</sup>	16.8 (9.8–29.3)	15.1 (9.4–24.1)	19.9 (12.0–39.0)	0.025	15.4 (9.9–20.8)	15.1 (8.9–24.9)	1.000
Age group				0.002			0.254
0–11 months	126 (32.8)	92 (37.1)	34 (25.0)		19 (34.6)	73 (37.8)	
12–23 months	136 (35.4)	92 (37.1)	44 (32.4)		25 (45.5)	67 (34.7)	
24–59 months	73 (19.0)	34 (13.7)	39 (28.7)		8 (14.6)	26 (14.0)	
>60 months	49 (12.8)	30 (12.1)	19 (14.0)		3 (5.5)	27 (14.0)	
RVA vaccine eligibility				0.327			0.063
Age eligible 2 dose	317 (82.6)	204 (82.3)	113 (83.1)		51 (92.7)	153 (79.3)	
Age eligible 1 dose	4 (1.0)	4 (1.6)	0 (0.0)		0 (0.0)	4 (2.1)	
Age ineligible	63 (16.4)	40 (16.1)	23 (16.9)		4 (7.3)	36 (18.7)	
Vaccination status ( <i>n</i> = 321)				0.273			0.209
Two dose eligible & received 2 doses	165 (51.4)	111 (53.4)	54 (47.8)		29 (56.9)	82 (52.2)	
Two dose eligible & received 1 dose	24 (7.5)	17 (8.2)	7 (6.2)		7 (13.7)	10 (6.2)	
One or 2 dose eligible but received none	6 (1.8)	2 (1.0)	4 (3.5)		0 (0.0)	2 (1.3)	
One or 2 dose eligible but status unknown	126 (39.3)	78 (37.5)	48 (42.5)		15 (29.4)	63 (40.1)	
Outcome ( <i>n</i> = 379)				<0.001			0.194
Died	38 (10.0)	13 (5.3)	25 (18.9)			12 (6.3)	
Alive	341 (90.0)	234 (94.7)	133 (81.1)			180 (93.8)	

<sup>¶</sup> SD stands for standard deviation; <sup>§</sup> IQR stands for interquartile range; <sup>§</sup> *p* value for comparison of sampled and not sampled groups; \* *p* value for comparison of RVA positive and negative groups.

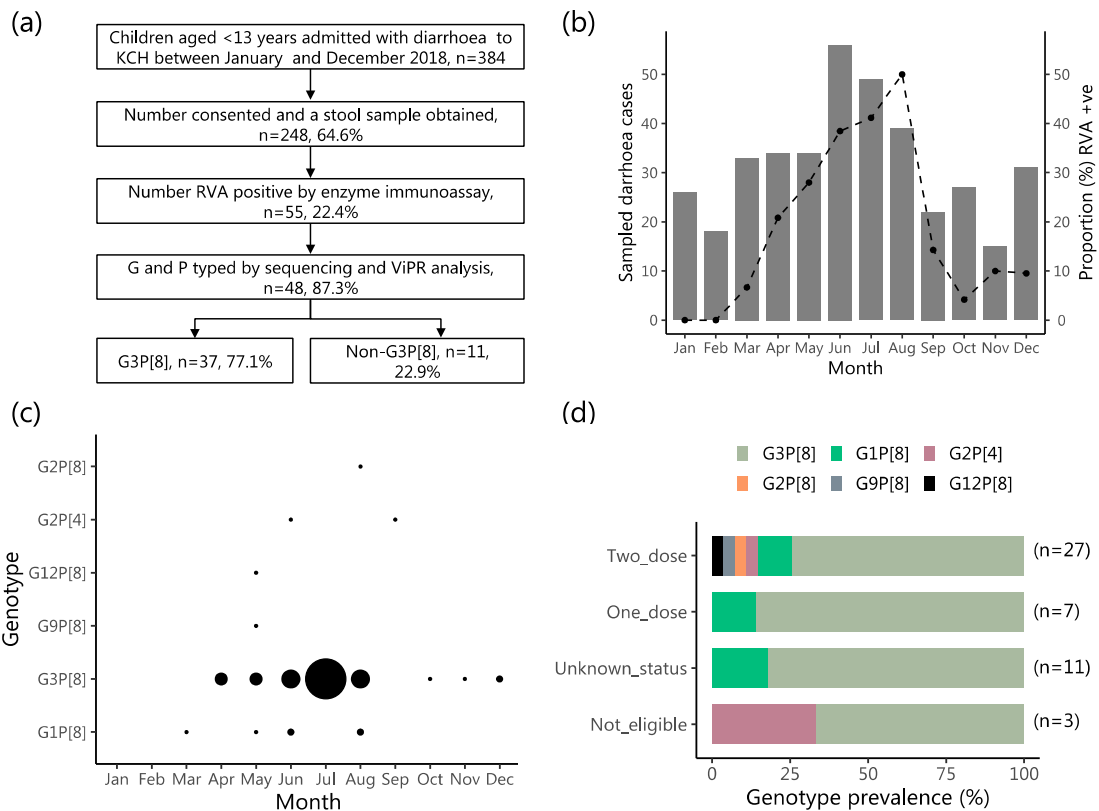


**Figure 1.** Summary of rotavirus group A (RVA) surveillance in Kilifi County Hospital (KCH) in 2018 and identified genotypes. Panel (a) sample flowgram from patient recruitment to VP4 and VP7 genotyping results for the RVA positives. Panel (b) monthly cases of diarrhea in children aged less than 13 years recorded at KCH in 2018 (grey bars) compared with monthly proportions of RVA positive samples (black dashed line on the secondary axis). Panel (c) the number of RVA positive samples by month in 2018 and by the GP genotype. The black circle size is proportional to the number of samples (the smallest indicates one sample and the largest is 13 samples). Panel (d) genotypes identified in children according to rotavirus vaccination status.

### 2.2. Characteristics of the RVA Infections and the Infected Children

RVA prevalence was higher in female compared to male children admitted with diarrhea (29.8% vs. 15.7%,  $p = 0.008$ ), Table 1. RVA was detected in all months of 2018 except January and February Figure 1b. Diarrhea cases peaked in June while RVA prevalence peaked in August (50% of all collected samples were RVA positive). Sequencing and GP typing was successful for 48 (87.3%) of the 55 RVA-positive samples. Five G types (G1, G2, G3, G9 and G12) and two P types (P[4] and P[8]) were identified in the successfully sequenced samples. From these, six GP combinations were identified, namely: G3P[8] ( $n = 37, 77.1%$ ), G1P[8] ( $n = 6, 12.5%$ ), G2P[4] ( $n = 2, 4.2%$ ), G2P[8] ( $n = 1, 2.1%$ ), G9P[8] ( $n = 1, 2.1%$ ) and G12P[8] ( $n = 1, 2.1%$ ). The G3P[8] and G1P[8] strains were the only genotypes detected for > 2 months while the other four genotypes were detected sporadically (1–2 months), Figure 1c. The distribution of the infecting genotype (summarized as G3P[8] versus non-G3P[8]) did not differ significantly by sex, patient age, vaccination status or discharge outcome, Table 2 and Figure 1d.

**Table 2.** Characteristics of children whom were infected with rotavirus G3P[8] versus those whom were infected with non-G3P[8].

Characteristic	Genotyped RVA (%)	G3P[8] (%)	Non-G3P[8] (%)	p Value
Number of patients	48	37 (77.1)	11 (22.9)	
Sex				0.248
Male	19 (39.6)	13 (35.1)	6 (55.6)	
Female	29 (60.4)	24 (64.9)	5 (45.5)	
Age				
Mean (SD #)	19.3 (14.8)	19.2 (13.3)	19.5 (18.6)	0.946
Median (IQR <sup>δ</sup> )	15.7 (9.9–20.4)	15.9 (9.8–20.4)	15.4 (7.8–23.1)	1.000
Age group				0.770
0–11 months	17 (35.4)	13 (35.1)	4 (36.4)	
12–23 months	22 (45.8)	17 (46.0)	5 (45.6)	
24–59 months	7 (14.6)	6 (16.2)	1 (9.1)	
>60 months	2 (4.2)	1 (2.7)	1 (9.1)	
RVA vaccine eligibility				0.658
Age eligible 2 dose	45 (93.8)	35 (94.6)	10 (90.9)	
Age eligible 1 dose	0 (0.0)	0 (0.0)	0 (0.0)	
Age ineligible	3 (6.3)	2 (5.4)	1 (9.1)	
RVA vaccination status among eligible (n = 45)				0.751
Two dose eligible & received two doses	27 (60.0)	20 (57.1)	7 (70.0)	
Two dose eligible & received one dose	7 (15.6)	6 (17.1)	1 (10.0)	
One or 2 dose eligible but received none	0 (0.0)	0 (0.0)	0 (0.0)	
One or 2 dose eligible but status unknown	11 (24.4)	9 (25.7)	2 (20.0)	
Outcome				0.064
Died	1 (2.1)	0 (0.0)	1 (9.1)	
Alive	47 (97.2)	37 (100.0)	10 (90.9)	

# SD stands for standard deviation, <sup>δ</sup> IQR stands for interquartile range.

### 2.3. Genetic Diversity in the Sequenced Viruses

For the VP4 segment, a 579 nt long region (~25%) was recovered for 47 viruses (88.5%) while for the VP7 segment, a 644 nt long region (~65%) was recovered for 48 viruses (87.3%). One virus (KEN/KLF0879/2018), genotyped G9P[8], yielded a significantly shorter VP4 fragment relative to the other viruses (<500 nt) due to low quality sequencing data and was excluded from subsequent analyses. Consistent with the greater number of assigned G types ( $n = 5$ ) compared to P types ( $n = 2$ ) types, the range of pairwise nt differences was much greater in the VP7 (up to 203 nt differences) compared to VP4 segment (up to 87 nt differences), Figure 2a,b, respectively. A multi-modal distribution of nt differences was observed for both VP4 and VP7 segments. A total of 328 (~51%) and 141 (~24%) SNP positions were identified in the sequenced VP7 and VP4 fragments, respectively. Of the 48 sequenced samples, 22 (45.8%) yielded unique VP7 sequences while 17 (36.2%) gave unique VP4 sequences.

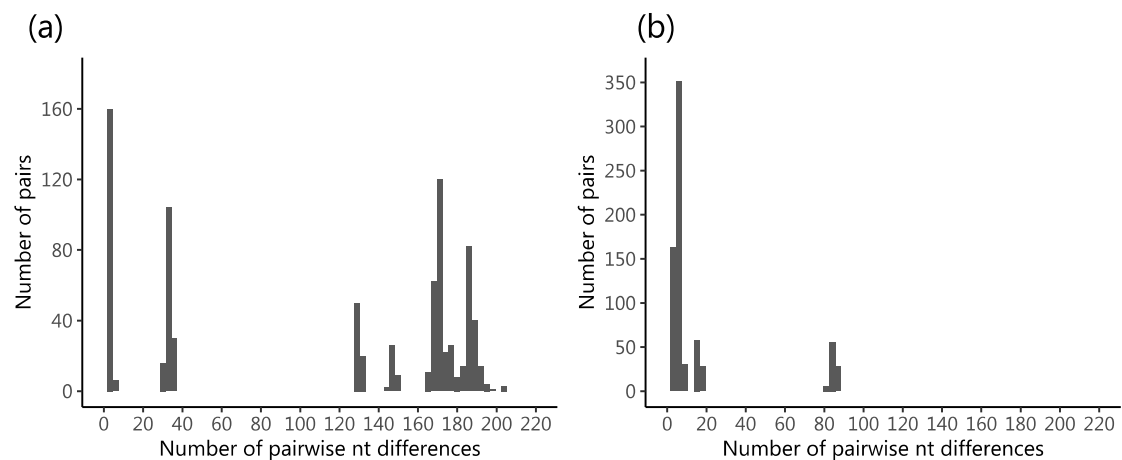


**Figure 2.** Genetic diversity in the sequenced RVA positives from Kilifi County Hospital (KCH). Panel (a) shows the distribution of pairwise nt differences in the sequenced portion of VP7 (644 nt long) of 48 RVA positives. Panel (b) shows the distribution of pairwise nt differences in the sequenced portion of VP4 (579 nt long) of 47 RVA positives.

### 2.4. Molecular Genetic Clusters

Using the range of pairwise nt differences observed in first modal distribution for the VP7 (0 to 20 nt differences, i.e., >97% nt similarity) to define a molecular genetic cluster, seven G clusters were assigned (named Clu\_1-7). Members of a cluster were universally of same G type. All G type sequences identified to be of the same type formed a single cluster except G3P[8] that occurred in three clusters, named Clu\_3/G3P[8], Clu\_4/G3P[8] and Clu\_5/G3P[8]. The temporal pattern of the assigned clusters is shown in Figure 3a. Most of the high incidence months (April to August) had multiple genetic clusters co-circulating, except for July, which had a single G3P[8] cluster. The reconstructed phylogenetic relationship between strains of the different G and P types sequenced is shown in Figure 3b,c. The VP7 phylogeny showed segregation of the seven clusters we identified from the pairwise nt difference analysis. The VP4 phylogeny showed less clear-cut phylogenetic clustering with respect to the assigned genetic clusters. The two phylogenies were not entirely congruent, a feature suggestive of reassortment in the local strains. The minimum spanning networks reconstructed for both the VP7 and VP4 sequences are shown in Figure 3d,e. Viruses in the same genetic cluster consistently had four or less nt differences to the closest next virus within the same genetic cluster.

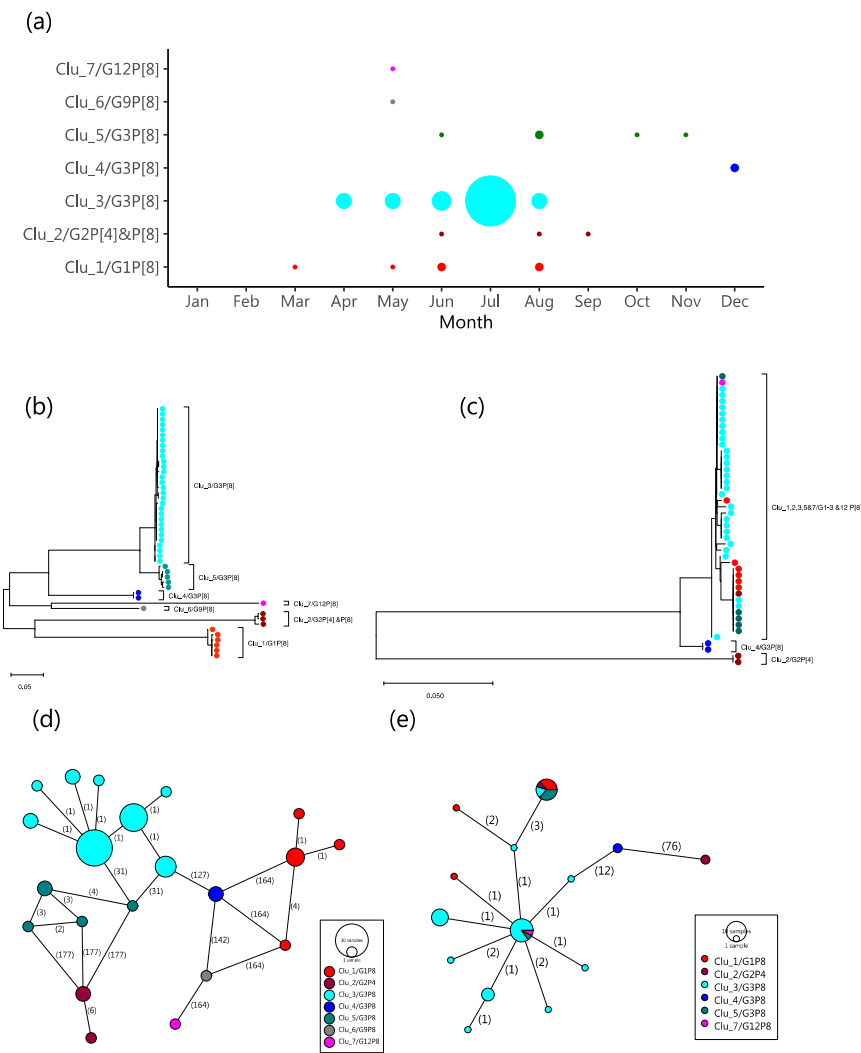


**Figure 3.** Temporal and genetic relatedness of the sequenced Kilifi rotaviruses. Panel (a) number of RVA positive samples by molecular genetic cluster and month. The circle sizes are proportional to the number of samples (the smallest indicates one sample and the largest is 13 samples). Panel (b) shows a Maximum Likelihood (ML) tree of the Kilifi 48 VP7 sequences. Panel (c) shows an ML tree of the Kilifi 47 VP4 sequences. Panel (d) shows the reconstructed POPART minimum spanning network from the 48 VP7 sequences. The vertices represent the sequenced VP7 haplotypes. The size of the vertex is proportional to the number of haplotypes (identical sequences) and is colored by the assigned molecular genetic cluster. The numbers shown on the edges represent the number of nucleotide changes from one vertex (haplotype) to the next. Panel (e) same as panel (d) above but for the Kilifi 47 VP4 sequences.

### 2.5. Spatial Distribution of the Kilifi G3 Genetic Clusters

A few viruses in different VP7-based genetic clusters had identical VP4 sequences and we explored if these were spatially clustered. Twenty-eight of the 48 genotyped samples were from KHDSS area residents. The geographical distribution of all diarrhea admissions and the RVA positives by genetic cluster is shown in Figure S1. Cases of the predominant Clu\_3/G3P[8] strains came from only a few locations although it appeared that road access (especially the Malindi-Mombasa highway) may have played a role in influencing which patients were turning up at KCH due to easier access.

## 2.6. Global Genetic Context of the Kilifi 2018 G3 Strains

A total of 338 G3 sequences from 26 countries fully met the criteria for inclusion as comparison data, including 39 previously collected in Kenya. The phylogeny derived from the combined Kilifi and global G3 viruses is shown in Figure 4a while Figure 4b shows the phylogenetic relatedness of all previous G3 sequences of RVA sampled in Kenya (5 locations including Kilifi).

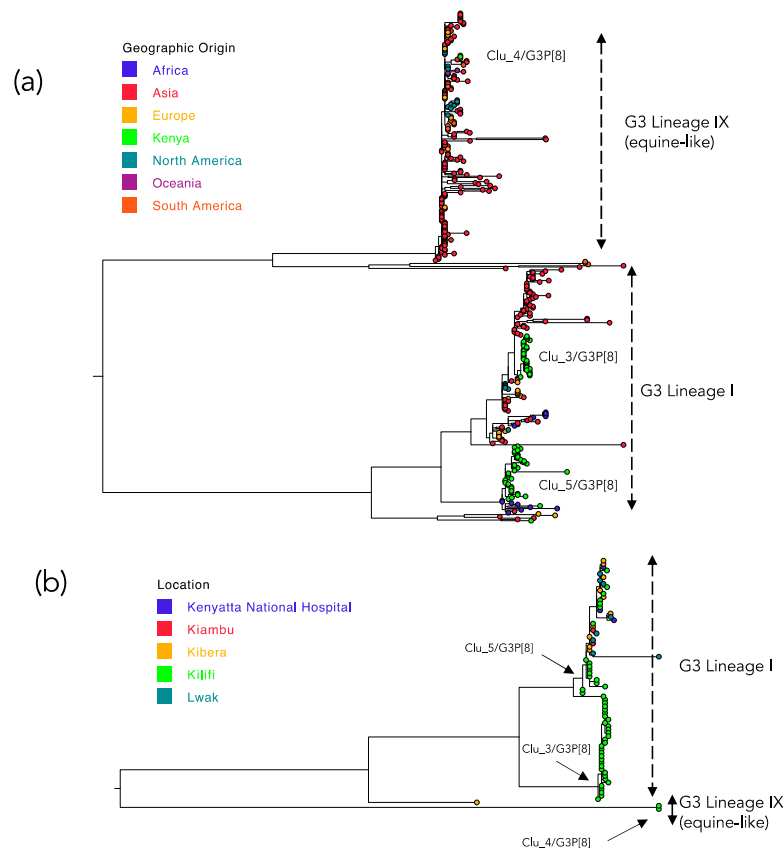


**Figure 4.** Global phylogeny derived from nucleotide sequences of G3 strains sampled between 2012–2018. (a) The phylogenetic tree reconstructed from 375 VP7 sequences of G3 type (338 collated from GenBank sampled across 26 countries including 39 from Kenya, and 37 G3 viruses sequenced in the current study) to determine the lineage and global context of the Kilifi sequences. The countries included were Australia, Belarus, Brazil, China, Dominican Republic, Ethiopia, Hungary, India, Indonesia, Italy, Japan, Kenya, South Korea, Kuwait, Nigeria, Pakistan, Peru, Russia, Spain, Taiwan, Thailand, USA, Uganda and Vietnam. The taxa for Kenya G3 sequences are provided by filled circles colored green and with the assigned Kilifi clusters names indicated next to the branches containing these sequences. Panel (b) a phylogeny of all Kenya G3 sequences ( $n = 76$ ). The different colors of the filled circle symbols indicate the Kenya taxa distinguished by their location of sampling. The names assigned to the Kilifi clusters are indicated next to the nodes leading to their branches as similarly shown in panel (a).

A majority of the global viruses fell within two of nine previously identified G3 lineages [25]; Lineage I and equine-like G3 lineage (named Lineage IX). The Kilifi G3 sequences had representation in both these two lineages: Lineage I ( $n = 35$ , 94.6%) and equine-like G3 Lineage ( $n = 2$ , 5.6%). Viruses of the genetic cluster Clu\_4/G3P[8] clustered with the equine-like G3 Lineage while the Kilifi G3 Lineage I viruses separated into two groups that corresponded to the Clu\_3/G3P[8] cluster ( $n = 30$ ) and the Clu\_5/G3P[8] cluster ( $n = 5$ ). The distribution of the pairwise nt differences in the compiled global G3 sequences dataset, like for the Kilifi G3 viruses, showed a multi-modal distribution (figure not shown). The first major trough was observed at 27 nt differences.

On applying the threshold used to identify the local molecular genetic clusters (>97% genetic similarity) on the global G3 dataset, 18 clusters were identified (Table S1). Of these, eight were singletons, six comprised of between 2 and 3 members and the remaining four clusters had 10, 47, 116 and 181 members. All the Kilifi G3 viruses fell in the three clusters that had the highest membership overall, Table S1. For each of the three Kilifi G3 genetic clusters we explored their closest genetic relative in the global dataset by network reconstructions (Figure 5). For the Kilifi Clu\_3/G3P[8] the closest similar sequences were from India (G3P[8] collected in 2016) and Singapore (G3P[8] collected in 2016) that had 2 nucleotide differences Figure 5a. For the Kilifi Clu\_4/G3P[8] (the equine-like G3 Lineage) the closest relative was from Taiwan (G3P[8] collected in 2016) with zero nucleotide difference in the sequenced region Figure 5b. For the Kilifi Clu\_5/G3P[8] the closest relatives were from Kenya (G3P[6] collected in 2014) and Uganda (G3P[6] collected in 2013) that had zero and 2 nucleotide difference, respectively, Figure 5c. Overall, within these three major global G3 genetic clusters, clustering by country was common.

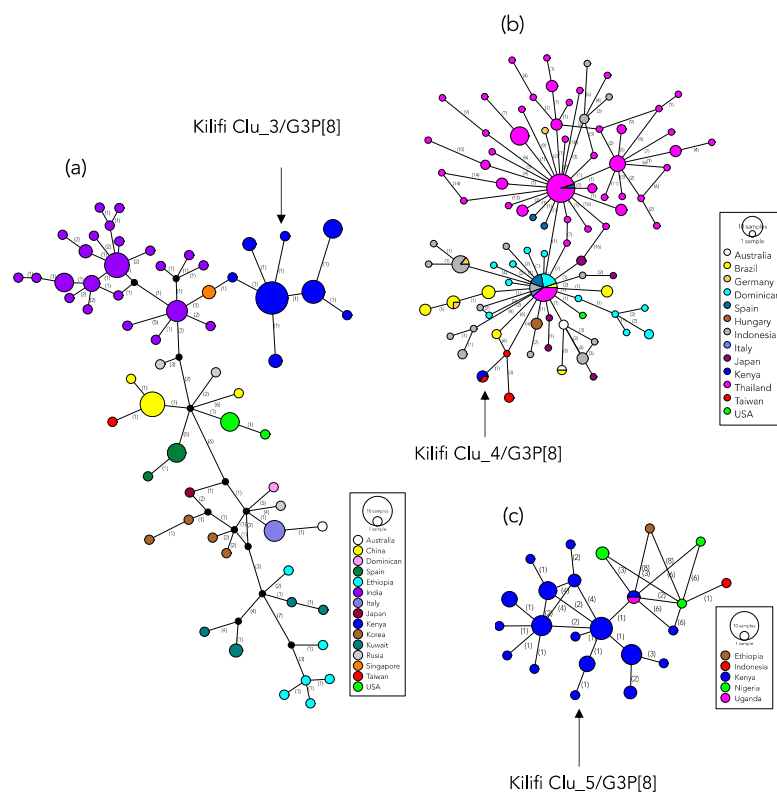


**Figure 5.** Haplotype network showing relationships of the identified global G3 lineages that included Kilifi viruses. Panel (a) shows the network for Lineage I cluster viruses that included the Kilifi Clu\_3/G3P[8] strains. The vertices represent the VP7 haplotypes. The size of the vertex is proportional to the number of haplotypes (identical sequences) and is colored by the country of sampling. The numbers shown on the edges represent the number of nucleotide changes from one vertex (haplotype) to the next. Panel (b) and (c) have the same description as panel (a) above but represent Lineage IX (equine-like G3) cluster that included Kilifi Clu\_4 G3P[8] and the Lineage I cluster that included Kilifi Clu\_5 G3P[8] sequences, respectively.

### 3. Discussion

Four years after Kenya introduced Rotarix<sup>®</sup> vaccine into its NIP, multiple RVA GP genotypes circulated during the 2018 season in Kilifi, Kenya, with the G3P[8] genotype predominating at 67.2%. At this study site, the preceding two years (2016 and 2017) were dominated by the G2P[4] and G1P[8] genotypes, respectively, with only six cases of G3P[8] detected from September 2009 to December

2017 [30] and an additional three partially genotyped G3P[x] detected in 2013 [31]. The G3P[8] strains are partially heterotypic to the monovalent Rotarix<sup>®</sup> vaccine, which is comprised of an attenuated G1P[8] strain. During 2018, this local G3P[8] predominance is consistent with the previously documented season-to-season spatial-temporal fluctuations in the prevalence of RVA genotypes [12], hypothesized to be driven by the prevailing population-level immunity derived from natural infections and the use of vaccines [14].

Vaccination records were available for 70.6% of the children with an RVA positive test. Of these, 92.7% were age eligible to have received the two doses of Rotarix<sup>®</sup> vaccine and, in that subgroup, the vast majority (80.6%) had indeed received the full 2-dose series. However, overall, the vaccination status of these children did not appear to predict either their RVA diagnosis result or the infecting GP genotype. These findings, albeit from a single season and site, suggest that for these children who acquired an RVA infection despite one or two-dose vaccination, host factors rather than viral characteristics or vaccine composition may explain the vaccine failures. A follow-up study is planned.

At least seven distinct genetic clusters constituted the 2018 coastal Kenya RVA season. The VP7 sequences showed greater genetic diversity and provided a better phylogenetic resolution compared to the VP4 sequences. Each of the identified G types corresponded to a single genetic cluster except G3 viruses that segregated into three genetically distinct clusters. Strikingly, some samples with different G types yielded identical VP4 sequences, indicating that some of the children may have been infected by reassortant viruses or harbored mixed infections [25]. Our analyses improve understanding on the recent composition and transmission patterns of local RVA seasons, providing insight into the design of final stretch RVA control strategies following vaccine introduction.

Several recent studies have reported the increased proportion of G3P[8] strains, e.g., in Australia [14], Japan [32], Thailand [28], Indonesia [29], Pakistan [33], Dominican Republic [25], Brazil [34], Spain [20], Mozambique [24], Malawi [35] and Botswana [36]. The global G3 sequences available from GenBank showed extensive genetic diversity. The significance of this diversity in relation to human immune recognition should be investigated. Notably, recent years have also observed the emergence and global spread of a new G3 lineage named equine-like G3, of putative equine origin, assigned G3 Lineage IX [25]. Strains of G3 Lineage IX were first detected in 2013 in Japan and have since been widely detected in several other countries (Australia [21], Taiwan (unpublished data in GenBank), Indonesia [29], Thailand [28], USA [26], Dominican Republic [25], Brazil [34], Italy [23], Germany [27], Hungary [22] and Spain [20]). Our study is the first to document African children infection with the G3 Lineage IX. Continued surveillance to monitor whether this particular strain becomes endemic in Kenya and the wider Africa continent in the face of increased RVA vaccine coverage is important to optimize RVA vaccine-mediated control. Notably, recent studies in Botswana [36], Mozambique [24], Malawi [35] and Ethiopia [37] reported increased prevalence of G3 type viruses but sequencing data from these studies are not yet available.

Based on sequence data deposited in GenBank, the predominant Kilifi G3 cluster (Clu\_3/G3P[8]) was the second most common genetic cluster globally. The closest sequences were from Singapore and India, both countries that did not yet have RVA vaccine in their NIP in 2018. The second most prevalent Kilifi G3 genetic cluster was Clu\_5/G3P[8]. Notably, this cluster has not been detected frequently around the globe and the closest genetic links were Kenyan strains collected in Kiambu County (Central province) in July and August 2014 [38], Kilifi in 2017, and strains from Ethiopia (collection date: April 2016 [39]) and Uganda (collection date: January 2013 [40]), neighboring countries which included RVA vaccines in their NIP in 2013 and 2018, respectively. Although the Kilifi Clu\_4/G3P[8] (equine-like G3 Lineage) was the least prevalent locally, it was the most prevalent globally. The closest relatives to the Kenyan strains were from Taiwan, a country yet to introduce RVA vaccination.

This study had some limitations. First, the sequence data from the cohort represents a single site and one season. Second, we only sequenced portions of the VP4 and VP7 segments. Whereas these data were adequate to assign genotypes, lineages and estimate the number of genetic clusters, whole genome sequences provide a better resolution in examining reassortment events, evolution in

internal genes and studying genetic clusters [18,25,41]. Third, to determine the origin and pathways of spread of the imported genetic clusters, background sequence data from more countries and including populations neighboring coastal Kenya would have been ideal. Unfortunately, sequence data in public sequence databases to facilitate such phylogeographic analysis are currently limited. Fourth, the absence of significant epidemiological data for some variables e.g., vaccine status for ~30% of the RVA positive children and geographic origin for children from outside the KHDSS area limited our analyses.

In conclusion, the finding that >20% of diarrheal stools from children admitted to KCH with diarrhea in 2018 were RVA positive highlights that RVA is still a significant contributor to severe childhood diarrhea in coastal Kenya, despite the introduction of Rotarix® into Kenya's NIP in 2014. The cross-continent detection of the emerging equine-like G3 viruses and other typical human G3 strains demonstrates the global nature of RVA transmission. Strikingly, strains found circulating in the Kilifi population were most closely related to strains circulating in countries that were yet to introduce RVA vaccines into their NIP. This observation reminds of the global connectedness regarding pathogen movement and emphasizes the importance of vaccinating all eligible populations across the world, as failure to do so builds a reservoir for strains that continue to seed transmission in vaccinated populations. Identifying factors responsible for RVA vaccine underperformance in low-income settings is a priority research area that may support efforts to further reduce RVA burden. Our study did not ascertain that viral genetic diversity is a contributor to the vaccine underperformance in this setting. Studies investigating the relationship between RVA vaccine immunogenicity and infant characteristics, such as malnutrition, age at first RVA dose, concomitant receipt of oral polio vaccine (OPV), enteric co-infections and enteric dysbiosis may provide better insight into RVA vaccine performance characteristics.

## **4. Materials and Methods**

### *4.1. Study Population and Location*

KCH is the main referral hospital in Kilifi County (population size ~1.5 million people). The major economic activities in the county are subsistence farming, fishing and tourism [42]. An area around KCH (~900 km<sup>2</sup> with a population of ~300,000 people) is monitored by the KWTRP and is known as the KHDSS area [42], Figure S1. A high proportion of the patients seeking care at the KCH are KHDSS area residents [42]. Vaccination data of admitted children were collected using an electronic registry [8,43,44].

In the current analysis, stool samples were collected from eligible and consented pediatric patients admitted to KCH between January and December 2018 (the surveillance period), as part of the ongoing rotavirus surveillance program [8,31,43]. All children aged <13 years old admitted with diarrhea (defined as passing three or more watery stools in the last 24-h) were eligible for inclusion [8,31,43]. Following a review of demographic and clinical data collected by a clinical staff, parents or caregivers of eligible children were approached for consent, and a single stool sample was collected. The samples were immediately transferred into a cool box with ice blocks before transportation to the KWTRP for RVA testing and long-term storage at -80 °C.

### *4.2. Specimen Laboratory Processing*

RVA in the stool samples was detected using ProSpecT™ enzyme immunoassay (EIA) kit (Oxoid, Basingstoke, UK) following the manufacturer's instructions. RVA positive samples were amplified in the VP4 and VP7 segments using One-step Reverse Transcriptase PCR Kit (Qiagen, Valencia, CA, USA) using previously published primers [45,46]. Successful amplification of the target regions was confirmed by the presence of expected bands (VP4: 660 bp and VP7: 881 bp) following gel electrophoresis of the PCR products. Products from successful PCRs were purified using GFX DNA purification kit (GFX-Amersham, Amersham, UK) and sequenced bi-directionally (both in forward and

reverse directions) using Big Dye Terminator 3.1 (Applied Biosystems, Foster City, CA, USA) chemistry. The primers used during PCR amplification were used for sequencing on an ABI Prism 3130xl Genetic Analyzer (Applied Biosystems, Foster City, CA, USA).

#### *4.3. Genotyping and Phylogenetic Analysis*

The sequence reads were assembled using Sequencher v5.4.6 (Gene Codes Corp Inc., Ann Arbor, MI, USA). Nucleotide (nt) sequence alignments were prepared using MAFFT v7.222 and visualized using Aliview v1.8. G and P genotypes were determined using Virus Pathogen Resource (ViPR) online classification tool [47]. The best nt substitution model for the alignments were determined IQ-Tree v1.6.6 [48]. Phylogenetic trees were reconstructed using the maximum likelihood (ML) method in RaxML v8.2.12 [49] and MEGA v7 [50]. Support for the tree branching patterns was evaluated by 1000 bootstrap iterations.

#### *4.4. Genetic Clusters*

Molecular genetic clusters were defined from the distribution of pairwise nt differences of VP7 segment sequences. Pairwise nt differences were determined using pairsnp (<https://github.com/gtonkinhill/pairsnp/>). Viruses within the same molecular genetic clusters were those which pairwise nt differences occurred within the first modal distribution. Using this threshold, clusters were identified using the USEARCH algorithm [51]. Single nucleotide polymorphic (SNP) positions in alignments were assessed using parseSNP [52]. The minimum spanning networks between the RVA positive patients were reconstructed using POPART v1.70 program [53].

#### *4.5. Comparison Dataset*

The phylogenetic context of the locally predominant genotype in global RVA populations was investigated by co-analysis with similar G type strains sequence data deposited in GenBank. The search in GenBank was conducted in October 2020. The criteria for comparison data inclusion were (i) detection in a human stool/rectal swab specimen, (ii) sequence fully overlapping with the VP7 region sequenced for the Kilifi viruses, (iii) information on country and date of sampling available and (iv) sample collected in 2012–2018. G3 sequences collected previously from around Kenya including Kilifi were included in the analysis.

#### *4.6. Statistical Analysis*

Numerical data were analyzed in STATA v15.1. Continuous variables were summarized using various measures of dispersion. Differences between groups were assessed using a t-test or Wilcoxon rank-sum test. Binary data were summarized using proportions and comparison between groups made using either  $\chi^2$  or Fisher's exact test (depending on group sample size). The 95% CI were presented for proportions and standard deviation for means. A *p*-value of <0.05 was considered significant.

#### *4.7. Data Availability*

Partial sequences for the VP7 and VP4 segments reported in this work have been deposited to GenBank database under the sequence accession numbers MN194408-MN194485 for VP7 and MN194325-MN194364 for VP4.

#### *4.8. Ethical Statement*

Before sample collection informed written consent was obtained from the child's parent or guardian. The Scientific Ethics Review Unit (SERU) board that sits at KEMRI, Nairobi, approved the study protocols (SERU#3049).

**Supplementary Materials:** The following are available online at <http://www.mdpi.com/2076-0817/9/12/981/s1>, Figure S1: Geographic origin distribution of sampled children who presented with diarrhea symptoms at KCH

and were Kilifi Health Demographic Surveillance System (KHDS) area residents; Table S1: The global distribution of the identified G3 global genetic clusters.

**Author Contributions:** Conceptualization, C.N.A., D.J.N., M.J.M. and R.F.B.; methodology, D.J.N., C.N.A. and M.J.M.; software, M.J.M. and C.N.A.; validation, C.N.A., E.G. and M.J.M.; formal analysis, C.N.A. and M.J.M.; investigation, C.N.A., M.J.M. and D.J.N. and E.G., resources, R.F.B., J.E.T., U.D.P. and D.J.N.; data curation, N.M., M.J.M. and C.N.A.; writing—original draft preparation, M.J.M. and C.N.A.; writing—review and editing, R.O., J.R.V., R.F.B., J.E.T., U.D.P. and D.J.N.; visualization, C.N.A. and M.J.M.; supervision, D.J.N. and C.N.A.; project administration, E.G., R.O., M.J.M., N.M. and D.J.N.; funding acquisition, D.J.N., R.O., J.R.V., J.E.T., U.D.P., R.F.B. All authors have read and agreed to the published version of the manuscript.

**Funding:** This work was funded by Gavi, The Vaccine Alliance through Emory University, to the Rotavirus Immunization Program and Evaluation in Kenya (RIPEK) and the Wellcome Trust (grant numbers 203077 and 102975). CNA is supported through the DELTAS Africa Initiative [DEL-15-003]. The DELTAS Africa Initiative is an independent funding scheme of the African Academy of Sciences (AAS)'s Alliance for Accelerating Excellence in Science in Africa (AESA) and supported by the New Partnership for Africa's Development Planning and Coordinating Agency (NEPAD Agency) with funding from the Wellcome Trust [107769/Z/10/Z] and the UK government. Views expressed in this publication are those of the authors and not necessarily those of Gavi, AAS, NEPAD Agency, Wellcome Trust or the UK government.

**Acknowledgments:** We thank the participants who provided samples for analysis, and the Clinical and Laboratory staff at Virus Epidemiology and Control group, KEMRI Wellcome Trust Research Programme for collection and processing the samples. This work is published with permission from Director KEMRI.

**Conflicts of Interest:** The authors declare no conflict of interest. The funders had no role in the design of the study; in the collection, analyses, or interpretation of data; in the writing of the manuscript, or in the decision to publish the results.

**Disclaimer:** The findings and conclusions in this report are those of the authors and do not necessarily represent the official position of the U.S. Centers for Disease Control and Prevention (CDC) or the authors' affiliated institutions.

## References

1. Burnett, E.; Jonesteller, C.L.; Tate, J.E.; Yen, C.; Parashar, U.D. Global Impact of Rotavirus Vaccination on Childhood Hospitalizations and Mortality From Diarrhea. *J. Infect. Dis.* **2017**, *215*, 1666–1672. [CrossRef] [PubMed]
2. Steele, A.D.; Groome, M.J. Measuring Rotavirus Vaccine Impact in Sub-Saharan Africa. *Clin. Infect. Dis.* **2020**, *70*, 2314–2316. [CrossRef] [PubMed]
3. Operario, D.J.; Platts-Mills, J.A.; Nadan, S.; Page, N.; Seheri, M.; Mphahlele, J.; Praharaj, I.; Kang, G.; Araujo, I.T.; Leite, J.P.G.; et al. Etiology of Severe Acute Watery Diarrhea in Children in the Global Rotavirus Surveillance Network Using Quantitative Polymerase Chain Reaction. *J. Infect. Dis.* **2017**, *216*, 220–227. [CrossRef] [PubMed]
4. Iturriza-Gómara, M.; Jere, K.C.; Hungerford, D.; Bar-Zeev, N.; Shioda, K.; Kanjerwa, O.; Houpt, E.R.; Operario, D.J.; Wachepa, R.; Pollock, L.; et al. Etiology of Diarrhea Among Hospitalized Children in Blantyre, Malawi, Following Rotavirus Vaccine Introduction: A Case-Control Study. *J. Infect. Dis.* **2019**, *220*, 213–218. [CrossRef] [PubMed]
5. Troeger, C.; Khalil, I.A.; Rao, P.C.; Cao, S.; Blacker, B.F.; Ahmed, T.; Armah, G.; Bines, J.E.; Brewer, T.G.; Colombara, D.V.; et al. Rotavirus Vaccination and the Global Burden of Rotavirus Diarrhea Among Children Younger Than 5 Years. *JAMA Pediatr.* **2018**, *172*, 958–965. [CrossRef]
6. Steele, D.; Victor, J.; Carey, M.; Tate, J.; Atherly, D.; Pecenska, C.; Diaz, Z.; Parashar, U.; Kirkwood, C. Experiences with rotavirus vaccines: Can we improve rotavirus vaccine impact in developing countries? *Hum. Vaccines Immunother.* **2019**, *15*, 1215–1227. [CrossRef]
7. Willame, C.; Noordegraaf-Schouten, M.V.; Gvozdenović, E.; Kochems, K.; Oordt-Speets, A.; Praet, N.; Van Hoorn, R.; Rosillon, D. Effectiveness of the Oral Human Attenuated Rotavirus Vaccine: A Systematic Review and Meta-analysis—2006–2016. *Open Forum Infect. Dis.* **2018**, *5*, ofy292. [CrossRef]
8. Khagayi, S.; Omoro, R.; Otieno, G.P.; Ogwel, B.; Ochieng, J.B.; Juma, J.; Apondi, E.; Bigogo, G.; Onyango, C.; Ngama, M.; et al. Effectiveness of Monovalent Rotavirus Vaccine Against Hospitalization With Acute Rotavirus Gastroenteritis in Kenyan Children. *Clin. Infect. Dis.* **2019**, *70*, 2298–2305. [CrossRef]
9. Walker, J.L.; Andrews, N.J.; Atchison, C.J.; Collins, S.; Allen, D.J.; Ramsay, M.E.; Ladhani, S.N.; Thomas, S.L. Effectiveness of oral rotavirus vaccination in England against rotavirus-confirmed and all-cause acute gastroenteritis. *Vaccine X* **2019**, *1*, 100005. [CrossRef]

10. Nair, N.; Feng, N.; Blum, L.K.; Sanyal, M.; Ding, S.; Jiang, B.; Sen, A.; Morton, J.M.; He, X.-S.; Robinson, W.H.; et al. VP4- and VP7-specific antibodies mediate heterotypic immunity to rotavirus in humans. *Sci. Transl. Med.* **2017**, *9*, eaam5434. [CrossRef]
11. RCWG. Rotavirus Classification Working Group: Newly Assigned Genotypes. Available online: <https://rega.kuleuven.be/cev/viralmetagenomics/virus-classification/rcwg> (accessed on 7 January 2020).
12. Sadiq, A.; Bostan, N.; Yinda, K.C.; Naseem, S.; Sattar, S. Rotavirus: Genetics, pathogenesis and vaccine advances. *Rev. Med. Virol.* **2018**, *28*, e2003. [CrossRef] [PubMed]
13. Leshem, E.; Lopman, B.; Glass, R.; Gentsch, J.; Bányai, K.; Parashar, U.; Patel, M. Distribution of rotavirus strains and strain-specific effectiveness of the rotavirus vaccine after its introduction: A systematic review and meta-analysis. *Lancet Infect. Dis.* **2014**, *14*, 847–856. [CrossRef]
14. Roczo-Farkas, S.; Kirkwood, C.D.; Cowley, D.; Barnes, G.L.; Bishop, R.F.; Bogdanovic-Sakran, N.; Boniface, K.; Donato, C.M.; Bines, J.E. The Impact of Rotavirus Vaccines on Genotype Diversity: A Comprehensive Analysis of 2 Decades of Australian Surveillance Data. *J. Infect. Dis.* **2018**, *218*, 546–554. [CrossRef] [PubMed]
15. Burke, R.M.; Tate, J.E.; Barin, N.; Bock, C.; Bowen, M.D.; Chang, D.; Gautam, R.; Han, G.; Holguin, J.; Huynh, T.; et al. Three Rotavirus Outbreaks in the Postvaccine Era—California, 2017. *MMWR Morb. Mortal. Wkly. Rep.* **2018**, *67*, 470–472. [CrossRef] [PubMed]
16. Pitzer, V.E.; Bilcke, J.; Heylen, E.; Crawford, F.W.; Callens, M.; De Smet, F.; Van Ranst, M.; Zeller, M.; Matthijssens, J. Did Large-Scale Vaccination Drive Changes in the Circulating Rotavirus Population in Belgium? *Sci. Rep.* **2015**, *5*, 18585. [CrossRef] [PubMed]
17. Ianiro, G.; Micolano, R.; Di Bartolo, I.; Scavia, G.; Monini, M.; RotaNet-Italy Study Group. Group A rotavirus surveillance before vaccine introduction in Italy, September 2014 to August 2017. *Eurosurveillance* **2019**, *24*, 1800418. [CrossRef]
18. Ogden, K.M.; Tan, Y.; Akopov, A.; Stewart, L.S.; McHenry, R.; Fonnesbeck, C.J.; Piya, B.; Carter, M.H.; Fedorova, N.B.; Halpin, R.A.; et al. Multiple Introductions and Antigenic Mismatch with Vaccines May Contribute to Increased Predominance of G12P[8] Rotaviruses in the United States. *J. Virol.* **2018**, *93*, e01476-18. [CrossRef]
19. Santos, N.; Hoshino, Y. Global distribution of rotavirus serotypes/genotypes and its implication for the development and implementation of an effective rotavirus vaccine. *Rev. Med. Virol.* **2005**, *15*, 29–56. [CrossRef]
20. Arana, A.; Montes, M.; Jere, K.C.; Alkorta, M.; Iturriza-Gómara, M.; Cilla, G. Emergence and spread of G3P[8] rotaviruses possessing an equine-like VP7 and a DS-1-like genetic backbone in the Basque Country (North of Spain), 2015. *Infect. Genet. Evol.* **2016**, *44*, 137–144. [CrossRef]
21. Cowley, D.; Donato, C.M.; Roczo-Farkas, S.; Kirkwood, C.D. Emergence of a novel equine-like G3P[8] inter-genogroup reassortant rotavirus strain associated with gastroenteritis in Australian children. *J. Gen. Virol.* **2016**, *97*, 403–410. [CrossRef]
22. Dóro, R.; Marton, S.; Bartókné, A.H.; Lengyel, G.; Agócs, Z.; Jakab, F.; Bányai, K. Equine-like G3 rotavirus in Hungary, 2015—Is it a novel intergenogroup reassortant pandemic strain? *Acta Microbiol. Immunol. Hung.* **2016**, *63*, 243–255. [CrossRef] [PubMed]
23. Esposito, S.; Camilloni, B.; Bianchini, S.; Ianiro, G.; Polinori, I.; Farinelli, E.; Monini, M.; Principi, N. First detection of a reassortant G3P[8] rotavirus A strain in Italy: A case report in an 8-year-old child. *Virol. J.* **2019**, *16*, 64. [CrossRef] [PubMed]
24. João, E.D.; Munlela, B.; Chissaque, A.; Chilaúle, J.; Langa, J.; Augusto, O.; Boone, S.S.; Anapakala, E.; Sambo, J.; Guimarães, E.; et al. Molecular Epidemiology of Rotavirus A Strains Pre- and Post-Vaccine (Rotarix®) Introduction in Mozambique, 2012–2019: Emergence of Genotypes G3P[4] and G3P[8]. *Pathogens* **2020**, *9*, 671. [CrossRef] [PubMed]
25. Katz, E.M.; Esona, M.D.; Betrapally, N.; Leon, L.A.D.L.C.D.; Neira, Y.R.; Rey, G.J.; Bowen, M.D. Whole-gene analysis of inter-genogroup reassortant rotaviruses from the Dominican Republic: Emergence of equine-like G3 strains and evidence of their reassortment with locally-circulating strains. *Virology* **2019**, *534*, 114–131. [CrossRef]
26. Perkins, C.; Mijatovic-Rustempasic, S.; Ward, M.L.; Cortese, M.M.; Bowen, M.D. Genomic Characterization of the First Equine-Like G3P[8] Rotavirus Strain Detected in the United States. *Genome Announc.* **2017**, *5*, e01341-17. [CrossRef]

27. Pietsch, C.; Liebert, U. Molecular characterization of different equine-like G3 rotavirus strains from Germany. *Infect. Genet. Evol.* **2018**, *57*, 46–50. [CrossRef]
28. Tacharoenuang, R.; Komoto, S.; Guntapong, R.; Upachai, S.; Singchai, P.; Ide, T.; Fukuda, S.; Ruchusatsawast, K.; Sriwantana, B.; Tatsumi, M.; et al. High prevalence of equine-like G3P[8] rotavirus in children and adults with acute gastroenteritis in Thailand. *J. Med. Virol.* **2020**, *92*, 174–186. [CrossRef]
29. Utsumi, T.; Wahyuni, R.M.; Doan, Y.H.; Dinana, Z.; Soegijanto, S.; Fujii, Y.; Juniastuti; Yamani, L.N.; Matsui, C.; Deng, L.; et al. Equine-like G3 rotavirus strains as predominant strains among children in Indonesia in 2015–2016. *Infect. Genet. Evol.* **2018**, *61*, 224–228. [CrossRef]
30. Mwanga, M.J.; Owor, B.E.; Ochieng, J.B.; Ngama, M.H.; Ogwel, B.; Onyango, C.; Juma, J.; Njeru, R.; Gicheru, E.; Otieno, G.P.; et al. Rotavirus group A genotype circulation patterns across Kenya before and after nationwide vaccine introduction, 2010–2018. *BMC Infect. Dis.* **2020**, *20*, 504. [CrossRef]
31. Owor, B.E.; Mwanga, M.J.; Njeru, R.; Mugo, R.; Ngama, M.; Otieno, G.P.; Nokes, D.J.; Agoti, C.N. Molecular characterization of rotavirus group A strains circulating prior to vaccine introduction in rural coastal Kenya, 2002–2013. *Wellcome Open Res.* **2018**, *3*, 150. [CrossRef]
32. Thongprachum, A.; Chan-It, W.; Khamrin, P.; Okitsu, S.; Nishimura, S.; Kikuta, H.; Yamamoto, A.; Sugita, K.; Baba, T.; Mizuguchi, M.; et al. Reemergence of new variant G3 rotavirus in Japanese pediatric patients, 2009–2011. *Infect. Genet. Evol.* **2013**, *13*, 168–174. [CrossRef] [PubMed]
33. Umair, M.; Abbasi, B.H.; Sharif, S.; Alam, M.M.; Rana, M.S.; Mujtaba, G.; Arshad, Y.; Fatmi, M.Q.; Zaidi, S.Z. High prevalence of G3 rotavirus in hospitalized children in Rawalpindi, Pakistan during 2014. *PLoS ONE* **2018**, *13*, e0195947. [CrossRef] [PubMed]
34. Guerra, S.F.S.; Soares, L.S.; Lobo, P.S.; Júnior, E.T.P.; Júnior, E.C.S.; Bezerra, D.A.M.; Vaz, L.R.; Linhares, A.C.; Mascarenhas, J.D.P. Detection of a novel equine-like G3 rotavirus associated with acute gastroenteritis in Brazil. *J. Gen. Virol.* **2016**, *97*, 3131–3138. [CrossRef] [PubMed]
35. Mhango, C.; Mandolo, J.J.; Chinyama, E.; Wachepa, R.; Kanjerwa, O.; Malamba-Banda, C.; Matambo, P.B.; Barnes, K.G.; Chaguzza, C.; Shawa, I.T.; et al. Rotavirus Genotypes in Hospitalized Children with Acute Gastroenteritis Before and After Rotavirus Vaccine Introduction in Blantyre, Malawi, 1997–2019. *J. Infect. Dis.* **2020**. [CrossRef]
36. Mokomane, M.; Esona, M.; Bowen, M.D.; Tate, J.; Steenhoff, A.; Lechiile, K.; Gaseitsiwe, S.; Seheri, L.; Magagula, N.; Weldegebriel, G.; et al. Diversity of Rotavirus Strains Circulating in Botswana before and after introduction of the Monovalent Rotavirus Vaccine. *Vaccine* **2019**, *37*, 6324–6328. [CrossRef]
37. Abebe, A.; Getahun, M.; Mapaseka, S.L.; Beyene, B.; Assefa, E.; Teshome, B.; Tefera, M.; Kebede, F.; Habtamu, A.; Haile-Mariam, T.; et al. Impact of rotavirus vaccine introduction and genotypic characteristics of rotavirus strains in children less than 5 years of age with gastroenteritis in Ethiopia: 2011–2016. *Vaccine* **2018**, *36*, 7043–7047. [CrossRef]
38. Wandera, E.A.; Komoto, S.; Mohammad, S.; Ide, T.; Bundi, M.; Nyangao, J.; Kathiiko, C.; Odoyo, E.; Galata, A.; Miring’U, G.; et al. Genomic characterization of uncommon human G3P[6] rotavirus strains that have emerged in Kenya after rotavirus vaccine introduction, and pre-vaccine human G8P[4] rotavirus strains. *Infect. Genet. Evol.* **2019**, *68*, 231–248. [CrossRef]
39. Gelaw, A.; Pietsch, C.; Liebert, U.G. Molecular epidemiology of rotaviruses in Northwest Ethiopia after national vaccine introduction. *Infect. Genet. Evol.* **2018**, *65*, 300–307. [CrossRef]
40. Bwogi, J.; Jere, K.C.; Karamagi, C.; Byarugaba, D.K.; Namuwulya, P.; Baliraine, F.N.; Desselberger, U.; Iturriza-Gomara, M. Whole genome analysis of selected human and animal rotaviruses identified in Uganda from 2012 to 2014 reveals complex genome reassortment events between human, bovine, caprine and porcine strains. *PLoS ONE* **2017**, *12*, e0178855. [CrossRef]
41. Jere, K.C.; Chaguzza, C.; Bar-Zeev, N.; Lowe, J.; Peno, C.; Kumwenda, B.; Nakagomi, O.; Tate, J.E.; Parashar, U.D.; Heyderman, R.S.; et al. Emergence of Double- and Triple-Gene Reassortant G1P[8] Rotaviruses Possessing a DS-1-Like Backbone after Rotavirus Vaccine Introduction in Malawi. *J. Virol.* **2017**, *92*, 92. [CrossRef]
42. Scott, J.A.G.; Bauni, E.; Moisi, J.C.; Ojal, J.; Gatakaa, H.; Nyundo, C.; Molyneux, C.S.; Kombe, F.; Tsofa, B.; Marsh, K.; et al. Profile: The Kilifi Health and Demographic Surveillance System (KHDSS). *Int. J. Epidemiol.* **2012**, *41*, 650–657. [CrossRef] [PubMed]

43. Otieno, G.P.; Bottomley, C.; Khagayi, S.; Adetifa, I.; Ngama, M.; Omore, R.; Ogwel, B.; Owor, B.E.; Bigogo, G.; Ochieng, J.B.; et al. Impact of the Introduction of Rotavirus Vaccine on Hospital Admissions for Diarrhea Among Children in Kenya: A Controlled Interrupted Time-Series Analysis. *Clin. Infect. Dis.* **2019**, *70*, 2306–2313. [CrossRef] [PubMed]
44. Adetifa, I.M.; Bwanaali, T.; Wafula, J.; Mutuku, A.; Karia, B.; Makumi, A.; Mwatsuma, P.; Bauni, E.; Hammitt, L.L.; Nokes, D.J.; et al. Cohort Profile: The Kilifi Vaccine Monitoring Study. *Int. J. Epidemiol.* **2016**, *46*, 792–792h. [CrossRef]
45. Gómara, M.I.; Cubitt, D.; Desselberger, U.; Gray, J. Amino Acid Substitution within the VP7 Protein of G2 Rotavirus Strains Associated with Failure To Serotype. *J. Clin. Microbiol.* **2001**, *39*, 3796–3798. [CrossRef] [PubMed]
46. Simmonds, M.K.; Armah, G.; Asmah, R.; Banerjee, I.; Damanka, S.; Esona, M.; Gentsch, J.R.; Gray, J.J.; Kirkwood, C.; Page, N.; et al. New oligonucleotide primers for P-typing of rotavirus strains: Strategies for typing previously untypeable strains. *J. Clin. Virol.* **2008**, *42*, 368–373. [CrossRef]
47. Pickett, B.E.; Greer, D.; Zhang, Y.; Stewart, L.; Zhou, L.; Sun, G.; Gu, Z.; Kumar, S.; Zaremba, S.; Larsen, C.N.; et al. Virus Pathogen Database and Analysis Resource (ViPR): A Comprehensive Bioinformatics Database and Analysis Resource for the Coronavirus Research Community. *Viruses* **2012**, *4*, 3209–3226. [CrossRef] [PubMed]
48. Nguyen, L.-T.; Schmidt, H.A.; Von Haeseler, A.; Minh, B.Q. IQ-TREE: A Fast and Effective Stochastic Algorithm for Estimating Maximum-Likelihood Phylogenies. *Mol. Biol. Evol.* **2015**, *32*, 268–274. [CrossRef]
49. Stamatakis, A. Using RAxML to Infer Phylogenies. *Curr. Protoc. Bioinform.* **2015**, *51*, 6–14. [CrossRef]
50. Kumar, S.; Stecher, G.; Tamura, K. MEGA7: Molecular Evolutionary Genetics Analysis Version 7.0 for Bigger Datasets. *Mol. Biol. Evol.* **2016**, *33*, 1870–1874. [CrossRef]
51. Edgar, R.C. Search and clustering orders of magnitude faster than BLAST. *Bioinformatics* **2010**, *26*, 2460–2461. [CrossRef]
52. Taylor, N.E.; Greene, E.A. PARSESNP: A tool for the analysis of nucleotide polymorphisms. *Nucleic Acids Res.* **2003**, *31*, 3808–3811. [CrossRef] [PubMed]
53. Leigh, J.W.; Bryant, D. POPART: Full-feature software for haplotype network construction. *Methods Ecol. Evol.* **2015**, *6*, 1110–1116. [CrossRef]

**Publisher’s Note:** MDPI stays neutral with regard to jurisdictional claims in published maps and institutional affiliations.



© 2020 by the authors. Licensee MDPI, Basel, Switzerland. This article is an open access article distributed under the terms and conditions of the Creative Commons Attribution (CC BY) license (<http://creativecommons.org/licenses/by/4.0/>).

Article

# Epidemiological Trends of Five Common Diarrhea-Associated Enteric Viruses Pre- and Post-Rotavirus Vaccine Introduction in Coastal Kenya

Arnold W. Lambisia <sup>1,2,\*</sup>, Sylvia Onchaga <sup>1,†</sup>, Nickson Murunga <sup>1</sup>, Clement S. Lewa <sup>1</sup>, Steven Ger Nyanjom <sup>2</sup> and Charles N. Agoti <sup>1,3</sup>

<sup>1</sup> Kenya Medical Research Institute (KEMRI)-Wellcome Trust Research Programme, Centre for Geographic Medicine Research-Coast, Kilifi 230-80108, Kenya; onchagasylvia@gmail.com (S.O.); nmurunga@kemri-wellcome.org (N.M.); clewa@kemri-wellcome.org (C.S.L.); cnyaigoti@kemri-wellcome.org (C.N.A.)

<sup>2</sup> Department of Biochemistry, Jomo Kenyatta University of Agriculture and Technology, Juja 62000-00200, Kenya; snyanjom@jkuat.ac.ke

<sup>3</sup> School of Health and Human Sciences, Pwani University, Kilifi 195-80108, Kenya

\* Correspondence: ALambisia@kemri-wellcome.org; Tel.: +254-708-164-077

† Joint First Authors.

Received: 8 July 2020; Accepted: 10 August 2020; Published: 15 August 2020



**Abstract:** Using real-time RT-PCR, we screened stool samples from children aged <5 years presenting with diarrhea and admitted to Kilifi County Hospital, coastal Kenya, pre- (2003 and 2013) and post-rotavirus vaccine introduction (2016 and 2019) for five viruses, namely rotavirus group A (RVA), norovirus GII, adenovirus, astrovirus and sapovirus. Of the 984 samples analyzed, at least one virus was detected in 401 (40.8%) patients. Post rotavirus vaccine introduction, the prevalence of RVA decreased (23.3% vs. 13.8%,  $p < 0.001$ ) while that of norovirus GII increased (6.6% vs. 10.9%,  $p = 0.023$ ). The prevalence of adenovirus, astrovirus and sapovirus remained statistically unchanged between the two periods: 9.9% vs. 14.2%, 2.4% vs. 3.2%, 4.6% vs. 2.6%, ( $p = 0.053, 0.585$  and  $0.133$ ), respectively. The median age of diarrhea cases was higher post vaccine introduction (12.5 months, interquartile range (IQR): 7.9–21 vs. 11.2 months pre-introduction, IQR: 6.8–16.5,  $p < 0.001$ ). In this setting, RVA and adenovirus cases peaked in the dry months while norovirus GII and sapovirus peaked in the rainy season. Astrovirus did not display clear seasonality. In conclusion, following rotavirus vaccine introduction, we found a significant reduction in the prevalence of RVA in coastal Kenya but an increase in norovirus GII prevalence in hospitalized children.

**Keywords:** viral diarrhea; real-time PCR; rotavirus vaccination; Kenya

## 1. Introduction

In the year 2016 alone, approximately 300,000 children aged <5 years succumbed to diarrhea in sub-Saharan Africa [1]. Viral pathogens including rotavirus group A (RVA), adenovirus (type 40/41), astrovirus, norovirus (genogroup GI and GII) and sapovirus are among the top causative agents of severe diarrhea globally [2,3]. Understanding their epidemiological patterns such as prevalence, incidence, seasonality, clinical severity and infection age distribution in local settings is essential for designing and prioritizing interventions. Historically, RVA has been the single most important cause of severe childhood diarrhea, responsible for ~38% (95% CI: 4.8–73.4%) of hospital cases (<5 years) pre-vaccine introduction [4]. However, RVA prevalence has been rapidly declining since 2009 and was approximately 23% (95% CI: 0.7–57.7%) in 2016, in settings where the rotavirus vaccine was in use [4]. Due to the shared ecological niche and the apparent decline of all-cause gastroenteritis-associated

hospital admissions, it has been hypothesized that rotavirus vaccination has likely impacted the epidemiology of the other enteric viruses [5]. However, there are contradicting reports on the specific impact of rotavirus vaccination on the prevalence of the individual enteric viruses—for example, norovirus [6,7]. This has not been adequately examined in African populations where diarrhea burden is highest. Kenya began rotavirus vaccination in July 2014 using the monovalent Rotarix® (RV1), derived from G1P[8] strain, administered at 6 and 10 weeks of life. RV1 vaccine coverage in Kenya has increased over time since 2014 but is varied by age group, number of doses and geographic region in Kenya [8]. Within Kilifi County, coastal Kenya, coverage in 2017 in <1-year-olds was 73% (at least one dose) vs. 65% (complete two doses), while in <12–24 month-olds, it was 86% (at least one dose) vs. 84% (complete two doses) [9].

The KEMRI/Wellcome Trust Research Programme (KWTRP) has been running surveillance of RVA since 2002 in children admitted to the Kilifi County Hospital (KCH). The current study screened archived diarrheal samples from KCH, spanning both the pre- and post-rotavirus vaccine introduction periods in Kenya for RVA, astrovirus, adenovirus (all serotypes), sapovirus and norovirus (only GII) using real-time reverse-transcription polymerase chain reaction (RT-PCR) approach. We update on the prevalence of these viral diarrheal agents and their seasonal patterns pre and post introduction of the rotavirus vaccination program in Kenya.

## 2. Results

### 2.1. Study Population Characteristics

Out of 2156 children aged <5 years who presented with diarrhea at KCH during the four selected years (2003, 2013, 2016 and 2019), 1397 (64.8%) provided a stool sample; see Table 1. Overall, the demographic characteristics of the eligible children sampled, and eligible children not sampled, differed in age strata distribution ( $p = 0.001$ ) and discharge outcome ( $p < 0.001$ ); see Table 1. The main reasons for failure to sample eligible children were as follows: death ( $n = 21$ , 2.8%), discharge or transfer before sample collection ( $n = 296$ , 40.0%), consent refusal ( $n = 315$ , 41.5%) or other ( $n = 127$ , 16.7%). Among the sampled cases, 984 (70.4%) had a specimen available and tested by real-time RT-PCR for the five enteric viruses, and these were included in subsequent analysis. The median age of the sampled participants was significantly higher for the post-vaccine introduction period compared to pre-vaccine introduction period ( $p < 0.001$ ); see Table 2.

**Table 1.** Characteristics of children under 5 years of age admitted to Kilifi County Hospital (KCH), coastal Kenya, with diarrhea symptoms that were sampled versus those who were not sampled in the study.

Characteristics	All Subjects	Sampled (%)	Not Sampled (%)	<i>p</i> -Value
<b>Total Admissions</b>	2156	1397 (64.8)	759 (35.2)	
<b>Admissions Per Year</b>				
2003	1007 (46.7)	587 (42.0)	420 (55.3)	
2013	332 (15.4)	254 (18.2)	78 (10.3)	
2016	334 (15.5)	257 (18.4)	77 (10.1)	
2019	483 (22.4)	299 (21.4)	184 (24.2)	
<b>Gender</b>				0.838
Male	1262 (58.5)	815 (58.3)	447 (58.9)	
Female	894 (41.5)	582 (41.7)	312 (41.1)	
<b>Age</b>				
Median (IQR)	12.4 (7.7–20.5)	11.7 (7.4–19.7)	13.8 (8.5–22.1)	<0.001
Mean (SD)	15.7 (11.4)	15.0 (11.1)	16.9 (12.0)	<0.001
<b>Age Group</b>				0.001
0–11 Months	1045 (48.4)	718 (51.4)	326 (43.0)	
12–23 Months	716 (33.2)	444 (31.8)	272 (35.8)	
24–59 Months	396 (18.4)	235 (16.8)	161 (21.2)	

Table 1. Cont.

Characteristics	All Subjects	Sampled (%)	Not Sampled (%)	<i>p</i> -Value
<b>Discharge Outcome (<i>n</i> = 2153) #</b>				<b>&lt;0.001</b>
<b>Alive</b>	1918 (88.9)	1306 (93.5)	612 (80.5)	
<b>Dead</b>	235 (10.9)	89 (6.4)	146 (19.3)	

SD means standard deviation; IQR means interquartile range. Not sampled: sample was not collected due to lack of consent, time-up, death and others. # Discharge outcome data for three subjects were missing.

**Table 2.** Characteristics of children under 5 years of age admitted to KCH, coastal Kenya, with diarrhea symptoms and tested pre-vaccine introduction versus those tested post-vaccine introduction.

Characteristics	Total	Pre-Vaccine Introduction (%)	Post-Vaccine Introduction (%)	<i>p</i> -Value
<b>Number of Samples Tested</b>	984	454 (46.1)	530 (53.9)	
<b>Samples Tested (Year)</b>				
2003	223	223	-	
2013	231	231	-	
2016	239	-	239	
2019	291	-	291	
<b>Gender</b>				0.847
<b>Male</b>	570 (57.9)	261 (57.5)	309 (58.3)	
<b>Female</b>	414 (42.1)	193 (42.5)	221 (41.7)	
<b>Age</b>				
<b>Mean (SD)</b>	15 (11.2)	13.4 (9.9)	16.3 (12)	<0.001
<b>Median (IQR)</b>	11.7 (7.3–19.3)	11.2 (6.8–16.5)	12.5 (7.9–21)	<0.001
<b>Age group</b>				0.003
<b>0–11 Months</b>	505 (51.3)	252 (55.5)	253 (47.7)	
<b>12–23 Months</b>	323 (32.8)	148 (32.6)	175 (33.0)	
<b>24–59 Months</b>	156 (15.9)	54 (11.9)	102 (19.3)	
<b>Disease Severity in RVA Cases = <i>n</i> (139)</b>				
<b>Mild</b>	12 (8.6)	7 (10.6)	5 (6.8)	0.441
<b>Moderate</b>	50 (36.0)	26 (39.4)	24 (32.9)	
<b>Severe</b>	77 (55.4)	33 (50)	44 (60.3)	
<b>Discharge Outcome = <i>n</i> (982) #</b>				0.556
<b>Alive</b>	925 (94.2)	425 (93.6)	500 (94.7)	
<b>Dead</b>	57 (5.8)	29 (6.4)	28 (5.3)	

SD means standard deviation; IQR means interquartile range; RVA means rotavirus group A. Values given are the counts and percentages are provided in brackets. # Discharge outcome for two subjects was missing. Disease Severity Was Calculated Using the Vesikari Clinical Severity Scoring System Manual [10].

## 2.2. Overall Virus Detection

Of the 984 samples analyzed, at least one of the viruses was detected in 401 samples (40.8%) at the real-time RT-PCR cycle threshold (Ct) value of <35.0. The lower the Ct value, the higher the virus titer in the sample. The detection frequency differed significantly for adenovirus ( $p = 0.001$ ) and sapovirus ( $p < 0.001$ ) pre- and post-rotavirus vaccine introduction when the Ct cut-off value was gradually lowered (<30, <35, <40), unlike for RVA, astrovirus and norovirus GII; see Figure 1. All our subsequent analyses were undertaken at Ct value <35.0 Single infections were detected in 354 specimens (36.0%) and included RVA ( $n = 149$ , 42.1%), adenovirus ( $n = 91$ , 25.7%), norovirus GII ( $n = 75$ , 21.2%), sapovirus ( $n = 20$ , 5.7%) and astrovirus ( $n = 18$ , 5.1%).

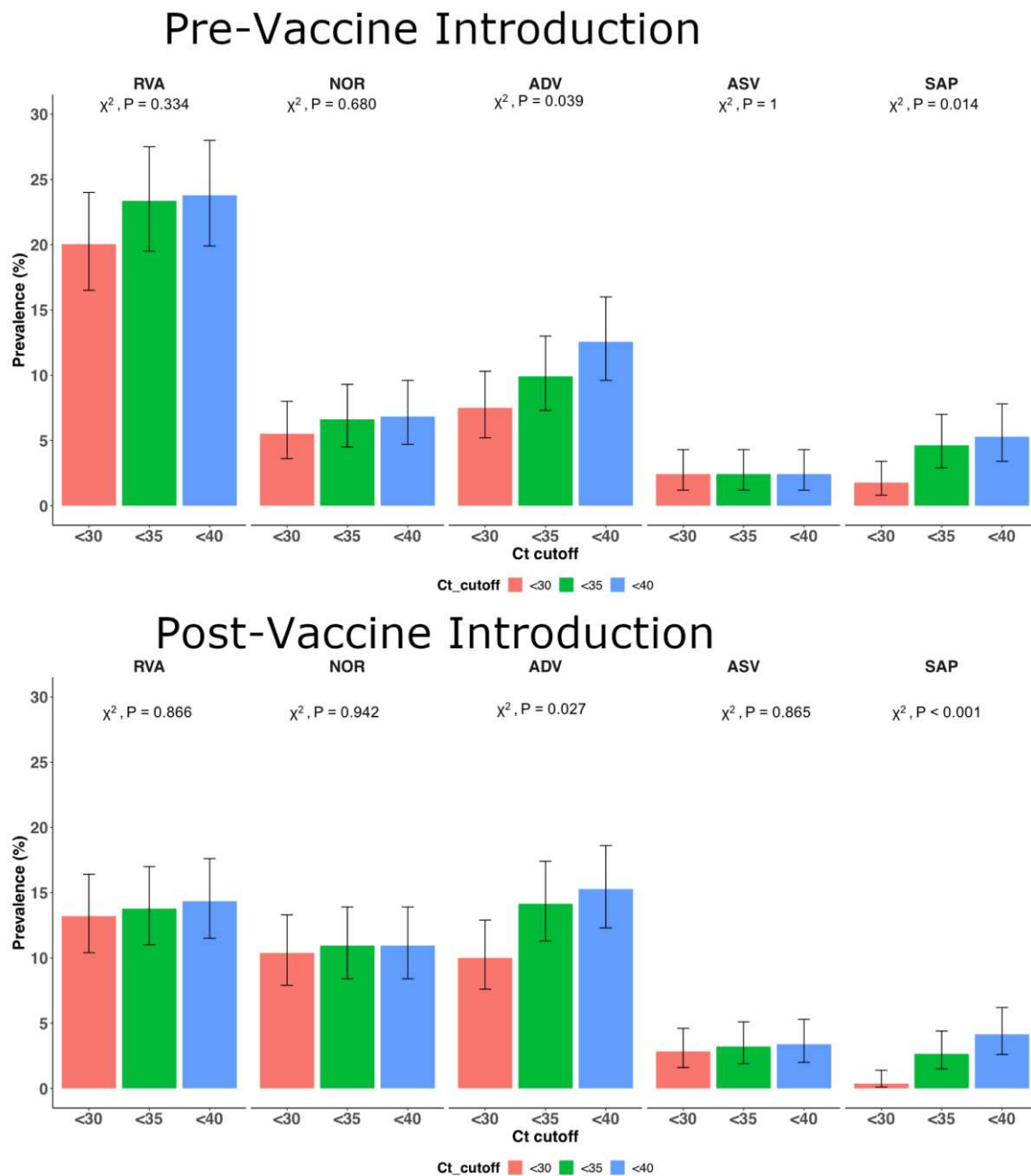


**Figure 1.** Detection frequency of RVA, adenovirus, norovirus GII, astrovirus and sapovirus at different cycle threshold (Ct) cutoffs for children under 5 years of age admitted to KCH Kenya with diarrhea symptoms. The error bars represent 95% confidence interval for the proportions. Proportions were compared using chi-square test. RVA stands for rotavirus group A, ADV stands for adenovirus, NOR stands for norovirus GII, ASV stands for astrovirus and SAP stands for sapovirus.

### 2.3. Patterns Pre-Post Vaccine Introduction

RVA showed a significant decrease (23.3% vs. 13.8%,  $p < 0.001$ ) in prevalence while norovirus GII showed a significant increase (6.6% vs. 10.9%,  $p = 0.02$ ) post-vaccine introduction compared to pre-vaccine introduction; see Table 3. There were no significant changes in the prevalence of astrovirus ( $p = 0.585$ ), adenovirus ( $p = 0.053$ ) and sapovirus ( $p = 0.133$ ) pre- and post-RVA vaccine introduction (chi-squared ( $\chi^2$ ) test); see Table 3. Notably, norovirus GII had a gradual increase in prevalence across the four years, from 6.7% (95% CI: 3.8–10.9%) to 12.4% (95% CI: 8.8–16.7%); see Figure 2. RVA was

the most commonly detected virus across all years, except in year 2019, in which adenovirus had the highest prevalence; see Figure 2.

**Table 3.** Comparison of the prevalence of viral detection in children under 5 years of age admitted to KCH Kenya with diarrhea symptoms pre- and post-rotavirus vaccine introduction.

Viruses Detected	Total	Pre-Vaccine Introduction (%)	Post-Vaccine Introduction (%)	<i>p</i> -Value
<b>Samples Tested</b>	984	454 (46.1)	530 (53.9)	
<b>Rotavirus Group A</b>	179 (18.2)	106 (23.3)	73 (13.8)	<0.001
<b>Adenovirus</b>	120 (12.2)	45 (9.9)	75 (14.2)	0.053
<b>Norovirus GII</b>	88 (8.9)	30 (6.6)	58 (10.9)	0.023
<b>Astrovirus</b>	28 (2.8)	11 (2.4)	17 (3.2)	0.585
<b>Sapovirus</b>	35 (3.6)	21 (4.6)	14 (2.6)	0.133

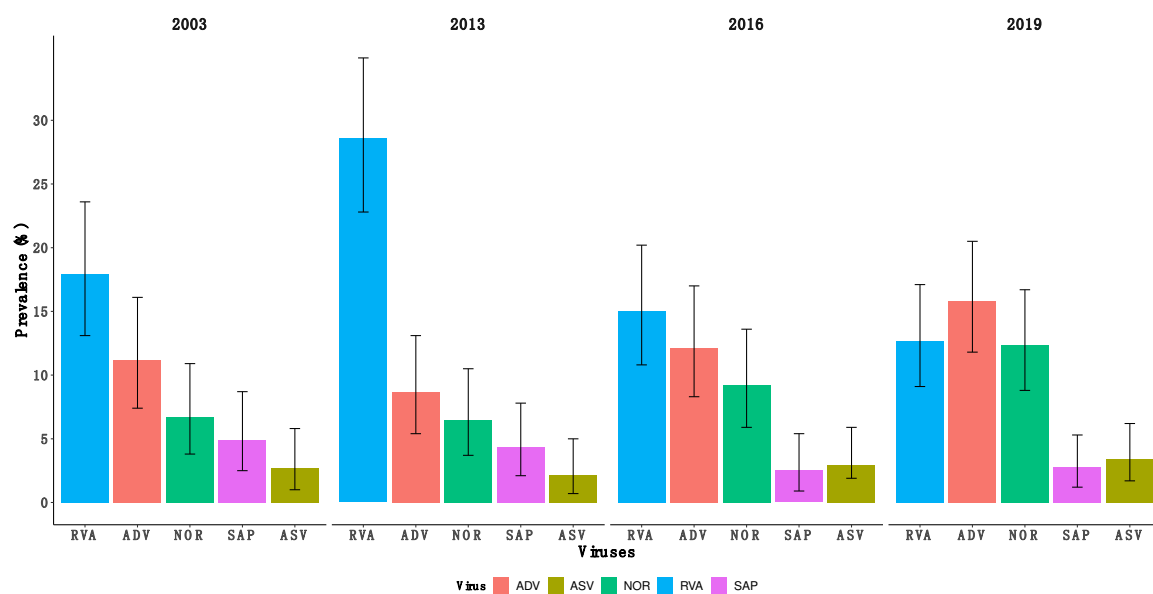


**Figure 2.** Prevalence of RVA, adenovirus, norovirus GII, astrovirus and sapovirus in 2003, 2013, 2016 and 2019 in children under 5 years of age admitted to KCH Kenya with diarrhea symptoms. The error bars represent 95% confidence interval for the proportions. Proportions were compared using chi-square test. Abbreviations used for viruses as in Figure 1.

Notably, RVA and sapovirus cases in the post-vaccine introduction period had statistically significant lower and higher median Ct values, respectively, compared to the pre-vaccine period (Wilcoxon, *p* value < 0.001); see Figure 3. This was not observed for the other three screened viruses pre- and post-rotavirus vaccine introduction. The median age of the RVA positive cases was significantly higher for the post-vaccine introduction period (14.0 months) compared to the pre-vaccine introduction period (10.4 months) (Wilcoxon, *p* < 0.001). A similar shift was not observed for the other viruses; see Figure 4.

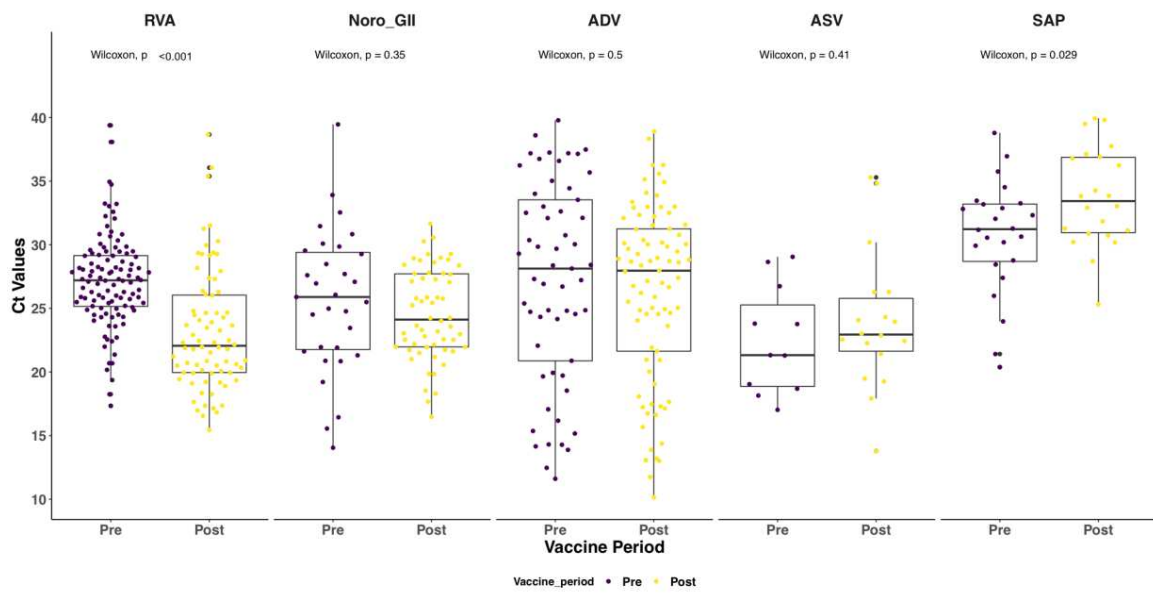


**Figure 3.** Distribution of Ct values among cases under 5 years of age admitted to KCH Kenya with diarrhea symptoms pre- and post-vaccine introduction. RVA stands for rotavirus group A, ADV stands for adenovirus, NOR GII stands for norovirus GII, ASV stands for astrovirus and SAP stands for sapovirus.

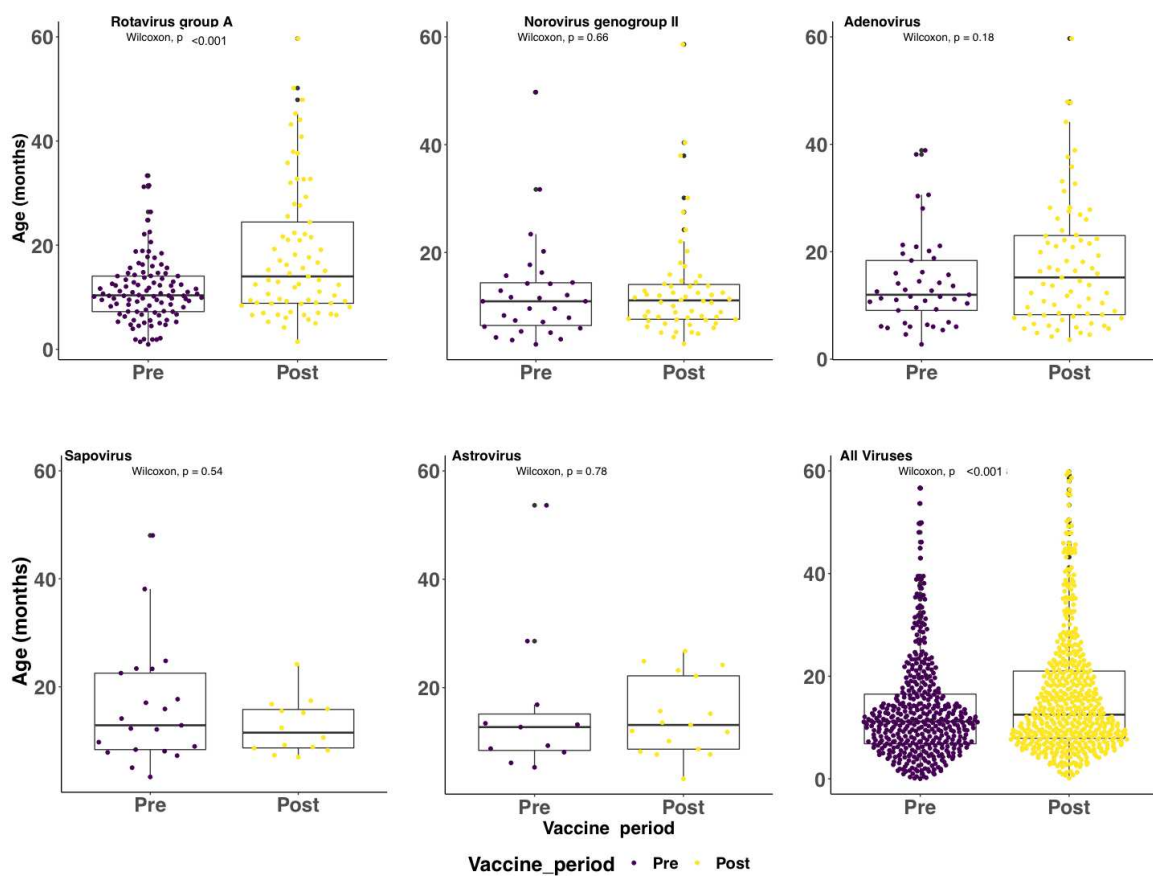


**Figure 4.** Distribution of age in months among cases under 5 years of age admitted to KCH Kenya with diarrhea symptoms pre- and post-vaccine introduction.

#### 2.4. Virus Coinfections (i.e., Two or More Viruses in a Single Specimen)

These were detected in 47 specimens (4.8%). In 583 specimens (59.2%), none of the targeted viruses was detected. The prevalence of coinfections pre-vaccine was 4.4% (95% CI: 2.7–6.7%), while in the post-vaccine introduction period, this value was 5.7% (95% CI: 3.9–8.0%),  $p = 0.454$ . RVA and astrovirus were the most common coinfections in the pre-vaccine introduction period ( $n = 6$ ), while in the post-vaccine introduction period, it was RVA and adenovirus ( $n = 15$ ); see Table 4.

**Table 4.** Coinfections pre- and post-rotavirus vaccine introduction. RVA stands for rotavirus group A, ADV stands for adenovirus, NOR GII stands for norovirus GII, ASV stands for astrovirus and SAP stands for sapovirus.

PATHOGEN COINFECTION	PRE-VACCINE INTRODUCTION	POST-VACCINE INTRODUCTION
RVA & NOR GII	1	2
RVA & ADV	2	15
RVA & ASV	3	0
RVA & SAP	6	1
NOR GII & ADV	3	4
NOR GII & ASV	0	1
NOVGII & SAP	2	1
ADV & ASV	1	3
ADV & SAP	1	1
ASV & SAP	1	2

Abbreviations used for viruses as in Figure 3.

#### 2.5. Circulating RVA Genotypes Pre- and Post-Vaccine Introduction

G1P[8] was the predominant RVA genotype pre vaccine introduction. However, in the post-vaccine introduction period, the predominant genotypes were G2P[4] (2016) and G3P[8] (2019); see Table 5.

**Table 5.** Frequency of RVA genotypes detected in coastal Kenya pre- (2003 and 2013) and post- (2016 and 2019) vaccine introduction.

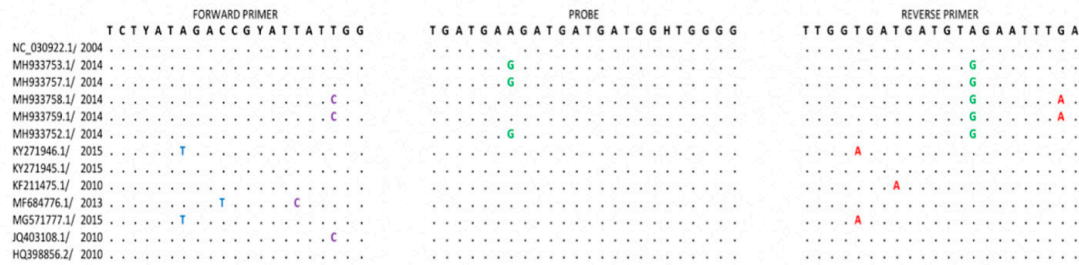
Year	2003		2013		2016		2019	
	No. of Cases	%						
<b>RVA Positive</b>	40		66		36		37	
<b>Genotyped</b>	2	5.0	48	72.7	34	94.4	36	97.3
<b>Genotypes</b>								
G1P[8]	1	50.0	43	89.6	5	14.7	1	2.8
G2P[4]	-	-	2	4.2	29	85.3	-	-
G3P[8]	-	-	1	2.1	-	-	34	94.4
G9P[8]	1	50.0	1	2.1	-	-	-	-
G10P[8]	-	-	1	2.1	-	-	-	-
G8P[8]	-	-	-	-	-	-	1	2.8

#### 2.6. Seasonality of the Detected Viruses

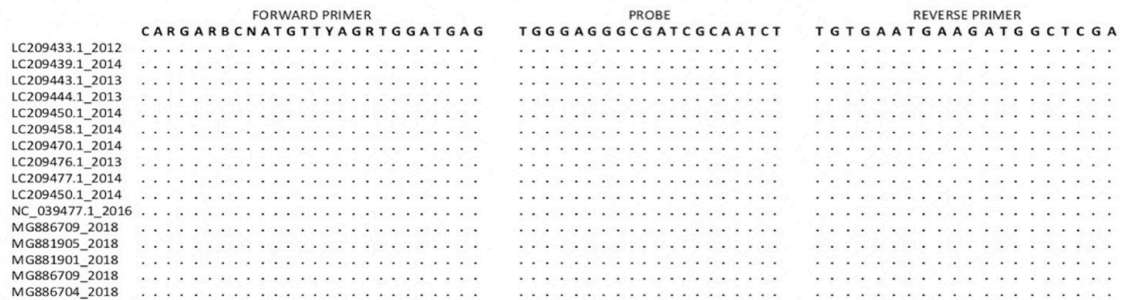
We constrained this analysis to the years 2013, 2016 and 2019, where >70% of the eligible patients had been analyzed. Pre-vaccine introduction (in 2013), for RVA, there were two peak months, in June and September. However, post-vaccine introduction (in 2016 and 2019), there was only a single peak month for RVA in September and August, respectively. For norovirus GII, cases were observed throughout the year, with peak months varying from year-to-year, in July, April and June in 2013, 2016 and 2019, respectively. Similarly, adenovirus cases appeared to occur throughout the year, with two peak months in 2013 (June and September) and one peak month in 2016 and 2019 (August for both). For sapovirus and astrovirus, we observed less than five cases monthly between January and August and no cases in the last quarter of each the three years; see Figure 5.



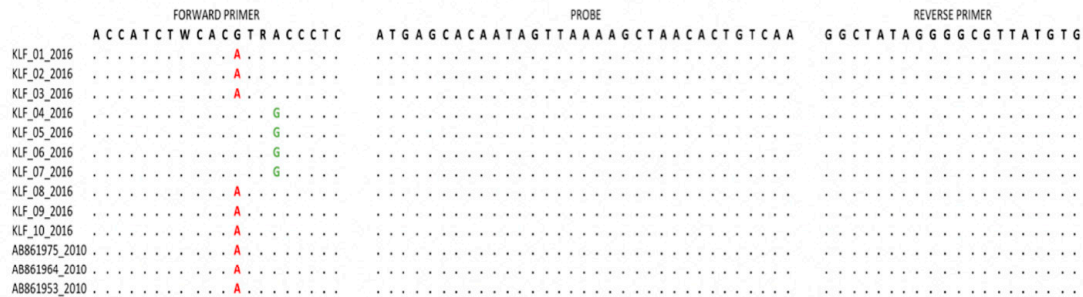
## Astrovirus



## Norovirus GII



## Rotavirus group A



## Sapovirus

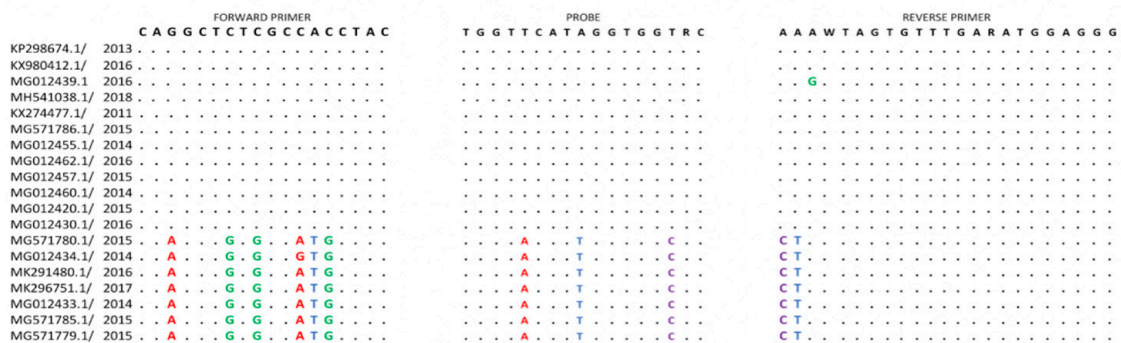


**Figure 6.** The primers and probes target sites for RVA, adenovirus and norovirus GII, sapovirus and astrovirus were aligned using MAFFT v.7.31313 and the alignments were trimmed to the region of the primer and probe target sites. Nucleotide differences between the expected primer and probe target sites and the viral sequences were identified and highlighted. Dots indicate identity with primer or probe sequences.

### 3. Discussion

We observed a significant decrease in the prevalence of RVA in the post-vaccine introduction period in KCH, concurring with findings of a recent multi-site study in Kenya that reported RVA vaccine effectiveness of ~64% (95% CI: 35–80%) and a reduction in rotavirus-associated hospital admissions two years post-vaccine introduction of ~80% (95% CI: 46–93%) [9,11]. Note that Kenya rotavirus vaccine coverage was considered medium in 2018 (70–79%) [12]. Our pre- and post-vaccine introduction analysis observed a significant increase in the prevalence of norovirus GII in KCH post-rotavirus vaccine introduction, as similarly observed in the United States, Nicaragua and Bolivia following RVA vaccine introduction [13–15]. It is unclear if this has been driven by an established biological interaction between these two viruses or that this reflects natural norovirus GII fluctuation in prevalence across multiple years.

The shift in the predominant genotypes pre- and post-vaccine introduction from G1P[8] to G2P[4] in 2016 and G3P[8] in 2019 in our setting has also been described elsewhere, e.g., in Belgium, Madagascar and Ethiopia [16–18]. G3P[8] was the predominant genotype in this setting in 2018 [19] and it continued being the dominant genotype in 2019. Although these dominant post-vaccine genotypes are either partially or fully heterotypic to the Rotarix G1P[8] strain, in their surface exposed immunodominant proteins, there is not enough evidence yet to directly attribute their increased incidence to vaccine introduction [20]. Additional analysis will help to bring better understanding on the reason behind their dominance.

Despite RV vaccine introduction in Kilifi, Kenya, no significant difference was observed in the discharge outcome for all causes of diarrhea pre- and post-rotavirus vaccine introduction. We suggest two explanations for this. Firstly, the majority of the children who were eligible to be in this study and died did not have a sample collected to determine their RVA and other enteric pathogens' status. Secondly, inpatient mortality of children treated for diarrhea in Kilifi County Hospital has been previously found to be predicted by a positive HIV test, bacteremia and poor nutritional status [21]. This may have not changed pre- or post-introduction of rotavirus vaccination.

RVA Ct values were decreased in post-vaccine samples compared to pre-vaccination years. This was despite RVA disease severity remaining unchanged between the two periods. Different extraction methods were used to process the samples between 2003, 2013 and 2016, 2019. However, according to Liu et al., the difference in the extraction methods for enteric pathogen studies is not significant, except for norovirus GII, which showed a higher Ct value with kits targeting RNA purification alone compared to those targeting total nucleic acid (TNA) (difference within 1 Ct value). Different extraction kits were used in this study because raw stool samples from 2003 to 2016 were already destroyed following a directive by the WHO in 2016 that was part of the larger global polio eradication effort.

It has been previously noted the introduction to rotavirus vaccines may result in the shift of diarrhea disease burden to slightly older age groups [20]. Our study found a significant increase in the median age of diarrhea cases post-vaccine introduction (12.5 months) compared 11.2 months pre-introduction. This in part may be explained by the higher immunity at both individual and population levels against rotavirus that wanes as children grow older.

On local seasonality patterns, in each year, a peak month(s) of occurrence was observed for RVA, norovirus GII, sapovirus and adenovirus but not astrovirus. The Kilifi area has a tropical climate with two rainy seasons; the main rains usually peak in May (up to July) while the short rains usually peak in November (can run from October to December). RVA and adenovirus appeared to peak in the dry months while norovirus GII and sapovirus peaked in the rainy season. Similar patterns in the seasonality of RVA, adenovirus, norovirus GII and sapovirus have been observed elsewhere [22–25]. The seasonality of astrovirus is not well described.

The performance of qPCR assays can be impacted by mismatches within the last five bases at the 3' end of primers and probe or/and the number of mismatches being more than five in the primers and probe [26,27]. The mismatches observed in the primer and probe binding sites of adenovirus,

astrovirus and sapovirus may have impaired the real-time PCR function by blocking the amplification or increasing the quantification cycles. Consequently, this may have impacted the estimated frequency of detection of these viruses. Unlike for RVA, the magnitude of the mismatches in qPCR function could have been shown better using recent local sequences of the other viruses.

This study had limitations: firstly, we did not analyze healthy children in the community to inform on the background prevalence of the five viruses in our study population. Secondly, the adenovirus assay was not specific to type 40/41 alone; thus, some of the adenoviruses detected may not be associated with diarrhea. Thirdly, a significant number of eligible cases were not sampled, including those who died before sampling. This potentially biased prevalence of the screened pathogens in the study population. Fourthly, extracting TNA from samples after many years of storage could lead to lower Ct values due to deterioration. Finally, the seasonality of examined pathogens will be best described if we examine more years.

In conclusion, we found a significant decline in the prevalence of rotavirus in hospitalized children in coastal Kenya after rotavirus vaccine introduction. This finding reinforces evidence of the continued benefit of rotavirus vaccination in this setting. Concomitantly, there has been a surge in norovirus GII prevalence, but the factors driving this increase are unclear and will require future investigation. The observation that the screened viruses peak at different times of the year also would benefit further investigation in order to understand drivers of their transmission and inform the design of effective intervention measures.

## **4. Materials and Methods**

### *4.1. Study Site and Population*

This study was undertaken at KCH, a referral hospital serving the Kilifi County population, which is majorly a rural population. We utilized stool specimens collected during routine surveillance of rotavirus in children with diarrhea as one of their illness symptoms, aged below five years and admitted to KCH [9,11]. Diarrhea was defined as observation of three or more loose stools in the preceding 24-h period. In this study, we selected two pre-vaccine years (2003 and 2013) and two post-vaccine years (2016 and 2019) for analysis. A stool specimen was collected from children who met the diarrhea case-definition following parental or guardian consent. The study protocol was approved by the Scientific and Ethics Review Unit (SSC#2861 and SERU#CGMRC/113/3624) based at KEMRI, Nairobi, Kenya.

### *4.2. Laboratory Methods*

Irrespective of their previously determined rotavirus status, TNA were extracted from 0.2 g of 2003 and 2013 specimens (or 200  $\mu$ L if liquid) using the cadon Pathogen 96 QIAcube HT Kit (Qiagen, Manchester, UK). For 2016 and 2019 specimens, TNA were extracted using QIAamp Fast DNA Stool Mini kit (Qiagen, Manchester, UK) as per the manufacturer's instructions. Fecal specimens from the post-vaccine period (0.2 mg or 200  $\mu$ L) were subjected to bead beating prior to TNA extraction and collected in a 200  $\mu$ L of elution buffer [28].

The TNA extracts were screened for the five viruses by a two-step real-time RT-PCR assay [29]. First, cDNA was synthesized in a total volume of 20  $\mu$ L using random hexamers and 5  $\mu$ L of TNA using the Omniscript Reverse Transcriptase kit (Qiagen, Manchester, UK), as per the manufacturer's instructions. Two  $\mu$ L of the cDNA was henceforth used for real-time RT-PCR in a total volume of 20  $\mu$ L using the QuantiFast RT-PCR Kit (Qiagen, Manchester, UK) and run on the ABI 7500 Real-Time PCR System (Applied Biosystems, Foster City, CA, USA). Primers and probes were adopted from previously published work [30]. The presence of nucleotide mismatches in the primer and probe binding sites was investigated by aligning the primers/probes to genomic sequences deposited in GenBank from 2010 to 2019, using MAFFT v.7.313 [31]. The adenovirus probe/primer pair used in this study detected adenovirus serotypes beyond type 40/41. We used three Ct cut-off values (<40.0, <35.0

and <30.0) to define positive samples. Samples that were positive for RVA in 2003, 2013, 2016 and 2019 were processed for RVA genotyping using VP4 and VP7 RT-PCR, followed by either dideoxy sanger sequencing, as described elsewhere [19], or next-generation sequencing on the Illumina Miseq platform [32].

#### 4.3. Statistical Analysis

All statistical analyses were performed using R version 3.6.1 [33]. Prevalence was defined as the proportion of these viruses in a hospital-admitted diarrhea patient population during the study period in Kilifi, Kenya. Means and medians of continuous variables were compared using a Kruskal Wallis and Wilcoxon rank-sum test, respectively. Binary data were summarized using proportions and comparisons between groups made using  $\chi^2$  statistics. A *p* value of <0.05 was considered statistically significant. Diarrhea severity in RVA positive cases pre- (year 2013) and post- (years 2016 and 2019) was assessed using the Vesikari Clinical Severity Scoring System Manual [10], with a modification in the treatment parameter. If the participant was given oral rehydration therapy or intravenous fluid therapy, they received a score of one or two, respectively.

**Author Contributions:** Conceptualization, A.W.L. and C.N.A.; methodology, A.W.L. and C.N.A.; formal analysis, A.W.L., N.M. and C.N.A.; investigation, A.W.L., S.O., C.S.L. and C.N.A.; resources, D.J.N. and C.N.A.; data curation, A.W.L. and N.M.; writing—original draft preparation, A.W.L.; writing—review and editing, A.W.L., S.O., N.M., C.S.L., S.G.N. and C.N.A.; visualization, A.W.L. supervision, S.G.N. and C.N.A., project administration, C.N.A.; funding acquisition, C.N.A. All authors have read and agreed to the published version of the manuscript.

**Funding:** This study was funded by the Wellcome Trust (102975,203077) The authors Arnold Lambisa, Sylvia Onchaga and Charles Agoti were supported by the Initiative to Develop African Research Leaders (IDeAL) through the DELTAS Africa Initiative (DEL-15-003). The DELTAS Africa Initiative is an independent funding scheme of the African Academy of Sciences (AAS)'s Alliance for Accelerating Excellence in Science in Africa (AESA) and supported by the New Partnership for Africa's Development Planning and Coordinating Agency (NEPAD Agency) with funding from the Wellcome Trust (107769/Z/10/Z) and the UK government. The views expressed in this publication are those of the authors and not necessarily those of AAS, NEPAD Agency, Wellcome Trust or the UK government. This paper is published with the permission of the Director of KEMRI.

**Acknowledgments:** We thank all the study participants for their contribution of study samples, their parents/guardians, members of the viral epidemiology and control research group (<http://virec-group.org/>) and colleagues at the KEMRI Wellcome Trust Research Programme for their useful discussions during the preparation of the manuscript. We are grateful to James Nokes of KEMRI-Wellcome Trust for his comments and suggestions on the presentation of this work This paper is published with the permission of the Director of KEMRI.

**Conflicts of Interest:** The authors declare no conflict of interest.

#### References

1. Troeger, C.; Blacker, B.F.; Khalil, I.A.; Rao, P.C.; Cao, S.; Zimsen, S.R.; Albertson, S.B.; Stanaway, J.D.; Deshpande, A.; Abebe, Z.; et al. Estimates of the global, regional, and national morbidity, mortality, and aetiologies of diarrhoea in 195 countries: A systematic analysis for the Global Burden of Disease Study 2016. *Lancet Infect. Dis.* **2018**, *18*, 1211–1228. [CrossRef]
2. Platts-Mills, J.A.; Liu, J.; Rogawski, E.T.; Kabir, F.; Lertsethtakarn, P.; Sigvas, M.; Khan, S.S.; Praharaj, I.; Murei, A.; Nshama, R.; et al. Use of quantitative molecular diagnostic methods to assess the aetiology, burden, and clinical characteristics of diarrhoea in children in low-resource settings: A reanalysis of the MAL-ED cohort study. *Lancet Glob. Health* **2018**, *6*, e1309–e1318. [CrossRef]
3. Liu, J.; Platts-Mills, J.A.; Juma, J.; Kabir, F.; Nkeze, J.; Okoi, C.; Operario, D.J.; Uddin, J.; Ahmed, S.; Alonso, P.L.; et al. Use of quantitative molecular diagnostic methods to identify causes of diarrhoea in children: A reanalysis of the GEMS case-control study. *Lancet* **2016**. [CrossRef]
4. Aliabadi, N.; Antoni, S.; Mwenda, J.M.; Weldegebriel, G.; Biey, J.N.M.; Cheikh, D.; Fahmy, K.; Teleb, N.; Ashmony, H.A.; Ahmed, H.; et al. Global impact of rotavirus vaccine introduction on rotavirus hospitalisations among children under 5 years of age, 2008–2016: Findings from the Global Rotavirus Surveillance Network. *Lancet Glob. Health* **2019**, *7*, e893–e903. [CrossRef]

5. Yu, W.J.; Chen, S.Y.; Tsai, C.N.; Chao, H.C.; Kong, M.S.; Chang, Y.J.; Chiu, C.H. Long-term impact of suboptimal rotavirus vaccines on acute gastroenteritis in hospitalized children in Northern Taiwan. *J. Formos. Med. Assoc.* **2018**, *117*, 720–726. [CrossRef] [PubMed]
6. Muhsen, K.; Kassem, E.; Rubenstein, U.; Goren, S.; Ephros, M.; Shulman, L.M.; Cohen, D. No evidence of an increase in the incidence of norovirus gastroenteritis hospitalizations in young children after the introduction of universal rotavirus immunization in Israel. *Hum. Vaccines Immunother.* **2019**, *15*, 1284–1293. [CrossRef]
7. Halasa, N.; Piya, B.; Stewart, L.S.; Rahman, H.; Payne, D.C.; Woron, A.; Thomas, L.; Constantine-Renna, L.; Garman, K.; McHenry, R.; et al. The Changing Landscape of Pediatric Viral Enteropathogens in the Post-Rotavirus Vaccine Era. *Clin. Infect. Dis.* **2020**, *53*, 1689–1699. [CrossRef]
8. Wandera, E.A.; Mohammad, S.; Ouko, J.O.; Yatitch, J.; Taniguchi, K.; Ichinose, Y. Variation in rotavirus vaccine coverage by sub-counties in Kenya. *Trop. Med. Health* **2017**. [CrossRef]
9. Otiemo, G.P.; Bottomley, C.; Khagayi, S.; Adetifa, I.; Ngama, M.; Omoro, R.; Ogwel, B.; Owor, B.E.; Bigogo, G.; Ochieng, J.B.; et al. Impact of the Introduction of Rotavirus Vaccine on Hospital Admissions for Diarrhea Among Children in Kenya: A Controlled Interrupted Time-Series Analysis. *Clin. Infect. Dis.* **2019**, 1–8. [CrossRef]
10. Lewis, K. Vesikari Clinical Severity Scoring System Manual. Path. 2011, pp. 1–50. Available online: [https://www.path.org/publications/files/VAD\\_vesikari\\_scoring\\_manual.pdf](https://www.path.org/publications/files/VAD_vesikari_scoring_manual.pdf) (accessed on 22 July 2020).
11. Khagayi, S.; Omoro, R.; Otiemo, G.P.; Ogwel, B.; Ochieng, J.B.; Juma, J.; Apondi, E.; Bigogo, G.; Onyango, C.; Ngama, M.; et al. Effectiveness of monovalent rotavirus vaccine against hospitalization with acute rotavirus gastroenteritis in Kenyan children. *Clin. Infect. Dis.* **2020**, *70*, 2298–2305. [CrossRef]
12. VIEW-hub, International Vaccine Access Center (IVAC), Johns Hopkins Bloomberg School of Public Health. Available online: <https://view-hub.org/map/?set=wuenic-coverage&group=vaccine-coverage&category=rv> (accessed on 31 July 2020).
13. Bucardo, F.; Reyes, Y.; Svensson, L.; Nordgren, J. Predominance of norovirus and sapovirus in nicaragua after implementation of universal rotavirus vaccination. *PLoS ONE* **2014**, *9*, e98201. [CrossRef] [PubMed]
14. McAtee, C.L.; Webman, R.; Gilman, R.H.; Mejia, C.; Bern, C.; Apaza, S.; Espetia, S.; Pajuelo, M.; Saito, M.; Challappa, R.; et al. Burden of norovirus and rotavirus in children after rotavirus vaccine introduction, Cochabamba, Bolivia. *Am. Trop. Med. Hyg.* **2016**. [CrossRef] [PubMed]
15. Payne, D.C.; Vinjé, J.; Szilagyi, P.G.; Edwards, K.M.; Staat, M.A.; Weinberg, G.A.; Hall, C.B.; Chappell, J.; Bernstein, D.I.; Curns, A.T.; et al. Norovirus and medically attended gastroenteritis in US children. *N. Engl. J. Med.* **2013**. [CrossRef] [PubMed]
16. Gelaw, A.; Pietsch, C.; Liebert, U.G. Molecular epidemiology of rotaviruses in Northwest Ethiopia after national vaccine introduction. *Infect. Genet. Evol.* **2018**. [CrossRef] [PubMed]
17. Rahajamanana, V.L.; Raboba, J.L.; Rakotozanany, A.; Razafindraibe, N.J.; Andriatahirintsoa, E.J.P.R.; Razafindrakoto, A.C.; Mioramalala, S.A.; Razaiarimanga, C.; Weldegebriel, G.G.; Burnett, E.; et al. Impact of rotavirus vaccine on all-cause diarrhea and rotavirus hospitalizations in Madagascar. *Vaccine* **2018**. [CrossRef] [PubMed]
18. Zeller, M.; Rahman, M.; Heylen, E.; De Coster, S.; De Vos, S.; Arijs, I.; Novo, L.; Verstoppen, N.; Van Ranst, M.; Matthijssens, J. Rotavirus incidence and genotype distribution before and after national rotavirus vaccine introduction in Belgium. *Vaccine* **2010**. [CrossRef]
19. Mwangi, M.J.; Owor, B.E.; Ochieng, J.B.; Ngama, M.H.; Ogwel, B.; Onyango, C.; Juma, J.; Njeru, R.; Gicheru, E.; Otiemo, G.P.; et al. Rotavirus group A genotype circulation patterns across Kenya before and after nationwide vaccine introduction, 2010–2018. *BMC Infect. Dis.* **2020**, *20*, 504. [CrossRef]
20. Pitzer, V.E.; Bilcke, J.; Heylen, E.; Crawford, F.W.; Callens, M.; De Smet, F.; Van Ranst, M.; Zeller, M.; Matthijssens, J. Did Large-Scale Vaccination Drive Changes in the Circulating Rotavirus Population in Belgium? *Sci. Rep.* **2015**, *5*, 1–14. [CrossRef]
21. Talbert, A.; Ngari, M.; Bauni, E.; Mwangome, M.; Mturi, N.; Otiemo, M.; Maitland, K.; Walson, J.; Berkley, J.A. Mortality after inpatient treatment for diarrhea in children: A cohort study. *BMC Med.* **2019**. [CrossRef]
22. Ahmed, S.M.; Lopman, B.A.; Levy, K. A Systematic Review and Meta-Analysis of the Global Seasonality of Norovirus. *PLoS ONE* **2013**, *8*, e75922. [CrossRef]
23. Dey, S.K.; Phathamavong, O.; Nguyen, T.D.; Thongprachum, A.; Chan-It, W.; Okitsu, S.; Mizuguchi, M.; Ushijima, H. Seasonal pattern and genotype distribution of sapovirus infection in Japan, 2003–2009. *Epidemiol. Infect.* **2012**, *140*, 74–77. [CrossRef] [PubMed]

24. Omore, R.; Tate, J.E.; O'Reilly, C.E.; Ayers, T.; Williamson, J.; Moke, F.; Schilling, K.A.; Awuor, A.O.; Jaron, P.; Ochieng, J.B.; et al. Epidemiology, seasonality and factors associated with rotavirus infection among children with moderate-to-severe diarrhea in rural western Kenya, 2008–2012: The Global Enteric Multicenter Study (GEMS). *PLoS ONE* **2016**, *11*, e0160060. [CrossRef] [PubMed]
25. Vetter, M.R.; Staggemeier, R.; Vecchia, A.D.; Henzel, A.; Rigotto, C.; Spilki, F.R. Seasonal variation on the presence of adenoviruses in stools from non-diarrheic patients. *Braz. J. Microbiol.* **2015**, *46*, 749–752. [CrossRef] [PubMed]
26. Stadhouders, R.; Pas, S.D.; Anber, J.; Voermans, J.; Mes, T.H.; Schutten, M. The effect of primer-template mismatches on the detection and quantification of nucleic acids using the 5' nuclease assay. *Mol. Diagn.* **2010**, *12*, 109–117. [CrossRef]
27. Lefever, S.; Pattyn, F.; Hellemans, J.; Vandesompele, J. Single-nucleotide polymorphisms and other mismatches reduce performance of quantitative PCR assays. *Clin. Chem.* **2013**, *59*, 1470–1480. [CrossRef]
28. Liu, J.; Gratz, J.; Amour, C.; Nshama, R.; Walongo, T.; Maro, A.; Mduma, E.; Platts-Mills, J.; Boisen, N.; Nataro, J.; et al. Optimization of quantitative PCR methods for enteropathogen detection. *PLoS ONE* **2016**, *11*, e0158199. [CrossRef]
29. Bennett, S.; Gunson, R.N. The development of a multiplex real-time RT-PCR for the detection of adenovirus, astrovirus, rotavirus and sapovirus from stool samples. *Viol. Methods* **2017**, *242*, 30–34. [CrossRef]
30. Van Maarseveen, N.M.; Wessels, E.; de Brouwer, C.S.; Vossen, A.C.; Claas, E.C. Diagnosis of viral gastroenteritis by simultaneous detection of Adenovirus group F, Astrovirus, Rotavirus group A, Norovirus genogroups I and II, and Sapovirus in two internally controlled multiplex real-time PCR assays. *Clin. Virol.* **2010**. [CrossRef]
31. Katoh, K.; Standley, D.M. MAFFT multiple sequence alignment software version 7: Improvements in performance and usability. *Mol. Biol. Evol.* **2013**. [CrossRef]
32. Magagula, N.B.; Esona, M.D.; Nyaga, M.M.; Stucker, K.M.; Halpin, R.A.; Stockwell, T.B.; Seheri, M.L.; Steele, A.D.; Wentworth, D.E.; Mphahlele, M.J. Whole genome analyses of G1P[8] rotavirus strains from vaccinated and non-vaccinated South African children presenting with diarrhea. *Med. Virol.* **2015**, *87*, 79–101. [CrossRef]
33. R Core Team. *R: A Language and Environment for Statistical Computing*; R Foundation for Statistical Computing: Vienna, Austria, 2019. Available online: <https://www.R-project.org/> (accessed on 22 October 2019).



© 2020 by the authors. Licensee MDPI, Basel, Switzerland. This article is an open access article distributed under the terms and conditions of the Creative Commons Attribution (CC BY) license (<http://creativecommons.org/licenses/by/4.0/>).

## Article

# Genotype Diversity before and after the Introduction of a Rotavirus Vaccine into the National Immunisation Program in Fiji

Sarah Thomas<sup>1,\*</sup>, Celeste M. Donato<sup>1,2</sup> , Sokoveti Covea<sup>3</sup>, Felisita T. Ratu<sup>3</sup>, Adam W. J. Jenney<sup>4,5,6</sup>, Rita Reyburn<sup>4,6</sup>, Aalisha Sahu Khan<sup>3</sup>, Eric Rafai<sup>3</sup>, Varja Grabovac<sup>7</sup>, Fatima Serhan<sup>8</sup>, Julie E. Bines<sup>1,2,9,†</sup>  and Fiona M. Russell<sup>4,6,†</sup>

- <sup>1</sup> Enteric Diseases Group, Murdoch Children's Research Institute, Parkville, VIC 3052, Australia; celeste.donato@mcri.edu.au (C.M.D.); jebines@unimelb.edu.au (J.E.B.)
- <sup>2</sup> Department of Paediatrics, The University of Melbourne, Parkville, VIC 3052, Australia
- <sup>3</sup> Ministry of Health and Medical Services, Suva, Fiji; soccovea@gmail.com (S.C.); tupou.ratu@gmail.com (F.T.R.); aalisha@gmail.com (A.S.K.); eric.rafaigovnet.gov.fj (E.R.)
- <sup>4</sup> Asia-Pacific Health Group, Murdoch Children's Research Institute, Parkville, VIC 3052, Australia; jenneya@unimelb.edu.au (A.W.J.J.); buaha@gmail.com (R.R.); fmruss@unimelb.edu.au (F.M.R.)
- <sup>5</sup> College of Medicine, Nursing and Health Sciences, Fiji National University, Suva, Fiji
- <sup>6</sup> Centre for International Child Health, Department of Paediatrics, The University of Melbourne, Parkville, VIC 3052, Australia
- <sup>7</sup> Western Pacific Regional Office, World Health Organization, Manila 1000, Philippines; grabovacv@who.int
- <sup>8</sup> World Health Organization, 1202 Geneva, Switzerland; serhanfa@who.int
- <sup>9</sup> Department of Gastroenterology and Clinical Nutrition, Royal Children's Hospital, Parkville, VIC 3052, Australia
- \* Correspondence: sarah.thomas@mcri.edu.au; Tel.: +61-3-8341-6451
- † These authors contributed equally.



**Citation:** Thomas, S.; Donato, C.M.; Covea, S.; Ratu, F.T.; Jenney, A.W.J.; Reyburn, R.; Sahu Khan, A.; Rafai, E.; Grabovac, V.; Serhan, F.; et al. Genotype Diversity before and after the Introduction of a Rotavirus Vaccine into the National Immunisation Program in Fiji. *Pathogens* **2021**, *10*, 358. <https://doi.org/10.3390/pathogens10030358>

Academic Editor: Thirumalaisamy P. Velavan

Received: 8 February 2021  
Accepted: 12 March 2021  
Published: 17 March 2021

**Publisher's Note:** MDPI stays neutral with regard to jurisdictional claims in published maps and institutional affiliations.



**Copyright:** © 2021 by the authors. Licensee MDPI, Basel, Switzerland. This article is an open access article distributed under the terms and conditions of the Creative Commons Attribution (CC BY) license (<https://creativecommons.org/licenses/by/4.0/>).

**Abstract:** The introduction of the rotavirus vaccine, Rotarix, into the Fiji National Immunisation Program in 2012 has reduced the burden of rotavirus disease and hospitalisations in children less than 5 years of age. The aim of this study was to describe the pattern of rotavirus genotype diversity from 2005 to 2018; to investigate changes following the introduction of the rotavirus vaccine in Fiji. Faecal samples from children less than 5 years with acute diarrhoea between 2005 to 2018 were analysed at the WHO Rotavirus Regional Reference Laboratory at the Murdoch Children's Research Institute, Melbourne, Australia, and positive samples were serotyped by EIA (2005–2006) or genotyped by heminested RT-PCR (2007 onwards). We observed a transient increase in the zoonotic strain equine-like G3P[8] in the initial period following vaccine introduction. G1P[8] and G2P[4], dominant genotypes prior to vaccine introduction, have not been detected since 2015 and 2014, respectively. A decrease in rotavirus genotypes G2P[8], G3P[6], G8P[8] and G9P[8] was also observed following vaccine introduction. Monitoring the rotavirus genotypes that cause diarrhoeal disease in children in Fiji is important to ensure that the rotavirus vaccine will continue to be protective and to enable early detection of new vaccine escape strains if this occurs.

**Keywords:** rotavirus; Fiji; Rotarix; genotype; equine-like G3P[8]

## 1. Introduction

Rotavirus is the most common cause of severe diarrhoea in children under 5 years of age worldwide. In 2016, rotavirus was responsible for 258 million episodes of diarrhoea and was attributed to ~128,500 deaths in children under 5 years, with the majority occurring in countries in Asia and Africa [1]. Genotyping of rotavirus strains underpins global rotavirus surveillance. The binomial classification of rotavirus genotypes is based on the outer capsid proteins VP7 and VP4 that define G and P genotypes, respectively [2]. There are 36 G

types and 51 P types described in humans and various animal species to date; however, the most common rotavirus genotypes observed in humans are the VP7 genotypes: G1, G2, G3, G4 and G9 and the VP4 genotypes: P[4] and P[8], representing three quarters of all genotypes causing human disease [3,4]. Previously uncommon genotypes including G12 and equine-like G3P[8] genotypes are increasingly being identified as a cause of rotavirus disease globally [5,6].

Fiji is a Pacific Island Nation with a population of approximately 837,271 [7]. Although designated as an upper middle-income country, it was estimated that prior to the COVID-19 pandemic, 24% of the population were living in poverty [7]. The child under-5-year mortality rate in Fiji was reported as 25.7 deaths per 1000 live births in 2019 [8]. Rotavirus was a major cause of diarrhoea-related hospitalisations in Fiji prior to rotavirus vaccine introduction, detected in 52% (2006) and 60% (2007) of children less than 5 years hospitalised with acute diarrhoea, with an annual incidence estimated at 486 per 100,000 children less than 5 years [9]. Due to this burden of rotavirus gastroenteritis, Fiji introduced a rotavirus vaccine (Rotarix, GlaxoSmithKline, Belgium) into the National Immunisation Program in October 2012. Rotarix is a monovalent vaccine containing a single, human, G1P[8] strain that is administered in a two-dose schedule at 6 and 14 weeks of age. The uptake of Rotarix in Fiji was prompt, reaching 85% coverage by 2013 and 99% coverage in eligible infants from 2014 onward [10]. The introduction of rotavirus vaccines in Fiji has been highly successfully resulting in an 82% reduction in rotavirus diarrhoea related hospitalisations in children less than 5 years of age [11].

The aim of this study was to describe the pattern of rotavirus genotype diversity from 2005 to 2018, specifically to describe any changes in genotype patterns that may have occurred following the introduction of the rotavirus vaccine in Fiji in 2012.

## 2. Results

### 2.1. Study Samples

During the study period 2005–2018, a total of 1504 stool samples was collected and sent to the WHO Rotavirus Regional Reference Laboratory (RRL) at the Murdoch Children’s Research Institute (MCRI). Of these, 1208 samples had sufficient data available on the date of collection and stool volume to enable analysis. Of the 1208 samples, a total of 576 were confirmed as rotavirus positive and proceeded to genotype characterisation (Figure 1). Thirty-four samples were not genotyped due to laboratory error, comprising 1 sample from 2010 and 33 samples from 2011, and were subsequently excluded from further analysis. The remaining 542 samples were proceeded with for further analysis (Figure 1).

### 2.2. Genotype Distribution and the Impact of Vaccine Introduction

In the pre-vaccine period (2005–2012), 58% (479/827) of samples received were confirmed as rotavirus positive, compared to only 18% (63/347) of samples in the post-vaccine era (2013–2018) (Table 1). These values may be affected by sampling changes over the study period. Between 2005 and 2009, only positive samples were received; between 2010 and 2016, all positive and negative samples were received; and from 2017 onward, all positive and 10% of all negatives were sent to MCRI. Overall, between 2005–2018, G1P[8] was the most commonly detected genotype ( $n = 157$ , 29%), with both G2P[4] ( $n = 155$ , 29%) and G3P[8] ( $n = 144$ , 27%) detected at similar frequencies, followed by G12P[8] ( $n = 33$ , 6%) (Table 1). Other genotypes including G2P[8], G3P[6], G8P[8], G9P[8] and G12P[4] as well as mixed or partially typed samples were infrequently detected ( $n = 1–5$ , 0.2–3%). However, marked differences were observed following vaccine introduction. Prior to vaccine introduction, genotype dominance varied across years, with G3P[8] dominant in 2006 ( $n = 74$ , 94%) and 2009 ( $n = 26$ , 59%), G2P[4] dominant in 2008 ( $n = 30$ , 40%) and 2010 ( $n = 88$ , 74%), and G1P[8] dominant in 2011 ( $n = 127$ , 85%) and 2012 ( $n = 4$ , 67%). However, the number of samples available for genotyping was low in 2005 and 2007 and no clear dominant genotype could be determined.

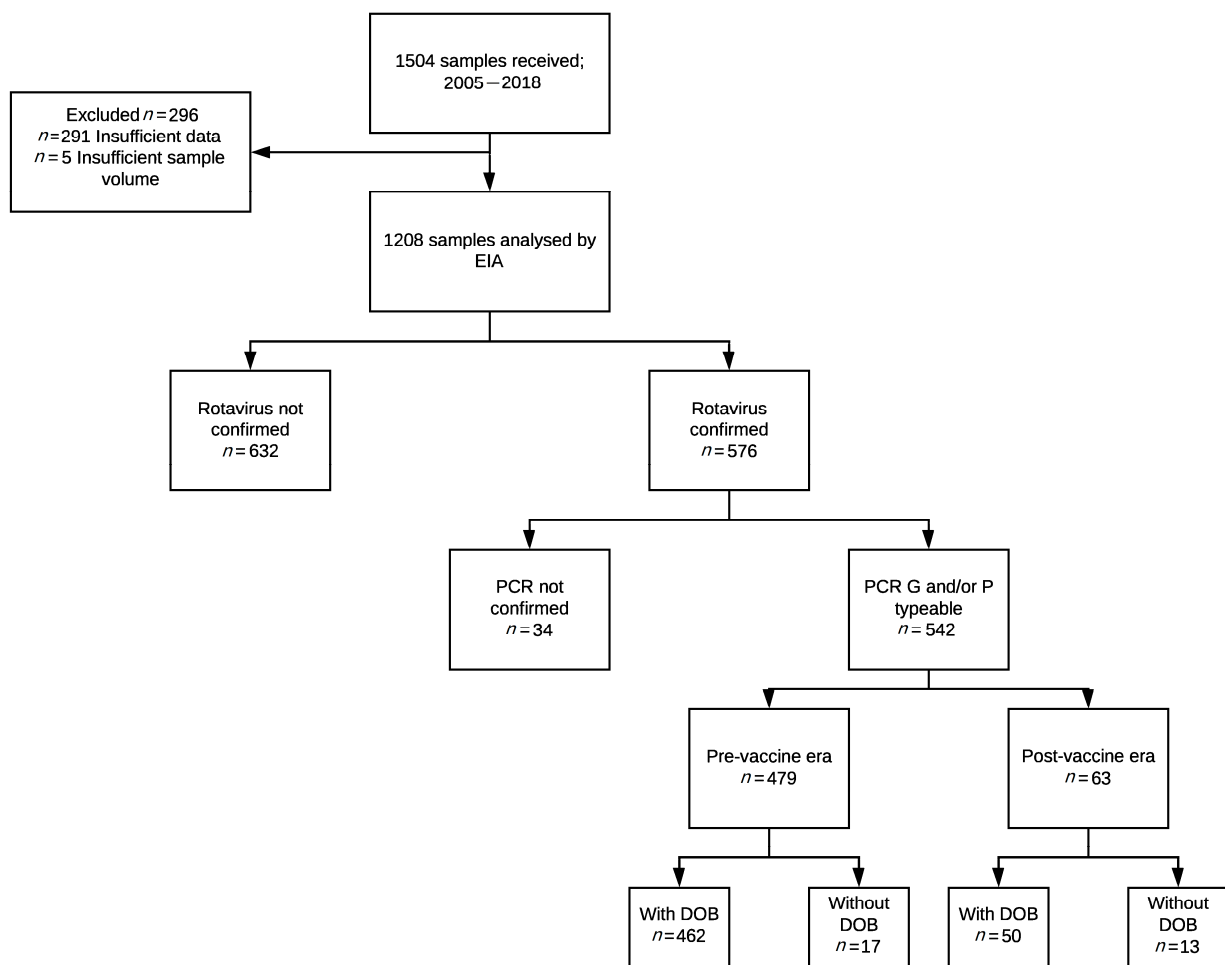


**Figure 1.** Consort diagram of samples included in this study.

Following vaccine introduction, there was a marked decrease in the number of rotavirus positive samples available for genotyping, reflecting the reduction in rotavirus disease observed (Table 1). The diversity of genotypes decreased following vaccine introduction (Figure 2) with some genotypes (G2P[8], G3P[6], G8P[8], G9P[8], G12P[4]) no longer detected. There was only one mixed genotype sample identified in the post-vaccine era, compared with 13 mixed genotype samples detected in the pre-vaccine era. The dominant genotype continued to vary annually following vaccine introduction, with G3P[8] dominant in 2013 ( $n = 6$ , 50%), G1P[8] in 2014 ( $n = 17$ , 71%), G12P[8] in 2017 ( $n = 11$ , 100%) and G3P[8] in 2018 ( $n = 6$ , 100%). The previously dominant G1P[8] disappeared 3 years after vaccine introduction, and G2P[4] strains were not detected after 2014 (Table 1). Emergence of the novel, equine-like G3P[8] reassortant strain, previously not detected in Fiji, was reported in the years following vaccine introduction. This equine-like G3P[8] was dominant for two consecutive years (2015–2016), accounting for 83% ( $n = 5/6$ ) and 100% ( $n = 4/4$ ) of samples genotyped. However, it was not detected in 2017 or 2018. G3P[8] re-emerged in 2018 after not being detected for 4 years.

Table 1. Genotype distribution in samples received by the WHO Regional Reference Laboratory.

Year	G1P[8]		G2P[4]		G2P[8]		G3P[6]		G3P[8]		G3P[8] EQUINE		G8P[8]		G9P[8]		G12P[4]		G12P[8]		Mixed		Partially Typed		Total Genotyped		Negative		Total Samples		
	n	%	n	%	n	%	n	%	n	%	n	%	n	%	n	%	n	%	n	%	n	%	n	%	n	%	n	%	n	%	
2005	1	20					1	20								1	20							2	40	5	71	2	29	7	
2006			1	1	74	94																	4	5	79	99	1	1	80		
2007					1	50																	1	50	2	100	0	0.0	2		
2008	5	7	30	40	4	5	1	1	3	4	2	3	22	29	8	11							75	100	0	0.0	0	0.0	75		
2009			9	21			26	59			1	2	1	2	2	5	5	5	11				2	5	44	96	2	4	46		
2010	1	1	88	74			23	19							3	3	4	3				3	3	119	62	74	38	193			
2011	127	85	15	10			6	4														1	1	149	37	255	63	404			
2012	4	67	2	33																			6	30	14	70	20				
Subtotal	138		144		4		1	132	0	1	5	2	22	13	17							479	348	6	30	14	70	20	827		
Rotarix Vaccine Introduced																															
2013	1	8	5	42			6	50														12	67	6	33	18					
2014	17	71	6	25										1	4							24	51	23	49	47					
2015	1	17							5	83												6	4	158	96	164					
2016									4	100												4	15	22	85	26					
2017													11	100								11	20	43	80	54					
2018							6	100														6	16	32	84	38					
Subtotal	19		11		0		0	12	9	0	0	11	1	0	0	0	0	0	11	1	0	63	284	6	30	14	70	20	347		

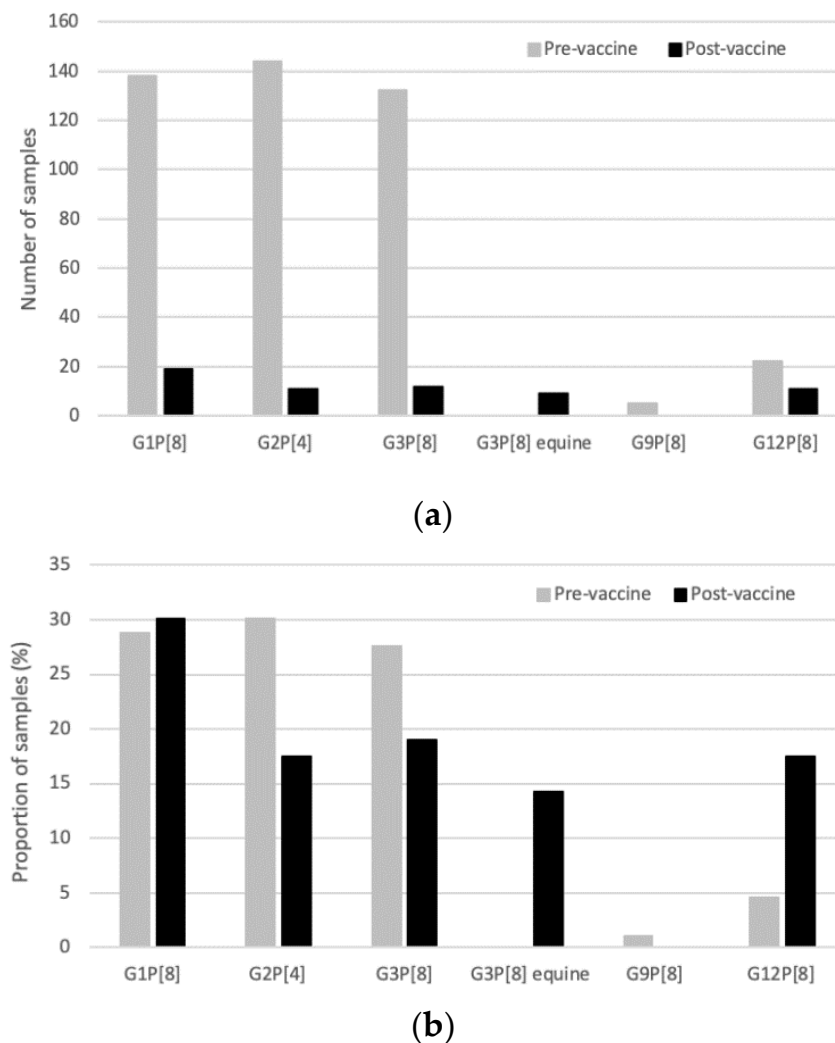


**Figure 2.** Distribution of main genotypes in samples collected in the pre-vaccine (2005–2012) and post-vaccine (2013–2018) period. (a) Number of samples in each of the main genotype groups. (b) Proportion of samples identified in each of the main genotype groups, of the total number of samples genotyped.

### 3. Discussion

This is the first study in a low- or middle-income country in the Western Pacific Region to describe rotavirus genotypes following national rotavirus vaccine introduction. Prior to rotavirus vaccine introduction, G1P[8], G2P[4] and G3P[8] were the predominant genotypes causing rotavirus diarrhoea in children less than 5 years of age in Fiji. Genotype diversity decreased following rotavirus vaccine introduction in Fiji; with G2P[8], G3P[6], G8P[8], G9P[8] and G12P[4], which all represented minor genotypes in the pre-vaccine period, subsequently undetected in the vaccine era. Following rotavirus vaccine introduction, G2P[4] has not been detected since 2014 and G1P[8] has not been detected since 2015. This is in contrast to changes in genotype distribution observed in Australia following introduction of the Rotarix (GlaxoSmithKline, Rixensart, Belgium) and RotaTeq (Merck, Kenilworth, NJ, USA) vaccines. In Australia, although there was an overall decrease in the common genotypes (G1, G2, G3, G4 and G9) from 83% to 63% observed following rotavirus vaccine introduction, an increase in G2P[4] (pre-vaccine era 5%; post-vaccine era 21%) was observed in states and territories implementing the Rotarix vaccine and G1P[8] continued to be detected [5].

We found that equine-like G3P[8] was the dominant genotype in 2015 to 2016 but was not detected in the following years (2017 or 2018). An increase in novel zoonotic strains such as equine-like G3P[8] following the introduction of Rotarix has also been observed in other countries (Australia, Japan, Hungary and Brazil) [12–16]. The segmented rotavirus genome allows reassortment to occur both within and between human and animal strains if the human host is infected with two different rotavirus strains, thus giving rise to novel and unusual genotype combinations [17]. In Australia, an increase in G12P[8], equine-like G3P[8], G8, G10 and other zoonotic reassortant strains has also been observed following rotavirus vaccine introduction [5]. In Fiji, human G3P[8] was not detected during 2015 and 2016 when the equine-like G3P[8] was circulating, but this strain re-emerged two years later when equine-like G3P[8] was no longer detected. This is consistent with reports from Asia, Australia, Europe and the U.S. [5,17].

The G12 genotype was first identified in Fiji in 2008, with both G12P[4] and G12P[8] detected. These strains accounted for 32% ( $n = 24/75$ ) of all rotavirus positive samples in 2008 but were not detected again until 2017 when all available samples ( $n = 11$ ) were identified as G12P[8] (Table 1). The emergence of G12 following vaccine introduction has been observed in other countries but does not appear to be dependent on vaccine coverage. In Finland, a 9% increase in G12P[8] was observed five years after vaccine introduction, with a higher frequency of G12P[8] detected in vaccinated children (14%) than observed in unvaccinated children (7%) [18]. In Australia, a small G12P[8] outbreak was reported in 2005 prior to vaccine introduction; however, since vaccine introduction G12P[8] has become common, detected in 18% of samples from children less than 5 years with acute diarrhoea [5]. Similarly, G12, originally detected in Brazil in 2008 following vaccine introduction (2006), has emerged to be the most prevalent genotype (G12P[8]) in 87% of samples in 2014 [19].

A key strength of this study is the ability to observe genotypic changes over time, following the introduction of Rotarix into a national program in a Pacific nation associated with very high vaccine coverage. Monitoring rotavirus genotypes that continue to cause diarrhoea in children provides critical information regarding the ongoing effectiveness of the vaccine program and can assist in outbreak investigation. It also enables early identification of the emergence or importation of new strains that may have a public health impact. This is particularly relevant for Fiji as an island nation with an economy highly dependent on tourism where there is potential for importation of novel strains resulting in disease outbreaks.

This study aligns with data on the impact of rotavirus vaccines on rotavirus disease hospitalisations in children less than 5 years of age in Fiji. Fiji has been notable within the Pacific as a country that has introduced new vaccines based on local data and is committed to monitoring vaccine impact. No other Pacific nation participates in WHO rotavirus surveillance. Data from Fiji may assist in informing vaccine decisions of neighbouring countries in the region. A limitation of this study is that it can only report on samples received for analysis by the WHO Rotavirus Regional Reference Laboratory. Despite attempts, not all children admitted to hospital with diarrhoea have a stool sample collected and sent for analysis. Following introduction of a rotavirus vaccine, the number of children hospitalised with rotavirus disease has dramatically decreased; as a result, the number of stool samples available to provide comparisons of genotypic distribution between the pre-vaccine and post-vaccine era has been impacted. As stool collection is still requested for hospitalised patients with acute diarrhoea in Fiji, it is unlikely that there is a bias impacting on stool collection between the period before and after introduction of the rotavirus vaccine.

The variation in the proportion of rotavirus negative samples reported reflects differences in the rotavirus detection status of stool samples submitted to MCRI for genotypic analysis over the 14-year surveillance period (Table 1). The lower proportion of rotavirus negative samples early in the surveillance period (2005–2009) has limited impact on the

outcome of this paper given the focus is the period following the introduction of the rotavirus vaccine.

In 2015, there was a marked increase in the number of negative samples tested. From 2010 to 2013, there was an increase in typhoid detection as the result of six typhoid outbreaks in Fiji, along with outbreaks of both Zika virus and Chikungunya virus, which were both initially detected in 2015, all which may have led to an increased number of negative samples being sent to MCRI for analysis during this time period [20–22]. Being negative samples only, this also would have had minimal impact on the rotavirus distribution observed in this study.

The effect of age on rotavirus detection in the stool following introduction of rotavirus vaccines in Fiji has recently been reported [11]. Due to the success of the rotavirus vaccination program, the ability to compare age related differences in genotype distribution in samples from the pre- and post-vaccine eras has been impacted by the limited number of samples available for analysis in the post-vaccine era (pre-vaccine era  $n = 462$ ; post-vaccine era  $n = 50$ ). This decline in number of available rotavirus positive samples was not likely to be due to a lack of sampling due to the ongoing surveillance program operating in Fiji.

In this study we report changes in the pattern of rotavirus genotypes causing diarrhoea in children in Fiji since rotavirus vaccine introduction. We observed a transient increase in the zoonotic strain equine-like G3P[8] and a reduction in the previously dominant G1P[8] and G2P[4]. A decrease in detection of rotavirus strains G2P[8], G3P[6], G8P[8] and G9P[8] was also detected in the years following rotavirus vaccine introduction. Monitoring rotavirus genotypes provides key information regarding the ongoing effectiveness of the vaccine program and can assist in outbreak investigation. It also enables early identification of the emergence or importation of new strains that may have a public health impact.

## 4. Materials and Methods

### 4.1. Population and Study Sites

Fiji has participated in the WHO Global Rotavirus Surveillance Program since 2006, monitoring rotavirus disease burden and rotavirus genotype diversity associated with hospitalisations in children less than 5 years of age. The samples from children hospitalised with acute diarrhoea are sent to the WHO Rotavirus Regional Reference Laboratory at Murdoch Children's Research Institute (MCRI) according to the case definitions and methods defined for the WHO Global Rotavirus Surveillance Program [11]. Two major hospitals admitting children with gastroenteritis in Fiji participated in this study. The Colonial War Memorial Hospital (CWMH) is Fiji's largest general hospital and is the main referral centre for the greater Suva area with approximately 34,920 children under 5 years of age. The Savusavu District Hospital is a secondary health inpatient and outpatient facility serving mainly a semiurban and rural population with an estimated 6563 children under 5 years of age. Samples were received from inpatients at Savusavu district hospital only in 2013 and 2014. Details on rotavirus surveillance in Fiji has previously been described [9,11].

### 4.2. Participants

A prospective rotavirus surveillance program was established in 2005 to effectively capture rotavirus detected in faecal samples from children less than 5 years with acute nonbloody diarrhoea in Fiji. Acute diarrhoea was defined as 3 or more loose, nonbloody stools within a 24-h period for <14 days. Eligible participants were identified by checking admission data and children's wards daily, parental/guardian consent was obtained, and stool was collected within 48 h of admission. Once rotavirus positivity was determined, demographics and clinical information were obtained via medical records.

Ethics approval for these studies was obtained from the Fiji National Research Ethics Review Committee (number 2013-40) and from the University of Melbourne Human Research Ethics Committee for the initial study surveillance in Colonial War Memorial Hospital from 2005–2012 (Ethics ID:050546X) and Savusavu from 2010–2012 (Ethics ID:0931282); during this period written informed consent was obtained from participants' parents. From

June 2012 onward, the Ministry of Health and Medical Services considered this public health surveillance and no longer required written consent.

#### 4.3. Genotyping

Faecal specimens were collected and stored at 4–8 °C prior to being transported to the Fiji Centre for Communicable Disease Control in Suva for rotavirus antigen testing via the ProSpecT Rotavirus test, a commercial rotavirus enzyme immunoassay (EIA) (ThermoFisher Scientific, Waltham, MA, USA) as per manufacturer's instructions. Stool samples were then stored at –70 °C. De-identified rotavirus specimens were transported on dry ice to the WHO Rotavirus Regional Reference Laboratory at the Murdoch Children's Research Institute, Parkville, Australia. Sample selection for shipment to MCRI varied during the surveillance program. Between 2005 and 2009 only stool samples that tested positive to rotavirus in the Fiji laboratory were sent to MCRI, with the negative samples reflected in Table 1 having been identified by EIA at MCRI. Between 2010 and 2016, stool samples were sent to MCRI for EIA and RT-PCR genotyping irrespective of whether they were rotavirus positive or negative via EIA conducted in Fiji. From 2017 onward, all rotavirus positive samples and 10% of rotavirus negative samples by EIA in Fiji were sent to MCRI for further analysis. All samples were retested at MCRI to confirm rotavirus positivity prior to proceeding with genotypic analysis. Rotavirus positivity (or negativity) was confirmed using the ProSpecT Rotavirus test, (EIA) (ThermoFisher Scientific, Waltham, MA, USA) as per the manufacturer's instructions. Stool samples that tested positive or equivocal for rotavirus antigen were further characterised to determine the G and P genotype. Samples from 2005 and 2006 were routinely serotyped using an in-house monoclonal antibody based serotyping EIA. This EIA consisted of a panel of monoclonal antibodies specific to the VP7 outer capsid protein of group A rotavirus serotypes G1, G2, G3, G4 and G9 [23]. Prior to 2007, P-typing and RT-PCR were not routinely performed. From 2007 onward, rotavirus G and P genotypes were determined by heminested multiplex RT-PCR assay. All samples collected prior to 2007 have retrospectively been characterised by heminested RT-PCR G and P genotyping. In brief, viral RNA was extracted from 20% (*w/v*) faecal extracts in a virus dilution buffer (0.01 M Tris-HCL [pH7.5], 10.5 mM CaCl, 145 mM NaCl) using the QIAamp Viral RNA mini extraction kit (QIAGEN, Hilden, Germany) according to the manufacturer's instructions.

The One-step RT-PCR kit (QIAGEN) was used to perform first round PCR, using VP7 primers VP7F and VP7R and VP4 primers VP4F and VP4R [24,25]. Second round genotyping PCR was performed using AmpliTaq DNA Polymerase with Buffer II (Applied Biosystems, Foster City, CA, USA), with specific G and P oligonucleotide primers for G typing (G1, G2, G3, G4, G8 and G9) or P typing (P[4], P[6], P[8], P[9], P[10] and P[11]) as described previously [26]. Amplified products were run on a 1.5% or 2% agarose gel for G and P types respectively, and genotypes were determined based on amplicon band size. PCR non-typeable samples were determined by Sanger sequencing. Strains including equine-like G3, G12 and unusual or uncommon strains were unable to be genotyped using standard primers. VP7 or VP4 amplicons from first round PCR products were purified for sequencing using the Wizard SV Gel and PCR Clean up System (Promega, Madison, WI, USA) as per manufacturer's protocol. Purified DNA with oligonucleotide primers (VP7F/R or VP4F/R) were sent to the Australian Genome Research Facility (AGRF) Melbourne and sequenced using an ABI PRISM BigDye Terminator Cycle Sequencing Reaction Kit (Applied Biosystems, Foster City, CA, USA) in an Applied Biosystems 3730xl DNA analyser. Sequencer version 4.10.1 (Gene Codes Corporation, Ann Arbor, MI, USA) was used to edit the sequences. BLAST (<http://blast.ncbi.nlm.nih.gov/Blast.cgi> (accessed on 10 October 2020)) and RotaC version 2.0 (<http://rotac.regatools.be> (accessed on 10 October 2020)) [27] were used to determine the genotype of each sample.

#### 4.4. Data Analysis

Samples were excluded if there was no date of stool collection available, if there was insufficient sample to process, if the sample was not confirmed as rotavirus positive by EIA at MCRI, or if samples were rotavirus positive by EIA at MCRI but genotype could not be determined. To describe the impact of rotavirus vaccine introduction on genotype distribution, samples were grouped into pre-vaccine (2005–2012) and post-vaccine (2013–2018) eras according to the date of collection. Analysis is by descriptive observations and comparisons between the pre-vaccine and post-vaccine introduction eras.

**Author Contributions:** Conceptualization, S.T., J.E.B. and F.M.R.; data curation, S.T. and C.M.D.; formal analysis, S.T., C.M.D. and J.E.B.; funding acquisition, J.E.B. and F.M.R.; investigation, S.T., C.M.D., S.C., F.T.R., A.W.J.J., R.R., A.S.K., E.R., V.G., F.S., J.E.B. and F.M.R.; methodology, S.T. and C.M.D.; project administration, J.E.B. and F.M.R.; resources, J.E.B. and F.M.R.; software, S.T. and C.M.D.; supervision, J.E.B. and F.M.R.; visualization, S.T. and C.M.D.; writing—original draft, S.T.; writing—review and editing, C.M.D., S.C., F.T.R., A.W.J.J., R.R., A.S.K., E.R., V.G., F.S., J.E.B. and F.M.R. All authors have read and agreed to the published version of the manuscript.

**Funding:** The identification, collection, transportation and laboratory analysis of surveillance samples was funded as part of the World Health Organization Rotavirus Regional Surveillance activity. The World Health Organization provided funds to set up the initial rotavirus surveillance (2005–2007) and an additional World Health Organization grant [Registry File No. V27-181-188] for data collected between 2006 and 2013. A Merck investigator grant (IISP ID#:35248) funded the early work in Savusavu (2009–2010). Surveillance data collected between 2014 and 2018 by the Department of Foreign Affairs and Trade of the Australian Government and Fiji Health Sector Support Program (FHSSP). FHSSP is implemented by Abt JTA on behalf of the Australian Government. The Murdoch Children’s Research Institute is supported by the Victorian Government’s Operational Infrastructure Support program. Funders had no role in study design, data collection, data analysis, interpretation, writing of the report. C.M.D. is supported through the Australian National Health and Medical Research Council with an Early Career Fellowship (1113269). F.M.R. is supported through Australian National Health and Medical Research Council with an Early Career Fellowship and Translating into Practice Fellowship.

**Institutional Review Board Statement:** The study was conducted according to the guidelines of the Declaration of Helsinki, and approved by the Fiji National Research Ethics Review Committee (number 2013-40) and from the University of Melbourne Human Research Ethics Committee for the initial study surveillance in Colonial War Memorial Hospital 2005–2012 (Ethics ID:050546X) and Savusavu from 2010–2012 (Ethics ID:0931282).

**Informed Consent Statement:** Informed consent was obtained from participant’s parents between 2005 and 2012; from June 2012, the Fiji Ministry of Health and Medical Services considered this public health surveillance and no longer required written consent.

**Data Availability Statement:** Data is contained within the article.

**Acknowledgments:** We gratefully acknowledge Rachel Devi; Kathryn Bright; Beth Temple; Lisi Tikoduadua; Joe Kado; E. Kim Mulholland; Kimberley K. Fox; and Mike Kama for assistance in collection of stool samples in Fiji. We acknowledge Josephine Logronio, WHO Western Pacific Regional Office. We gratefully acknowledge Carl D. Kirkwood, Nada Bogdanovic-Sakran, Huy Tran and the Enteric Disease Group MCRI for their assistance within the laboratory.

**Conflicts of Interest:** C.M.D. has served on a rotavirus advisory board for GSK (2019); all payments were paid directly to an administrative fund held by Murdoch Children’s Research Institute. J.E.B. is lead for the Rotavirus Vaccine Program at Murdoch Children’s Research Institute that aims to develop an affordable rotavirus vaccine, RV3-BB. J.E.B. is Director of the Australia Rotavirus Surveillance Program that receives funding from the Australian Commonwealth Department of Health and Aging and GlaxoSmithKline. The funders had no role in the design of the study; in the collection, analyses, or interpretation of data; in the writing of the manuscript, or in the decision to publish the results. All other authors declare no conflict of interest.

## References

1. Troeger, C.; Khalil, I.A.; Rao, P.C.; Cao, S.; Blacker, B.F.; Ahmed, T.; Armah, G.; Bines, J.E.; Brewer, T.G.; Colombara, D.V.; et al. Rotavirus Vaccination and the Global Burden of Rotavirus Diarrhea Among Children Younger Than 5 Years. *JAMA Pediatr.* **2018**, *172*, 958–965. [[CrossRef](#)] [[PubMed](#)]
2. Desselberger, U. Rotaviruses. *Virus Res.* **2014**, *190*, 75–96. [[CrossRef](#)]
3. Rotavirus Classification Working Group. List of Accepted Genotypes. Available online: <https://rega.kuleuven.be/cev/viralmetagenomics/virus-classification/rcwg> (accessed on 1 October 2020).
4. Clarke, E.; Desselberger, U. Correlates of protection against human rotavirus disease and the factors influencing protection in low-income settings. *Mucosal Immunol.* **2015**, *8*, 1–17. [[CrossRef](#)] [[PubMed](#)]
5. Roczo-Farkas, S.; Kirkwood, C.D.; Cowley, D.; Barnes, G.L.; Bishop, R.F.; Bogdanovic-Sakran, N.; Boniface, K.; Donato, C.M.; Bines, J.E. The impact of rotavirus vaccines on genotype diversity: A comprehensive analysis of two decades of Australian surveillance data. *J. Infect. Dis.* **2018**, *218*, 546–554. [[CrossRef](#)] [[PubMed](#)]
6. Aliabadi, N.; Antoni, S.; Mwenda, J.M.; Weldegebriel, G.; Biey, J.N.M.; Cheikh, D.; Fahmy, K.; Teleb, N.; Ashmony, H.A.; Ahmed, H.; et al. Global impact of rotavirus vaccine introduction on rotavirus hospitalisations among children under 5 years of age, 2008–2016: Findings from the Global Rotavirus Surveillance Network. *Lancet Glob. Health* **2019**, *7*, e893–e903. [[CrossRef](#)]
7. United Nations Pacific. Socio-Economic Impact Assessment of COVID-19 in Fiji July 2020. Available online: <https://www.pacific.undp.org/content/pacific/en/home/library/socio-economic-impact-assessment-of-covid-19-in-fiji.html> (accessed on 8 December 2020).
8. World Health Organization. Fiji Key Indicators. Available online: <https://apps.who.int/gho/data/node.cco.ki-FJI?lang=en> (accessed on 15 October 2020).
9. Jenney, A.; Tikoduadua, L.; Buadromo, E.; Barnes, G.; Kirkwood, C.D.; Boniface, K.; Bines, J.; Mulholland, K.; Russell, F. The burden of hospitalised rotavirus infections in Fiji. *Vaccine* **2009**, *27* (Suppl. 5), F108–F111. [[CrossRef](#)]
10. World Health Organization. WHO and UNICEF Estimates of National Immunization Coverage. 2020. Available online: [https://www.who.int/immunization/monitoring\\_surveillance/data/fji.pdf](https://www.who.int/immunization/monitoring_surveillance/data/fji.pdf) (accessed on 14 January 2020).
11. Jenney, A.W.; Reyburn, R.; Ratu, F.T.; Tuivaga, E.; Nguyen, C.; Covea, S.; Thomas, S.; Rafai, E.; Devi, R.; Bright, K.; et al. The impact of the rotavirus vaccine on diarrhoea five years following national introduction in Fiji. *Lancet Reg. Health-West. Pac.* **2020**. [[CrossRef](#)]
12. Dóró, R.; Marton, S.; Bartókné, A.H.; Lengyel, G.; Agócs, Z.; Jakab, F.; Bányai, K. Equine-like G3 rotavirus in Hungary, 2015—Is it a novel intergenogroup reassortant pandemic strain? *Acta Microbiol. Immunol. Hung.* **2016**, *63*, 243–255. [[CrossRef](#)]
13. Malasao, R.; Saito, M.; Suzuki, A.; Imagawa, T.; Nukiwa-Soma, N.; Tohma, K.; Liu, X.; Okamoto, M.; Chaimongkol, N.; Dapat, C.; et al. Human G3P[4] rotavirus obtained in Japan, 2013, possibly emerged through a human-equine rotavirus reassortment event. *Virus Genes* **2015**, *50*, 129–133. [[CrossRef](#)] [[PubMed](#)]
14. Luchs, A.; Da Costa, A.C.; Cilli, A.; Komninakis, S.C.V.; Carmona, R.D.C.C.; Boen, L.; Morillo, S.G.; Sabino, E.C.; Timenetsky, M.D.C.S.T. Spread of the emerging equine-like G3P[8] DS-1-like genetic backbone rotavirus strain in Brazil and identification of potential genetic variants. *J. Gen. Virol.* **2019**, *100*, 7–25. [[CrossRef](#)]
15. Jain, S.; Vashist, J.; Changotra, H. Rotaviruses: Is their surveillance needed? *Vaccine* **2014**, *32*, 3367–3378. [[CrossRef](#)] [[PubMed](#)]
16. Matthijnsens, J.; Bilcke, J.; Ciarlet, M.; Martella, V.; Bányai, K.; Rahman, M.; Zeller, M.; Beutels, P.; Van Damme, P.; Van Ranst, M. Rotavirus disease and vaccination: Impact on genotype diversity. *Future Microbiol.* **2009**, *4*, 1303–1316. [[CrossRef](#)] [[PubMed](#)]
17. Perkins, C.; Mijatovic-Rustempasic, S.; Ward, M.L.; Cortese, M.M.; Bowen, M.D. Genomic Characterization of the First Equine-Like G3P[8] Rotavirus Strain Detected in the United States. *Genome Announc.* **2017**, *5*. [[CrossRef](#)] [[PubMed](#)]
18. Markkula, J.; Hemming-Harlo, M.; Salminen, M.T.; Savolainen-Kopra, C.; Pirhonen, J.; Al-Hello, H.; Vesikari, T. Rotavirus epidemiology 5–6 years after universal rotavirus vaccination: Persistent rotavirus activity in older children and elderly. *Infect. Dis.* **2017**, *49*, 388–395. [[CrossRef](#)] [[PubMed](#)]
19. Luchs, A.; Cilli, A.; Morillo, S.G.; Gregório, D.D.S.; De Souza, K.A.F.; Vieira, H.R.; Fernandes, A.D.M.; Carmona, R.D.C.C.; Timenetsky, M.D.C.S.T. Detection of the emerging rotavirus G12P[8] genotype at high frequency in Brazil in 2014: Successive replacement of predominant strains after vaccine introduction. *Acta Trop.* **2016**, *156*, 87–94. [[CrossRef](#)]
20. Parry, C.M.; Crump, J.A.; Rosa, V.; Jenney, A.; Naidu, R.; Mulholland, K.; Strugnell, R.A. A retrospective study of patients with blood culture-confirmed typhoid fever in Fiji during 2014–2015: Epidemiology, clinical features, treatment and outcome. *Trans. R. Soc. Trop. Med. Hyg.* **2019**, *113*, 764–770.
21. Kama, M.; Aubry, M.; Al, M.K.E.; Vanhomwegen, J.; Mariteragi-Helle, T.; Teissier, A.; Paoaafaite, T.; Hué, S.; Hibberd, M.L.; Manuguerra, J.-C.; et al. Sustained Low-Level Transmission of Zika and Chikungunya Viruses after Emergence in the Fiji Islands. *Emerg. Infect. Dis.* **2019**, *25*, 1535–1538. [[CrossRef](#)]
22. Aubry, M.; Kama, M.; Henderson, A.D.; Teissier, A.; Vanhomwegen, J.; Mariteragi-Helle, T.; Paoaafaite, T.; Manuguerra, J.-C.; Christi, K.; Watson, C.H.; et al. Low chikungunya virus seroprevalence two years after emergence in Fiji. *Int. J. Infect. Dis.* **2020**, *90*, 223–225. [[CrossRef](#)] [[PubMed](#)]
23. Coulson, B.S.; Unicomb, L.E.; Pitson, G.A.; Bishop, R.F. Simple and specific enzyme immunoassay using monoclonal antibodies for serotyping human rotaviruses. *J. Clin. Microbiol.* **1987**, *25*, 509–515. [[CrossRef](#)] [[PubMed](#)]

24. Gomara, M.I.; Cubitt, D.; Desselberger, U.; Gray, J. Amino acid substitution within the VP7 protein of G2 rotavirus strains associated with failure to serotype. *J. Clin. Microbiol.* **2001**, *39*, 3796–3798. [[CrossRef](#)]
25. Simmonds, M.K.; Armah, G.; Asmah, R.; Banerjee, I.; Damanka, S.; Esona, M.; Gentsch, J.R.; Gray, J.J.; Kirkwood, C.; Page, N.; et al. New oligonucleotide primers for P-typing of rotavirus strains: Strategies for typing previously untypeable strains. *J. Clin. Virol.* **2008**, *42*, 368–373. [[CrossRef](#)] [[PubMed](#)]
26. Kirkwood, C.D.; Roczo-Farkas, S.; Australian Rotavirus Surveillance Group. Australian Rotavirus Surveillance Program annual report, 2013. *Commun. Dis. Intell. Q. Rep.* **2014**, *38*, E334–E342. [[PubMed](#)]
27. Maes, P.; Matthijssens, J.; Rahman, M.; Van Ranst, M. RotaC: A web-based tool for the complete genome classification of group a rotaviruses. *BMC Microbiol.* **2009**, *9*, 238. [[CrossRef](#)] [[PubMed](#)]



## Article

# Rotavirus Strain Distribution Before and After Introducing Rotavirus Vaccine in India

Tintu Varghese <sup>1</sup>, Shainey Alokith Khakha <sup>1</sup> , Sidhartha Giri <sup>1</sup>, Nayana P. Nair <sup>1</sup>, Manohar Badur <sup>2</sup>, Geeta Gathwala <sup>3</sup>, Sanjeev Chaudhury <sup>4</sup>, Shayam Kaushik <sup>5</sup>, Mrutunjay Dash <sup>6</sup>, Nirmal K. Mohakud <sup>7</sup> , Rajib K. Ray <sup>8</sup>, Prasantajyoti Mohanty <sup>8</sup>, Chethrapilly Purushothaman Girish Kumar <sup>9</sup> , Seshadri Venkatasubramanian <sup>9</sup>, Rashmi Arora <sup>10</sup>, Venkata Raghava Mohan <sup>11</sup> , Jacqueline E. Tate <sup>12</sup>, Umesh D. Parashar <sup>12</sup> and Gagandeep Kang <sup>1,\*</sup>

- <sup>1</sup> The Wellcome Trust Research Laboratory, Division of Gastrointestinal Sciences, Christian Medical College, Vellore 632004, India; tintu.varghese@cmcvellore.ac.in (T.V.); shainey.rnc0411@gmail.com (S.A.K.); sidharthgiri@gmail.com (S.G.); nayana.arun@cmcvellore.ac.in (N.P.N.)
- <sup>2</sup> Department of Pediatrics, Sri Venkateshwara Medical College, Tirupati 517507, India; punya\_manohar2002@yahoo.com
- <sup>3</sup> Department of Pediatrics, Post Graduate Institute of Medical Sciences, Medical Road, Rohtak, Haryana 124001, India; geetagathwala@gmail.com
- <sup>4</sup> Department of Pediatrics, Dr Rajendra Prasad Government Medical College, Tanda, Himachal Pradesh 176001, India; s\_chaudhary@ymail.com
- <sup>5</sup> Department of Pediatrics, Indira Gandhi Medical College, Shimla, Himachal Pradesh 171001, India; shayam.kaushik@live.in
- <sup>6</sup> Department of Pediatrics, Institute of Medical Sciences and SUM Hospital, Bhubaneswar, Odisha 751003, India; m.dash74@gmail.com
- <sup>7</sup> Department of Pediatrics, Kalinga Institute of Medical Sciences, 5 KIIT Road, Bhubaneswar, Odisha 751024, India; nkmohakud@yahoo.co.in
- <sup>8</sup> Department of Pediatrics, Hi-Tech Hospital, Bhubaneswar, Odisha 751025, India; drrajib2007@gmail.com (R.K.R.); prasantij53@gmail.com (P.M.)
- <sup>9</sup> ICMR National Institute of Epidemiology, Chennai, Tamil Nadu 600077, India; girishmicro@gmail.com (C.P.G.K.); subramanianv89@yahoo.co.in (S.V.)
- <sup>10</sup> Translational Health Science and Technology Institute, Faridabad, Haryana 121001, India; arorarashmi2015@gmail.com
- <sup>11</sup> Department of Community Health, Christian Medical College, Vellore 632002, India; venkat@cmcvellore.ac.in
- <sup>12</sup> Centers for Disease Control and Prevention, Atlanta, GA 30333, USA; jqt8@cdc.gov (J.E.T.); uap2@cdc.gov (U.D.P.)
- \* Correspondence: gkang@cmcvellore.ac.in



**Citation:** Varghese, T.; Alokith Khakha, S.; Giri, S.; Nair, N.P.; Badur, M.; Gathwala, G.; Chaudhury, S.; Kaushik, S.; Dash, M.; Mohakud, N.K.; et al. Rotavirus Strain Distribution Before and After Introducing Rotavirus Vaccine in India. *Pathogens* **2021**, *10*, 416. <https://doi.org/10.3390/pathogens10040416>

Academic Editors: Julie Bines and Celeste Donato

Received: 22 February 2021

Accepted: 18 March 2021

Published: 1 April 2021

**Publisher's Note:** MDPI stays neutral with regard to jurisdictional claims in published maps and institutional affiliations.



**Copyright:** © 2021 by the authors. Licensee MDPI, Basel, Switzerland. This article is an open access article distributed under the terms and conditions of the Creative Commons Attribution (CC BY) license (<https://creativecommons.org/licenses/by/4.0/>).

**Abstract:** In April 2016, an indigenous monovalent rotavirus vaccine (Rotavac) was introduced to the National Immunization Program in India. Hospital-based surveillance for acute gastroenteritis was conducted in five sentinel sites from 2012 to 2020 to monitor the vaccine impact on various genotypes and the reduction in rotavirus positivity at each site. Stool samples collected from children under 5 years of age hospitalized with diarrhea were tested for group A rotavirus using a commercial enzyme immunoassay, and rotavirus strains were characterized by RT-PCR. The proportion of diarrhea hospitalizations attributable to rotavirus at the five sites declined from a range of 56–29.4% in pre-vaccine years to 34–12% in post-vaccine years. G1P[8] was the predominant strain in the pre-vaccination period, and G3P[8] was the most common in the post-vaccination period. Circulating patterns varied throughout the study period, and increased proportions of mixed genotypes were detected in the post-vaccination phase. Continuous long-term surveillance is essential to understand the diversity and immuno-epidemiological effects of rotavirus vaccination.

**Keywords:** rotavirus diarrhea; rotavirus genotyping; Rotavac vaccine

## 1. Introduction

Rotavirus is the leading etiology of acute gastroenteritis in children under 5 years old worldwide, causing high mortality, especially in middle- and low-income countries. India accounts for 22% of the total global rotavirus mortality [1]. In India, 40% of all diarrhea-related hospitalizations among children under 5 years of age is caused by group A rotavirus [2].

The genome of group A rotavirus is composed of 11 double-stranded RNA segments, of which the VP7 and VP4 genes coding for the outer capsid proteins are used for the classification of the virus into G and P types, respectively. Studies have been conducted across the globe to understand the natural evolution of rotavirus and its relevance in the context of vaccine introduction. Globally, G1P[8], G2P[4], G3P[8], and G9P[8] are the most common genotypes associated with rotavirus diarrhea [3]. However, it is hypothesized that large-scale vaccination may exert pressure on circulating strains, leading to possible changes in strain circulation.

In 2009, the World Health Organization (WHO) recommended the inclusion of rotavirus vaccines in the national immunization program of all countries. Currently, four live-attenuated oral vaccines are prequalified by WHO, which includes Rotarix (Glaxo-SmithKline Biologicals, Rixensart, Belgium), RotaTeq (Merck & Co., Inc., West Point, PA, USA), Rotavac (Bharath Biotech, India), and Rotasiil (Serum Institute of India PVT. LTD., Pune, India). These rotavirus vaccines differ in their genotypic composition, with Rotarix and Rotavac being the monovalent vaccines and RotaTeq and Rotasiil being the pentavalent vaccines [4]. Rotarix and RotaTeq vaccines have been available on the market since 2006 and are currently used by nearly 90 countries in their immunization programs [4]. Early studies reported a decline in G1P[8] and the emergence of G2P[4] after Rotarix vaccination [5,6], while others showed no change [7]. The emergence of G9P[8] and G12P[8] was reported with the use of the RotaTeq vaccine [8]. However, such changes were also observed in other countries without rotavirus vaccination [9,10]. Hence, the vaccine impact on the circulating pattern of rotavirus strains is not clearly understood.

In India, the indigenously developed Rotavac vaccine, based on the human-bovine reassortant neonatal attenuated 116E strain, is a monovalent vaccine with the genotypic composition G9P [11]. It was introduced to the Universal Immunization Program (UIP) in April 2016 in a phased manner [11]. Other rotavirus vaccines like Rotateq and Rotarix were available in the private sectors for immunization before nationwide rotavirus vaccine implementation. India is the first Asian country to introduce rotavirus vaccines to the national immunization schedule, and currently, the Rotavac vaccine is used only in India and a few smaller countries [4]. The National Rotavirus Surveillance Network was established in India in 2005 to generate data on disease burden and monitor the trends of circulating genotypes [12,13]. This study describes the reduction in rotavirus prevalence and temporal trends in rotavirus strain distribution before and after Rotavac vaccine introduction in five sites in India.

## 2. Results

### 2.1. Prevalence of Rotavirus Diarrhea

Between September 2012 and June 2020, 8499 children under 5 years of age were enrolled in the surveillance study at the five sites. The details of enrollment and rotavirus testing are summarized in Table 1.

**Table 1.** Enrollment and rotavirus testing details from 5 surveillance sites (September 2012–June 2020).

Site Name	Pre-Vaccination Period and Enrollment	Pre-Vaccination Rotavirus Positivity	Post-Vaccination Period and Enrollment	Post-Vaccination Rotavirus Positivity	Percentage Reduction in Rotavirus Positivity
Rohtak	489	153 (31.2%)	1103	169 (15.3%)	50.96%
Tanda	423	237 (56.0%)	573	104 (18.1%)	67.67%
Tirupati	930	401 (43.1%)	1089	131 (12.0%)	72.15%
Bhubaneswar	723	395 (54.6%)	1113	379 (34.0%)	37.72%
Vellore	1598	470 (29.4%)	458	91 (19.8%)	32.65%
Total	4163	1656 (39.7%)	4336	874 (20.1%)	49.37%

The proportion of diarrhea hospitalizations attributable to rotavirus at the five sites declined from a range of 56–29.4% in pre-vaccine years to 34–12% in post-vaccine years. The maximum annual positivity rate was in 2014 (46.2%), and the minimum was in 2019 (13.3%). The positivity rates declined steadily after vaccine implementation and were more marked towards the later years with higher vaccine coverage (Figure 1). The maximum reduction in rotavirus diarrhea was seen in Tirupati (72.1%), the site with maximum vaccine coverage, compared to a 32.5% reduction in Vellore, which was the last to introduce the vaccine and hence had the lowest overall vaccine coverage among the five sites.

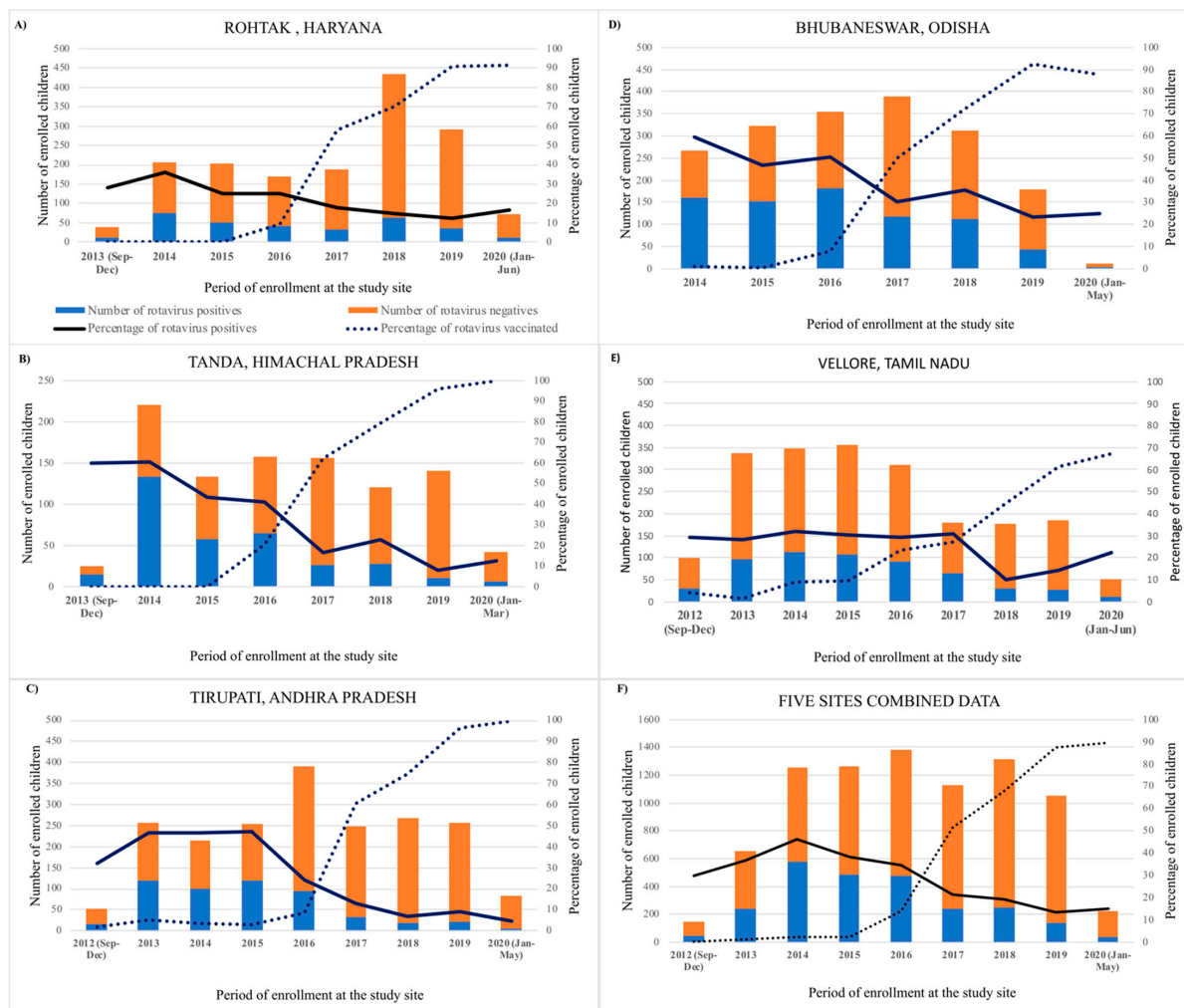


**Figure 1.** Impact of rotavirus vaccine after its introduction into the universal immunization programme in India, pre-vaccination and post-vaccination introduction surveillance comparison data from study sites at Rohtak (A), Tandak (B), Tirupati (C) Bhubaneswar (D), Vellore (E), and all the sites combined (F).

## 2.2. Rotavirus Genotype Distribution in India

During the study period, genotyping was performed for 76.04% of the samples. The proportion of positive samples tested by genotyping PCR was greater in the post-vaccination period (97.02%) compared to the pre-vaccination period (64.97%), when the protocol changed for genotyping of a subset of samples.

G1P[8] was the most common strain (49.5%) in the pre-vaccine period. The other common genotypes were G2P[4] (8%), G9P[4] (7.5%), G9P[8] (4.5%), and G12P[6] (3.8%). Conversely, G3P[8] (44.3%) was the most common genotype in the post-vaccine period, with G1P[8] (15.4%), G2P[4] (7.4%), G9P[4] (4.9%), and G1P[6] (3.7%) being the next most common genotypes (Figure 2). Marked yearly changes were seen among the circulating strains. Circulation of G9P[8] peaked during the year 2013, while G12P[6] increased in 2014/2015. Some reassortant strains like G1P[4], G2P[6], G2P[8], G3P[4], G3P[6], and G4P[6] were occasionally reported during the study period (Figure 2).

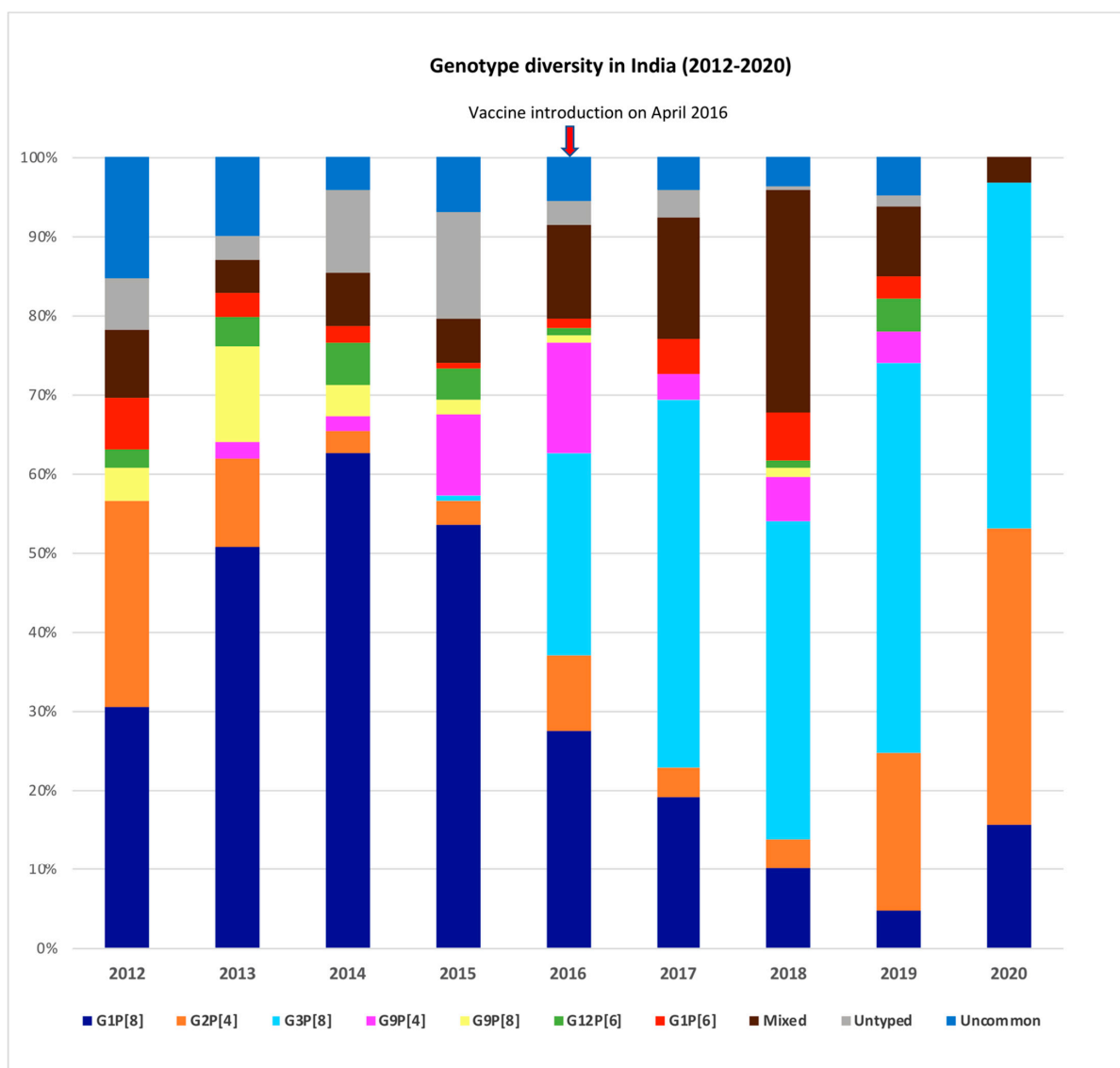


**Figure 2.** Data represented as the proportion of a specific genotype compared to the total genotype results. Uncommon genotype: <1% of total results; Mixed genotypes: those with >1 G or P-type; Untypables: those with either G or P untyped.

The genotype distribution also varied across the sentinel sites in North India (Tanda and Rohtak) and South India (Vellore, Tirupati, and Bhubaneswar). G1P[6] was seen predominantly in northern sites, while G9P[8] and G12P[6] were seen in southern sites

during the pre-vaccination period. In the post-vaccination period, the major circulating strains remained the same in northern sites, with G3P[8] topping the list. G3P[8] emerged in the southern sites as well, with a decline in G9P[8] and G12P[6] (Figure 3).

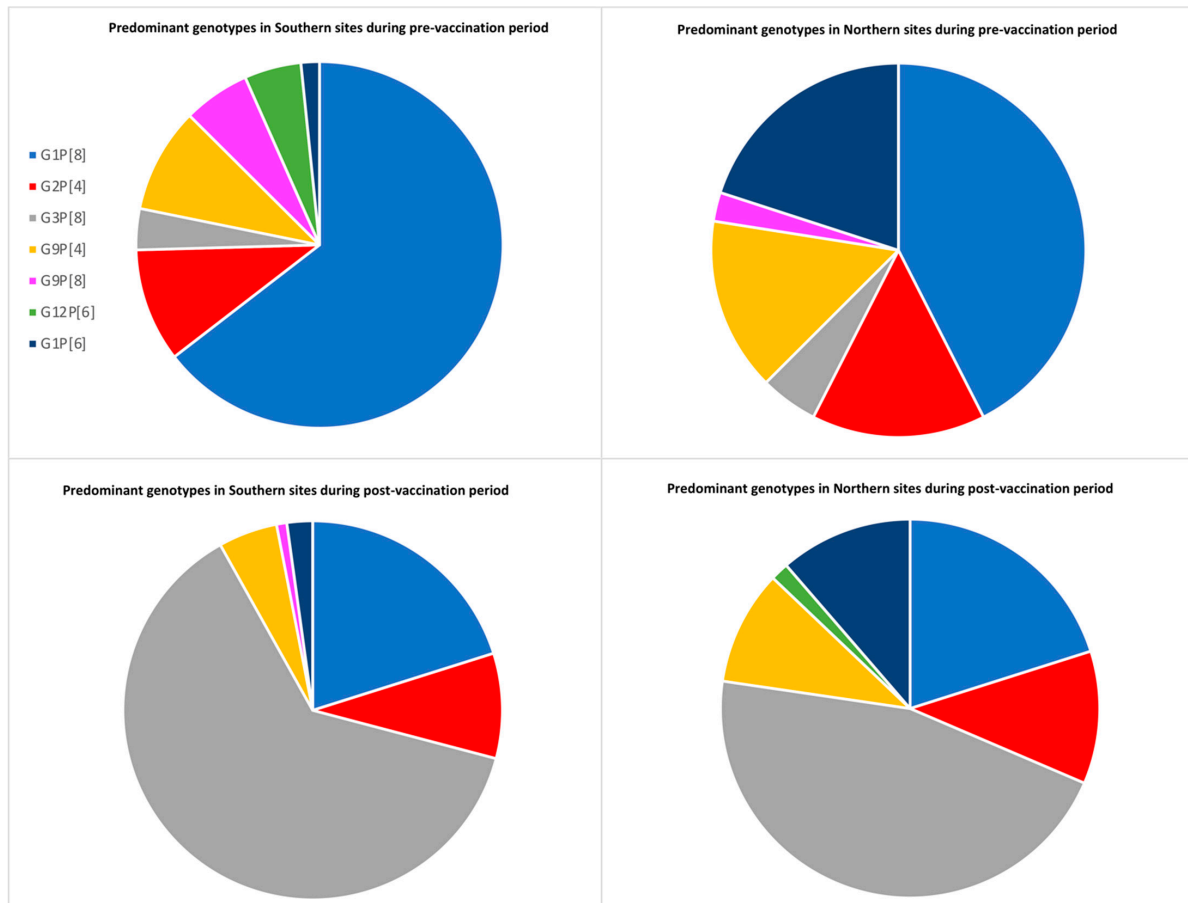


**Figure 3.** Comparison of genotype distribution between Northern sites (Tanda and Rohtak) and Southern sites (Vellore, Tirupati and Bhubaneswar). The major genotypes are compared during pre-vaccination (September 2012–April 2016) and post-vaccination period (May 2016–June 2020). The mixed genotype infections were excluded from the analysis.

An increased prevalence of G3P[8] and decreased prevalence of G1P[8] were noted in the post-vaccination period compared to the pre-vaccination period. G1P[8] peaked during the year 2014 (62.6%) and has declined steadily since then. G3P[8] started appearing in 2015 and was the predominant genotype in the following years. No novel strains were detected during the post-vaccination period. Mixed genotype infections occurred in a higher proportion in the post-vaccine period (17.4%) compared to the pre-vaccine period (6.4%). G1 (33%) was the most common G-type found in mixed infections, mainly in combination with G12 (10.8%) and G3 (9%). Similarly, P[8] (93.4%) was the most common P-type in mixed infections, along with P[4] (55.6%) and P[6] (37.8%).

### 3. Discussion

Pre- and post-introduction surveillance at five sites in India indicate that vaccination is impacting severe rotavirus gastroenteritis. The overall prevalence of rotavirus in children with hospitalized gastroenteritis decreased after vaccine introduction, reaching 13.3% by the third year post-vaccine introduction, indicating the effectiveness predicted by clinical trials and modeling [14,15]. The maximum reduction rate was seen in Tirupati (72.1%), and the minimum was observed in Vellore (32.45%), which are the sites with maximum and minimum vaccine coverage, respectively.

During the study period, from 2012 to 2020, the major genotypes were G1P[8], G3P[8], G2P[4], G9P[4], G9P[8], G12P[6], and G1P[6], which include some reassortants that are not common in other parts of the world. There was marked temporal fluctuation, with G9P[8] detected at a high frequency in 2013/2014, only to disappear by 2019/2020, while G12P[6] was high in 2014/2015. Our findings are consistent with surveillance data from India and neighboring countries that also saw the emergence of G12 strains [16]. We also noted a geographic variation, with G12P[6] and G9P[8] seen more in the southern sites in 2012-2016 and G1P[6] observed more in the northern sites. These findings are in agreement with other studies conducted in the northern and southern parts of India [17–20]. The genotypic pattern in the northern sites had a rise in G3P[8] in the post-vaccine period compared to the pre-vaccine period, along with the disappearance of G9P[8] and the emergence of G12P[6]. However, the southern sites had a greater proportion of G3P[8] in the post-vaccination period, with a decline in both G12P[6] and G9P[8]. Variation in the geographic and temporal trends of rotavirus strains emphasizes the importance of multicentric studies.

Changes in genotype distribution and increased diversity are seen with other rotavirus vaccines. In Brazil, G2P[4] emerged as the major strain, while no change in genotype distribution was seen in Kenya after Rotarix introduction [7,21]. An increase in G3P[8] strain prevalence was seen in the United States after RotaTeq introduction [21,22]. In our study, G1P[8] was the predominant strain in the pre-vaccine period, coinciding with other studies conducted during this period [17,23,24], which declined thereafter with the emergence of G3P[8]. However, the rise in G3P[8] in 2017/2018 is likely to be a natural fluctuation rather than the effect of the vaccine, as there was a similar trend seen in other countries without rotavirus immunization [25,26]. There are currently ongoing efforts to examine rotavirus vaccine effectiveness against diseases caused by specific strains, which will help further address this issue.

Globally, the rate of mixed rotavirus infections is similar to our findings [23,27]. Mixed rotavirus infections can facilitate the evolution of novel strains by genetic reassortment between the segmented genes of rotavirus, eventually increasing its diversity. Other studies have reported an increased frequency of unusual and novel strains in the post-vaccine surveillance period [24,28]. In our study, reassortant strains including G1P[4], G2P[6], G3P[6], G3P[4], and G4P[6] were occasionally seen, with no specific increase in the post-vaccination phase. Whole-genome sequencing and phylogenetic analysis will help to identify possible reassortment of rotavirus genes and detect mutational events. This will help us in tracking the virus evolution over time, which might give us more insight into the drivers of viral strain circulation and the impact of vaccines.

To conclude, our study showed a reduction in rotavirus diarrhea across five sites in India after Rotavac vaccine introduction. Changes in circulating strains with an increased rate of mixed infections were also seen in the post-vaccine period. In our study from 2016, additional methods were used for the genotyping of samples that remained untyped with standard laboratory protocols. Some of the differences in genotypes before and after vaccination introduction may have been caused by the change in genotyping methods. Due to the short period of surveillance, it is difficult to determine whether the changes were due to natural strain variations or vaccine pressure. Continued surveillance is warranted to determine the long-term effects of rotavirus vaccination.

## 4. Materials and Methods

### 4.1. Study Sites

Active hospital-based surveillance for diarrhea was established in five sentinel sites consisting of major referral hospitals from September 2012 to June 2020. The hospitals included were Christian Medical College (Vellore, Tamil Nadu), Sri Venkateshwara Medical College (Tirupati, Andhra Pradesh), Hi-Tech hospital (Bhubaneswar, Odisha), Pt. Bhagwat Dayal Sharma Postgraduate Institute of Medical Sciences (Rohtak, Haryana), and Rajendra Prasad Government Medical College (Tanda, Himachal Pradesh).

#### 4.2. Sample Collection and Laboratory Testing

Sample collection and laboratory methods are detailed in the study protocol [2]. In brief, children under 5 years of age hospitalized with diarrhea were enrolled in the study. A stool sample, vaccination card copy, and case report form with clinical and demographic details were collected from each child. Samples were stored at the appropriate temperature until transported to CMC, Vellore, which served as the main testing laboratory. All testing was done as per the modified WHO generic protocol for rotavirus surveillance [29]. Stool samples were screened for rotavirus VP6 antigen using a commercial enzyme immunoassay (EIA). All EIA positive samples were further characterized by reverse transcription-polymerase chain reaction (RT-PCR) for VP7 (G Type) and VP4 (P Type) genes. In brief, RNA was extracted from 20% fecal suspension using the QIAamp Viral RNA Mini Kit (Qiagen). Complementary DNA (cDNA) synthesized by reverse transcription using Moloney murine reverse transcriptase enzyme (Superscript II MMLV-RT, Invitrogen) and random primers (Invitrogen) were used as templates for VP7 and VP4 typing by a hemi-nested multiplex PCR using published primers [30,31]. For the samples collected in the post-vaccination period, additional typing methods were used if they remained untyped with standard laboratory testing protocols [32]. The negative samples by genotyping PCR were confirmed for rotavirus positivity by VP6 PCR [32]. The untyped samples and unusual rotavirus strains were sequenced by the Sanger sequencing method.

**Author Contributions:** Conceptualization, G.K., U.D.P., and J.E.T.; methodology, G.K., S.G., S.A.K., T.V.; software, S.V.; validation, G.K., S.G., C.P.G.K.; formal analysis, T.V.; investigation, all authors; resources, U.D.P., J.E.T., G.K.; data curation, S.V., V.R.M.; writing—original draft preparation, T.V.; writing—review and editing, G.K.; visualization, T.V., N.P.N., S.G.; supervision, S.G., R.A., G.K.; project administration, G.K.; funding acquisition, G.K., U.D.P., J.E.T. All authors have read and agreed to the published version of the manuscript.

**Funding:** This work was supported by the Indian Council of Medical Research [5/8-1(189)/TF/2011-12-ECD] and the Bill and Melinda Gates Foundation [OPP1053989]. SG was supported on TW0007392.

**Institutional Review Board Statement:** The study was conducted according to the guidelines of the Declaration of Helsinki and approved by the Institutional Review Board of Christian Medical College, Vellore, and all participating institutions.

**Informed Consent Statement:** Written informed consent was obtained from parents/guardian of all children enrolled in this study.

**Data Availability Statement:** Since the study is continuing in some settings, the data are still being generated and have not yet been placed in a public repository. The data analyzed during the period reported will be made available on request after de-identification.

**Acknowledgments:** We would like to thank the families of infants and children who participated in the surveillance study, the sentinel site study teams, and Christian Medical College laboratory team.

**Conflicts of Interest:** The authors declare no conflict of interest.

**Disclaimer:** The findings and conclusions in this report are those of the authors and do not necessarily represent the official position of the Centers for Disease Control and Prevention.

#### References

1. Parashar, U.D.; Gibson, C.J.; Bresee, J.S.; Glass, R.I. Rotavirus and Severe Childhood Diarrhea. *Emerg. Infect. Dis.* **2006**, *12*, 304–306. [[CrossRef](#)]
2. Nair, N.P.; Giri, S.; Mohan, V.R.; Parashar, U.; Tate, J.; Shah, M.P.; Arora, R.; Gupte, M.; Mehendale, S.M. Rotavirus vaccine impact assessment surveillance in India: Protocol and methods. *BMJ Open* **2019**, *9*, e024840. [[CrossRef](#)]
3. Santos, N.; Hoshino, Y. Global distribution of rotavirus serotypes/genotypes and its implication for the development and implementation of an effective rotavirus vaccine. *Rev. Med. Virol.* **2004**, *15*, 29–56. [[CrossRef](#)] [[PubMed](#)]
4. Burke, R.M.; Tate, J.E.; Kirkwood, C.D.; Steele, A.D.; Parashar, U.D. Current and new rotavirus vaccines. *Curr. Opin. Infect. Dis.* **2019**, *32*, 435–444. [[CrossRef](#)] [[PubMed](#)]

5. Zeller, M.; Rahman, M.; Heylen, E.; De Coster, S.; De Vos, S.; Arijs, I.; Novo, L.; Verstappen, N.; Van Ranst, M.; Matthijnsens, J. Rotavirus incidence and genotype distribution before and after national rotavirus vaccine introduction in Belgium. *Vaccine* **2010**, *28*, 7507–7513. [[CrossRef](#)]
6. Hungerford, D.; Allen, D.J.; Nawaz, S.; Collins, S.; Ladhani, S.; Vivancos, R.; Iturriza-Gómara, M. Impact of rotavirus vaccination on rotavirus genotype distribution and diversity in England, September 2006 to August 2016. *Eurosurveillance* **2019**, *24*, 1700774. [[CrossRef](#)]
7. Mwangi, M.J.; Owor, B.E.; Ochieng, J.B.; Ngama, M.H.; Ogwel, B.; Onyango, C.; Juma, J.; Njeru, R.; Gicheru, E.; Otieno, G.P.; et al. Rotavirus group A genotype circulation patterns across Kenya before and after nationwide vaccine introduction, 2010–2018. *BMC Infect. Dis.* **2020**, *20*, 1–12. [[CrossRef](#)]
8. Markkula, J.; Hemming-Harlow, M.; Salminen, M.T.; Savolainen-Kopra, C.; Pirhonen, J.; Al-Hello, H.; Vesikari, T. Rotavirus epidemiology 5–6 years after universal rotavirus vaccination: Persistent rotavirus activity in older children and elderly. *Infect. Dis.* **2017**, *49*, 388–395. [[CrossRef](#)]
9. Verberk, J.; Bruijning-Verhagen, P.; de Melker, H.E. *Rotavirus in the Netherlands: Background information for the Health Council; National Institute for Public Health and the Environment; RIVM: Bilthoven, The Netherlands*, 2017. [[CrossRef](#)]
10. Kaplon, J.; Grangier, N.; Pillet, S.; Minoui-Tran, A.; Vabret, A.; Wilhelm, N.; Prieur, N.; Lazrek, M.; Alain, S.; Mekki, Y.; et al. Predominance of G9P[8] rotavirus strains throughout France, 2014–2017. *Clin. Microbiol. Infect.* **2018**, *24*, 660.e1–660.e4. [[CrossRef](#)]
11. Malik, A.; Haldar, P.; Ray, A.; Shet, A.; Kapuria, B.; Bhadana, S.; Santosham, M.; Ghosh, R.S.; Steinglass, R.; Kumar, R. Introducing rotavirus vaccine in the Universal Immunization Programme in India: From evidence to policy to implementation. *Vaccine* **2019**, *37*, 5817–5824. [[CrossRef](#)] [[PubMed](#)]
12. Kang, G.; Arora, R.; Chitambar, S.D.; Deshpande, J.; Gupte, M.D.; Kulkarni, M.; Naik, T.N.; Mukherji, D.; Venkatasubramanian, S.; Gentsch, J.R.; et al. Multicenter, Hospital-Based Surveillance of Rotavirus Disease and Strains among Indian Children Aged. *J. Infect. Dis.* **2009**, *200* (Suppl. 1), S147–S153. [[CrossRef](#)]
13. Mehendale, S.; Venkatasubramanian, S.; Kumar, C.P.G.; Kang, G.; Gupte, M.D.; Arora, R. Expanded Indian national rotavirus surveillance network in the context of rotavirus vaccine introduction. *Indian Pediatr.* **2016**, *53*, 575–581. [[CrossRef](#)] [[PubMed](#)]
14. Bhandari, N.; Rongsen-Chandola, T.; Bavdekar, A.; John, J.; Antony, K.; Taneja, S.; Goyal, N.; Kawade, A.; Kang, G.; Rathore, S.S.; et al. Efficacy of a monovalent human-bovine (116E) rotavirus vaccine in Indian infants: A randomised, double-blind, placebo-controlled trial. *Lancet* **2014**, *383*, 2136–2143. [[CrossRef](#)]
15. Debellut, F.; Jaber, S.; Bouzuya, Y.; Sabbah, J.; Barham, M.; Abu-Awwad, F.; Hjajja, D.; Ramlawi, A.; Pecenka, C.; Clark, A.; et al. Introduction of rotavirus vaccination in Palestine: An evaluation of the costs, impact, and cost-effectiveness of ROTARIX and ROTAVAC. *PLoS ONE* **2020**, *15*, e0228506. [[CrossRef](#)]
16. Giri, S.; Kumar, C.P.G.; Khakha, S.A.; Chawla-Sarkar, M.; Gopalkrishna, V.; Chitambar, S.D.; Ray, P.; Venkatasubramanian, S.; Borkakoty, B.J.; National Rotavirus Surveillance Network investigators; et al. Diversity of rotavirus genotypes circulating in children <5 years of age hospitalized for acute gastroenteritis in India from 2005 to 2016: Analysis of temporal and regional genotype variation. *BMC Infect. Dis.* **2020**, *20*, 740. [[CrossRef](#)] [[PubMed](#)]
17. Jain, S.; Thakur, N.; Vashist, J.; Grover, N.; Krishnan, T.; Changotra, H. Predominance of unusual rotavirus G1P[6] strain in North India: An evidence from hospitalized children and adult diarrheal patients. *Infect. Genet. Evol.* **2016**, *46*, 65–70. [[CrossRef](#)] [[PubMed](#)]
18. Babji, S.; Arumugam, R.; Priyhemavathy, R.; Sriraman, A.; Sarvanabhavan, A.; Manickavasagam, P.; Simon, A.; Aggarwal, I.; Moses, P.D.; Arora, R.; et al. Genotype distribution of Group A rotavirus from southern India, 2005–2016. *Vaccine* **2018**, *36*, 7816–7819. [[CrossRef](#)]
19. Giri, S.; Nair, N.P.; Mathew, A.; Manohar, B.; Simon, A.; Singh, T.; Kumar, S.S.; Mathew, M.A.; Babji, S.; Arora, R.; et al. Rotavirus gastroenteritis in Indian children < 5 years hospitalized for diarrhoea, 2012 to 2016. *BMC Public Health* **2019**, *19*, 69. [[CrossRef](#)]
20. Tiku, V.R.; Sharma, S.; Verma, A.; Kumar, P.; Raghavendhar, S.; Aneja, S.; Paul, V.K.; Bhan, M.K.; Ray, P. Rotavirus diversity among diarrheal children in Delhi, India during 2007–2012. *Vaccine* **2014**, *32*, A62–A67. [[CrossRef](#)]
21. Carvalho-Costa, F.A.; Volotão, E.D.M.; de Assis, R.M.S.; Fialho, A.M.; Andrade, J.D.S.R.D.; Rocha, L.N.; Tort, L.F.L.; da Silva, M.F.M.; Gómez, M.M.; de Souza, P.M.; et al. Laboratory-based Rotavirus Surveillance During the Introduction of a Vaccination Program, Brazil, 2005–2009. *Pediatr. Infect. Dis. J.* **2011**, *30*, S35–S41. [[CrossRef](#)]
22. Hull, J.J.; Teel, E.N.; Kerin, T.K.; Freeman, M.M.; Esona, M.D.; Gentsch, J.R.; Cortese, M.M.; Parashar, U.D.; Glass, R.I.; Bowen, M.D. United States Rotavirus Strain Surveillance from 2005 to 2008. *Pediatr. Infect. Dis. J.* **2011**, *30*, S42–S47. [[CrossRef](#)] [[PubMed](#)]
23. Bányai, K.; László, B.; Duque, J.; Steele, A.D.; Nelson, E.A.S.; Gentsch, J.R.; Parashar, U.D. Systematic review of regional and temporal trends in global rotavirus strain diversity in the pre rotavirus vaccine era: Insights for understanding the impact of rotavirus vaccination programs. *Vaccine* **2012**, *30*, A122–A130. [[CrossRef](#)] [[PubMed](#)]
24. Roczo-Farkas, S.; Kirkwood, C.D.; Cowley, D.; Barnes, G.L.; Bishop, R.F.; Bogdanovic-Sakran, N.; Boniface, K.; Donato, C.M.; Bines, J.E. The Impact of Rotavirus Vaccines on Genotype Diversity: A Comprehensive Analysis of 2 Decades of Australian Surveillance Data. *J. Infect. Dis.* **2018**, *218*, 546–554. [[CrossRef](#)] [[PubMed](#)]
25. Sadiq, A.; Bostan, N.; Bokhari, H.; Matthijnsens, J.; Yinda, K.C.; Raza, S.; Nawaz, T. Molecular characterization of human group A rotavirus genotypes circulating in Rawalpindi, Islamabad, Pakistan during 2015–2016. *PLoS ONE* **2019**, *14*, e0220387. [[CrossRef](#)]
26. Umair, M.; Salman, M.; Alam, M.M.; Rana, M.S.; Zaidi, S.S.Z.; Bowen, M.D.; Aamir, U.B.; Abbasi, B.H. Rotavirus surveillance in Pakistan during 2015–2016 reveals high prevalence of G12P[6]. *J. Med. Virol.* **2018**, *90*, 1272–1276. [[CrossRef](#)] [[PubMed](#)]

27. Nyaga, M.M.; Jere, K.C.; Esona, M.D.; Seheri, M.L.; Stucker, K.M.; Halpin, R.A.; Akopov, A.; Stockwell, T.B.; Peenze, I.; Diop, A.; et al. Whole genome detection of rotavirus mixed infections in human, porcine and bovine samples co-infected with various rotavirus strains collected from sub-Saharan Africa. *Infect. Genet. Evol.* **2015**, *31*, 321–334. [[CrossRef](#)]
28. Tanaka, T.; Kamiya, H.; Asada, K.; Suga, S.; Ido, M.; Umemoto, M.; Ouchi, K.; Ito, H.; Kuroki, H.; Nakano, T.; et al. Changes in Rotavirus Genotypes before and after Vaccine Introduction: A Multicenter, Prospective Observational Study in Three Areas of Japan. *Jpn. J. Infect. Dis.* **2017**, *70*, 448–452. [[CrossRef](#)] [[PubMed](#)]
29. World Health Organization. Manual of Rotavirus Detection and Characterization Methods. (2009)WHO\_IVB\_08.17\_eng.Pdf. Available online: [https://apps.who.int/iris/bitstream/handle/10665/70122/WHO\\_IVB\\_08.17\\_eng.pdf?sequence=1](https://apps.who.int/iris/bitstream/handle/10665/70122/WHO_IVB_08.17_eng.pdf?sequence=1) (accessed on 19 March 2021).
30. Kang, G.; Desai, R.; Arora, R.; Chitamabar, S.; Naik, T.N.; Krishnan, T.; Deshpande, J.; Gupte, M.D.; Venkatasubramaniam, S.; Gentsch, J.R.; et al. Diversity of circulating rotavirus strains in children hospitalized with diarrhea in India, 2005–2009. *Vaccine* **2013**, *31*, 2879–2883. [[CrossRef](#)]
31. Iturriza-Gomara, M.; Green, J.; Brown, D.; Desselberger, U.; Gray, J. Comparison of specific and random priming in the reverse transcriptase polymerase chain reaction for genotyping group A rotaviruses. *J. Virol. Methods* **1999**, *78*, 93–103. [[CrossRef](#)]
32. Babji, S.; Arumugam, R.; Sarvanabhavan, A.; Gentsch, J.R.; Kang, G. Approach to molecular characterization of partially and completely untyped samples in an Indian rotavirus surveillance program. *Vaccine* **2014**, *32*, A84–A88. [[CrossRef](#)]



Article

# Molecular Epidemiology of Rotavirus A Strains Pre- and Post-Vaccine (Rotarix<sup>®</sup>) Introduction in Mozambique, 2012–2019: Emergence of Genotypes G3P[4] and G3P[8]

Eva D. João <sup>1,2,\*</sup>, Benilde Munlela <sup>1,3</sup>, Assucênio Chissaque <sup>1,2</sup>, Jorfélia Chilaúle <sup>1</sup>, Jerónimo Langa <sup>1</sup>, Orvalho Augusto <sup>4,5</sup>, Simone S. Boene <sup>1,3</sup>, Elda Anapakala <sup>1</sup>, Júlia Sambo <sup>1,2</sup>, Esperança Guimarães <sup>1,2</sup>, Diocreciano Bero <sup>1</sup>, Marta Cassocera <sup>1,2</sup>, Idalécia Cossa-Moiane <sup>1</sup>, Jason M. Mwenda <sup>6</sup>, Isabel Maurício <sup>2,7</sup>, Hester G. O'Neill <sup>8</sup> and Nilsa de Deus <sup>1,9</sup>

<sup>1</sup> Instituto Nacional de Saúde (INS), Maputo 1008, Mozambique; benildeantnio@gmail.com (B.M.); assucenyoo@gmail.com (A.C.); Jorfeliachilaule@gmail.com (J.C.); langajeronimo@gmail.com (J.L.); simonboene@gmail.com (S.S.B.); elda.muianga07@gmail.com (E.A.); juliassiat@yahoo.com.br (J.S.); espeguima@hotmail.com (E.G.); dmbero@gmail.com (D.B.); marti.life@hotmail.com (M.C.); idaleciacossa@yahoo.com.br (I.C.-M.); ndeus1@yahoo.com (N.d.D.)

<sup>2</sup> Instituto de Higiene e Medicina Tropical, Universidade Nova de Lisboa, 1349-008 Lisbon, Portugal; isabel.mauricio@ihmt.unl.pt

<sup>3</sup> Centro de Biotecnologia, Universidade Eduardo Mondlane, Maputo 3453, Mozambique

<sup>4</sup> Faculdade de Medicina, Universidade Eduardo Mondlane, Maputo, P.O. Box 257, Mozambique; orvaquim@gmail.com

<sup>5</sup> Harris Hydraulics Laboratory, Department of Global Health, University of Washington, Seattle, WA 98195-7965, USA

<sup>6</sup> African Rotavirus Surveillance Network, Immunization, Vaccines and Development Program, WHO Regional Office for Africa, Brazzaville, P.O. Box 2465, Congo; mwendaj@who.int

<sup>7</sup> Global Health and Tropical Medicine, Instituto de Higiene e Medicina Tropical, Universidade Nova de Lisboa, 1349-008 Lisbon, Portugal

<sup>8</sup> Department of Microbial, Biochemical and Food Biotechnology, University of the Free State, Bloemfontein 9301, South Africa; oneillhg@ufs.ac.za

<sup>9</sup> Departamento de Ciências Biológicas, Universidade Eduardo Mondlane, Maputo 3453, Mozambique

\* Correspondence: evadora1@hotmail.com; Tel.: +258-827479229

Received: 1 July 2020; Accepted: 14 August 2020; Published: 19 August 2020



**Abstract:** Group A rotavirus (RVA) remains the most important etiological agent associated with severe acute diarrhea in children. *Rotarix*<sup>®</sup> monovalent vaccine was introduced into Mozambique's Expanded Program on Immunization in September 2015. In the present study, we report the diversity and prevalence of rotavirus genotypes, pre- (2012–2015) and post-vaccine (2016–2019) introduction in Mozambique, among diarrheic children less than five years of age. Genotyping data were analyzed for five sentinel sites for the periods indicated. The primary sentinel site, Mavalane General Hospital (HGM), was analyzed for the period 2012–2019, and for all five sites (country-wide analyses), 2015–2019. During the pre-vaccine period, G9P[8] was the most predominant genotype for both HGM (28.5%) and the country-wide analysis (46.0%). However, in the post-vaccine period, G9P[8] was significantly reduced. Instead, G3P[8] was the most common genotype at HGM, while G1P[8] predominated country-wide. Genotypes G9P[4] and G9P[6] were detected for the first time, and the emergence of G3P[8] and G3P[4] genotypes were observed during the post-vaccine period. The distribution and prevalence of rotavirus genotypes were distinct in pre- and post-vaccination periods, while uncommon genotypes were also detected in the post-vaccine period. These observations support the need for continued country-wide surveillance to monitor changes in strain diversity, due to possible vaccine pressure, and consequently, the effect on vaccine effectiveness.

**Keywords:** rotavirus type A; Mozambique vaccine surveillance; G3 genotype; Rotarix

---

## 1. Introduction

Group A rotavirus (RVA) remains the most important etiological agent associated with severe acute diarrhea in children worldwide [1–3]. In 2016, RVA was estimated to cause more than 128,000 deaths among children younger than five years throughout the world, with more than 104,000 deaths occurring in sub-Saharan Africa [3].

RVA is a non-enveloped, double-stranded RNA virus. The segmented genome has 11 gene segments which encode six structural viral proteins (VP1, VP2, VP3, VP4, VP6, and VP7) and six non-structural viral proteins (NSP1, NSP2, NSP3, NSP4, and NSP5/6) [4–6]. The viral capsid is composed of three concentric layers which encapsulate the 11-segmented genome. The outer layer is composed of the viral spike protein, protease-sensitive VP4, and glycoprotein VP7. A dual typing system for RVA is based on the gene segments encoding VP4 (P genotypes) and VP7 (G types). The rotavirus classification-working group has identified 36 G and 51 P genotypes globally in humans and in the young of many mammalian and avian species [7–10]. Six G types (G1, G2, G3, G4, G9, G12) and 3 P types (P[8], P[4], P[6]) predominate globally [11–14], although in Africa and Asia genotypes, such as G5, G6, and G8, are also described as important [15]. The six most frequently reported G/P combinations associated with infections in humans worldwide are G1P[8], G2P[4], G3P[8], G4P[8], G9P[8], and G12P[8] [10–14,16].

In 2009, the World Health Organization (WHO) recommended the introduction of rotavirus vaccines in national immunization programs worldwide and particularly in countries with a high under-five mortality rate associated with diarrhea [17]. The WHO has coordinated the Global Network of Rotavirus surveillance (GNRS) since 2006 to support countries with evidence-based decision-making [10]. Mozambique has actively participated in WHO rotavirus surveillance since 2016. Continuous surveillance of circulating genotypes, as well as the monitoring of disease burden, is important to evaluate the effectiveness of rotavirus vaccines.

Before the introduction of rotavirus vaccines, a high rotavirus disease burden was reported in particular the southern Mozambican region. However, due to a lack of surveillance, no information was available from the center and northern regions of the country [18–20]. In the Global Enteric Multicenter Study (GEMS), which determined the burden and etiology of diarrhea in children under five years of age in four sub-Saharan African and three Asian countries, Mozambique had the highest attributable fraction (27.0%) of rotavirus-associated diarrhea among infants [20]. In Mozambique, the prevalence of rotavirus in under-five year old children from urban (Maputo City) and rural (Manhiça District) areas in 2012 and 2013 was higher than 40.0% [19]. A lower infection rate (24.0%) was, however, reported in 2011 in Gaza province, a rural area [18]. Data from the National Surveillance of Diarrhea also showed a high rotavirus infection rate of 40.2% and 38.3% in 2014 and 2015, respectively, before vaccine introduction in Mozambique [21]. The monovalent vaccine, *Rotarix*<sup>®</sup> (GlaxoSmithKline, Rixensart, Belgium), was introduced into the Expanded Program on Immunization of Mozambique in September 2015. Since then, the prevalence of rotavirus infections of 12.2% and 13.5% in 2016 and 2017, respectively, has been reported [21].

The evolution of RVA through the accumulation of point mutations, gene reassortment, recombination and interspecies transmission [5,22,23], call for rotavirus strain surveillance to elucidate the effect, if any, of rotavirus vaccine usage on the circulation of rotavirus genotypes in Mozambique. The main objective of the present study was to evaluate the distribution of rotavirus genotypes prior to (2012–2015) and following (2016–2019) rotavirus vaccine introduction in Mozambique, among diarrheic children less than five years of age.

## 2. Results

### 2.1. Comparison of Rotavirus G- and P-Types in Mozambique Pre- and Post-Vaccine Introduction

From May 2014 to December 2019, a total of 1736 diarrheal stool samples were collected in five sentinel sites as part of the National Surveillance of Diarrhea program in Mozambique. Of these stool samples, 468 tested positive for RVA by ELISA (27.0%) (Supplementary Table S1). A total of 94.0% (440/468) of these samples were genotyped,  $n = 245$  from Maputo (HGM and HJM),  $n = 149$  from Nampula (HCN),  $n = 34$  from Quelimane (HGQ) and  $n = 12$  from Beira (HCB) (Supplementary Table S2). During the pre-vaccine period (2014–2015) a total of 246 samples were genotyped and in the post-vaccine period (2016–2019) 194 samples (Supplementary Table S1). In total, 6.0% (28/468) were excluded from genotyping as an insufficient amount of sample was available.

For HGM, a total of 200 genotyped samples corresponded to the pre-vaccine period (2012–2015) and 43 to the post-vaccine period (2016–2019) (Supplementary Table S3). The samples from the pre-vaccine period also included 91 genotyped samples collected at HGM between 2012 and 2013 from a cross-sectional study [24] to extend the analyses for this particular site (Supplementary Table S3).

The analyses for HGM showed that G9 was the most prevalent G type (30.5%) in the pre-vaccine period ( $n = 200$ ), but was significantly reduced to 9.3% during the post-vaccination period ( $n = 43$ ). Similarly, G12 was also significantly reduced (from 18.5% to 2.3%) (Table 1). In contrast, during the pre-vaccination period, no G3 strains were detected; but during the post-vaccine period, the genotype was the most prevalent genotype (48.8%). Interestingly, a small increase in prevalence was observed for the G1 genotype, although this increase was not statistically significant (Table 1).

**Table 1.** Prevalence of G and P types at Mavalane General Hospital pre- and post-vaccine introduction in Mozambique (2012–2019).

<sup>1</sup> G Type	Pre-Vaccine		Post-Vaccine		OR (95% CI)	p-Value
	<sup>5</sup> 2012–2015 n	%	2016–2019 n	%		
G1	34	<b>17.0</b>	10	<b>23.3</b>	1.47 (0.59–3.44)	0.330
G12	37	<b>18.5</b>	1	2.3	0.10 (0.003–0.66)	0.008
G2	25	<b>12.5</b>	1	2.3	0.16 (0.004–1.08)	0.054
G3	0	0.0	21	<b>48.8</b>	-	-
G8	6	3.0	1	2.3	0.76 (0.02–6.61)	0.810
G9	61	<b>30.5</b>	4	9.3	0.23 (0.01–0.69)	0.004
<sup>2</sup> Mix G	10	5.0	1	2.3	0.45 (0.01–3.30)	0.440
<sup>3</sup> Gx	27	13.5	4	9.3	0.65 (0.16–2.04)	0.450
Total	200	100.0	43	100.0	-	-
<sup>1</sup> P type	-	-	-	-	-	-
P[4]	31	15.5	16	<b>37.2</b>	3.23 (1.44–7.04)	<0.001
P[6]	32	16.0	3	7.0	0.39 (0.07–1.36)	0.120
P[8]	108	<b>54.0</b>	22	<b>51.2</b>	0.89 (0.43–1.83)	0.740
Mix P	8	4.0	0	0.0	-	-
<sup>4</sup> P[x]	21	10.5	2	4.7	0.42 (0.05–0.82)	0.230
Total	200	100.0	43	100.0	-	-

<sup>1</sup> It is not possible to calculate the Odds-ratio (OR) for cells with a value of 0; <sup>2</sup> Mix G: 2012–2015: G12G8 (2.0%), G12G9 (1.5%), G9G2 (1.5%); 2016–2019: G12G3 (2.3%); <sup>3</sup> x—refers to strains that were non-typeable for G; <sup>4</sup> x—refers to strains that were non-typeable for P; <sup>5</sup> Reference category: Pre-vaccine; Bold: The most prevalent genotypes per period.

P[8] was the most predominant P type in the pre-vaccine period (54.0%) (Table 1), as well as the post-vaccine period (51.2%). Only P[4] (37.2%) (Table 1) had a statistically significant increase during the post-vaccine period ( $p < 0.001$ ). No mixed P types were detected during the post-vaccine period.

When all five sentinel sites (including HGM) were analyzed for the period of 2015–2019, a similar trend was observed for the G9 genotype. During the pre-vaccine period ( $n = 213$ ), G9 was the

most prevalent G type at 49.3%, but a significant reduction for G9 (25.3%) was reported during the post-vaccine period ( $n = 194$ ). The emergence of G3 was also observed, becoming the most prevalent genotype, although only at 26.3% (Table 2). In contrast, a reduction in the prevalence of the G1 genotype was observed (31.5% reduced to 21.6%) for all five sentinel sites.

**Table 2.** Prevalence of G and P types at five sentinel sites in Mozambique during surveillance pre- and post-vaccine introduction (2015–2019).

<sup>1</sup> G Type	<sup>5</sup> Pre-Vaccine		Post-Vaccine		OR (95% CI)	p-Value
	2015		2016–2019			
	n	%	n	%		
G1	67	<b>31.5</b>	42	<b>21.6</b>	0.60 (0.37–0.96)	0.030
G12	2	0.9	2	1.0	1.18 (0.08–15.29)	0.930
G2	10	4.7	11	5.7	1.22 (0.46–3.28)	0.660
G3	0	0	51	<b>26.3</b>	-	-
G8	0	0	3	1.5	-	-
G9	105	<b>49.3</b>	49	<b>25.3</b>	0.35 (0.22–0.54)	<0.001
<sup>2</sup> Mix G	0	0	12	6.2	-	-
<sup>3</sup> Gx	29	13.6	24	12.4	0.90 (0.48–1.66)	0.710
Total	213	100.0	194	100.0	-	-
<sup>1</sup> P type	-	-	-	-	-	-
P[4]	1	0.5	71	<b>36.6</b>	-	-
P[6]	10	4.7	37	19.1	4.78 (2.23–11.10)	<0.001
P[8]	182	<b>85.4</b>	76	<b>39.2</b>	0.10 (0.06–0.16)	<0.001
<sup>4</sup> P[x]	20	9.4	10	5.2	0.57 (0.23–1.32)	0.100
Total	213	100.0	194	100.0	-	-

<sup>1</sup> It is not possible to calculate the Odds-ratio (OR) for cells with a value of 0; <sup>2</sup> Mix G—2016–2019: G12G3 (0.5%), G2G1 (0.5%), G3G1 (2.1%), G9G3 (3.1%); <sup>3</sup> x—refers to strains that were non-typeable for G; <sup>4</sup> x—Refers to strains that were non-typeable for P; <sup>5</sup> Reference category: Pre-vaccine; Bold: The most prevalent genotypes per period.

During the pre-vaccine period, P[8] was the most frequently detected P genotype accounting for 85.4% of all genotypes detected (Table 2). However, this high frequency was significantly reduced in the post-vaccination period to less than half (39.2%). An increase in the detection of P[6] (19.1%) and P[4] (36.6%), from almost undetectable, were recorded during this period (Table 2).

Analyses of the data recorded for samples collected at the HGM, showed a slight increase in the odds ratio for G1 type from pre-vaccine to the post-vaccine period of 1.47 times (OR = 1.47, 95CI = 0.59–3.44,  $p > 0.330$ ), but a decrease in the odds ratio for genotypes G12 of 90.0% (OR = 0.10, 95CI = 0.003–0.66,  $p < 0.008$ ) and G9 of 77.0% (OR = 0.23, 95CI = 0.01–0.69,  $p < 0.004$ ), respectively (Table 1). Considering all the sentinel sites, a significant decrease was observed in the odds ratio for G1 genotype from pre-vaccine to the post-vaccine period of 40.0% (OR = 0.60, 95CI = 0.37–0.96,  $p < 0.030$ ), as well as a reduction for G9 of 65.0% (OR = 0.35, 95CI = 0.22–0.54,  $p < 0.001$ ) (Table 2).

A reduction for genotype P[8] from pre-vaccine to the post-vaccine period was also observed at HGM (11.0%, OR = 0.89, 95CI = 0.43–1.83,  $p > 0.740$ , Table 1), as well as for the country-wide sentinel sites (90.0% (OR = 0.10, 95CI = 0.06 to 0.16,  $p < 0.001$ , Table 2). In contrast, a significant increase in the odds ratio of genotype P[4] of 3.23 times (OR = 3.23, 95CI = 1.44–7.04,  $p < 0.001$ ) was observed at the HGM (Table 1). Analyses for all the sentinel sites showed a high prevalence for P[4] during the post-vaccine period (36.6%) compared to the pre-vaccine period (0.5%).

## 2.2. Comparison of G/P Genotype Combinations in Mozambique Pre- and Post-Vaccine Introduction

At HGM, the most predominant combinations during the pre-vaccine period were G9P[8] (28.5%), G1P[8] (17.0%), G12P[6] (13.0%) and G2P[4] (10.0%), comprising a total of 68.5% of all genotypes analyzed (Table 3). During the post-vaccine period, G1P[8] (20.9%) was still one of the predominant combinations, although G3P[8] and G3P[4] strains were detected at 25.6% and 18.6%, respectively

(Table 3). A significant reduction in G9P[8] detection was observed following vaccine introduction ( $p < 0.001$ ). Instead, the G9 genotype was now detected in combination with P[4] and P[6] both at a frequency of 4.7% (Table 3).

**Table 3.** G/P type combinations prevalent at Mavalane General Hospital pre- and post-vaccine introduction in Mozambique (2012–2019).

<sup>1</sup> G/P Genotype Combination	<sup>5</sup> Pre-Vaccine		Post-Vaccine		OR (95% CI)	<i>p</i> -Value
	2012–2015		2016–2019			
	n	%	n	%		
G1P[8]	34	<b>17.0</b>	9	<b>20.9</b>	1.29 (0.50–3.07)	0.540
G9P[8]	57	<b>28.5</b>	1	2.3	0.06 (0.002–0.40)	< 0.001
G12P[6]	26	<b>13.0</b>	0	0.0	-	-
G2P[4]	20	10.0	1	2.3	0.21 (0.01–1.42)	0.100
G12P[8]	6	3.0	0	0.0	-	-
G3P[4]	0	0.0	8	<b>18.6</b>	-	-
G3P[8]	0	0.0	11	<b>25.6</b>	-	-
G8P[4]	5	2.5	1	2.3	0.93 (0.02–8.61)	0.950
G9P[4]	0	0.0	2	4.7	-	-
G9P[6]	0	0.0	2	4.7	-	-
<sup>2</sup> Other genotypes	5	2.5	3	7.0	2.93 (0.43–15.65)	0.140
<sup>3</sup> Mixed types	13	6.5	1	2.3	0.34 (0.01–2.41)	0.290
<sup>4</sup> Partial G/P types	20	10.0	2	4.7	0.44 (0.05–1.93)	0.270
Untypeables	14	7.0	2	4.7	0.64 (0.07–3.00)	0.570
Total	200	100.0	43	100.0	-	-

<sup>1</sup> It is not possible to calculate the Odds-ratio (OR) for cells with a value of 0; <sup>2</sup> Other genotypes: 2012–2015: G12P[4] (0.5%), G2P[6] (1.0%), G2P[8] (0.5%), G8P[8] (0.5%); 2016–2019: G1P[4] (2.3%), G3P[6] (2.3%), G12P[4] (2.3%); <sup>3</sup> Mixed types: 2012–2015: G12G8P[4] (1.0%), G12G8P[6] (0.5%), G12G8P[6]P[4] (0.5%), G12G9P[6] (0.5%), G12G9P[8]P[6] (1.0%), G12P[8]P[6] (1.0%), G9G2P[4] (0.5%), G9G2P[6] (0.5%), G9G2P[8] (0.5%), G9P[8]P[4] (0.5%); 2016–2019: G12G3P[4] (2.3%); <sup>4</sup> Partial G/P types: 2012–2015: G12P[x] (1.0%), G2P[x] (1.0%), G9P[x] (1.5%), GxP[4] (1.0%), GxP[6] (0.5%), GxP[6]P[4] (0.5%), GxP[8] (4.0%), GxP[8]P[6] (0.5%); 2016–2019: GxP[4] (2.3%), GxP[8] (2.3%); <sup>5</sup> Reference category: Pre-vaccine; Bold: The most prevalent genotypes per period.

The most frequent G/P combinations observed for all the sites participating in the National Surveillance of Diarrhea program during the pre-vaccine period were G9P[8] and G1P[8] at 46.0% and 31.0%, respectively. These combinations comprised a total of 77.0% of all genotypes analyzed (Table 4).

In the post-vaccine period, G1P[8] remained the most frequent G/P combination, but at a reduced frequency of 20.6%. G2P[4] (at a slightly higher frequency) and G2P[6] (similar frequency as in 2015) were, again, detected in the post-vaccine period. Similar to the analysis for HGM, G3 in combination with P[4] (14.4%) and P[8] (9.8%) were detected during the post-vaccine period, together with G9P[4] (12.4%) and G9P[6] (8.8%). Mixed infections, as determined with RT-PCR, was detected for 6.2% of the samples (Table 4).

Analyses for HGM showed an increase in the odds for G1P[8] at 1.29 times (95CI = 0.50–3.07,  $p > 0.54$ ), but a significant decrease in the odds ratio for G9P[8] at 94.0% (OR = 0.06, 95CI = 0.002–0.40,  $p < 0.001$ ) (Table 3).

In contrast, a significant decrease in the odds ratio for all the sentinel sites was observed for G1P[8] at 42.0% (OR = 0.58, 95CI = 0.36–0.93,  $p < 0.020$ ) and G9P[8] at 96.0% (OR = 0.04, 95CI = 0.02–0.10,  $p < 0.001$ ) (Table 4).

**Table 4.** G/P type combinations prevalent at five sentinel sites in Mozambique during surveillance pre- and post-vaccine introduction (2015–2019).

<sup>1</sup> G/P Genotype Combination	<sup>5</sup> Pre-Vaccine		Post-Vaccine		OR (95% CI)	p-Value
	2015		2016–2019			
	n	%	n	%		
G1P[8]	66	<b>31.0</b>	40	<b>20.6</b>	0.58 (0.36–0.93)	0.020
G3P[4]	0	0.0	28	<b>14.4</b>	-	-
G3P[6]	0	0.0	3	1.5	-	-
G3P[8]	0	0.0	19	9.8	-	-
G8P[4]	0	0.0	3	1.5	-	-
G9P[4]	0	0.0	24	<b>12.4</b>	-	-
G9P[6]	0	0.0	17	8.8	-	-
G2P[4]	1	0.5	3	1.5	-	-
G2P[6]	9	4.2	8	4.1	0.97 (0.32–2.91)	0.959
G9P[8]	98	<b>46.0</b>	7	3.6	0.04 (0.02–0.10)	<0.001
<sup>2</sup> Other genotypes	3	1.4	4	2.1	1.47 (0.25–10.18)	0.612
<sup>3</sup> Mixed types	0	0	12	6.2	-	-
<sup>4</sup> Partial G/P types	23	10.8	18	9.3	0.84 (0.41–1.70)	0.611
Untypeables	13	6.1	8	4.1	0.66 (0.23–1.77)	0.370
Total	213	100.0	194	100.0	-	-

<sup>1</sup> It is not possible to calculate the Odds-ratio (OR) for cells with a value of 0; <sup>2</sup> Other genotypes: 2015: G12P[8] (0.9%), G1P[6] (0.5%); 2016–2019: G12P[4] (0.5%), G12P[8] (0.5%), G1P[4] (1.0%); <sup>3</sup> Mixed types: 2016–2019: G12G3P[4] (0.5%), G2G1P[8] (0.5%), G3G1P[8] (2.6%), G9G3P[6] (2.6%); <sup>4</sup> Partial G/P types: 2015: G9P[x] (3.3%), GxP[6] (0.5%), GxP[8] (7.0%); 2016–2019: G9P[x] (1.0%), GxP[4] (4.6%), GxP[6] (1.6%), GxP[8] (2.1%); <sup>5</sup> Reference category: Pre-vaccine; Bold: The most prevalent genotypes per period.

### 2.3. Yearly Distribution of Rotavirus Genotypes at the Mavalane General Hospital (HGM) and National Surveillance Sites

As reported before, G12P[6] (28.6%) and G2P[4] (23.1%) were the most predominant genotype combinations at HGM during 2012–2013 [24]. In 2014 and 2015, G1P[8] and G9P[8] with 84.8% and 73.7%, respectively, were detected at the highest frequencies. In 2016, during the post-vaccine period, the most frequent genotype was G1P[8] with 66.7%. The emergence of new genotypes was observed in 2016 (G3P[4]), which increased in 2017, to the most prevalent genotype (25.0%) followed by G1P[8] (18.8%) (Table 5). In 2018, G3P[8] and G3P[4] became the most prevalent genotype combinations with 36.4% and 27.3%, respectively. Finally, in 2019, only G3P[8] were detected at the HGM. No G1P[8] strains were, therefore, detected in 2018 and 2019 (Table 5).

Since data is available for only one year for all five participating sentinel sites during the pre-vaccine period, yearly analysis for the national surveillance sites are presented from 2015–2019. The results showed that in 2015 the most frequent G/P combination was G9P[8] (46.0%), followed by G1P[8] (31.0%). In 2016, G1P[8] was detected at the highest frequency (43.6%) (Table 6). Other genotype combinations, such as G2P[6] (17.9%), G9P[6] (12.8%), G9P[4] (7.7%), and G3P[4] (2.6%), were also observed in 2016 (Table 6). These results were comparable to those from HGM.

In 2017, G1P[8], as well as G9P[4], were detected at similar frequencies (19.2%), while G3P[4] was detected at 13.5% (Table 6). In 2018 and 2019, G3P[4] and G3P[8] became the most frequently detected genotype combination with 38.7% and 60.0%, respectively (Table 6). G3 was also observed in combination with P[4] (13.5%) and P[6] (1.9%) in 2017, whereas G1P[8] genotype was not detected in 2018, although this genotype was detected at 15.0% in 2019 (Table 6). The results reported for all the sentinel sites participating in the National Surveillance of Diarrhea program is comparable to that observed for HGM for the reporting period (2015–2019), except that G1P[8] was not detected in 2019 for HGM.

**Table 5.** Prevalence of G/P type combinations at Mavalane General Hospital in Mozambique by year.

G/P Genotype Combination	2012		2013		2014		2015		2016		2017		2018		2019	
	n	%	n	%	n	%	n	%	n	%	n	%	n	%	n	%
G1P[8]	2	3.0	0	0.0	28	84.8	4	5.3	6	66.7	3	18.8	0	0.0	0	0.0
G9P[8]	1	1.5	0	0.0	0	0.0	56	73.7	0	0.0	1	6.3	0	0.0	0	0.0
G12P[6]	26	38.8	0	0.0	0	0.0	0	0.0	0	0.0	0	0.0	0	0.0	0	0.0
G2P[4]	5	7.5	16	66.7	0	0.0	0	0.0	0	0.0	0	0.0	1	9.1	0	0.0
G12P[8]	5	7.5	0	0.0	0	0.0	1	1.3	0	0.0	0	0.0	0	0.0	0	0.0
G3P[4]	0	0	0	0.0	0	0.0	0	0.0	1	11.1	4	25.0	3	27.3	0	0.0
G3P[8]	0	0	0	0.0	0	0.0	0	0.0	0	0.0	0	0.0	4	36.4	7	100.0
G8P[4]	5	7.5	0	0.0	0	0.0	0	0.0	0	0.0	0	0.0	0	0.0	1	9.1
G9P[4]	0	0	0	0.0	0	0.0	0	0.0	0	0.0	2	12.5	0	0.0	0	0.0
G9P[6]	0	0	0	0.0	0	0.0	0	0.0	0	0.0	0	0.0	2	18.2	0	0.0
<sup>1</sup> Other genotypes	3	4.5	0	0.0	0	0.0	2	2.6	1	11.1	2	12.5	0	0.0	0	0.0
<sup>2</sup> Mixed types	13	19.4	0	0.0	0	0.0	0	0.0	1	11.1	0	0.0	0	0.0	0	0.0
<sup>3</sup> Partial G/P types	5	7.5	4	16.7	4	12.1	7	9.2	0	0.0	2	12.5	0	0.0	0	0.0
Untypeables	2	3.0	4	16.7	1	3.0	6	7.9	0	0.0	2	12.5	0	0.0	0	0.0
Total	67	100.0	24	100.0	33	100.0	76	100.0	9	100.0	16	100.0	11	100.0	7	100.0

<sup>1</sup> Other genotypes: 2012: G12P[4] (1.5%), G2P[8] (1.5%), G8P[8] (1.5%); 2015: G2P[6] (2.6%); 2016: G12P[4] (11.1%); 2017: G1P[4] (6.3%), G3P[6] (6.3%); <sup>2</sup> Mixed types: 2012: G12G8P[4] (3.0%), G12G8P[6] (1.5%), G12G8P[6]P[4] (1.5%), G12G9P[6] (1.5%), G12G9P[8]P[6] (3.0%), G12P[8]P[6] (3.0%), G9G2P[4] (1.5%), G9G2P[6] (1.5%), G9G2P[8] (1.5%), G9P[8]P[4] (1.5%); 2016: G12G3P[4] (11.1%); <sup>3</sup> Partial G/P types: 2012: G12P[x] (3.0%), GxP[6]P[4] (1.5%), GxP[6]P[4] (1.5%), GxP[8]P[6] (1.5%); 2013: G2P[x] (8.3%), GxP[4] (8.3%); 2014: GxP[6] (3.0%), GxP[8] (9.1%); 2015: G9P[x] (4.0%), GxP[8] (5.3%); 2017: GxP[4] (6.3%), GxP[8] (6.3%); Grey: The most prevalent genotypes per year.

**Table 6.** Prevalence of G/P type combinations at five sentinel sites in Mozambique during surveillance by year.

G/P Genotype Combination	2015		2016		2017		2018		2019	
	n	%	n	%	n	%	n	%	n	%
G1P[8]	66	31.0	17	43.6	20	19.2	0	0.0	3	15.0
G3P[4]	0	0.0	1	2.6	14	13.5	12	38.7	1	5.0
G3P[6]	0	0.0	0	0.0	2	1.9	1	3.2	0	0.0
G3P[8]	0	0.0	0	0.0	0	0	7	22.6	12	60.0
G8P[4]	0	0.0	0	0.0	1	1.0	2	6.5	0	0.0
G9P[4]	0	0.0	3	7.7	20	19.2	1	3.2	0	0.0
G9P[6]	0	0.0	5	12.8	9	8.7	3	9.7	0	0.0
G2P[6]	9	4.2	7	17.9	0	0	1	3.2	0	0.0
G9P[8]	98	46.0	0	0.0	6	5.8	1	3.2	0	0.0
<sup>1</sup> Other genotypes	4	1.9	3	7.7	3	2.9	1	3.2	0	0.0
<sup>2</sup> Mixed types	0	0.0	2	5.1	10	9.6	0	0.0	0	0.0
<sup>3</sup> Partial G/P types	23	10.8	0	0.0	14	13.5	2	6.5	2	10.0
Untypeables	13	6.1	1	2.6	5	4.8	0	0.0	2	10.0
Total	213	100.0	39	100.0	104	100.0	31	100.0	20	100.0

<sup>1</sup> Other genotypes: 2015: G12P[8] (0.9%), G1P[6] (0.5%), G2P[4] (0.5%); 2016: G12P[4] (2.6%), G2P[4] (5.1%); 2017: G12P[8] (1.0%), G1P[4] (1.9%); 2018: G2P[4] (3.2%); <sup>2</sup> Mixed types: 2016: G12G3P[4] (2.6%), G2G1P[8] (2.6%); 2017: G3G1P[8] (3.9%), G9G3P[6] (5.8%); <sup>3</sup> Partial G/P types: 2015: G9P[x] (3.3%), GxP[6] (0.5%), GxP[8] (7.0%); 2017: G9P[x] (1.9%), GxP[4] (6.7%), GxP[6] (1.9%), GxP[8] (2.9%); 2018: GxP[4] (3.2%), GxP[6] (3.2%); 2019: GxP[4] (5.0%), GxP[8] (5.0%); Grey: The most prevalent genotypes per year.

2.4. Geographical Distribution of Rotavirus Genotypes

A variation in rotavirus genotypes between the five sentinel sites in Mozambique was observed (Supplementary Table S4).

In the pre-vaccine period (2015), it was observed that G1P[8] occurred in all regions included in this study, with the highest frequency (78.0%) detected in the northern region, at Nampula (HCN) (Supplementary Table S4). In contrast, the G9P[8] genotype combination was mostly detected in the southern region, Maputo (HGM and HJM) at 68.8%. Other uncommon genotypes, such as G2P[6], were mostly detected at Nampula at 10.2% but were not detected in Quelimane (HGQ) or Beira (HCB) (Supplementary Table S4). Similarly, in the post-vaccine period (2016–2019), the combination G1P[8]

was observed across the country. In 2016 at Maputo and Nampula, G1P[8] was the most prevalent genotype with 66.7% and 43.5%, respectively. The G1P[8] genotype was, however, also detected in Quelimane and Beira, which had small sample sizes.

In 2017 the genotype combination G3P[4] was the most prevalent (29.7%) in Maputo, while in Nampula and Quelimane G9P[4] and G9P[6] were the most prevalent at 32.7% and 35.7%, respectively. In 2018 and 2019, the G3 genotypes were predominantly detected in Maputo and Quelimane in combination with P[4] and P[8]. In Nampula and Beira, G3 was detected in combination with P[4] (Supplementary Table S4).

### **3. Discussion**

Before rotavirus vaccine introduction in Mozambique, RVA surveillance studies focused in the southern region of the country [18–20]. Instituto Nacional de Saúde (INS) initiated national RVA surveillance in the southern region of Mozambique in 2014, which was expanded to other regions (center and north) in 2015. Following the country-wide introduction of *Rotarix*<sup>®</sup> in September 2015, its impact has been monitored and a substantial reduction in the prevalence of RVA infection rate to 12.2% and 13.5% in 2016 and 2017, respectively, was reported [21]. Since the country is vast, it is important to expand strain surveillance to include the entire country.

In the present analysis, rotavirus surveillance that form part of the National Surveillance of Diarrhea during 2014–2019, as well as data from a cross-section study at the HGM from 2012 and 2013, are reported [24].

During the surveillance at HGM (2012–2019), as well as country-wide sentinel sites (2015–2019), variations in the prevalence of genotypes in the pre- and post-vaccine periods were observed. Genotypes G9 and P[8] were consistently the most prevalent in the pre-vaccine period and in the post-vaccine period, genotypes G3 and P[8] were the most prevalent. However, the proportion of P[8] was reduced, and the prevalence of genotype P[4] increased. These results suggest that genotype prevalence can vary from year to year pre- or post-vaccination in Mozambique.

When comparing the most predominant G/P combinations before and after vaccine introduction at the HGM, G9P[8] was the most predominant genotype combination in the pre-vaccine period, while G1P[8] was the most prevalent genotype combination in the post-vaccine period. The country-wide surveillance also revealed a decreased odds ratio for G9P[8] after the introduction of the vaccine. However, this reduction was accompanied by the emergence of G9P[4] and G9P[6], especially in the northern part of Mozambique, after vaccine introduction. Finally, the emergence of G3P[4] and G3P[8] was also observed. These results showed that in this early phase of rotavirus strain surveillance, it is not clear whether these variations in genotype combinations between both periods were due to the rotavirus vaccine or simply natural variation in genotype frequency. Our results are consistent with previously published studies, as a number of countries from Africa, Europe and America reported a variation in the strain diversity between the two periods [16,25–30].

Countries that introduced the monovalent *Rotarix*<sup>®</sup> vaccine similar to Mozambique, reported a decline of genotype G1P[8] with a concurrent rise in other combinations in the post-vaccine period. For example, South Africa reported an increase in non-G1P[8] strains [25]. In contrast, in Malawi, the reduction of G1P[8] was not significant [27]. In Ghana, G1P[8] returned as one of the dominant strains in the fourth year post-vaccine introduction [26]. Other studies reported from England, Brazil, Belgium, Scotland, a decline in the proportion of G1P[8] with a rise in the proportion of heterotypic strains, such as G2P[4], was observed [28–31].

Additionally, Belgium reported a slightly lower vaccine effectiveness against G2P[4], and in Malawi, a lower vaccine effectiveness against G2 strains than G1 strains was reported [27].

In our analyses, HGM, with at least four years pre-vaccine data showed a slight increase of G1P[8] after vaccine introduction, although in the country-wide analyses the G1P[8] prevalence was reduced. This needs careful interpretation, due to the difference in the number of years in the pre-vaccine period, one of the limitations of this analysis.

Regarding the variation in the prevalence of some uncommon genotypes (e.g., G9P[4] G9P[6], G3P[4], G3P[6]) detected after vaccine introduction in Mozambique, it is important to mention that a number of studies in Africa [16,25,32] and Asia (India and Japan) also reported these uncommon genotypes before vaccine introduction in low frequency [33,34]. These uncommon genotypes, apart from G9P[6], were also observed in Ireland before vaccine introduction [35–37]. However, a study conducted in Ghana reported the emergence of G9P[4] at a low frequency only during the fourth rotavirus season after vaccine introduction [26].

The emergence of the genotype combinations G3P[4], detected in 2016, 2017, 2018, and G3P[8] in 2018 and 2019 was observed in Mozambique. These strains were also reported in the same period in Botswana after vaccine introduction in 2012 [38]. Botswana also reported an outbreak of G3P[8] in 2018 [39]. In addition, several countries reported G3 in combination with P[4] and P[8] during the 12th African Rotavirus Symposium 2019 [40–42]: Malawi (introduced vaccine in 2012, reported G3P[8] in 2018), South Africa (introduced vaccine in 2009, reported G3P[4] in 2015–2016), Kingdom of Eswatini (introduced vaccine in 2015, reported G3P[8] in 2018). These observations suggest that G3 strains were circulating in Southern Africa during 2015–2018, with a sharp increase in 2018. Around the world, the emergence of genotype G3P[8] and equine-like G3P[8] in 2013 in Australia and re-emergence of G3P[8] were observed in Brazil in the post-vaccine introduction [43–45]. The European Rotavirus Network (EuroRotaNet) reported 2017–2018 for the first time since inception, G3P[8] as the most prevalent strain [28].

Temporal variation of rotavirus strains was observed in Mozambique, in particular in the model site, Mavalane General Hospital (HGM), as data from a cross-sectional study that characterized rotavirus strains at the HGM from 2012 and 2013 [24], was combined with data generated at the same site as part of the National Surveillance program with its inception in 2014. As already mentioned, G12P[6] was the most predominant genotype in 2012, and in 2013, G2P[4] was the most prevalent [24]. In a similar time period, G12P[6] was also reported in the Manhiça District, while in 2011 in the Chókwè district, G12P[8] was the most prevalent genotype [18,24]. These results suggest circulation of G12 during 2011–2012 in southern Mozambique. The G12 genotype was detected at a prevalence of almost 20% in Sub-Saharan Africa during 2012–2013 [10,16]. In 2013 the G2P[4] was the predominant genotype in the Manhiça district [24] and also in South Africa in 2013 [46]. A shift in genotypes was observed in 2014 and 2015 when mostly G1P[8] and G9P[8] strains were detected.

In the post-vaccine period (2016–2019), G9P[8] was replaced by G1P[8] in 2016, while in 2017, G3P[4] was the most predominant followed by G1P[8]. In 2018 and 2019, no G1P[8] strains were detected; instead, the G3P[8] genotype was the most prevalent. The G3P[8] genotype combination is one of the most prevalent strains associated with human rotavirus infection globally [11–14]. However, G3P[4], which is considered an uncommon combination, was also detected. Studies published previously in Mozambique during the pre-vaccine period did not detect these strains. These temporal analyses clearly showed a yearly variation of rotavirus strains, complicating the assessment of vaccine introduction impact on changes in strain diversity [11–14]. These observations are further supported by data generated by the National Surveillance of Diarrhea that also showed a temporal variation of rotavirus strains and may rather represent the natural variation in rotavirus strains.

Evaluation of strains detected at the various sentinel sites between 2015–2019, showed that G1P[8] was detected at all sentinel sites, albeit at a variation in frequency. It is interesting to note that G9P[8] occurred mostly in Maputo (HGM and HJM) in the southern region of the country, while G9 in combination with P[4] and P[6] were observed mostly in the north, Nampula (HCN), and central region, Quelimane (HGQ). The occurrence of G2P[6] was mostly observed in Nampula. The emergence of G3 strains was, however, detected at all sites under surveillance suggesting that the occurrence of these strains was not location bound. Differences in the geographical distribution of genotypes within a country was previously reported [11].

Various challenges and limitations were experienced during the study. These include logistical issues, which led to a delay in the start of surveillance at some sentinel sites. The study was limited

by its small sample size; therefore, it was not possible to perform in-depth temporal analyses by the site to access the genetic variability of strains. Furthermore, bias in strain diversity is possible since a low number of strains were characterized at some sentinel sites. Extended pre-vaccine genotyping data (four years) was available for only one sentinel site, whereas only one year genotyping data were available for the remainder of the sentinel sites.

Despite the circulation of diverse rotavirus strains and the emergence of some genotypes, the National Surveillance of Diarrhea reported a reduction in rotavirus prevalence during the early impact study of the rotavirus vaccine after vaccine introduction.

The whole genome characterization of rotavirus strains circulating pre- and post-vaccine introduction will be useful to evaluate any potential vaccine-induced selection of specific antigenic profiles. Moreover, with recent reports related to the emergence of double-reassortant G1P[8] on a DS-1-like genetic backbone [47–49], whole-genome characterization will be important for strains surveillance.

#### **4. Materials and Methods**

##### *4.1. Study Population and Stool Samples Collection*

RVA positive samples, as tested by Enzyme-Linked Immunosorbent Assay (ELISA), were included. Samples were obtained from children under five years of age suffering from moderate-to-severe acute and non-acute diarrhea. These samples were collected as part of an ongoing hospital-based diarrhea surveillance program, called the National Surveillance of Diarrhea (ViNaDia) that commenced in May 2014. Samples were included for this study up to December 2019. In addition, data from a cross-sectional study conducted at the Mavalane General Hospital (HGM) from January 2012 to September 2013 were also included in the analyses [24].

The National Surveillance of Diarrhea in children was led by the “Instituto Nacional de Saúde” (INS), started in May 2014 at the Mavalane General Hospital (HGM, first sentinel site) in the Maputo province (Figure 1). In March 2015, José Macamo General Hospital (HJM), also Maputo Province, and Nampula Central Hospital (HCN), in Nampula province in the northern region of the country were added. Surveillance was extended to two additional sentinel sites in June 2015: Beira Central Hospital (HCB) in Sofala Province and Quelimane General Hospital (HGQ) in the Zambézia province (Figure 1). Since 2016, Mozambique participates and actively report data to the WHO African Rotavirus Surveillance Network (ARSN). ARSN monitors rotavirus infection in children with severe acute watery diarrhea as part of a hospital-based sentinel-site surveillance program.

In the surveillance at HGM and HJM samples were collected and immediately transferred to the INS laboratory, while at HCB, HCN and HGQ, samples were collected and stored at  $-20\text{ }^{\circ}\text{C}$ . Samples were transported on a weekly basis on dry ice to the INS laboratories located in Maputo City for testing and stored in  $-70\text{ }^{\circ}\text{C}$  as previously described [21]. The cross-sectional study was conducted at the Centro de Investigação em Saúde de Manhiça (CISM). The sampling, testing procedures, clinical, socio-demographic information and characterization of rotavirus strains, as previously described [19,24].

##### *4.2. Ethical Approval*

The National Surveillance of Diarrhea in children protocol was reviewed and approved by the Mozambican National Committee on Bioethics for Health (CNBS) (reference N<sup>o</sup>: 348/CNBS/13; IRB00002657), as well as the rotavirus cross-sectional study (reference N<sup>o</sup>286/CNBS/10; IRB00002657).

### 4.3. Laboratory Testing

#### 4.3.1. Rotavirus Detection and RNA Extraction

All samples analyzed, were tested for rotavirus using the commercial Enzyme-immuno-sorbent assay (ELISA) kit (Prospect, Oxoid Ltd., Hampshire, UK) following the manufacturer’s instructions. Total RNA was extracted from ELISA-positive samples using the QIAamp Viral RNA protocol (QIAGEN, Hilden, Germany), and stored at  $-70^{\circ}\text{C}$ .

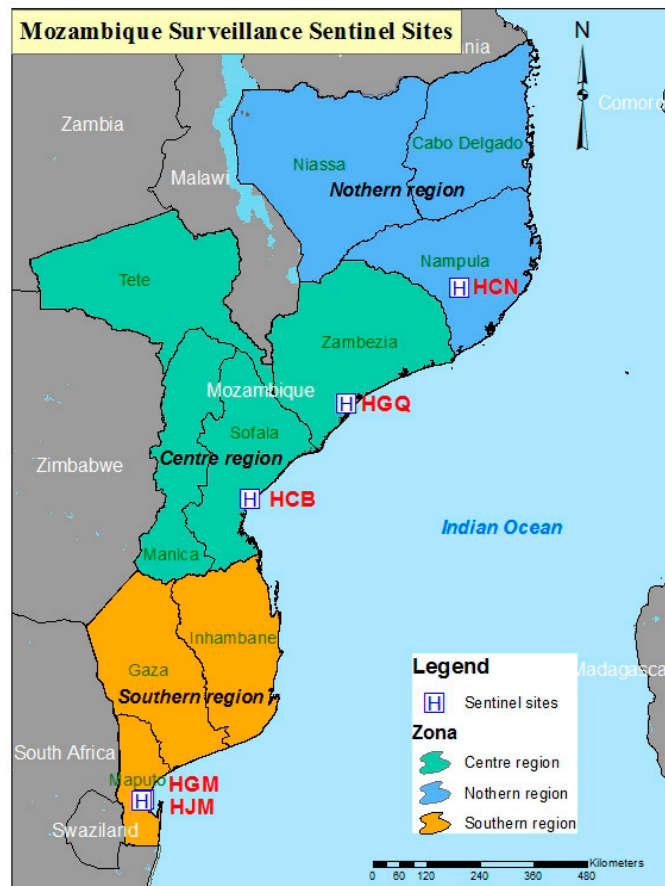


**Figure 1.** Map of Mozambique indicating the geographical location of study sites. Abbreviations for hospitals are indicated in red. HGM (Mavalane General Hospital), HJM (Jose Macamo General Hospital), HCB (Beira Central Hospital), HGQ (Quelimane General Hospital) and HCN (Nampula Central Hospital).

#### 4.3.2. Reverse Transcriptase (RT) and G/P Typing PCR

Extracted RNA (8  $\mu\text{L}$ ) was reverse transcribed using Con2/Con3 for the partial VP4-encoding gene (VP8\*, 876 bp) and sBeg9/End9 for the VP7-encoding gene. G genotypes were subsequently determined using a multiplex semi-nested PCR as described before [24]. Specific primers that identified the VP7-encoding gene with the following G genotypes: G1, aBT1; G2, aCT2; G3, aET3 or mG3; G4, aDT4; G8, aAT8; G9, aFT9, or mG9; G12, G12b; G10, mG10 in combination with the common primer RVG9 were used as described previously [50–52].

Similarly, Con3 was used in combination with specific primers that identify P genotypes: P[8], 1T-1D or 1T-1v; P[4], 2T-1; P[6], 3T-1; P[9], 4T-1, and P[10], 5T-1, P[11], mp11, P[14], P4943, as described previously [53–55]. The PCR product was analyzed using 2% agarose gel electrophoresis, stained with ethidium bromide and visualized under ultraviolet illumination.

#### 4.4. Data Management and Statistical Analyses

The rotavirus vaccine, *Rotarix*<sup>®</sup>, was introduced in September 2015 in Mozambique. Therefore, the pre-vaccine period was considered to be before December 2015, due to logistical problems associated with vaccine introduction across the country.

The genotyping data from the primary sentinel site, Mavalane General Hospital (HGM), was analyzed separately from other sites because data at this site was available from 2012 and other sites from 2015.

Frequencies of identified genotypes are reported. To assess the magnitude of change in genotypes from the pre- to post-vaccine periods, unadjusted odds ratios (OR) and their 95% confidence intervals (95CI) were computed. In this analysis, the genotype was the dependent variable and time the predictor. All statistical analysis was conducted using Stata software version 15.0 (Stata Corp., College Station, TX, USA). A *p*-value of <0.05 was considered statistically significant.

## 5. Conclusions

This is the first report describing the circulation of rotavirus genotypes in three regions of Mozambique. A comparison between the pre- and post-vaccine introduction periods showed a shift in circulating genotypes following vaccine introduction. However, due to the short surveillance period, it is not clear if the observed changes were due to the introduction of the vaccine or a consequence of natural strain variation. In addition, the emergence of unusual strains, such as G3P[4] and G3P[8], was also observed, which support the need for continued country-wide surveillance to monitor changes, due to possible vaccine pressure, and consequently, the effect on vaccine effectiveness.

**Supplementary Materials:** The following are available online at <http://www.mdpi.com/2076-0817/9/9/671/s1>: Table S1: Total number of stool samples collected at sentinel sites in Mozambique during surveillance between May 2014 and December 2019; Table S2: Total number of stool samples collected per sentinel sites in Mozambique during surveillance between May 2014 and December 2019; Table S3: Total number of stool samples collected at Mavalane General Hospital during a cross-sectional study (2012–2013) and the National Surveillance of Diarrhea program (2014–2019); Table S4: Distribution of rotavirus genotypes between geographical regions.

**Author Contributions:** N.d.D. and E.D.J conceptualized the main project. E.D.J., B.M., J.C., J.L., A.C., E.A., J.S., E.G., D.B., M.C., I.C.-M. and S.S.B. performed investigations. Formal analysis and methodology was done by E.D.J. and O.A. Data curation was performed by A.C., M.C. and O.A. Writing of the original draft preparation was performed by E.D.J. Review and editing was done by E.D.J., N.d.D., I.M., J.M.M. and H.G.O. Visualizations was performed by A.C. Project administration was done by J.C. Validation was done by N.d.D., H.G.O. and I.M. Supervision and funding acquisition was done by N.d.D. All authors have read and agreed to the published version of the manuscript.

**Funding:** The National Surveillance of Diarrhea was supported by European Foundation Initiative into African Research in Neglected Tropical Diseases (EFINTD) through a senior fellowship awarded to N.D. (grant number 89539), World Health Organization (WHO), Gavi, the Vaccine Alliance and Fundo Nacional de Investigação (FNI). E.D.J. Ph.D. was supported by Calouste Gulbenkian Foundation. B.M., A.C. and S.B. received a scholarship from the Deutsche Forschungsgemeinschaft (DFG; JO369/5-1).

**Acknowledgments:** We would like to thank the surveillance teams in Maputo, Nampula, Beira and Quelimane, as well as the parents that provided consent for the collection of stool samples and data from children. We are grateful for Centro de Investigação da Polana Caniço, INS, for providing the map illustration and to Adilson Bauhofer for assistance with data analyses.

**Conflicts of Interest:** The authors declare no conflict of interest.

## References

1. Troeger, C.; Khalil, I.A.; Rao, P.C.; Cao, S.; Blacker, B.F.; Ahmed, T.; Armah, G.; Bines, J.E.; Brewer, T.G.; Colombara, D.V.; et al. Rotavirus Vaccination and the Global Burden of Rotavirus Diarrhea Among Children Younger Than 5 Years. *JAMA Pediatr.* **2018**, *172*, 958–965. [CrossRef]
2. Tate, J.E.; Burton, A.H.; Boschi-Pinto, C.; Parashar, U.D. Global, Regional, and National Estimates of Rotavirus Mortality in Children <5 Years of Age, 2000–2013. *Clin. Infect. Dis.* **2016**, *62*, S96–S105. [PubMed]

3. GBD. Estimates of the global, regional, and national morbidity, mortality, and aetiologies of diarrhoea in 195 countries: A systematic analysis for the Global Burden of Disease Study 2016. *Lancet Infect. Dis.* **2018**, *18*, 1211–1228.
4. Estes, M.K.; Cohen, J. Rotavirus gene structure and function. *Microbiol. Rev.* **1989**, *53*, 410–449. [CrossRef] [PubMed]
5. Crawford, S.E.; Ramani, S.; Tate, J.E.; Parashar, U.D.; Svensson, L.; Hagbom, M.; Francco, M.A.; Greenberg, H.B.; O’Ryan, M.; Kang, G.; et al. Rotavirus infection. *Nat. Rev. Dis. Primers.* **2017**, *3*, 17083. [CrossRef]
6. Desselberger, U. Rotaviruses. *Virus Res.* **2014**, *190*, 75–96. [CrossRef]
7. Matthijssens, J.; Ciarlet, M.; McDonald, S.M.; Attoui, H.; Banyai, K.; Brister, J.R.; Buesa, J.; Esona, M.D.; Estes, M.K.; Gentsch, J.R.; et al. Uniformity of rotavirus strain nomenclature proposed by the Rotavirus Classification Working Group (RCWG). *Arch. Virol.* **2011**, *156*, 1397–1413. [CrossRef]
8. Matthijssens, J.; Ciarlet, M.; Heiman, E.; Arijs, I.; Delbeke, T.; McDonald, S.M.; Palombo, E.A.; Iturriza-Gómara, M.; Maes, P.; Patton, J.T.; et al. Full genome-based classification of rotaviruses reveals a common origin between human Wa-Like and porcine rotavirus strains and human DS-1-like and bovine rotavirus strains. *J. Virol.* **2008**, *82*, 3204–3219. [CrossRef]
9. Virus Classification- Laboratory of Viral Metagenomics. Available online: <https://rega.kuleuven.be/cev/viralmetagenomics/virus-classification/rcwg> (accessed on 20 May 2020).
10. Mwenda, J.M.; Tate, J.E.; Parashar, U.D.; Mihigo, R.; Agocs, M.; Serhan, F.; Nshimirimana, D. African rotavirus surveillance network: A brief overview. *Pediatr. Infect. Dis. J.* **2014**, *33*, S6–S8. [CrossRef]
11. Banyai, K.; Laszlo, B.; Duque, J.; Steele, A.D.; Nelson, E.A.; Gentsch, J.R.; Parashar, U.D. Systematic review of regional and temporal trends in global rotavirus strain diversity in the pre rotavirus vaccine era: Insights for understanding the impact of rotavirus vaccination programs. *Vaccine* **2012**, *30*, A122–A130. [CrossRef]
12. Gentsch, J.R.; Laird, A.R.; Bielfelt, B.; Griffin, D.D.; Banyai, K.; Ramachandran, M.; Jain, V.; Cunliffe, N.A.; Nakagomi, O.; Kirkwood, C.D.; et al. Serotype diversity and reassortment between human and animal rotavirus strains: Implications for rotavirus vaccine programs. *J. Infect. Dis.* **2005**, *192*, S146–S159. [CrossRef]
13. Leshem, E.; Lopman, B.; Glass, R.; Gentsch, J.; Banyai, K.; Parashar, U.; Patel, M. Distribution of rotavirus strains and strain-specific effectiveness of the rotavirus vaccine after its introduction: A systematic review and meta-analysis. *Lancet Infect. Dis.* **2014**, *14*, 847–856. [CrossRef]
14. Matthijssens, J.; Bilcke, J.; Ciarlet, M.; Martella, V.; Banyai, K.; Rahman, M.; Zeller, M.; Beutels, P.; van Damme, P.; van Ranst, M. Rotavirus disease and vaccination: Impact on genotype diversity. *Fut. Microbiol.* **2009**, *4*, 1303–1316. [CrossRef]
15. Todd, S.; Page, N.A.; Duncan Steele, A.; Peenze, I.; Cunliffe, N.A. Rotavirus strain types circulating in Africa: Review of studies published during 1997–2006. *J. Infect. Dis.* **2010**, *202*, S34–S42. [CrossRef]
16. Seheri, L.M.; Magagula, N.B.; Peenze, I.; Rakau, K.; Ndadza, A.; Mwenda, J.M.; Weldegebriel, G.; Steele, A.D.; Mphahlele, M.J. Rotavirus strain diversity in Eastern and Southern African countries before and after vaccine introduction. *Vaccine* **2017**, *36*, 7222–7230. [CrossRef] [PubMed]
17. Rotavirus vaccines. WHO position paper—January 2013. *Wkly. Epidemiol. Rec.* **2013**, *88*, 49–64.
18. Langa, J.S.; Thompson, R.; Arnaldo, P.; Resque, H.R.; Rose, T.; Enosse, S.M.; Fialho, A.; Assis, R.M.S.; Silva, M.F.M.; Paulo, J.; et al. Epidemiology of Rotavirus A diarrhea in Chókwè, Southern Mozambique, from February to September, 2011. *J. Med. Virol.* **2016**, *88*, 1751–1758. [CrossRef]
19. De Deus, N.; João, E.; Cuamba, A.; Cassocera, M.; Luís, L.; Acácio, S.; Mandomando, I.; Augusto, O.; Page, N. Epidemiology of Rotavirus Infection in Children from a Rural and Urban Area, in Maputo, Southern Mozambique, before Vaccine Introduction. *J. Trop. Pediatr.* **2018**, *64*, 141–145. [CrossRef]
20. Kotloff, K.L.; Nataro, J.P.; Blackwelder, W.C.; Nasrin, D.; Farag, T.H.; Panchalingam, S.; Wu, Y.; O Sow, S.; Sur, D.; Breiman, R.F.; et al. Burden and aetiology of diarrhoeal disease in infants and young children in developing countries (the Global Enteric Multicenter Study, GEMS): A prospective, case-control study. *Lancet* **2013**, *382*, 209–222. [CrossRef]
21. De Deus, N.; Chilaule, J.J.; Cassocera, M.; Bambo, M.; Langa, J.S.; Siteo, E.; Chissaque, A.; Anapakala, E.; Sambo, J.; Lourenço Guimarães, E.; et al. Early impact of rotavirus vaccination in children less than five years of age in Mozambique. *Vaccine* **2018**, *36*, 7205–7209. [CrossRef]

22. Matthijnssens, J.; de Grazia, S.; Piessens, J.; Heylen, E.; Zeller, M.; Giammanco, G.M.; Bányai, K.; Buonavoglia, C.; Ciarlet, M.; Martella, V.; et al. Multiple reassortment and interspecies transmission events contribute to the diversity of feline, canine and feline/canine-like human group A rotavirus strains. *Infect. Genet. Evol.* **2011**, *11*, 1396–1406. [CrossRef]
23. Matthijnssens, J.; Taraporewala, Z.F.; Yang, H.; Rao, S.; Yuan, L.; Cao, D.; Hoshino, Y.; Mertens, P.P.C.; Carner, G.R.; McNeal, M.; et al. Simian rotaviruses possess divergent gene constellations that originated from interspecies transmission and reassortment. *J. Virol.* **2009**, *84*, 2013–2026. [CrossRef] [PubMed]
24. Joao, E.D.; Strydom, A.; O’Neill, H.G.; Cuamba, A.; Cassocera, M.; Acacio, S.; Mandomando, I.; Motanyane, L.; Page, N.; de Deus, N. Rotavirus A strains obtained from children with acute gastroenteritis in Mozambique, 2012–2013: G and P genotypes and phylogenetic analysis of VP7 and partial VP4 genes. *Arch. Virol.* **2018**, *163*, 153–165. [CrossRef] [PubMed]
25. Page, N.A.; Seheri, L.M.; Groome, M.J.; Moyes, J.; Walaza, S.; Mphahlele, J.; Kahn, K.; Kapongo, C.N.; Zar, H.J.; Tempia, S.; et al. Temporal association of rotavirus vaccination and genotype circulation in South Africa: Observations from 2002 to 2014. *Vaccine* **2017**, *36*, 7231–7237. [CrossRef]
26. Lartey, B.L.; Damanka, S.; Dennis, F.E.; Enweronu-Laryea, C.C.; Addo-Yobo, E.; Ansong, D.; Kwarteng-Owusu, S.; Sagoe, K.W.; Mwenda, J.M.; Diamenu, S.K.; et al. Rotavirus strain distribution in Ghana pre- and post- rotavirus vaccine introduction. *Vaccine* **2018**, *36*, 7238–7242. [CrossRef]
27. Bar-Zeev, N.; Jere, K.C.; Bennett, A.; Pollock, L.; Tate, J.E.; Nakagomi, O.; Iturriza-Gomara, M.; Costello, A.; Mwanambo, C.; Parashar, U.D.; et al. Population Impact and Effectiveness of Monovalent Rotavirus Vaccination in Urban Malawian Children 3 Years After Vaccine Introduction: Ecological and Case-Control Analyses. *Clin. Infect. Dis.* **2016**, *62*, S213–S219. [CrossRef]
28. Hungerford, D.; Allen, D.J.; Nawaz, S.; Collins, S.; Ladhani, S.; Vivancos, R.; Iturriza-Gómara, M. Impact of rotavirus vaccination on rotavirus genotype distribution and diversity in England, September 2006 to August 2016. *Eurosurveillance* **2019**, *24*, 1700774.
29. Matthijnssens, J.; Zeller, M.; Heylen, E.; de Coster, S.; Vercauteren, J.; Braeckman, T.; van Herck, K.; Meyer, N.; Pircon, J.-Y.; Soriano-Gabarro, M.; et al. Higher proportion of G2P[4] rotaviruses in vaccinated hospitalized cases compared with unvaccinated hospitalized cases, despite high vaccine effectiveness against heterotypic G2P[4] rotaviruses. *Clin. Microbiol. Infect.* **2014**, *20*, O702–O710. [CrossRef]
30. Luchs, A.; Cilli, A.; Morillo, S.G.; de Cássia Compagnoli, C.R.; Timenetsky, M.C.S.T. Rotavirus Genotypes Circulating in Brazil, 2007–2012: Implications for the Vaccine Program. *Rev. Inst. Med. Trop.* **2015**, *57*, 305–313. [CrossRef] [PubMed]
31. Mukhopadhyaya, I.; Murdoch, H.; Berry, S.; Hunt, A.; Iturriza-Gomara, M.; Smith-Palmer, A.; Cameron, J.C.; Hold, G.L. Changing molecular epidemiology of rotavirus infection after introduction of monovalent rotavirus vaccination in Scotland. *Vaccine* **2016**, *35*, 156–163. [CrossRef] [PubMed]
32. Cunliffe, N.A.; Ngwira, B.M.; Dove, W.; Thindwa, B.D.; Turner, A.M.; Broadhead, R.L.; Molyneux, M.E.; Hart, A.C. Epidemiology of rotavirus infection in children in Blantyre, Malawi, 1997–2007. *J. Infect. Dis.* **2010**, *202*, S168–S174. [CrossRef] [PubMed]
33. Yamamoto, S.P.; Kaida, A.; Ono, A.; Kubo, H.; Iritani, N. Detection and characterization of a human G9P[4] rotavirus strain in Japan. *J. Med. Virol.* **2015**, *87*, 1311–1318. [CrossRef]
34. Giri, S.; Nair, N.P.; Mathew, A.; Manohar, B.; Simon, A.; Singh, T.; Suresh Kumar, S.; Mathew, M.A.; Babji, S.; Arora, R.; et al. Rotavirus gastroenteritis in Indian children < 5 years hospitalized for diarrhoea, 2012 to 2016. *BMC Public Health* **2019**, *19*, 69.
35. Cashman, O.; Collins, P.J.; Lennon, G.; Cryan, B.; Martella, V.; Fanning, S.; Staines, A.; O’Shea, H. Molecular characterization of group A rotaviruses detected in children with gastroenteritis in Ireland in 2006–2009. *Epidemiol. Infect.* **2011**, *140*, 247–259. [CrossRef]
36. Collins, P.J.; Mulherin, E.; O’Shea, H.; Cashman, O.; Lennon, G.; Pidgeon, E.; Coughlan, S.; Hall, W.; Fanning, S. Changing patterns of rotavirus strains circulating in Ireland: Re-emergence of G2P[4] and identification of novel genotypes in Ireland. *J. Med. Virol.* **2015**, *87*, 764–773. [CrossRef]

37. Lennon, G.; Reidy, N.; Cryan, B.; Fanning, S.; O’Shea, H. Changing profile of rotavirus in Ireland: Predominance of P[8] and emergence of P[6] and P[9] in mixed infections. *J. Med. Virol.* **2008**, *80*, 524–530. [CrossRef]
38. Mokomane, M.; Esona, M.D.; Bowen, M.D.; Tate, J.E.; Steenhoff, A.P.; Lechiile, K.; Gaseitsiwe, S.; Seheri, L.M.; Magagula, N.B.; Weldegebriel, G.; et al. Diversity of Rotavirus Strains Circulating in Botswana before and after introduction of the Monovalent Rotavirus Vaccine. *Vaccine* **2019**, *37*, 6324–6328. [CrossRef]
39. WHO-Botswana. Available online: <https://www.afro.who.int/news/who-supports-botswana-respond-outbreak-diarrhoea-children-below-five-years-age>. (accessed on 29 May 2020).
40. Rakau, K.; Gededzha, M.; Peenze, I.; Seheri, M. Rotavirus strains detected in Dr George Mukhari academic hospital and Oukasie primary healthcare, Pretoria from 2015-2016. In Proceedings of the 12th African Rotavirus Symposium, Johannesburg, South Africa, 30 July–1 August 2019.
41. Gugu, M.; Nomcebo, P.; Sindisiwe, D.; Susan, K.; Gilbert, M.; Goitom, W.; Lonkululeko, K.; Xolsile, D.; Getahun, T.; Michael, L.; et al. G3P[8] rotavirus strain causing diarrheal outbreak in the Kingdom of Eswatini, 2018. In Proceedings of the 12th African Rotavirus Symposium, Johannesburg, South Africa, 30 July–1 August 2019.
42. Mhango, C.; Chinyama, E.; Mandolo, J.; Malamba, C.; Wachepa, R.; Kanjerwa, O.; Kamng’ona, A.W.; Shawa, I.T.; Jere, K.C. Changes in rotavirus strains circulating in Malawi before vaccine introduction and six years post vaccine era. In Proceedings of the 12th African Rotavirus Symposium, Johannesburg, South Africa, 30 July–1 August 2019.
43. Carvalho-Costa, F.A.; de Assis, R.M.S.; Fialho, A.M.; Araujo, I.T.; Silva, M.F.; Gomez, M.M.; Andrade, J.S.; Rose, T.L.; Fumian, T.M.; Voloato, E.M. The evolving epidemiology of rotavirus A infection in Brazil a decade after the introduction of universal vaccination with Rotarix(R). *BMC Pediatr.* **2019**, *19*, 42. [CrossRef]
44. Roczo-Farkas, S.; Kirkwood, C.D.; Cowley, D.; Barnes, G.L.; Bishop, R.F.; Bogdanovic-Sakran, N.; Boniface, K.; Donato, C.M.; Bines, J.E. The Impact of Rotavirus Vaccines on Genotype Diversity: A Comprehensive Analysis of 2 Decades of Australian Surveillance Data. *J. Infect. Dis.* **2018**, *218*, 546–554. [CrossRef]
45. Cowley, D.; Donato, C.M.; Roczo-Farkas, S.; Kirkwood, C.D. Emergence of a novel equine-like G3P[8] inter-genogroup reassortant rotavirus strain associated with gastroenteritis in Australian children. *J. Gen. Virol.* **2015**, *97*, 403–410. [CrossRef]
46. Page, N.; Mapuroma, F.; Seheri, M.; Kruger, T.; Peenze, I.; Walaza, S.; Cohen, C.; Groome, M.; Madhi, S. Rotavirus surveillance report, South Africa, 2013. *Commun Dis Surveill Bull.* **2014**, *12*, 130–135.
47. Jere, K.C.; Chaguza, C.; Bar-Zeev, N.; Lowe, J.; Peno, C.; Kumwenda, B.; Nakagomi, O.; Tate, J.E.; Parashar, U.D.; Heyderman, R.S.; et al. Emergence of Double- and Triple-Gene Reassortant G1P[8] Rotaviruses Possessing a DS-1-Like Backbone after Rotavirus Vaccine Introduction in Malawi. *J. Virol.* **2018**, *92*, e01246-17. [CrossRef] [PubMed]
48. Komoto, S.; Tacharoenmuang, R.; Guntapong, R.; Ide, T.; Haga, K.; Katayama, K.; Kato, T.; Ouchi, Y.; Kurahashi, H.; Tsjui, T.; et al. Emergence and Characterization of Unusual DS-1-Like G1P[8] Rotavirus Strains in Children with Diarrhea in Thailand. *PLoS ONE* **2015**, *10*, e0141739. [CrossRef] [PubMed]
49. Mwangi, P.N.; Mogotsi, M.T.; Rasebotsa, S.P.; Seheri, M.L.; Mphahlele, M.J.; Ndze, V.N.; Dennis, F.E.; Jere, K.C.; Nyaga, M.M. Uncovering the First Atypical DS-1-like G1P[8] Rotavirus Strains That Circulated during Pre-Rotavirus Vaccine Introduction Era in South Africa. *Pathogens* **2020**, *9*, 391. [CrossRef]
50. Gouvea, V.; Glass, R.I.; Woods, P.; Taniguchi, K.; Clark, H.F.; Forrester, B.; Fang, Z.Y. Polymerase chain reaction amplification and typing of rotavirus nucleic acid from stool specimens. *J. Clin. Microbiol.* **1990**, *28*, 276–282. [CrossRef]
51. Iturriza Gomara, M.; Kang, G.; Mammen, A.; Jana, A.K.; Abraham, M.; Desselberger, U.; Brown, D.; Gray, J. Characterization of G10P[11] rotaviruses causing acute gastroenteritis in neonates and infants in Vellore, India. *J. Clin. Microbiol.* **2004**, *42*, 2541–2547. [CrossRef]
52. Aladin, F.; Nawaz, S.; Iturriza-Gomara, M.; Gray, J. Identification of G8 rotavirus strains determined as G12 by rotavirus genotyping PCR: Updating the current genotyping methods. *J. Clin. Virol.* **2010**, *47*, 340–344. [CrossRef]
53. Gentsch, J.R.; Glass, R.I.; Woods, P.; Gouvea, V.; Gorziglia, M.; Flores, J.; Das, B.K.; Bhan, M.K. Identification of group A rotavirus gene 4 types by polymerase chain reaction. *J. Clin. Microbiol.* **1992**, *30*, 1365–1373. [CrossRef]

54. Iturriza-Gomara, M.; Green, J.; Brown, D.W.; Desselberger, U.; Gray, J.J. Diversity within the VP4 gene of rotavirus P [8] strains: Implications for reverse transcription-PCR genotyping. *J. Clin. Microbiol.* **2000**, *38*, 898–901. [CrossRef]
55. Mphahlele, M.J.; Peenze, I.; Steele, A.D. Rotavirus strains bearing the VP4P[14] genotype recovered from South African children with diarrhoea. *Arch. Virol.* **1999**, *144*, 1027–1034. [CrossRef]



© 2020 World Health Organization; Licensee MDPI, Basel, Switzerland. This is an open access article distributed under the terms of the Creative Commons Attribution IGO License (CC BY) license (<http://creativecommons.org/licenses/by/3.0/igo/legalcode>), which permits unrestricted use, distribution, and reproduction in any medium, provided the original work is properly cited. In any reproduction of this article there should not be any suggestion that WHO or this article endorse any specific organisation or products. The use of the WHO logo is not permitted.

Article

# Whole Genome Characterization and Evolutionary Analysis of G1P[8] Rotavirus A Strains during the Pre- and Post-Vaccine Periods in Mozambique (2012–2017)

Benilde Munlela <sup>1,2,\*</sup>, Eva D. João <sup>1,3,\*</sup>, Celeste M. Donato <sup>4,5,6</sup>, Amy Strydom <sup>7</sup>, Simone S. Boene <sup>1,2</sup>, Assucênio Chissaque <sup>1,3</sup>, Adilson F. L. Bauhofer <sup>1,3</sup>, Jerónimo Langa <sup>1</sup>, Marta Cassocera <sup>1,3</sup>, Idalécia Cossa-Moiane <sup>1,8</sup>, Jorfélia J. Chilaúle <sup>1</sup>, Hester G. O'Neill <sup>7</sup> and Nilsa de Deus <sup>1,9</sup>

<sup>1</sup> Instituto Nacional de Saúde (INS), Distrito de Marracuene, Maputo 3943, Mozambique; simone.boene@ins.gov.mz (S.S.B.); assucenio.chissaque@ins.gov.mz (A.C.); adilson.bauhofer@ins.gov.mz (A.F.L.B.); Jeronimo.Langa@ins.gov.mz (J.L.); marta.Cassocera@ins.gov.mz (M.C.); idalecia.moiane@ins.gov.mz (I.C.-M.); jorfelia.chilaule@ins.gov.mz (J.J.C.); nilsa.dedeus@ins.gov.mz (N.d.D.)

<sup>2</sup> Centro de Biotecnologia, Universidade Eduardo Mondlane, Maputo 3453, Mozambique

<sup>3</sup> Instituto de Higiene e Medicina Tropical (IHMT), Universidade Nova de Lisboa, UNL, Rua da Junqueira 100, 1349-008 Lisbon, Portugal

<sup>4</sup> Enteric Diseases Group, Murdoch Children's Research Institute, 50 Flemington Road, Parkville, Melbourne 3052, Australia; celeste.donato@mcri.edu.au

<sup>5</sup> Department of Paediatrics, the University of Melbourne, Parkville 3010, Australia

<sup>6</sup> Biomedicine Discovery Institute and Department of Microbiology, Monash University, Clayton 3800, Australia

<sup>7</sup> Department of Microbial, Biochemical and Food Biotechnology, University of the Free State, 205 Nelson Mandela Avenue, Bloemfontein 9301, South Africa; strydoma@ufs.ac.za (A.S.); oneillhg@ufs.ac.za (H.G.O.)

<sup>8</sup> Institute of Tropical Medicine (ITM), Kronenburgstraat 43, 2000 Antwerp, Belgium

<sup>9</sup> Departamento de Ciências Biológicas, Universidade Eduardo Mondlane, Maputo 3453, Mozambique

\* Correspondence: benilde.munlela@ins.gov.mz or benildeantnio@gmail.com (B.M.); evadora1@hotmail.com (E.D.J.); Tel.: +258-848814087 (B.M.); +258-827479229 (E.D.J.)

† These authors contributed equally in this work.

Received: 26 October 2020; Accepted: 3 December 2020; Published: 6 December 2020



**Abstract:** Mozambique introduced the Rotarix<sup>®</sup> vaccine (GSK Biologicals, Rixensart, Belgium) into the National Immunization Program in September 2015. Although G1P[8] was one of the most prevalent genotypes between 2012 and 2017 in Mozambique, no complete genomes had been sequenced to date. Here we report whole genome sequence analysis for 36 G1P[8] strains using an Illumina MiSeq platform. All strains exhibited a Wa-like genetic backbone (G1-P[8]-I1-R1-C1-M1-A1-N1-T1-E1-H1). Phylogenetic analysis showed that most of the Mozambican strains clustered closely together in a conserved clade for the entire genome. No distinct clustering for pre- and post-vaccine strains were observed. These findings may suggest no selective pressure by the introduction of the Rotarix<sup>®</sup> vaccine in 2015. Two strains (HJM1646 and HGM0544) showed varied clustering for the entire genome, suggesting reassortment, whereas a further strain obtained from a rural area (MAN0033) clustered separately for all gene segments. Bayesian analysis for the VP7 and VP4 encoding gene segments supported the phylogenetic analysis and indicated a possible introduction from India around 2011.7 and 2013.0 for the main Mozambican clade. Continued monitoring of rotavirus strains in the post-vaccine period is required to fully understand the impact of vaccine introduction on the diversity and evolution of rotavirus strains.

**Keywords:** rotavirus group A; G1P[8]; whole genome sequencing; Rotarix®; Bayesian analysis; Mozambique

---

## 1. Introduction

Rotavirus is one of the leading causes of diarrheal disease in children under five years of age [1,2]. Worldwide, the number of deaths due to rotavirus infection in children under five years of age in 2016 was estimated to be 128,500, of which 104,733 occurred in sub-Saharan Africa [2]. Rotavirus is a member of the *Reoviridae* family. The genome is comprised of 11 double-stranded ribonucleic acid (dsRNA) segments. The mature virus has an icosahedral capsid formed by three concentric protein layers. The 11 segments of the rotavirus genome encode 12 viral proteins: 6 structural proteins VP1-VP4, VP6 and VP7 and 6 non-structural proteins (NSP1-NSP6) [3–6].

The gene segments encoding the external capsid proteins, VP7 and VP4, are used in a binary classification system defining G and P genotypes, respectively [5,7]. Currently, 36 G and 51 P genotypes have been described in humans and various animal species [7–10]. At least 73 combinations of human rotavirus group A (RVA) G/P genotypes have been described, of which the most common combinations are G1P[8], G2P[4], G3P[8], G4P[8], G9P[8] and G12P[8] [10,11]. However, the implementation of whole genome sequencing has led to comprehensive sequence-based classification of all RVA genes into genotypes, which are identified and differentiated according to particular cut-off values of nucleotide sequence identities [9,11]. Currently, 26 I (VP6), 22 R (VP1), 20 C (VP2), 20 M (VP3), 31 A (NSP1), 22 N (NSP2), 22 T (NSP3), 27 E (NSP4) and 22 H (NSP5) genotypes have been described [8]. The whole genome constellation of a strain can be described following the nomenclature Gx-P[x]-Ix-Rx-Cx-Mx-Ax-Nx-Tx-Ex-Hx. Two major genotype constellations have been designated for strains that commonly infect humans: Wa-like (I1-R1-C1-M1-A1-N1-T1-E1-H1) and DS-1-like (I2-R2-C2-M2-A2-N2-T2-E2-H2). A third constellation also observed in human strains, called AU-1-like (I3-R3-C3-M3-A3-N3-T3-E3-H3), has been shown to have a feline/canine origin [9,11].

Four live oral vaccines, namely Rotarix® (GlaxoSmithKline Biologics, Rixensart, Belgium), RotaTeq® (Merck & Co., Kenilworth, NJ, USA), Rotavac® (Bharat Biotech, Hyderabad, India) and Rotasiil® (Serum Institute of India Pvt. Ltd., Pune, India) have been prequalified by the World Health Organization [12,13]. Rotarix® and RotaTeq® have been introduced into the immunization programs of more than 100 countries [13]. Rotarix® is a monovalent vaccine containing a single human G1P[8] strain and is administered from the age of six weeks [13]. Prior to vaccine introduction in Mozambique, a high burden of rotavirus disease was reported in children under five years old. The rate of rotavirus infection in urban (Maputo City) and rural (Manhiça District) areas between 2012 and 2013 was 42.4% [6]. In 2011, a 24.0% infection rate was reported in the Gaza province, another rural area in southern Mozambique [14]. In both studies G1P[8] was detected at a low frequency [14,15]. Data from the National Surveillance of Diarrhea (ViNaDia) revealed a high rotavirus infection rate of 40.2% and 38.3% in 2014 and 2015, respectively [16]. The Rotarix® vaccine was introduced in Mozambique in 2015 with increasing vaccine coverage of 70% and 80% in 2016 and 2017, respectively [16,17]. Post vaccine introduction, the rotavirus infection rate was reduced to 12.2% and 13.5% in 2016 and 2017, respectively [16]. During ViNaDia surveillance, G1P[8] strains were consistently observed in the pre- (2012–2015) and post-vaccination period (2016–2019). However, in the post-vaccine period a decrease in G1P[8] strains was observed which coincided with the emergence of other non-G1P[8] genotypes such as G3P[4] and G3P[8] [18].

The whole genomes of Mozambican G2P[4], G8P[4], G12P[6] and G12P[8] RVA strains from the pre-vaccination period have been described [19,20]. However, there are no reports of the whole genome analyses of G1P[8] strains from Mozambique. To address this, the consensus sequences of 36 G1P[8] strains collected between 2012–2017 from vaccinated and non-vaccinated children were analyzed to investigate the diversity and evolution of G1P[8] strains.

## **2. Results**

### *2.1. Genome Constellation*

A total of 36 G1P[8] (12 from the pre-vaccine period and 24 from the post-vaccine period) strains were successfully sequenced with an average coverage ranging from 450.0 to 46060.5 per sequence (Supplementary Table S1). Complete open reading frames (ORFs) were obtained for 393 of the 396 genome segments analyzed. A partial ORF (99.0%) for segment four of RVA/Human-wt/MOZ/HCN0690/2015/G1P[8] was obtained, while two genome segments (encoding VP2 and VP3, respectively) of RVA/Human-wt/MOZ/HGM0059/2014/G1P[8] could not be determined as insufficient data were generated for these two segments (Supplementary Table S1). The genotype constellations were determined and all strains exhibited a Wa-like genetic backbone (G1-P[8]-I1-R1-C1-M1-A1-N1-T1-E1-H1). The nucleotide (nt) identities among Mozambican strains varied from 92.5–100.0% and the comparison between Rotarix® and the 11 genes of the Mozambican strains revealed 84.0–97.9% nt identity (Supplementary Table S2).

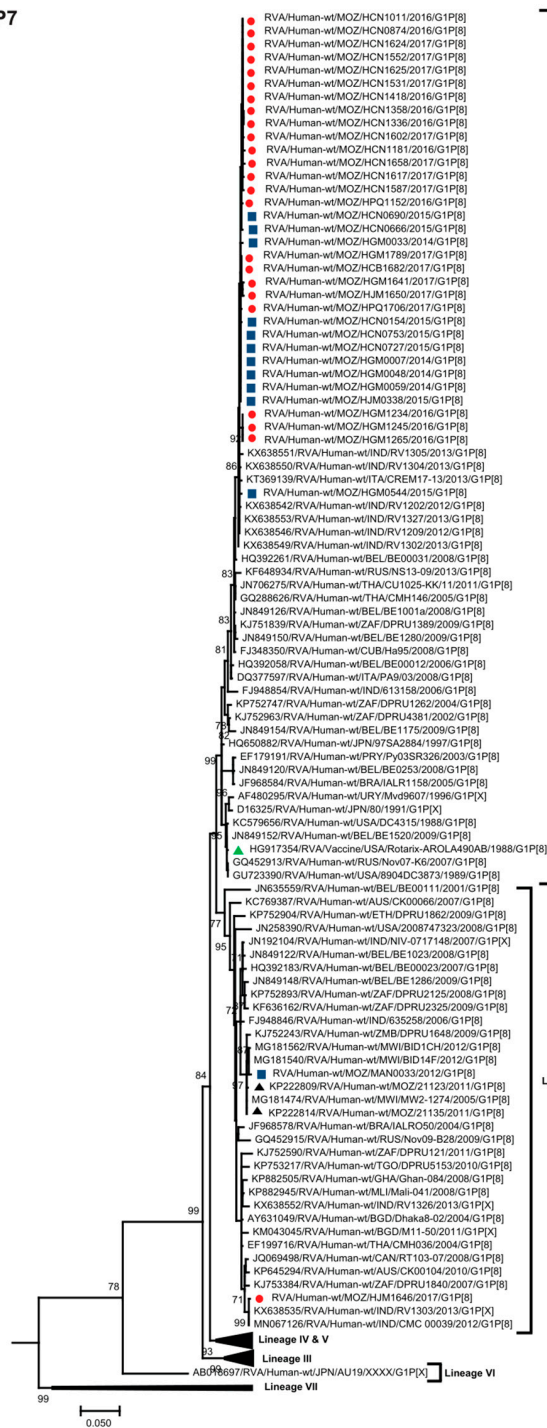
### *2.2. Phylogenetic Analyses*

#### **2.2.1. Sequence Analyses of VP7 and VP4**

The VP7 encoding sequences of the 36 Mozambican G1P[8] strains, collected between 2012 to 2017 from non-vaccinated and vaccinated children (Supplementary Table S3), were compared with human rotavirus sequences representing VP7 G1 lineages (I–VII) [21–28]. The Mozambican strains clustered into two distinct lineages, I and II (Figure 1a). The majority of Mozambican strains formed a highly conserved clade, and were closely related to various Indian strains circulating between 2012 and 2013. HGM0544 was moderately divergent to the rest of the strains in the clade sharing 99.2–99.7% nucleotide (nt) identity and 98.8–99.4% amino acid (aa) identity. Strains from the pre- and post-vaccine era were intermingled in lineage II. Only two Mozambican strains from this study clustered in the VP7 lineage I and were more diverse than the 34 strains clustering in lineage II. MAN0033, collected in a rural area in southern Mozambique before vaccine introduction, was closely related to Malawian strains from 2012 and to previously characterized Mozambican strains detected in 2011 [14]. HJM1646, collected in southern Mozambique after vaccine introduction, clustered distinctly and only shared 92.5–92.9% nt and 92.7–93.3% aa identity to the other Mozambican strains. HJM1646 clustered with contemporary Indian strains in a sub-lineage of African and global strains (Figure 1a).

The P[8] encoding sequences of the 36 Mozambican strains were compared with human rotavirus sequences representing the four lineages (I–IV) [21–27] (Figure 1b). The Mozambican strains clustered in the major P[8] lineage III. Similar to the VP7 tree, the majority of Mozambican P[8] sequences formed a highly conserved clade, and were closely related to various Indian strains circulating between 2012 and 2013. The P[8] encoding sequence of HJM1646 clustered with HGM0544, despite clustering in different VP7 lineages. These two strains were moderately divergent to the rest of the study strains in the Mozambican clade and clustered close to another Mozambican strain, RVA/Human-wt/MOZ/0060a/2012/G12P[8]P[14], which was previously detected in the Manhica district in southern Mozambique [19]. MAN0033 clustered distinctly to the rest of the Mozambican strains sharing 95.7–96.2% nt and 98.3–98.7% aa identity and was closely related to contemporary Malawian strains isolated in 2012 (Figure 1b, Supplementary Table S1).

a) VP7



b) VP4

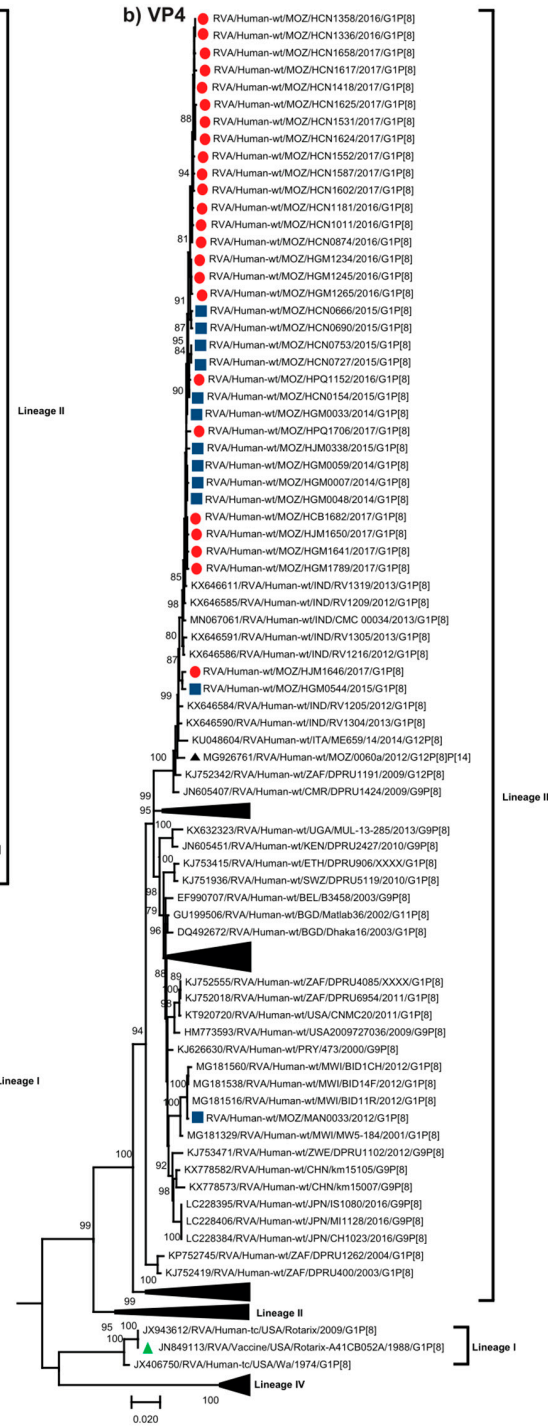


**Figure 1.** Phylogenetic trees based on the ORF (open reading frame) nucleotide sequence of the (a) VP7 and (b) VP4 genes of G1P[8] strains circulating in Mozambique and global strains obtained from GenBank. The trees were constructed based on the maximum likelihood method implemented in MEGA X [29], applying the best-fit nucleotide substitution model Tamura-3-parameter (T92+G+I) for VP7 and General Time Reversible (GTR-G) for VP4, determined by JModelTest [30]. Bootstrap values (1000 replicates)  $\geq 70\%$  are shown with DS-1 serving as an out-group (not shown in the final tree). Scale bar indicates genetic distance expressed as the number of nucleotide substitutions per site. Pre-vaccine Mozambican strains are indicated by blue squares, post-vaccine by red circles, the Rotarix® vaccine strain by a green triangle and Mozambican strains from previous studies [14,19] are indicated by black triangles. Lineages are defined from I-VIII for VP7 and I-IV for VP4 [21–23,25–28].

### 2.2.2. Sequence Analyses of VP1-VP3 and VP6

Thirty-three Mozambican strains formed conserved, monophyletic clades that were observed in the VP1, VP2 and VP3 trees, closely related to RVA/Human-wt/IND/CMC00034/2013/G1P[8], and within lineages comprising of contemporary African and global strains (Figure 2a–c). In the VP6 tree, the 35 Mozambican strains clustered together but did not form a discrete monophyletic clade, and were closely related to contemporary Indian G1P[8] strains (Figure 2d). HJM1646 and HGM0544 clustered together in the VP1 tree were moderately divergent from the main Mozambican clade (Figure 2a). In the VP2 tree, HJM1646 clustered close to the monophyletic clade while HGM0544 fell within the Mozambican clade (Figure 2b). In the VP3 tree, these strains clustered together, distinct from the Mozambican clade, adjacent to previously characterized G12P[6] Mozambican strains (Figure 2c) [19]. MAN0033 fell within the same lineage as the main Mozambican clade, showing minor divergence in the VP1 and VP2 tree and more pronounced divergence in the VP3 tree, closely related to contemporary Malawian G1P[8] strains (Figure 2a–c). This strain clustered within a different lineage in the VP6 tree, closely related to the same group of Malawian G1P[8] strains and adjacent to the Mozambican G12P[6] strains (Figure 2d).

### 2.2.3. Sequence Analyses of NSP1-NSP5/6

The conserved monophyletic clade, comprised of 33 Mozambican strains, was observed in the NSP1–NSP4 trees, with RVA/Human-wt/IND/CMC00034/2013/G1P[8] interspersed within the clade in the NSP2 tree (Figure 2e–h). HJM1646 and HGM0544 continued to show varied clustering patterns across the trees. In the NSP3 tree these strains clustered together and were divergent from the main Mozambican clade, clustering with Indian strains including RVA/Human-wt/IND/CMC00034/2013/G1P[8], and close to Mozambican G12P[6] strains (Figure 2g). HJM1646 was divergent to the Mozambican clade in the NSP1 and NSP4 trees, but clustered close to the monophyletic clade in the NSP2 tree. HGM0544 clustered with the main Mozambican clade in the NSP1, NSP2 and NSP4 trees. In the NSP5 tree, HJM1646 and HGM0544, along with 33 other Mozambican strains, formed a monophyletic clade that was interspersed with global strains (Figure 2i). MAN0033 clustered distinctly to the rest of the Mozambican strains and was closely related to contemporary Malawian strains isolated in 2012 across these trees (Figure 2e–i). The five G12P[6] [19] Mozambican strains fell within neighboring clusters to MAN0033 in the VP6 and NSP2 trees (Figure 2d,f).

### 2.3. Evolutionary Analysis of VP7 and VP4 Genes

A randomly subsampled dataset of 378 G1 genes that were representative of global strains temporally and genetically were analyzed (Supplementary Figure S1). The Mozambican strains detected between 2012 and 2017 shared a common ancestral strain circulating in 2009.9 (95% HPD 2008.1–2010.9). Of the Mozambican strains characterized in this study, 34 clustered within the same lineage and shared a most recent common ancestor in 2011.7 (95% HPD 2011.1–2012.0) and diverged from the closest related Indian strains around the same time. MAN0033 and HJM1646 clustered in the other major lineage present in the tree. MAN0033 and closely related Malawian strains shared a common ancestor in 2010.1 (95% HPD 2008.5–2010.9). These variants, circulating in Malawi, Zambia and Mozambique, diverged from a group of Indian G1P[8] strains in 2001.3 (95% HPD 1998.4–2003.5). HJM1646 was divergent to the other G1 strains from Mozambique in this lineage and shared its most recent common ancestor with Indian strains in 2012.9 (95% HPD 2012.4–2013.0) (Supplementary Figure S1).

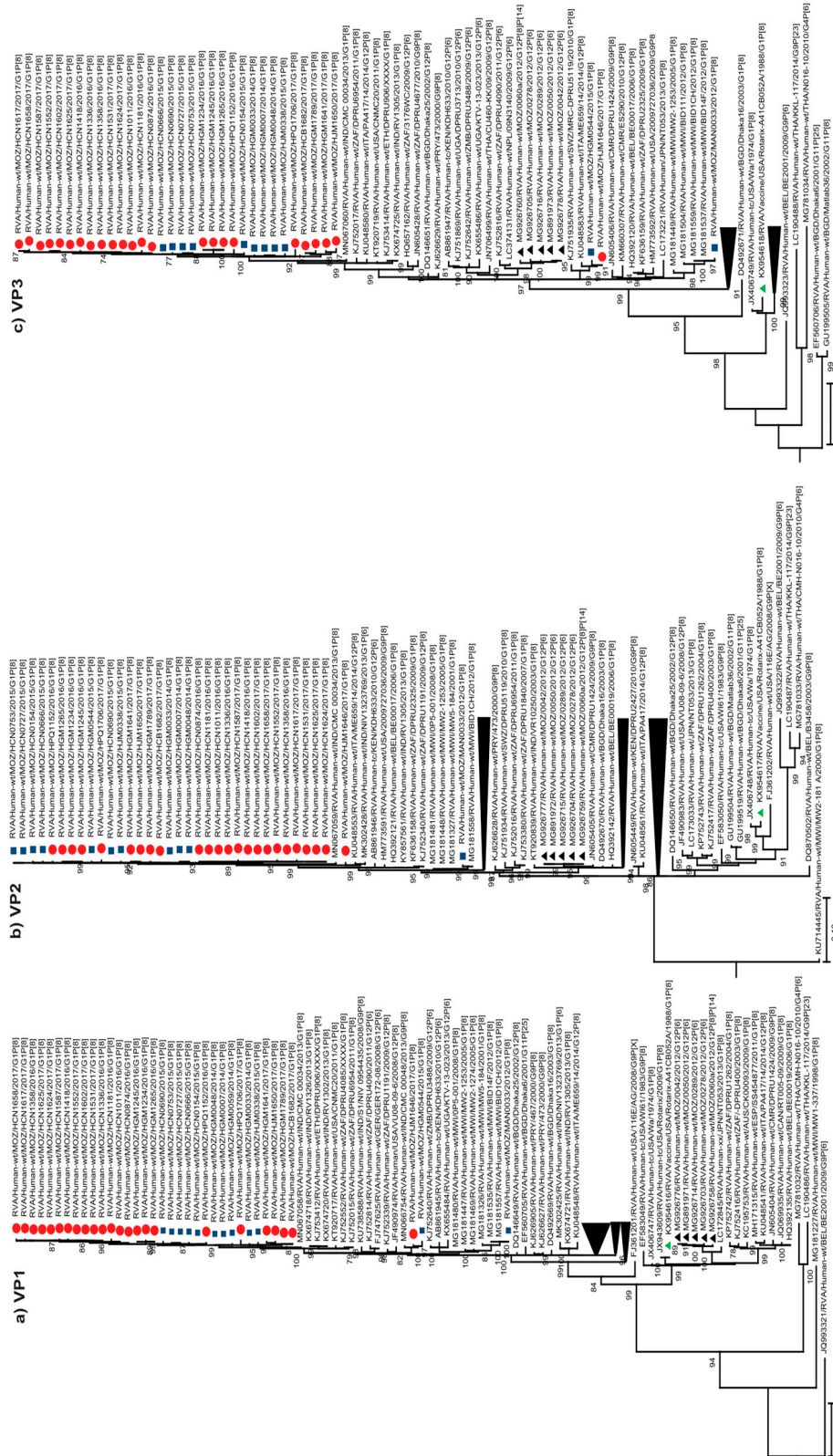


Figure 2. Cont.

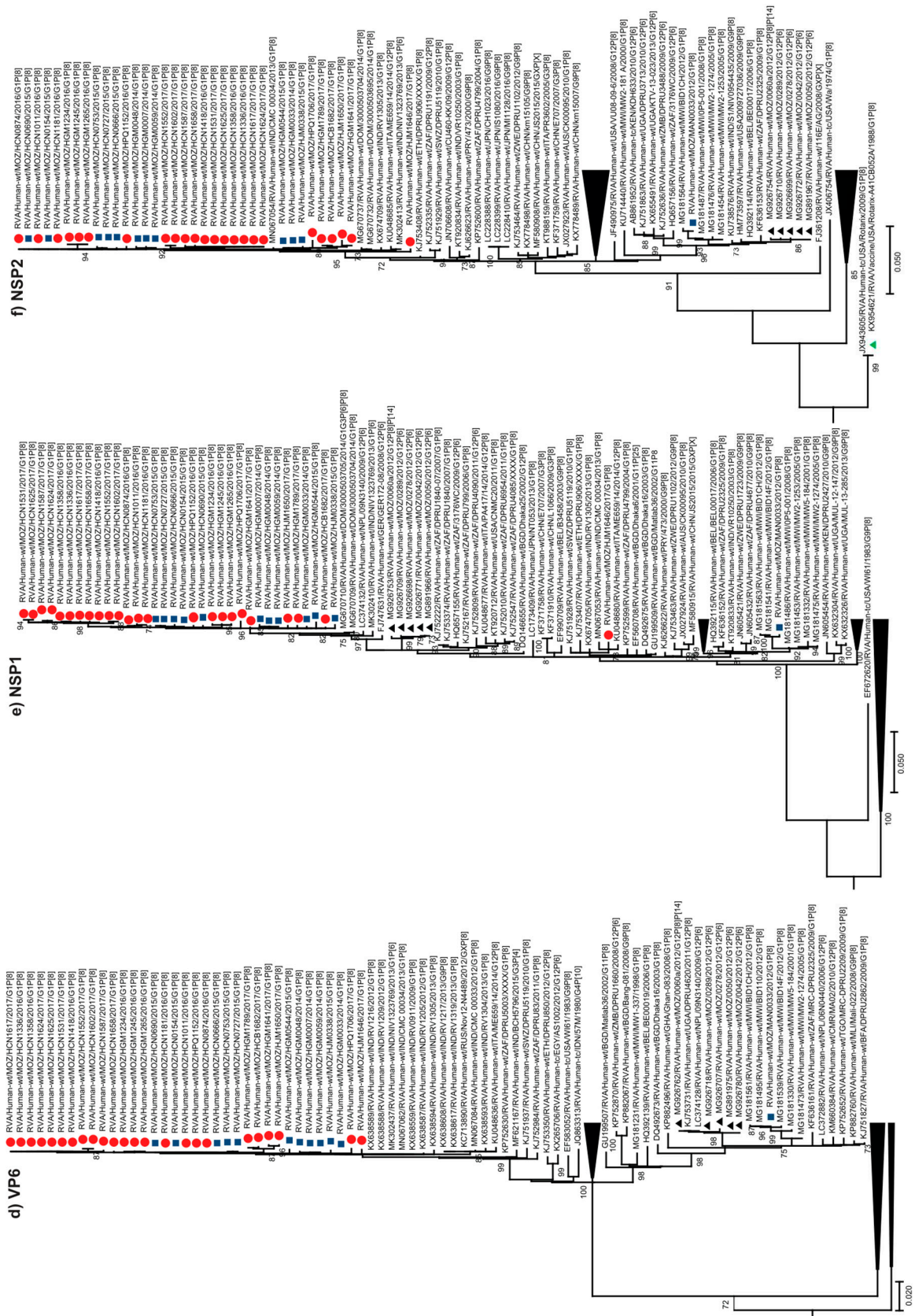


Figure 2. Cont.

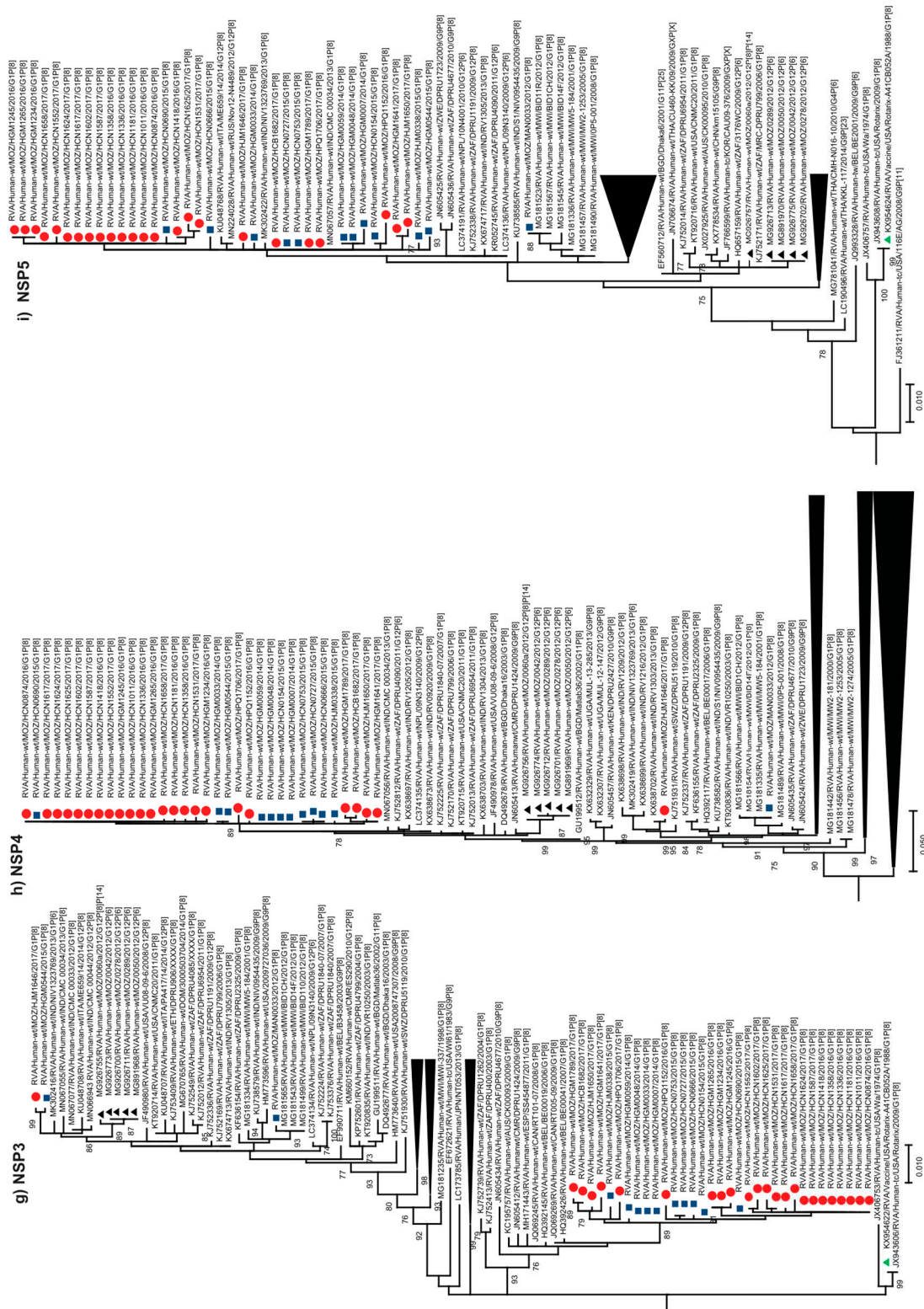


Figure 2. Phylogenetic trees based on the ORF nucleotide sequences of the (a) VP1, (b) VP2, (c) VP3, (d) VP6, (e) NSP1, (f) NSP2, (g) NSP3, (h) NSP4 and (i) NSP5

genes of G1P[8] strains circulating in Mozambique and global strains obtained from GenBank. The trees were constructed based on the maximum likelihood method implemented in MEGA X [29], using the best-fit nucleotide substitution model General Time Reversible (GTR+G+I) for VP3, GTR+G for VP2, NSP2 and NSP3, Hasegawa Kishino Yano (HKY+G+I) for VP6 and NSP1, HKY+G for VP1, NSP4 and NSP5/6, determined by JModelTest [30]. Bootstrap values (1000 replicates)  $\geq 70\%$  are shown with DS-1 serving as an out-group (not shown in the final tree). Scale bar indicates genetic distance expressed as the number of nucleotide substitutions per site. Pre-vaccine Mozambican strains are indicated by blue squares, post-vaccine by red circles, the Rotarix<sup>®</sup> vaccine strain by a green triangle and Mozambican strains from a previous study [19] are indicated by black triangles.

A subsampled dataset of 235 P[8] genes, representative of global strains temporally and genetically, was also analyzed. Thirty-three Mozambican strains characterized in this study clustered within the same lineage and shared a common ancestor in 2013.0 (95% HPD 2012.1–2013.6) and diverged from the closest related Indian strains around 2011.6 (95% HPD 2011.2–2011.9) (Supplementary Figure S2). The most recent common ancestor of HGM0544 and HJM1646 (that was moderately divergent to the rest of the Mozambican strains in the major clade), was estimated to be 2014.1 (95% HPD 2013.0–2014.9). Clustering in a separate lineage to the other Mozambican G1P[8] strains, MAN0033 diverged from the closest Malawian strain in 2010.9 (95% HPD 2009.5–2011.7) (Supplementary Figure S2).

2.4. Comparative Analysis of Neutralizing Antigenic Epitopes of the VP7 and VP4 Genes of Mozambican Strains and the Rotarix® Vaccine Strain

The rotavirus VP7 protein consists of two antigenic epitopes, 7-1 and 7-2, with 7-1 subdivided into 7-1a and 7-1b [31]. The comparative analysis of the VP7 antigenic epitopes between Mozambican strains and the Rotarix® vaccine strain revealed amino acid substitutions in all three antigenic sites. However, most of the amino acid substitutions were observed in antigenic region 7-2. A total of 30 strains shared conserved amino acid differences at positions N147D and 25 strains at M217I. Sporadic mutations were observed in MAN0033 (unvaccinated) and HJM1646 (fully vaccinated) (S123N, K291R and M217T). The HJM1646 strain contained an additional amino acid substitution at N96S (Figure 3).

Antigenic regions	7-1a													7-1b						7-2									
	87	91	94	96	97	98	99	100	104	123	125	129	130	291	201	211	212	213	238	242	143	145	146	147	148	190	217	221	264
Rotarix®	T	T	N	G	E	W	K	D	Q	S	V	V	D	K	Q	N	V	D	N	T	K	D	Q	N	L	S	M	N	G
HCB1682	.	.	.	.	.	.	.	.	.	.	.	.	.	.	.	.	.	.	.	.	.	.	.	D	.	.	.	.	.
HCN0154	.	.	.	.	.	.	.	.	.	.	.	.	.	N	.	.	.	.	.	.	.	.	.	D	.	.	I	.	.
HCN0666	.	.	.	.	.	.	.	.	.	.	.	.	.	.	.	.	.	.	.	.	.	.	.	D	.	.	I	.	.
HCN0690	.	.	.	.	.	.	.	.	.	.	.	.	.	.	.	.	.	.	.	.	.	.	.	D	.	.	I	.	.
HCN0727	.	.	.	.	.	.	.	.	.	.	.	.	.	.	.	.	.	.	.	.	.	.	.	D	.	.	I	.	.
HCN0753	.	.	.	.	.	.	.	.	.	.	.	.	.	.	.	.	.	.	.	.	.	.	.	D	.	.	I	.	.
HCN0874	.	.	.	.	.	.	.	.	.	.	.	.	.	.	.	.	.	.	.	.	.	.	.	D	.	.	I	.	.
HCN1011	.	.	.	.	.	.	.	.	.	.	.	.	.	.	.	.	.	.	.	.	.	.	.	D	.	.	I	.	.
HCN1181	.	.	.	.	.	.	E	.	.	.	.	.	.	.	.	.	.	.	.	.	.	.	.	D	.	.	I	.	.
HCN1336	.	.	.	.	.	.	.	.	.	.	.	.	.	.	.	.	.	.	.	.	.	.	.	D	.	.	I	.	.
HCN1358	.	.	.	.	.	.	.	.	.	.	.	.	.	.	.	.	.	.	.	.	.	.	.	D	.	.	I	.	.
HCN1418	.	.	.	.	.	.	.	.	.	.	.	.	.	.	.	.	.	.	.	.	.	.	.	D	.	.	I	.	.
HCN1531	.	.	.	.	.	.	.	.	.	.	.	.	.	.	.	.	.	.	.	.	.	.	.	D	.	.	I	.	.
HCN1552	.	.	.	.	.	.	.	.	.	.	.	.	.	.	.	.	.	.	.	.	.	.	.	D	.	.	I	.	.
HCN1587	.	.	.	.	.	.	.	.	.	.	.	.	.	.	.	.	.	.	.	.	.	.	.	D	.	.	I	.	S
HCN1602	.	.	.	.	.	.	.	.	.	.	.	.	.	.	.	.	.	.	.	.	.	.	.	D	.	.	I	.	.
HCN1617	.	.	.	.	.	.	.	.	.	.	.	.	.	.	.	.	.	.	.	.	.	.	.	D	.	.	I	.	.
HCN1624	.	.	.	.	.	.	.	.	.	.	.	.	.	.	.	.	.	.	.	.	.	.	.	D	.	.	I	.	.
HCN1625	.	.	.	.	.	.	.	.	.	.	.	.	.	.	.	.	.	.	.	.	.	.	.	D	.	.	I	.	.
HCN1658	.	.	.	.	.	.	.	.	.	.	.	.	.	.	.	.	.	.	.	.	.	.	.	D	.	.	I	.	.
HGM0007	.	.	.	.	.	.	.	.	.	.	.	.	.	.	.	.	.	.	.	.	.	.	.	D	.	.	I	.	.
HGM0033	.	.	.	.	.	.	.	.	.	.	.	.	.	.	.	.	.	.	.	.	.	.	.	D	.	.	I	.	.
HGM0048	.	.	.	.	.	.	.	.	.	.	.	.	.	.	.	.	.	.	.	.	.	.	.	D	.	.	I	.	.
HGM0059	.	.	.	.	.	.	.	.	.	.	.	.	.	.	.	.	.	.	.	.	.	.	.	D	.	.	I	.	.
HGM0544	.	.	.	.	.	.	.	.	.	.	.	.	.	.	.	.	.	I	.	.	.	.	.	.	.	.	.	.	.
HGM1234	.	.	.	.	.	.	.	.	.	.	.	.	.	.	.	.	.	.	.	.	.	.	.	.	.	.	I	.	.
HGM1245	.	.	.	.	.	.	.	.	.	.	.	.	.	.	.	.	.	.	.	.	.	.	.	.	.	.	I	.	.
HGM1265	.	.	.	.	.	.	.	.	.	.	.	.	.	.	.	.	.	.	.	.	.	.	.	.	.	.	I	.	.
HGM1641	.	.	.	.	.	.	.	.	.	.	.	.	.	.	.	.	.	.	.	.	.	.	.	D	.	.	.	.	.
HGM1789	.	.	.	.	.	.	.	.	.	.	.	.	.	.	.	.	.	.	.	.	.	.	.	D	.	.	.	.	.
HJM0338	.	.	.	.	.	.	.	.	.	.	.	.	.	.	.	.	.	.	.	.	.	.	.	D	.	.	.	.	.
HJM1646	.	.	S	.	.	.	.	.	.	N	.	.	.	R	.	.	.	.	.	.	.	.	.	.	.	.	.	T	.
HJM1650	.	.	.	.	.	.	.	.	.	.	.	.	.	.	.	.	.	.	.	.	.	.	.	D	.	.	.	.	.
HPQ1152	.	.	.	.	.	.	.	.	.	.	.	.	.	.	.	.	.	.	.	.	.	.	.	D	.	.	I	.	.
HPQ1706	.	.	.	.	.	.	.	.	.	.	.	.	.	.	.	.	.	.	.	.	.	.	.	D	.	.	.	.	.
MAN0033	.	.	.	.	.	.	.	.	N	.	.	.	R	.	.	.	.	.	.	.	.	.	.	.	.	.	T	.	

Figure 3. The alignment of amino acids corresponding to three VP7 antigenic epitopes (7-1a, 7-1b and 7-2). The amino acid sequence of Rotarix® is the reference strain and the conserved residues between the Rotarix® to Mozambican strains are indicated by dots (.) and residues that differ are in bold.

Activation of the protein VP4 requires proteolytic cleavage to produce the VP8\* and VP5\* subunits. These regions contain four (8-1 to 8-4) and five (5-1 to 5-5) antigenic epitopes, respectively [32,33]. The amino acid substitutions between the Rotarix® vaccine strain and Mozambican P[8] strains were concentrated in the 8-1 and 8-3 epitopes. There were five conserved amino acid substitutions, at positions E150D, N195D/G, S125N, S131R and N135D. Sporadic mutations were observed in MAN0033 (N195S and N113D), HJM0338 (S146N) and HGM1789 (P114T) (Figure 4).



### 3. Discussion

In the present study, whole genome sequencing was performed for 36 G1P[8] RVA strains obtained from Mozambican children with gastroenteritis between 2012–2017 (12 from the pre-vaccine period and 24 from the post-vaccine period). This is the first study to perform whole genome analysis of G1P[8] strains in Mozambique, facilitating the description of genetic diversity and the origins of Mozambican strains.

Of the 36 strains characterized, 33 clustered within the same conserved Mozambican clade across all trees. Two strains, HGM0544 and HJM1646, showed varied patterns by clustering within and were distinct from the Mozambican clade across trees, suggesting these strains had undergone reassortment events. The strain, MAN0033, clustered distinctly from the rest of the Mozambican strains in all trees. This strain was closely related to a conserved group of Malawian G1P[8] strains suggesting that this strain may have been recently introduced from a neighboring country. No distinct clustering patterns were observed based on the year of isolation or vaccination status, which suggests that strains with limited sequence diversity may have circulated among children in the country over the five year period investigated (2012–2017). The homogeneous population of G1P[8] strains suggests that the introduction of Rotarix® has not resulted in a dramatic shift in the diversity of G1P[8] strains circulating in Mozambique. A similar finding was reported in South Africa where no distinct clustering was observed for strains from the pre- and post-vaccine introduction period [26]. Analysis of G1P[8] strains in Brazil over a 27 year period also did not detect any evidence of a selective pressure exerted by the mass introduction of Rotarix® [34]. In contrast, Australia and Belgium reported some unique clusters of G1P[8] strains following vaccine introduction, which may have been due to natural fluctuation or the first signs of vaccine-driven evolution [35]. In Rwanda, unique clusters of G1P[8] strains were identified following RotaTeq introduction [36]. Although neighboring countries reported the widespread (Malawi) and sporadic (South Africa) detection of G1P[8] strains that had undergone reassortment with DS-1 like strains [28,37], all Mozambican strains characterized in this study exhibited a typical Wa-like genetic backbone. Despite some reports of vaccine-derived G1P[8] strains detected in Australia and England, none of the strains identified in this study were derived from the Rotarix® vaccine [38,39].

Although there are seven recognized lineages described for global G1 sequences [40], the majority of Mozambican strains from this study clustered in lineage II, with only two strains clustering in lineage I. However, one strain that clustered in lineage I represented the oldest Mozambican strain sequenced in this study from 2012, which clustered with previously characterized G1P[8] Mozambican strains from 2011 [14]. This may suggest that lineage I strains were replaced in later years by G1 strains associated with lineage II [26,41]. The VP7 lineage I strains were detected in the south of Mozambique which may suggest geographical restriction in the circulation of strains. However, these results can be in part due to the short sampling period of this study. Of the four established lineages of the P[8] genotype [21], all Mozambican strains clustered in lineage III and shared a high level of genetic similarity, except strain MAN0033 which clustered in a distinct sub-lineage.

Maximum likelihood phylogenetic analysis showed that the majority of the Mozambican strains, with the exception of MAN0033, were most closely related to a conserved group of Indian strains across most genes. Even the two reassortant strains (HJM1646 and HGM0544) were most closely related to Indian strains. This suggests that there may have been multiple, contemporary introductions of diverse strains from a similar origin, perhaps India, into Mozambique. This was further supported by the results of the Bayesian analysis, where the time to the most recent common ancestor for the VP7 and VP4 genes of the main Mozambican clade were 2011.7 and 2013.0, respectively, and which had diverged from the closest Indian strain in 2011.7 and 2011.6, respectively. This suggests that the strains became endemic shortly after being introduced and became the dominant variant circulating in the population. These Indian strains were submitted directly to the GenBank database and no associated manuscripts were found, so it is unclear if these strains were associated with any particular outbreak or were detected as part of routine surveillance.

Overall, the VP7 and VP4 antigenic epitopes exhibited conserved substitutions among the Mozambican strains when compared to Rotarix<sup>®</sup>. The substitutions in the 7-2 VP7 epitope at position M217I, N147D and 8-1, 8-3 VP4 at positions E150D, N195D and S125N, S131R, N135D were observed in pre- and post-vaccine introduction strains, suggesting that these substitutions are not due to the vaccine introduction.

The main limitation of the study was the limited number of strains successfully sequenced, and that fewer strains were sequenced from the pre-vaccine period.

There is a need to expand the whole genome analysis to other strains detected in Mozambique such as G3, G9 in combination with P[4], P[6] and P[8] genotypes reported previously [18] in order to evaluate the possible influence of vaccine introduction on other rotavirus genotypes.

Mozambique has introduced the Rotarix<sup>®</sup> vaccine, however cases of rotavirus infection associated with G1P[8] strains resulting in hospitalization of children are still being reported. The present analysis showed that G1P[8] strains detected in the post-vaccine period did not undergo significant mutations in the epitope regions that could result in vaccine escape. However, the short post vaccine period analyzed (three years) may have influenced these results, as it may be too early to see major genetic changes associated with vaccine pressure. These results highlight the need for future studies to understand host factors such as the role of histo-blood group antigen status, nutritional status and enteric co-infections that can influence the vaccine effectiveness in Mozambique.

#### **4. Materials and Methods**

##### *4.1. Ethics Approval*

The ViNaDia Protocol was approved by the National Health Bioethics Committee of Mozambique (CNBS) under number (IRB00002657, reference Nr: 348/CNBS/13). Participants' anonymity and confidentiality were guaranteed.

##### *4.2. Sample Collection*

Forty-three fecal samples, collected between 2012 and 2017 that were positive for RVA by ELISA (Prospect EIA rotavirus, Basingstoke, UK) and identified as genotype G1P[8] by multiplex RT-PCR according to described protocols [42,43], were selected for sequencing according to year of isolation, location of collection (region of Mozambique) and the child's vaccination status. The samples were obtained from children <5 years of age, hospitalized with acute gastroenteritis, and collected at five sentinel sites of the National Diarrheal Surveillance (ViNaDia), which are Hospital Geral de Mavalane (HGM), Hospital Geral Jose Macamo (HJM), Hospital Central da Beira (HCB), Hospital Geral de Quelimane (HGQ) and Hospital Central de Nampula (HCN), and from a previous study of Centro de Investigação em Saúde da Manhiça (CISM) in Mozambique between 2012 and 2013 (Supplementary Figure S3) [15]. Clinical information was collected through a structured questionnaire from ViNaDia which included metadata such as age, gender, site and vaccination status.

##### *4.3. RNA Extraction and cDNA Synthesis*

Total RNA was extracted from stool samples with TRI-reagent (Sigma, Darmstadt, Germany) and single-stranded RNA was precipitated with lithium chloride. The self-priming PC3-T7 loop primer (Integrated DNA Technologies, Coralville, IA, USA) was ligated to dsRNA in order to obtain full-length sequences and cDNA was synthesized using the Maxima H Minus double-stranded cDNA kit (Thermo Fisher Scientific, Massachusetts, MA, USA) as previously described [20,44].

##### *4.4. Next Generation Sequencing*

The whole genome sequencing was performed using an Illumina MiSeq sequencing platform (Illumina, Inc. San Diego, CA, USA) at the Next Generation Sequencing Unit at the University of the

Free State (NGS-UFS). Sequencing was completed using the Nextera XT DNA Library Preparation Kit (Illumina, Inc., San Diego, CA, USA) using protocols previously describe [19].

#### *4.5. Data Analyses*

A de novo assembly was performed for all samples using CLC Bio Genomics Workbench (12.0.3; Qiagen, Aarhus, Denmark); all contigs with an average coverage above 100 were identified on the Nucleotide Basic Local Alignment Search Tool (BLASTn at the National Center for Biotechnology information (NCBI). References were chosen based on the Blastn results for reference mapping and extraction of consensus sequences for each segment. The genotyping tools, Virus Pathogenic database and analysis resource (ViPR) [45] and RotaC v2.0 [46], were used to determine the genotype of each gene. The sequences were submitted to GenBank and accession numbers MT737379-MT737772 were assigned.

#### *4.6. Phylogenetic Analysis*

Multiple nucleotide sequence alignments with strains obtained from GenBank [24] were made with multiple sequence alignment program (MAFFT v7.450) [47] on Geneious prime v2020.0.3 and Multiple Sequence Comparison by Log Expectation (MUSCLE) [48] alignment available in Molecular Evolutionary Genetic Analysis X (MEGA X) [29]. The optimal nucleotide substitution model for phylogenetic analysis was selected based upon the Akaike information criterion (corrected) (AICc) ranking implemented in the model selection algorithm available on JModelTest [30] and the models selected for each segment were: Tamura-3 parameter (T92+G+I) [49] for VP7; General Time Reversible (GTR+G+I) [50] for VP3; GTR+G for VP2, VP4, NSP2 and NSP3; Hasegawa Kishino Yano (HKY+G+I) for VP6 and NSP1; and HKY+G for VP1, NSP4 and NSP5/6 [51]. The maximum-likelihood trees were generated using MEGA X [29] using 1000 bootstrap replicates to estimate branch support. Pairwise distance matrix nucleotides were obtained in MEGA X using the p-distance algorithm [29]. Amino acid sequences of the VP7 and VP4 Mozambican strains were aligned and epitopes were identified and compared to those of the vaccine strain Rotarix<sup>®</sup> (A41CB052A, with accession numbers JN849114 and JN849113 for VP7 and VP4) using MEGA X [23,31].

#### *4.7. Evolutionary Analysis*

Maximum likelihood trees were generated using the Randomized Accelerated Maximum Likelihood (RAxML) program (v2.0.0) [52], applying the nucleotide substitution model GTR+G. The trees were used as the input for TempEst 1.5.3 to plot root-to-tip genetic distances, and sequences not conforming to a linear evolutionary pattern were discarded [53]. Time-measured evolutionary histories were reconstructed using the Bayesian Evolutionary Analysis Sampling Trees (BEAST) Program package (v 1.7.5) [54]. The nucleotide substitution model Hasegawa-Kishino-Yano model (HKY+G) for VP7 and GTR+G for VP4 were selected based on AICc raking in jModelTest [30].

The parameters applied included a relaxed uncorrelated lognormal molecular clock to account for varied evolutionary rates among lineages and a coalescent Gaussian Markov random field (GMRF) Bayesian Skyride tree prior. Three independent Markov chain Monte Carlo (MCMC) chains were run for 200 million generations with sampling every 20,000 generations, with the first 10% discarded as burn-in. Convergence and mixing of the chains was assessed using Tracer (v1.7.1) and all parameters yielded effective sample sizes  $\geq 200$  [55]. The Maximum Clade Credibility (MCC) trees were summarized using TreeAnnotator (v1.10.4) [54]. The time-ordered MCC trees were visualized in FigTree (v1.4.4) (<http://tree.bio.ed.ac.uk/software/figtree/>).

## **5. Conclusions**

This study provides important insights into the whole genome sequences of G1P[8] strains in Mozambique. Whilst similar strains were detected prior to and following vaccine introduction, multiple introductions of diverse strains from India highlight the importance of continuously monitoring the

strains detected in Mozambique to determine if the strains are evolving by vaccine-induced selection or by natural evolutionary pressures.

**Supplementary Materials:** The following are available online at <http://www.mdpi.com/2076-0817/9/12/1026/s1>: Table S1: Genome assembly of Mozambican Wa-like G1P[8] strains from 2012 to 2017. The percentage identity was determined with BLASTn; Table S2: Nucleotide identities of the Mozambican and Rotarix<sup>®</sup> vaccine strains; Table S3: Mozambican G1P[8] strains. Figure S1: A simplified maximum clade credibility trees (MCC) for the G1 VP7 strains characterized between 1978 and 2017; Figure S2: A simplified maximum clade credibility trees (MCC) for the P[8] VP4 strains characterized between 2000 and 2017; Figure S3: Mozambique Map with the geographical location of study sentinel sites.

**Author Contributions:** Conceptualization: N.d.D., B.M. and E.D.J.; methodology: B.M., C.M.D., A.S. and E.D.J.; validation: N.d.D., C.M.D. and H.G.O.; formal analysis: B.M., E.D.J., C.M.D. and A.S.; investigation: B.M., E.D.J., J.J.C., J.L., A.C., A.F.L.B., M.C., I.C.-M. and S.S.B.; resources: N.d.D.; data curation: C.M.D. and A.S.; writing—original draft preparation: B.M. and E.D.J.; writing—review and editing: B.M., E.D.J., C.M.D., N.d.D., A.S., H.G.O., A.F.L.B. and A.C.; visualization: B.M., E.D.J., C.M.D., N.d.D., A.S. and H.G.O.; supervision: C.M.D. and N.d.D.; project administration: J.J.C. and funding acquisition: N.d.D. and H.G.O. All authors have read and agreed to the published version of the manuscript.

**Funding:** The study was supported by European Foundation Initiative into African Research in Neglected Tropical Diseases that awarded a senior fellowship to ND (EFINTD; 89539); World Health Organization (WHO); Deutsche Forschungsgemeinschaft (DFG; JO369/5-1) to ND and HGO which supported scholarship of BM, AC, AFLB, AS and SSB; Fundo Nacional de Investigação (FNI) fellowships to BM, AC, and JC. EDJ Ph.D. was supported by Calouste Gulbenkian Foundation. CMD is supported through the Australian National Health and Medical Research Council with an Early Career Fellowship (1113269).

**Acknowledgments:** We want to thank the caretakers who consented for their children to be enrolled in the surveillance. For their efforts with recruitment, data collection and shipment of specimens to Maputo, we would like to thank Elda Anapakala, Esperança Guimarães, Júlia Sambo, Diocreciano Bero, Lena Manhique, Judite Salência, Félix Gundane, Aunésia Marurele, Délcio Muteto, Angelina Pereira, Mulaja Kabeya Étienne, Celso Gabriel, Titos Maulate, Julieta Ernesto, Francisca Ricardo, Siasa Mendes, Hércio Simbine, Susete de Carvalho, Marcos Joaquim, Elvira Sarguene, Fernando Vilanculos, Felicidade Martins, Dulce Graça, Edma Samuel, Vivaldo Pedro, Lúcia Matabel, Maria Safrina, Natércia Abreu, Vanessa da Silva, Nazareth Mabutana, Carlos Guilamba and Celina Nhamuave and Rui Cossa for providing the map illustration. For technical ICT support we thank Stephanus Riekert.

**Conflicts of Interest:** CMD has served on an advisory board for GSK (2019), all payments were paid directly to an administrative fund held by Murdoch Children’s Research Institute. All other authors declare no conflicts of interest.

## References

1. Tate, J.E.; Burton, A.H.; Boschi-Pinto, C.; Parashar, U.D. Global, Regional, and National Estimates of Rotavirus Mortality in Children <5 Years of Age, 2000–2013. *Clin. Infect. Dis.* **2016**, *62* (Suppl. 2), S96–S105. [CrossRef] [PubMed]
2. Troeger, C.; Khalil, I.A.; Rao, P.C.; Cao, S.; Blacker, B.F.; Ahmed, T.; Armah, G.; Bines, J.E.; Brewer, T.G.; Colombara, D.V.; et al. Rotavirus Vaccination and the Global Burden of Rotavirus Diarrhea Among Children Younger Than 5 Years. *JAMA Pediatr.* **2018**, *172*, 958–965. [CrossRef] [PubMed]
3. Estes, M.K.; Cohen, J. Rotavirus gene structure and function. *Microbiol. Rev.* **1989**, *53*, 410–449. [CrossRef] [PubMed]
4. Jayaram, H.; Estes, M.; Prasad, B.V. Emerging themes in rotavirus cell entry, genome organization, transcription and replication. *Virus Res.* **2004**, *101*, 67–81. [CrossRef]
5. Desselberger, U. Rotaviruses. *Virus Res.* **2014**, *190*, 75–96. [CrossRef]
6. De Deus, N.; João, E.; Cuamba, A.; Cassocera, M.; Luís, L.; Acácio, S.; Mandomando, I.; Augusto, O.; Page, N. Epidemiology of Rotavirus Infection in Children from a Rural and Urban Area, in Maputo, Southern Mozambique, before Vaccine Introduction. *J. Trop. Pediatr.* **2017**, *64*, 141–145. [CrossRef]
7. Matthijnssens, J.; Ciarlet, M.; McDonald, S.M.; Attoui, H.; Banyai, K.; Brister, J.R.; Buesa, J.; Esona, M.D.; Estes, M.K.; Gentsch, J.R.; et al. Uniformity of rotavirus strain nomenclature proposed by the Rotavirus Classification Working Group (RCWG). *Arch. Virol.* **2011**, *156*, 1397–1413. [CrossRef]
8. Rotavirus Classification Working Group. Virus Classification. Available online: <https://rega.kuleuven.be/cev/viralmetagenomics/virus-classification> (accessed on 5 June 2020).

9. Matthijnssens, J.; Ciarlet, M.; Heiman, E.; Arijs, I.; Delbeke, T.; McDonald, S.M.; Palombo, E.A.; Iturriza-Gómara, M.; Maes, P.; Patton, J.T.; et al. Full Genome-Based Classification of Rotaviruses Reveals a Common Origin between Human Wa-Like and Porcine Rotavirus Strains and Human DS-1-Like and Bovine Rotavirus Strains. *J. Virol.* **2008**, *82*, 3204–3219. [CrossRef]
10. Mwenda, J.M.; Tate, J.E.; Parashar, U.D.; Mihigo, R.; Agócs, M.; Serhan, F.; Nshimirimana, D. African Rotavirus Surveillance Network. *Pediatr. Infect. Dis. J.* **2014**, *33*, S6–S8. [CrossRef]
11. Matthijnssens, J.; Van Ranst, M. Genotype constellation and evolution of group A rotaviruses infecting humans. *Curr. Opin. Virol.* **2012**, *2*, 426–433. [CrossRef]
12. World Health Organization. WHO Prequalifies New Rotavirus Vaccine. Available online: [http://www.who.int/medicines/news/2018/prequalified\\_new-rotavirus\\_vaccine/en/](http://www.who.int/medicines/news/2018/prequalified_new-rotavirus_vaccine/en/) (accessed on 5 June 2020).
13. Burke, R.M.; Tate, J.E.; Kirkwood, C.D.; Steele, A.D.; Parashar, U.D. Current and new rotavirus vaccines. *Curr. Opin. Infect. Dis.* **2019**, *32*, 435–444. [CrossRef] [PubMed]
14. Langa, J.S.; Thompson, R.; Arnaldo, P.; Resque, H.R.; Rose, T.; Enosse, S.M.; Fialho, A.; De Assis, R.M.S.; Da Silva, M.F.M.; Leite, J.P.G. Epidemiology of rotavirus A diarrhea in Chókwè, Southern Mozambique, from February to September, 2011. *J. Med. Virol.* **2016**, *88*, 1751–1758. [CrossRef] [PubMed]
15. João, E.D.; Strydom, A.; O’Neill, H.G.; Cuamba, A.; Cassocera, M.; Acácio, S.; Mandomando, I.; Motanyane, L.; Page, N.; De Deus, N. Rotavirus A strains obtained from children with acute gastroenteritis in Mozambique, 2012–2013: G and P genotypes and phylogenetic analysis of VP7 and partial VP4 genes. *Arch. Virol.* **2017**, *163*, 153–165. [CrossRef] [PubMed]
16. De Deus, N.; Chilaúle, J.J.; Cassocera, M.; Bambo, M.; Langa, J.S.; Siteo, E.; Chissaque, A.; Anapakala, E.; Sambo, J.; Guimarães, E.L.; et al. Early impact of rotavirus vaccination in children less than five years of age in Mozambique. *Vaccine* **2018**, *36*, 7205–7209. [CrossRef]
17. World Health Organization. WHO and UNICEF Estimates of National Immunization Coverage. Available online: [http://www.who.int/immunization/monitoring\\_surveillance/routine/coverage/en/index4.html](http://www.who.int/immunization/monitoring_surveillance/routine/coverage/en/index4.html) (accessed on 1 April 2020).
18. João, E.; Munlela, B.; Chissaque, A.; Chilaúle, J.; Langa, J.S.; Augusto, O.; Boene, S.; Anapakala, E.; Sambo, J.; Guimarães, E.; et al. Molecular Epidemiology of Rotavirus A Strains Pre- and Post-Vaccine (Rotarix®) Introduction in Mozambique, 2012–2019: Emergence of Genotypes G3P[4] and G3P[8]. *Pathogens* **2020**, *9*, 671. [CrossRef]
19. Strydom, A.; Motanyane, L.; Nyaga, M.M.; João, E.D.; Cuamba, A.; Mandomando, I.; Cassocera, M.; De Deus, N.; O’Neill, H.G. Whole-genome characterization of G12 rotavirus strains detected in Mozambique reveals a co-infection with a GXP[14] strain of possible animal origin. *J. Gen. Virol.* **2019**, *100*, 932–937. [CrossRef]
20. Strydom, A.; João, E.D.; Motanyane, L.; Nyaga, M.M.; Potgieter, A.C.; Cuamba, A.; Mandomando, I.; Cassocera, M.; De Deus, N.; O’Neill, H.G. Whole genome analyses of DS-1-like Rotavirus A strains detected in children with acute diarrhoea in southern Mozambique suggest several reassortment events. *Infect. Genet. Evol.* **2019**, *69*, 68–75. [CrossRef]
21. Le, V.P.; Chung, Y.-C.; Kim, K.; Chung, S.-I.; Lim, I.; Kim, W. Genetic variation of prevalent G1P[8] human rotaviruses in South Korea. *J. Med. Virol.* **2010**, *82*, 886–896. [CrossRef]
22. Arista, S.; Giammanco, G.M.; De Grazia, S.; Ramirez, S.; Biundo, C.L.; Colomba, C.; Cascio, A.; Martella, V. Heterogeneity and Temporal Dynamics of Evolution of G1 Human Rotaviruses in a Settled Population. *J. Virol.* **2006**, *80*, 10724–10733. [CrossRef]
23. Zeller, M.; Patton, J.T.; Heylen, E.; De Coster, S.; Ciarlet, M.; Van Ranst, M.; Matthijnssens, J. Genetic Analyses Reveal Differences in the VP7 and VP4 Antigenic Epitopes between Human Rotaviruses Circulating in Belgium and Rotaviruses in Rotarix and RotaTeq. *J. Clin. Microbiol.* **2012**, *50*, 966–976. [CrossRef]
24. Ianiro, G.; Delogu, R.; Fiore, L.; Ruggeri, F.M. Genetic variability of VP7, VP4, VP6 and NSP4 genes of common human G1P[8] rotavirus strains circulating in Italy between 2010 and 2014. *Virus Res.* **2016**, *220*, 117–128. [CrossRef] [PubMed]
25. Almeida, T.N.V.; De Sousa, T.T.; Da Silva, R.A.; Fiaccadori, F.S.; Souza, M.; Badr, K.R.; de Paula Cardoso, D.d.D. Phylogenetic analysis of G1P[8] and G12P[8] rotavirus A samples obtained in the pre- and post-vaccine periods, and molecular modeling of VP4 and VP7 proteins. *Acta Trop.* **2017**, *173*, 153–159. [CrossRef] [PubMed]

26. Magagula, N.B.; Esona, M.D.; Nyaga, M.M.; Stucker, K.M.; Halpin, R.A.; Stockwell, T.B.; Seheri, M.L.; Steele, A.D.; Wentworth, D.E.; Mphahlele, M.J. Whole genome analyses of G1P[8] rotavirus strains from vaccinated and non-vaccinated South African children presenting with diarrhea. *J. Med. Virol.* **2015**, *87*, 79–101. [CrossRef] [PubMed]
27. Damanka, S.; Kwofie, S.; Dennis, F.E.; Lartey, B.L.; Agbemabiese, C.A.; Doan, Y.H.; Adiku, T.K.; Katayama, K.; Enweronu-Laryea, C.C.; Armah, G.E. Whole genome characterization and evolutionary analysis of OP354-like P[8] Rotavirus A strains isolated from Ghanaian children with diarrhoea. *PLoS ONE* **2019**, *14*, e0218348. [CrossRef] [PubMed]
28. Jere, K.C.; Chaguza, C.; Bar-Zeev, N.; Lowe, J.; Peno, C.; Kumwenda, B.; Nakagomi, O.; Tate, J.E.; Parashar, U.D.; Heyderman, R.S.; et al. Emergence of Double- and Triple-Gene Reassortant G1P[8] Rotaviruses Possessing a DS-1-Like Backbone after Rotavirus Vaccine Introduction in Malawi. *J. Virol.* **2017**, *92*, e01246-17. [CrossRef] [PubMed]
29. Kumar, S.; Stecher, G.; Li, M.; Nnyaz, C.; Tamura, K. MEGA X: Molecular Evolutionary Genetics Analysis across Computing Platforms. *Mol. Biol. Evol.* **2018**, *35*, 1547–1549. [CrossRef]
30. Darriba, D.; Taboada, G.L.; Doallo, R.; Posada, D. jModelTest 2: More models, new heuristics and parallel computing. *Nat. Methods* **2012**, *9*, 772. [CrossRef]
31. Aoki, S.T.; Settembre, E.C.; Trask, S.D.; Greenberg, H.B.; Harrison, S.C.; Dormitzer, P.R. Structure of Rotavirus Outer-Layer Protein VP7 Bound with a Neutralizing Fab. *Science* **2009**, *324*, 1444–1447. [CrossRef]
32. Dormitzer, P.R.; Sun, Z.J.; Wagner, G.; Harrison, S.C. The rhesus rotavirus VP4 sialic acid binding domain has a galectin fold with a novel carbohydrate binding site. *EMBO J.* **2002**, *21*, 885–897. [CrossRef]
33. Dormitzer, P.R.; Nason, E.B.; Prasad, B.V.V.; Harrison, S.C. Structural rearrangements in the membrane penetration protein of a non-enveloped virus. *Nat. Cell Biol.* **2004**, *430*, 1053–1058. [CrossRef]
34. Da Silva, M.F.M.; Rose, T.L.; Gómez, M.M.; Carvalho-Costa, F.A.; Fialho, A.M.; De Assis, R.M.; Sde Andrade, J.d.S.R.; Volotão, E.D.M.; Leite, J.P.G. G1P[8] species A rotavirus over 27 years—Pre- and post-vaccination eras—in Brazil: Full genomic constellation analysis and no evidence for selection pressure by Rotarix<sup>®</sup> vaccine. *Infect. Genet. Evol.* **2015**, *30*, 206–218. [CrossRef] [PubMed]
35. Zeller, M.; Donato, C.; Trovão, N.S.; Cowley, D.; Heylen, E.; Donker, N.C.; McAllen, J.K.; Akopov, A.; Kirkness, E.F.; Lemey, P.; et al. Genome-Wide Evolutionary Analyses of G1P[8] Strains Isolated Before and After Rotavirus Vaccine Introduction. *Genome Biol. Evol.* **2015**, *7*, 2473–2483. [CrossRef] [PubMed]
36. Rasebotsa, S.; Mwangi, P.N.; Mogotsi, M.T.; Sabiu, S.; Magagula, N.B.; Rakau, K.; Uwimana, J.; Mutesa, L.; Muganga, N.; Murenzi, D.; et al. Whole genome and in-silico analyses of G1P[8] rotavirus strains from pre- and post-vaccination periods in Rwanda. *Sci. Rep.* **2020**, *10*, 1–22. [CrossRef] [PubMed]
37. Mwangi, P.N.; Mogotsi, M.; Rasebotsa, S.P.; Seheri, M.L.; Mphahlele, M.J.; Ndze, V.N.; Dennis, F.E.; Jere, K.C.; Nyaga, M.M. Uncovering the First Atypical DS-1-like G1P[8] Rotavirus Strains That Circulated during Pre-Rotavirus Vaccine Introduction Era in South Africa. *Pathogens* **2020**, *9*, 391. [CrossRef]
38. Donato, C.M.; Ch'Ng, L.S.; Boniface, K.F.; Crawford, N.W.; Buttery, J.P.; Lyon, M.; Bishop, R.F.; Kirkwood, C.D. Identification of Strains of RotaTeq Rotavirus Vaccine in Infants With Gastroenteritis Following Routine Vaccination. *J. Infect. Dis.* **2012**, *206*, 377–383. [CrossRef]
39. Gower, C.M.; Dunning, J.; Nawaz, S.; Allen, D.; Ramsay, M.E.; Ladhani, S.N. Vaccine-derived rotavirus strains in infants in England. *Arch. Dis. Child.* **2019**, *105*, 553–557. [CrossRef]
40. Arora, R.; Chitambar, S. Full genomic analysis of Indian G1P[8] rotavirus strains. *Infect. Genet. Evol.* **2011**, *11*, 504–511. [CrossRef]
41. Kulkarni, R.; Arora, R.; Arora, R.; Chitambar, S.D. Sequence analysis of VP7 and VP4 genes of G1P[8] rotaviruses circulating among diarrhoeic children in Pune, India: A comparison with Rotarix and RotaTeq vaccine strains. *Vaccine* **2014**, *32*, A75–A83. [CrossRef]
42. Gouvea, V.; Glass, R.I.; Woods, P.; Taniguchi, K.; Clark, H.F.; Forrester, B.; Fang, Z.Y. Polymerase chain reaction amplification and typing of rotavirus nucleic acid from stool specimens. *J. Clin. Microbiol.* **1990**, *28*, 276–282. [CrossRef]
43. Gentsch, J.R.; Glass, R.I.; Woods, P.; Gouvea, V.; Gorziglia, M.; Flores, J.; Das, B.K.; Bhan, M.K. Identification of group A rotavirus gene 4 types by polymerase chain reaction. *J. Clin. Microbiol.* **1992**, *30*, 1365–1373. [CrossRef]

44. Potgieter, A.C.; Page, N.A.; Liebenberg, J.; Wright, I.M.; Landt, O.; Van Dijk, A. Improved strategies for sequence-independent amplification and sequencing of viral double-stranded RNA genomes. *J. Gen. Virol.* **2009**, *90*, 1423–1432. [CrossRef] [PubMed]
45. Pickett, B.E.; Sadat, E.L.; Zhang, Y.; Noronha, J.M.; Squires, R.B.; Hunt, V.; Liu, M.; Kumar, S.; Zaremba, S.; Gu, Z.; et al. ViPR: An open bioinformatics database and analysis resource for virology research. *Nucleic Acids Res.* **2012**, *40*, D593–D598. [CrossRef] [PubMed]
46. Maes, P.; Matthijnsens, J.; Rahman, M.; Van Ranst, M. RotaC: A web-based tool for the complete genome classification of group A rotaviruses. *BMC Microbiol.* **2009**, *9*, 238. [CrossRef]
47. Katoh, K.; Standley, D.M. MAFFT multiple sequence alignment software version 7: Improvements in performance and usability. *Mol. Biol. Evol.* **2013**, *30*, 772–780. [CrossRef] [PubMed]
48. Edgar, R.C. MUSCLE: Multiple sequence alignment with high accuracy and high throughput. *Nucleic Acids Res.* **2004**, *32*, 1792–1797. [CrossRef]
49. Hazkani-Covo, E.; Graur, D. A Comparative Analysis of numt Evolution in Human and Chimpanzee. *Mol. Biol. Evol.* **2006**, *24*, 13–18. [CrossRef]
50. Nei, M.; Kumar, S. *Molecular Evolution and Phylogenetics*; Oxford University Press: Oxford, UK, 2000.
51. Hasegawa, M.; Kishino, H.; Yano, T.-A. Dating of the human-ape splitting by a molecular clock of mitochondrial DNA. *J. Mol. Evol.* **1985**, *22*, 160–174. [CrossRef]
52. Stamatakis, A. RAxML version 8: A tool for phylogenetic analysis and post-analysis of large phylogenies. *Bioinformatics* **2014**, *30*, 1312–1313. [CrossRef]
53. Rambaut, A.; Lam, T.T.; Carvalho, L.M.; Pybus, O.G. Exploring the temporal structure of heterochronous sequences using TempEst (formerly Path-O-Gen). *Virus Evol.* **2016**, *2*, vew007. [CrossRef]
54. Suchard, M.A.; Lemey, P.; Baele, G.; Ayres, D.L.; Drummond, A.J.; Rambaut, A. Bayesian phylogenetic and phylodynamic data integration using BEAST 1.10. *Virus Evol.* **2018**, *4*, vey016. [CrossRef]
55. Rambaut, A.; Drummond, A.J.; Xie, D.; Baele, G.; Suchard, M.A. Posterior Summarization in Bayesian Phylogenetics Using Tracer 1.7. *Syst. Biol.* **2018**, *67*, 901–904. [CrossRef] [PubMed]

**Publisher’s Note:** MDPI stays neutral with regard to jurisdictional claims in published maps and institutional affiliations.



© 2020 by the authors. Licensee MDPI, Basel, Switzerland. This article is an open access article distributed under the terms and conditions of the Creative Commons Attribution (CC BY) license (<http://creativecommons.org/licenses/by/4.0/>).



MDPI  
St. Alban-Anlage 66  
4052 Basel  
Switzerland  
Tel. +41 61 683 77 34  
Fax +41 61 302 89 18  
[www.mdpi.com](http://www.mdpi.com)

*Pathogens* Editorial Office  
E-mail: [pathogens@mdpi.com](mailto:pathogens@mdpi.com)  
[www.mdpi.com/journal/pathogens](http://www.mdpi.com/journal/pathogens)





MDPI  
St. Alban-Anlage 66  
4052 Basel  
Switzerland

Tel: +41 61 683 77 34  
Fax: +41 61 302 89 18

[www.mdpi.com](http://www.mdpi.com)



ISBN 978-3-0365-2590-7